

PROJECT ADMINISTRATION DATA SHEET

ORIGINAL REVISION NO. _____

Project No./(Center No.) E-19-672 (R6343-OAO) GTRC/~~GHX~~ DATE 7 / 24 / 87

Project Director: Dr. Aryn S. Teja CO School/~~XXH~~ Chemical Engineering

Sponsor: American Society of Heating, Refrigerating and Air Conditioning Engineers, Inc.

Agreement No.: Research Agreement No. 527-RP

Award Period: From 7/1/87 To 12/31/88 (Performance) 1/15/89 Reports

Sponsor Amount:	<u>New With This Change</u>	<u>Total to Date</u>
Contract Value: \$	<u>72,124</u>	\$ <u>72,124</u>
Funded: \$	<u>72,124</u>	\$ <u>72,124</u>

Cost Sharing No./(Center No.) N/A Cost Sharing: \$ N/A

Title: Thermophysical Property Data for Lithium Bromide-Water at High Temperatures and Concentrations.

ADMINISTRATIVE DATA

OCA Contact Ina R. Lashley Ext. 4820

1) Sponsor Technical Contact:

2) Sponsor Issuing Office:

ASHRAE

1791 Tullie Circle

Atlanta, GA 30329

ATTN: William W. Seaton

(404) 636-8400

Military Security Classification: N/A

ONR Resident Rep. is ACO: N/A Yes No

(or) Company/Industrial Proprietary: N/A

Defense Priority Rating: N/A

RESTRICTIONS

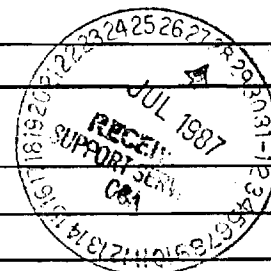
See Attached N/A Supplemental Information Sheet for Additional Requirements.

Travel: Foreign travel must have prior approval — Contact OCA in each case. Domestic travel requires sponsor approval where total will exceed greater of \$500 or 125% of approved proposal budget category.

Equipment: Title vests with Sponsor. See Article VII

COMMENTS:

- This is a fixed-price agreement.
- Sub-Project is E-25-M25/R6343-OA1, Dr. Sheldon M. Jeter, Project Director (Mechanical Engineering)



COPIES TO:

SPONSOR'S I.D. NO. 02.500.001.87.001

- Project Director
- Research Administrative Network
- Research Property Management
- Accounting

- Procurement/GTRI Supply Services
- Research Security Services
- Contract Support Div.(OCA)(2) *Pat*
- Research Communications

- GTRC
- Library
- Project File
- Other _____

GEORGIA INSTITUTE OF TECHNOLOGY
OFFICE OF CONTRACT ADMINISTRATION

NOTICE OF PROJECT CLOSEOUT

Closeout Notice Date 06/26/90

Project No. E-19-672 _____ Center No. R6343-0A0 _____
Project Director TEJA A S _____ School/Lab CHEM ENGR _____
Sponsor AM SOC HEAT REF AIR CON ENGR/ATLANTA, GA _____
Contract/Grant No. 527-RP _____ Contract Entity GTRC
Prime Contract No. _____
Title THERMOPHYSICAL PROPERTY DATA FOR LITHIUM BROMIDE-WATER AT HIGH TEMPS _____
Effective Completion Date 881231 (Performance) 890115 (Reports)

Closeout Actions Required:	Y/N	Date Submitted
Final Invoice or Copy of Final Invoice	Y	910708
Final Report of Inventions and/or Subcontracts	N	_____
Government Property Inventory & Related Certificate	N	_____
Classified Material Certificate	N	_____
Release and Assignment	N	_____
Other _____	N	_____
Comments _____		

Subproject Under Main Project No. _____

Continues Project No. _____

Distribution Required:

Project Director	Y
Administrative Network Representative	Y
GTRI Accounting/Grants and Contracts	Y
Procurement/Supply Services	Y
Research Property Management	Y
Research Security Services	N
Reports Coordinator (OCA)	N
GTRC	N
Project File	Y
Other _____	N
_____	N



Georgia Institute of Technology
School of Chemical Engineering
Atlanta, Georgia 30332-0100
(404) 894- 3098

DESIGNING TOMORROW TODAY

October 22, 1987

Mr. Wm. W. Seaton
Manager of Research
ASHRAE
1791 Tullie Circle NE
Atlanta, GA 30329

ASHRAE Research Project 527-RP "Thermophysical Property Data for Lithium Bromide-Water"

Dear Mr. Seaton:

I am enclosing four copies of the first progress report on the above project. The report covers the period from July 1, 1987 to September 30, 1987.

Yours sincerely,

Aryn S. Teja
Professor

AST/jvl

PROGRESS REPORT #1

PROJECT: E-19-672 (Research Agreement No. 572-RP)

SPONSOR: American Society of Heating, Refrigeration and Air Conditioning Engineers, Inc.

PROJECT TITLE: Thermophysical Property Data for Lithium Bromide-Water at High Temperatures and Concentrations

PRINCIPAL INVESTIGATORS: Aryn S. Teja and Sheldon T. Jeter

GRADUATE STUDENTS: Ralph DiGuilio, Jean-Louis Lenard and Joe Moran

PERIOD COVERED: July 1, 1987 to September 30, 1987

This report covers the first three months of the project and, as such, is limited in its scope. Three students (Ralph DiGuilio, Jean-Louis Lenard and Joe Moran) have begun research work on the physical properties of Lithium Bromide-Water solutions under the supervision of the two principal investigators. In particular, the following specific tasks have been initiated:

- (1) Specific heats: A new drop capsule and a data acquisition system have been purchased for the adiabatic drop calorimeter. Work has begun on interfacing the data acquisition system to the calorimeter. Temperature calibrations of the thermocouples are in progress, as is a literature search of available experimental data.

- (2) Vapor-liquid equilibria: The first measurements on the Fischer recirculation still have been carried out. In this first instance, we have measured the vapor pressure (P vs T behavior) of pure water up to 120°C. Our measured vapor pressures agreed with literature values to $\pm 0.5\%$. An improved pressure control device will be added to further improve our accuracy.

- (3) Thermal conductivity: A tantalum hot-wire cell has been constructed for the measurement of thermal conductivity. The data acquisition system acquired for the adiabatic drop calorimeter will also be interfaced with this thermal conductivity apparatus.

- (4) Density: A literature search of density data for Lithium bromide + water solutions is in progress.

- (5) Viscosity: New high-temperature valves have been added to the capillary viscometer to extend the range of our measurements 200°C and beyond.

In summary, work on all proposed experiments has been initiated, and literature searches for data and correlation techniques are in progress.

E-10-695

3098

January 20, 1988

Mr. Wm. W. Seaton
Manager of Research
ASHRAE
1791 Tullie Circle NE
Atlanta, GA 30329

ASHRAE Research Project 527-RD "Thermophysical Property Data for Lithium Bromide-Water"

Dear Mr. Seaton:

I am enclosing four copies of the second progress report on the above project. The report covers the period from October 1, 1987 to December 31, 1987.

Yours sincerely,

Aryn S. Teja
Professor

AST/jvl

PROGRESS REPORT

(1) Specific Heat

Work on specific heat measurements have been proceeding since summer 1987. Preliminary work included a review of the pertinent literature. No substantive publications were discovered other than the well known work in this area.

Our preliminary laboratory work involved rehabilitating the drop calorimeter and adapting it to this experiment. The apparatus was functionally tested and found to be in basically good working condition. The receiver was plated with a bright nickel alloy to minimize radiation losses. An attempt was made to repair the the defective electromechanical printer that was supplied with the calorimeter. This was an effort to provide a redundant, independent data display in addition to the PC based data acquisition system (DAS) to be used in production runs. This effort was not successful.

The next effort was to interface the calorimeter to the DAS. The DAS can accommodate calibrated thermocouple inputs as well as millivolt level inputs. Standard thermocouple input is used to monitor the sample temperature while in the furnace chamber. Precision resistance networks were constructed to condition the signal from the receiver thermistor. For our purposes two receiver temperature ranges may be necessary (0 to 40°C and 0 to 100°C) so two interface bridges have been designed and constructed.

Some upgrading of the calorimeter has been accomplished to improve its performance and reliability. The most critical functional change is in the measurement of the sample temperature in the heater. In the stock design, a thermocouple is imbedded in the heating element outside the furnace tube. This arrangement is unsatisfactory for at least two reasons. Since the thermocouple is

permanently installed, it cannot be removed for recalibration. Secondly, since the stock thermocouple is attached to the tube wall, it cannot be assured that an accurate sample temperature measurement is being attained. To alleviate these problems, the apparatus was augmented with a calibrated thermocouple that is inserted directly into the capsule. To allow this access, a modified cap was designed and fabricated. Some other minor improvements were made to insure the integrity of electrical connections, minimize mechanical problems caused by dust shedded from thermal insulation, and eliminate jams caused by interference between the heater tube and the capsule.

Some additional analytical work has begun on the analysis of the receiver cooling curves and reduction of heat transfer data to energy changes and specific heats.

(2) Vapor-liquid Equilibria

We are continuing with improvements to the pressure control system to obtain better accuracy using the Fischer VLE apparatus. In addition, the temperature measurement system has been calibrated against a standard platinum resistance thermometer.

(3) Thermal Conductivity

Two new tantalum thermal conductivity cells have been constructed. The cells were being tested with toluene as the test fluid when the toluene reacted with the teflon parts of the cell. A new set of parts made of bakelite is therefore under construction. In addition, several improvements to the measuring apparatus have been made. New differential amplifiers have been added and key components have been rewired. Conversion of data to computer is still in progress.

(4) Density

Initial tests with m-xylene have been carried out. Our results agreed with literature values to a disappointing 1.5%. Several improvements to the apparatus and procedure are therefore being undertaken.

(5) Viscosity

We are awaiting several key components (including a capillary U-tube) to complete construction of this apparatus.



ASHRAE American Society of Heating, Refrigerating and Air-Conditioning Engineers, Inc.

1791 Tullie Circle, NE • Atlanta, Georgia 30329 ☎ (404) 636-8400 • Tlx 705343 ASHRAE

RESEARCH PROGRESS REPORT

1. **Project Number and Title:** 527-RP: Thermophysical data for lithium bromide-water at high temperatures and concentrations
2. **Sponsoring ASHRAE Technical Committee or Task Group:**
3. **Research Institution:** Georgia Tech Research Corporation
4. **Objective of Research:** Measurement of specific heat, thermal conductivity, vapor pressure, viscosity and density of concentrated aqueous lithium bromide solutions at high temperatures
5. **Period of Report:** January 1, 1988 to March 31, 1988
6. **Summary of Activity including specific accomplishments, trends or conclusions (use additional sheets if needed.)**

(see attached)
7. **Any Condition(s) which effect the scheduled completion or cost of the project or which suggests a modification to the scope is reported on a separate sheet. Such a sheet is _____, is not X attached.**

(Signature of Principal Investigator)

Amy S. Teja 404-894-3098

(Typed Name and phone number
of Principal Investigator)

4/25/88

(Date)

Submit Four Copies of this Report to:

Manager of Research
ASHRAE

1791 Tullie Circle, NE
Atlanta, GA 30329

PROGRESS REPORT SPECIFIC HEAT MEASUREMENTS

As originally proposed, these specific heat measurements are being conducted using a commercially fabricated drop calorimeter. A drop calorimeter comprises a heater section and a receiver along with auxiliaries and controls. In operation, the material sample is confined in a rigid capsule or "bomb". The sample is brought up to temperature in the tube heater and inserted, by dropping, into the receiver. The receiver is a massive metal block, a copper cylinder in this case. The heat interaction between the sample and receiver can be monitored with a temperature probe installed in the receiver.

Work on specific heat measurements have been proceeding since summer 1987. Preliminary work included a review of the pertinent literature. No substantive publications were discovered other than the well known work in this area.

Our preliminary laboratory work involved rehabilitating the drop calorimeter and adapting it to this experiment. The apparatus was functionally tested and found to be in basically good working condition. The receiver was plated with a bright nickel alloy to minimize radiation losses. An attempt was made to repair the defective electromechanical printer that was supplied with the calorimeter. This was an effort to provide a redundant, independent data display in addition to the PC based data acquisition system (DAS) to be used in production runs. This effort was not successful.

The next effort was to interface the calorimeter to the DAS. The DAS can accommodate calibrated thermocouple inputs as well as millivolt level inputs. Standard thermocouple input is used to monitor the sample temperature while in the furnace chamber. Precision resistance networks were constructed to condition the signal from the receiver thermistor. For our purposes two receiver temperature ranges may be necessary (0 to 40 C and 0 to 100 C) so two interface bridges have been designed and constructed.

Some upgrading of the calorimeter has been accomplished to improve its performance and reliability. The most critical functional change is in the measurement of the sample temperature in the heater. In the stock design, a thermocouple is imbedded in the heating element outside the furnace tube. This arrangement is unsatisfactory for at least two reasons. Since the thermocouple is permanently installed, it cannot be removed for recalibration. Secondly, since the stock thermocouple is attached to the tube wall, it can not be assured that an accurate sample temperature measurement is being attained. To alleviate these problems, the apparatus was augmented with a calibrated thermocouple that is inserted directly into the capsule. To allow this access, a modified cap was designed and fabricated. Some other minor improvements were made to insure the integrity of electrical connections, minimize mechanical problems caused by dust shedded from thermal insulation, and eliminate jams caused by interference between the heater tube and the capsule. These mechan-

cal and electrical upgrades were completed by January 1988.

An important upgrading of the calorimeter has been the provision of an insulated enclosure. This enclosure when permanently equipped with a temperature controller will eliminate measure error induced by varying ambient temperatures. The enclosure is a necessity for high concentration experiments since the receiver must be kept at an elevated temperature to avoid heat effects from phase changes that would disrupt the sensible specific heat determinations.

The present operation of the drop calorimeter is relatively simple in principle although demanding in practice. The experimental procedure is as follows:

1. A solution sample is placed in the capsule. The sample is measured to allow for expansion from room temperature to furnace temperature. The mass of the sample is determined by weighing the loaded sample and subtracting the mass of the empty sample.

2. The capsule is installed in the furnace of the calorimeter. The furnace temperature setting is adjusted to an elevated temperature and the receiver is readied to accept the drop.

3. A delay of 40 to 60 minutes is imposed to insure that the receiver is at an equilibrium temperature, essentially the same as the enclosure temperature.

4. Just prior to a drop, the receiver temperature is monitored for ten minutes to ensure that it has stabilized. This is the initial receiver temperature T_i . If the receiver temperature is stable, a drop is initiated about 3 seconds before a minute on the PC clock. This will insure that the capsule enters the receiver nearly on the minute. With data being logged on the minute, the drop time is then precisely identified. The initial sample temperature T_s is also determined at this time.

5. The data logger then continues to record receiver temperature for two to three hours. This time is required for a full presentation of the receiver heating and cooling process.

6. Data is then retrieved from the PC and analyzed on a VAX.

Some analytical work has been accomplished on the analysis of the receiver cooling curves and reduction of heat transfer data to energy changes and specific heats. While some additional work in this area may be desirable to utilize the available data to the maximum extent, a preliminary procedure has been developed and applied with apparent success. A search procedure is conducted to find the time maximum empirical receiver temperature. The cooling curve is then extrapolated from twice this time to the time at which the receiver achieves 60% of the empirical maximum. The extrapolated value approximates the hypothetical maximum temperature that the receiver would attain in the absence of heat loss from the receiver. This procedure gives the final receiver temperature T_f .

Assuming that heat loss from the receiver has been compensated by the cooling curve analysis outlined above, the energy increase of the receiver equals the energy decrease of the capsule and sample, or

$$C_r * DTr = (C_c + C_s) * DTs$$

where:

C_r = heat capacity of receiver

C_c = heat capacity of capsule

C_s = (unknown) heat capacity of sample

DTr = temperature change of receiver, $T_f - T_i$

DTs = temperature change of sample and capsule, $T_s - T_f$

Solving for the sample heat capacity one has:

$$C_s = C_r * DTr/DTs - C_c$$

Or in experimentally more convenient terms:

$$C_s = C_r * DTr/DTs - C_r * K$$

Where $K = C_c/C_r$ and is determined from a series of empty drops.

With C_r determined from a series of drops using a sample with standard heat capacity, the heat capacity of the sample can be determined. Note that this is the average heat capacity over the range T_f to T_s . The specific heat capacity, c , is determined by dividing by the mass of the sample, and point specific heats are determined from an RMS fit to a series of drops from different sample temperatures. A first order model, for fixed concentration, seems to be adequate such that :

$$c = a + b * T$$

Representative results are displayed on the attached Figure 1. These results show reasonably good agreement with Differential Scanning Calorimeter (DSC) data graciously provide by Dr. Uwe Rockenfelder of Rocky Research. As is evident in the graph the specific heats from the current investigation and the alternative data are in general agreement. A problematical situation is evident in that the drop calorimeter data for the 65% solution is anomalous. This data was collected using the heated enclosure. It is planned to repeat the drops for this concentration and compare with literature results for a compound with well established specific heat values in the same temperature range.

The lower concentration specific heats are in better agreement, possibly to near the inherent accuracy of the two instruments. The drop calorimeter shows systematically higher values and greater increase with temperature. It is planned to repeat some or all of these runs and scrutinize the data processing techniques in an attempt to either reduce the disagreement or substantiate the current results.

45%–65% LiBr

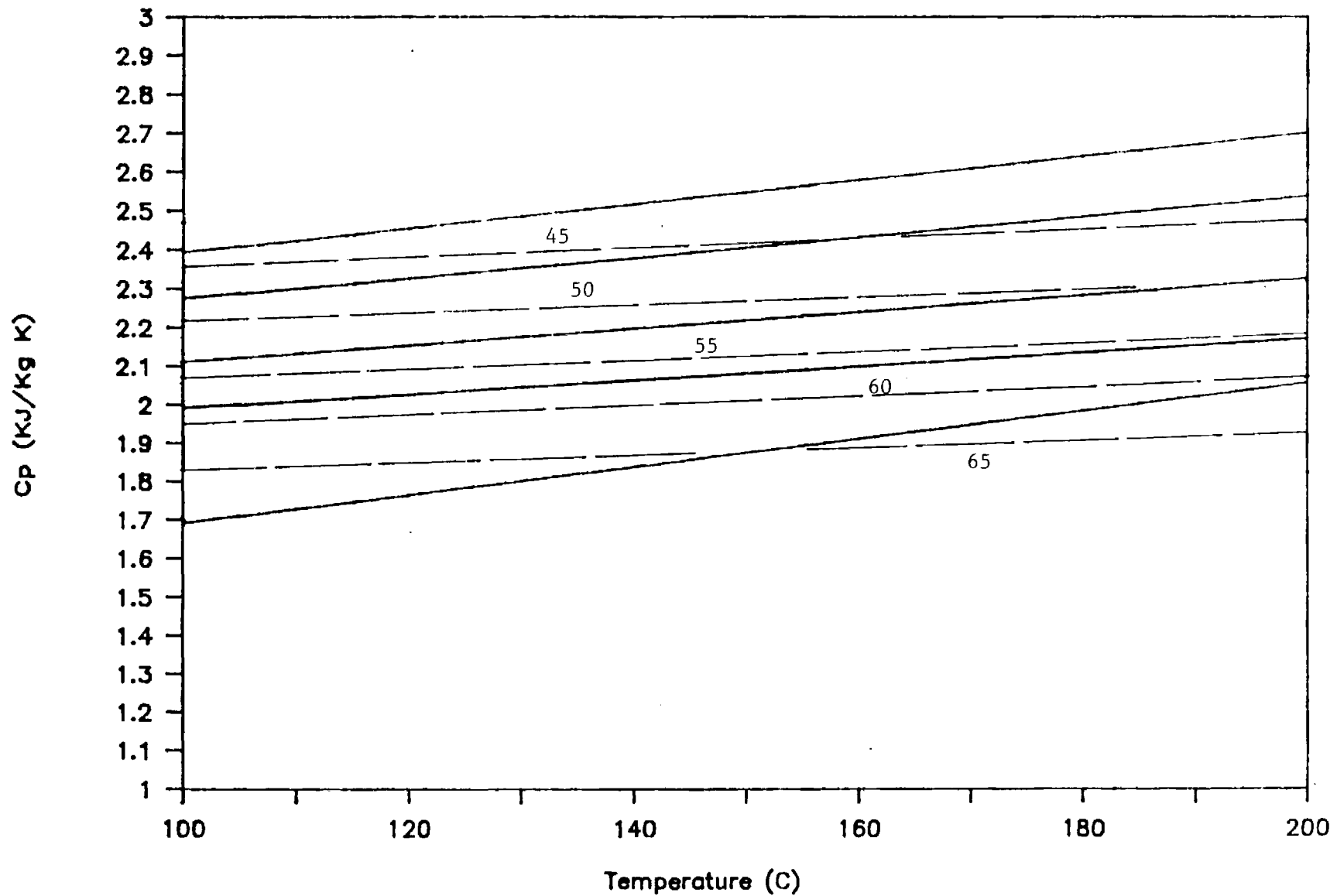


Figure 1: Comparison of Specific Heats from Current Study with Alternative Results (broken lines). concentration by Mass Fraction in Percent.

Thermal Conductivity of Lithium Bromide Solutions

It is now established that the most accurate method for the measurement of thermal conductivity is the transient hot wire method [1]. This method generally employs platinum for the electrically heated wire. The platinum wire is not satisfactory in the case of electrolytes. The electrolyte solution interferes with the measurement in two ways. In the first, some of the current intended to heat the wire is lost directly to the solution. In the second, constituents of the electrolyte polarize onto the wire, thus destroying the homogeneity of the liquid [2]. The solution is to insulate the wire from the fluid. Nagaska et. al. [3] tried applying a polymer coating but were limited in temperature. Wakeham et. al. [2], employed a tantalum filament with a tantalum oxide coating produced on the filament in situ. The cell was then used to measure aqueous lithium bromide solutions.

The data shown below in figure 1 were reported by Wakeham [2] in 1982. The accuracy is claimed to be $\pm 3\%$.

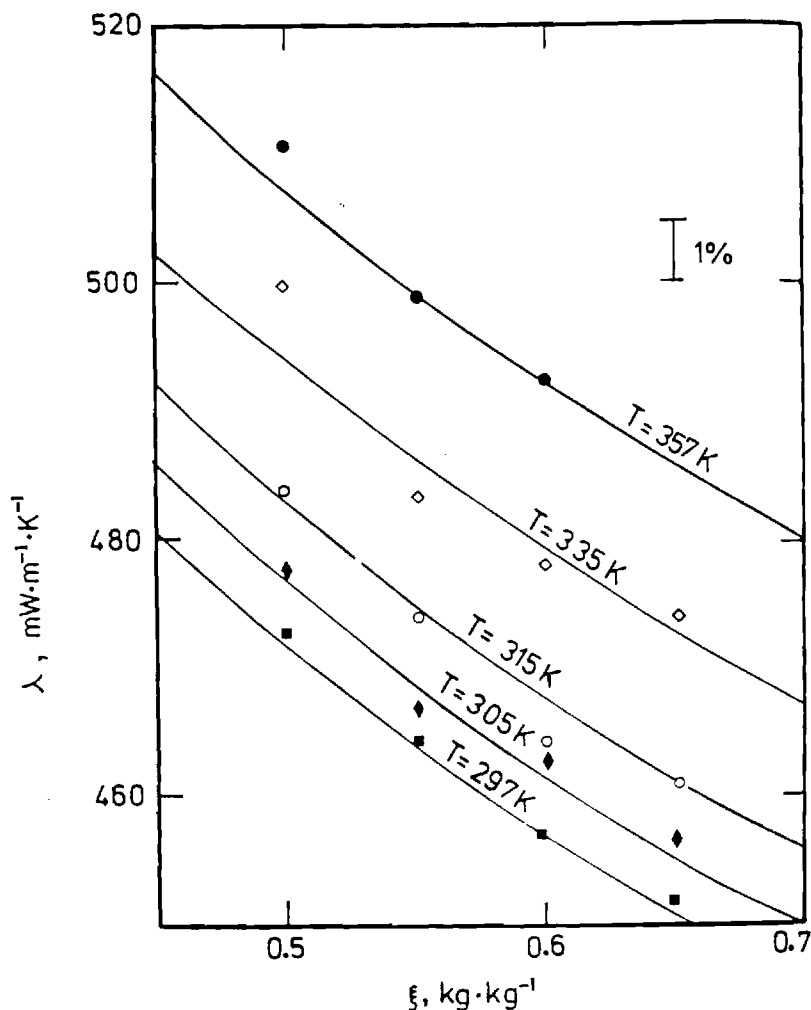


Figure 1: Thermal Conductivity of Libr solutions over a range of temperature and concentrations.

The following equation is given to represent the data [2]:

$$k = 434.14 - 367.69Z + 191.64Z^2 + .5875T$$

k = thermal conductivity [mW/ m K]

Z = mass fraction LiBr

T = absolute temperature [K]

Deviation from the correlation is less than $\pm 0.8\%$. The method is limited in temperature to about 420 K because of the unequal expansion of the tantalum and its oxide.

Our measurements will be done in a similiar manner as those of Wakeham et. al. [2]. Specifically we will use the transient hot wire technique with the oxide coated tantalum wire. Prior to these measurements, however, we planned to computerize our apparatus. The data acquisition system has been installed and the necessary software developed. The apparatus was checked by testing toluene, an accepted standard [1], with platinum cells. Results are shown in figure 2. Agreement with the standard is within 1.5%.

Toluene (P = 1 atm)

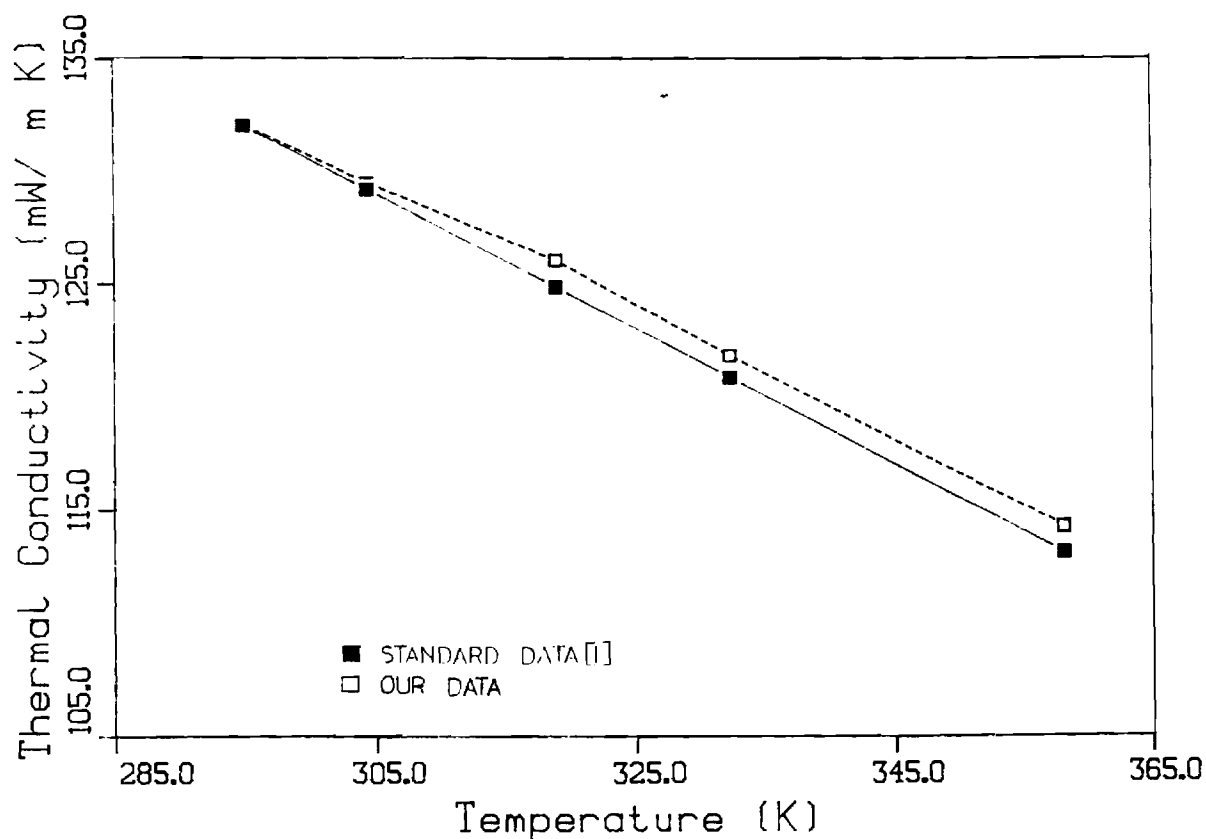


Figure 2: Results obtained for Toluene with our apparatus using platinum cells.

The design of the tantalum cells is complete. The next step is to test our tantalum cells without the oxide coating. Figure 3 below is a drawing of the cell. We will then proceed to coat the tantalum and verify that the cell works by measuring a suitable substance such as toluene or pure water. Finally, we will measure the LiBr solutions.

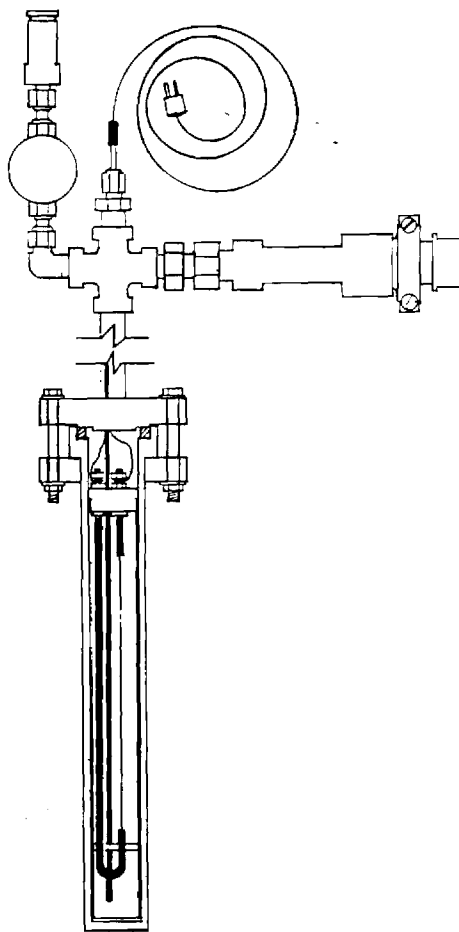


Figure 3: Tantalum thermal conductivity cell.

References

1. Nieto de Castro C. A., Li S. F. Y., Nagashima A.,
Trenngrove R. D., Wakeham W. A., *J Phys Chem Ref Data*
15:1073 (1986)
2. Wakeham W. A., Alloush A., Gosney W. B., *Int J*
Thermophysics, 3:225 (1982)
3. Nagasaka Y., Nagashima A., *J Phys E: Sci Instrum* 14:
1435 (1981)

VAPOR PRESSURE OF AQUEOUS SOLUTIONS OF LITHIUM BROMIDE

Numerous techniques are available for measuring the vapor pressures of salt solutions [1], [2]. Our original intentions were to use the dynamic recirculation method available in our laboratory [3]. A more promising technique for salts solutions seems to be the determination of vapor pressure by a static apparatus. Figure 1 shows the main features of such a device designed in our laboratory (For clarity, only one cell is represented).

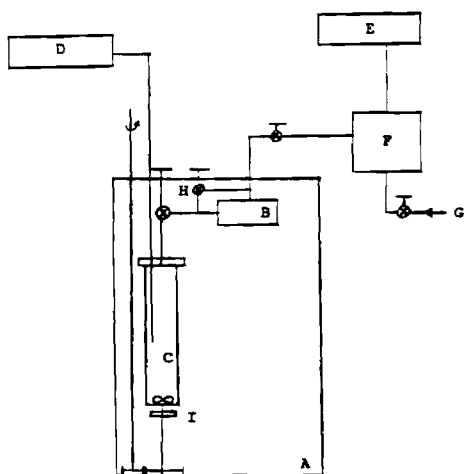


Figure 1.

- A. constant temperature bath
- B. differential pressure transducer
- C. equilibrium chamber
- D. electronic thermometer
- E. pressure gauge
- F. surge tank
- G. high pressure inert gas
- H. by-pass valve for zeroing B in situ
- I. magnet

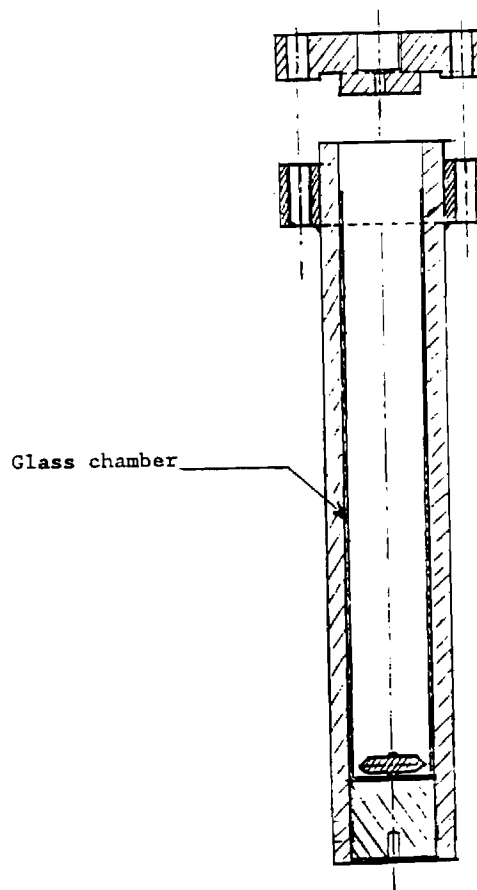
The glass chamber inside the high pressure equilibrium cell eliminates the problem of corrosion inherent to the system H₂O-LiBr. The mixing of the solution is done by a magnetically driven glass coated bar and enables a quick approach to equilibrium. The vapor pressure is measured through an external gauge; the equality between the cell pressure and the inert gas pressure is ensured by the balancing of the differential pressure transducer. This design eliminates the problem of condensation in the lines. The temperature of the cell is

controlled by placing the whole assembly in an oil bath. The temperature is measured by a platinum resistance thermometer. The composition of the solutions are determined gravimetrically during the loading of the cells.

This apparatus will allow us to extend substantially the data base of vapor pressures of concentrated aqueous solutions of lithium bromide at high temperatures. We are, however, still in the final design and testing stages of this apparatus.

Figure 2.

Equilibrium cell



References

- [1]. PYTKOWICZ R.M., " Activity coefficients in electrolyte solutions ", vol I, CRC press, Inc, 1979.
- [2]. WILHOIT R.C., " Current status of experimental knowledge of thermodynamics of aqueous solutions ", in " Thermodynamics of aqueous systems with industrial applications ", ACS symposium series 133, 1980
- [3]. WILLMAN B.T. and TEJA A.S., J. Chem. Eng. Data, 30, 116, 1985

Measurement of the Absolute Viscosity of Aqueous Lithium Bromide Solutions under Pressure

The apparatus used to measure the viscosity of liquids under pressure is the absolute capillary viscometer shown in Figure 1. This apparatus is designed to pass a precise flow of fluid through a capillary tube of known dimensions at a controlled temperature (up to 600K) and pressure (up to 70MPa). By measuring the pressure drop across the capillary, the viscosity of the fluid μ can be determined using Poisselle's law:

$$\mu = \frac{\pi r^4 \Delta P}{8LQ}$$

where r is the capillary radius, L is the capillary length, ΔP is the pressure drop, and Q is the fluid flow rate.

The fluid initially held in the feed tank is fed into the Ruska piston pump. The delivery range of the pump is from 0.1 to 10 cm³/min. The fluid then passes through a pre-heater and into the capillary assembly. The capillary assembly consists of a number of tubes which permit the selection of the proper radius for the fluid viscosity range. The differential pressure is measured with a differential pressure gauge. Upon exiting the capillary assembly, the fluid is cooled, depressurized, and collected.

The system pressure is measured by a Heise gauge calibrated with a Bundenberg dead-weight gauge and is accurate to ± 0.3 MPa. The system temperature is measured with a thermocouple calibrated with an NBS-certified platinum resistance thermometer, and is accurate to ± 0.1 K. The differential pressure gauge has been calibrated with a manometer.

Corrections to the viscosity for non-idealities such as capillary curvature and entrance and exit effects have been developed. The operation and accuracy of this apparatus have been confirmed using several test fluids--water, n-propanol, and cyclohexane. The average reproducibility of the measured viscosity is approximately ± 2 percent and, by comparison with literature data, the accuracy is also approximately ± 2 percent.

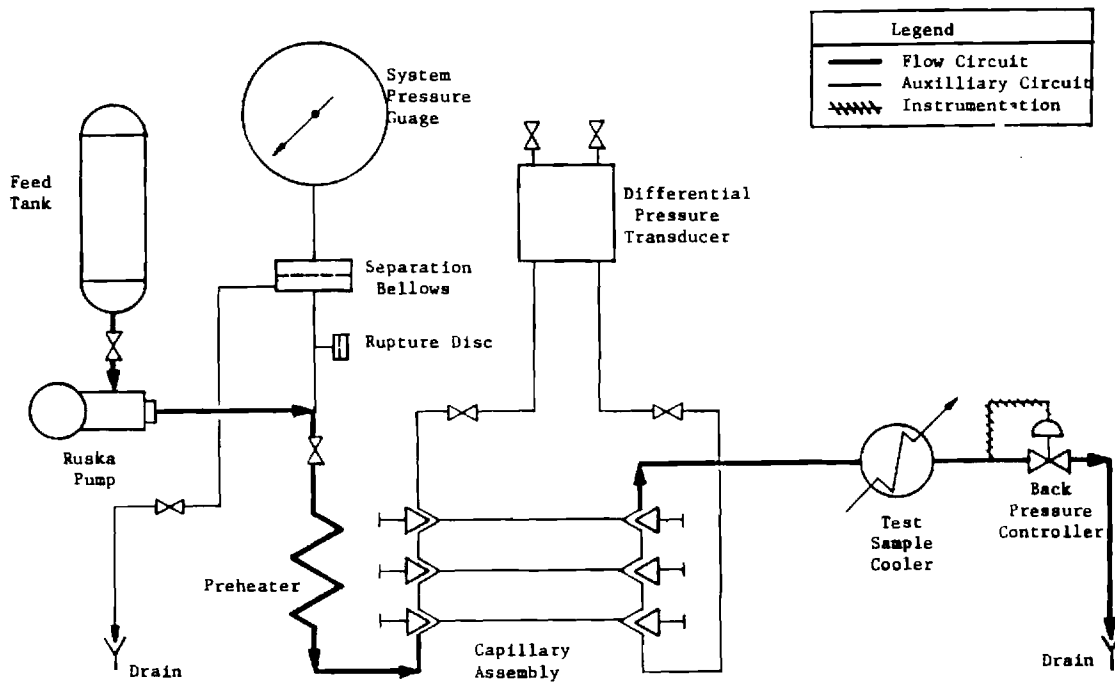


Figure 1.
Schematic Flow Diagram of Absolute Viscometer
Experimental Apparatus

Density of LiBr - Water Solutions

Density of a fluid is an important parameter in aiding the design of many systems. Therefore, we see the density as a worthwhile investigation for the LiBr salt solutions. The density of several compositions of LiBr-water solutions are being examined. This density investigation employs two techniques: one consists of a vibrating densitometer and the other uses a high pressure pycnometer. By using two different experiments, we are able to confirm our results thus leading to higher reliability.

The densitometer (Fig. 1) works by electronic measurement of a time period from which, upon calibration, density can be calculated. The measuring principle of the instrument is based on the change of the natural frequency of a hollow oscillator when filled with different liquids or gases. The mass, and thus the density, of the liquid changes this natural frequency of vibration. The oscillator consists of a hollow steel tube which is electronically excited in an undamped harmonic fashion. The frequency of the oscillator is only influenced by that fraction of the volume of liquid which is actually in the vibrating part of the sample tube. It is essential to ensure that the sample tube is completely filled; over filling does not affect the measurement since the vibrating volume is always the same inside the tube.

Our high pressure pycnometer (Fig. 2) consists of a stainless steel cylinder containing a high pressure fitting and valve. The cell contains a thermowell to allow the temperature inside the cell to be measured. In order to make an experimental density determination, the cylinder is cleaned thoroughly and then weighed. By loading the cylinder with a fluid of well known density, the volume of the cell can also be determined. Once the characteristics of the cell have been found, the cell is evacuated and filled with the sample. The cell is attached to a surge bottle then immersed in a constant temperature oil bath. As the liquid expands, it flows freely between the pycnometer and the surge bottle. Once temperature and pressure equilibrium have been achieved, the valve on the full pycnometer is closed and the complete cell is removed from the bath, allowed to cool, and then weighed. This enables the weight of the sample to be determined and, knowing the volume of the cell, the density can be determined.

Currently, both apparatuses have been calibrated using pure water and N₂. The results obtained from the pycnometer are reliable to within 0.1%. The vibrating tube densitometer is being used to measure LiBr-H₂O densities from 30 C to 80 C, and the pycnometer from 80 C to 200 C. This will allow a cross-check of the data.

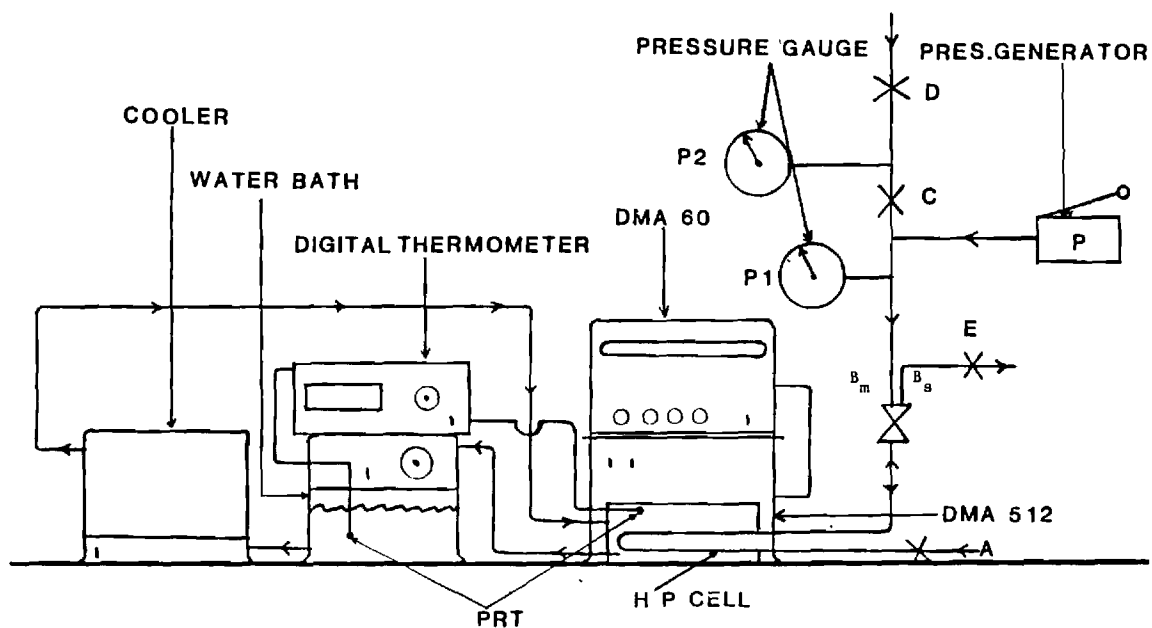


Figure 1

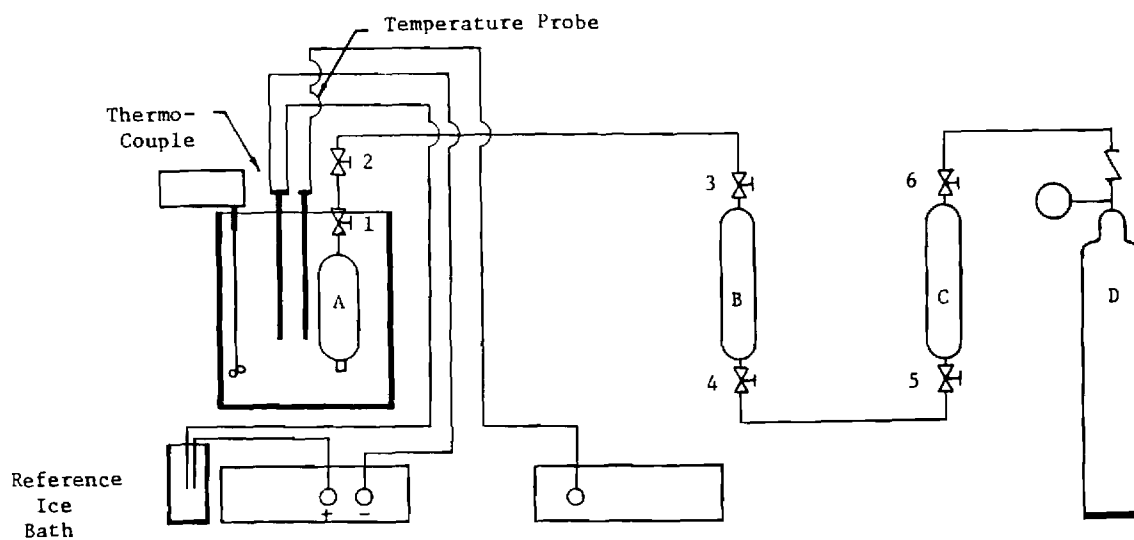


Figure 2. The Pycnometer Schematically Shown

A. Hoke 2HD30 pressure cylinder



ASHRAE American Society of Heating, Refrigerating and Air-Conditioning Engineers, Inc.

1791 Tullie Circle, NE • Atlanta, Georgia 30329 ☎ (404) 636-8400 • Tlx 705343 ASHRAE

RESEARCH FINANCIAL REPORT

- A. Project Number and Title: Thermophysical Property Data for Li Br/Water
Project 527-RP
- B. Research Institution: Georgia Tech
- C. Period Covered by Report: 1 April to 31 May, 1988

1.0 Total ASHRAE Funds Appropriated: \$ 72,124.00

2.0 Expenditures prior to period reported: \$ 43,239.49

3.0 Expenditures during period reported:

a) Professional Salaries	\$ 0
b) Research Assistants	<u>2,771.00</u>
c) Fringe Benefits	<u>0</u>
d) Equipment	<u>0</u>
e) Supplies & Materials	<u>345.50</u>
f) Computer Costs	<u>0</u>
g) Travel & Communications	<u>0</u>
h) Special Expenses (explain below)	<u>0</u>
i) Total Direct Costs	<u>3,116.50</u>
j) Indirect Costs	<u>1,870.00</u>
k) TOTAL	<u>4,986.50</u>

4.0 Total expenditures to date: 48,225.99

5.0 Balance of appropriated funds: 23,898.01

6.0 Explanation of any Special Expenses:

7.0 Statement of anticipated deviation from estimated fund requirements:

8.0 Signature of Project Director: _____

Title: Associate Professor

Date: 8 June, 1988

Submit four copies to:

Manager of Research
ASHRAE
1791 Tullie Circle, N. E.
Atlanta, Georgia 30029

SUMMARY OF ACTIVITY

THERMOPHYSICAL PROPERTY DATA FOR LiBr/WATER

1. **DENSITY.** Preliminary results have been obtained with the vibrating tube densitometer. These results show acceptable internal consistency. Vibrating tube densitometer measurements will be conducted over the range of 25 to 150 C. Higher temperatures cannot be attempted because of pressure limitations on glass components. At higher temperatures, the high pressure pycnometer must be used. Preliminary measurements with this instrument have not been internally consistent or consistent with published values for suggested reference fluids within 1 %. Improvements in technique and apparatus are being implemented. Simplified fittings and careful technique will insure that the bulb is absolutely full. To improve temperature data, an immersed thermowell is now installed in the sample bulb. This gives better thermal contact between temperature sensor and sample fluid. It may be necessary to passivate the inner surface of the stainless steel bulb to eliminate corrosion. With these enhancements and improved operational technique, it should be possible to make accurate pycnometer measurements over the range of 100 to 200 C. These overlapping measurements by independent means should reinforce the credibility of the density data.

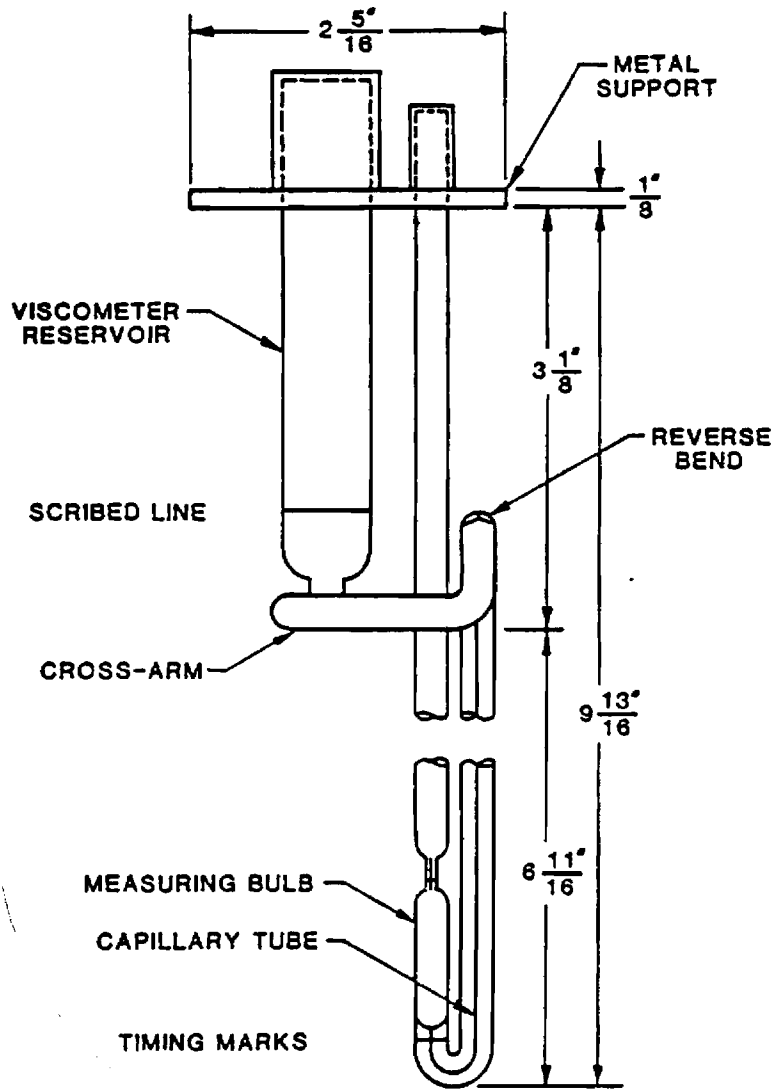
2. **THERMAL CONDUCTIVITY.** The transient hot wire thermal conductivity cell has been tested with nonconductive organic liquids and is being readied for measurements on the conductive Li Br solutions. All software for data acquisition and analysis have been developed and tested. The next critical step is the formation of a stable oxide coating on the filament and its supports by an electrochemical process.

3. **SPECIFIC HEAT.** Preliminary results have been reported previously. These data agree well with recent independent data. Both data sets agree that the specific heat trends up with increasing temperature and down with increasing salt concentration. Both trends are in agreement with a microscopic model of water molecules highly polarized by electrolyte ions. Increasing salt concentration and consequent polarization enhances the microscopic restoring forces and raises the characteristic frequency and energy of microscopic oscillations. These higher energy modes are not so readily excited leading to a lower specific heat with increased salt concentration. Higher solution temperatures increase the population of excited states and raise the specific heat.

Improvements continued on the drop calorimeter including the implementation of a controlled temperature enclosure. Comparison drops using ethanol as a reference fluid have yielded results agreeing with published data when the initial receiver temperature drift has been small. This small drift can be effected by allowing a longer equilibration time between drops. It may also be possible to improve the cooling curve analysis to compensate for any residual drift.

4. **VAPOR PRESSURE.** Design of the static vapor pressure cell is complete and required components are on hand or on order. This apparatus should yield very accurate results at the required high pressures. A cover gas is used to maintain and indicate the pressure in the sample vessel. This eliminates the concern about possible condensation in external tubing and consequent degradation of pressure measurements. Since it will not be necessary to measure the composition of the vapor phase, this apparatus, being simpler and more reliable, is preferable to the dynamic recirculating system originally proposed.

5. **VISCOSITY.** Review of established techniques has revealed a very promising technique that has now been adopted for these measurements. This technique utilizes the cross-arm variant of the capillary viscometer, see attached figure. The cross arm allows remote manipulation of the fluid so the device can be installed in a pressure vessel for the required high temperature measurements. Flow of the fluid will be monitored visually through high pressure windows.



SCHEMATIC OF CROSS-ARM CAPILLARY VISCOMETER



ASHRAE American Society of Heating, Refrigerating and Air-Conditioning Engineers, Inc.

1791 Tullie Circle, NE • Atlanta, Georgia 30329 ☎ (404) 636-8400 • Tlx 705343 ASHRAE

RESEARCH PROGRESS REPORT

1. Project Number and Title: 527-RD Thermophysical Data for Lithium Bromide-Water
2. Sponsoring ASHRAE Technical Committee or Task Group:
3. Research Institution: Georgia Institute of Technology
4. Objective of Research: Measurement of specific heat, density, viscosity, thermal conductivity and vapor pressure of concentrated aqueous lithium bromide solutions at high temperatures.
5. Period of Report: June 1, 1988 to Sept. 30, 1988
6. Summary of Activity including specific accomplishments, trends or conclusions (use additional sheets if needed.)

(SEE ATTACHED)

7. Any Condition(s) which effect the scheduled completion or cost of the project or which suggests a modification to the scope is reported on a separate sheet. Such a sheet is _____, is not x attached.

C. S. Teja
(Signature of Principal Investigator)

10/14/88
(Date)

AMYN S. TEJA 404-894-3098
(Typed Name and phone number
of Principal Investigator)

Submit Four Copies of this Report to:
Manager of Research
ASHRAE
1791 Tullie Circle, NE
Atlanta, GA 30329

ASHRAE Project 527-RD Thermophysical Data for Lithium Bromide-Water

Research Progress Report

June-Sept. 1988

1. DENSITY. Density measurements have been completed for Lithium Bromide-Water solutions containing 45.07, 49.85, 55.0 and 59.9 wt% Lithium Bromide. A high pressure pycnometer designed in our laboratory was used in the experiments and measurements were made at temperatures between 25°C and 200°C. The data were consistent with data obtained (in our laboratory) using a vibrating tube densitometer at the lower temperatures and also agreed with the lower temperature data of Vemura and Hasaba (Technical Reports of Kansai University, Japan, 6, 31-55, 1964) and Bagatykh and Evnovich (Zh. Prikl. Khim. 38, 945, 1965) within $\pm 0.2\%$. Our data are given in Table 1 and comparisons with literature values are given in Fig. 1. Each reported value represents an average of four measurements. The standard deviations are also given.

2. VISCOSITY. Kinematic viscosities of 45.0, 49.85, 55.0 and 59.9 wt% Lithium Bromide-water solutions were measured using a capillary viscometer described in an earlier report. A schematic diagram of the apparatus is given in Fig. 2. Problems were experienced with the temperature controller at high temperatures and therefore only data between temperatures of 30°C and 110°C are reported in Table 2. We are in the process of replacing the controller and will report data up to 200°C in the next report. Each value reported in Table 2 represents the average of at least four runs and therefore standard deviations are also reported. Kinematic viscosities were converted to dynamic

viscosities using density data measured by us and these values are plotted in Figs. 3 and 4. Also shown in the figures are the viscosity data of Vemura and Hasabe (Technical Reports of Kansai University, Japan, 6, 31-55, 1964) and Bogatykh and Evnovich (Zh. Prikl. Khim. 36, 1867, 1963). Our results generally fall between the values of these two sources.

3. THERMAL CONDUCTIVITY. Construction of the transient hot wire thermal conductivity cell for aqueous electrolyte solutions has been completed. The coating of the tantalum wire with a stable oxide layer has also been successfully completed after much trial and error. The thermal conductivity of water has been measured and will serve as the reference for the work on lithium bromide solutions. A problem encountered recently is the shorting of the electrical circuit at high temperatures caused by evolution of vapors from the epoxy plugs used in the cell. We expect to overcome this problem and have the Lithium bromide thermal conductivities in the very near future.

4. VAPOR PRESSURES. The apparatus shown in Fig. 5 has been constructed for the direct measurement of the vapor pressure over lithium bromide-water solutions. The apparatus consists of a bank of six stainless steel equilibrium cells connected via a manifold to a pressure measurement system. Lithium bromide-water solutions will be placed in five of the cells and pure water in the sixth. The measurement of the vapor pressure of pure water will provide a means for determining the accuracy of the vapor pressure measurements for Lithium bromide-water solutions. The pressure measurement system consists of a Heise 710A pressure transducer and readout, as well as a pressure transmitting fluid, Gallium was chosen as the pressure transmitting fluid because of its very low vapor pressure at high temperatures (10^{-5} Torr

at 500°C) and because it is inert to metals, water and other substances. However, because the melting point of gallium is 29.7°C, an auxiliary water bath will be used to keep its temperature above 30°C. It is expected that vapor pressure measurements will be completed by Dec. 1988.

Table 1. Densities of Lithium Bromide-Water Solutions

45.07 wt% LiBr

49.85 wt% LiBr

<u>Temp (°C)</u>	<u>ρ (g/cm³)</u>	<u>Std. dev.</u>	<u>Temp (°C)</u>	<u>ρ (g/cc)</u>	<u>Std. dev.</u>
28.48	1.4554	4.2×10^{-4}	25.55	1.5328	8.8×10^{-4}
45.98	1.4470	5.6×10^{-4}	45.30	1.5206	4.7×10^{-4}
60.02	1.4389	1.6×10^{-3}	60.03	1.5128	8.4×10^{-4}
74.95	1.4323	1.4×10^{-3}	74.79	1.5042	6.0×10^{-4}
88.45	1.4255	1.7×10^{-3}	89.89	1.4954	7.5×10^{-4}
108.12	1.4144	1.0×10^{-3}	109.49	1.4833	7.6×10^{-4}
129.20	1.4041	9.0×10^{-4}	129.61	1.4705	7.6×10^{-4}
150.32	1.3919	6.9×10^{-4}	150.51	1.4568	6.9×10^{-4}
174.25	1.3782	5.4×10^{-4}	175.43	1.4397	9.2×10^{-4}
			201.64	1.4216	1.1×10^{-3}

55.0% LiBr

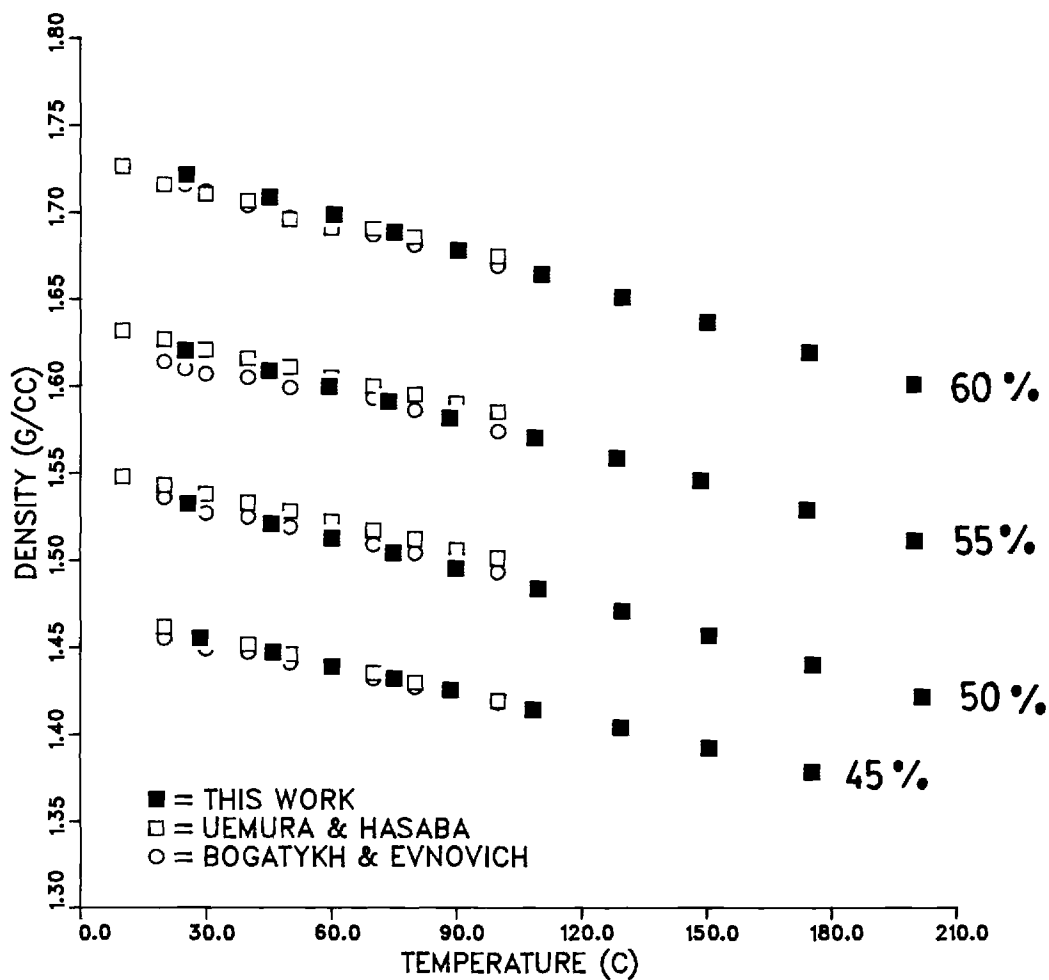
59.90% LiBr

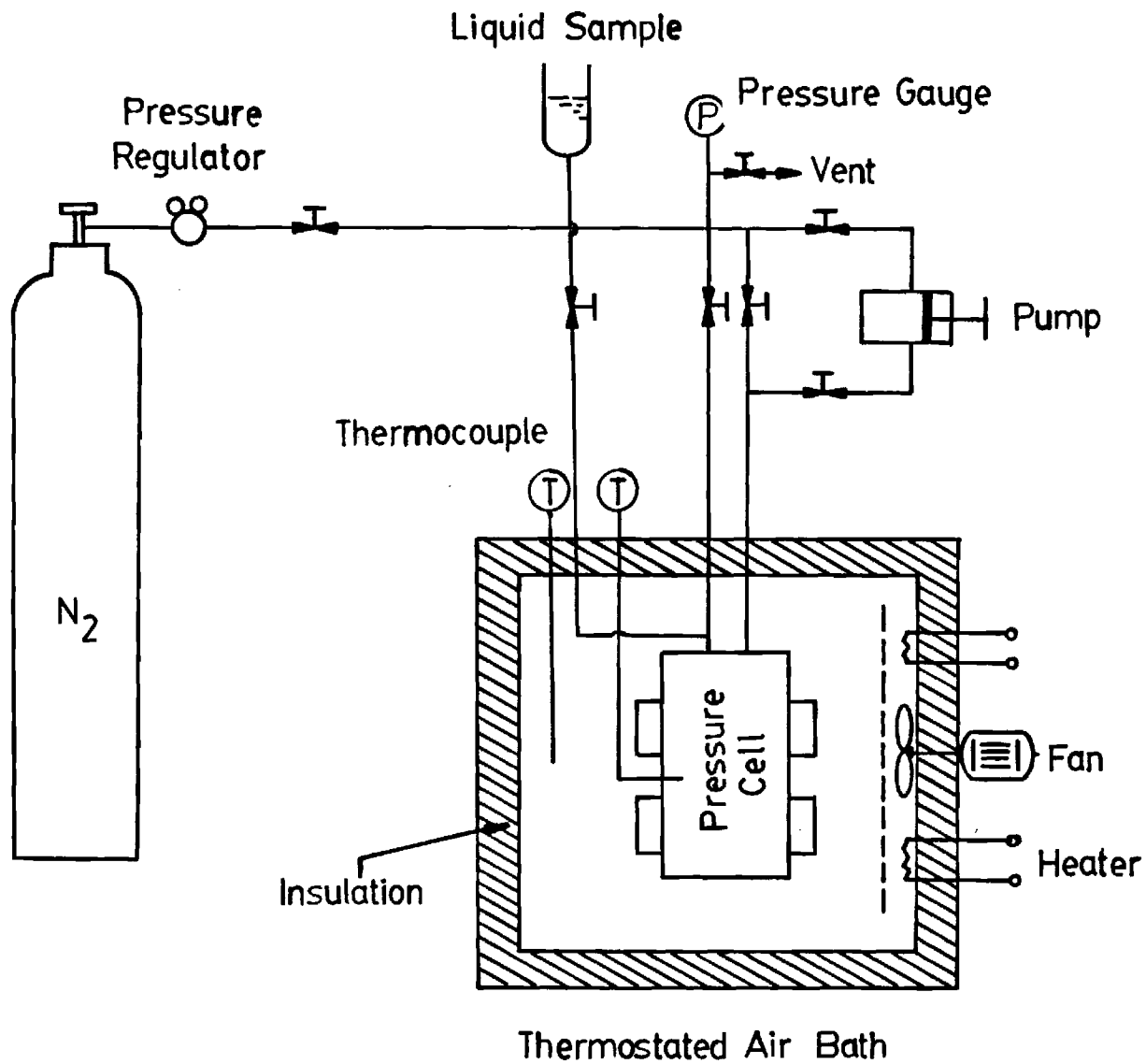
<u>Temp (°C)</u>	<u>ρ (g/cc)</u>	<u>Std. dev.</u>	<u>Temp (°C)</u>	<u>ρ (g/cc)</u>	<u>Std. dev.</u>
25.05	1.6205	1.2×10^{-3}	25.30	1.7217	7.2×10^{-4}
45.00	1.6089	1.4×10^{-3}	45.08	1.7087	7.1×10^{-4}
59.40	1.5997	1.2×10^{-3}	60.55	1.6986	6.9×10^{-4}
73.70	1.5912	1.2×10^{-3}	74.98	1.6884	8.5×10^{-4}
88.38	1.5816	1.1×10^{-3}	90.40	1.6779	8.6×10^{-4}
108.90	1.5703	6.9×10^{-4}	110.39	1.6642	9.5×10^{-4}
128.48	1.5584	8.6×10^{-4}	129.87	1.6512	1.0×10^{-3}
148.40	1.5453	8.6×10^{-4}	150.28	1.6365	1.2×10^{-3}
174.20	1.5287	2.1×10^{-4}	174.71	1.6192	1.2×10^{-3}
199.90	1.5110	1.3×10^{-4}	200.01	1.6008	1.5×10^{-3}

Table 2. Viscosities of Lithium Bromide - Water Solutions

<u>45.0 wt% LiBr</u>			<u>49.85 wt% LiBr</u>		
<u>T(°C)</u>	<u>ν (cSt.) $\pm \sigma$</u>	<u>μ (cP)</u>	<u>T(°C)</u>	<u>ν (cSt.) $\pm \sigma$</u>	<u>μ (cP)</u>
30.22	1.5293 \pm 0.0004	2.2244	30.22	1.9181 \pm 0.0005	2.9345
45.28	1.1886 \pm 0.0002	1.7203	45.29	1.4791 \pm 0.0005	2.2491
60.29	0.9604 \pm 0.0003	1.3819	60.28	1.1869 \pm 0.0002	1.7954
75.25	0.8014 \pm 0.0002	1.1482	75.26	0.9821 \pm 0.0001	1.4770
90.20	0.6854 \pm 0.0002	0.9763	90.24	0.8339 \pm 0.0002	1.2468
109.85	0.5711 \pm 0.0003	0.8073	110.08	0.6910 \pm 0.0004	1.0247
<u>55.0 wt% LiBr</u>			<u>59.9 wt% LiBr</u>		
<u>T(°C)</u>	<u>ν (cSt.) $\pm \sigma$</u>	<u>μ (cP)</u>	<u>T(°C)</u>	<u>ν (cSt.) $\pm \sigma$</u>	<u>μ (cP)</u>
30.22	2.6930 \pm 0.0013	4.3560	30.22	3.9457 \pm 0.0014	6.7804
45.29	2.0350 \pm 0.0013	3.2737	45.35	2.8704 \pm 0.0011	4.9042
60.28	1.6066 \pm 0.0007	2.5692	60.38	2.1863 \pm 0.0009	3.7139
75.26	1.3102 \pm 0.0015	2.0835	75.32	1.7339 \pm 0.0020	2.9270
90.24	1.0992 \pm 0.0007	1.7374	90.31	1.4293 \pm 0.0002	2.3982
110.09	0.9021 \pm 0.0008	1.4161	110.11	1.1355 \pm 0.0003	1.8899

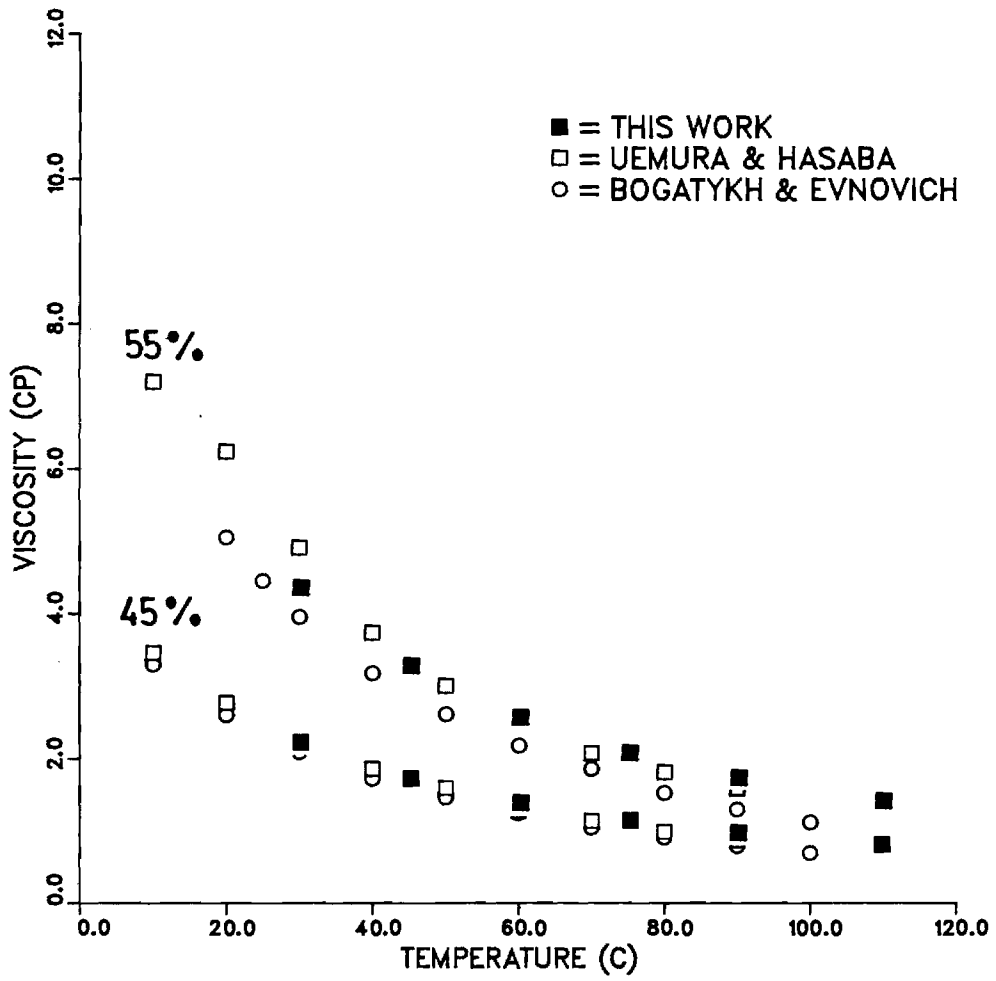
DENSITY OF AQUEOUS LiBr SOLUTION





SCHEMATIC DIAGRAM OF VISCOSITY APPARATUS

VISCOSITY OF AQUEOUS LIBR SOLUTION



VISCOSITY OF AQUEOUS LIBR SOLUTION

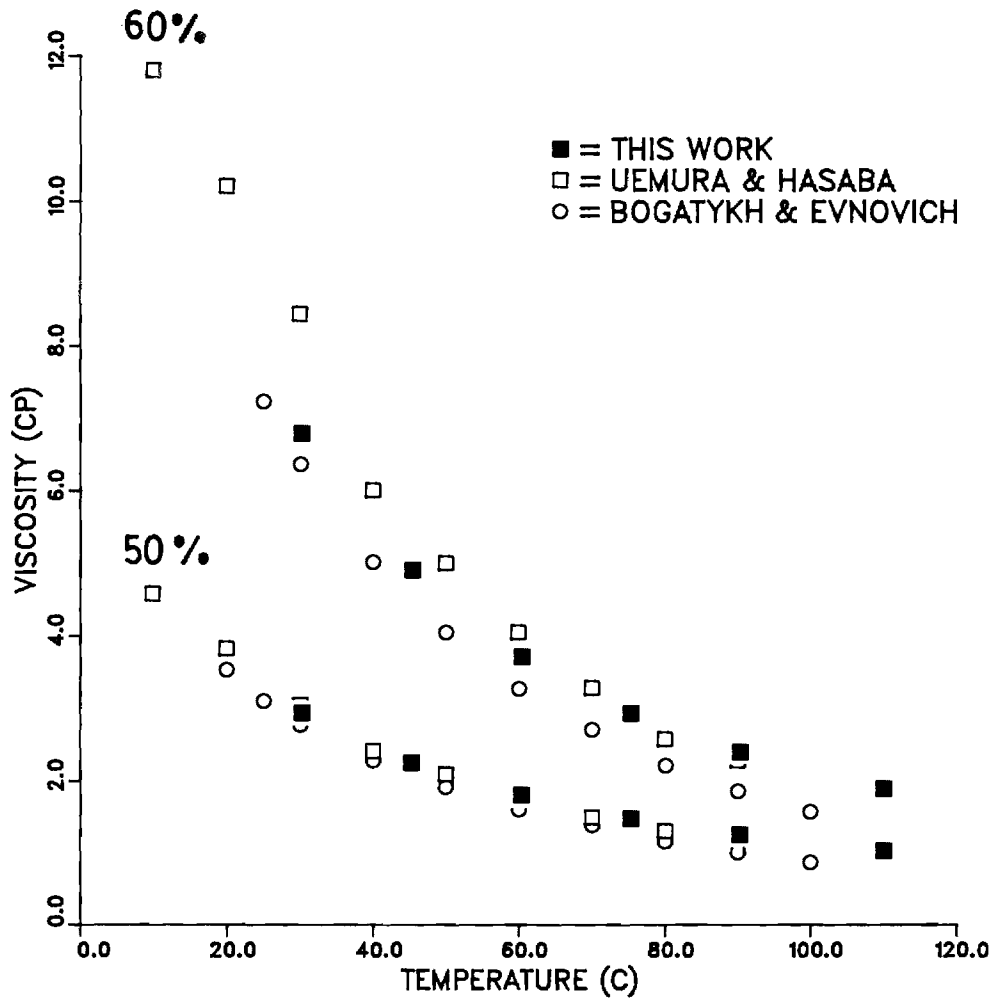
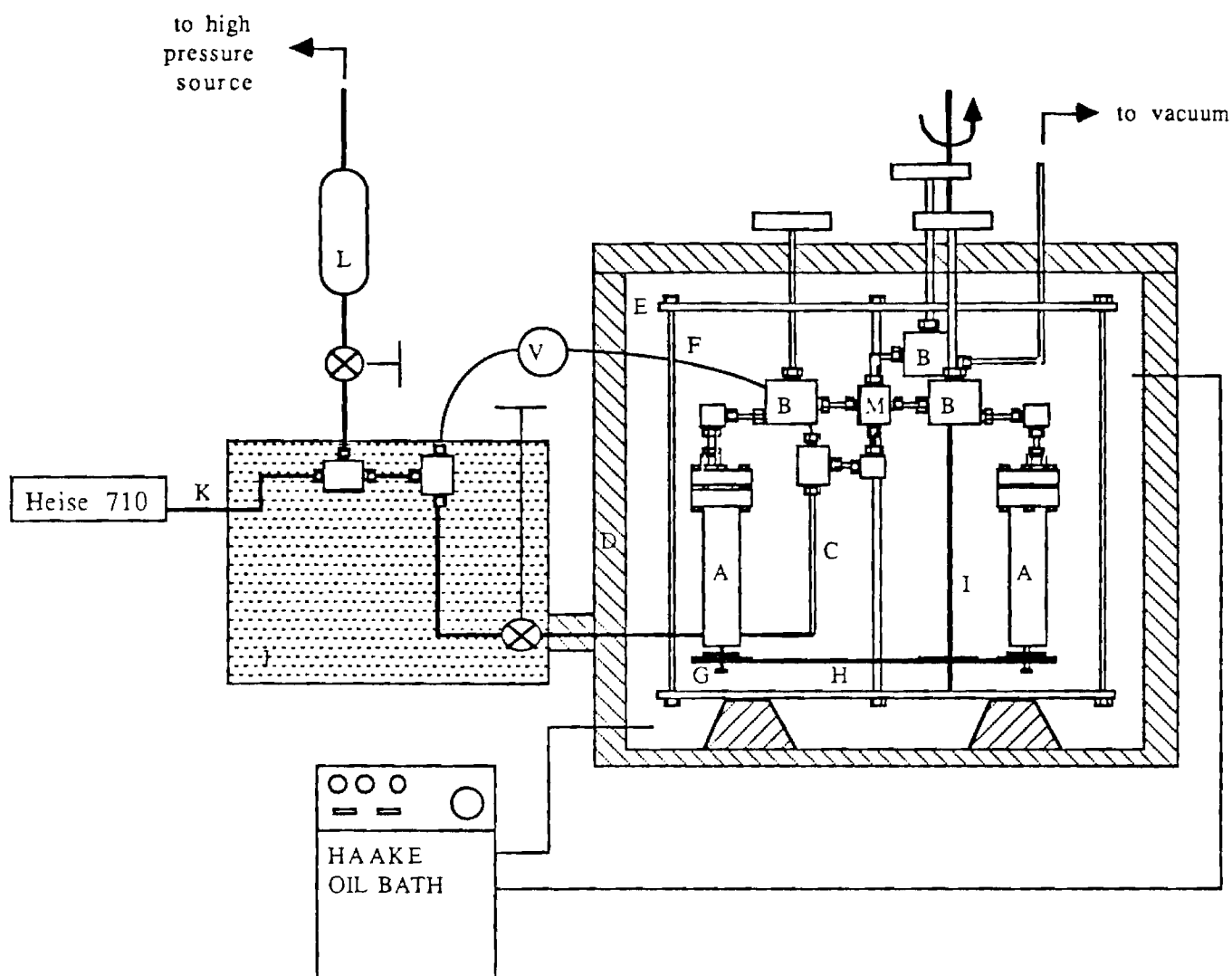


FIGURE 6



- A CELL
- B VALVE
- C GALLIUM LINE
- D BATH INSULATION
- E OUTER OIL BATH
- F INNER BAFFLE TANK (WALL NOT SHOWN)
- G MAGNETIC BAR AND DRIVEN WHEEL UNIT
- H DRIVING BELT
- I STIRRING SHAFT
- J WATER BATH
- K OIL LINE
- L OIL RESERVOIR
- V VOLTMETER

**SKETCH OF THE
STATIC VLE STILL**

FINAL REPORT

**THERMOPHYSICAL PROPERTY DATA FOR
LITHIUM BROMIDE/WATER SOLUTIONS
AT ELEVATED TEMPERATURES**

PREPARED FOR

**THE AMERICAN SOCIETY OF HEATING, REFRIGERATING AND
AIR-CONDITIONING ENGINEERS**

UNDER PROJECT 526-RP

SUPERVISED BY

**TECHNICAL COMMITTEE 8.3
(ABSORPTION AND HEAT OPERATED MACHINES)**

PREPARED BY

**GEORGIA INSTITUTE OF TECHNOLOGY
SCHOOL OF CHEMICAL ENGINEERING
AND
THE GEORGE W. WOODRUFF SCHOOL OF MECHANICAL ENGINEERING**

AUTHORS:

**A. S. TEJA, PRINCIPAL INVESTIGATOR
S. M. JETER, CO-PRINCIPAL INVESTIGATOR**

**R. J. LEE, RESEARCH ENGINEER
R. M. DIGUILIO, GRADUATE RESEARCH ASSISTANT
J.-L. Y. LENARD, GRADUATE RESEARCH ASSISTANT
J. P. MORAN, GRADUATE RESEARCH ASSISTANT**

TABLE OF CONTENTS

1. Introduction
2. Thermal Conductivity
3. Density
4. Kinematic Viscosity
5. Liquid Specific Heat
6. Vapor Pressure

INTRODUCTION

Aqueous lithium bromide (LiBr) solutions and similar mixtures have long been used in absorption refrigeration. Accurate thermophysical data including thermodynamic and transport data are needed for adequate design analysis and evaluations of such systems. In the past, much of available thermophysical property data had been based on proprietary data or on the results of measurements that had not been fully disclosed or described. To alleviate this shortcoming, Technical Committee 8.3 initiated a project for the measurement of the following properties:

1. Thermal Conductivity
2. Density
3. Kinematic Viscosity
4. Liquid Specific Heat
5. Vapor Pressure

The Georgia Institute of Technology was selected as the contractor on this project. With assistance and forbearance from the sponsoring Technical Committee, the required measurements and data reduction and analysis are now (nearly) complete. This report represents the completion of the project.

Important accomplishments of this project include the following:

1. The development and successful operation of a fused quartz thermal conductivity cell using a liquid metal thermometric fluid suitable for implementing the hot wire thermal conductivity measurement in an electrically conductive fluid.
2. The demonstration of a high pressure capillary viscometer system successfully used for measurements of the viscosity of a volatile fluid at elevated temperature.
3. Successful demonstration of an innovative static vapor pressure measurement system using water as the pressure transmitting fluid which is capable of highly accurate measurements of the pressure of water vapor above water solutions with non-volatile solutes.
4. Successful application of classical drop calorimetry with design improvements in temperature measurement and environmental control.

Details of the experimental procedures and designs are given in the following sections along with raw data and correlations.

The entire research team expresses its gratitude for the opportunity to be involved in this challenging and worthwhile project.

Thermal Conductivity of Lithium Bromide and Water Solutions

Abstract

The thermal conductivity of lithium bromide and water solutions was measured over the temperature range 20 ° - 190 °C using a modified hot wire technique. Solutions containing 30.2, 44.3, 49.1, 56.3, 60.0, 62.9, and 64.9 wt % lithium bromide were studied and comparisons were made with reported data on aqueous lithium bromide solutions at lower temperatures. The data were correlated as a function of temperature and weight percent lithium bromide with an average deviation of 0.6%. The accuracy of the measurements was estimated to be $\pm 2\%$.

1 Introduction

The design of refrigeration and heat pump systems which use aqueous lithium bromide solutions requires accurate thermal conductivity data. Most literature data, however, are limited to low temperature and low concentrations of lithium bromide. The objectives of this work were therefore to measure lithium bromide solutions at high temperatures and concentrations of lithium bromide.

The most accurate technique for the measurement of the thermal conductivity of liquids is the transient hot wire method [1] in which a thin wire immersed in the liquid is electrically heated. The temperature rise of the wire is used to determine the thermal conductivity of the liquid. Electrically conducting solutions can be measured with this technique if the wire is electrically insulated from the liquid under study. The insulation blocks current paths through the liquid which would interfere with the small voltages which must be measured. However, the addition of an insulating layer to the wire has proved difficult to achieve in practice, especially at higher temperatures. In 1981, Nagasaka and Nagashima [2] successfully insulated a platinum wire with a polyester coating and reported measurements up to 150 °C. In 1982, Alloush et al. [3] used a tantalum filament coated with a layer of tantalum oxide to obtain data on LiBr solutions at temperatures up to 80 °C. Recently Nagashima et al. [4] used the tantalum - tantalum oxide filament to make measurements on LiBr solutions up to 100 °C. However, they noted that the oxide coating failed to insulate the wire properly above 100 °C. This limitation was confirmed by our own efforts to use the tantalum - tantalum oxide filament at temperatures above 100 °C as shown in Figure 1 where the thermal conductivity of water as measured with a tantalum wire is plotted as a function of temperature. Above 100 °C, deviation from the ESDU [5] recommended values occurs. The probable reasons for failure are the cracks that develop in the insulation due

to the unequal expansion coefficients of the base metal and the oxide and the decrease in dielectric strength with temperature of the oxide. Both effects might permit current paths into the liquid and allow polarization of the fluid near the wire. A different technique was pioneered by Nagashima et al. [6,7] in 1981 and 1982. This technique uses a fine glass capillary filled with liquid mercury instead of the insulated wire. The apparatus was used to measure the thermal conductivity of molten salts up to 300 °C. The accuracy of these measurements was verified by Le Neindre et al. [8] using a coaxial cylinder method to measure the thermal conductivities of some of the same systems. Since the liquid metal technique has been validated at the temperatures of interest in this study, it was adopted in this work. Measurements were made in the range of concentration from 30 % to 65 wt % LiBr and of temperature between 20 °C to 190 °C.

2 Apparatus and Procedure

The transient hot wire apparatus employed in this work is shown in Figure 2. The major components of the apparatus are a Wheatstone bridge, a power supply, and a data acquisition system.

The Wheatstone bridge consists of two $100 \pm 0.01 \Omega$ precision resistors, a resistance decade box (General Radio Model 1433 U) with a range of 0 - 111.11 Ω , and a hot wire cell. The hot wire cell was constructed of quartz and is shown in Figure 3. The cell is in the shape of a U tube with one leg consisting of a quartz capillary tube (13.6 cm long, 0.05 mm ID, 0.08 mm OD) and the other a larger bore quartz tube (2 mm ID by 4 mm OD). The open end of the U tube is supported with a piece of machinable ceramic. The connection between the larger tube and the capillary tube is achieved by drawing down the larger tubing and sealing the capillary tubing into place with silicone rubber (General

Electric RTV-106). Originally, it was intended to use liquid gallium to fill the U tube. Liquid gallium has the advantages of low toxicity and very low vapor pressures. However, the reactivity of gallium with water vapor at high temperatures forced the choice of mercury as the liquid metal. The entire U tube was filled with liquid mercury with the thread of mercury in the capillary tube serving as the hot wire. A small piece of tungsten wire was inserted into the liquid mercury at each end of the open U-tube to serve as electrodes. The tungsten wires were, in turn, connected to copper wires which attached to the bridge. The cell itself was placed in a glass sleeve with ceramic supports at the top and bottom of the U-tube to ensure that the U-tube remained centered in the sleeve. The sleeve was then placed inside a pressure vessel. A 0.0625 in Type E thermocouple was inserted through both ceramic supports along the axis of the larger bore tube. The bridge was powered by a precision power supply (Hewlett-Packard Model 6213A) which served as a constant voltage source. The supply was used both to balance the bridge and provide the voltage for heating. A lab quality multimeter (Fluke Model 8840A) was used to indicate a balanced condition in the bridge. A data acquisition system consisting of an IBM PC XT with a 16 bit analog to digital converter card (Strawberry Tree ACPC-16) was used to read both the offset voltage and the applied voltage.

The test fluid was loaded into the glass sleeve and the sleeve inserted into a stainless steel pressure vessel. The quartz cell was then lowered into the glass sleeve and the pressure vessel sealed. The apparatus was then placed in a fluidized sand bath (Techne Model SBL-2D) which maintained the temperature to ± 0.1 °K. The sample was pressurized to 15 bar with nitrogen to prevent boiling during measurement. A Type E thermocouple, calibrated against a PRT (Leeds and Northup SN 709892), was used to determine the stability of the bath and the sample equilibrium temperatures. After temperature equilibrium had been

achieved, the air flow to the sand bath was stopped to prevent any vibration of the cell during measurement.

The procedure for each measurement was as follows. The bridge was first balanced and the computer program started. The program initiated a step input to the bridge using an electromechanical relay (Magnecraft W172DIP-1). The relay settled in less than 0.3 ms. The program sampled the offset voltage on one channel, then switched channels to sample the applied voltage to insure its constancy. The time between any two samples was 0.0084 s and that between two successive readings of the same channel was 0.0168 s. The delay between the closing of the relay and the first sampling was found to be 0.0132 s using an oscilloscope. Two hundred points were measured during each run and the experiment lasted about 3.4 seconds. From a previous calibration of the temperature versus resistance, the temperature of the wire was found. A plot of ΔT versus \ln time was made and the slope in the time interval from 0.7 to 2.2 s was calculated using a least squares fit as described in the analysis section. The applied voltage was varied from about 2.5 to 3.5 V so that a more or less constant temperature rise in the quartz capillary surface of about 1.7 °K was achieved. This resulted in offset voltages on the order of 5 mV. The A/D card has 16 bit resolution and the ± 25 mV range was used. Thus the card is capable of 0.08 μ V resolution.

3 Source and Purity of Materials

Anhydrous lithium bromide was obtained from Morton Thiokol Inc. (Lots F06H, L02F, and H26G). The minimum stated purity of the sample was 99 wt% LiBr. Distilled water was used to prepare the solutions. Solutions were first prepared gravimetrically based on weight percent LiBr. To ensure that no change in the composition of a solution occurred during the measurement procedure, samples of each composition were taken before and

after measurement and checked by titration. Titration was done with silver nitrate using a computer aided titrimeter (Fisher, Controller Model 450, Buret Model 400, Stirrer Model 460). The compositions reported are the averages of two measurements. No variation in composition during the measurement procedure was observed.

4 Analysis

The model for the experiment is an infinite line source of heat submersed in an infinite fluid medium. By monitoring the temperature response of the wire to a step voltage input, the thermal conductivity of the fluid can be deduced. For an infinite line source of heat in an infinite fluid medium, the ideal temperature rise of the wire can be calculated using an expression derived by Carslaw and Jaeger [9] and Healy et al. [10] for $t \gg \frac{r_w^2}{4\alpha}$. The inequality is satisfied shortly after heating is started, that is, for $10 \text{ ms} < t < 100 \text{ ms}$. The expression is:

$$\Delta T_{id} = \frac{q}{4\pi\lambda} \ln \left(\frac{4\lambda t}{r_w^2 \rho C_p C} \right) \quad (1)$$

where q is the heat dissipation per unit length, λ is the thermal conductivity, ρ the density, C_p the heat capacity, r_w the radius of the filament and C is equal to $\exp(\gamma)$ where γ is Euler's constant. If it is assumed that all physical properties are independent of temperature over the small range of temperature considered (ca. 1.7 °K), then,

$$\lambda = \frac{q}{4\pi \left(\frac{d\Delta T_{id}}{d \ln t} \right)} \quad (2)$$

where $\frac{d\Delta T_{id}}{d \ln t}$ is found experimentally from a plot of ΔT_{id} vs $\ln t$.

Healy et al. [10] also derived several corrections for the deviation of the model from reality. These may be written as:

$$\Delta T_{id} = \Delta T_w(t) + \sum_i \delta T_i \quad (3)$$

δT_1 accounts for the finite physical properties of the wire (liquid mercury) and is given by [9]:

$$\delta T_1 = \frac{r_w^2 [(\rho C_p)_w - (\rho C_p)]}{2\lambda t} \Delta T_{id} - \frac{q}{4\pi\lambda} \frac{r_w^2}{4\alpha t} \left(2 - \frac{\alpha}{\alpha_w} \right) \quad (4)$$

where $(\rho C_p)_w$ is the volumetric heat capacity of the liquid mercury and α and α_w are the thermal diffusivity of the fluid and mercury respectively.

The correction due to the finite extent of the fluid is given by [10]:

$$\delta T_2 = \frac{q}{4\pi\lambda} \left(\ln \frac{4\alpha t}{b^2 C} + \sum_{\nu=1}^{\infty} \exp^{-g_\nu^2 \alpha t / b^2} [\pi Y_0(g_\nu)]^2 \right) \quad (5)$$

where b is the inside diameter of the cell, Y_0 is the zero order Bessel function of the second kind and g_ν are the roots of J_0 , the zero order Bessel function of the first kind. Although the first several roots are readily available, the higher roots can be found to sufficient accuracy from [11]:

$$g_\nu = (\pi\nu - \pi/4) + \frac{1}{8(\pi\nu - \pi/4)} - \frac{31}{385(\pi\nu - \pi/4)^3} + \frac{3779}{15366(\pi\nu - \pi/4)^5} \quad (6)$$

Values of Y_0 were calculated using the polynomial approximation given by Abramowitz and Stegun [12].

The effect of the quartz capillary tube on the measurement has been evaluated analytically by Nagasaka and Nagashima [2]. The correction is given by:

$$\delta T_3 = \frac{-q}{4\pi\lambda} \left[\ln \left(\frac{r_w}{r_l} \right)^2 + \frac{2\lambda}{\lambda_l} \ln \frac{r_l}{r_w} + \frac{\lambda}{\lambda_l} + A \right] \quad (7)$$

with :

$$\begin{aligned} A &= \frac{1}{t} (C0 + B \ln t) \\ C0 &= C1 + C2 + B \ln \left(\frac{4\alpha}{r_l^2 C} \right) \\ C1 &= \frac{r_w^2}{8} \left[\left(\frac{\lambda - \lambda_l}{\lambda_w} \right) \left(\frac{1}{\alpha_w} - \frac{1}{\alpha_l} \right) + \frac{4}{\alpha_l} - \frac{2}{\alpha_w} \right] \end{aligned}$$

$$C2 = \frac{r_l^2}{2} \left(\frac{1}{\alpha} - \frac{1}{\alpha_l} \right) + \frac{r_w^2}{\lambda_l} \left(\frac{\lambda_l}{\alpha_l} - \frac{\lambda_w}{\alpha_w} \right) \ln \left(\frac{r_l}{r_w} \right)$$

$$B = \frac{r_w^2}{2\lambda} \left(\frac{\lambda_l}{\alpha_l} - \frac{\lambda_w}{\alpha_w} \right) + \frac{r_l^2}{2\lambda} \left(\frac{\lambda}{\alpha} - \frac{\lambda_w}{\alpha_w} \right)$$

where r_l, α_l, λ_l are the radius, thermal diffusivity, and thermal conductivity of the quartz capillary.

Radiation by the fluid can be accounted for using an analytical expression for the temperature rise of the mercury thread given by Wakeham et al. [13] :

$$\Delta T = \frac{q}{4\pi\lambda} \left(1 + \frac{Br_w^2}{4\alpha} \right) \ln \frac{4\alpha t}{r_w^2 C} + \frac{Bqr_w^2}{16\pi\alpha\lambda} - \frac{Bqt}{4\pi\lambda} \quad (8)$$

where B is the radiation parameter and is a measure of the contribution of radiant emission by the fluid to the heat transfer process. From equation (8) Wakeham et al. [13] derived the following expression for the correction to the observed temperature rise:

$$\delta T_4 = \frac{-qB}{4\pi\lambda} \left(\frac{r_w^2}{4\alpha} \ln \frac{4\alpha t}{r_w^2 C} + \frac{r_w^2}{4\alpha} - t \right) \quad (9)$$

They used equation (8) to show that emission from a fluid causes the ΔT vs $\ln t$ slope to exhibit a slight curvature, concave to the $\ln t$ axis.

ΔT , after correction for the other effects mentioned, can be fit to equation (8) to obtain B as suggested by Wakeham et al. [13]. Equation (9), then can be used to calculate δT_4 . If there is no radiation contribution, B is equal zero and thus there is no danger of biasing the data.

Since both sides of the U tube are made of quartz and the mercury is free to expand, there are no effects due to wire-slackening which must be accounted for in hot wire methods. End effects must, however, still be considered. End effects result mostly from conduction of heat axially away from the mercury thread to the thicker leads. No analytical correction exists for this source of error and it is generally compensated for experimentally using

either potential leads or a long and a short wire [1]. However, liquid mercury has a thermal conductivity only about 10% of that of platinum, which is commonly used in hot wire apparatus. Therefore, any end effects were expected to be small or negligible. This expectation was experimentally verified by the excellent agreement of our data with the IUPAC [14] data for water and with the data of Nagashima et al. [4] for LiBr solutions. Nagashima et al. used a two wire technique to account for end effects.

The actual temperature at which the thermal conductivity is reported is the average temperature of the fluid during the heating process. That is:

$$T_R = T_o + \frac{\Delta T(t_I) + \Delta T(t_F)}{2} \quad (10)$$

where T_o is the temperature of the fluid at the start of a measurement, and t_I and t_F refer to the initial and final times of the data used to find the slope of ΔT vs $\ln t$. ΔT in the case of an insulated wire is given by the temperature at the surface of the insulation adjacent to the liquid. This temperature has been determined by Nagasaka and Nagashima [2] and is given by:

$$\Delta T_i = \frac{q}{4\pi\lambda} \left[\frac{(P3 + P2 + P1)}{t_i} + \ln \left(\frac{4\alpha t_i}{r_i^2 C} \right) \right] \quad (11)$$

with :

$$\begin{aligned} P3 &= \frac{r_w^2}{4} \left(\frac{1}{\alpha_l} - \frac{1}{2\alpha_w} \right) + \frac{r_l^2}{4} \left(\frac{1}{\alpha} - \frac{1}{\alpha_l} \right) \\ P2 &= \frac{r_w^2}{2\lambda_l} \left(\frac{\lambda_l}{\alpha_l} - \frac{\lambda_w}{\alpha_w} \right) \ln \left(\frac{r_l}{r_w} \right) \\ P1 &= \ln \left(\frac{4\alpha t_i}{r_i^2 C} \right) \left[\frac{r_w^2}{2\lambda} \left(\frac{\lambda_l}{\alpha_l} - \frac{\lambda_w}{\alpha_w} \right) + \frac{r_l^2}{2\lambda} \left(\frac{\lambda}{\alpha} - \frac{\lambda_l}{\alpha_l} \right) \right] \end{aligned}$$

where the subscript i refers to t_I or t_F .

In order to apply the temperature corrections, various physical properties are required. The density and heat capacity of mercury were obtained from the CRC handbook [15], and

the thermal conductivity from the compilation of Ho et al. [16], and the electrical resistivity from the work of Williams [17]. The thermal conductivity and the thermal diffusivity of quartz were obtained from a manufacturer's catalog [18]. Finally, the heat capacity and density of lithium bromide solutions were measured in our laboratory.

The radiation parameter B for all fluids measured here was found to be negligible (less than 0.0007). Nevertheless, the correction was uniformly applied for consistency.

5 Results

Water was measured at room temperature to validate the liquid metal capillary technique. The agreement with the IUPAC data was excellent, with deviations between our measurements and IUPAC data being within 0.6%. However, the thermal conductivity of water at higher temperatures could not be measured because the low viscosity of water allowed convection to occur during the heating process. Fortunately, the viscosities of lithium bromide solutions were high enough to prevent the rapid onset of convection. In order to verify the linearity of the ΔT vs $\ln t$ curves, the deviation from the linear fit was checked. Figure 4 shows a plot of the deviation from the fitted line for a typical ΔT vs $\ln t$ curve. The points are evenly scattered so that no bias is evident.

Seven compositions of lithium bromide - water solutions were measured (30.2, 44.3, 49.1, 56.3, 60.0, 62.9, and 64.9 wt% LiBr) in the temperature range from 20 ° to 190 °C. The data are compiled in Table I and are shown graphically in Figure 5. Each data point represents the average of five experimental runs. The maximum deviation from the average value never exceeded 1.0%. Thus the precision of the data is 1.0% and the accuracy is estimated to be $\pm 2.0\%$. Direct comparison of our data with literature data is difficult due to differences in concentrations. Table II is a comparison of the correlation found using only our data

with the data of Nagashima et al. [4], Wakeham et al. [3], Uemura and Hasaba[19], and Riedel [20]. The agreement between our data and Nagashima et al. who claim an accuracy of $\pm 0.5\%$ is excellent. The average deviation on 15 data points is 0.65% and the maximum is 1.8%. Agreement with Uemura and Hasaba is also excellent. The average deviation on 25 data points is 0.63% and the maximum is 1.9%. The single point in our concentration range of Reidel agrees within 1.1%. The data of Wakeham et al. show much larger deviation. The average deviation for 19 points is 2.1% with a maximum deviation of 4.4%. However, Wakeham et al. claimed an accuracy of only $\pm 3.0\%$. Therefore, the overall agreement is within the accuracy of their experiments.

Nagashima et al. [4] measured the thermal conductivity of LiBr solutions at three concentrations (30.3, 46.5, and 56.6 wt % LiBr) at pressures up to 40 MPa. The effect of pressure was found to be small. For example, at 56.6 wt% LiBr and 100 °C, the change in thermal conductivity from .1 MPa to 40 MPa was 1.7%.

6 Correlation

The thermal conductivity of the lithium bromide solutions was correlated with temperature T in ° K and composition X in wt % as follows:

$$\lambda(T, X) = A(T) + B(T)X + C(T)X^2 \quad (12)$$

$$\text{with : } A(T) = a_1 + a_2T + a_3T^2$$

$$B(T) = b_1 + b_2T + b_3T^2$$

$$C(T) = c_1 + c_2T + c_3T^2$$

Values of the constants $a_1, a_2, a_3, b_1, b_2, c_1, c_2, c_3$ were obtained by regression of the data obtained in this work and are given in Table III. The average absolute deviation between correlation and experiment was found to be .6% for 47 data points and the maximum deviation was found to be 1.6%. The fitted curves are shown on Figure 5.

7 Conclusions

The thermal conductivity of aqueous solutions of lithium bromide ranging in composition from 30 to 65 wt % and in temperature from 20 ° to 190 °C were measured. A correlation was developed which was able to fit the data with an average absolute deviation of 0.6% and a maximum deviation of 1.6%. The estimated accuracy ($\pm 2\%$) of the thermal conductivity measurements is supported by comparison with the literature.

References

- [1] C. A. Nieto de Castro, S. F. Y. Li, A. Nagashima, R. D. Trengrove, and W. A. Wakeham. *J Phys Chem Ref Data*, 15:1073, 1986.
- [2] Y. Nagasaka and A. Nagashima. *J Phys E: Sci Instrum*, 14:1435, 1981.
- [3] A. Alloush, W. B. Gosney, and W. A. Wakeham. *Int J Thermophysics*, 3:225, 1982.
- [4] K. Kawamata, Y. Nagasaka, and A. Nagashima. *Int J Thermophysics*, 9:317, 1988.
- [5] ESDU. *Thermal Conductivity of Water Substance*. Technical Report 67031, Engineering Sciences Data Unit, London, 1967.
- [6] M. Hoshi, T. Omotani, and A. Nagashima. *Rev Sci Instrum*, 52:755, 1981.
- [7] T. Omotani, Y. Nagasaka, and A. Nagashima. *Int J Thermophysics*, 3:17, 1982.
- [8] R. Tufeu, J. P. Petitet, L. Denielou, and B. Le Neindre. *Int J Thermophysics*, 6:315, 1985.
- [9] H. S. Carslaw and J. C. Jaeger. *Conduction of Heat in Solids*. Oxford University Press, London, second edition, 1959.
- [10] J. J. Healy, J. J. de Groot, and J. Kestin. *Physica*, 82C:392, 1976.
- [11] G. N. Watson. *A Treatise on the Theory of Bessel Functions*. Cambridge University Press, Cambridge, England, second edition, 1962.
- [12] M. Abramowitz and I. A. Stegun, editors. *Handbook of Mathematical Functions*. Dover, New York, 1965.
- [13] C. A. Nieto de Castro, S. F. Y. Li, C. Maitland, and W. A. Wakeham. *Int J Thermophysics*, 4:311, 1983.

- [14] K. N. Marsh, editor. *Recommended Reference Materials for the Realization of Physicochemical Properties*. Blackwell Scientific Publications, Boston, 1987.
- [15] R. C. Weast, editor. *CRC Handbook of Chemistry and Physics*. CRC Press, Inc., Boca Raton, Florida, 69 edition, 1988.
- [16] C. Y. Ho, R. W. Powell, and P. E. Liley. *J Phys Chem Ref Data*, 1:279, 1972.
- [17] E. J. Williams. *Phil Mag*, 50:589, 1925.
- [18] *General Products Catalog*. Quartz Scientific, Inc., Fairport Harbor, Ohio, 1988.
- [19] T. Uemura and S. Hasaba. *Refrig Japan*, 38:19, 1963.
- [20] L. Riedel. *Chem Ingr Tech*, 23:59, 1951.

Table I: Thermal Conductivity of LiBr - Water Solutions

Wt% LiBr	T [K]	λ [mW/M K]	Wt% LiBr	T [K]	λ [mW/M K]	
0.0	293.8	602.3	49.1	401.2	513.5	
	296.7	607.6		430.0	522.0	
	323.4	646.0		460.0	523.0	
30.2	292.9	508.1	56.3	294.1	419.0	
	296.9	512.1		329.4	453.5	
	326.1	544.6		362.3	468.4	
	329.1	545.9		397.6	484.2	
	359.5	570.7		430.1	493.5	
	365.0	579.5		461.1	501.6	
	385.2	592.0		60.0	299.6	408.8
	388.9	592.8			329.2	432.9
	404.7	597.5			369.7	457.5
	434.0	591.1			402.5	473.4
44.3	435.7	590.2	62.9	430.8	476.5	
	461.3	573.8		460.6	485.8	
	295.1	467.5		339.8	429.5	
	321.4	495.4		371.0	447.2	
	353.5	521.4		400.4	457.3	
	378.6	535.5		430.7	465.4	
	407.2	550.9		460.9	476.1	
	439.2	557.3		64.9	343.4	421.0
	463.3	553.4			370.5	432.1
	298.0	446.7			400.7	442.0
49.1	328.9	478.1	49.1	428.8	453.0	
	371.6	503.9		461.0	458.2	

Table II: Comparison of this Work with the Literature [P = 1 atm]

T [K]	Wt% LiBr	λ [mW/M K] Literature	Ref.	λ [mW/M K] This Work ¹	Claimed Accuracy [\pm %]	% Dev.
293.8	0.0	599.1	[14]	602.3 ²		0.55
296.7		604.1	[14]	607.6 ²		0.58
323.4		642.6	[14]	646.0 ²		0.52
323	26.04	557	[19]	558.0		0.18
313	26.05	551	[19]	545.5		-1.01
353	26.08	581	[19]	586.7		0.97
303	26.28	426	[19]	530.9		0.82
333	26.52	564	[19]	567.4		0.60
304.2	30.3	527.7	[4]	520.7	0.5	-1.35
313.9		536.0	[4]	533.2	0.5	-0.53
333.9		558.6	[4]	555.3	0.5	-0.60
353.5		575.1	[4]	572.1	0.5	-0.53
373.5		588.5	[4]	584.2	0.5	-0.73
313	34.93	521	[19]	516.8		-0.81
303	35.61	503	[19]	502.6		-0.09
323	35.90	521	[19]	524.4		0.65
293	36.21	492	[19]	487.8		-0.87
333	36.29	533	[19]	532.8		-0.04
343	36.50	547	[19]	540.8		-1.15
353	36.53	538	[19]	548.4		1.89
293	40	471	[20]	476.2		1.08
297.0	41.4	473	[3]	476.5	3.0	0.74
305.0		478	[3]	485.7	3.0	1.58
315.0		484	[3]	496.3	3.0	2.49
335.0		500	[3]	515.1	3.0	2.94
357.0		511	[3]	531.9	3.0	3.93
303	44.84	465	[19]	471.5		1.37
333	44.94	501	[19]	499.5		-0.30
323	44.98	489	[19]	490.6		0.33
313	44.99	486	[19]	481.1		-1.01
353	45.42	509	[19]	512.6		0.71
297.0	45.6	465	[3]	462.4	3.0	-0.56
305.0		467	[3]	470.9	3.0	0.82
315.0		469	[3]	480.8	3.0	2.45
335.0		483	[3]	498.5	3.0	3.10
357.0		499	[3]	514.6	3.0	3.02
293	46.05	459	[19]	456.5		-0.55
302.4	46.5	468.2	[4]	464.9	0.5	-0.70
313.8		477.3	[4]	476.2	0.5	-0.22
333.3		490.8	[4]	493.4	0.5	0.54
353.6		501.4	[4]	508.5	0.5	1.40
373.2		510.9	[4]	520.3	0.5	1.81

¹Values calculated from correlation of our data²Experimental Value (pure water not included in correlation).

Table II: Comparison of this Work with the Literature (Continued)

T [K]	Wt% LiBr	λ [mW/M K] Literature	Ref.	λ [mW/M K] This Work ¹	Claimed Accuracy [\pm %]	% Dev.
297.0	49.7	457	[3]	448.0	3.0	-2.01
305.0		463	[3]	455.8	3.0	-1.57
315.0		464	[3]	465.0	3.0	0.22
335.0		478	[3]	481.6	3.0	0.75
357.0		493	[3]	497.0	3.0	0.80
297.0	53.8	452	[3]	432.9	3.0	-4.40
305.0		457	[3]	440.2	3.0	-3.82
315.0		461	[3]	448.7	3.0	-2.74
335.0		474	[3]	464.2	3.0	-2.11
313	54.25	444	[19]	445.2		0.28
302.8	56.6	428.6	[4]	427.3	0.5	-0.31
313.6		438.0	[4]	436.1	0.5	-0.43
333.5		452.4	[4]	451.0	0.5	-0.32
353.7		464.0	[4]	464.1	0.5	0.01
373.5		473.7	[4]	475.0	0.5	0.27
353	56.61	463	[19]	463.6		0.13
323	56.62	442	[19]	443.3		0.30
293	56.70	416	[19]	418.4		0.57
303	56.71	429	[19]	427.0		-0.46
333	56.75	451	[19]	450.0		-0.23
313	60.35	418	[19]	420.0		0.47

Table III: Constants for Correlation

Constant	Value
a_1	-1407.5255
a_2	11.051253
a_3	$-1.4674147 \times 10^{-2}$
b_1	38.985550
b_2	-0.24047484
b_3	3.4807273×10^{-4}
c_1	-0.26502516
c_2	1.5191536×10^{-3}
c_3	$-2.3226242 \times 10^{-6}$

WATER MEASURED WITH TANTALUM CELL

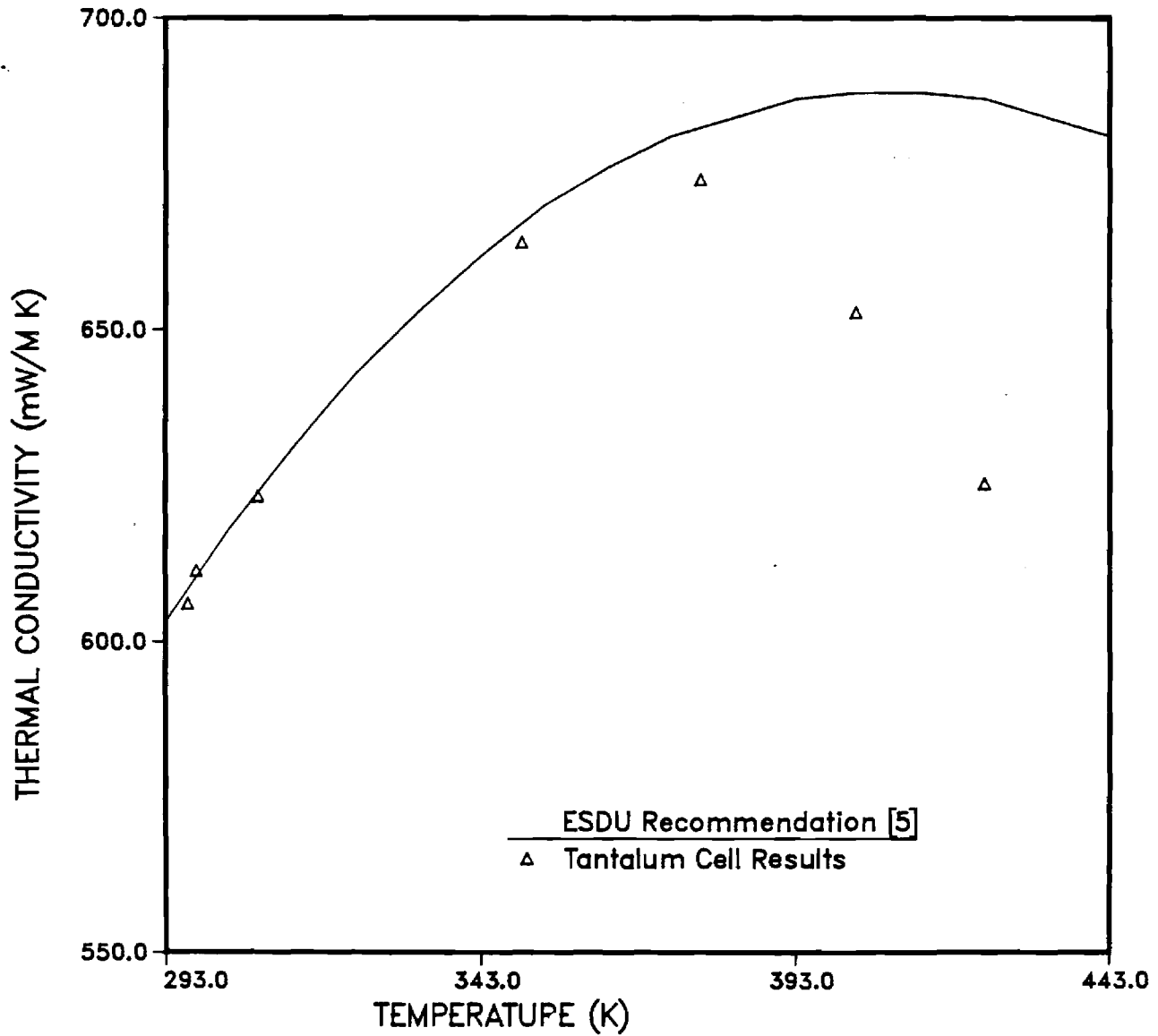


Figure 1: Thermal conductivity of water measured with a tantalum filament insulated with tantalum oxide. The oxide coating fails to insulate above 100 °C.

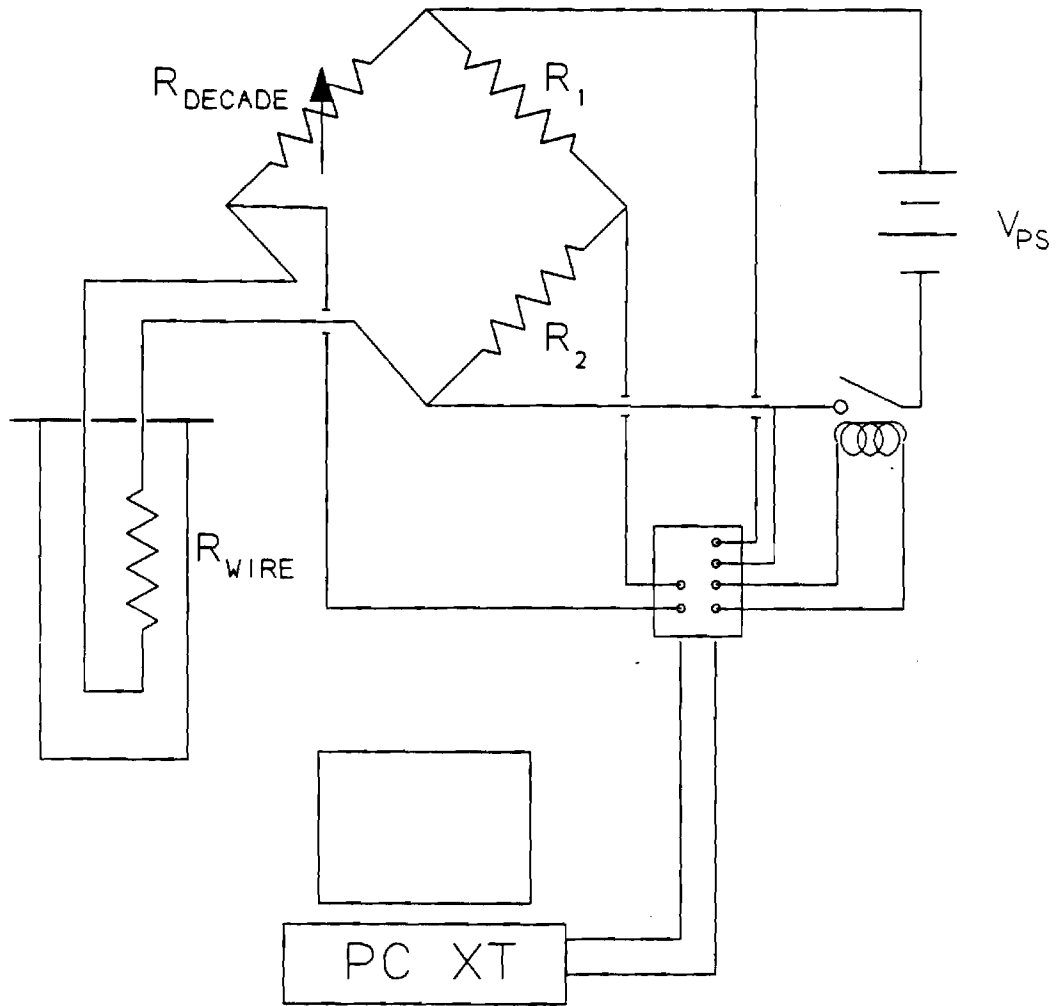


Figure 2: Schematic diagram of apparatus.

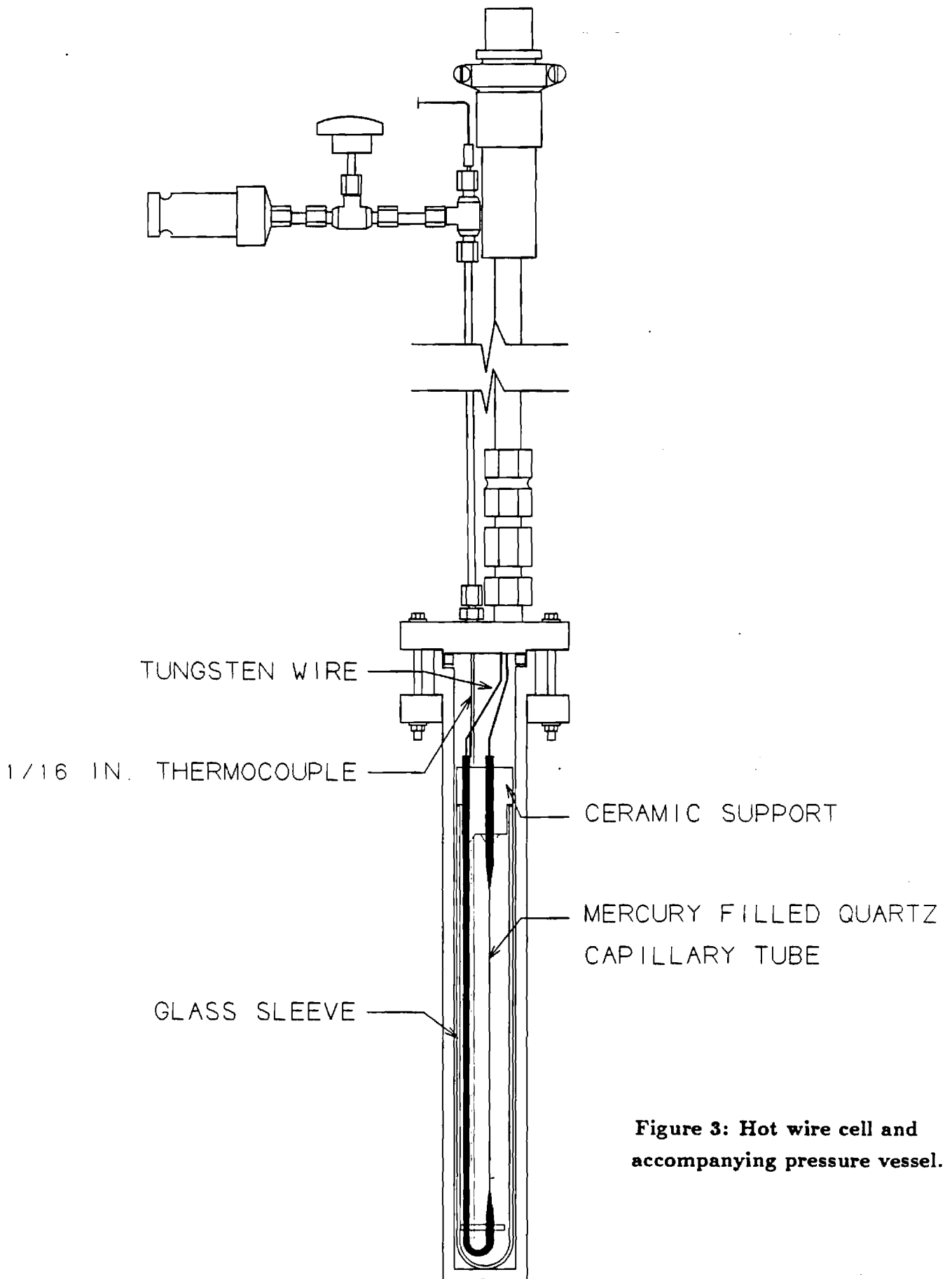


Figure 3: Hot wire cell and accompanying pressure vessel.

LINEARITY OF TEMPERATURE VS LN(t) CURVE

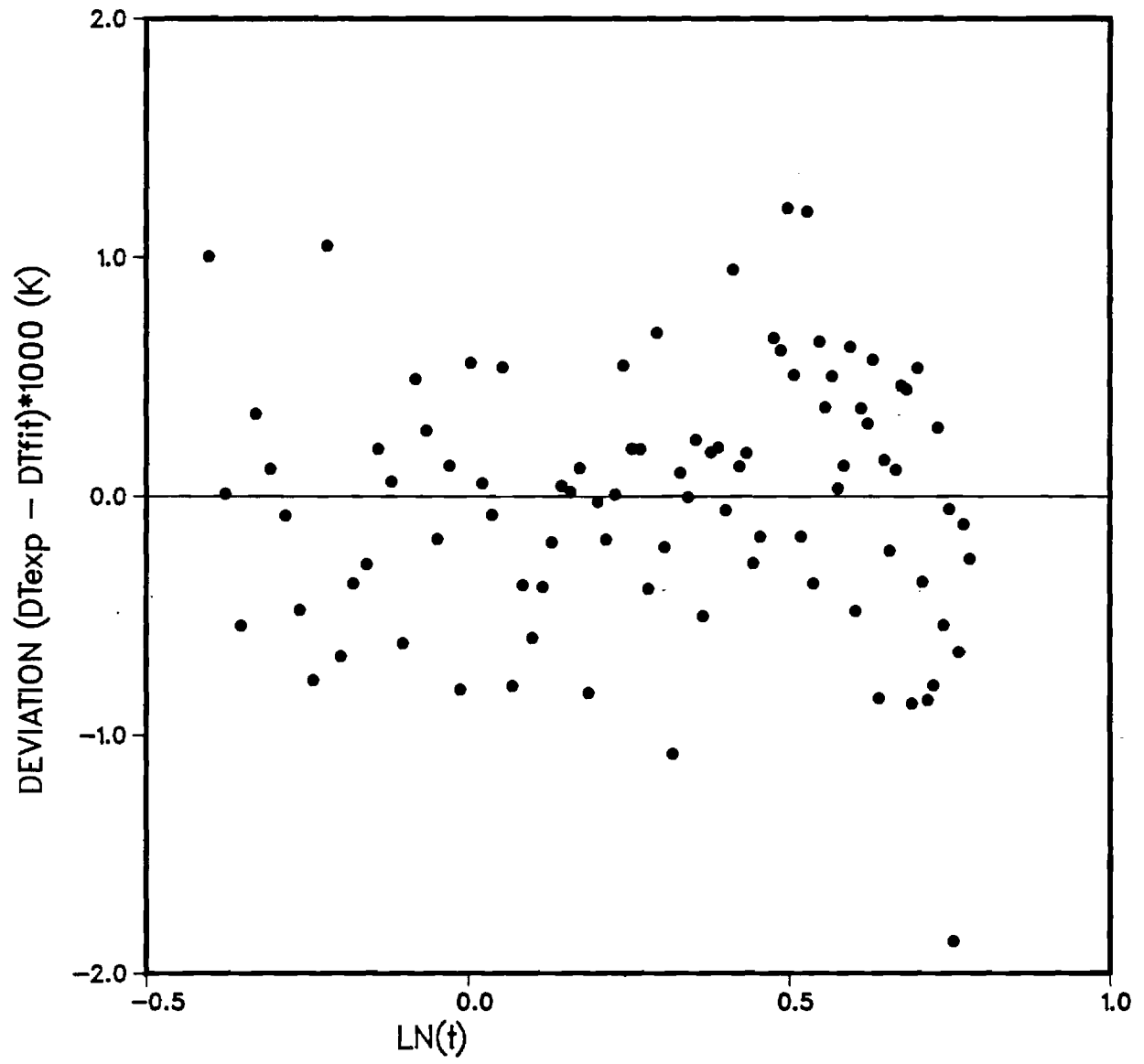


Figure 4: Plot of ΔT vs $\ln t$ to verify function linearity.

THERMAL CONDUCTIVITY OF AQUEOUS LiBr

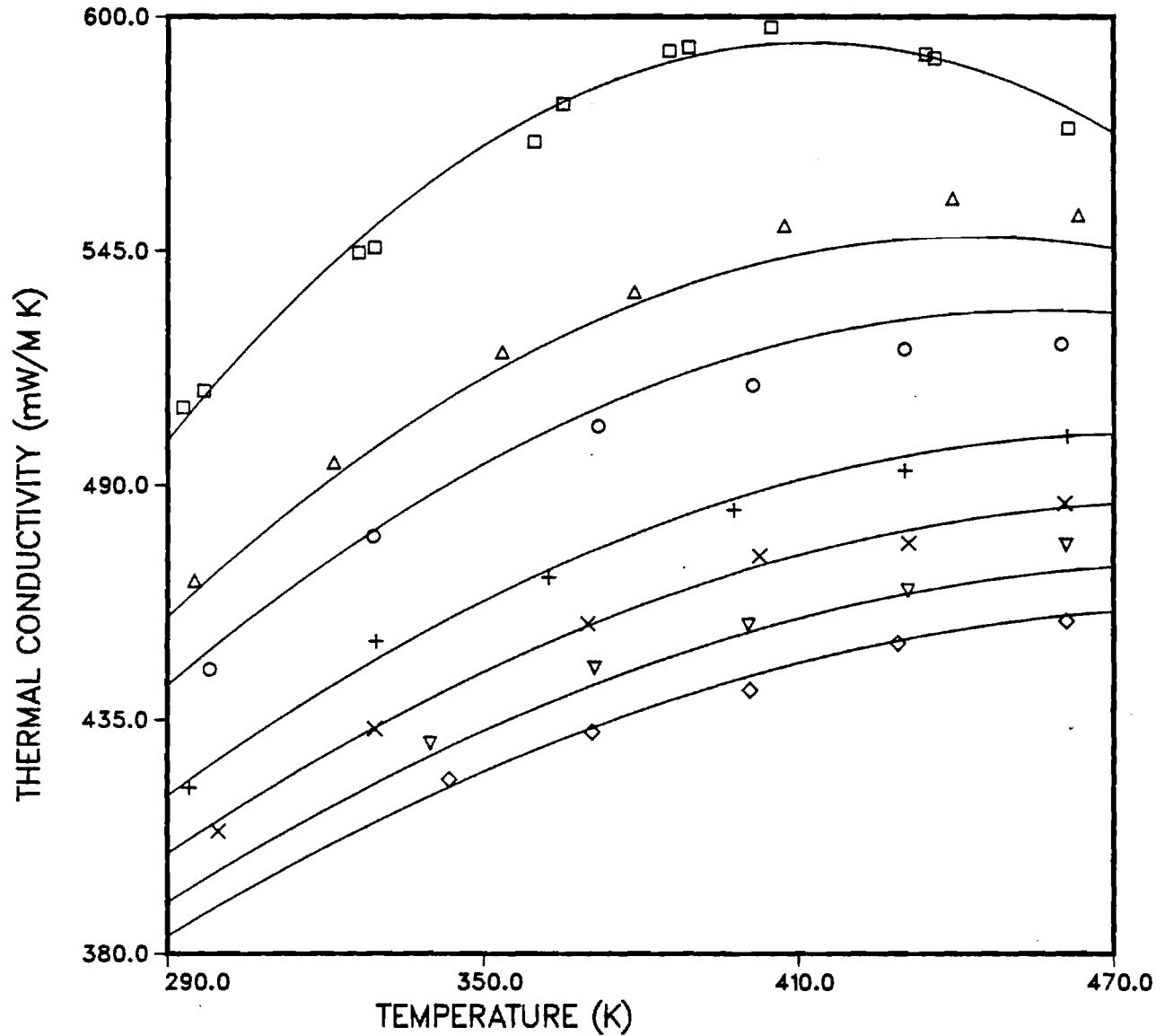


Figure 5: Thermal Conductivity of aqueous lithium bromide solutions. Solid curves are from the correlation. □ = 30.2 wt% LiBr, △ = 44.3 wt% LiBr, ○ = 49.1 wt% LiBr, + = 56.3 wt% LiBr, x = 60.0 wt% LiBr, ▽ = 62.9 wt% LiBr, ◇ = 64.9 wt% LiBr.

Density of Lithium Bromide - Water Solutions

1 Introduction

Improvements to the performance of absorption refrigeration equipment require a knowledge of the thermophysical properties of aqueous lithium bromide solutions. The density of such solutions at temperatures up to 100 °C has been investigated by several workers (ref. 1,3,4). An extension of these measurements to higher temperatures and concentrations is reported in this paper. The densities of aqueous lithium bromide solutions at four concentrations, namely 45.1, 49.9, 55.0, and 59.9 weight % and temperatures up to 200 °C were measured. A correlation of the experimental data is also presented.

2 Experiment

Principle of Operation The principle used to determine the liquid density (ρ) of a fluid in this study is based on its definition, namely the mass (M) per unit volume (V), and is expressed as

$$\rho = \frac{M}{V} \quad (1)$$

Experimentally, we measured the mass of the test fluid required to fill in a density cell where its internal volume has previously been calibrated. The density is therefore calculated accordingly.

Apparatus and Procedure The densities of lithium bromide - water solutions were measured in a high pressure pycnometer shown schematically in Figure 1. The pycnometer was rated up to 300 °C and 100 bar and consisted of four sampling cylinders (Whitey). One end of each cylinder was capped by a high pressure fitting and the other was attached to a pipe fitting (Cajon HLN), a shut-off valve, and a high pressure hand pump (High Pressure Equip. Co., model 50-6-15). The pump was used to maintain pressure to suppress boiling in the system. Each stainless steel cylinder was equipped with a thermowell for temperature measurement and had an internal volume of approximately 40 ml. The exact volume of each cell assembly was obtained by calibration with pure mercury at temperatures up to 150 °C. Figure 2 shows a typical calibration curve for density cell No. 1. The data were fitted to an appropriate function (either linear, as in Figure 1, or quadratic) for interpolation or extrapolation. Temperature control within ± 0.05 °C was achieved by a constant temperature circulating bath (Haake-Buchler, model N3B) filled with silicon oil.

The solution temperature was measured using a type K thermocouple which had previously been calibrated against a platinum resistance thermometer (Leeds and Northrup Co., Ser. No. 709892). The accuracy of the temperature measurement was estimated to be ± 0.1 °C. The system pressure was monitored by a precision pressure gauge (3D Instruments Inc.) rated at 1500 psi with an accuracy of $\pm 0.25\%$ of the full scale. An electronic balance (Sartorius, type 1580) with a precision of ± 0.001 g was used for weight measurement.

Material and Solution Preparation N-methylpyrrolidinone (99.5% purity) and HPLC grade water were purchased from Pfatz & Bauer, Inc. and Fisher Scientific respectively. Anhydrous lithium bromide was provided by Alfa Products (Lot No. H26G) and had certified purity of 99.5 % by weight. These chemicals were used without further purification. Aqueous lithium bromide solutions were prepared by adding degassed water to

fresh anhydrous lithium bromide. The solutions were degassed by alternating freeze-thaw procedure. About 0.2% of impurities by weight (excluding water) was ignored in calculating the concentrations of the prepared solutions. The concentrations were determined gravimetrically. A computer-aided titrator (Fisher Scientific, CAT system) was also used to check the concentration. As shown in Table 1, excellent agreement between solution concentrations determined by these two methods was obtained. The accuracy of concentration measurement was estimated to be within ± 0.1 wt % lithium bromide.

Test Run In order to test the apparatus and procedure, the densities of N-methylpyrrolidinone at atmospheric pressure were measured and compared with data in the literature. As illustrated in Figure 3 our measurements were in good agreement with those reported by Kneisl and Zondlo (1987).

3 Results and Discussion

Table 2 summarizes the measured densities of four lithium bromide - water solutions containing 45.1, 49.9, 55.0, and 59.9 weight % of lithium bromide respectively. Measurements were performed at temperatures from ambient to 200 °C. The system pressure was maintained at 150 psig throughout the experiments. At least three samples were taken at each condition to give the average reported in Table 2. The reproducibility of the results was ± 0.15 %.

The densities of aqueous lithium bromide solutions at lower temperatures have been reported by Uemura and Hasaba (1964) and Bogatykh and Evnovich (1965). Figure 4 shows that our data are in good agreement with those of the earlier workers, with average

absolute deviations being 0.3% when compared with those of Uemura and Hasaba and 0.2% with those of Bogatykh and evnovich, although the data from these two references are at concentration of 45.0, 50.0, 55.0, and 60.0 wt% LiBr respectively.

4 Correlation

Our results were fitted to the following polynomial function in temperature

$$\rho = A_0 + A_1T + A_2T^2 \quad (2)$$

where ρ is in gm/ml and T is in K. The values of A_0 , A_1 , and A_2 were determined by minimizing the sum of squares of the relative deviations: $\sum_i [(\rho_{expt,i} - \rho_{cal,i})/\rho_{expt,i}]^2$. The constants A_0 , A_1 , and A_2 were further interpolated in terms of weight fraction of lithium bromide (X) as follows

$$A_0 = 1.09763 + 0.071244X + 2.21446X^2 \quad (3)$$

$$A_1 = (0.679620 - 1.48247X - 0.89696X^2) \times 10^{-3} \quad (4)$$

$$A_2 = (-0.035097 - 3.24312X + 4.97020X^2) \times 10^{-6} \quad (5)$$

All data could be correlated with the above equation with an overall AAD of 0.06% and MAD of 0.19%. However, nine parameters are required. A simpler form with five parameters is given by:

$$\rho = 1.40818 - 0.713995X + 2.64232X^2 - \frac{(0.12318 + 0.946268X)T}{1000} \quad (6)$$

with an AAD of 0.08% and MAD of 0.39%. Figure 4 shows the comparison between the values calculated by this equation and the observed values.

It should be noted that the correlatin is based on lithium bromide concentrations between 0.45 and 0.6. Extrapolation to other concentrations is not recommended. To cover a wider range of X, we included the data available in the literature at lower temperatures. The following equation is obtained

$$\rho = 1.14536 + 0.47084X + 1.37479X^2 - \frac{(0.333393 + 0.571749X)T}{1000} \quad (7)$$

The average deviation (AAD%) between the calculated and experimental values was found to be 0.19% for 86 data points covering a weight fraction of LiBr from 0.2 to 0.65. The maximum deviation was 0.51% for this case.

5 References

1. Bogatykh, S. A., and I. D. Evnovich, *Zh. Prikl. Klim.*, 38, 945 (1965).
2. Kneisl, P., and J. W. Zondlo, *J. Chem. Eng. Data*, 32, 11 (1987).
3. Sohnel, O., and P. Novotny, 'Densities of Aqueous Solutions of Inorganic Substances', Elsevier, Amsterdam, 1985.
4. Uemura, T., and S. Hasaba, *Technol. Rept.*, Kansai Univ., 6, 31 (1964).

Table 1. Comparison of Solution Concentration
Determined by Different Methods.

No.	Weight Fraction of LiBr	
	Gravimetric	Titrametric
1	0.4506	0.4507
2	0.4985	0.4993
3	0.5500	0.5495
4	0.5990	0.5988

Table 2. Experimental Densities of Aqueous Lithium Bromide Solutions.

Wt% LiBr	T [K]	ρ [gm/ml]	Wt% LiBr	T [K]	ρ [gm/ml]
45.1	301.6	1.4554	49.9	298.7	1.5328
	319.1	1.4470		318.5	1.5206
	333.2	1.4389		333.2	1.5128
	348.1	1.4323		348.0	1.5042
	361.6	1.4255		363.1	1.4954
	381.3	1.4144		382.7	1.4833
	402.4	1.4041		402.8	1.4705
	423.5	1.3919		423.7	1.4568
	448.4	1.3782		448.6	1.4397
				474.8	1.4216
55.0	298.2	1.6205	59.9	298.5	1.7217
	318.2	1.6089		318.2	1.7087
	332.6	1.5997		333.7	1.6986
	346.9	1.5912		348.1	1.6884
	361.5	1.5816		363.6	1.6779
	382.1	1.5703		383.6	1.6642
	401.6	1.5584		403.0	1.6512
	421.6	1.5453		423.4	1.6365
	447.4	1.5287		447.9	1.6192
	473.1	1.5110		473.2	1.6008

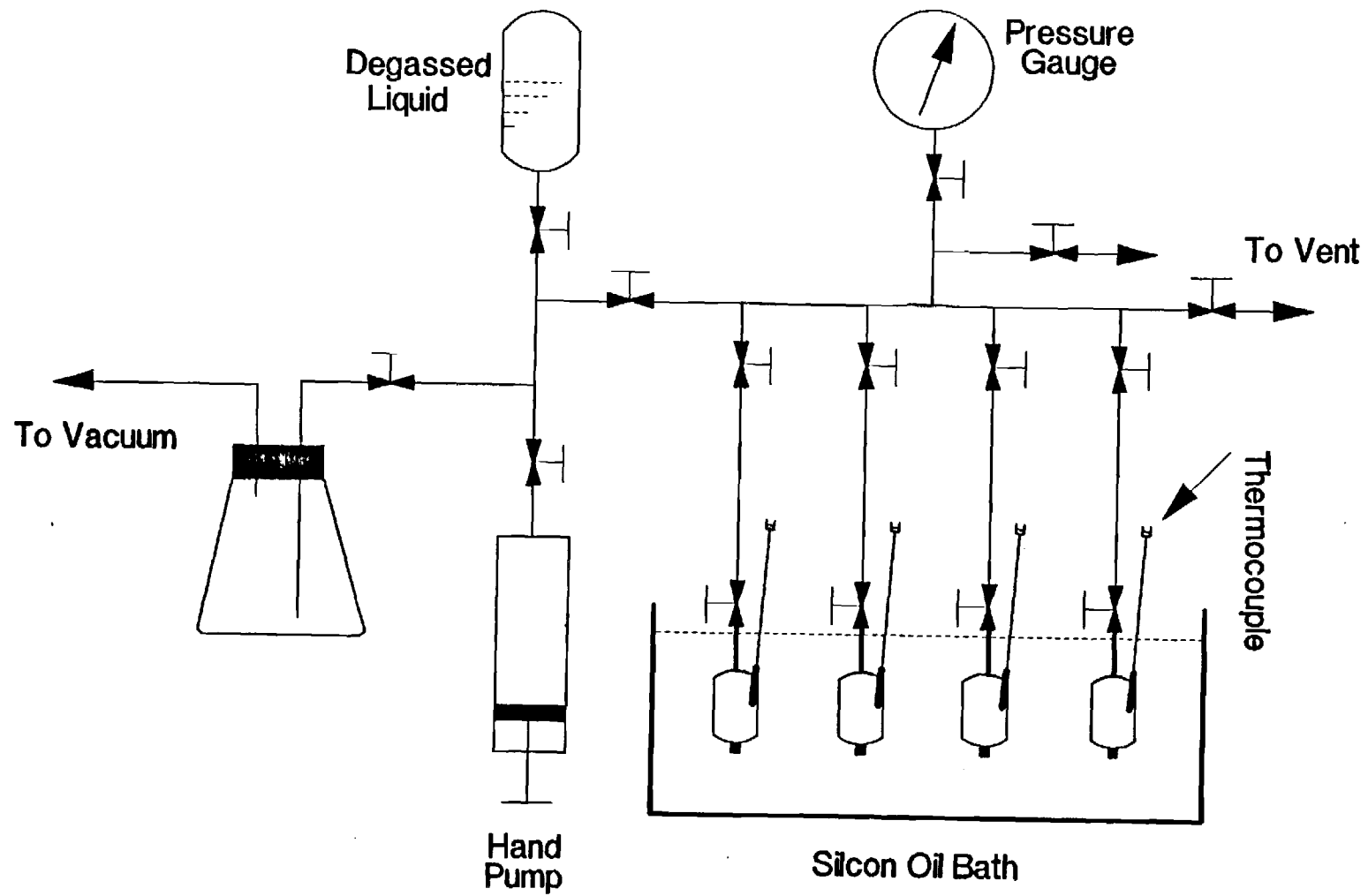


Figure 1. Schematic diagram of the high pressure pycnometer.

INTERNAL VOLUME OF DENSITY CELL 1

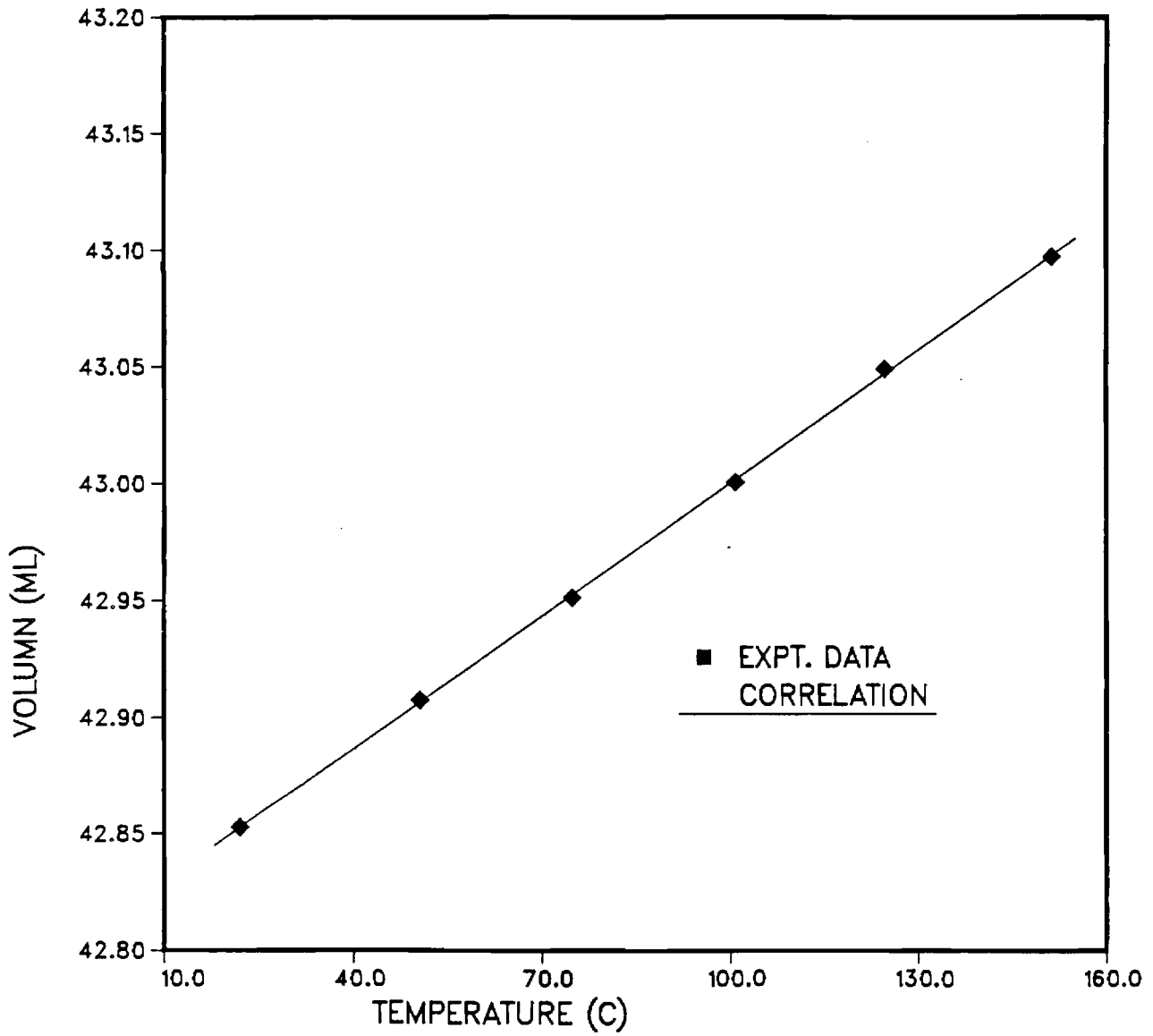


Figure 2. Volume of density cell 1.

DENSITY OF N,METHYLPYRROLIDINONE

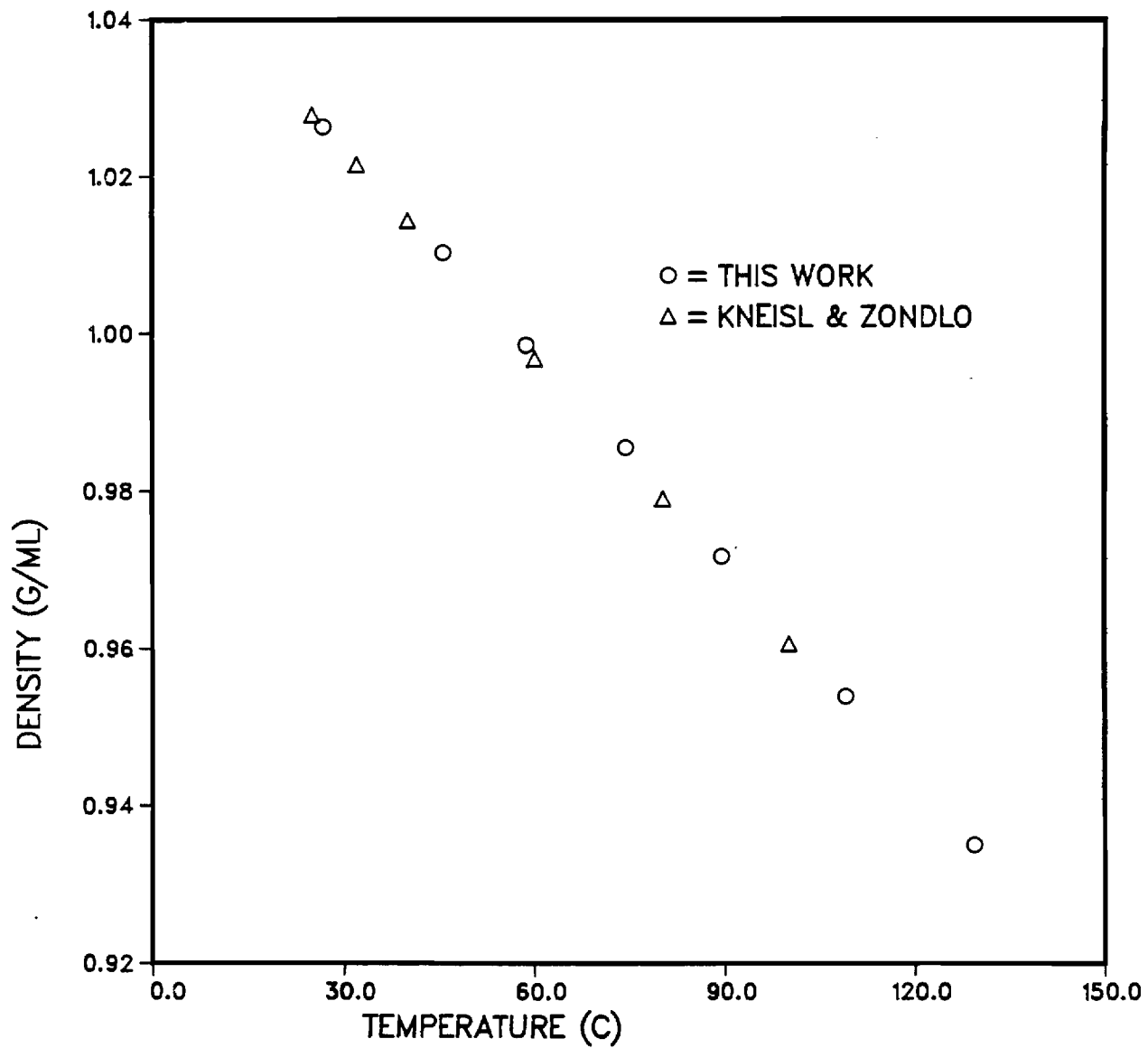


Figure 3. Liquid density of N,methylpyrrolidinone.

DENSITY OF AQUEOUS LiBr SOLUTION

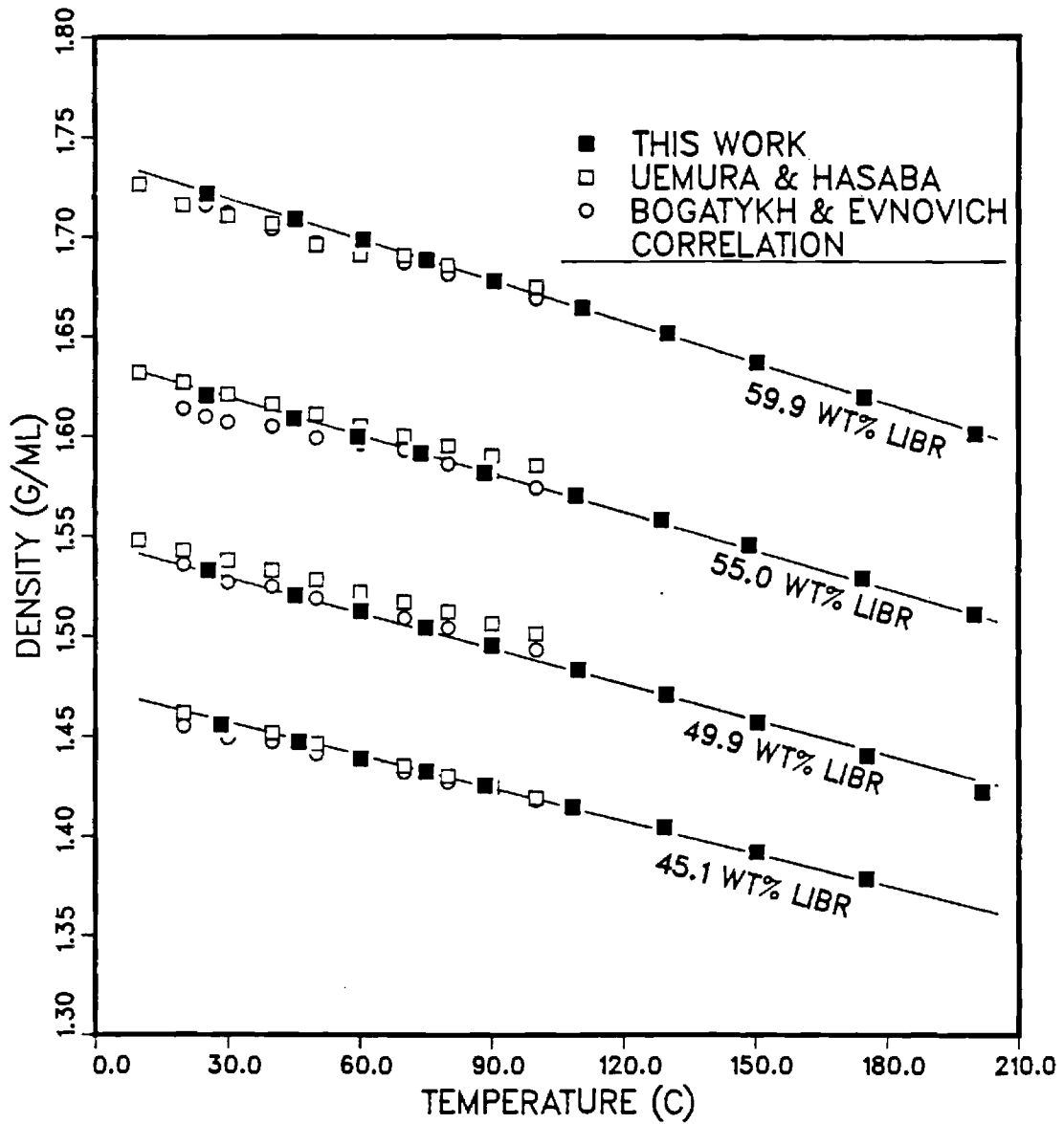


Figure 4. Liquid density of LiBr - water solutions.

Viscosity of Lithium Bromide - Water Solutions

1 Introduction

The transport properties of concentrated aqueous lithium bromide solutions are important in the design of absorption refrigeration systems. Although the viscosities of such solutions have been measured at low temperatures, the results are not consistent (more than 15% difference between values reported by different workers). Therefore, the viscosities of solutions with weight fractions of lithium bromide ranging from 0.45 to 0.65 and at temperatures up to 200 °C were measured and are reported below.

2 Experiment

Principle of Operation The equation used to represent the absolute viscosity, μ , of a fluid flowing through a capillary is based on Poiseuille's law,

$$\mu = \frac{\pi r^4 g h}{8LV} \rho t - \frac{\zeta V}{8\pi L} \frac{\rho}{t} \quad (1)$$

where

- r : radius of the capillary
 g : gravitational constant
 h : average head of the fluid
 L : length of the capillary
 V : efflux volume of the fluid
 t : efflux time
 ρ : density of the fluid
 ζ : kinetic energy coefficient

For a specific capillary viscometer, the kinematic viscosity ν can therefore be related to the efflux time using:

$$\nu = \frac{\mu}{\rho} = C_1 t - \frac{C_2}{t} \quad (2)$$

where C_1 is the viscometric constant and is determined by calibration with a fluid of known viscosity. The second term on the right hand side represents the correction due to the kinetic energy and is usually neglected if an appropriate size of viscometer is used.

Apparatus and Procedure A high pressure viscometer was designed and constructed for viscosity measurement of highly corrosive solutions. The design of the apparatus is similar to that proposed by Al-Harbi (1982). Figure 1 shows the schematic diagram of this apparatus, which consists of a capillary viscometer, a pressure cell, a thermostated air bath, and a pressure distribution section. This apparatus was designed for temperatures up to 200 °C and pressures up to 30 atm.

A size 1 Zeitfuchs cross-arm capillary viscometer (International Research Glassware) was used for determination of the kinematic viscosity (Figure 2). The calibration factor was determined using pure water and a wetted capillary viscometer. After calibration, the

viscometer was placed inside the pressure cell and the capillary end was connected to the pressure distribution section through V5. The reservoir end was opened to the cell chamber such that the pressure over the viscometer was balanced. The pressure cell which was designed to withstand the system pressure during an experiment, is shown schematically in Figure 3. The cell is equipped with four glass view ports (tempered borosilicate glass) to allow visual observation of the reservoir and the measuring bulb of the viscometer. An insulated air bath, heated by a primary (800 W) as well as a secondary (200 W) heater, was used to establish the desired temperature. A stable temperature in the air bath was maintained by a commercial temperature control unit (Omega, model CN5000) and a circulating fan. Temperature fluctuations were minimized by the material of the pressure cell, which was made of a heavy steel. The test fluid was moved back and forth through the capillary tube by a high pressure hand pump (High Pressure Equipment Co., model 50-6-15). Helium was used as the pressurizing fluid.

The temperature was measured inside the pressure cell by a chromel-alumel thermocouple, calibrated with a NBS calibrated Leeds and Northrop platinum resistance thermometer (Serial No. 709892). The accuracy of the temperature measurement was estimated to be ± 0.1 °C. Pressure measurement was accomplished by a precision gauge (3D Instruments Inc.) with an accuracy of 0.25% of the full scale (0-1500 psi). An electronic timer accurate to 1/100 second was used to obtain the efflux time.

Before an experiment was performed, a clean dry viscometer loaded with the appropriate test solution was attached to the top flange of the pressure cell. The top flange was then bolted into place, and the cell was connected to the pressure distribution section and pressurized slowly to the desired pressure. To eliminate loss of vapor from the solution, about 40 ml of slightly dilute lithium bromide solution was placed at the bottom of the cell

chamber so that the solution in the viscometer was always under its vapor pressure.

At the beginning of an experiment, all valves were closed except for V4 and V5. The pressure on the capillary end was reduced by the use of the hand pump, causing the solution to flow into the reverse bend of the capillary. Once the flow had been initiated, valve V3 was opened to balance the pressures over both ends of the viscometer. The efflux time for the solution to flow through the timing marks on the measuring bulb was then measured. At the end of the measurement, valve V3 was closed and the solution was then forced to return to the reservoir by increasing the pressure on the capillary end with the hand pump. Measurements were repeated until consistent efflux times were obtained.

Material and Solution Preparation Anhydrous lithium bromide, with certified purity of 99.3% from Alfa Products (Lot No. F06H), was used for preparation of solution. The lithium bromide - water solutions were prepared the same way as described in the section on density measurement. The concentrations of the solutions were determined either by gravimetric or titrametric methods and are summarized in Table 1.

Test Run To test the apparatus and procedures, the kinematic viscosity of pure water was measured and compared with values reported by the National Bureau Standard (ref. 3). Figure 4 shows this comparison. Good agreement was obtained with the density of water reported by Gildseth et al. (1972) being used to obtain the absolute viscosity shown in this diagram.

3 Results and Discussion

The experimental kinematic viscosities of aqueous lithium bromide solutions of 45.0, 50.0, 55.0, 59.9, 63.0, and 65.0 wt% LiBr are presented in Table 2. The temperature range of the measurements varied from 40 to 200 °C, and the pressure was maintained at 200 psig throughout the experiments. Absolute viscosity data, in which the liquid densities were obtained from the correlation previously described, are also included in Table 2. The average of at least four samples was taken to obtain each value reported in this table. The viscosities were reproducible within $\pm 1.5\%$. A graphical presentation of the experimental results is given in Figure 5. As shown, a linear relationship between $\ln(\mu)$ and $1/T$ exists at low temperatures. However, the relationship is nonlinear at higher temperatures, in particular for less concentrated solutions (eg. 45.0 wt% LiBr).

Comparison of our data with data available in the literature was attempted though the system pressures were different. Two sets of experimental data studied at atmospheric pressure by Uemura and Hasaba (1964), and by Bogatykh and Evnovich (1963) were selected. Figure 6 illustrates a comparison of 50.0 and 59.9 wt% LiBr solutions. The literature data shown in this figure were for 50.0 and 60.0 wt% LiBr respectively. The agreement between the literature data is poor, with the experimental data of Bogatykh and Evnovich being consistently lower than the data of Uemura and Hasaba. The literature data bracket our data at lower temperatures, while our data are higher at the higher temperatures. It is also apparent that our data are smoother than the literature data.

4 Correlation

The viscosity of lithium bromide - water solutions at each concentration can be described by the following equation

$$\ln \mu = A_1 + \frac{A_2}{T} + A_3 \ln T \quad (3)$$

where the unit of viscosity (μ) is in centipoise and temperature is in K. Values of A_1 , A_2 , and A_3 obtained by regression are listed in Table 3, as are the AAD% and MAD% between experimental and calculated viscosities. The MAD% was less than 1.1 % in all cases. The dependence of A_1 , A_2 , and A_3 on the weight fraction (X) is illustrated graphically in Figure 7. A regression of all data yields

$$A_1 = (-0.494122 + 1.63967X - 1.45110X^2) \times 10^3 \quad (4)$$

$$A_2 = (2.86064 - 9.34568X + 8.52755X^2) \times 10^4 \quad (5)$$

$$A_3 = (0.703848 - 2.35014X + 2.07809X^2) \times 10^2 \quad (6)$$

This correlation results in an AAD of 1.1% and a MAD of 3.1% over the entire region of T and X covered by this study. Figure 8 shows the good agreement between experimental data and the values calculated using the above correlation.

5 References

1. Al-Harbi, D. K., 'Viscosity of Selected Hydrocarbons Saturated with Gas', Ph. D. Dissertation, Oklahoma State University, Stillwater, OK, 1982.
2. Bogatykh, S. A., and I. D. Evnovich, *Zh. Prikl. Klim.*, 36, 186 (1963).
3. CRC Handbook of Chemistry and Physics, 63rd Edition, CRC Press, 1982.
4. Gildseth, W., A. Habenschus, and F. H. Spedding, *J. Chem. Eng. Data*, 17, 402 (1972).
5. Uemura, T. and S. Hasaba, *Technol. Rept.*, Kansai, Univ., 6, 31 (1964).

Table 1. Comparison of Solution Concentration
Determined by Different Methods.

No.	Weight Fraction of LiBr	
	Gravimetric	Titrametric
1	0.4500	0.4503
2	0.4999	0.5000
3	0.5499	0.5507
4	0.5993	0.6002
5	0.6300	0.6289
6	0.6495	0.6504

Table 2. Experimental Viscosities of Aqueous Lithium Bromide Solutions

Wt% LiBr	T [K]	ν [cst]	μ [cp]	Wt% LiBr	T [K]	ν [cst]	μ [cp]
45.0	312.9	1.325	1.919	50.0	314.9	1.605	2.446
	333.0	0.947	1.363		333.2	1.204	1.822
	353.2	0.738	1.054		353.7	0.932	1.400
	373.9	0.602	0.854		373.2	0.759	1.131
	393.2	0.515	0.725		393.3	0.637	0.942
	413.2	0.453	0.632		412.3	0.554	0.813
	433.0	0.407	0.564		432.6	0.490	0.712
	453.2	0.376	0.516		453.2	0.451	0.650
	472.5	0.353	0.480		472.6	0.413	0.589
55.0	314.2	2.120	3.418	59.9	316.0	2.897	4.952
	333.6	1.547	2.476		333.5	2.122	3.603
	353.1	1.193	1.895		353.6	1.577	2.657
	373.1	0.954	1.503		372.9	1.236	2.066
	393.5	0.786	1.228		394.3	0.986	1.634
	412.7	0.669	1.037		412.7	0.834	1.372
	433.0	0.586	0.900		433.0	0.714	1.164
	453.2	0.523	0.796		453.2	0.630	1.018
	472.3	0.477	0.720		472.9	0.553	0.886
63.0	333.1	2.826	4.964	65.0	333.4	3.162	5.680
	353.2	2.030	3.537		352.4	2.331	4.158
	373.6	1.542	2.665		372.3	1.749	3.095
	393.8	1.219	2.090		393.6	1.352	2.372
	413.2	1.011	1.720		413.2	1.106	1.925
	432.9	0.867	1.463		433.4	0.946	1.633
	452.9	0.744	1.245		452.6	0.820	1.405
	472.8	0.662	1.099		472.7	0.730	1.240

Table 3. Correlation of Experimental Data by Equation 3.

WT% LiBr	A_1	A_2	A_3	AAD%	MAD%
45.0	-49.8181	3813.29	6.66101	0.48	1.09
50.0	-40.1023	3357.43	5.27316	0.36	1.06
55.0	-33.6317	3118.48	4.33620	0.18	0.43
59.9	-32.5247	3222.14	4.15643	0.37	1.04
63.0	-37.3241	3605.41	4.83769	0.27	0.85
65.0	-46.3684	4167.00	6.13288	0.23	0.71

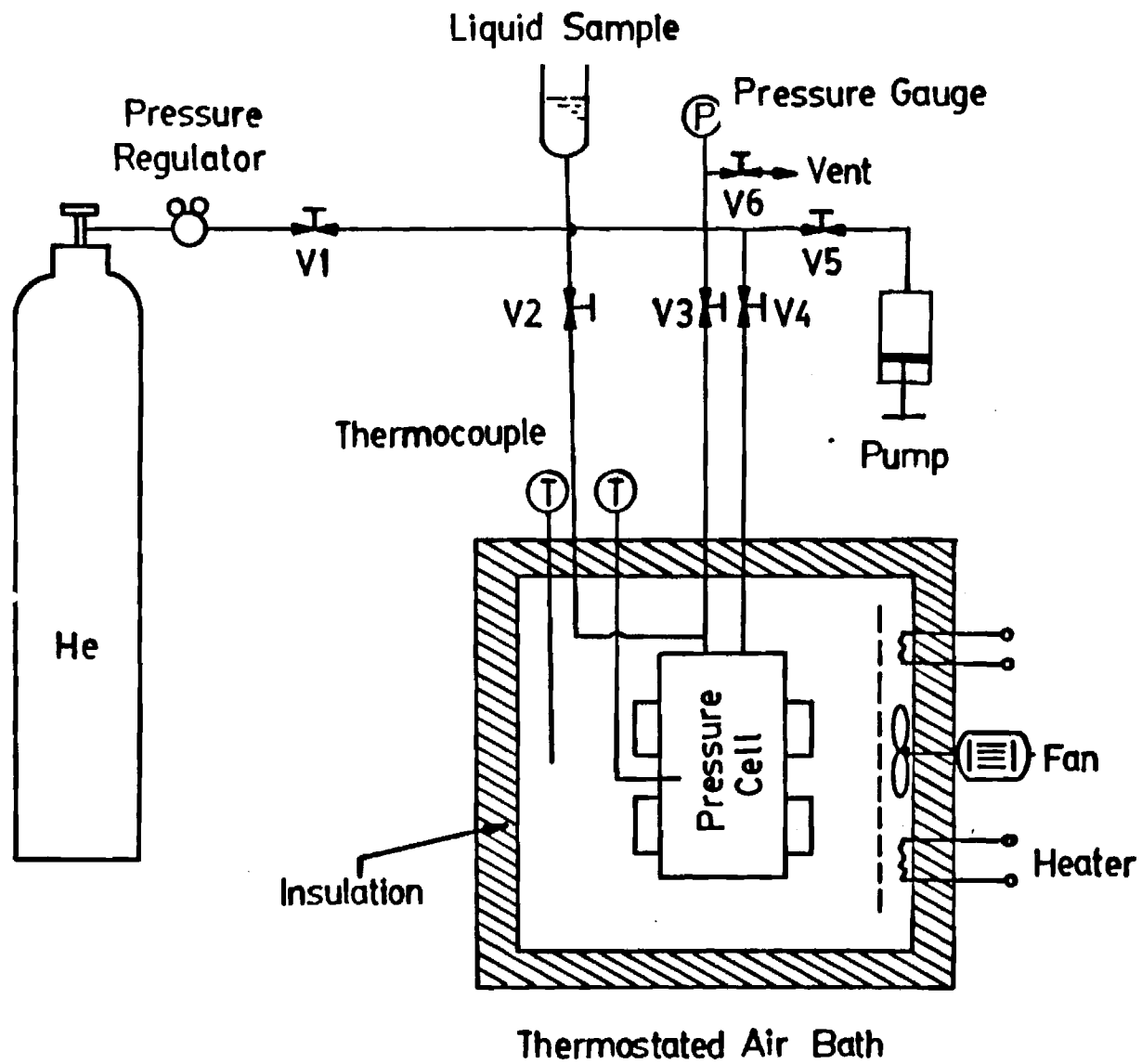


Figure 1. Schematic diagram of the high pressure viscometer.

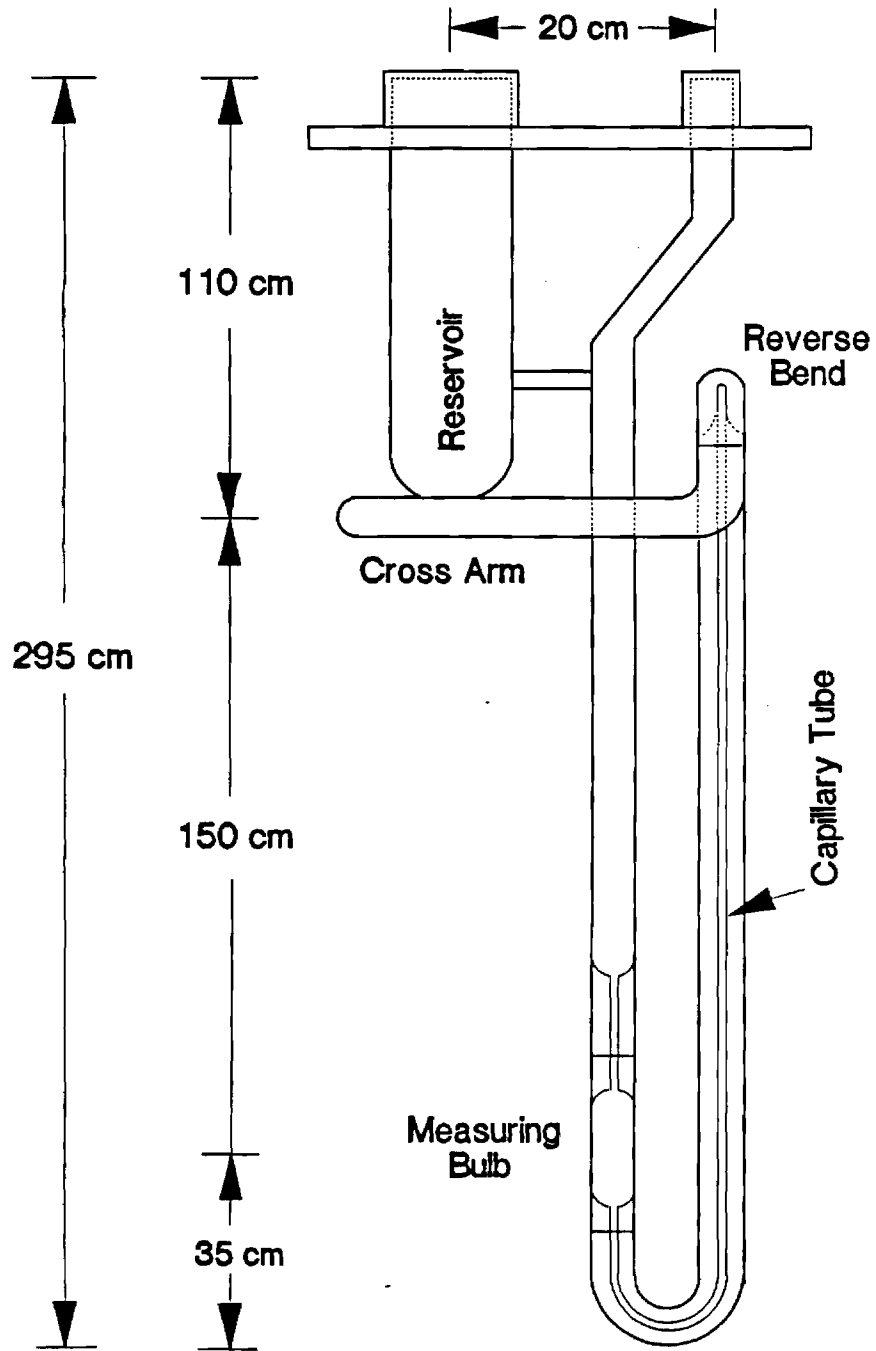


Figure 2. Zeitfuchs cross-arm viscometer.

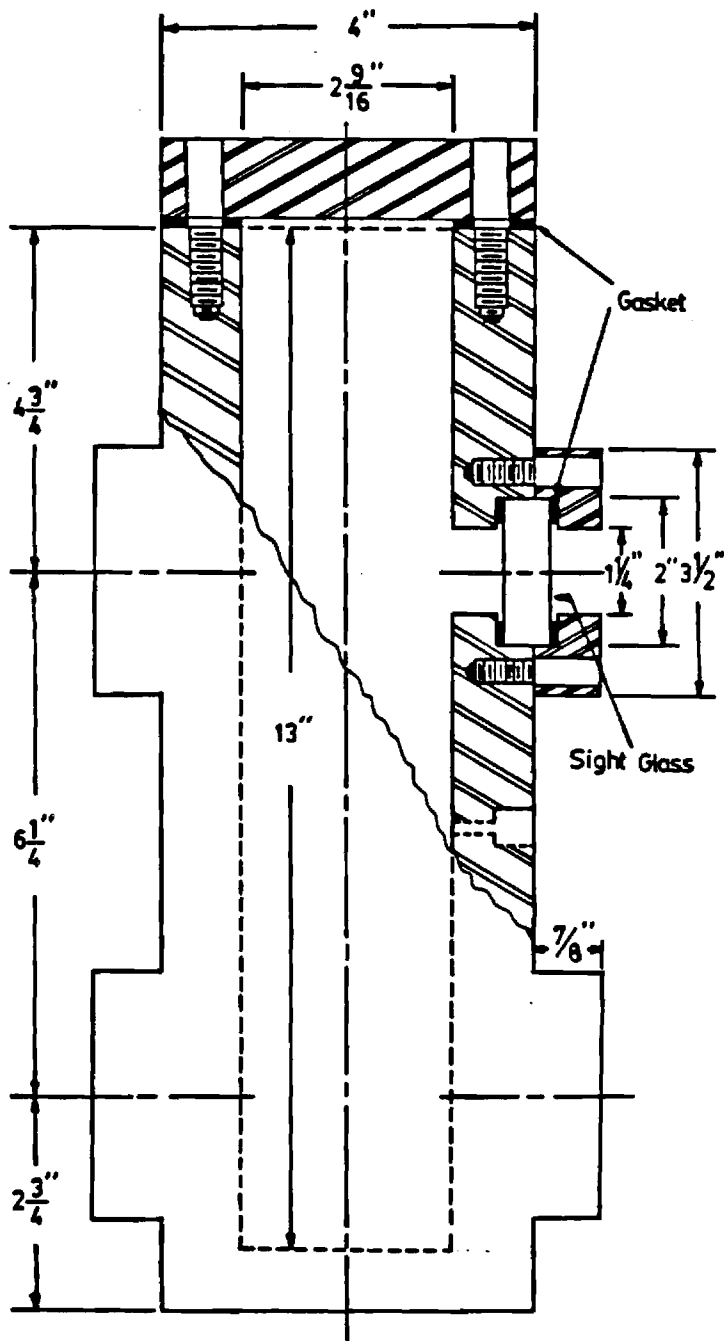


Figure 3. Detail design of the pressure cell.

VISCOSITY OF WATER

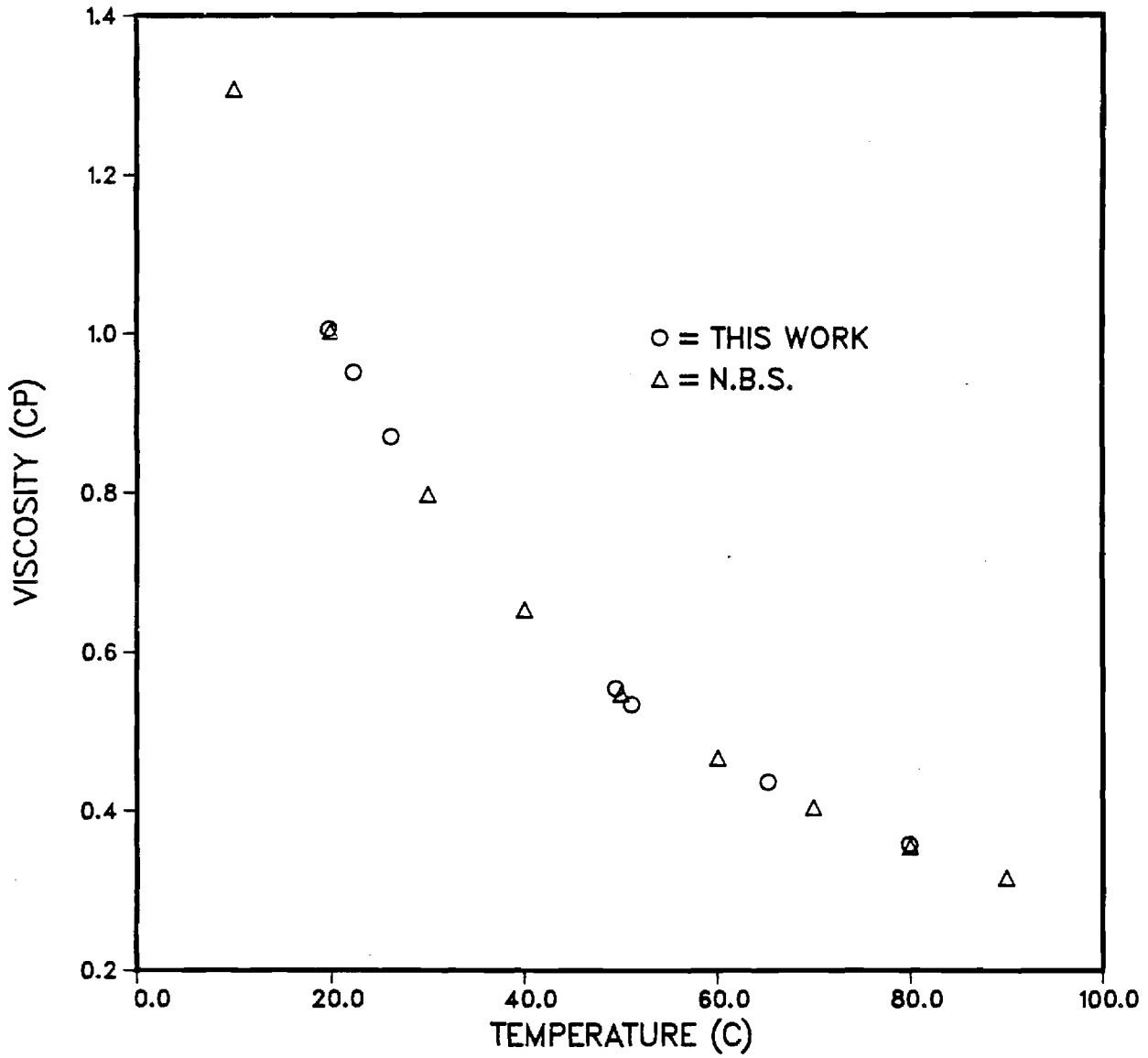


Figure 4. Viscosity of liquid water.

VISCOSITY OF AQUEOUS LiBr SOLUTION

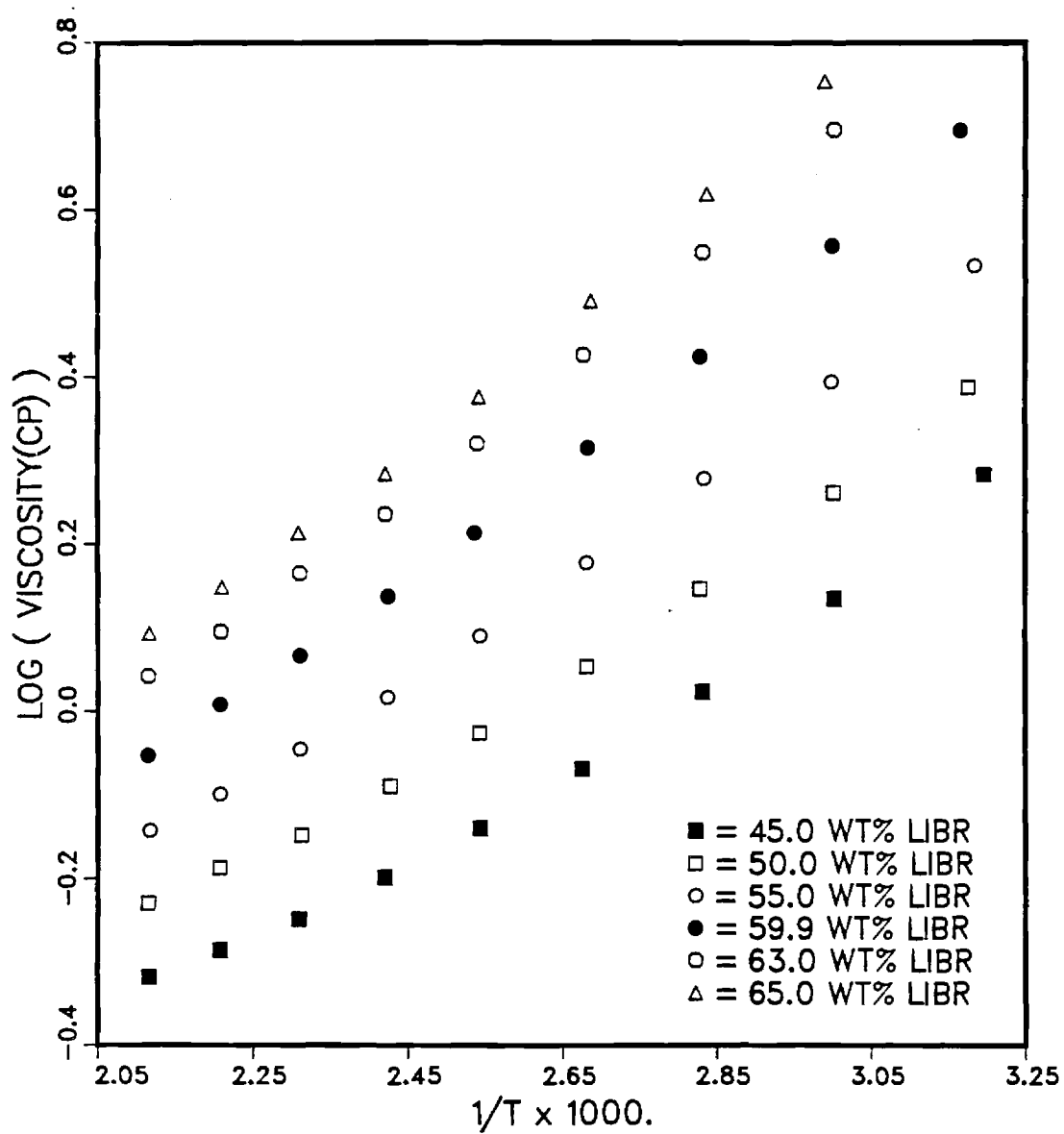


Figure 5. Viscosity of aqueous LiBr solutions.

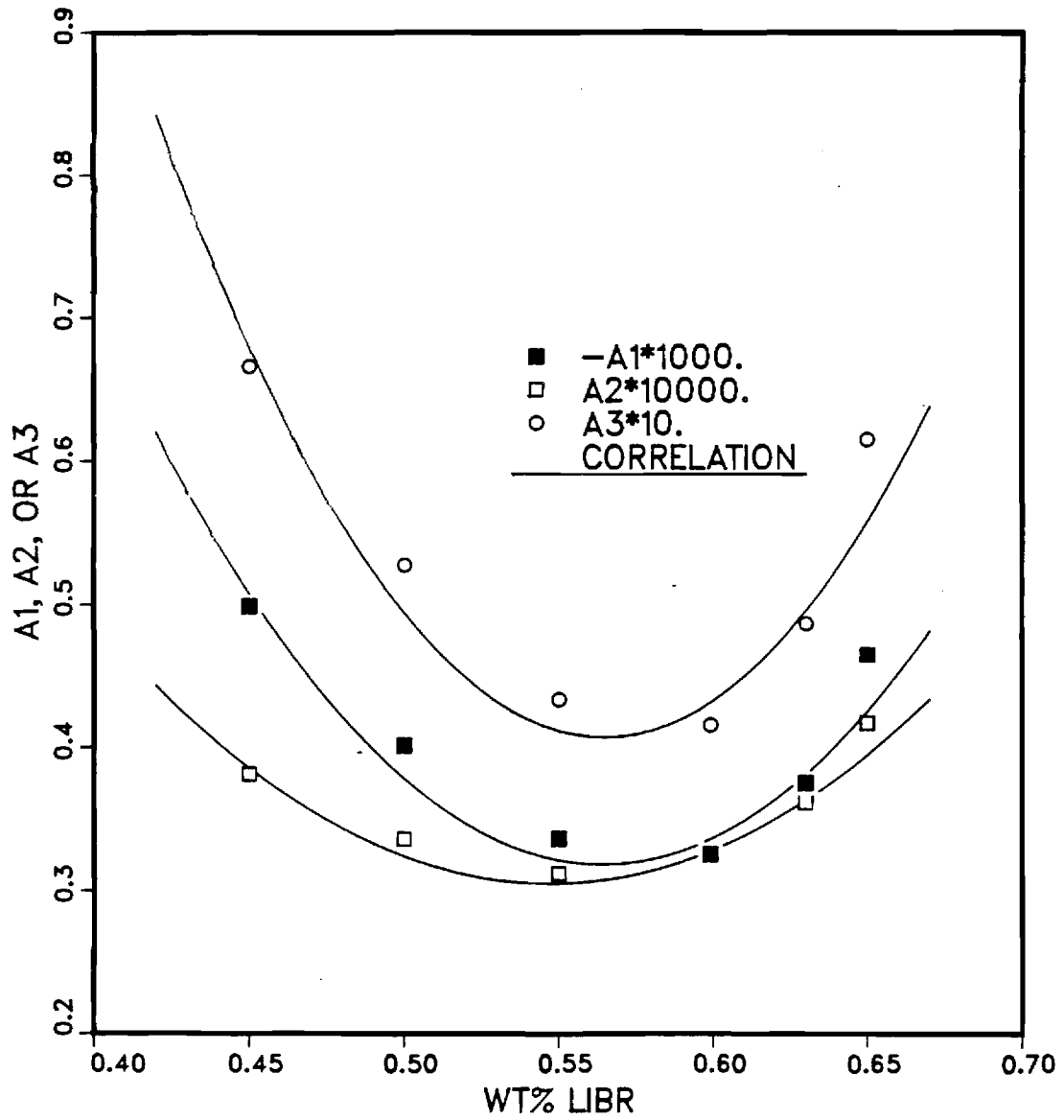


Figure 7. The values of A_1 , A_2 , and A_3 as a function of concentration.

VISCOSITY OF AQUEOUS LIBR SOLUTION

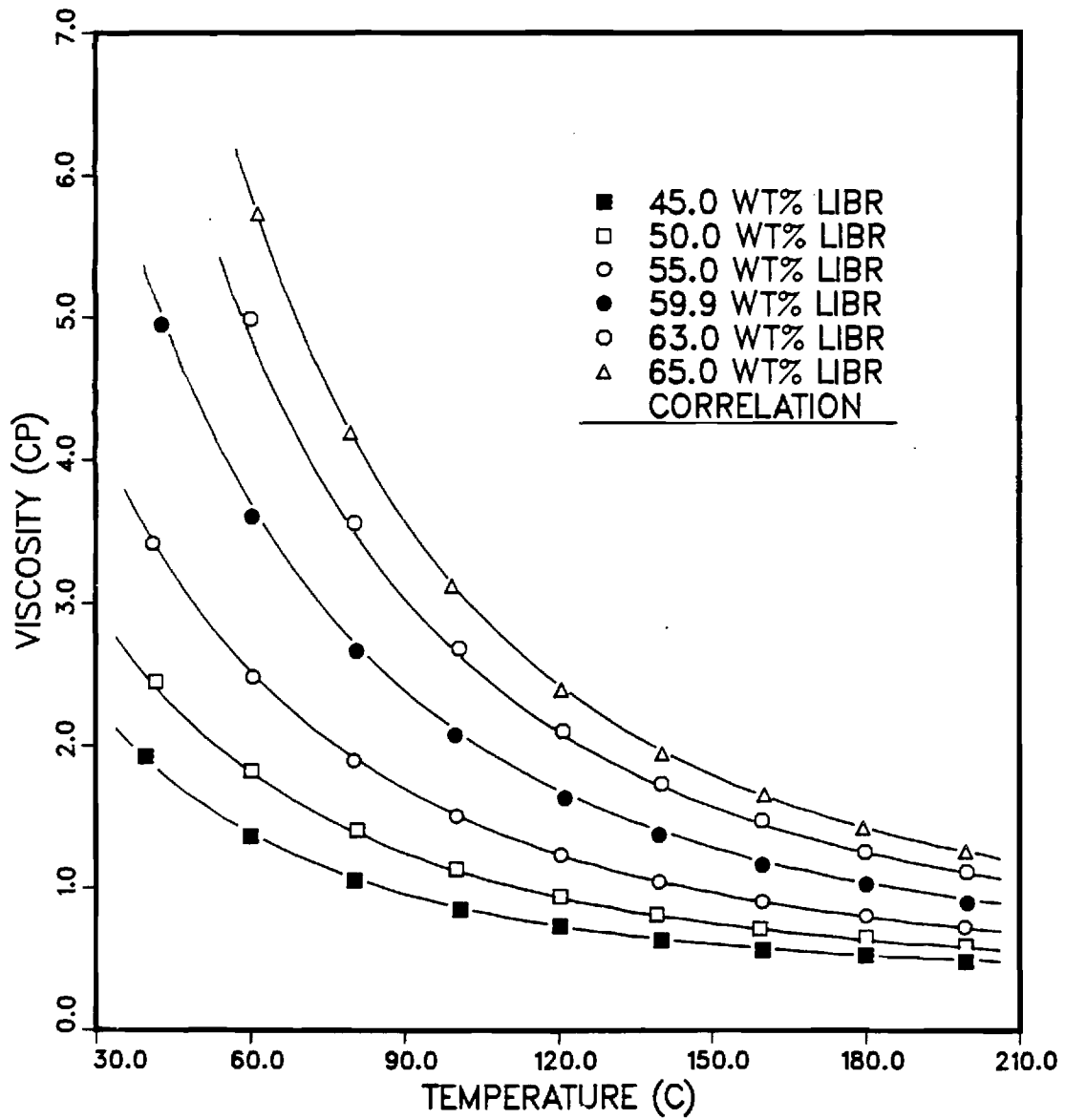


Figure 8. Comparison of the correlation with experimental data.

SPECIFIC HEAT MEASUREMENTS

1. INTRODUCTION:

As originally proposed, the specific heat measurements were conducted using a modified drop calorimeter. Proper application of this instrument produces accurate values for average specific heats over a finite temperature interval. These average specific heats can be fitted to a suitable function, such as a polynomial, of the temperature and concentration. Continuous values for the specific heat over the temperature range can be obtained by differentiating the average specific heat function. This general procedure has been followed resulting in data from this investigation that is in good agreement with independent data. The new data presented herein along with data from two alternative sources are demonstrated to be mutually confirming.

A schematic of the particular instrument used in this investigation is shown in Figure 1. A drop calorimeter implements the classical "method of mixing" in which the system being "mixed" (i.e. brought to thermal equilibrium) consists of a small, ca. 100 gm, capsule containing the sample and a large, ca. 15 kg, receiver. The receiver is well insulated but not quite adiabatic. In addition to the sample capsule and receiver, a drop calorimeter comprises a heater section and auxiliaries and controls. In operation, the material sample is confined in the rigid capsule or "bomb". The capsule containing the sample is brought up to temperature in the tube heater and inserted, by dropping, into the receiver. The receiver is a massive metal block, a copper cylinder in this case, with a central well to accept the capsule. The heat interaction between the sample and receiver is then monitored by a temperature probe installed in the receiver.

Quantitatively, the heat interaction can be interpreted in terms of energy changes in the receiver and the sample by consideration of two closed thermodynamic systems. The first system is the combination of the receiver and the capsule, which is charged with the sample. The second system is the capsule and sample alone. With reference to the closed system consisting of the charged capsule and the receiver, one has the following total energy at the instant before a drop:

$$E_{\text{com},i} = U_{\text{cs}}(T_s) + PE_{\text{cs}} + U_{\text{r}}(T_{\text{ri}})$$

Where:

$E_{\text{com},i}$ = energy of the combined system at the initial state, i

$U_{\text{cs}}(T_s)$ = internal energy of the capsule and sample at drop temperature, T_s

PE_{cs} = potential energy of the capsule and sample which are elevated with respect to the receiver

$U_{\text{r}}(T_{\text{ri}})$ = internal energy of the receiver at its initial temperature, before the drop, T_{ri} .

After the drop and after the capsule, sample, and receiver have reached temperature equilibrium and have achieved a uniform final temperature, T_p , the energy is distributed as follows:

$$E_{\text{com},f} = U_{\text{cs}}(T_f) + U_r(T_f)$$

For the entire process beginning just before a drop and ending with temperature equilibrium, the principle of conservation of energy gives the following:

$$E_{\text{com},f} - E_{\text{com},i} + W_{\text{cs}} + W_r = Q_{\text{com}}$$

Where:

W_{cs} = work done by the capsule and sample during the process

W_r = work done by the receiver during the process

Q_{com} = heat interaction between combined system and its environment

It can be verified that the change in potential energy of the sample due to its drop of about 0.5 meter is an entirely negligible .005 kJ/kg. The work terms can only involve boundary work on the atmosphere, $W_r = P_o \Delta V_r$ and $W_{\text{cs}} = P_o \Delta V_c$, and these quantities are also negligible. Ignoring the potential energy change and accepting for now the approximation, for which compensation is later introduced, that the combined system is adiabatic the energy balance reduces to the following:

$$U_r(T_f) - U_r(T_i) + P_o \Delta V_r = - \{U_{\text{cs}}(T_f) - U_{\text{cs}}(T_s) + P_o \Delta V_c\}$$

or

$$\Delta H_r = - \Delta H_{\text{cs}}$$

Since the thermal expansion of both the receiver and capsule are entirely negligible, one could just as well write:

$$\Delta U_r = - \Delta U_{\text{cs}}$$

Clearly then the heat interaction from the capsule to the receiver, Q_x , is equal to the change in either the enthalpy or the energy of the sample and the capsule, or:

$$-Q_x = \Delta H_{\text{cs}} \text{ or } \Delta U_{\text{cs}}$$

Where the the indicated energy change is the sum of the component changes of the energies of the capsule and sample, or

$$\Delta U_{\text{cs}} = \Delta U_c + \Delta U_s$$

Proceeding from the assumption that the capsule undergoes an essentially constant volume process, the energy change of the sample, ΔU_s , can be readily evaluated. Ignoring the presence of a tiny quantity of air, the capsule can be considered to be filled with a known mass of fluid, m_s , such that:

$$V_s = m_s(v_f + x v_{fg})$$

Where V_s is the 14.8 ml sample volume.

Similarly, the internal energy of the sample is given as follows:

$$U_s = m_s(u_f + x u_{fg})$$

For a constant volume process proceeding from the initial sample temperature, T_s , and ending at T_f , the change in energy is as follows:

$$(U_s - U_f)/m_s = (u_{fs} - u_{ff}) + (x_s u_{fgs} - x_f u_{fgf})$$

Where:

u_{fs} = specific internal energy of the saturated liquid sample at T_s

u_{ff} = specific internal energy of the saturated liquid sample at T_f

x_s = quality of the sample at initial temperature, T_s

x_f = quality of the sample at final temperature, T_f

u_{fgs} = specific internal energy of evaporation of the sample at T_s

u_{fgf} = specific internal energy of evaporation of the sample at T_f

For a representative process, cooling a 12 gm sample of water from 200 C to 50 C, the first difference on the right is 641.33 kJ/kg while the second is around 1.02 kJ/kg. The influence of the phase change is only .0016 of the overall difference. Consequently, the heat effect on the sample can be considered to be just the change in energy of the saturated liquid. In terms of a heat capacity, the energy change can be quantified as the specific heat of the saturated liquid, often symbolized as " c_s ", as follows:

$$c_{s,ave} = (u_{fs} - u_{ff})/(T_s - T_f)$$

Generation of the saturated liquid specific heat data presented herein required a phased project beginning with a review of the pertinent literature, followed by upgrading and modifying the apparatus. The next steps were the development of a reliable experimental procedure and collecting the experimental data. The final step was the statistical analysis of the data and development of correlations for the average specific heats and the continuous specific heats. Work on the project has been proceeding since the summer of 1987. Preliminary work focused on a review of the pertinent literature. One source of data is especially well known, a dissertation by Lower [1]. Specific heats at 50% concentration from Lower were relied upon by McNeely [2] in the production of enthalpy versus concentration and temperature charts. These charts were prepared using a procedure developed by Haltenberger [3]. This procedure requires specific heats at only one concentration for the range of temperature along with vapor pressure data for the ranges of temperature and concentration. The data produced by McNeely have been fitted to a polynomial representation of the enthalpy by Patterson and Perez-Blanco [4]. Differentiation of these data provide an additional resource for specific heat data for ranges of temperature and concentration. A third alternative source is the previously unpublished data graciously provided by Dr. Uwe Rockenfeller, president of Rocky

Research. An additional source of data is a report by Uemura and Hasaba [5] which includes data subsequently quoted elsewhere [6]. A final data source, by Pennington and Daetwyler [7], has been mentioned, but this data is for such a low temperature as to have no direct implication to the current work.

Our preliminary laboratory work involved rehabilitating the drop calorimeter, adapting it to this experiment, and interfacing to a personal computer (PC) based data acquisition system (DAS). The apparatus was functionally tested and found to be in basically good working condition. The receiver surface was oxidized after years of use so it was plated with a bright nickel alloy to minimize radiation losses. An attempt was made to repair the defective electromechanical printer that was supplied with the calorimeter. This was an effort to provide a redundant, independent data display in addition to the PC-based DAS to be used in production runs. This effort was not successful.

The next effort was to interface the calorimeter to the DAS. The DAS can accommodate calibrated thermocouple inputs as well as millivolt level inputs. A standard thermocouple input is used to monitor the sample temperature while in the furnace chamber. Precision resistance networks were constructed to condition the signal from the receiver thermistor. It was anticipated that initial runs would be made at low concentrations in open air while the heated enclosure necessary to elevate the calorimeter temperature to forestall phase change at high concentrations was under preparation. Consequently, it was necessary to design and build bridge circuits for two receiver temperature ranges, 0 to 40 C and 0 to 100 C.

Some upgrading of the calorimeter was accomplished to improve its performance and reliability. The most critical functional change is in the measurement of the sample temperature while the capsule is in the heater. In the stock design, a thermocouple is imbedded in the heating element outside the furnace tube. This arrangement is unsatisfactory for at least two reasons. Since the thermocouple is permanently installed, it cannot be removed for recalibration. Secondly, since the stock thermocouple is attached to the tube wall, it can not be assured that an accurate sample temperature measurement is being attained. To alleviate these problems, the apparatus was augmented with a calibrated thermocouple that is inserted directly into the capsule. To allow this access, a modified capsule was designed and fabricated. Some other minor improvements were made to insure the integrity of electrical connections, minimize mechanical problems caused by dust shedded from thermal insulation, and eliminate jams caused by interference between the heater tube and the capsule.

Some additional analytical work was also completed on the analysis of the receiver cooling curves and reduction of heat transfer data to energy changes and specific heats. These efforts complicated our initial preparation and allowed for the initiation of the final tasks: development of the experimental procedure and collection of the data in production runs and analysis of the results and production of the property correlations.

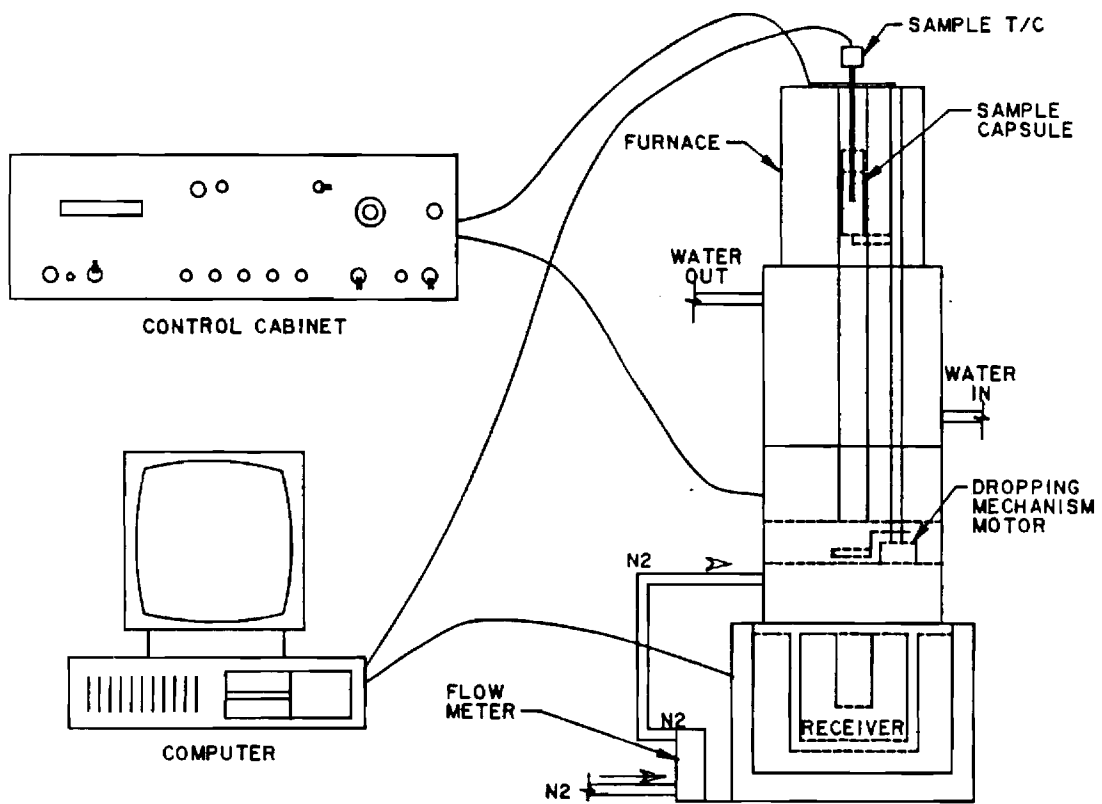


Figure 1. Schematic of Drop Calorimeter

2. EXPERIMENTAL DESIGN:

Experimental Apparatus. A single calorimeter, a Unitherm Model 7100 Drop Calorimeter, was used in all tests. For low concentrations, the calorimeter was operated in open air in the laboratory. For the higher concentrations, 60% and 65% by weight of LiBr, the calorimeter was operated in an elevated temperature enclosure as shown in Figure 2. The addition of the heated enclosure was necessary to prevent a phase transition to a crystalline hydrated complex, $\text{LiBr} \cdot n\text{H}_2\text{O}$, when the concentrated solutions are cooled to near room temperature. The enclosure was also thought desirable to provide a temperature stable environment.

Obtaining an accurate sample temperature is thought to be one of the important challenges in drop calorimetry. In the design of the original equipment, the sample thermocouple is installed outside the tube heater. This location is undesirable because the thermocouple cannot be removed for calibration and because an unknown temperature gradient must exist between the heater and capsule. To enhance this measurement, the capsule was modified to include a removable thermocouple well as shown in Figure 3. The entire construction is stainless steel. The thermowell port also serves as the capsule spout, and the thermowell tube serves as the stopper. A standard two piece, ring and ferrule, compression fitting secures the thermowell tubing. This reliable high pressure fitting can be reused indefinitely providing an inexpensive, leak-free assembly. In addition to the operational advantages, the integral thermowell has two thermometric advantages. In the modified design, the sample thermocouple can readily be removed for calibration and, as importantly, the thermocouple is immersed within the sample providing a highly accurate measure of the sample temperature. The sample thermocouple output from the DAS was calibrated by comparison with a field standard platinum RTD (Leeds and Northrop platinum resistance thermometer, Serial No. 709892) in a Muller bridge. The field standard RTD is traceable to the International Practical Temperature Scale in force when it was manufactured, the IPTS-48, and has been adjusted to correspond to IPTS-68, the current standard. Note that the calibration procedure used the production DAS in the calibration step. This allowed for the entire sample temperature measurement subsystem, including the thermocouple and its reference temperature compensation circuit as well as the instrumentation amplifier and ADC in the DAS, to be calibrated simultaneously. This inclusive calibration, while somewhat more demanding and inflexible, should allow for improved accuracy as calibration compensation is provided for all the critical measuring components and not just the temperature probe alone.

The other critical temperature measurement is the receiver temperature. For the present purposes, it is most important that the receiver temperature probe produce a linear response over the range of expected use, around 20 C to 30 C in open air or around 50 C to 60 C in the enclosure. A commercially packaged thermistor pair in a parallel arrangement with compensating resistors, similar to the manufacturers original equipment, was selected for the receiver temperature sensor. Semiconducting thermistors exhibit decreasing electrical resistance with increasing temperature. This resistance change can be measured as a voltage change in a suitable auxiliary circuit. The parallel, compensated arrangement of the thermistors produces a very nearly linear temperature

dependence in the overall resistance. This linear response is important for drop calorimetry. Circuits for both temperature ranges are similar. In the higher temperature device, the resistance is converted into a voltage signal in an external voltage divider with a nominal sensitivity of 6.7 mV/C°. The voltage divider was further incorporated into a Wheatstone bridge to allow the establishment of an arbitrary zero output voltage near 0 C. The completed circuit and DAS were calibrated by comparing computer output of the voltage with the field standard platinum RTD with the resulting relation:

$$T_r = 148.5964 \text{ (C/volt)} V_{\text{DAS}} + 5.781795 \text{ C}$$

This response allows service over a range of 5.8 C (at $V_{\text{DAS}} = 0$) to 80 C (at $V_{\text{DAS}} = 500$ mV) since the analog to digital converter will be used with a span of 0 to 500 mV. The temperature range is more than adequate in this or similar applications. The calibrated sensitivity of 6.73 mV/C° provides a resolution of .001 C°/count in the receiver temperature with the 16 bit ADC in use here. This is about .05% of the expected temperature change in a typical drop and represents the limit of accuracy in the system due to resolution. In the room temperature device, a sensitivity of 9.92 mV/C° was obtained for a similar resolution of .0008 C°/count and an operating temperature range of 0 to 50 C.

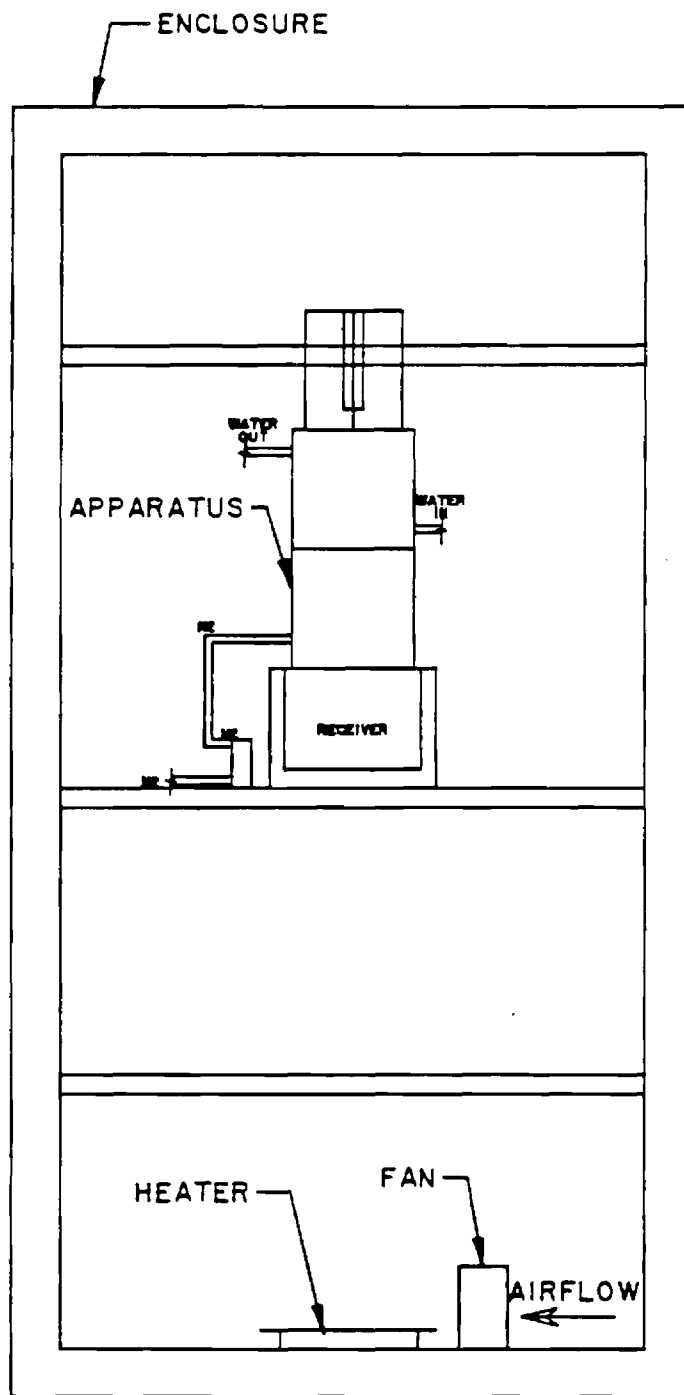
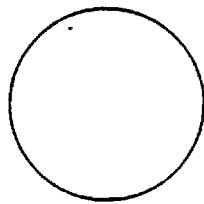
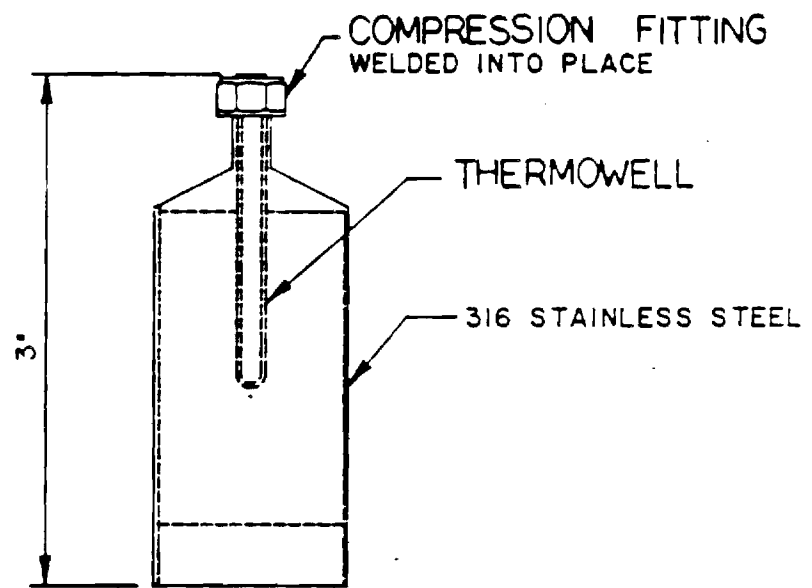


Figure 2. Drop Calorimeter in Temperature Controlled Enclosure



BOTTOM VIEW

Figure 3. Sample Capsule with Integral Thermowell

Experimental Procedure. The most crucial aspects of the experimental procedure are loading an accurate and appropriate mass of sample in the capsule and establishing stable sample and receiver temperatures before a drop and maintaining a stable environmental temperature during a drop.

The sample volume has been determined gravimetrically, using water, to be around 14.8 ml. A sample mass should be installed such that after thermal expansion a small ullage space remains as it is a practical impossibility to seal the capsule against the expansion of a compressed liquid. Typically, a volume of around 12 to 13 ml is installed. A minimal ullage volume is preferable primarily to maximize the mass of the sample and thereby increase the temperature response of the receiver and secondarily to reduce the effect of vaporization. The capsule is accurately weighed before and after installation of the sample to accurately determine the mass of the sample and to monitor against the possibility of leaks. No leaks have been observed in practice.

Establishing stable temperatures begins with the initial preparation for a drop with the receiver lowered after a previous drop. It is first necessary to return the receiver to near its environmental temperature whether this is room temperature or, preferably, the enclosure temperature. In the enclosure, it was found desirable to ventilate the exposed receiver with a small fan. Usually it was convenient to ventilate the receiver for several hours to allow complete cooling. During this cooling process, it is desirable to proceed with installing the sample capsule in the tube heater and preheating the sample. If the sample is preheated while the receiver is being ventilated, the heater will operate only intermittently later after the receiver has been raised and even later after the sample drop. Excessive operation of the sample heater later is likely to disturb the temperatures in the receiver or in the enclosure.

After the receiver is cooled and the sample preheated, the receiver is raised to its operational position where it is ready to accept the dropped capsule. Heat leak from the heater to the receiver cannot be eliminated by the insulation, water jacket, and cover gas so it is typical for the temperature of a properly cooled receiver to rise slightly subsequently to raising the receiver. In contrast, a receiver improperly left too warm from a previous drop will continue to cool even after being raised. It is critical to minimize any temperature drift prior to a drop. Otherwise the results of the drop will be impaired. Typically, the receiver is left in the raised position for at least 90 minutes to reestablish a stable receiver temperature. Prior to a drop, the receiver temperature should be closely monitored. Usually, the receiver temperature is studied for 10 minutes before the drop to verify a stable condition.

Once stable temperatures in the heated sample and receiver have been established, it is appropriate to drop the sample into the receiver. The drop mechanism can then be activated. The drop pin and insulated shutter move to allow the capsule to enter the receiver and then quickly return to their original position to allow the insulated shutter to continue to prevent excessive heat leak from the furnace tube to the receiver.

Figure 16.

Rocky Research Data and its Correlation

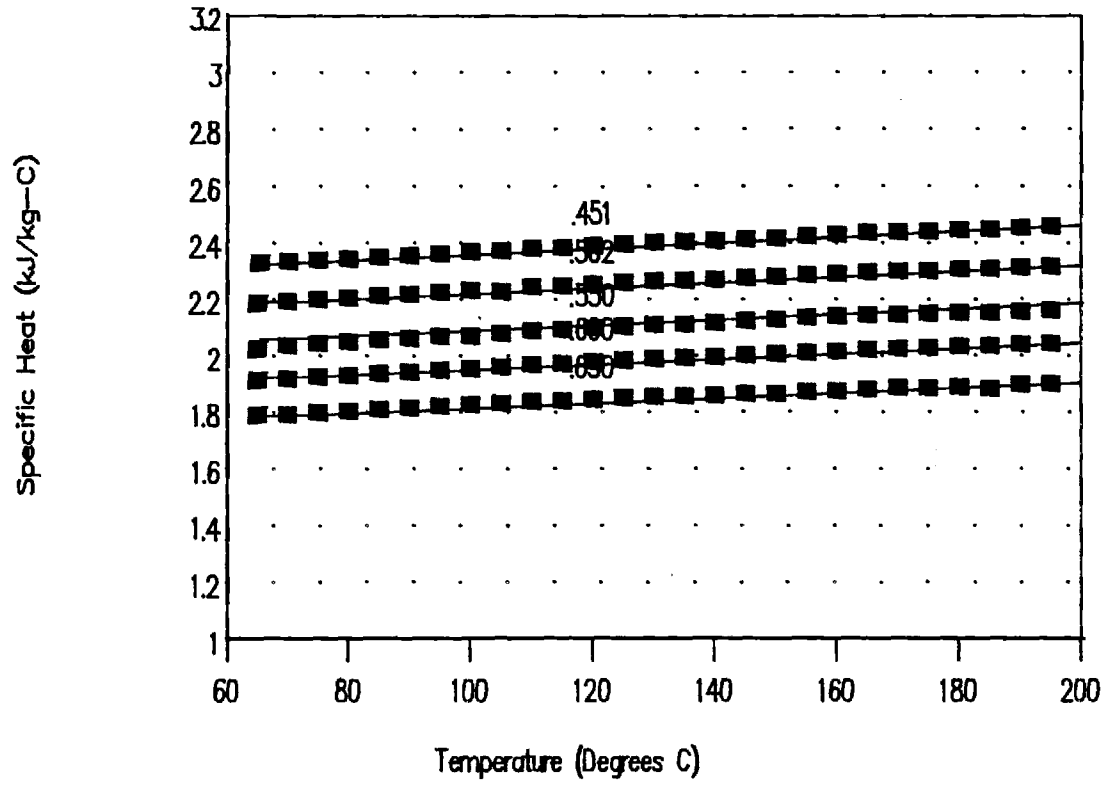


Figure 17: Rocky Research Data Compared
with Patterson and Perez-Blanco

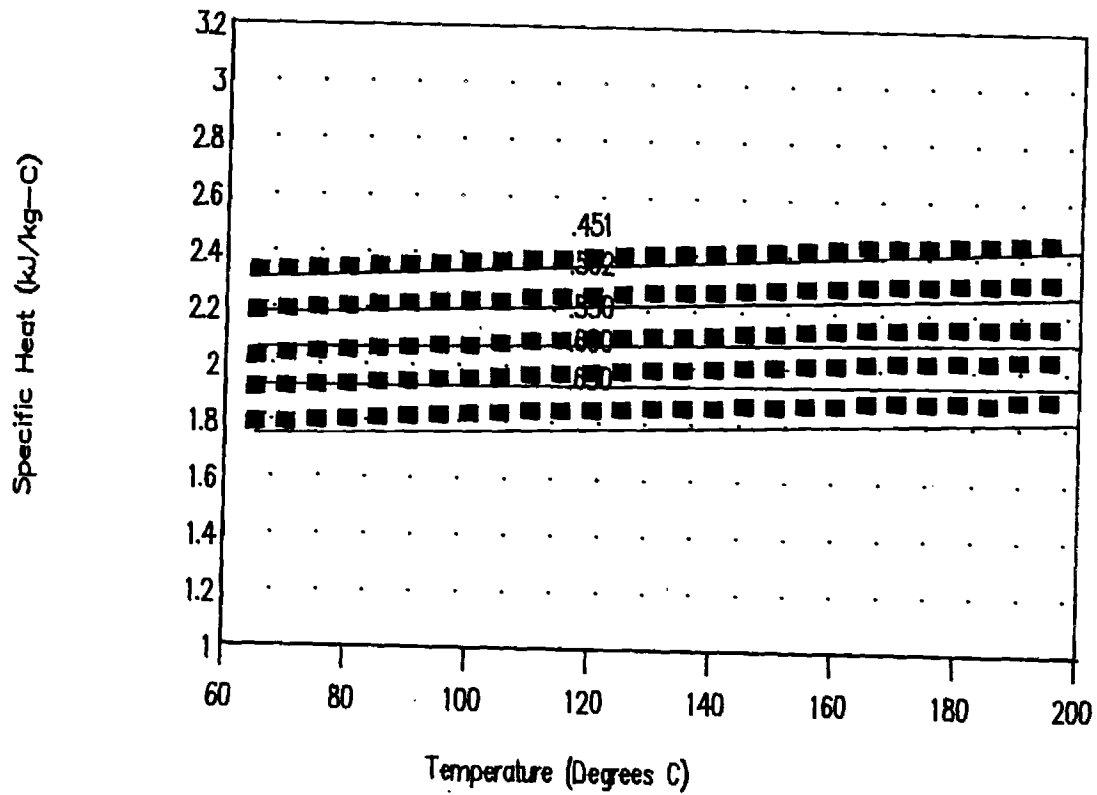


Figure 18: Rocky Research Data
and GIT Linear-Linear Correlation

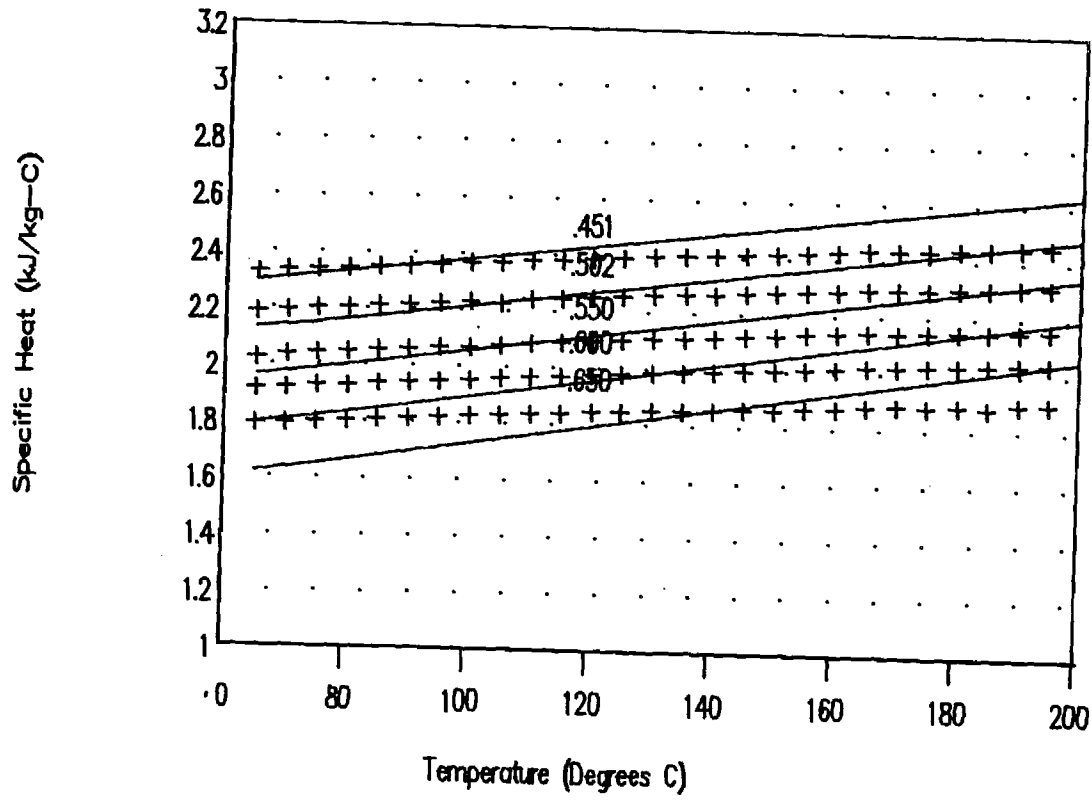


Fig. 19: Rocky Research data and GIT

linear-linear error bands

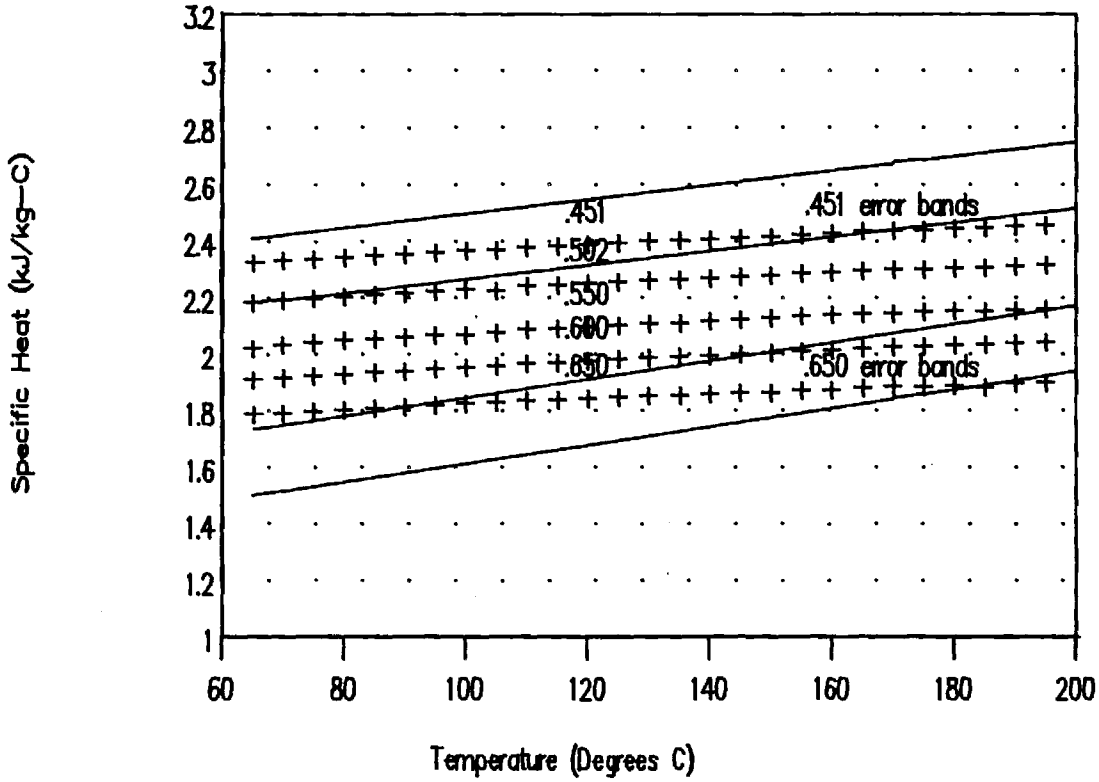


Table 9

CORRELATION RESULTS FROM DATA OF OTHERS

Coefficient	Regression of Rocky Research Data on Model of Form: Linear-Linear Quadratic-Linear		Differentiation of Enthalpy Fit by Patterson and Perez-Blanco	
	a_0	3.462023	3.818560	4.124891
a_1	-2.679895	-3.996355	-7.643903	E-02
a_2		1.195485	2.589577	E-03
a_3			-9.500522	E-05
a_4			1.708026	E-06
a_5			-1.102363	E-08
b_0	.0013499	.0013499	0.0011487386	
b_1	-.000655	-.000655	0.00011741842	
b_2			-1.4750638	E-05
b_3			6.555184	E-07
b_4			-1.2124608	E-08
b_5			7.803794	E-11
Standard Error of Estimate	.0096	.0081		
Coefficient of Correlation	.9977	.9984		

6. CONCLUSIONS:

Two data bases, the DSC measurements from Rocky Research and specific heats obtained by differentiation of enthalpy correlations prepared by Patterson and Perez-Blanco, are in agreement with the results of the current investigation. The data of Uemura and Hasaba are clearly lower than the results of the three mutually consistent data bases. The data of Lower are only marginally supported by the three later data bases, even though one of them, the enthalpy correlation, incorporated Lower's data in its preparation. The Rocky Research data are supported by excellent agreement with the results from the Patterson and Perez-Blanco correlation and are confirmed by statistically significant agreement with the results of the current investigation. Since the Rocky Research data are purely empirical, they should be preferred over the numerical results.

It may be possible to make a finer distinction among the three preferred data bases by improving the current measurements. Two possibilities exist. Initially the temperature range of the measurements should be extended, at least for the higher concentrations where the vapor pressure will be low enough for safe operation with the existing calorimeter capsule. This will not only provide additional data points but also relieve the leverage of possible outliers at lower temperatures which can distort the temperature dependence. Additionally, the data base should be scanned for outliers and suspected outliers should be replaced with measurements from carefully conducted measurements. Outliers are especially likely at higher concentrations where the lower specific heats magnify the influence of inadequate procedures or environmental influences.

At present, additional measurements are in progress. These measurements may improve the confidence in the present data set; however, until these additional measurements are successful the Rocky Research data which demonstrate excellent internal consistency as well as being confirmed by both alternative sets is preferred.

7. ACKNOWLEDGEMENTS

The contributions of Dr. Uwe Rockenfeller both for his guidance and encouragement as the technical monitor of this project and for providing the previously unpublished specific heat data is gratefully acknowledged. The assistance of Professor K. E. Herold for helpful discussions and his assistance with the literature review is also gratefully acknowledged.

7. REFERENCES:

1. Lower, H., "Thermodynamische und physikalische Eigenschaften der wässrigen Lithiumbromid-Lösung", Dissertation, Technischen Hochschule Karlsruhe, Karlsruhe, Germany, 1960.
2. McNeely, L. A., "Thermodynamic Properties of Aqueous Solutions of Lithium Bromide", *ASHRAE Transactions*, Vol. 85, Part 2, pp. 413-434, 1979.
3. Haltenberger, W., "Enthalpy-Concentration Charts from Vapor Pressure Data", *Industrial and Engineering Chemistry*, pp. 783-786, June, 1939.
4. Patterson, M. R. and H. Perez-Blanco, "Numerical Fits of the Properties of Lithium-Bromide Water Solutions", *ASHRAE Transactions*, Vol. 94, Part 2, 1988.
5. Uemura, T. and S. Hasaba, "Studies on the Lithium Bromide-Water Absorption Refrigerating Machine", Technical Report, Kansai University, Vol. 6, pp. 31-55, 1964.
6. "Technical Data: Lithium Bromide", Commercial Brochure, Foote Mineral Company, Exton, PA.
7. Pennington, W. A. and C. Daetwyler, "Heat Capacity and Heat of Dilution of some Concentrated Water Solutions of LiBr at 25 C", Carrier Confidential Report, Project R1011-S1 Report No. 6, Carrier Corporation, Syracuse NY, 18 April 1952.
8. "Operating Manual, Unitherm Model 7100 Calorimeter", Anter Laboratories, 15 December 1976.
9. Lee, M. C. and R. N. Maddox, "Measuring Heat Capacity Using the Unitherm Model 7100 Drop Calorimeter", Liquid Heat Capacity Report No. 6, Fluid Properties Research Institute, January 1979.
10. Moran, J. P., "Specific Heats of Aqueous Lithium Bromide Solutions", M. S. Thesis, The George W. Woodruff School of Mechanical Engineering, Georgia Institute of Technology, August 1988.
11. Pan, W. P. and R. N. Maddox, "Improved Technique for Heat Capacity Measurements using the Unitherm Model 7100 Drop Calorimeter", Liquid Heat Capacity Report No. 7, Fluid Properties Research Institute, August 1979.
12. McClintock, R. B. and G. J. Silvestri, "Some Improved Steam Property Calculation Procedures", *Journal of Engineering for Power*, American Society of Mechanical Engineers, pp. 123-134, April 1970.
13. Rockenfeller, U., "Laboratory Results: Solution = LiBr-H₂O, Properties = P-T-x, Heat Capacity", Unpublished Data, Rocky Research, Inc, Boulder City, NV, 1987.

8. APPENDIX:

For completeness the following graphs are appended which illustrate the scatter plots of raw data along with correlation lines and error bands for the quadratic-quadratic and quadratic-linear models:

Figure A.1: Specific Heat Data for 43.95% Solution of LiBr by Weight with Corresponding Quadratic-Quadratic Correlation Model.

Figure A.2: Specific Heat Data for 50.595% Solution of LiBr by Weight with Corresponding Quadratic-Quadratic Correlation Model.

Figure A.3: Specific Heat Data for 54.10% Solution of LiBr by Weight with Corresponding Quadratic-Quadratic Correlation Model.

Figure A.4: Specific Heat Data for 59.48% Solution of LiBr by Weight with Corresponding Quadratic-Quadratic Correlation Model.

Figure A.5: Specific Heat Data for 64.83% Solution of LiBr by Weight with Corresponding Quadratic-Quadratic Correlation Model.

Figure A.6: Specific Heat Data for 43.95% Solution of LiBr by Weight with Corresponding Quadratic-Linear Correlation Model.

Figure A.7: Specific Heat Data for 50.595% Solution of LiBr by Weight with Corresponding Quadratic-Linear Correlation Model.

Figure A.8: Specific Heat Data for 54.10% Solution of LiBr by Weight with Corresponding Quadratic-Linear Correlation Model.

Figure A.9: Specific Heat Data for 59.48% Solution of LiBr by Weight with Corresponding Quadratic-Linear Correlation Model.

Figure A.10: Specific Heat Data for 64.83% Solution of LiBr by Weight with Corresponding Quadratic-Linear Correlation Model.

Figure A.1: 43.95% LiBr by weight

Quadratic-Quadratic Correlation

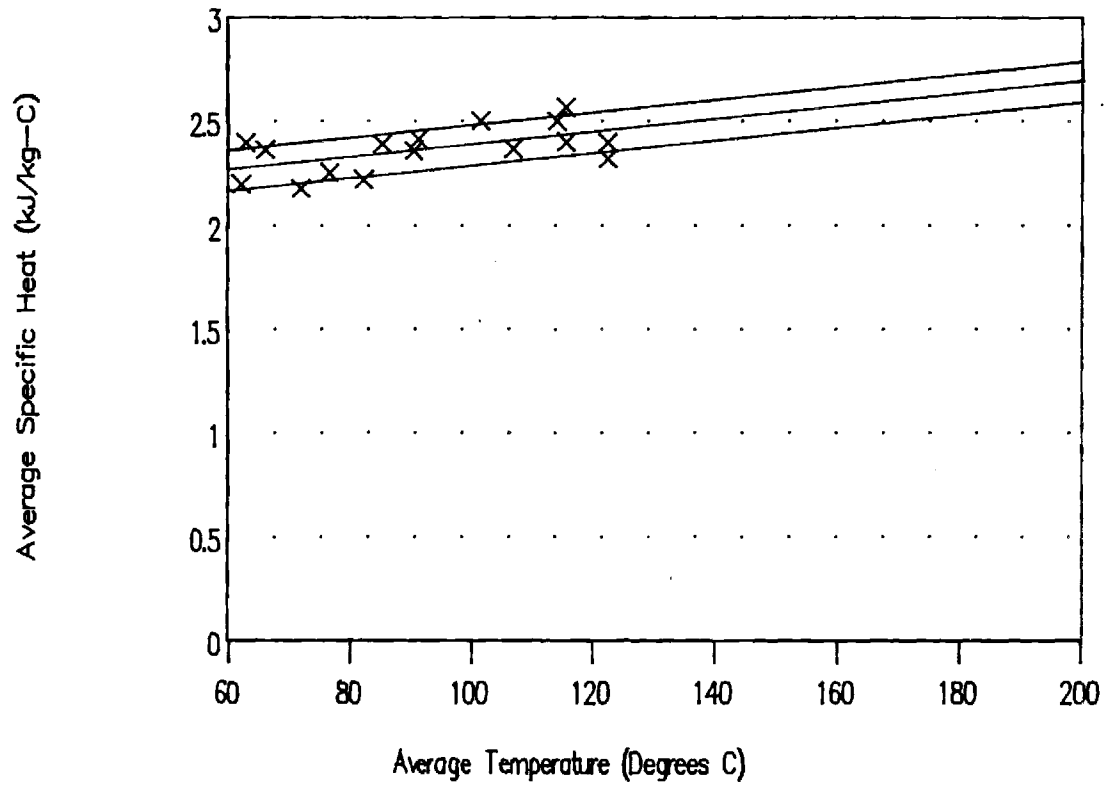
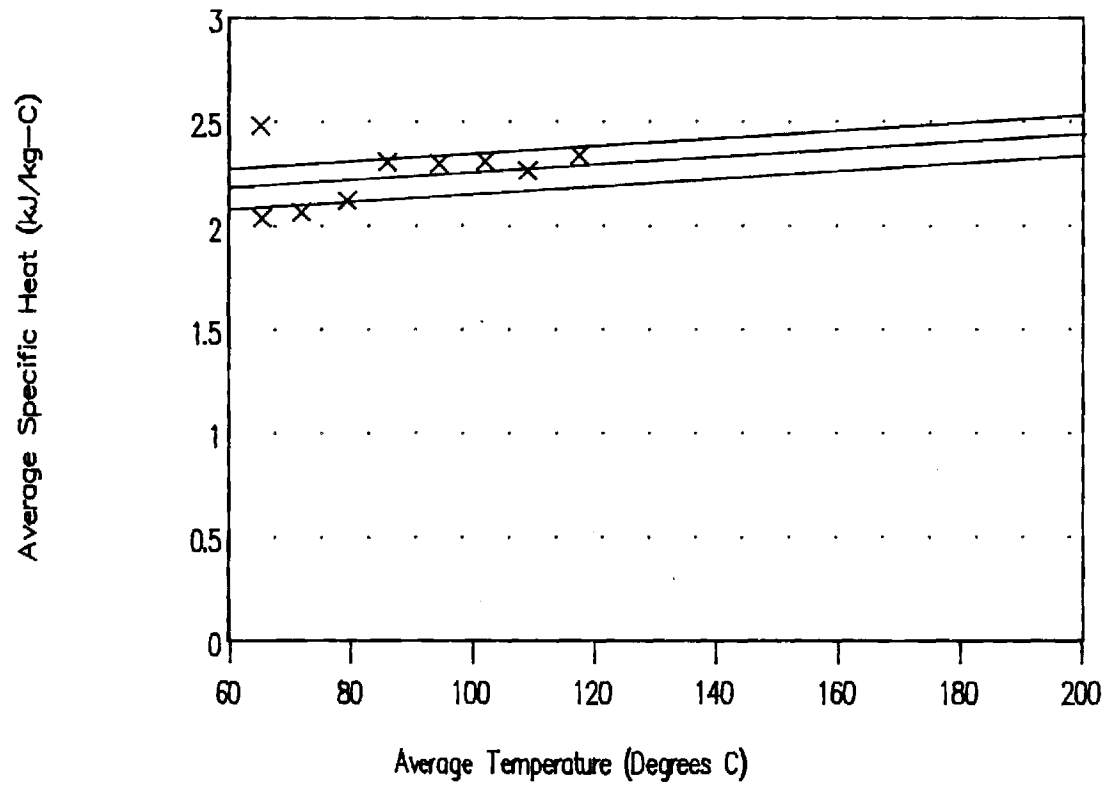


Figure A.2: 50.59% LiBr by weight

Quadratic-Quadratic Correlation



After the drop, the receiver temperature is monitored for several hours until the receiver has passed through its temperature maximum and is well along its cooling curve. For reference, the DAS continues to monitor the enclosure and room temperatures. After the cooling period, the temperature data is retrieved for further analysis.

3. DATA REDUCTION AND ANALYSIS:

Data reduction and analysis involves two steps, cooling curve analysis to determine the ultimate heat transfer from the capsule to the receiver followed by interpretation of the heat interaction in terms of calibration data for the capsule and receiver.

The cooling curve analysis results in an estimate of the ultimate temperature which would be reached by the receiver in the absence of heat loss. With this correction, the receiver, capsule, and sample constitute the adiabatic combined system envisaged as the principle of operation of the drop calorimeter. The correction is illustrated in Figure 4. The numerical procedure is as follows:

1. Identify the time, t_{max} , at which the maximum temperature is reached. For accuracy, this is done by fitting a smooth quadratic curve through the 10 data points nearest the peak and solving for the peak time and temperature analytically.

2. Next, identify the slope of the temperature versus time curve, also called the temperature drift, at some convenient instant. This slope should be evaluated well after the maximum so that the temperature drift due to heat loss from the receiver to the ambient is dominant and its trend is well established. A convenient time is $2 \cdot t_{max}$. Numerically this is done by fitting a straight line through the 11 data centering on $2 \cdot t_{max}$.

3. The temperature drift is next extrapolated backwards to a unique time after the drop at which time the extrapolated temperature is predicted to equal the ultimate receiver temperature that would have been achieved in a perfectly adiabatic process. The time suggested, [8] and [9], for this evaluation corresponds to the time at which the receiver has attained 60% of its observed maximum value. Analysis of a thermal resistance network containing two lumped capacitances presented in [10] confirms this suggestion for the parameters of the drop calorimeter used in these measurements.

4. The temperature computed from the extrapolated drift, T_p , is used as the final temperature for the capsule and sample as well as the receiver. Note that this correction has the advantage of being strictly based on physical observations and current conditions, such as the temperature difference between the receiver and ambient, and should provide at least a first order correction for any casual environmental influences.

The cooling curve analysis also identifies the initial sample temperature, T_s , and the initial receiver temperature, T_{ri} . In later modifications, a linear fit was applied to minimize the effect of any initial drift or irregularity in these two measurements. The heat interaction is interpreted in terms of heat capacities from the following result of the energy balance:

$$-\Delta U_{cs} = (C_c + C_{sam})(T_s - T_f) = \Delta U_r = C_r(T_f - T_{ri})$$

Where:

C_c = the average heat capacity, $m \cdot c_{ave}$, of the capsule
 C_{sam} = the average heat capacity of the sample
 C_r = the average heat capacity of the receiver

Then solving for the average heat capacity of the sample:

$$C_{sam} = C_r(T_f - T_{ri}) / (T_s - T_f) - C_c$$

Upon introducing the experimentally convenient ratio, $K_{cr} = C_c / C_r$, which is the ratio of the average heat capacity of the capsule to that of the receiver one has:

$$C_{sam} = C_r(T_f - T_{ri}) / (T_s - T_f) - C_r K_{cr}$$

The specific heat of the saturated liquid sample can then be determined from the mass of the sample and its average heat capacity:

$$c_{s,ave} = C_{sam} / m_s$$

Clearly, the specific heat determination requires the two calibration values, C_r and K_{cr} . The values are determined as functions of the experimental conditions to further enhance accuracy in accord with the procedure suggested in [11]. The heat capacity ratio, K_{cr} , is determined by a series of empty capsule calibration drops. For a zero mass sample, the combined energy balance gives:

$$K_{cr} = C_c / C_r = (T_f - T_{ri}) / (T_s - T_f)$$

The results for a range of furnace temperatures, T_s , were correlated against the sample temperatures with the following results:

For the open air system:

$$K_{cr} = .0000088 T_s + .011551$$

For the temperature controlled enclosure:

$$K_{cr} = .0000085 T_s + .01149$$

The slight temperature dependency of this ratio is not necessarily due to thermal property differences alone but can also account for heat leaks from the furnace to the receiver during drops, when the insulated shutter is momentarily open, and any (much smaller) heat leak following the drop.

The heat capacity of the receiver can be calibrated by either a "relative" or an "absolute" procedure. An absolute calibration would rely on electric heating of the receiver and the subsequent temperature response. While the electric energy input can obviously be determined with great precision, the success of an absolute calibration is entirely dependent on a full understanding and characterization of the systematic behavior of the calorimeter. Accounting for systematic errors in the form of heat leaks between the

receiver and the ambient and the heater is enormously challenging; consequently, a relative calibration was adopted. In a relative calibration, the response of the receiver to a reference sample is measured. Two stable and well characterized materials were used as the reference substances, alumina and water. According to the energy balance, the receiver heat capacity for a calibration drop when the reference sample has a specific energy change of $u_{ref}(T_s)$ to $u_{ref}(T_f)$ is given by:

$$C_r = m_s [u_{ref}(T_s) - u_{ref}(T_f)] / [(T_f - T_{ri}) - K_{cr}(T_s - T_f)]$$

In accordance with the suggested procedure, C_r in units of kJ/K, was correlated against the overall temperature change of the receiver with the following results:

For the open air system:

$$C_r = 4.321664 + .052339 \Delta T_r$$

For the system in temperature controlled enclosure:

$$C_r = 4.312143 + .019233 \Delta T_r$$

The variation of apparent heat capacity of the receiver as explained by the receiver temperature change is unlikely to bear much relation to thermodynamic property changes since the receiver temperature rise is only a couple of degrees at most. More likely, this effect comes from a somewhat enhanced heat leak to the environment in higher temperature drops as well as from residual variation in the leak from the heater not accounted for by the K_{cs} correlation.

The calibration procedure described above represents one of the obstacles to rapid specific heat evaluations using the drop calorimeter since the entire calibration procedure for both K_{cr} and C_r should be repeated if the capsule or any other critical component such as the temperature sensors or their signal conditioning and data conversion circuits must be changed or significantly altered. In this investigation the calorimeter environment was changed once along with the receiver temperature circuit. This necessary change doubled the effort required for calibration. Obtaining stable initial conditions and collecting data for the extensive cooling curve analysis present another drawback. Several hours of phased cooling of the exposed receiver and an hour or two or more of temperature stabilization of the raised receiver must precede every drop, and several hours of monitored receiver response must follow the drop. Consequently, not even a single drop can be completed in an ordinary working day, and it takes considerable coordination to arrange for a drop to be prepared during the day and completed overnight. The resulting data rate, especially if allowing for interrupted data and spoiled drops, is not very high. An advantage is, however, that the physical principles of the device are simple and well founded in thermodynamic fundamentals. Another advantage is that an average specific heat is obtained which represents the behavior of the sample over a broad range, e.g. 100 Celsius degrees or more, on each drop.

The experimental data are presented in Tables 1 through 5 which present the measured average specific heat data, at specified concentrations near 45%, 50%, 55%,

60% and 65%. Also tabulated are the initial and final sample temperatures T_s and T_f and the average temperature for the drop, $T_{ave} = (T_s + T_f)/2$.

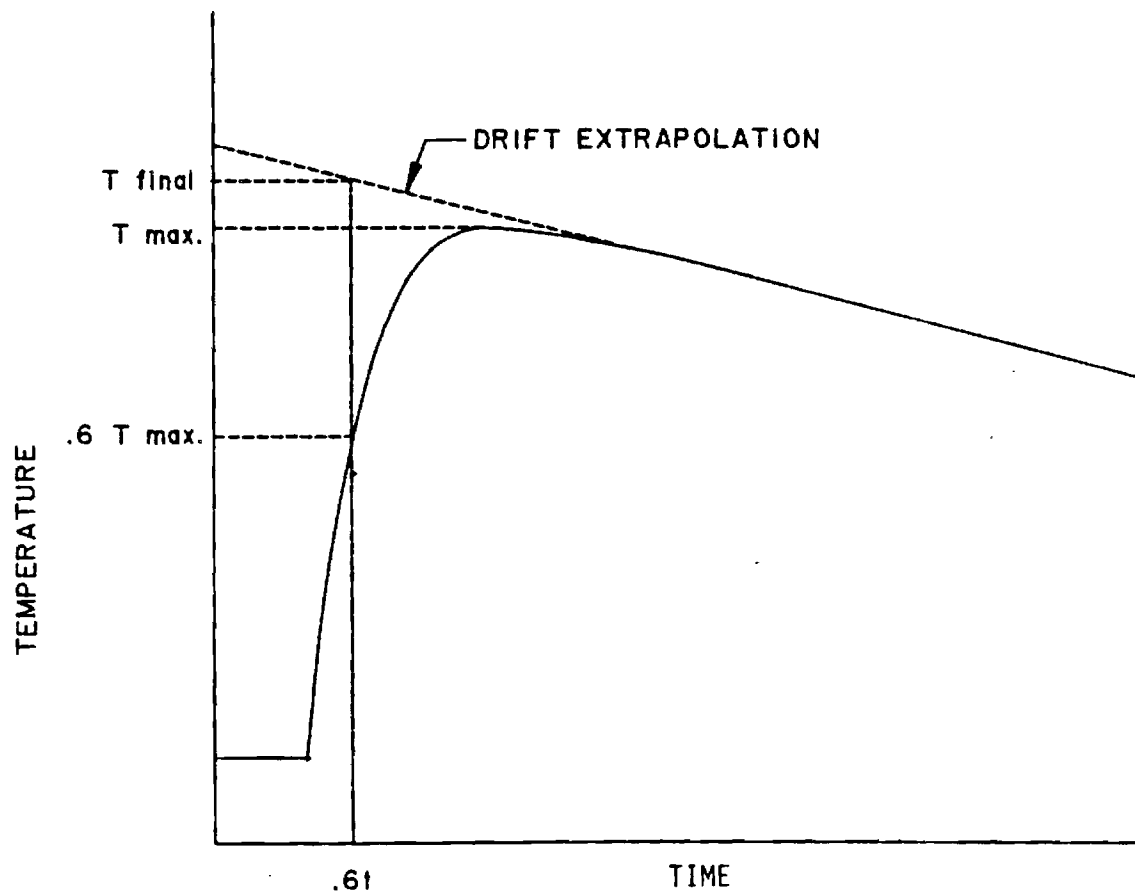


Figure 4. Graphical Representation of Cooling Curve Analysis

Table 1.
Average Specific Heat Results
for Concentrations near 45%

Mass Fraction	Average Temperature	Average Specific Heat	Initial Temperature	Final Temperature
0.4395	61.9125	2.1924	23.741	100.084
0.4395	62.566	2.3932	25.193	99.939
0.4395	81.747	2.2153	25.345	138.149
0.4395	89.781	2.3525	26.454	153.108
0.4395	90.456	2.4056	26.627	154.285
0.4395	100.5785	2.4956	26.614	174.543
0.4395	114.605	2.3915	28.039	201.171
0.4395	105.7915	2.3589	28.402	183.181
0.4395	113.103	2.4931	25.701	200.505
0.4395	65.237	2.3546	25.603	104.871
0.4395	75.818	2.2437	26.324	125.312
0.4395	71.082	2.1682	25.461	116.703
0.4395	114.5565	2.5604	29.214	199.899
0.4395	84.36055	2.3824	49.0448	119.6763
0.4395	121.4709	2.3117	53.0417	189.9001
0.4395	121.4293	2.39	53.1895	189.669

Table 2.
Average Specific Heat Results
for Concentrations near 50%

Mass Fraction	Average Temperature	Average Specific Heat	Initial Temperature	Final Temperature
0.5059	64.9115	2.4772	25.309	104.514
0.5059	85.564	2.3021	27.102	144.026
0.5059	108.394	2.2599	28.781	188.007
0.5059	71.2325	2.059	26.785	115.68
0.5059	93.616	2.2912	28.739	158.493
0.5059	116.522	2.3296	29.971	203.073
0.5059	78.5505	2.113	27.687	129.414
0.5059	101.093	2.3024	28.666	173.52
0.5059	64.6	2.029	23.094	106.106

Table 3.
Average Specific Heat Results
for Concentrations near 55%

Mass Fraction	Average Temperature	Average Specific Heat	Initial Temperature	Final Temperature
0.541	68.3	2.0767	20.92	115.68
0.541	98.0085	1.9805	23.51	172.507
0.541	92.3355	2.1271	26.043	158.628
0.541	76.532	2.0097	23.988	129.076
0.541	87.2585	2.1565	25.443	149.074
0.541	114.661	2.167	27.089	202.233
0.541	64.459	1.949	22.281	106.637
0.541	71.3375	2.1536	22.449	120.226
0.541	105.565	2.2025	23.905	187.225
0.541	102.4675	2.0443	23.404	181.531

Table 4.
Average Specific Heat Results
for Concentrations near 60%

Mass Fraction	Average Temperature	Average Specific Heat	Initial Temperature	Final Temperature
0.5948	88.001	1.8122	57.88	118.122
0.5948	95.21	1.9684	58.381	132.039
0.5948	103.0425	1.9254	59.318	146.767
0.5948	109.453	2.1008	61.387	157.519
0.5948	110.8975	2.0566	60.638	161.157
0.5948	117.207	1.9555	59.784	174.63
0.5948	118.488	2.0738	61.439	175.537
0.5948	126.6605	2.0113	63.731	189.59
0.5948	132.867	2.0438	62.42	203.314
0.5948	133.33	1.8606	62.593	204.067

Table 5.
Average Specific Heat Results
for Concentrations near 65%

Mass Fraction	Average Temperature	Average Specific Heat	Initial Temperature	Final Temperature
0.6483	110.465	1.8476	60.796	160.134
0.6483	133.0425	1.7396	62.231	203.854
0.6483	100.1705	1.6356	59.307	141.034
0.6483	114.8285	1.7726	59.708	169.949
0.6483	127.694	1.7973	61.996	193.392
0.6483	104.864	1.6391	59.178	150.55
0.6483	120.3965	1.815	61.057	179.736
0.6483	87.973	1.4063	57.891	118.055
0.6483	126.0605	1.9652	62.222	189.899
0.6483	95.731	1.5161	59.539	131.923

4. CORRELATION OF DATA:

Inspection of the available data indicates that a polynomial temperature dependence constitutes an adequate model. For this behavior, the general dependence of the specific heat on temperature, T , is of the form:

$$c_s = a + b \cdot T$$
for a linear dependence on temperature, and

$$c_s = a + b \cdot T + c \cdot T^2$$
for a quadratic dependence.

In either case the coefficient functions can be polynomials in the salt concentration such as the following general formula:

$$a = \sum a_k \cdot x^k, \text{ with } k = 1 \text{ to } n.$$

In the current experimental work, statistically valid values for n were limited to 1 or 2 while in some numerical work quoted below n is as large as 5. As discussed below, no statistical support was found for a quadratic temperature dependence compared with the linear relationship; consequently, consideration of the linear temperature functions will be emphasized. In the preceding relationships, the coefficient functions, a and b and c , can be functions of the concentration. Herein, the concentration, x , will be expressed in terms of mass fraction of the salt (i.e. $0 < x < 1.0$). Both linear and quadratic functions of concentration, and combinations, have been investigated. Expanding the coefficient functions, the relationships that are linear in temperature can have one of the following functional forms:

A linear-linear (in x) model:

$$c_s = (a_0 + a_1 x) + (b_0 + b_1 x)T$$

A quadratic-linear model:

$$c_s = (a_0 + a_1 x + a_2 x^2) + (b_0 + b_1 x)T$$

A quadratic-quadratic model:

$$c_s = (a_0 + a_1 x + a_2 x^2) + (b_0 + b_1 x + b_2 x^2)T$$

For quantitative comparison, the following model quadratic in temperature was also considered:

T-Quadratic model:

$$c_s = (a_0 + a_1 x + a_2 x^2) + (b_0 + b_1 x + b_2 x^2)T + c_0 T^2$$

Regression calculation were performed on the four preceding models with the following results:

Table 6.

CORRELATION RESULTS FROM DROP CALORIMETER DATA

Model	Coefficient of Correlation	Statistical Significance	Standard Error of Estimate
Linear-Linear	.808409	< < .0005	.1166 (ca. 5.8%)
Quadratic-Linear	.848651	ca. .0005	.1047 (ca. 5.2%)
Quadratic-Quadratic	.859522	ca. .025	.1019 (ca. 5.1%)
T-Quadratic	.867427	> .05	.1000 (ca. 5.0%)

In the preceding table, salient statistical results are presented for each model. The first statistical result is the Coefficient of Correlation which is the ratio of the variation explained by the model to the total variation in the data set. The balance of the variation is called the residual variation. The residual variation is due to both systematic errors and noise in the data as well as any inadequacy in the model. Any augmentation of the model is sure to decrease the residual variation, but continued augmentation of the model is not justifiable. According to the preceding results, the model with both coefficients quadratic in the concentration is the most inclusive model that remains significant at the probability criterion of .05 or lower. All of the models that are linear in temperature remain statistically significant while the model quadratic in temperature is not significant. Basically, this result implies that the improvement in the Coefficient of Correlation obtained by expanding the model to include the quadratic temperature term is no more than a random improvement. This model decreases the residual variation but probably only by reducing the random component not because the model really better suits the data set. Therefore, it is the quadratic-quadratic form that is the most likely model in a purely statistical sense. For any of the models with linear dependence on temperature such as the first three models, the average specific heat has the following especially simple form:

$$c_{s,ave} = a + b(T_s + T_f)/2$$

or using the quadratic-quadratic model as an example,

$$c_{s,ave} = (a_0 + a_1 x + a_2 x^2) + (b_0 + b_1 x + b_2 x^2)T_{ave}$$

This simple dependence conveniently allows even average specific heat data to be plotted as a function of the average temperature on a two dimensional graph. Figures 5, 6, and 7 illustrate the correlation lines superimposed on the entire data set. Note that while the quadratic-quadratic model has the best statistics, it is unreasonable physically because the concentration lines cross unrealistically. The quadratic-linear model also appears to be marginally realistic as some of its constant concentration lines nearly cross. The

Figure 5.

Linear-Linear Model with Data

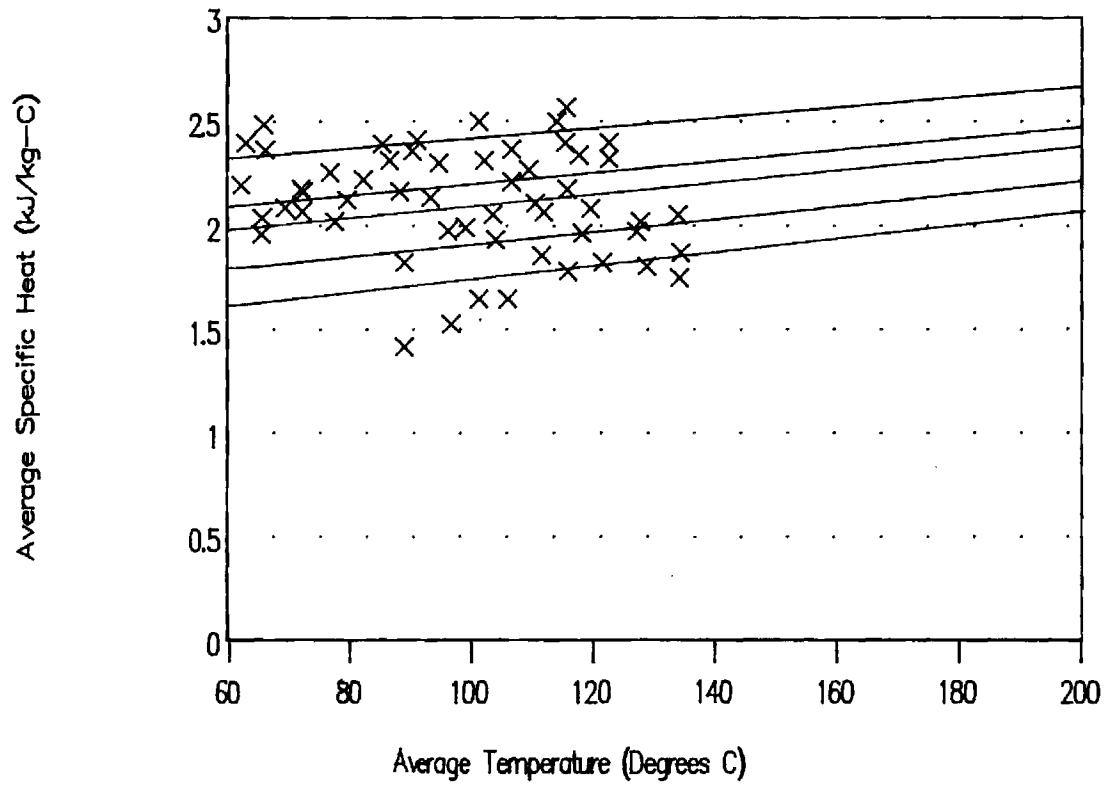


Figure 6.

Quadratic-Linear Model with Data

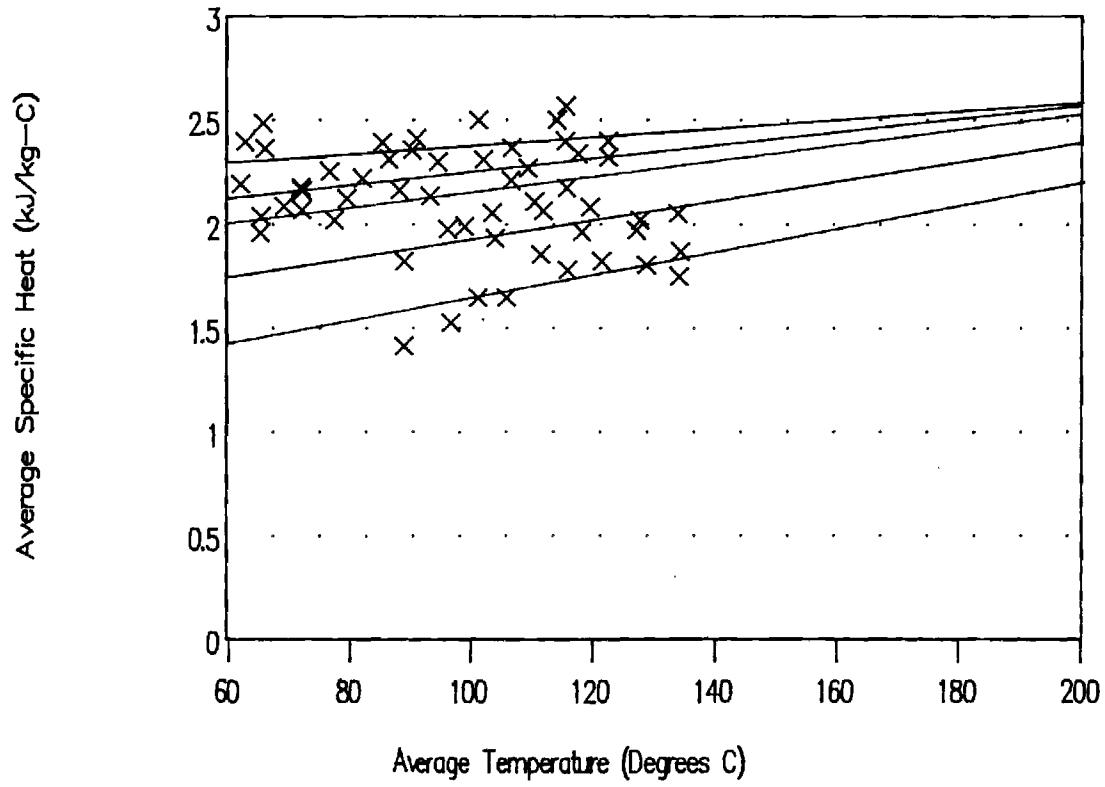
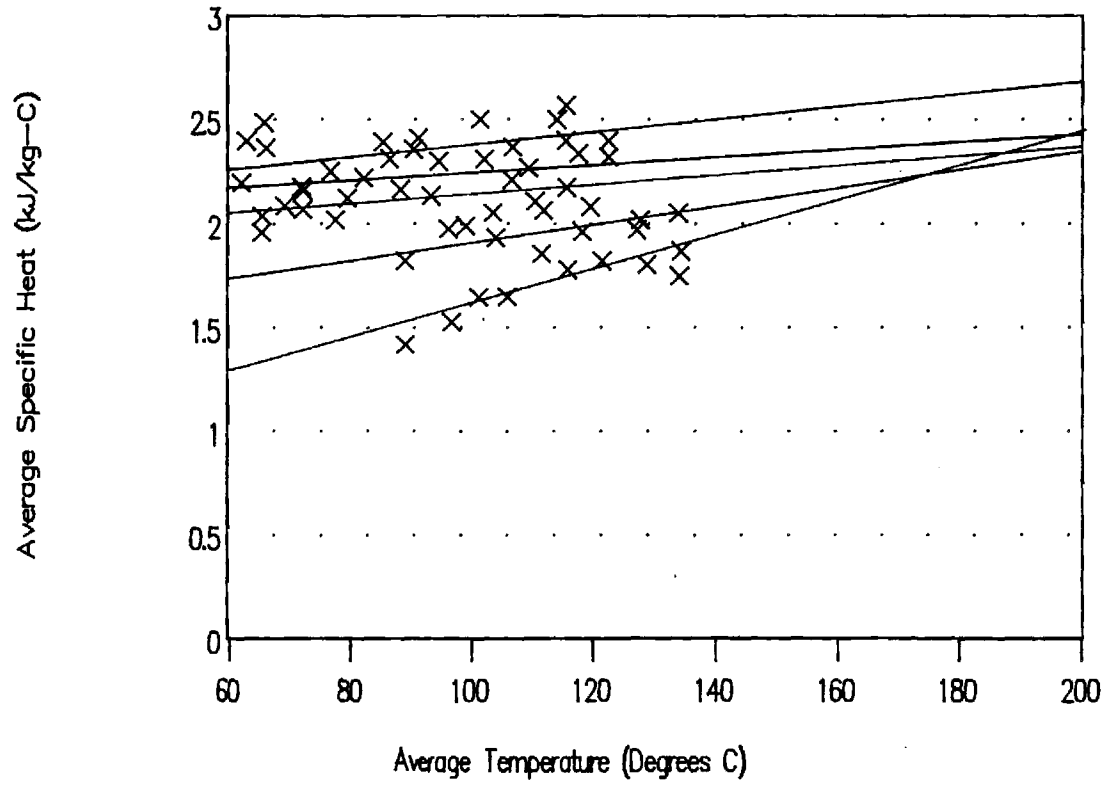


Figure 7.

Quadratic-Quadratic Model with Data



necessary conclusion is that the linear-linear model is the best choice as it is acceptable both statistically and physically.

The linear-linear correlation results are plotted in Figures 8 to 12 for the five different concentrations. Plotted along with the correlation lines are confidence limits above and below the correlation line displaced by the amount of the Standard Error of Estimate. There is, unfortunately, some significant scatter in the data so the confidence limits are rather broad. Note that the error estimates are on the order of .10 kJ/kg. This uncertainty is about 5% of the typical value of the specific heat which is around 2 kJ/kg. Finally, the correlation model at evenly spaced values of the LiBr concentration is shown in Figure 13. Also shown in this figure is the c_p curve for water determined from quadratic interpolation of results from a program [12] that reproduces the 1967 version of the ASME Steam Tables. Note that the steady increase in c_p exhibited by water is reflected in the increase demonstrated by the solutions.

Note that for completeness the correlation lines and correlation lines with error limits for the quadratic-linear and quadratic-quadratic models have been plotted and are included in an appendix. The coefficients for all three models are given in the following table:

Table 7

Coefficients for Three Models Linear in Temperature

Algebraic Formulation of Model:

Coefficient	Linear-Linear	Quadratic-Linear	Quadratic-Quadratic
a_0	3.782593	1.116787	-7.13462
a_1	-3.66412	7.529969	39.34921
a_2		-11.687133	-41.8392
b_0	.00602	-.005177	.07826
b_1	.003761	.016532	-.30412
b_2			.302543

Fig. 8: 43.95% LiBr by weight

Linear-Linear Correlation

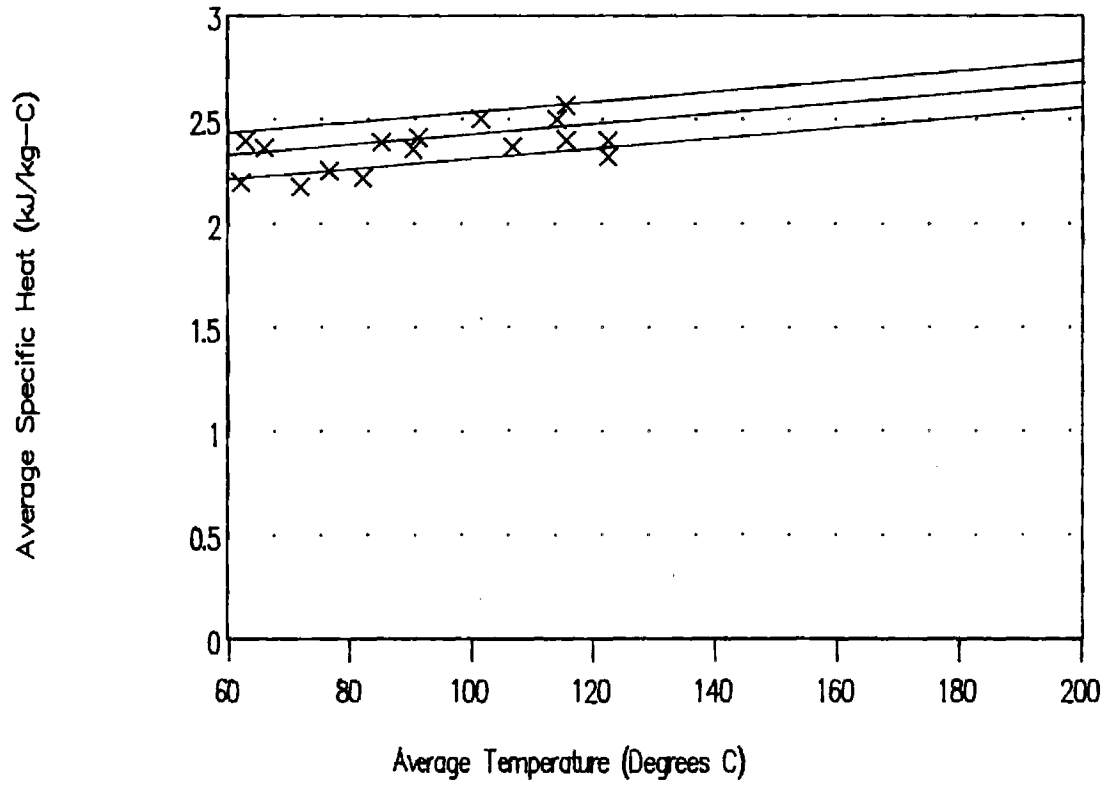


Fig. 9: 50.59% LiBr by weight

Linear-Linear Correlation

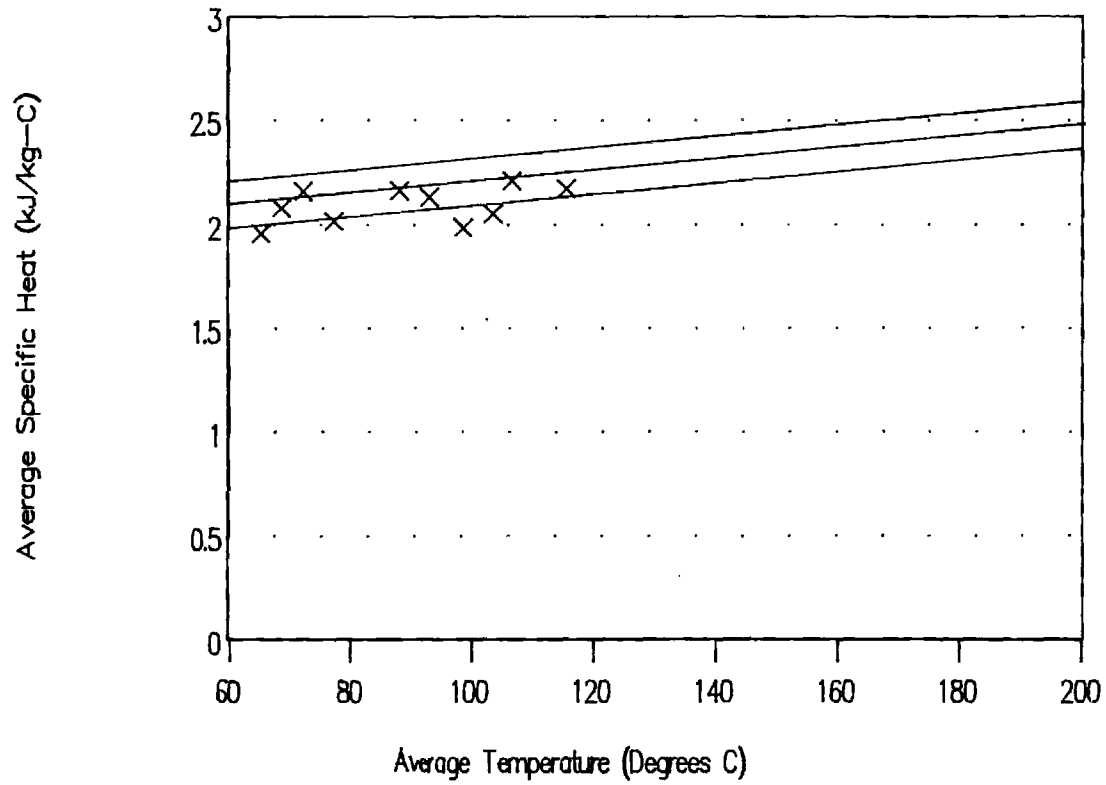


Fig. 10: 54.10% LiBr by weight

Linear-Linear Correlation

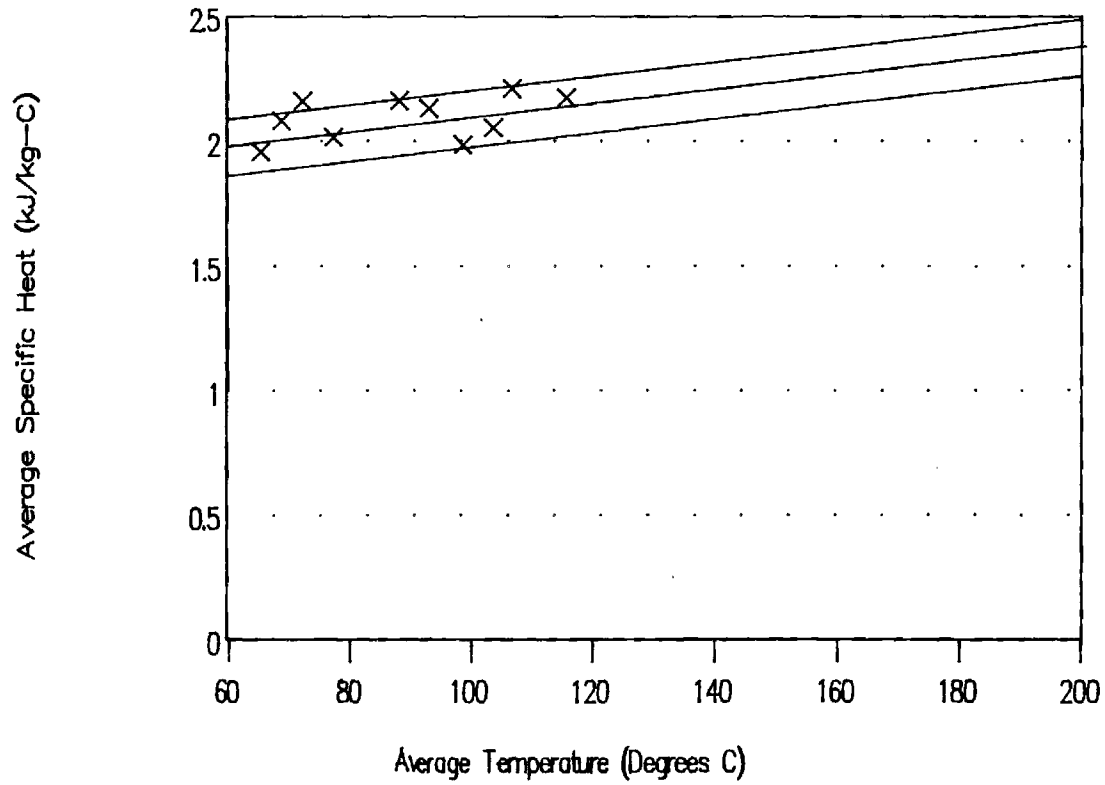


Fig 11: 59.48% LiBr by weight

Linear-Linear Correlation

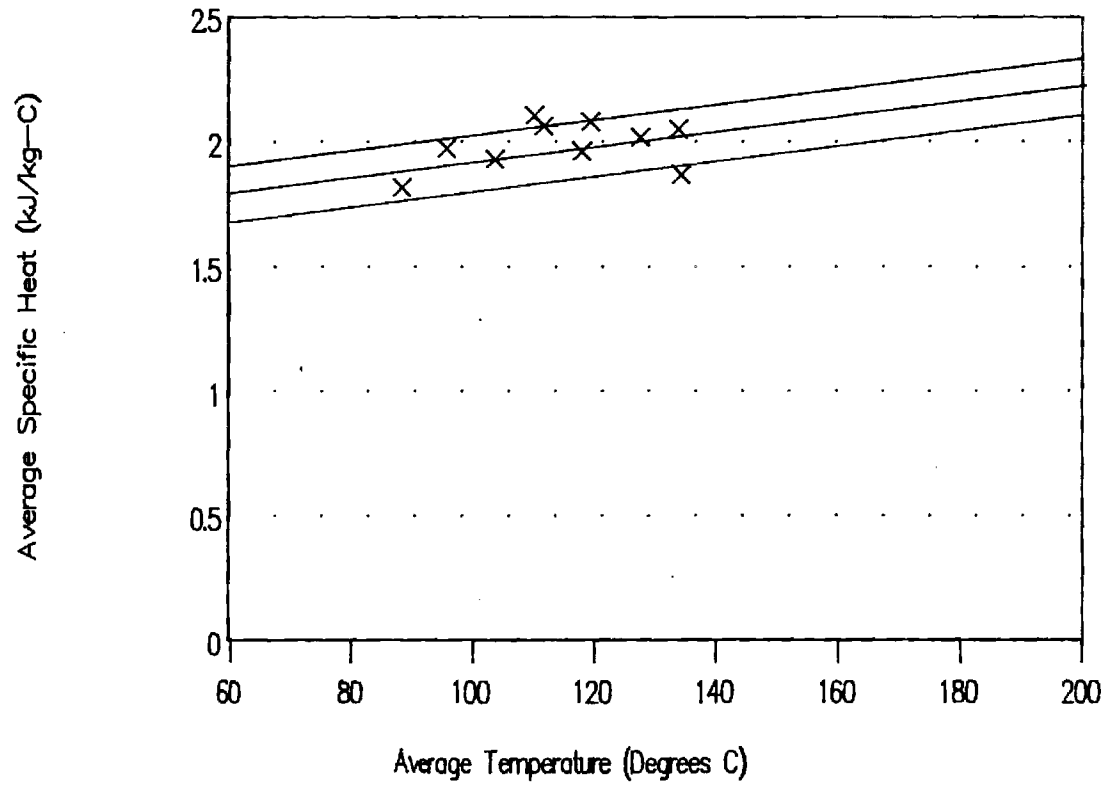
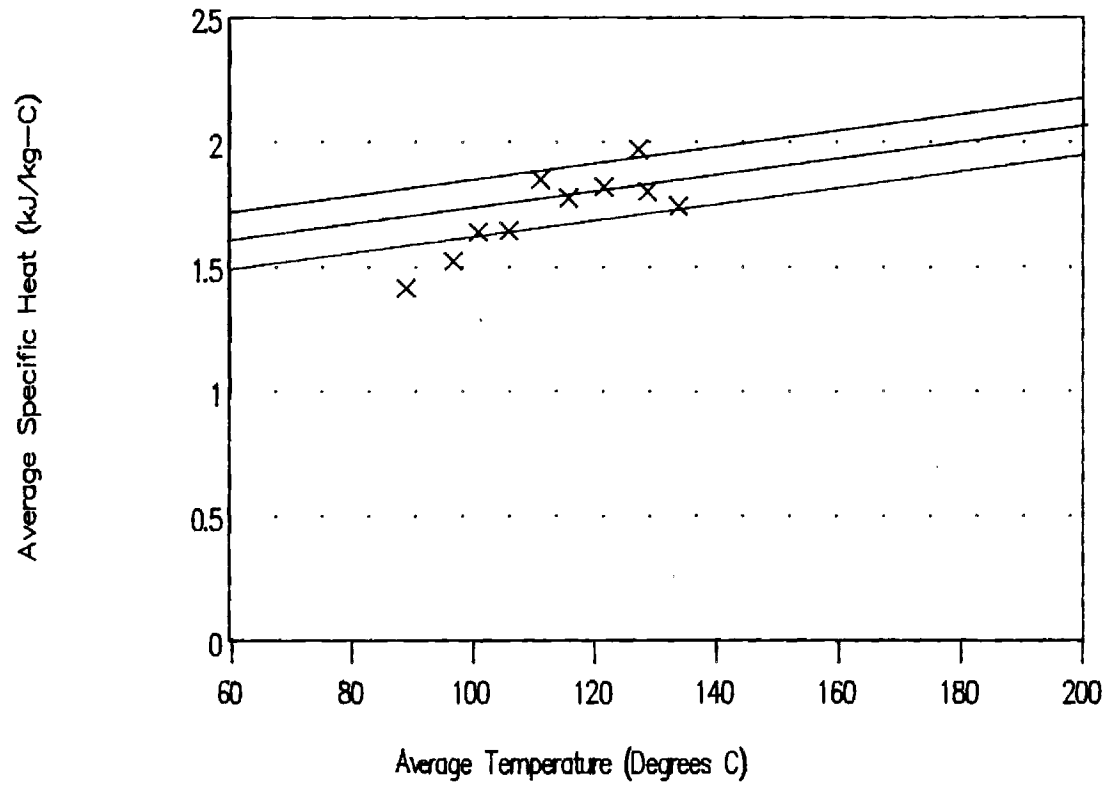


Fig. 12: 64.83% LiBr by weight

Linear-Linear Correlation



5. ERROR ANALYSIS AND COMPARISON WITH OTHER RESULTS:

Error Estimate. Since the drop calorimeter is a relatively complex device especially as regards heat leaks to the environment, an error analysis based on and proceeding from elementary principles appears to be formidably challenging at a minimum. Rather than attempt such an analysis a series of drops using water as a standard reference fluid were conducted in November and December of 1988. Note that these drops are independent of the water drop used to calibrate the receiver: different samples were used and the latter drops were not used to adjust the calibration curves. Results of these drops are detailed in the following table.

Table 8

RESULTS OF STANDARDIZATION TESTS WITH WATER

Sample Temperature	Final Temperature	Empirical Average Specific Heat	Tabulated Average Specific Heat	Relative Error
142.77	51.59	4.21	4.219	-.002
165.98	52.36	4.29	4.239	.012
189.81	54.09	4.23	4.267	-.009
190.28	53.79	4.24	4.267	-.006
165.61	55.25	4.22	4.241	-.005
119.43	53.04	4.19	4.204	-.003
Root Mean Squared Error				.007

The preceding reveals an inherent calorimeter error on the order of $\pm 0.7\%$ with the samples of water. Over a similar temperature range, water has about twice the specific heat capacity of a typical LiBr solution (e.g. $4.2/2.4 = 1.75$). Consequently, for a typical LiBr solution the calorimeter error, ϵ_{cal} , is estimated to be about 1.2% (i.e. $.007 \cdot 1.75 = .012$).

In the current situation, inaccuracy in the composition of the solution is also a source of error. For the linear-linear model, the dependence of the specific heat on concentration is given by the following partial derivative:

$$\partial c_s / \partial x = a_1 + b_1 T$$

At 150 C, the value of the derivative is about $-3.1 \text{ kJ}/(\text{kg} \cdot \text{K} \cdot \text{kg}/\text{kg})$. Uncertainty in the composition is probably on the order of 0.1% ; but even if it is as great as 1% , this component can contribute a relative composition error, ϵ_x , of only $.013$ (i.e. $3.1 \cdot .01/2.4$) which is only of the same order as the calorimeter error. Using the central limit theorem, the combined error is given as follows:

$$\epsilon = \{ \epsilon_{\text{cal}}^2 + \epsilon_x^2 \}^{1/2} = .018$$

In the production drops, this accuracy has not been achieved probably because of imperfect attention to all procedures over the many weeks of effort required to complete the series of drops. The production drops have at least twice this inaccuracy as indicated by Standard Errors of Estimate in the correlations of around 5%.

Comparison with Other Results. As indicated above, five other sources of comparative data are available. The data of Pennington [7] are at room temperature and are not helpful for a comparison with the current results. The data of Uemura and Hasaba [5] are significantly lower than the values obtained herein or the values in the other three remaining sources. The comparison is illustrated in Figure 13 which shows both the reported data and the correlation provided by Uemura and Hasaba. Data obtained by Uemura and Hasaba are limited to the range of 51.7 C to 130.2 C for the concentration shown, 66.2%. At lower concentrations, 110.4 C was the highest experimental temperature. Both the data and the correlation are 10% to 17% lower than the present linear-linear correlation over the range of their experimental basis, which is approximately 50 C to 130 C. For example, Uemura and Hasaba obtained 1.51 kJ/(kg K) at $x = .662$ and $T = 130.2$ C compared with 1.79 kJ/(kg K) with the linear-linear correlation from the current investigation. The relative error between these data is 17%. Error limits are also plotted on the graph at one standard error above and below the correlation results from the present study. It is notable that all the data points reported by Uemura and Hasaba as well as their correlation line are fully outside the error bounds over their valid temperature range. This divergence from the present correlation indicates that there is no statistical support for the older results from the current data. The error in the results of Uemura and Hasaba appears to be excessive, and their results should probably not be employed. The reason for this error cannot be explained from the sketchy description in the literature. Possibly their apparatus was unsuitable for higher temperature operation since the temperature quoted above, only 130.2 C, was the highest in the data set. Note that the Uemura and Hasaba correlation converges on the linear-linear correlation at higher temperatures, but this is beyond the range of their experimental data base and is, therefore, only unsupported extrapolation.

A third source of comparative data is the thesis by Lower [1]. These data at concentrations of 45, 50, 55, and 60 weight percent are plotted in Figure 14 along with the corresponding linear-linear correlation lines from the present investigation. Agreement between the two set of results of data is not perfect and ranges from good agreement near 45% to poor agreement near 60%. In Figure 15, the standard error limits for 45% and 60% are plotted along in comparison with the data of Lower. As is evident in the figure the data from Lower is marginally in agreement with the results for the present study at near 45%. At 60% the data do not agree well with most of Lower's data out of the error band defined by the current investigation. Consequently, support for the results of Lower from the current study is marginal at most.

Two more important sources of data are the numerical results of Patterson and Perez-Blanco [4] and the experimental data provided by Dr. Uwe Rockenfeller of Rocky

Research Inc. [13]. The Rocky Research data were measured with a Differential Scanning Calorimeter (DSC) manufactured by Perkin-Elmer. These data are reported to include compensation for the difference in heat capacity between the cells holding the samples and the cell holding the reference. In addition corrections have been applied for vaporization effects. The Rocky Research data are illustrated in Figure 16 along with linear-linear correlation lines for these same data. Because the DSC data are very smooth, the linear-linear correlation produces an excellent fit with a Coefficient of Correlation over 99%. The numerical results of Patterson and Perez-Blanco are curve fits to the enthalpy data generated by McNeely [2]. Specific heats are obtained from the enthalpy function by taking the partial derivative with respect to temperature while holding constant the concentration. McNeely employed the procedure of Haltenberger [3] to produce enthalpy-concentration charts from vapor-pressure data over a range of temperatures and concentrations and specific heat data over a range of temperature. In particular, to produce the published results, McNeely used the specific heat data from Lower at 50% concentration. As shown in Figure 17, the results from differentiation of the correlations of Patterson and Perez-Blanco agree very well with the Rocky Research data. It is notable that the differentiation does not precisely return the specific heat data of Lower. This is to be expected since both vapor properties and specific heat data are required to define the enthalpies, and the vapor properties have a significant impact. In addition, the numerical curve fit is defined over the entire range of the enthalpy chart which tends to somewhat obscure the influence of any particular contributing data. The following table provides the coefficients for both correlations and statistical results for the Rocky Research data.

Since the Rocky Research data agree very well with the correlation from Patterson and Perez-Blanco, it should be sufficient to illustrate and discuss the comparison between the results of the present investigation and the data from Rocky Research. The Rocky Research data are illustrated along with the corresponding linear-linear correlations in Figure 18. As is evident in the figure, there is good agreement between the two data sets which is very reassuring since disparate procedures are used in the two measurements. The linear correlation ranges from 4% above the Rocky Research correlation at 45.1% and 150 C to 2% below at 65% and 150 C. The RMS error at mid range is only about 3%. This is hardly greater than the estimated inherent accuracy of the drop calorimeter and is less than the standard error estimate in the specific heat correlation for the drop calorimeter data. The Rocky Research data are illustrated in Figure 19 along with representative error bands for the linear-linear correlation. Nearly all of the Rocky Research data fall within the error bands. Consequently, the results of the current investigation are not statistically divergent from the Rocky Research data, and the two sets of data are mutually reinforcing. The principal difference is in the slope of the temperature dependence with the current investigation having the greater temperature effect. The specific heats from the enthalpy correlation of Patterson and Perez-Blanco are similarly in agreement with the current investigation and the with the Rocky Research data. Error bounds on the other two sources cannot be quantified, but they may be very small in the case of the Rocky Research data. In the absence of further uncertainty estimates, no distinction can be drawn from the three data bases.

Fig. 13: 64.83% Linear-Linear Model

Compared with Uemura and Hasaba

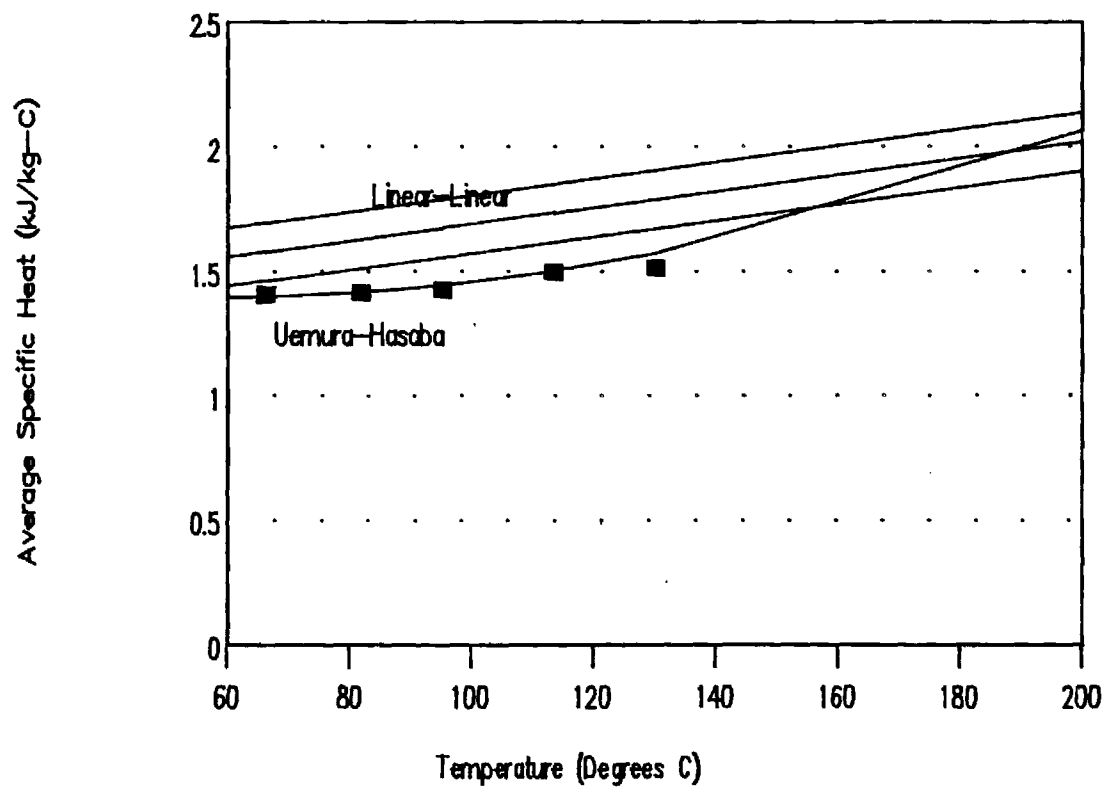


Figure 14: Data of Lower
and GIT Linear-Linear Correlation

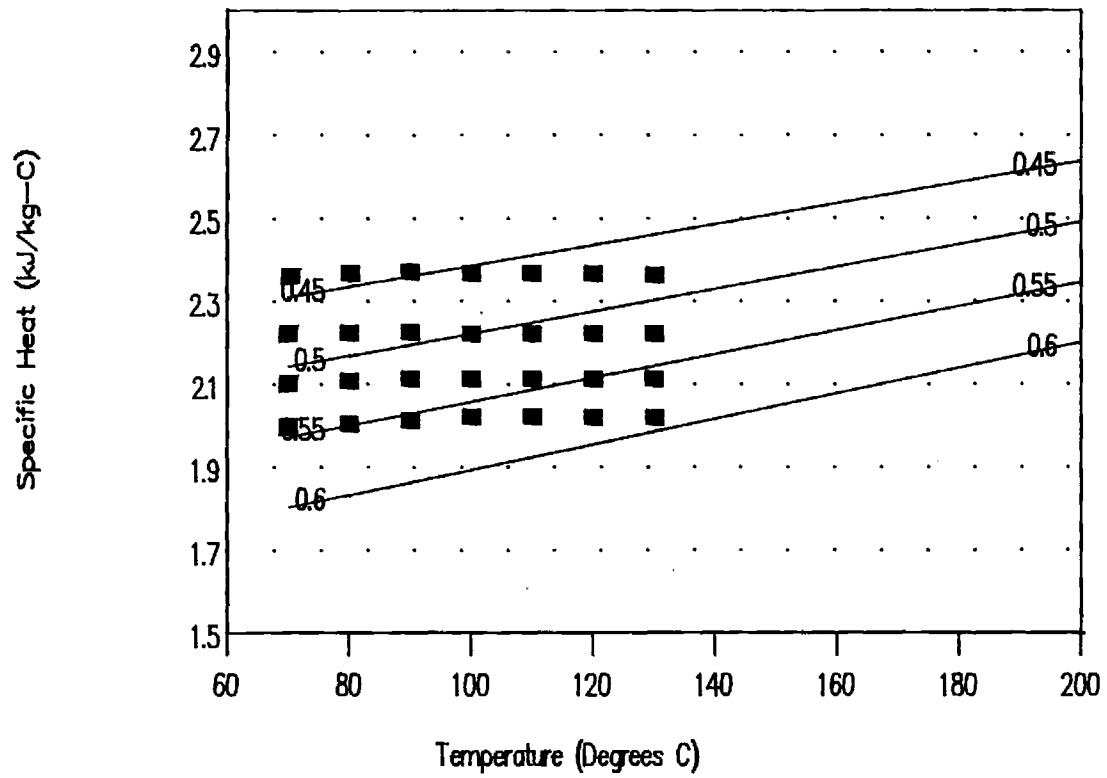


Fig. 15: Data of Lower and GIT

Error Bands at 40% and 60%

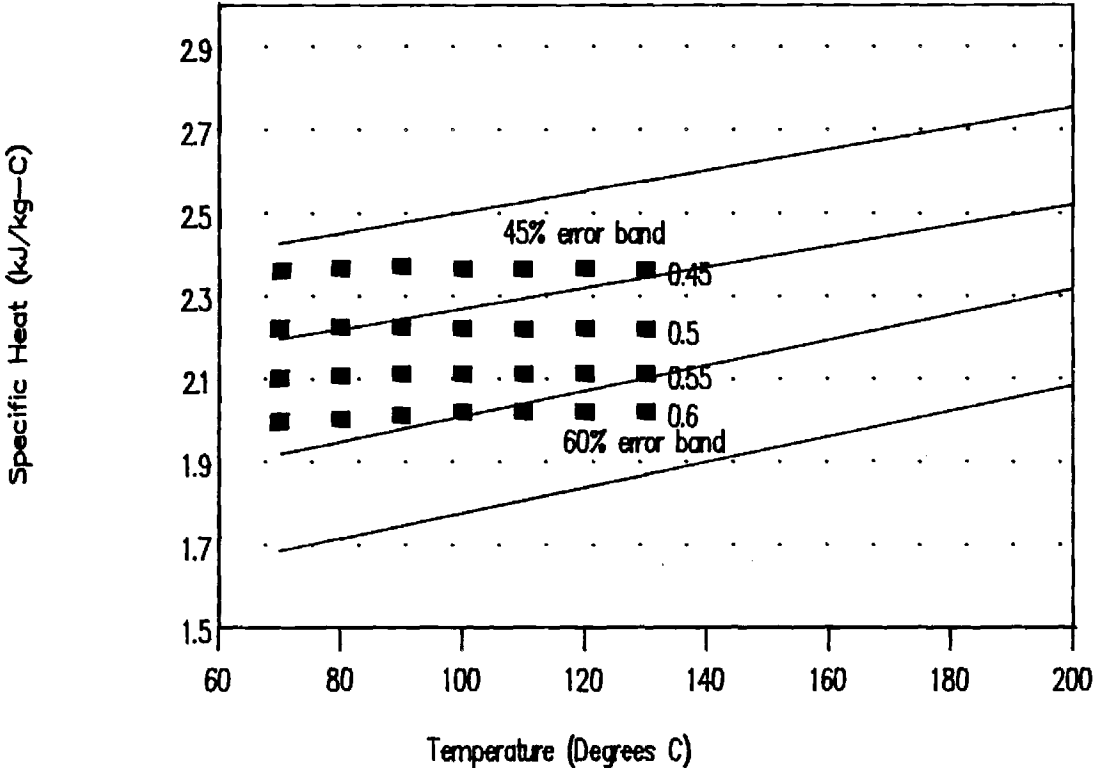


Figure A.3: 54.10% LiBr by weight

Quadratic-Quadratic Correlation

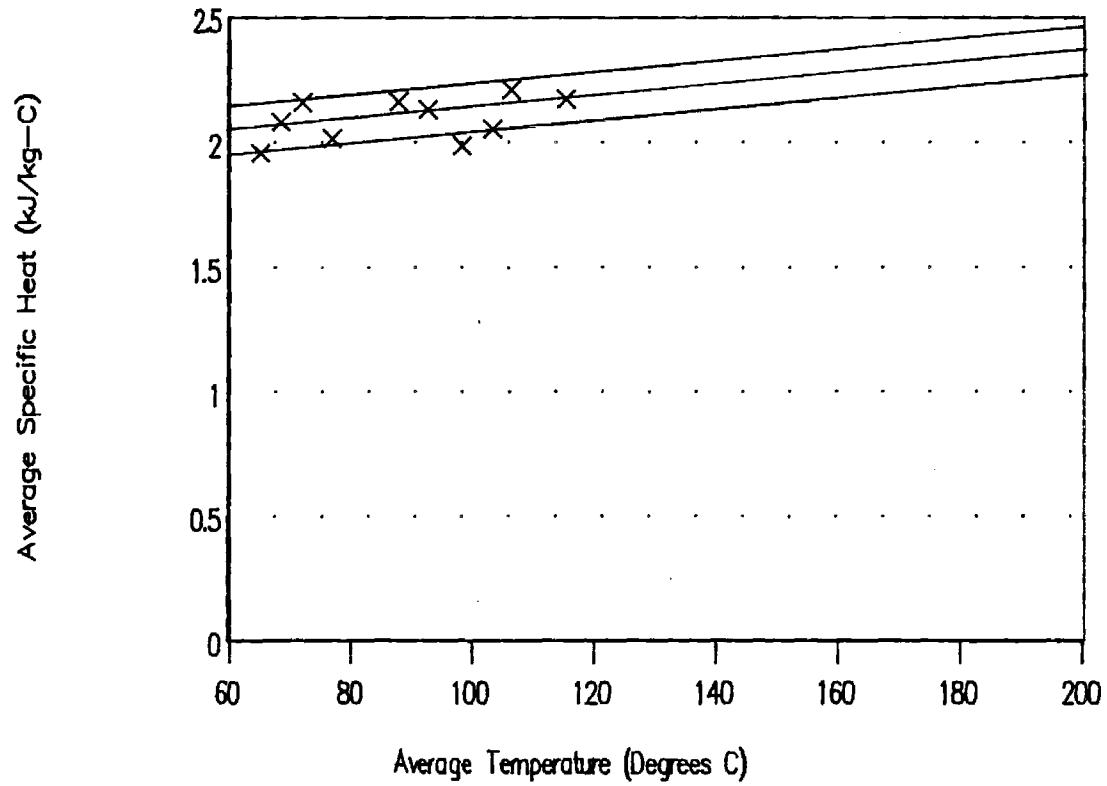


Figure A.4: 59.48% LiBr by weight

Quadratic-Quadratic Correlation

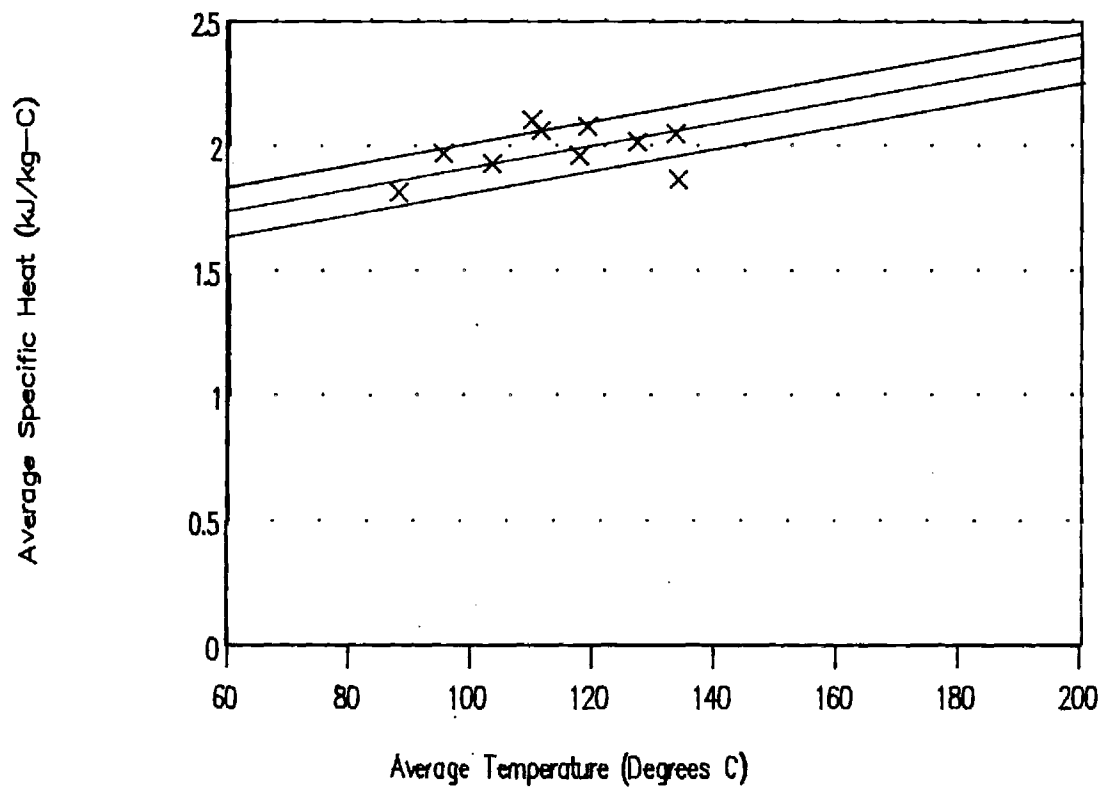


Figure A.5: 64.83% LiBr by weight

Quadratic-Quadratic Correlation

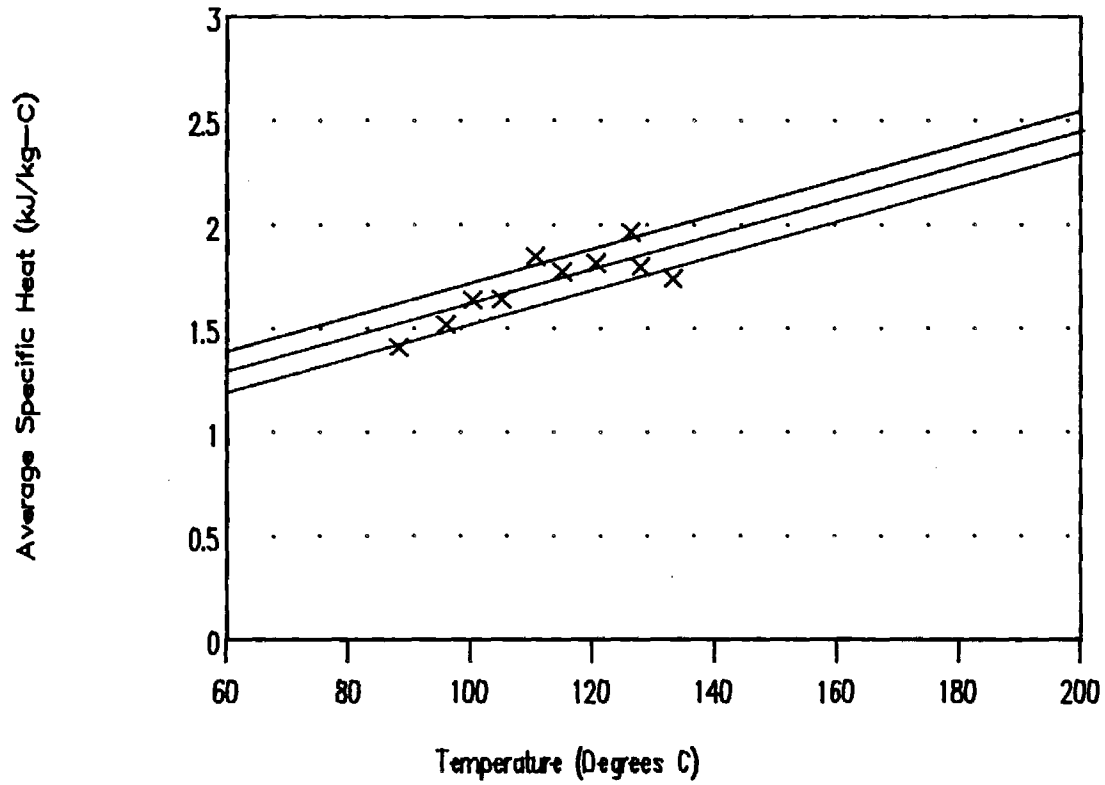


Figure A.6: 43.95% LiBr by weight

Quadratic-Linear Correlation

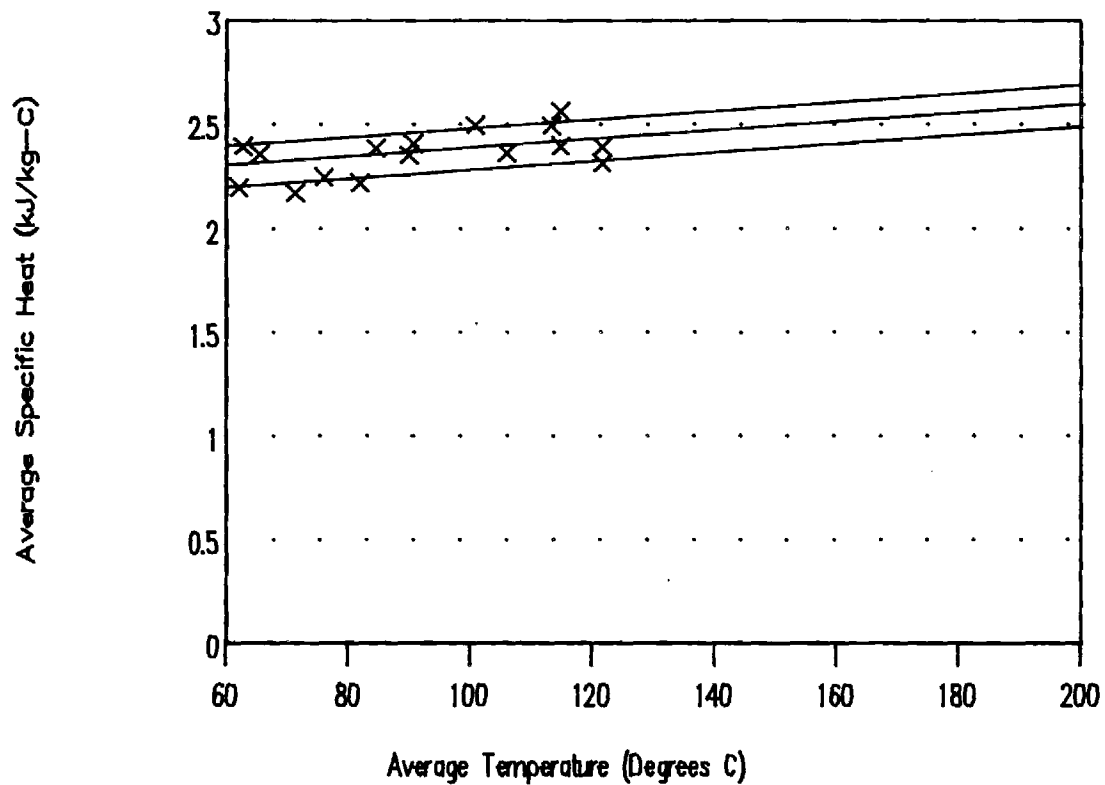


Figure A.7: 50.59% LiBr by weight

Quadratic-Linear Correlation

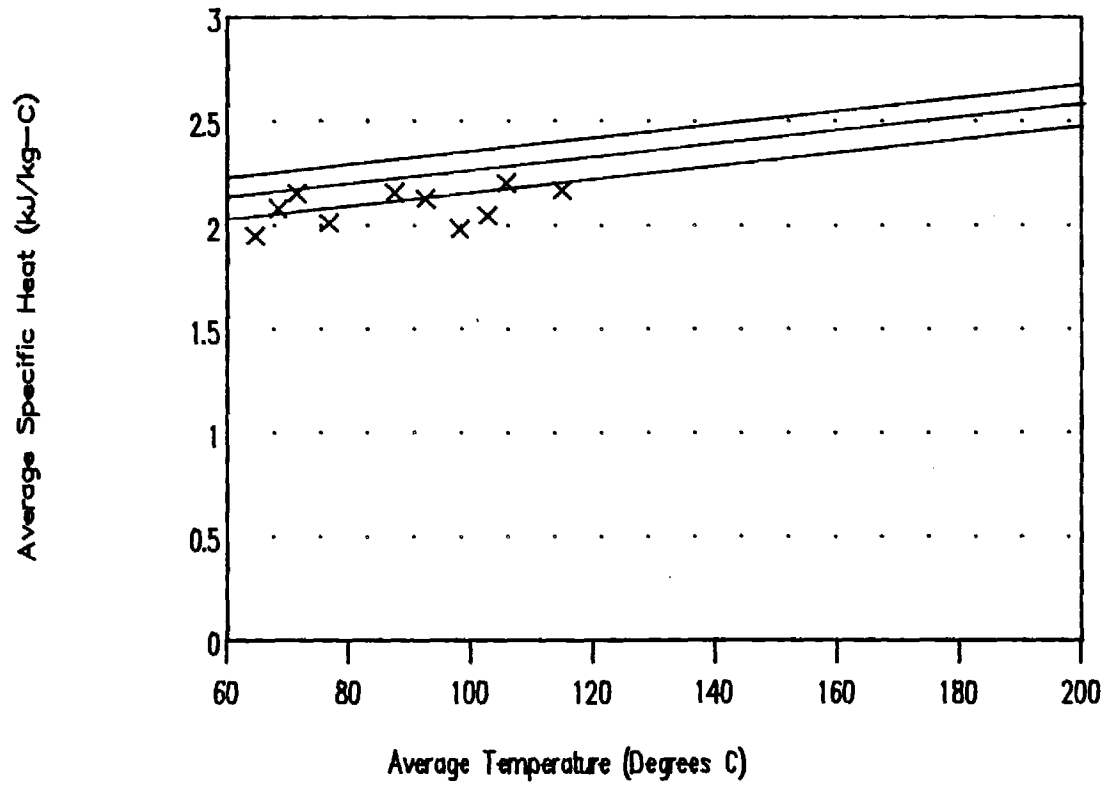


Figure A.8: 54.10% LiBr by weight

Quadratic-Linear Correlation

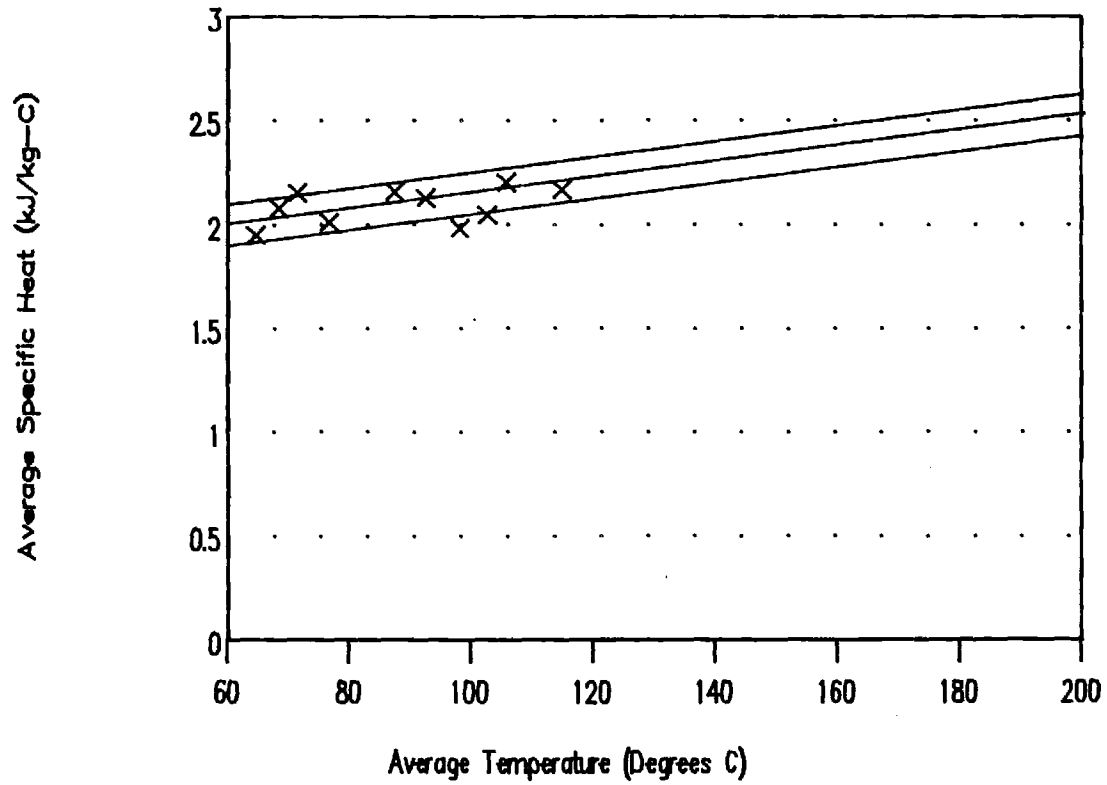


Figure A.9: 59.48% LiBr by weight

Quadratic-Linear Correlation

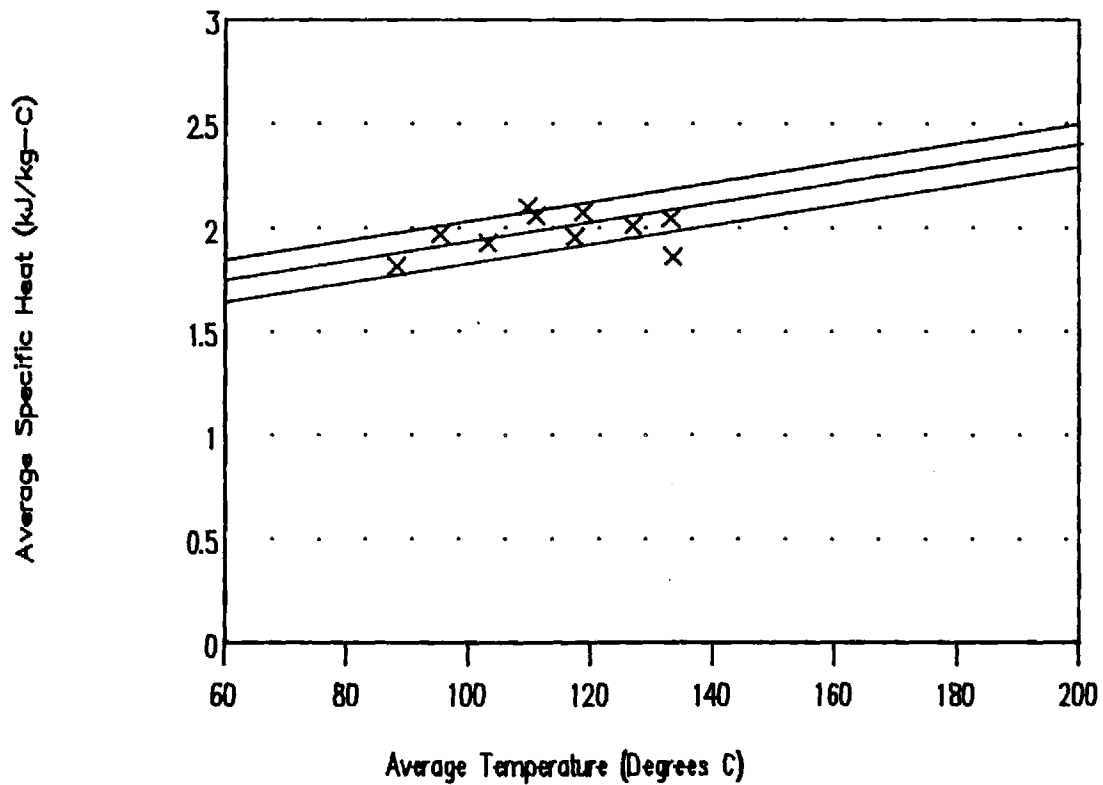
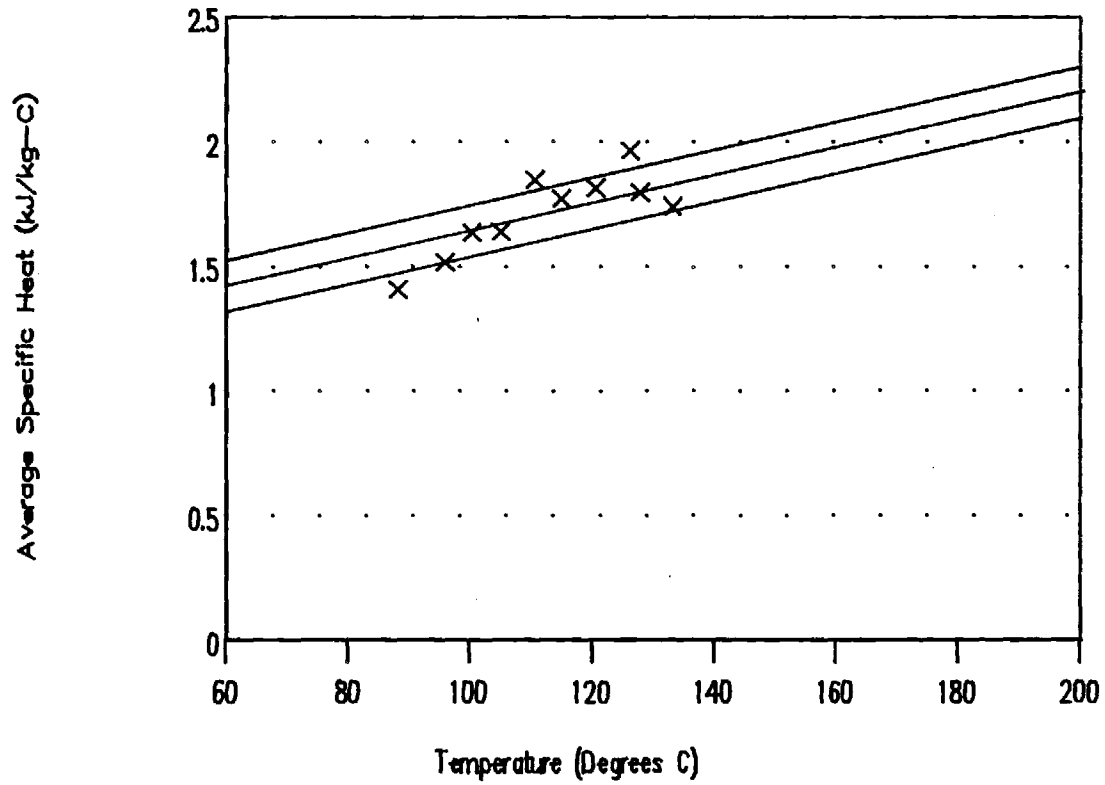


Figure A.10: 64.83% LiBr by weight

Quadratic-Linear Correlation



VAPOR PRESSURE OF AQUEOUS LITHIUM BROMIDE SOLUTIONS

Abstract: Vapor pressure measurements of aqueous solutions of lithium bromide have been reviewed and checked for consistency. A correlation of the literature data as a function of temperature and composition was also developed. A static apparatus was constructed for the measurement of the vapor pressures of lithium bromide solutions and new data are presented in this report.

Aqueous solutions of lithium bromide are common working fluids in absorption refrigeration applications [3]. A knowledge of the physical properties of such solutions and, in particular, of the P-T-x behavior is necessary for process design. The objective of this work was to measure the vapor pressure of aqueous solutions of lithium bromide at temperatures ranging from 100 ° to 200 ° C and concentrations ranging from 30 to 65 weight % LiBr. The majority of phase equilibrium data on salt solutions have been obtained using isopiestic measurements [11]. In such measurements, a sample solution is allowed to equilibrate with a reference solution in a sealed container at a specified temperature. However, this technique requires a great deal of skill and the availability of a standard salt solution over the range of temperature and concentration of interest. In the case of LiBr-H₂O mixtures, the usual standard (NaCl-H₂O) is inapplicable because of the saturation limits of NaCl. Furthermore, very few salt data can be considered reliable at the experimental conditions of interest in this study. These limitations can be overcome by the use of static methods [1]. Therefore a static apparatus was constructed for the determination of the vapor pressure of LiBr-H₂O mixtures at pressures greater than one atmosphere. Preliminary results are presented in this report. In addition, a review of previous work and a new correlation of the data are also discussed.

I) REVIEW OF PREVIOUS WORK

Numerous investigators have reported data for the vapor pressures of LiBr-H₂O mixtures. For example, nine references are

cited in the International Critical Tables [6], published in 1923. Work done before 1970 has been summarized by McNeely [9], who compiled published data as well as data measured by the major manufacturers of lithium bromide absorption equipment in the USA. More recent work is reviewed in the following paragraphs. Note that osmotic coefficient data and mean ionic activity data are not reviewed, although their conversion to vapor pressure values is generally straightforward.

The range of temperatures and concentrations covered by the most recent measurements is shown in figure 1. The studies of Greeley [5], Pennington [10], Maust [8] and Boryta [2] cover the range of variables commonly found in absorption refrigeration applications. The agreement between these workers is generally fair. The highest temperature range was studied by Federov [4]. However, he did not publish his raw experimental data but listed instead smoothed values of vapor pressures. He claimed an accuracy of $\pm 0.5\%$. The more recent work of Rocky Research [14] covers the same range of temperature and concentrations as the present study. The original data of Löwer [7], Renz [13] and Zimmermann [17] were not available; although the approximate range covered by Renz is shown in Figure 1. Uemura [16] presented graphical results as well as a nine parameter correlation of his unpublished data. However, the temperature and concentrations covered in his study were the same as those covered by Pennington and Boryta. His vapor pressure results are not considered further in this work.

Vapor pressure-temperature-concentration diagrams for the system $\text{LiBr-H}_2\text{O}$ are quite common in the literature. These diagrams are generally produced by extrapolating data measured over a small temperature or concentration range. Disagreement among the data of different workers is quite common, especially when extrapolated values are compared. A general correlation of all the then available data was developed by McNeely [9]. An updating of this correlation to include the most recent published data will be attempted in this work. A preliminary correlation of the Rocky Research data which cover the range of temperatures and concentrations of this study is presented below. Several functional forms for the dependence of the

vapor pressure on temperature and concentration were examined. The most efficient form was one where the properties of lithium bromide solutions were referred to those of pure water, as in Dürhing's law type of approach. In the final correlation, the ratio of the vapor pressure of the solution to the saturation pressure of water at the solution temperature is expressed as a function of the weight fraction of lithium bromide (x) and the temperature T (C) as follows:

$$\frac{P_{\text{solution}}(T,x)}{P_{\text{water}}^{\text{sat}}(T)} = A_1 + A_2(x - 0.5) + A_3 T \cdot x + A_4(x - 0.5)^2 + A_5 T$$

The saturation pressure of water was computed using the International Association for the Properties of Steam recommendations [15]. The least square estimators of A_1 , A_2 , A_3 , A_4 and A_5 are given in table 1. The objective function used was the sum of squares of the deviations between the predicted and the experimental values of the ratio of pressures and was minimized using a stepwise regression algorithm. The regression coefficient was found to be 0.997 and the quality of the fit is shown in figure 2. At this stage of the correlation work, no data have been removed from the data set, even when discrepancies were evident.

II) EXPERIMENTAL

2-1) Apparatus

The static apparatus used in this work is shown in Figure 3 and consisted of five parts: the equilibrium cells, the manifold, the pressure reading unit, the temperature reading unit and the oven.

The cells were made from 316 stainless steel and have an internal volume of 90 cm³ and a wall thickness of 0.635 cm (1/4 in). A glass liner and passivation of the steel by nitric acid were employed to minimize corrosion problems inherent to the system LiBr-H₂O. A 0.32 cm (1/8 in) thick graphite washer (Grafoil) was used

to provide a pressure-tight seal for each cell. High pressure fittings (High pressure Autoclave Engineering) were used with NPT threads for lid/tubing connections. Cells were closed individually by non rotating stem valves (High pressure Autoclave Engineering, model 30-VM).

A high pressure manifold (High pressure Autoclave Engineering) was used to connect the six cells (only two are shown in fig. 11 for clarity) to the pressure reading unit and the vacuum line. For increased precision, two pressure gauges (Heise 710-A, range 0-150 psig and Heise 710-A, range 0-200 bar) were used in this study. Initially we attempted to use gallium as a pressure transmitting fluid. However, this was abandoned when it was discovered that gallium oxide reacts with water at high temperature and pressure. An attempt to use various silicon oils was also abandoned because of problems with degassing. Finally, a novel approach was adopted with water as the pressure transmitting fluid. This will be explained further in the next section. The use of an inert pressure transmitting fluid improves the accuracy of the pressure measurements. This was preferred over the use of electronic transducers, since the latter generally cannot withstand high temperatures.

The oven consisted of an insulated metal cabinet containing a heater and a fan. An inside enclosure was used to separate the heater and the fan from the rest of the contents of the oven. A platinum resistance thermometer (Fluke Model Y2039) buried in a metal block was used to measure the temperature in the oven. The PRT was connected to a high precision digital thermometer (Fluke Model 2180A) allowing direct reading of the temperature. The six cells, the manifold, the temperature sensor for the control unit and the PRT were placed in the inside enclosure where the temperature could be maintained constant within ± 0.07 K for periods of up to three days.

2-2) Procedure

Gravimetrically prepared lithium bromide solutions were charged into five of the cells. Their salt contents were 30.0, 40.0, 50.0, 60.0 and 65.0 weight% respectively. The sixth cell was filled with pure water. Due to the importance of thorough degassing in static VLE experiments, several techniques for degassing the solutions were tried. The most successful was repeated freeze-pump-thaw cycles. The pressure in the cells during the freeze-pump steps was monitored by a vacuum gauge (Sargent-Welch Model 11-278). Six to ten cycles were found to be sufficient to get a constant vapor pressure in the cells.

After connecting the cells to the manifold, the system was checked for leaks under pressure (up to 80 bar) and under vacuum. With the valve V1 closed, the lines leading from the pressure gauges and the pressure generator (Ruska proportioning pump, model 2272) were charged with degassed water. The manifold was kept under vacuum (valve V2 open) at this stage. The oven temperature was then set at a predetermined value. The valve V1 was then opened slowly (with valve V2 closed) and liquid water was allowed to enter the manifold, until the line from the valve V1 to the oven wall was filled. Owing to the sharp gradient of temperature across the wall of the oven (estimated at 25 °C/cm), the intrusion of liquid water in this gradient of temperature was accompanied by an increase of the pressure in the manifold due to the generation of water vapor. In fact, the pressure in the manifold could be adjusted to any value by carefully controlling the position of the water meniscus in the temperature gradient region, as shown in Figure 4. By displacing the piston of the pressure generator, the position of the water meniscus could be changed. Adjustments of a few hundredths of psi could also be made by moving the position of the stem of the valve V1.

The vapor pressure in the cell was measured after opening the cell to the manifold. If the cell pressure (determined by the temperature of the oven and the composition of the solution) was higher than the set manifold pressure (determined by the position of the water meniscus), then a transfer of water from the cell to the meniscus occurs. If the cell pressure was lower than the manifold pressure, then the transfer is reversed. Due to the very small tubing

flow area (0.0323 cm^2) and to the exponential nature of the dependence of the saturation pressure of water on temperature, only a minute amount of water is transferred. Furthermore, it was found that mechanical equilibrium (ie equilibration of the pressure in the system) occurred much faster than thermal equilibrium of the meniscus at its new position in the temperature gradient region. Thus, by closing the valve of the cell (valve V3) before any significant transfer of water occurs, it is possible to make many measurements without affecting the concentration of the solutions. This is particularly true when the manifold pressure is near the equilibrium pressure to be measured. Generally three to five adjustments of manifold pressure were sufficient to achieve equilibrium conditions. The constancy of the reading was then checked by adjusting alternatively the manifold pressure to values a few hundredths of psi higher and a few hundredths of psi lower than the cell pressure. At the equilibrium pressure, these small perturbations did not affect the readings.

After closing the valve of the cell (valve V3), the manifold pressure was checked to see that it had returned to its initial value, thus confirming that no significant transfer of water had occurred. At the end of a run, some isotherms were remeasured to check any drift in the water content of the cells. The pressure gauges were zeroed periodically by opening the manifold (valve V2) to the atmosphere. Barometric pressures were determined using a Fortin barometer; mercury elevations were corrected for temperature and local gravity effects. The static VLE technique also allows a check for the presence of inerts in the system during a experimental run. If a measurement is repeated after evacuating the manifold and recharging it with degassed water, any decrease in the reading indicates the presence of inerts.

At the end of the experiment, the concentrations of the solutions were verified by titration with silver nitrate using a computer aided titrator (Fisher, Controller model 450, Buret Model 400). The accuracy of the titration procedure was checked by titrating a standard 0.1 M NaBr solution. The measured

concentrations of salt were within the accuracy of the standard solution (± 0.0005 Molar).

2-3) Materials

Anhydrous lithium bromide was obtained from Morton Thiokol Inc. (lot F06H). The manufacturer's certificate of analysis stated a purity of 99.3 weight%, the remaining being water (0.5 weight%) and diverse salts. However, during the preparation of the lithium bromide solutions, the presence of fiber-like materials and of black and orange pellets was noticed. These impurities were assumed to come from the manufacturing process and it was assumed that these impurities did not affect the vapor pressures measurements. The water used in this study was distilled in an all-glass still (Corning Mega-Pure System Model MP-6A). Standard 0.1 N silver nitrate and standard NaBr solutions, used in the titration studies, were purchased from Fisher.

III) PRELIMINARY RESULTS AND DISCUSSION

Some of the data collected in this work are shown in Table I. Run 1, Run 2, and Run 3 correspond essentially to a different air flow pattern in the oven. For each tabulated pair of temperatures and vapor pressures, an apparent concentration of LiBr can be inferred from the correlation developed in this study. The results are shown in Figure 5. On average, the apparent concentration in each cell was found to be higher than the concentrations determined by gravimetry. Therefore, loss of solvent occurred during the initial stages of the experiment, and especially during degassing. However, since the readings were reproducible, it seems very unlikely that

any further loss of water occurred after the initial period. The actual concentrations of LiBr will be obtained by titration at the end of the experiment.

Figure 5 shows also that there is considerable scatter of the data around their mean values. This indicates that either the pressure or temperature measurement is in error. The accuracy of the pressure transmitting set-up was checked by applying a known pressure of nitrogen to the manifold (vacuum line side). No discrepancies in pressure readings were noted. Therefore, it must be assumed that the temperature in the cells is not the same as the temperature of the oven, measured with the PRT, because the temperature distribution was not really uniform. A thermowell is presently being inserted into each cell to obtain an accurate indication of the temperature. The measurements will be repeated as soon as this is completed.

BIBLIOGRAPHY

- [1] Abbott M.M. in *Phase equilibria and fluid properties in chemical industry*, p.87, Dechema 1980
- [2] Boryta D.A., Maas A.J. and Grant C.B., *Journal of Chemical and Engineering Data*, vol 20, 3, 316-319, 1975
- [3] Ellington R.T., Kunst G, Peck R.E. and Reed J.F., *Institute of Gas Technology Research Bulletin*, 14, 1957
- [4] Federov M.K., Antonov N.A. and L'vov S.N., translated from *Zhurnal prikladnoi Khimii*, vol 49, 6, 1226-1232, 1976
- [5] Greeley E.M., data published in [9]
- [6] *International Critical Tables*, vol 3, New-york, Mc Graw-Hill, 1928
- [7] Löwer H. *Kältetechnik*, 13(5), 178-184, 1961
- [8] Maust Jr E.E., PhD dissertation, University of Maryland, College Park, Md, 1966
- [9] Mc Neely L.A., *ASHRAE Transactions*, 3, 413-434, 1979
- [10] Pennington W., *Refrigerating Engineering*, 63, 57-61, 1955
- [11] Platford R.F., *Experimental methods* , in [11], 65
- [12] Pytkowicz R.M., *Activity Coefficient in Electrolyte Solutions*, CRC Press, 1979
- [13] Renz M., Dissertation, University of Essen (1981)
- [14] Rocky Research , private communication, 1989
- [15] Saul A. and Wagner W., *Journal of Physical and Chemical Reference Data*, vol 16, 4, 893-901, 1987

- [16] Uemura T. and Hasaha S., *Technical Report of Kansai University*, 6, 31-55, 1964
- [17] Zimmerman A and Keller J.U., paper presented at the Fifth International Conference on *Fluid Properties and Phase Equilibria for Chemical Process Design*, Banff, Canada, 1989

FIGURE 1.

VAPOR PRESSURE LITERATURE DATA

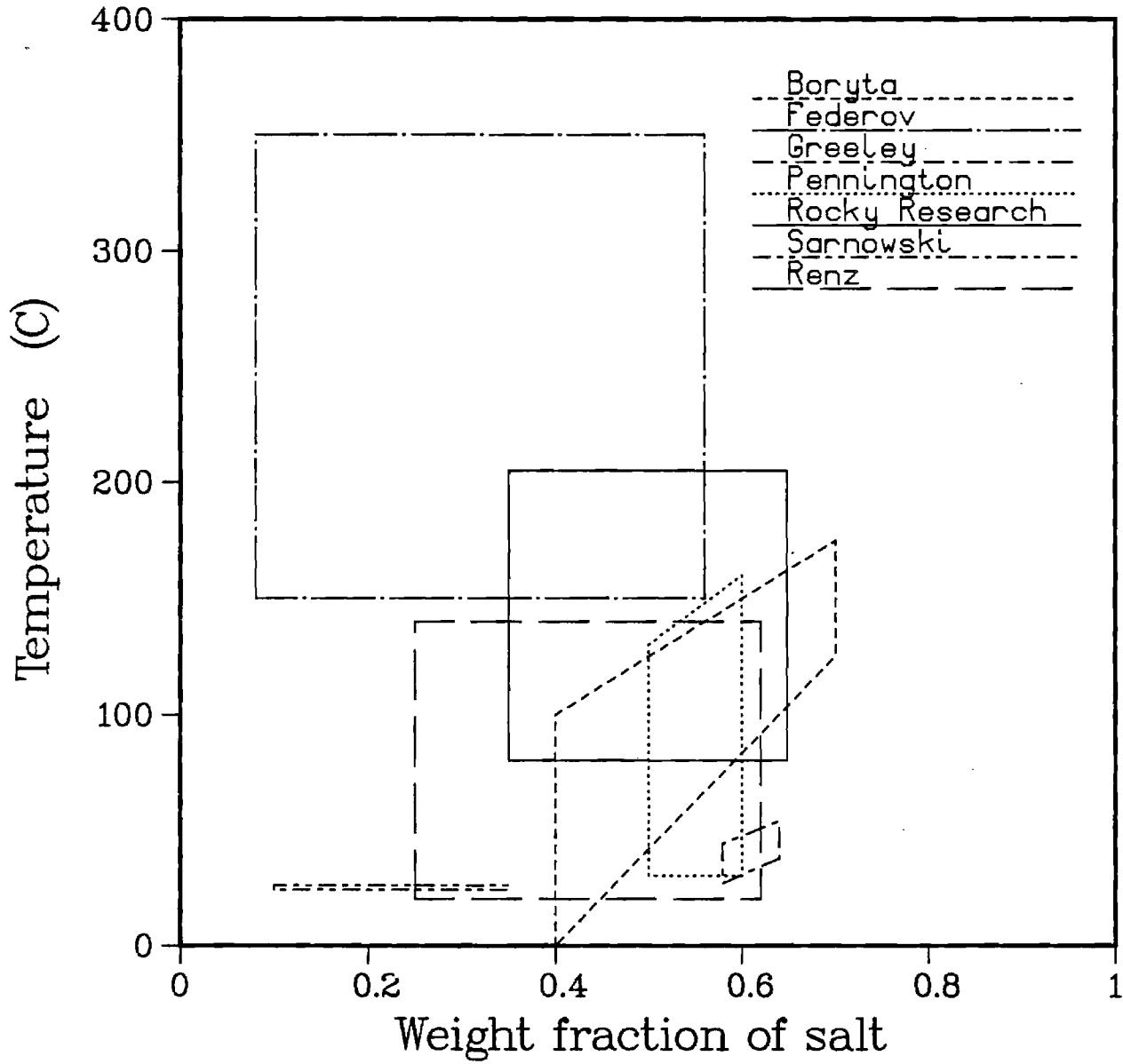


FIGURE 2.

CORRELATION OF RECENT DATA [14]

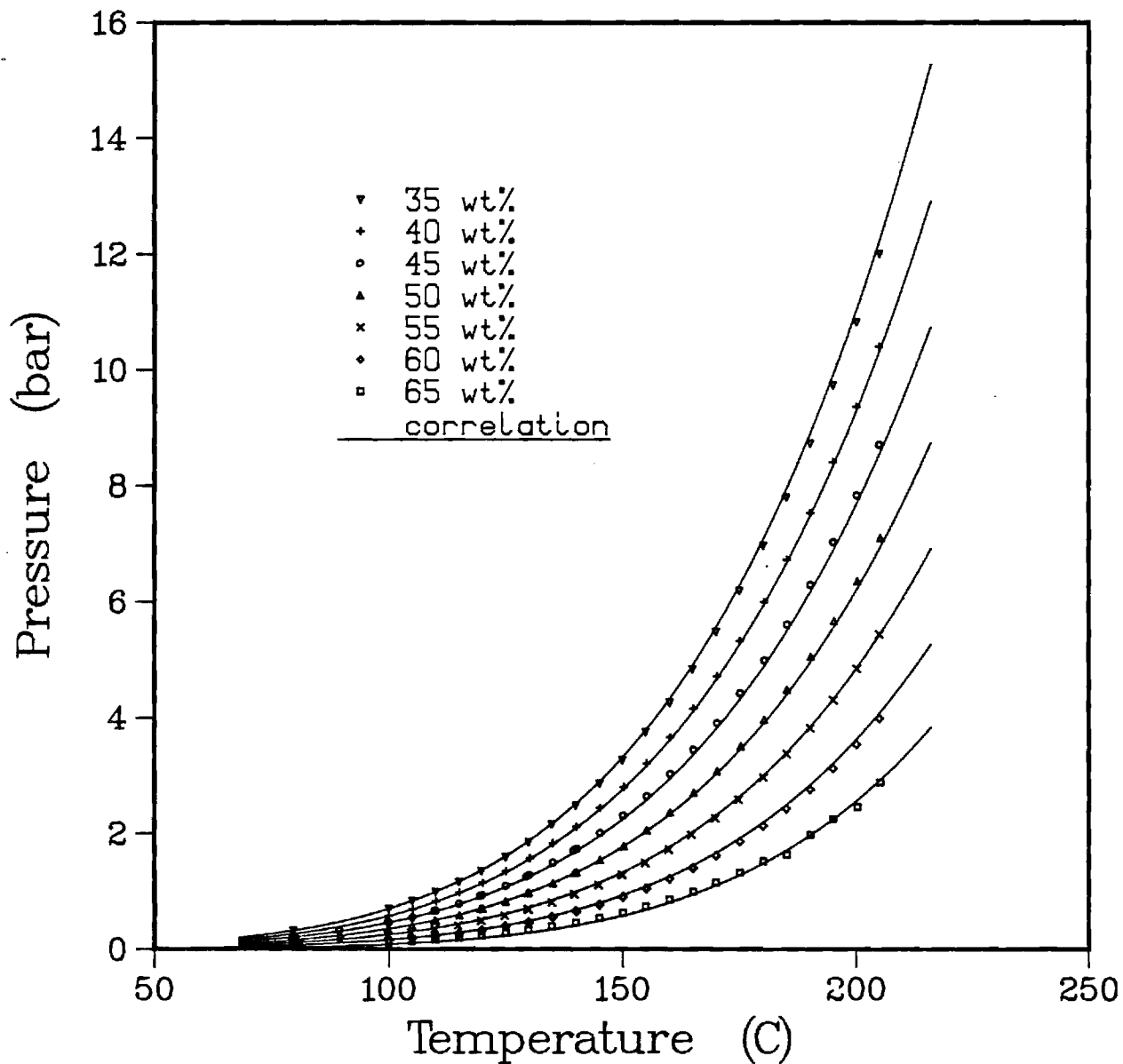
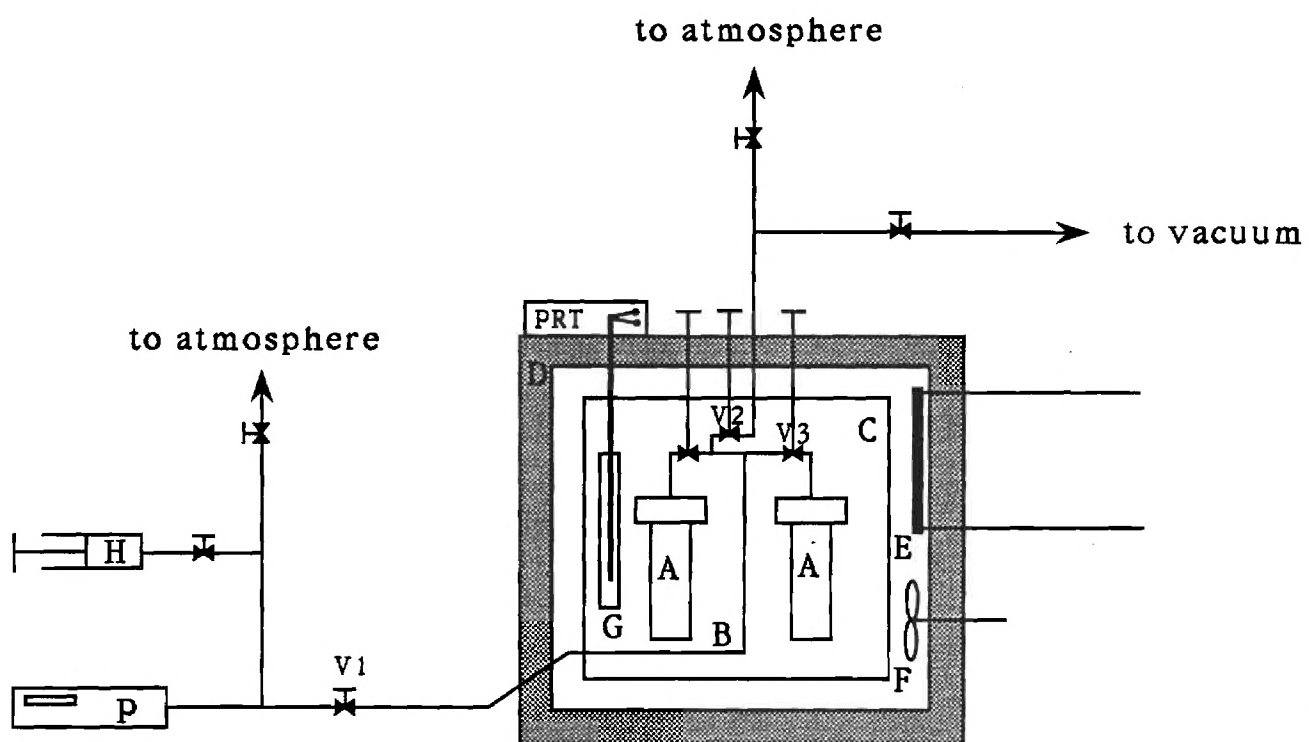


FIGURE 3.

SCHEMATIC OF THE STATIC VLE APPARATUS



- A cell
- B manifold
- C inner bath
- D insulating oven wall
- E heater
- F fan
- G Platinum Resistance Thermometer
- H pressure generator
- P pressure gauge

FIGURE 4.

PRESSURE TRANSMITTING PRINCIPLE

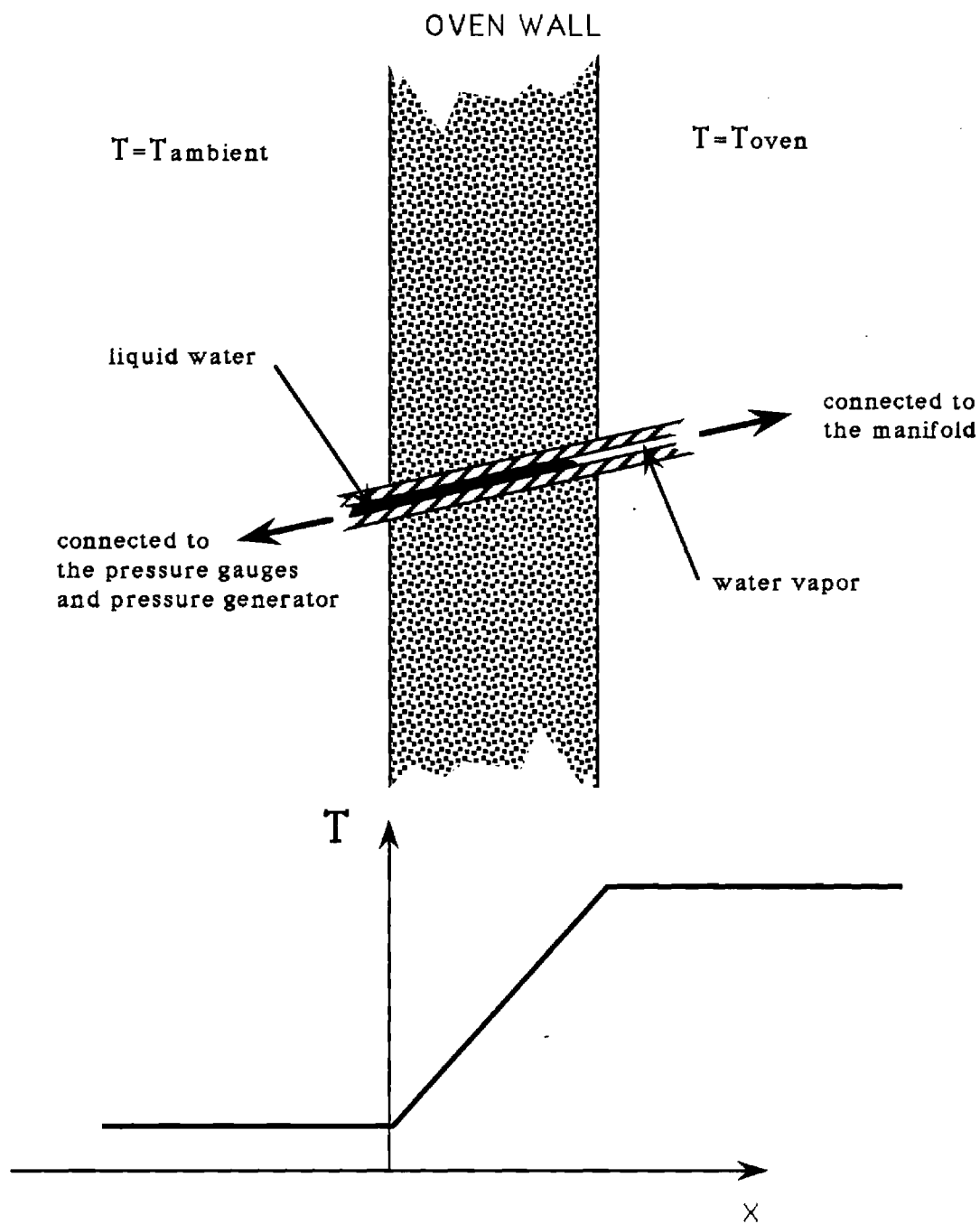


TABLE 1: CORRELATION PARAMETERS

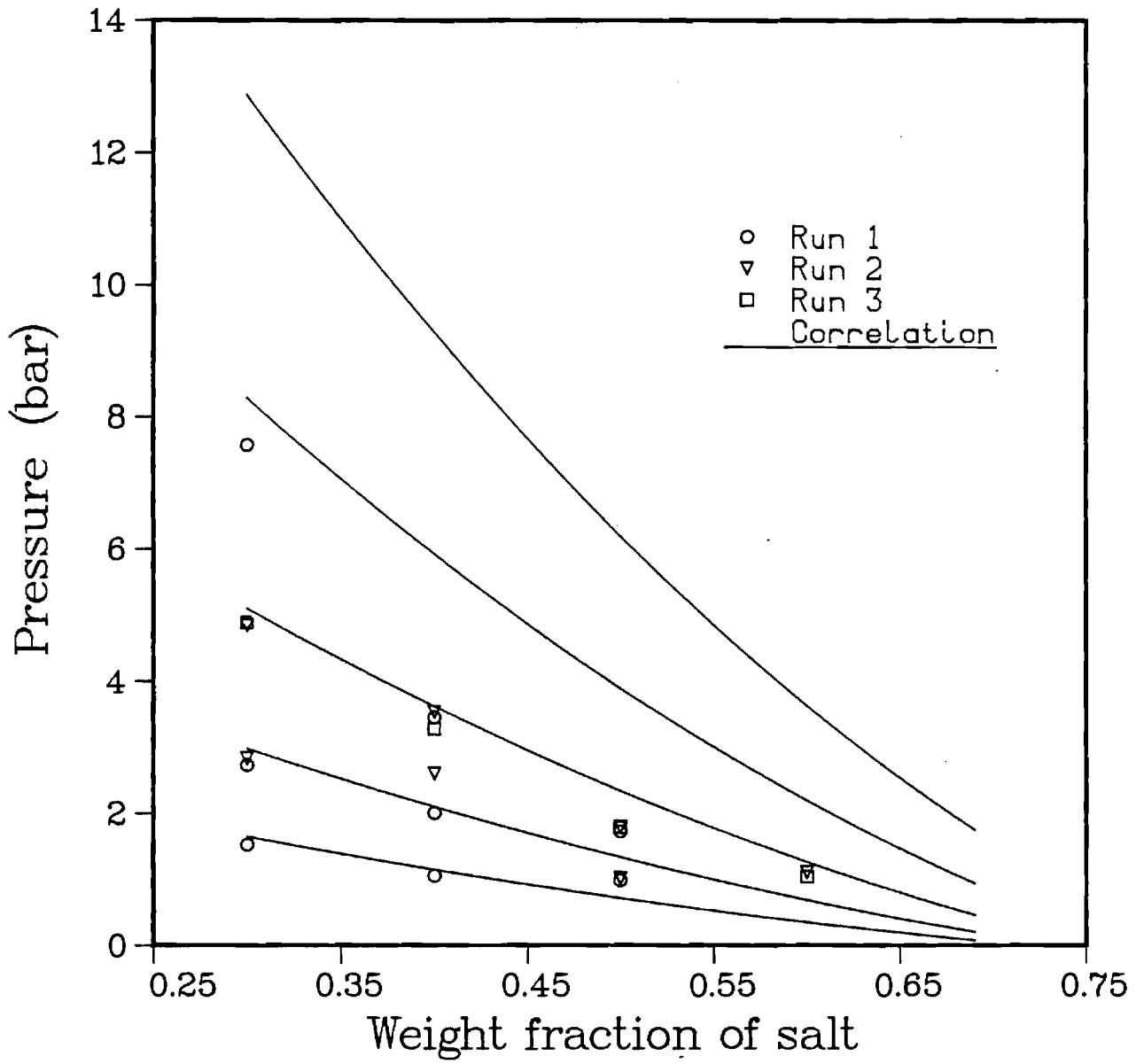
PARAMETER	VALUE
A1	0.293864
A2	-2.27627
A3	0.0022881
A4	1.64234
A5	-0.0006203

TABLE 2 : PRELIMINARY RESULTS

	RUN 1		RUN 2		RUN 3	
CELL	T (C)	P (bar)	T (C)	P (bar)	T (C)	P (bar)
1			159.80	1.105	160.00	1.035
2	119.77 139.70 159.78	1.046 1.998 3.449	139.95 159.80	2.600 3.536	160.11	3.273
5	139.70 159.79	0.980 1.723	139.90 159.80	1.014 1.794	160.00	1.782
6	119.80 139.71 180.00	1.513 2.726 7.572	139.98 159.80	2.832 4.845	160.10	4.896

FIGURE 5.

COMPARISON WITH LITERATURE



E-19-670

FINAL REPORT

**THERMOPHYSICAL PROPERTY DATA FOR
LITHIUM BROMIDE/WATER SOLUTIONS
AT ELEVATED TEMPERATURES**

PREPARED FOR

**THE AMERICAN SOCIETY OF HEATING, REFRIGERATING AND
AIR-CONDITIONING ENGINEERS**

UNDER PROJECT ⁵²⁶526-RP

PREPARED BY

GEORGIA INSTITUTE OF TECHNOLOGY

SCHOOL OF CHEMICAL ENGINEERING

AND

**THE GEORGE W. WOODRUFF SCHOOL
OF MECHANICAL ENGINEERING**

MARCH 1991

FINAL REPORT

March 1991

**THERMOPHYSICAL PROPERTY DATA FOR
LITHIUM BROMIDE/WATER SOLUTIONS
AT ELEVATED TEMPERATURES**

PREPARED FOR

**THE AMERICAN SOCIETY OF HEATING, REFRIGERATING AND
AIR-CONDITIONING ENGINEERS**

UNDER PROJECT 526-RP

SUPERVISED BY

**TECHNICAL COMMITTEE 8.3
(ABSORPTION AND HEAT OPERATED MACHINES)**

PREPARED BY

**GEORGIA INSTITUTE OF TECHNOLOGY
SCHOOL OF CHEMICAL ENGINEERING
AND
THE GEORGE W. WOODRUFF SCHOOL OF MECHANICAL ENGINEERING**

AUTHORS:

**A. S. TEJA, PRINCIPAL INVESTIGATOR
S. M. JETER, CO-PRINCIPAL INVESTIGATOR**

**R. J. LEE, RESEARCH ENGINEER
R. M. DIGUILIO, GRADUATE RESEARCH ASSISTANT
J.-L. Y. LENARD, GRADUATE RESEARCH ASSISTANT
J. P. MORAN, GRADUATE RESEARCH ASSISTANT**

TABLE OF CONTENTS

1. Introduction
2. Thermal Conductivity
3. Density
4. Kinematic Viscosity
5. Liquid Specific Heat
6. Vapor Pressure

Appendices

- I. ASHRAE Paper AT-90-30-4 (3380, RP-527): "Properties of Lithium Bromide - Water Solutions at High Temperatures and Concentrations - I. Thermal Conductivity", R. M. DiGuilio, R. J. Lee, S. M. Jeter, and A. S. Teja, **ASHRAE Transactions 1990**, Vol. 96, Part 1, 1990.
- II. ASHRAE Paper AT-90-30-5 (3381, RP-527): "Properties of Lithium Bromide - Water Solutions at High Temperatures and Concentrations - II. Density and Viscosity", R. J. Lee, R. M. DiGuilio, S. M. Jeter, and A. S. Teja, **ASHRAE Transactions 1990**, Vol. 96, Part 1, 1990.

INTRODUCTION

Aqueous lithium bromide (LiBr) solutions and similar mixtures have long been used in absorption refrigeration. Accurate thermophysical data including thermodynamic and transport data are needed for adequate design analysis and evaluations of such systems. In the past, much of available thermophysical property data had been based on proprietary data or on the results of measurements that had not been fully disclosed or described. To alleviate this shortcoming, Technical Committee 8.3 initiated a project for the measurement of the following properties:

1. Thermal Conductivity
2. Density
3. Kinematic Viscosity
4. Liquid Specific Heat
5. Vapor Pressure

The Georgia Institute of Technology was selected as the contractor on this project. With assistance and forbearance from the sponsoring Technical Committee, the required measurements and data reduction and analysis are now been conducted. This report represents the completion of the project.

Important accomplishments of this project include the following:

1. The development and successful operation of a fused quartz thermal conductivity cell using a liquid metal thermometric fluid suitable for implementing the hot wire thermal conductivity measurement in an electrically conductive fluid.

2. The demonstration of a high pressure capillary viscometer system successfully used for measurements of the viscosity of a volatile fluid at elevated temperature.

3. Successful development and demonstration of an innovative static vapor pressure measurement system using water as the pressure transmitting fluid which is capable of highly accurate measurements of the pressure of water vapor above water solutions with non-volatile solutes.

4. Successful application of classical drop calorimetry with design improvements in temperature measurement and environmental control.

Details of the experimental procedures and designs are given in the following sections along with raw data and correlations. Two ASHRAE papers have already been generated reporting the results of this research. Copies of these papers are appended (see Appendix I and Appendix II).

The entire research team expresses its gratitude for the opportunity to be involved in this challenging and worthwhile project.

(This page intentionally left blank.)

Chapter 2

Thermal Conductivity of Lithium Bromide and Water Solutions

1 Introduction

The design of refrigeration and heat pump systems which use aqueous lithium bromide solutions requires accurate thermal conductivity data. Most literature data, however, are limited to low temperatures and low concentrations of lithium bromide. The objectives of this work were therefore to measure the properties of lithium bromide solutions at high temperatures and concentrations of lithium bromide.

The most accurate technique for the measurement of the thermal conductivity of liquids is the transient hot wire method (Nieto de Castro et al. (1986)) in which a thin wire immersed in the liquid is electrically heated. The temperature rise of the wire is used to determine the thermal conductivity of the liquid. Electrically conducting solutions can be measured with this technique, if the wire is electrically insulated from the liquid under study. The insulation blocks the flow of current through the liquid, which would confuse the interpretation of the voltage measurements. However, the addition of an insulating layer to the wire has proved difficult to achieve in practice, especially at higher temperatures. Nagasaka and Nagashima (1981) successfully insulated a platinum wire with a polyester coating and reported measurements up to 150 °C. Alloush et al. (1982) used a tantalum

filament coated with a layer of tantalum oxide to obtain data on LiBr solutions at temperatures up to 80 °C. Recently Kawamata et al. (1988) used the tantalum - tantalum oxide filament to make measurements on LiBr solutions up to 100 °C. However, they noted that the oxide coating failed to insulate the wire properly above 100 °C. This limitation was confirmed by our own efforts to use the tantalum - tantalum oxide filament at temperatures above 100 °C. This is shown in Figure 1, where the thermal conductivity of water measured with a tantalum wire is plotted as a function of temperature. Above 100 °C, deviation from the ESDU (1967) recommended values occurs. The probable reasons for failure are the cracks that develop in the insulation due to the unequal expansion coefficients of the base metal and the oxide and the decrease in dielectric strength with temperature of the oxide. Both effects might permit current paths into the liquid and allow polarization of the fluid near the wire. A different technique was pioneered by Omotani et al. (1981, 1982). This technique uses a fine glass capillary filled with liquid mercury instead of the insulated wire. The apparatus was used to measure the thermal conductivity of molten salts up to 300 °C. The accuracy of these measurements was verified by Tufeu et al. (1985) using a coaxial cylinder method to measure the thermal conductivities of some of the same systems. Since the liquid metal technique has been validated at the temperatures of interest in this study, it was adopted in this work. Measurements were made in the range of concentration from 30 weight percent (wt%) to 65 wt% LiBr and of temperature between 20 °C to 190 °C.

2 Apparatus and Procedure

The transient hot wire apparatus employed in this work is shown in Figure 2. The major components of the apparatus are a Wheatstone bridge, a power supply, and a data acquisition system.

The Wheatstone bridge consists of two $100 \pm 0.01 \Omega$ precision resistors, a resistance decade box (General Radio Model 1433 U) with a range of 0 - 111.11 Ω , and a hot wire cell. The hot wire cell was constructed of quartz and is shown in Figure 3. The cell is in the shape of a U tube with one leg consisting of a quartz capillary tube (13.6 cm long, 0.05 mm ID, 0.08 mm OD) and the other a larger bore quartz tube (2 mm ID by 4 mm OD). The open end of the U tube is supported with a piece of machinable ceramic. The connection between the larger tube and the capillary tube is achieved by drawing down the larger tubing and sealing the capillary tubing into place with silicone rubber (General Electric RTV-106). Originally, it was intended to use liquid gallium to fill the U tube since liquid gallium has the advantages of low toxicity and very low vapor pressures. However, the reactivity of gallium with water vapor at high temperatures forced the choice of mercury as the liquid metal. The entire U tube was filled with liquid mercury with the thread of mercury in the capillary tube serving as the hot wire. Small pieces of tungsten wire were inserted into the liquid mercury at each end of the open U-tube to serve as electrodes. The tungsten wires were, in turn, connected to copper wires attached to the bridge. The cell itself was placed in a glass sleeve with ceramic supports at the top and bottom of the U-tube to ensure that the U- tube remained centered in the sleeve. The sleeve was then placed inside a pressure vessel. A 0.0625 inch diameter Type E thermocouple probe was inserted through both ceramic supports along the axis of the larger bore tube. The bridge was powered by a precision power supply (Hewlett-Packard Model 6213A) which served as a constant voltage source. The supply was used both to balance the bridge and provide the voltage for heating. A lab quality multimeter (Fluke Model 8840A) was used to indicate a balanced condition in the bridge. A data acquisition system consisting of an IBM PC XT with a 16 bit analog to digital converter card (Strawberry Tree ACPC-16) was used to read both the offset voltage and the applied voltage.

The test fluid was loaded into the glass sleeve and the sleeve was inserted into a stainless steel pressure vessel. The quartz cell was then lowered into the glass sleeve and the pressure vessel was sealed. The apparatus was then placed in a fluidized sand bath (Techne Model SBL-2D) which maintained the temperature to ± 0.1 °K. The sample was pressurized to 15 bar with nitrogen to prevent boiling during measurement. A Type E thermocouple, calibrated against a PRT (Leeds and Northrup SN 709892), was used to determine the stability of the bath and the sample equilibrium temperatures. After temperature equilibrium had been achieved, the air flow to the sand bath was stopped to prevent any vibration of the cell during measurement.

The procedure for each measurement was as follows. The bridge was first balanced and the computer program started. The program initiated a step input to the bridge using an electromechanical relay (Magnecraft W172DIP-1). The relay settled in less than 0.3 milliseconds. The program sampled the offset voltage on one channel, then switched channels to sample the applied voltage to insure its constancy. The time between any two samples was 0.0084 seconds and that between two successive readings of the same channel was 0.0168 seconds. The delay between the closing of the relay and the first sampling was found to be 0.0132 seconds using an oscilloscope. Two hundred points were measured during each run and the experiment lasted about 3.4 seconds. From a previous calibration of the temperature versus resistance, the temperature of the wire was found. A plot of ΔT versus the logarithm of time was made and the slope in the time interval from 0.7 to 2.2 seconds was calculated using a least squares fit as described in the analysis section. The applied voltage was varied from about 2.5 to 3.5 V so that a more or less constant temperature rise in the quartz capillary surface of about 1.4 °C was achieved. This resulted in offset voltages on the order of 5 mV. The A/D card has 16 bit resolution and the ± 25 mV range was used. Thus the card is capable of 0.8 μV resolution.

3 Source and Purity of Materials

Anhydrous lithium bromide was obtained from Morton Thiokol Inc. (Lots F06H, L02F, and H26G). The minimum stated purity of the sample was 99 wt% LiBr. Distilled water was used to prepare the solutions. Solutions were first prepared gravimetrically based on weight percent LiBr. To ensure that no change in the composition of a solution occurred during the measurement procedure, samples of each composition were taken before and after the thermal conductivity measurement and checked using a computer aided titrimer (Fisher CAT System including Controller Model 450, Buret Model 400 and Stirrer Model 460). The precipitation titration was done using a 0.1 Normal standard silver nitrate solution as the titrant (Fisher, Cat. No. SS72-500, .1000 \pm 0.0002 Normality). A silver specific electrode (Fisher Cat. No. 13-620-122) was used to indicate the equivalence point, and a standard calomel electrode (Fisher Cat. No. 13-620-51) was used as the reference electrode. The compositions reported are the averages of two titrations. The average deviation between any pair of measurements was 0.4% and the maximum deviation was 0.8%. This agreement indicates that there was little variation in composition during the thermal conductivity measurement.

4 Analysis

The model for the experiment is an infinite line source of heat submersed in an infinite fluid medium. By monitoring the temperature response of the wire to a step voltage input, the thermal conductivity of the fluid can be deduced. For an infinite line source of heat in an infinite fluid medium, the ideal temperature rise of the wire ΔT_{id} can be calculated using an expression derived by Carslaw and Jaeger (1959) and Healy et al. (1976) for $t \gg \frac{r_w^2}{4\alpha}$, where r_w is the radius of the filament and α is the thermal diffusivity of the fluid. The

inequality is satisfied shortly after heating is started, that is, for 10 milliseconds $< t <$ 100 milliseconds. The expression is:

$$\Delta T_{id} = \frac{q}{4\pi\lambda} \ln \left(\frac{4\lambda t}{r_w^2 \rho C_p C} \right) \quad (1)$$

where q is the heat dissipation per unit length, λ is the thermal conductivity, ρ the density, C_p the heat capacity, t the time from the application of the step voltage and C is equal to $\exp(\gamma)$ where γ is Euler's constant. If it is assumed that all physical properties are independent of temperature over the small range of temperature considered (ca. 1.4 °C), then,

$$\lambda = \frac{q}{4\pi \left(\frac{d\Delta T_{id}}{d \ln t} \right)} \quad (2)$$

where $\frac{d\Delta T_{id}}{d \ln t}$ is found experimentally from a plot of ΔT_{id} vs $\ln t$.

Healy et al. (1976) also derived several corrections for the deviation of the model from reality. These may be written as:

$$\Delta T_{id} = \Delta T_w(t) + \sum_i \delta T_i \quad (3)$$

δT_1 accounts for the finite physical properties of the wire (liquid mercury) and is given by Healy et al. (1976):

$$\delta T_1 = \frac{r_w^2 [(\rho C_p)_w - (\rho C_p)]}{2\lambda t} \Delta T_{id} - \frac{q}{4\pi\lambda} \frac{r_w^2}{4\alpha t} \left(2 - \frac{\alpha}{\alpha_w} \right) \quad (4)$$

where $(\rho C_p)_w$ is the volumetric heat capacity of the liquid mercury and α and α_w are the thermal diffusivity of the fluid and mercury respectively.

The correction due to the finite extent of the fluid is given by Healy et al. (1976):

$$\delta T_2 = \frac{q}{4\pi\lambda} \left(\ln \frac{4\alpha t}{b^2 C} + \sum_{\nu=1}^{\infty} \exp^{-g_\nu^2 \alpha t / b^2} [\pi Y_0(g_\nu)]^2 \right) \quad (5)$$

where b is the inside diameter of the cell, Y_0 is the zero order Bessel function of the second kind and g_ν are the roots of J_0 , the zero order Bessel function of the first kind. Although the

first several roots are readily available, the higher roots can be found to sufficient accuracy using an expression from the work of Watson (1962):

$$g_\nu = (\pi\nu - \pi/4) + \frac{1}{8(\pi\nu - \pi/4)} - \frac{31}{385(\pi\nu - \pi/4)^3} + \frac{3779}{15366(\pi\nu - \pi/4)^5} \quad (6)$$

Values of Y_o were calculated using the polynomial approximation given by Abramowitz and Stegun (1965).

The effect of the quartz capillary tube on the measurement has been evaluated analytically by Nagasaka and Nagashima (1981). The correction is given by:

$$\delta T_3 = \frac{-q}{4\pi\lambda} \left[\ln \left(\frac{r_w}{r_l} \right)^2 + \frac{2\lambda}{\lambda_l} \ln \frac{r_l}{r_w} + \frac{\lambda}{\lambda_l} + A \right] \quad (7)$$

with :

$$\begin{aligned} A &= \frac{1}{t} (C0 + B \ln t) \\ C0 &= C1 + C2 + B \ln \left(\frac{4\alpha}{r_l^2 C} \right) \\ C1 &= \frac{r_w^2}{8} \left[\left(\frac{\lambda - \lambda_l}{\lambda_w} \right) \left(\frac{1}{\alpha_w} - \frac{1}{\alpha_l} \right) + \frac{4}{\alpha_l} - \frac{2}{\alpha_w} \right] \\ C2 &= \frac{r_l^2}{2} \left(\frac{1}{\alpha} - \frac{1}{\alpha_l} \right) + \frac{r_w^2}{\lambda_l} \left(\frac{\lambda_l}{\alpha_l} - \frac{\lambda_w}{\alpha_w} \right) \ln \left(\frac{r_l}{r_w} \right) \\ B &= \frac{r_w^2}{2\lambda} \left(\frac{\lambda_l}{\alpha_l} - \frac{\lambda_w}{\alpha_w} \right) + \frac{r_l^2}{2\lambda} \left(\frac{\lambda}{\alpha} - \frac{\lambda_w}{\alpha_w} \right) \end{aligned}$$

where r_l, α_l, λ_l are the radius, thermal diffusivity, and thermal conductivity of the quartz capillary.

Radiation by the fluid can be accounted for using an analytical expression for the temperature rise of the mercury thread given by Nieto de Castro et al. (1983):

$$\Delta T = \frac{q}{4\pi\lambda} \left(1 + \frac{Br_w^2}{4\alpha} \right) \ln \frac{4\alpha t}{r_w^2 C} + \frac{Bqr_w^2}{16\pi\alpha\lambda} - \frac{Bqt}{4\pi\lambda} \quad (8)$$

where B is the radiation parameter and is a measure of the contribution of radiant emission by the fluid to the heat transfer process. From Equation 8 Nieto de Castro et al. (1983) derived the following expression for the correction to the observed temperature rise:

$$\delta T_4 = \frac{-qB}{4\pi\lambda} \left(\frac{r_w^2}{4\alpha} \ln \frac{4\alpha t}{r_w^2 C} + \frac{r_w^2}{4\alpha} - t \right) \quad (9)$$

They used Equation 8 to show that emission from a fluid causes the ΔT vs $\ln t$ slope to exhibit a slight curvature, concave to the $\ln t$ axis.

ΔT , after correction for the other effects mentioned, can be fit to Equation 8 to obtain B as suggested by Nieto de Castro et al. (1983). Equation 9, then can be used to calculate δT_4 . If there is no radiation contribution, B is equal zero and thus there is no danger of biasing the data.

Since both sides of the U tube are made of quartz and the mercury is free to expand, there are no effects due to wire-slackening which must be accounted for in conventional hot wire methods. End effects however, must still be considered. These effects result mostly from conduction of heat axially away from the mercury thread to the thicker leads. No analytical correction exists for this source of error and it is generally compensated for experimentally using either potential leads at the top and bottom of the filament or by using a long and a short wire. However, liquid mercury has a thermal conductivity only about 10% of that of platinum, which is commonly used in hot wire apparatus. Therefore, any end effects were expected to be small or negligible in our experiments. This expectation was experimentally verified by the excellent agreement of our data with the IUPAC (1987) data for water and with the data of Kawamata et al. (1988) for LiBr solutions. Kawamata et al. (1988) used a two wire technique to account for end effects.

The actual temperature at which the thermal conductivity is reported is the average temperature of the fluid during the heating process. That is:

$$T_R = T_o + \frac{\Delta T(t_I) + \Delta T(t_F)}{2} \quad (10)$$

where T_o is the temperature of the fluid at the start of a measurement, and t_I and t_F refer to the initial and final times of the data used to find the slope of ΔT vs $\ln t$. In the case of an insulated wire, ΔT refers to the temperature at the surface of the insulation adjacent to the liquid. This temperature has been determined by Nagasaka and Nagashima (1981) and is given by:

$$\Delta T_i = \frac{q}{4\pi\lambda} \left[\frac{(P3 + P2 + P1)}{t_i} + \ln \left(\frac{4\alpha t_i}{r_i^2 C} \right) \right] \quad (11)$$

with :

$$P3 = \frac{r_w^2}{4} \left(\frac{1}{\alpha_l} - \frac{1}{2\alpha_w} \right) + \frac{r_l^2}{4} \left(\frac{1}{\alpha} - \frac{1}{\alpha_l} \right)$$

$$P2 = \frac{r_w^2}{2\lambda_l} \left(\frac{\lambda_l}{\alpha_l} - \frac{\lambda_w}{\alpha_w} \right) \ln \left(\frac{r_l}{r_w} \right)$$

$$P1 = \ln \left(\frac{4\alpha t_i}{r_i^2 C} \right) \left[\frac{r_w^2}{2\lambda} \left(\frac{\lambda_l}{\alpha_l} - \frac{\lambda_w}{\alpha_w} \right) + \frac{r_l^2}{2\lambda} \left(\frac{\lambda}{\alpha} - \frac{\lambda_l}{\alpha_l} \right) \right]$$

where the subscript i refers to t_I or t_F .

In order to apply the temperature corrections, various physical properties are required. The density and heat capacity of mercury were obtained from the CRC handbook (1988), and the thermal conductivity from the compilation of Ho et al. (1972), and the electrical resistivity from the work of Williams (1925). The thermal conductivity and the heat capacity of quartz were obtained from the Thermophysical Properties Research Center compilations (1972a,b). Finally, the heat capacity and density of lithium bromide solutions were measured in our laboratory.

The maximum correction δT_1 for the physical properties of the wire was 0.23% of ΔT_{id} . The correction for the finite extent of the fluid δT_2 was negligible, never exceeding 0.0002% of ΔT_{id} . The maximum correction for radiation δT_4 was less than 0.0004% of ΔT_{id} . Both δT_2 and δT_4 were included for consistency, although they were negligible. As expected, the correction for the insulation layer, δT_3 , was significant. The magnitude of δT_3 varied from about 12% to 16% of ΔT_{id} over the time interval of the measurement. Thus, the correction adds an offset to the temperature rise measured, although the slope $\frac{d\Delta T_{id}}{d \ln t}$ is only slightly affected. A typical ΔT_{id} vs $\ln t$ curve is shown in Figure 4. Only the data from about 0.7 seconds to 2.2 seconds were used to calculate $\frac{d\Delta T_{id}}{d \ln t}$. In order to calculate the corrections, an estimate of the thermal conductivity of the fluid is needed. This estimate was obtained by using ΔT_w , the measured temperature rise of the wire instead of ΔT_{id} to calculate the thermal conductivity. Using this estimate, the corrections δT_1 , δT_2 and δT_3 could be calculated and the corrected temperature rise data fit to Equation 8 to obtain B. The radiation parameter was then used to calculate δT_4 and hence ΔT_{id} . Finally, the thermal conductivity of the fluid was obtained using ΔT_{id} . This new thermal conductivity estimate generally differed from the original estimate. Furthermore, the physical properties required in the calculations had to be adjusted to reflect the actual average temperature of the system between 0.7 seconds and 2.2 seconds. This was done with Equation 10. In practice, the temperature of the system increased from about 0.8° to 1.2°C above the original equilibrium temperature during the time interval 0.7 seconds to 2.2 seconds. This resulted in an average temperature adjustment of about 1°C. The temperature corrections were re-evaluated using the new value of the thermal conductivity of the fluid and the adjusted temperature of the system. This series of calculations was repeated until no change in the thermal conductivity occurred. Three iterations were typically required for convergence.

5 Results

Water was measured at room temperature to validate the liquid metal capillary technique. The agreement with the IUPAC data was excellent, with deviations between our measurements and IUPAC data being within 0.6%. However, the thermal conductivity of water at higher temperatures could not be measured because the low viscosity of water allowed convection to occur during the heating process. Fortunately, the viscosities of lithium bromide solutions were high enough to prevent the rapid onset of convection. In order to verify the linearity of the ΔT vs $\ln t$ curves, the deviation from the linear fit was checked. Figure 5 shows a plot of the deviation from the fitted line for the same ΔT vs $\ln t$ curve shown in Figure 4. The points are evenly scattered so that no bias is evident.

Seven compositions of lithium bromide - water solutions were measured (30.2, 44.3, 49.1, 56.3, 60.0, 62.9, and 64.9 wt% LiBr) in the temperature range from 20 ° to 190 °C. The data are compiled in Table 1 and are shown graphically in Figure 5. Each data point represents the average of five experimental runs. The maximum deviation from the average value never exceeded 1.0%, and the precision of the data is therefore 1.0%.

The accuracy of the data was estimated from the sum of the bias error ϵ_b and the random error ϵ_r . The bias error was estimated from:

$$\epsilon_b = \epsilon_{b,LT} + \frac{\partial \epsilon_b}{\partial T} \Delta T_M \quad (12)$$

where $\epsilon_{b,LT}$ is the low temperature bias and ΔT_M is the temperature difference between the highest temperature at which the thermal conductivity was measured and the reference temperature. The low temperature bias was obtained by comparing our data on water with IUPAC data. Since our data were consistently about 0.6% high by comparison with the IUPAC data, we estimate the low temperature bias error to be 0.6%. Comparison of our data with literature data for temperatures up to 100°C (see Table 2) showed no apparent

trends in the bias error with temperature. Thus we concluded that $\frac{\partial \epsilon_r}{\partial T}$ is approximately zero and the bias is 0.6% at all temperatures. Random error was estimated from three sources: the uncertainty in the thermal conductivity measurement, the uncertainty in the reported concentration and the uncertainty in the equilibrium temperature of the fluid, with

$$\epsilon_r^2 = \epsilon_m^2 + \left(\frac{\partial \lambda}{\partial W} \frac{\delta W}{\lambda} \right)^2 + \left(\frac{\partial \lambda}{\partial T} \frac{\delta T}{\lambda} \right)^2 \quad (13)$$

The uncertainty in the measurement ϵ_m was 1%. The sensitivity of the thermal conductivity to temperature and concentration were found using the correlation for thermal conductivity reported in the next section of this paper. The maximum value of $\frac{\partial \lambda}{\partial W} \frac{1}{\lambda}$ was found to be $-0.011 \text{ wt}\%^{-1}$ and the maximum uncertainty in the composition was $\pm 0.8 \text{ wt}\%$. The maximum value of $\frac{\partial \lambda}{\partial T} \frac{1}{\lambda}$ was found to be 0.003 K^{-1} and the maximum uncertainty in the temperature measurement was $\pm 0.2 \text{ K}$. The total random error was thus less than 1.4% and the total error was $\pm 2\%$.

Direct comparison of our data with literature data is difficult due to differences in concentrations. Table 2 is a comparison of the correlation found using only our data with the data of Kawamata et al. (1988), Alloush et al. (1982), Uemura and Hasaba (1963), and Riedel (1951). The agreement between our data and Kawamata et al. who claim an accuracy of $\pm 0.5\%$ is excellent. The average deviation on 15 data points is 0.65% and the maximum is 1.8%. Agreement with Uemura and Hasaba is also excellent. The average deviation on 25 data points is 0.63% and the maximum is 1.9%. The single point from Riedel that lies in our concentration range agrees within 1.1%. The data of Alloush et al. show much larger deviation. The average deviation for 19 points is 2.1% with a maximum deviation of 4.4%. However, Alloush et al. claimed an accuracy of only $\pm 3.0\%$. Therefore, the overall agreement is within the accuracy of their experiments.

Kawamata et al. (1988) measured the thermal conductivity of LiBr solutions at three concentrations (30.3, 46.5, and 56.6 wt % LiBr) at pressures up to 40 MPa. The effect of pressure was found to be small. For example, at 56.6 wt% LiBr and 100 °C, the change in thermal conductivity from .1 MPa to 40 MPa was only 1.7%. Consequently, any dependence of the thermal conductivity on pressure is insignificant both in engineering calculations and as an influence on the measurements reported herein.

6 Correlation

The thermal conductivity of the lithium bromide solutions was correlated with temperature T in K and composition X in wt % as follows:

$$\lambda(T, X) = A(T) + B(T)X + C(T)X^2 \quad (14)$$

with :

$$A(T) = a_1 + a_2T + a_3T^2$$

$$B(T) = b_1 + b_2T + b_3T^2$$

$$C(T) = c_1 + c_2T + c_3T^2$$

Values of the constants $a_1, a_2, a_3, b_1, b_2, c_1, c_2, c_3$ were obtained by regression of the data obtained in this work and are given in Table 3. The average absolute deviation between correlation and experiment was found to be .6% for 47 data points and the maximum deviation was found to be 1.6%. The fitted curves are shown on Figure 6.

7 Conclusions

The thermal conductivity of aqueous solutions of lithium bromide ranging in composition from 30 to 65 wt % and in temperature from 20 ° to 190 °C were measured. The precision of the data is $\pm 1\%$ and the accuracy is estimated to be $\pm 2\%$. A correlation was developed which was able to fit the data with an average absolute deviation of 0.6% and a maximum deviation of 1.6%.

References

- [1] M. Abramowitz and I. A. Stegun, editors. *Handbook of Mathematical Functions*. Dover, New York, 1965.
- [2] A. Alloush, W. B. Gosney, and W. A. Wakeham. *Int J Thermophysics*, 3:225, 1982.
- [3] H. S. Carslaw and J. C. Jaeger. *Conduction of Heat in Solids*. Oxford University Press, London, second edition, 1959.
- [4] C. A. Nieto de Castro, S. F. Y. Li, C. Maitland, and W. A. Wakeham. *Int J Thermophysics*, 4:311, 1983.
- [5] C. A. Nieto de Castro, S. F. Y. Li, A. Nagashima, R. D. Trengrove, and W. A. Wakeham. *J Phys Chem Ref Data*, 15:1073, 1986.
- [6] ESDU. *Thermal Conductivity of Water Substance*. Technical Report 67031, Engineering Sciences Data Unit, London, 1967.
- [7] J. J. Healy, J. J. de Groot, and J. Kestin. *Physica*, 82C:392, 1976.
- [8] C. Y. Ho, R. W. Powell, and P. E. Liley. *J Phys Chem Ref Data*, 1:279, 1972.
- [9] M. Hoshi, T. Omotani, and A. Nagashima. *Rev Sci Instrum*, 52:755, 1981.
- [10] K. Kawamata, Y. Nagasaka, and A. Nagashima. *Int J Thermophysics*, 9:317, 1988.
- [11] K. N. Marsh, editor. *Recommended Reference Materials for the Realization of Physicochemical Properties*. Blackwell Scientific Publications, Boston, 1987.
- [12] Y. Nagasaka and A. Nagashima. *J Phys E: Sci Instrum*, 14:1435, 1981.
- [13] T. Omotani, Y. Nagasaka, and A. Nagashima. *Int J Thermophysics*, 3:17, 1982.

- [14] L. Riedel. *Chem Ingr Tech*, 23:59, 1951.
- [15] Y. S. Touloukian and C. Y. Ho, editors. *Specific Heat of Nonmetallic Solids*. Volume 5 of *The Thermophysical Properties Research Center Data Series*, Plenum Press, New York, 1972.
- [16] Y. S. Touloukian and C. Y. Ho, editors. *Thermal Conductivity of Nonmetallic Solids*. Volume 2 of *The Thermophysical Properties Research Center Data Series*, Plenum Press, New York, 1972.
- [17] R. Tufeu, J. P. Petitet, L. Denielou, and B. Le Neindre. *Int J Thermophysics*, 6:315, 1985.
- [18] T. Uemura and S. Hasaba. *Refrig Japan*, 38:19, 1963.
- [19] G. N. Watson. *A Treatise on the Theory of Bessel Functions*. Cambridge University Press, Cambridge, England, second edition, 1962.
- [20] R. C. Weast, editor. *CRC Handbook of Chemistry and Physics*. CRC Press, Inc., Boca Raton, Florida, 69 edition, 1988.
- [21] E. J. Williams. *Phil Mag*, 50:589, 1925.

Table I: Thermal Conductivity of LiBr - Water Solutions

Wt% LiBr	T [K]	λ [mW/M K]	Wt% LiBr	T [K]	λ [mW/M K]	
0.0	293.8	602.3	49.1	401.2	513.5	
	296.7	607.6		430.0	522.0	
	323.4	646.0		460.0	523.0	
30.2	292.9	508.1	56.3	294.1	419.0	
	296.9	512.1		329.4	453.5	
	326.1	544.6		362.3	468.4	
	329.1	545.9		397.6	484.2	
	359.5	570.7		430.1	493.5	
	365.0	579.5		461.1	501.6	
	385.2	592.0		60.0	299.6	408.8
	388.9	592.8			329.2	432.9
	404.7	597.5			369.7	457.5
	434.0	591.1			402.5	473.4
44.3	435.7	590.2	62.9	430.8	476.5	
	461.3	573.8		460.6	485.8	
	295.1	467.5		339.8	429.5	
	321.4	495.4		371.0	447.2	
	353.5	521.4		400.4	457.3	
	378.6	535.5		430.7	465.4	
	407.2	550.9		460.9	476.1	
	439.2	557.3		64.9	343.4	421.0
	463.3	553.4			370.5	432.1
	298.0	446.7			400.7	442.0
49.1	328.9	478.1	64.9	428.8	453.0	
	371.6	503.9		461.0	458.2	

Table II: Comparison of this Work with the Literature [P = 1 atm]

T [K]	Wt% LiBr	λ [mW/M K] Literature	Ref.	λ [mW/M K] This Work ¹	Claimed Accuracy [\pm %]	% Dev.
293.8	0.0	599.1	[14]	602.3 ²		0.55
296.7		604.1	[14]	607.6 ²		0.58
323.4		642.6	[14]	646.0 ²		0.52
323	26.04	557	[19]	558.0		0.18
313	26.05	551	[19]	545.5		-1.01
353	26.08	581	[19]	586.7		0.97
303	26.28	426	[19]	530.9		0.82
333	26.52	564	[19]	567.4		0.60
304.2	30.3	527.7	[4]	520.7	0.5	-1.35
313.9		536.0	[4]	533.2	0.5	-0.53
333.9		558.6	[4]	555.3	0.5	-0.60
353.5		575.1	[4]	572.1	0.5	-0.53
373.5		588.5	[4]	584.2	0.5	-0.73
313	34.93	521	[19]	516.8		-0.81
303	35.61	503	[19]	502.6		-0.09
323	35.90	521	[19]	524.4		0.65
293	36.21	492	[19]	487.8		-0.87
333	36.29	533	[19]	532.8		-0.04
343	36.50	547	[19]	540.8		-1.15
353	36.53	538	[19]	548.4		1.89
293	40	471	[20]	476.2		1.08
297.0	41.4	473	[3]	476.5	3.0	0.74
305.0		478	[3]	485.7	3.0	1.58
315.0		484	[3]	496.3	3.0	2.49
335.0		500	[3]	515.1	3.0	2.94
357.0		511	[3]	531.9	3.0	3.93
303	44.84	465	[19]	471.5		1.37
333	44.94	501	[19]	499.5		-0.30
323	44.98	489	[19]	490.6		0.33
313	44.99	486	[19]	481.1		-1.01
353	45.42	509	[19]	512.6		0.71
297.0	45.6	465	[3]	462.4	3.0	-0.56
305.0		467	[3]	470.9	3.0	0.82
315.0		469	[3]	480.8	3.0	2.45
335.0		483	[3]	498.5	3.0	3.10
357.0		499	[3]	514.6	3.0	3.02
293	46.05	459	[19]	456.5		-0.55
302.4	46.5	468.2	[4]	464.9	0.5	-0.70
313.8		477.3	[4]	476.2	0.5	-0.22
333.3		490.8	[4]	493.4	0.5	0.54
353.6		501.4	[4]	508.5	0.5	1.40
373.2		510.9	[4]	520.3	0.5	1.81

¹Values calculated from correlation of our data²Experimental Value (pure water not included in correlation).

Table II: Comparison of this Work with the Literature (Continued)

T [K]	Wt% LiBr	λ [mW/M K] Literature	Ref.	λ [mW/M K] This Work ¹	Claimed Accuracy [\pm %]	% Dev.
297.0	49.7	457	[3]	448.0	3.0	-2.01
305.0		463	[3]	455.8	3.0	-1.57
315.0		464	[3]	465.0	3.0	0.22
335.0		478	[3]	481.6	3.0	0.75
357.0		493	[3]	497.0	3.0	0.80
297.0	53.8	452	[3]	432.9	3.0	-4.40
305.0		457	[3]	440.2	3.0	-3.82
315.0		461	[3]	448.7	3.0	-2.74
335.0		474	[3]	464.2	3.0	-2.11
313	54.25	444	[19]	445.2		0.28
302.8	56.6	428.6	[4]	427.3	0.5	-0.31
313.6		438.0	[4]	436.1	0.5	-0.43
333.5		452.4	[4]	451.0	0.5	-0.32
353.7		464.0	[4]	464.1	0.5	0.01
373.5		473.7	[4]	475.0	0.5	0.27
353	56.61	463	[19]	463.6		0.13
323	56.62	442	[19]	443.3		0.30
293	56.70	416	[19]	418.4		0.57
303	56.71	429	[19]	427.0		-0.46
333	56.75	451	[19]	450.0		-0.23
313	60.35	418	[19]	420.0		0.47

Table III: Constants for Correlation

Constant	Value
a_1	-1407.5255
a_2	11.051253
a_3	$-1.4674147 \times 10^{-2}$
b_1	38.985550
b_2	-0.24047484
b_3	3.4807273×10^{-4}
c_1	-0.26502516
c_2	1.5191536×10^{-3}
c_3	$-2.3226242 \times 10^{-6}$

WATER MEASURED WITH TANTALUM CELL

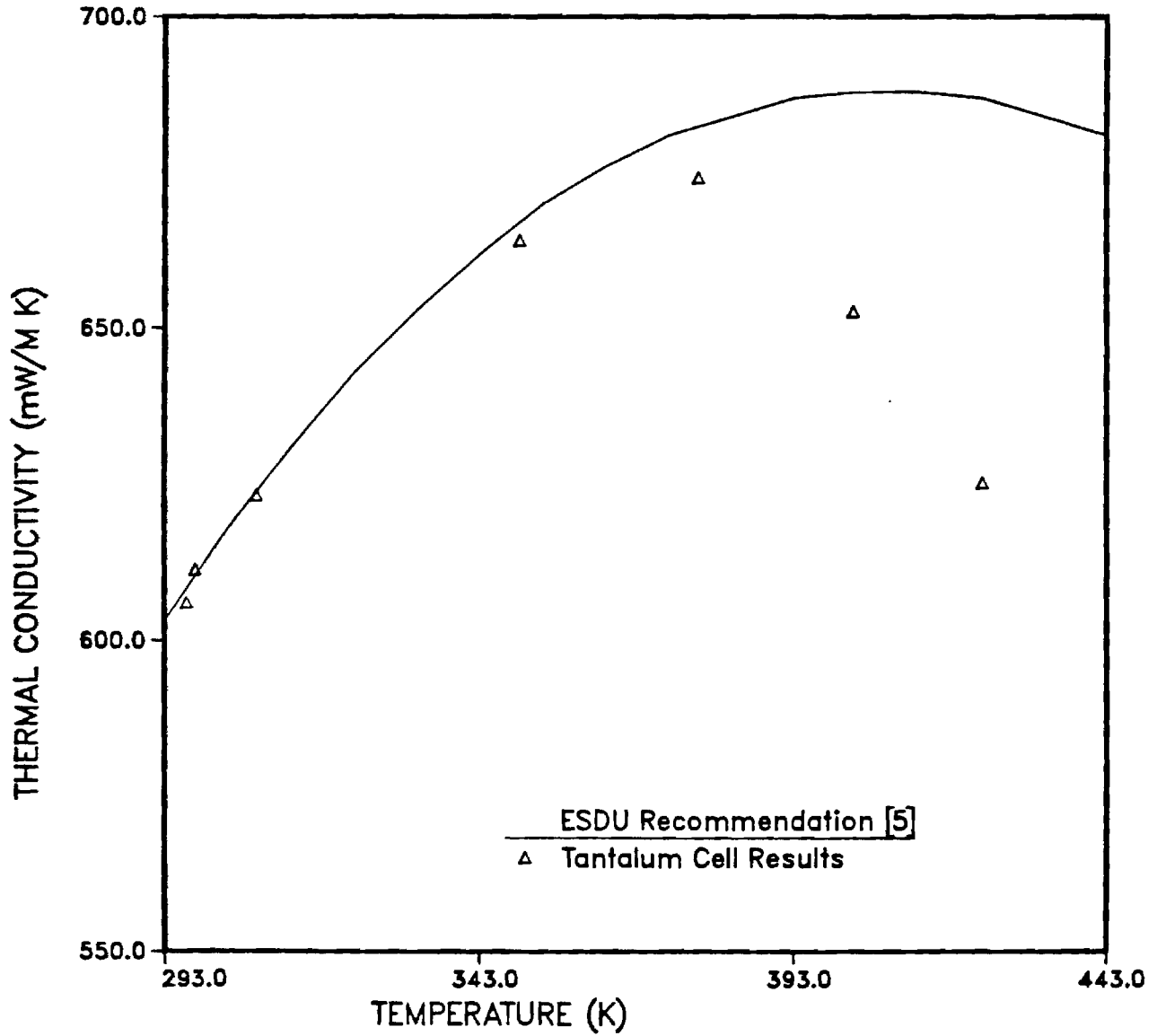


Figure 1: Thermal conductivity of water measured with a tantalum filament insulated with tantalum oxide. The oxide coating fails to insulate above 100 °C.

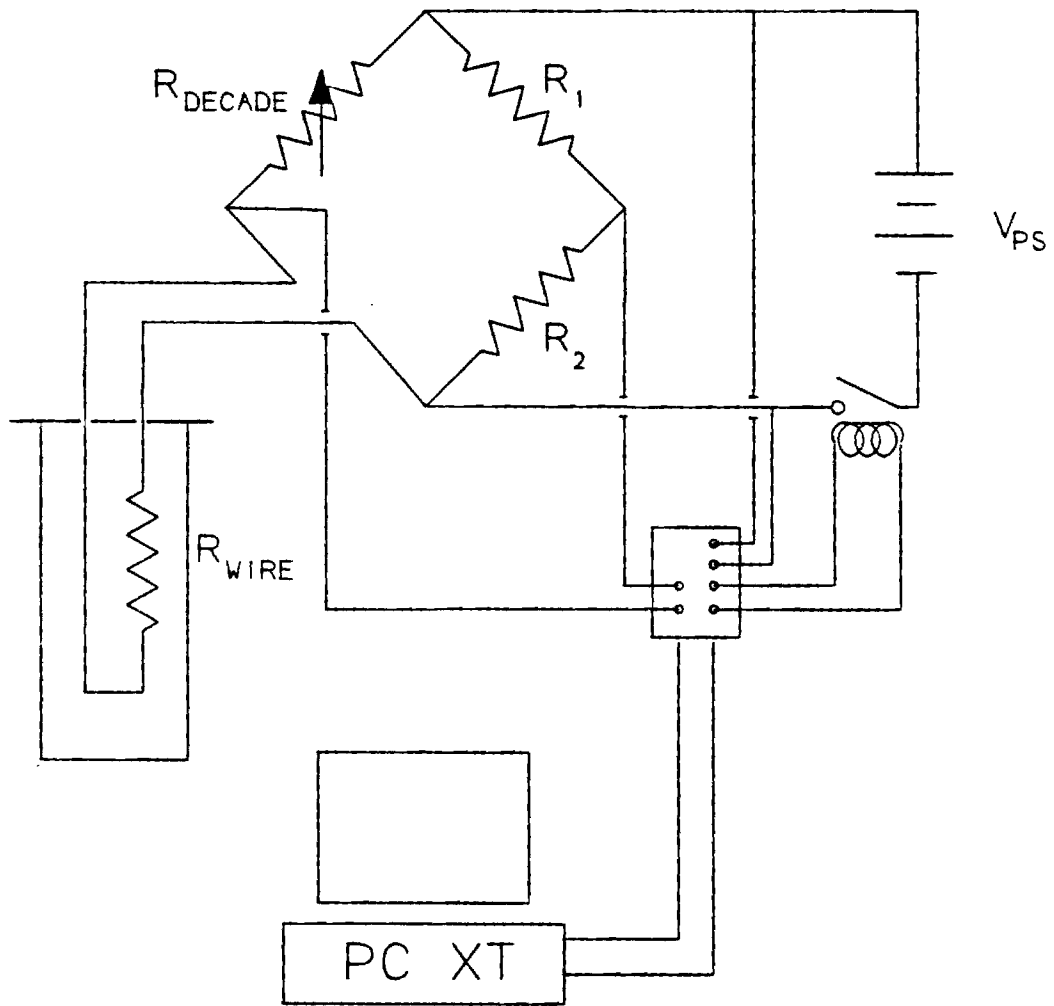


Figure 2: Schematic diagram of apparatus.

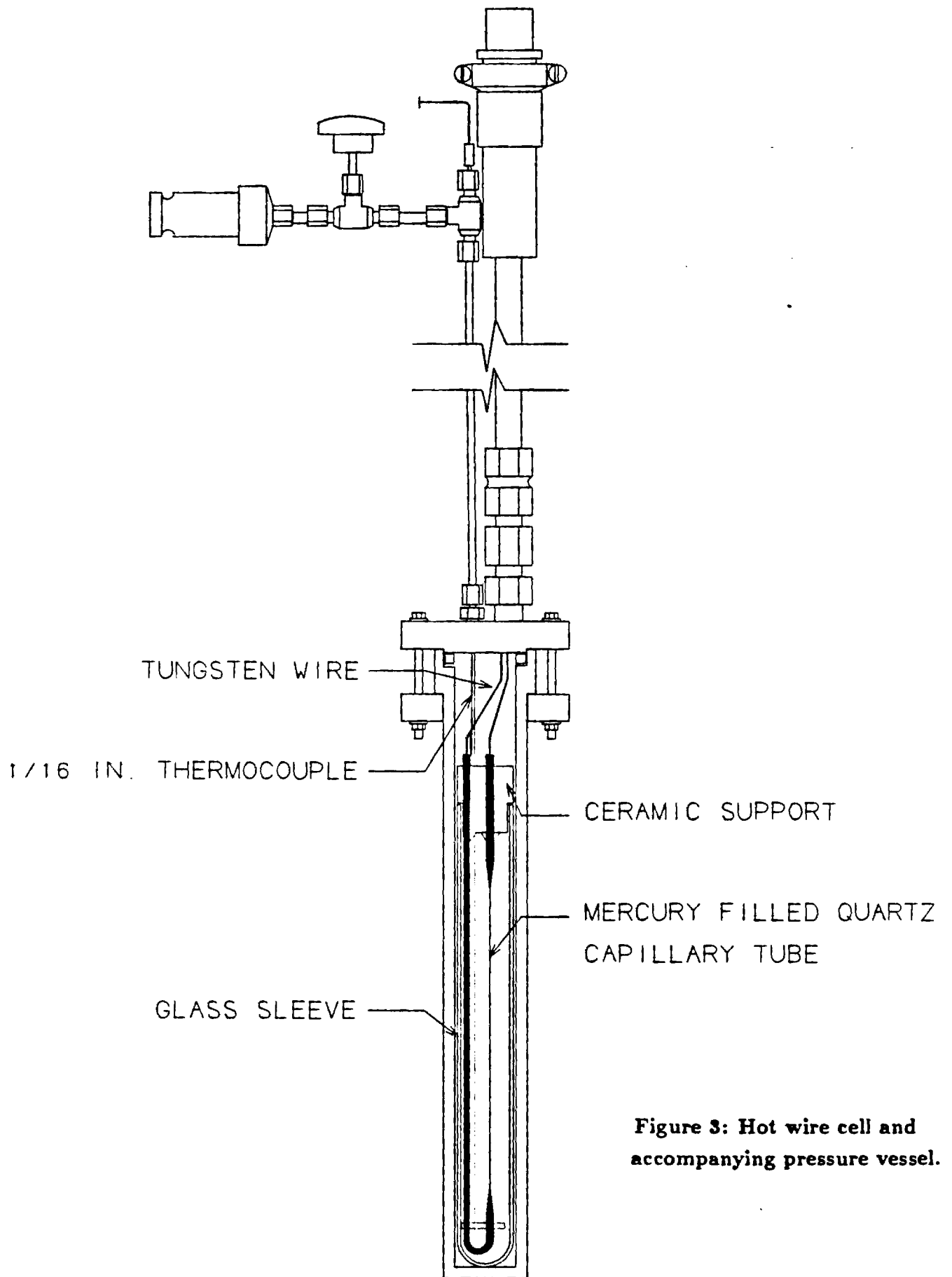


Figure 3: Hot wire cell and accompanying pressure vessel.

TEMPERATURE RISE VS $\ln(t)$

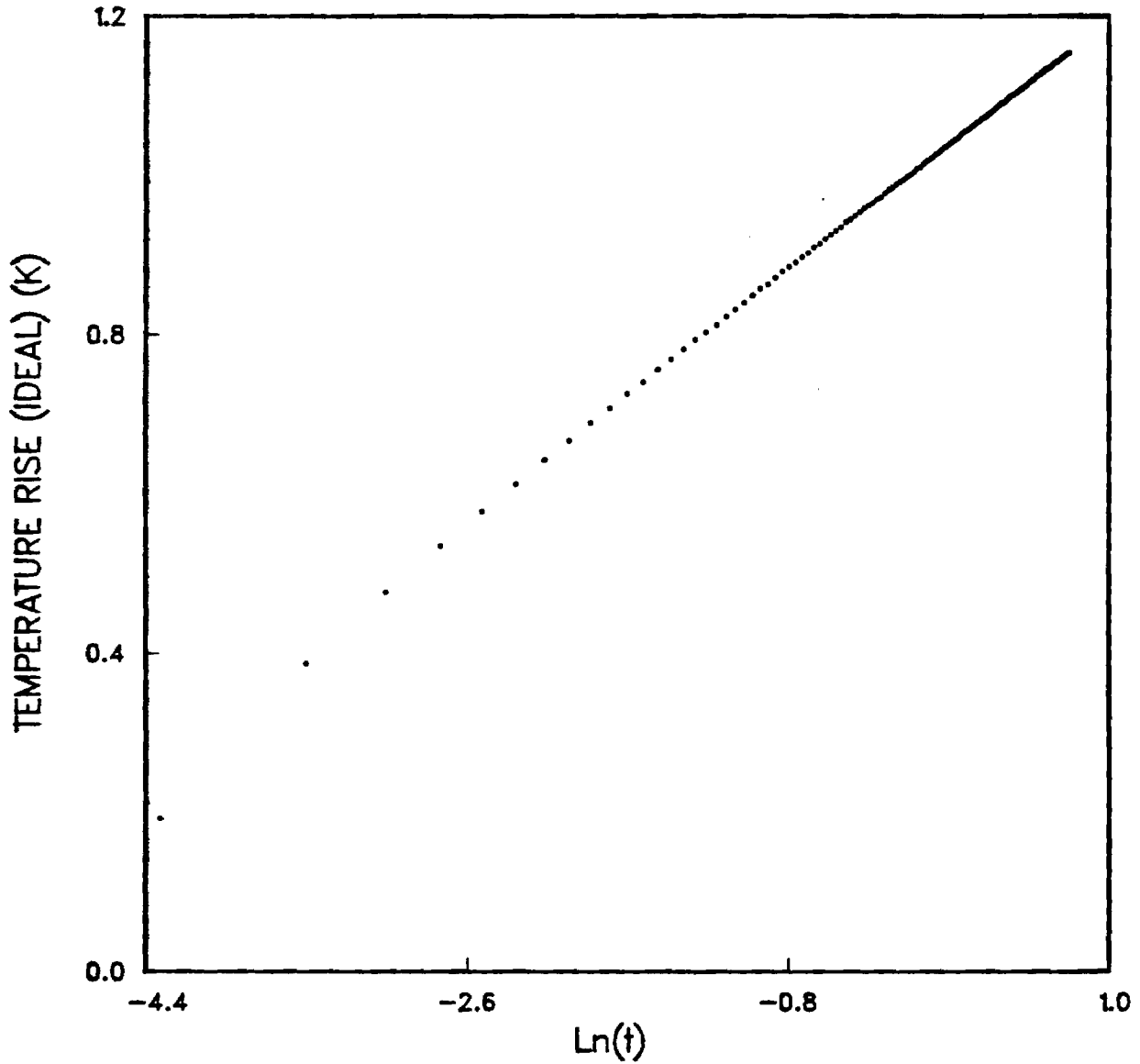


Figure 4: Plot of ΔT_{id} vs $\ln t$ obtained from experiment. Only data from 0.7 s to 2.2 s (-.35 to .79) was used in the calculation of the slope.

LINEARITY OF TEMPERATURE VS LN(t) CURVE

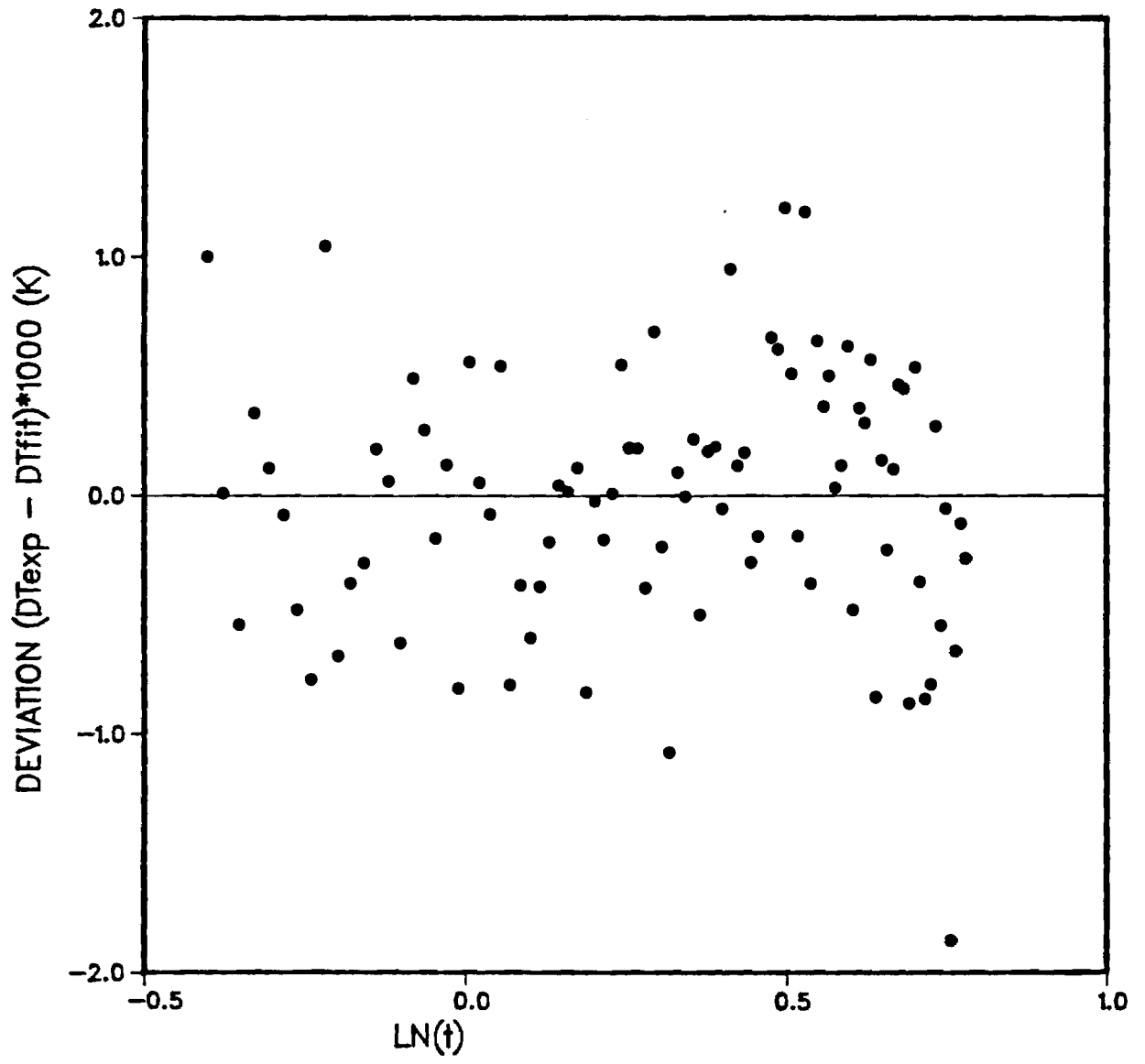


Figure 5: Plot of ΔT vs $\ln t$ to verify function linearity.

THERMAL CONDUCTIVITY OF AQUEOUS LiBr

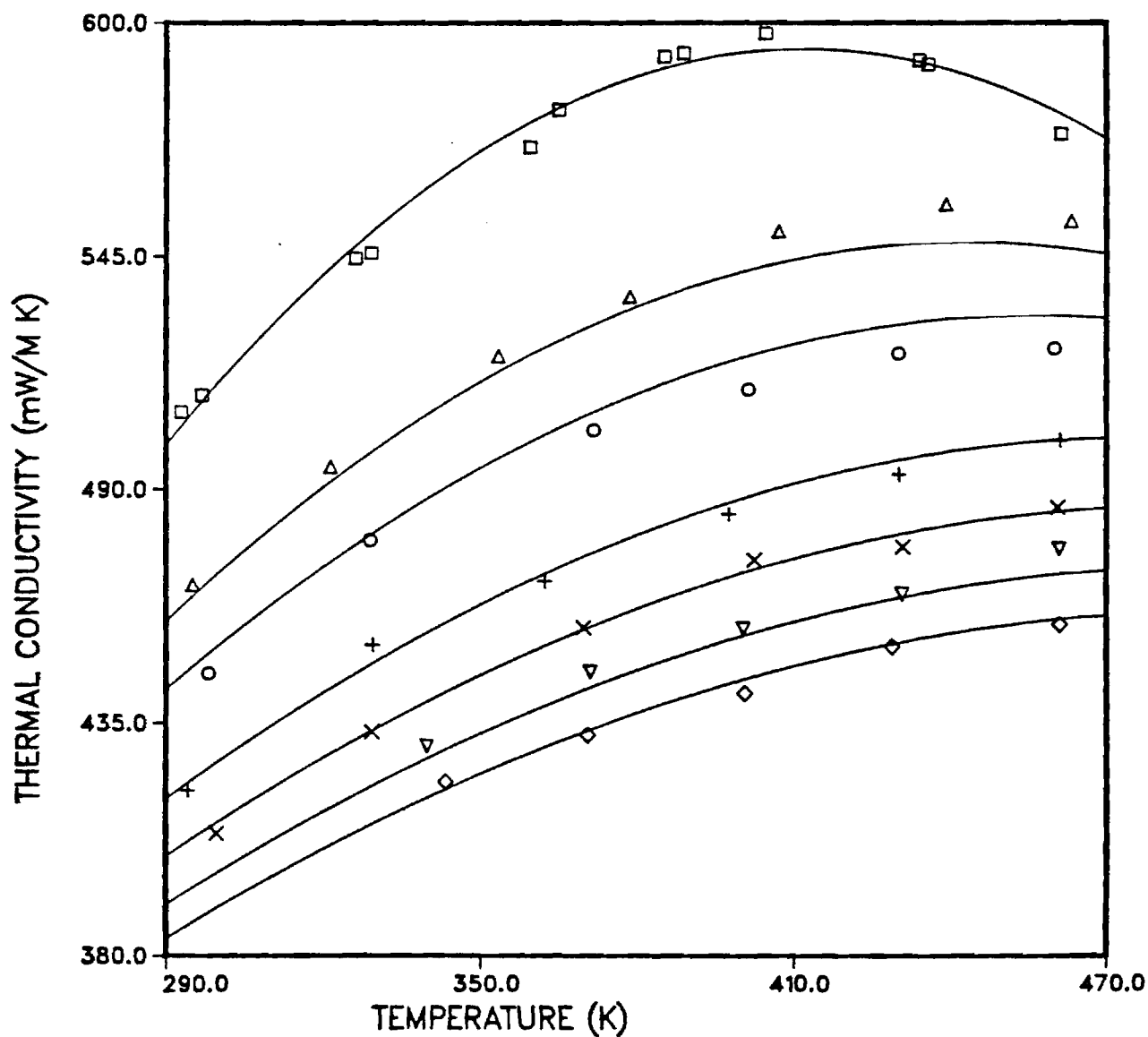


Figure 6: Thermal Conductivity of aqueous lithium bromide solutions. Solid curves are from the correlation. \square = 30.2 wt% LiBr, \triangle = 44.3 wt% LiBr, \circ = 49.1 wt% LiBr, $+$ = 56.3 wt% LiBr, \times = 60.0 wt% LiBr, ∇ = 62.9 wt% LiBr, \diamond = 64.9 wt% LiBr.

Chapter 3

Density of Lithium Bromide - Water Solutions

1 Introduction

Improvements to the performance of absorption refrigeration equipment require a knowledge of the thermophysical properties of aqueous lithium bromide solutions. The density of such solutions at temperatures up to 100 °C has been investigated by Uemura and Hasaba (1964) and by Bogatykh and Evnovich (1965). An extension of these measurements to higher temperatures and concentrations is reported in this paper. The densities of aqueous lithium bromide solutions at four concentrations, namely 45.1, 49.9, 55.0, and 59.9 weight % (wt%) and temperatures up to 200 °C were measured. A correlation of the experimental data is also presented.

2 Experiment

Principle of Operation The principle used to determine the liquid density (ρ) of a fluid in this study is based on the definition:

$$\rho = \frac{M}{V} \quad (1)$$

where M is the mass and V the volume of the fluid. Experimentally, we measured the mass of the fluid required to fill a calibrated volume (density cell).

Apparatus and Procedure The densities of lithium bromide - water solutions were measured in a high pressure pycnometer shown schematically in Figure 1. The pycnometer is rated up to 300 °C and 100 bar and consists of four sampling cylinders (Whitey, HDF2-40) capped at one end by a high pressure fitting. The other end of each cylinder was attached through a pipe nipple (Cajon HLN), an isolation valve (Whitey, ORF2), and a quick connect coupling to a high pressure hand pump (High Pressure Equipment Co., model 50-6-15). The pump was used to maintain pressure in the system in order to suppress boiling. Each stainless steel sampling cylinder was equipped with a thermowell for temperature measurement and had an internal volume of approximately 40 ml. The exact volume of each cell assembly was obtained by calibration with triple-distilled mercury at temperatures up to 150 °C. Figure 2 shows a typical calibration curve for density cell No. 1. The data were fitted to an appropriate function (either linear, as in Figure 1, or quadratic) for interpolation or extrapolation. Temperature control within ± 0.05 °C was achieved by a constant temperature circulating bath (Haake-Buchler, model N3B) filled with silicone oil.

At the beginning of an experiment, the four density cells were cleaned thoroughly, weighed, and then connected to the system. The density cell assembly was then evacuated, filled with the test liquid and placed in the oil bath. Usually, two hours were allowed for temperature equilibrium to be attained. Once equilibrium had been established, the isolation valves were closed and the pycnometers removed from the oil bath and weighed on an electronic balance (Sartorius, type 1580).

The solution temperature was measured using a type K thermocouple which had previously been calibrated against a platinum resistance thermometer (Leeds and Northrup Co., Serial No. 709892). The accuracy of the temperature measurement was estimated to be ± 0.1 °C. The system pressure was monitored by a precision pressure gauge (3D Instruments

Inc.) rated at 1500 psi with an accuracy of $\pm 0.25\%$ of full scale. The electronic balance used for weight measurement has a precision of $\pm 0.001\text{g}$.

Material and Solution Preparation N-Methylpyrrolidinone (99.5% purity), mercury (99.999+% purity) and HPLC grade water were purchased from Pfatz & Bauer, Inc., Bethlehem Apparatus Co., and Fisher Scientific respectively. Anhydrous lithium bromide was provided by Alfa Products (lot No. H26G) and had a certified purity of 99.5 % by weight. These chemicals were used without further purification. Aqueous lithium bromide solutions were prepared by adding degassed water to fresh anhydrous lithium bromide. The solutions were degassed by an alternating freeze-thaw procedure. About 0.2% of impurities by weight (excluding water) were ignored in calculating the concentrations of the prepared solutions. The concentrations were determined gravimetrically and checked on a computer-aided titrameter (Fisher Scientific, CAT system). As shown in Table 1, excellent agreement between solution concentrations determined by these two methods was obtained. The precision of concentration measurement was estimated to be ± 0.1 wt% lithium bromide.

Reference Experiment In order to test the apparatus and procedure, the densities of N-methylpyrrolidinone at atmospheric pressure were measured and compared with data in the literature. As illustrated in Figure 3, our measurements are in good agreement with those reported recently by Kneisl and Zondlo (1987).

3 Results and Discussion

Table 2 summarizes the measured densities of four lithium bromide - water solutions containing 45.1, 49.9, 55.0, and 59.9 wt% of lithium bromide respectively. Since high concentration

solutions are supersaturated at room temperature, the 65 wt% solution could not be measured with this apparatus because the solution would crystallize in unheated sections of the apparatus (such as the pressure gauge or exposed tubing). Measurements on the remaining solutions were performed at temperatures from ambient to 200 °C. The system pressure was maintained at 150 psig throughout the experiments. At least three samples were taken at each condition to give the average reported in Table 2. The reproducibility of the results was $\pm 0.1\%$.

The accuracy of the data was estimated as the sum of the bias error ϵ_b and the random error ϵ_r . The bias error was estimated from:

$$\epsilon_b = \epsilon_{b,MT} + \frac{\partial \epsilon_b}{\partial T} \Delta T_M \quad (2)$$

where $\epsilon_{b,MT}$ is the moderate temperature bias and the ΔT_M is the temperature difference between the moderate temperature reference test and the temperature range over which the data were measured. The moderate temperature bias error was estimated to be 0.1% by comparing our data on N-methylpyrrolidinone with data of Kneisl and Zondlo at temperatures up to 100 °C. The comparison showed no apparent trend in the bias error with temperature. Thus, we concluded that $\frac{\partial \epsilon_b}{\partial T}$ is approximately zero and the bias error is 0.1% at all temperatures. Random error was estimated from three sources: the uncertainty in the measurement, the uncertainty in the reported concentration and the uncertainty in the equilibrium temperature of the fluid, with

$$\epsilon_r^2 = \epsilon_m^2 + \left(\frac{\partial \rho}{\partial X} \frac{\partial X}{\rho} \right)^2 + \left(\frac{\partial \rho}{\partial T} \frac{\partial T}{\rho} \right)^2 \quad (3)$$

The uncertainty in the measurement ϵ_m^2 was 0.1%. The sensitivity of the density to temperature and concentration were found using the correlation for density reported in the next section of this chapter. The maximum value of $\frac{\partial \rho}{\partial X} \frac{1}{\rho}$ was found to be $0.012 \text{ wt}\%^{-1}$. Allowing

for experimental variation, the maximum uncertainty in the composition was ± 0.5 wt%. The maximum value of $\frac{\partial \rho}{\partial T} \frac{1}{\rho}$ was found to be -0.0002 K^{-1} and the maximum uncertainty in the temperature measurement was ± 0.2 K. The total random error was then less than 0.15% and the total error was ± 0.25 %.

The densities of aqueous lithium bromide solutions at lower temperatures have been reported by Uemura and Hasaba (1964) and Bogatykh and Evnovich (1965). Figure 4 shows that our data are in good agreement with those of the earlier workers. The average absolute deviation between our data and the data of Uemura and Hasaba was found to be 0.3%, while that between our data and the data of Bogatykh and Evnovich was 0.2%. Note that the data from these two references are at concentrations of 45.0, 50.0, 55.0, and 60.0 wt% LiBr which differ only slightly from the experimental concentrations in this investigation (45.1, 49.9, 55.0, and 59.9 wt%).

4 Correlation

Our results were fitted to the following polynomial function in temperature

$$\rho = A_0 + A_1T + A_2T^2 \quad (4)$$

where ρ is in gm/ml and T is in K. The values of A_0 , A_1 , and A_2 were determined by minimizing the sum of squares of the relative deviations: $\sum_i [(\rho_{expt,i} - \rho_{cal,i})/\rho_{expt,i}]^2$. The constants A_0 , A_1 , and A_2 were further interpolated in terms of weight fraction of lithium bromide (X) as follows

$$A_0 = 1.09763 + 0.071244X + 2.21446X^2 \quad (5)$$

$$A_1 = (0.679620 - 1.48247X - 0.89696X^2) \times 10^{-3} \quad (6)$$

$$A_2 = (-0.035097 - 3.24312X + 4.97020X^2) \times 10^{-6} \quad (7)$$

All data could be correlated with the above equation with an overall average absolute deviation (AAD) of 0.06% and maximum absolute deviation (MAD) of 0.19%. However, nine parameters are required. A simpler form with five parameters is given by:

$$\rho = 1.40818 - 0.713995X + 2.64232X^2 - \frac{(0.12318 + 0.946268X)T}{1000} \quad (8)$$

with an AAD of 0.08% and MAD of 0.39%. Figure 4 shows the comparison between the values calculated by this equation and the observed values.

It should be noted that the correlation of Equation 8 is based only on lithium bromide concentrations between 45 wt% and 60 wt% measured in this investigation. Extrapolation to other concentrations is not recommended. To cover a wider range of X, we included the data available in the literature at lower temperatures in the following equation:

$$\rho = 1.14536 + 0.47084X + 1.37479X^2 - \frac{(0.333393 + 0.571749X)T}{1000} \quad (9)$$

Figure 5 illustrates good agreement between the calculated values and experimental data of this work and of Bogatykh and Evnovich (1965), Sohnel and Novotny (1985), and Uemura and Hasaba (1964). The average deviation (AAD%) between the calculated and experimental values was found to be 0.19% for the 86 data points, which covered a weight fraction of LiBr from 0.2 to 0.65. The maximum deviation was 0.51%. Note that Equation 9, which is also shown in the figure, does not extrapolate well to lower concentrations.

References

- [1] Bogatykh, S. A.; and Evnovich, I. D. 1965. *Zh. Prikl. Klim.*, Vol. 38, p. 945.
- [2] Kneisl, P.; and Zondlo J. W. 1987. *J. Chem. Eng. Data*, Vol. 32, p. 11.
- [3] Sohnel, O.; and Novotny P. 1985. "Densities of Aqueous Solutions of Inorganic Substances", Elsevier, Amsterdam.
- [4] Uemura, T.; and Hasaba S. 1964. *Technol. Rept.*, Kansai Univ., Vol. 6, p. 31.

**Table 1. Comparison of Solution Concentration
Determined by Different Methods.**

No.	Weight Fraction of LiBr	
	Gravimetric	Titrametric
1	0.4506	0.4507
2	0.4985	0.4993
3	0.5500	0.5495
4	0.5990	0.5988

Table 2. Experimental Densities of Aqueous Lithium Bromide Solutions.

Wt% LiBr	T [K]	ρ [gm/ml]	Wt% LiBr	T [K]	ρ [gm/ml]
45.1	301.6	1.4554	49.9	298.7	1.5328
	319.1	1.4470		318.5	1.5206
	333.2	1.4389		333.2	1.5128
	348.1	1.4323		348.0	1.5042
	361.6	1.4255		363.1	1.4954
	381.3	1.4144		382.7	1.4833
	402.4	1.4041		402.8	1.4705
	423.5	1.3919		423.7	1.4568
	448.4	1.3782		448.6	1.4397
				474.8	1.4216
55.0	298.2	1.6205	59.9	298.5	1.7217
	318.2	1.6089		318.2	1.7087
	332.6	1.5997		333.7	1.6986
	346.9	1.5912		348.1	1.6884
	361.5	1.5816		363.6	1.6779
	382.1	1.5703		383.6	1.6642
	401.6	1.5584		403.0	1.6512
	421.6	1.5453		423.4	1.6365
	447.4	1.5287		447.9	1.6192
	473.1	1.5110		473.2	1.6008

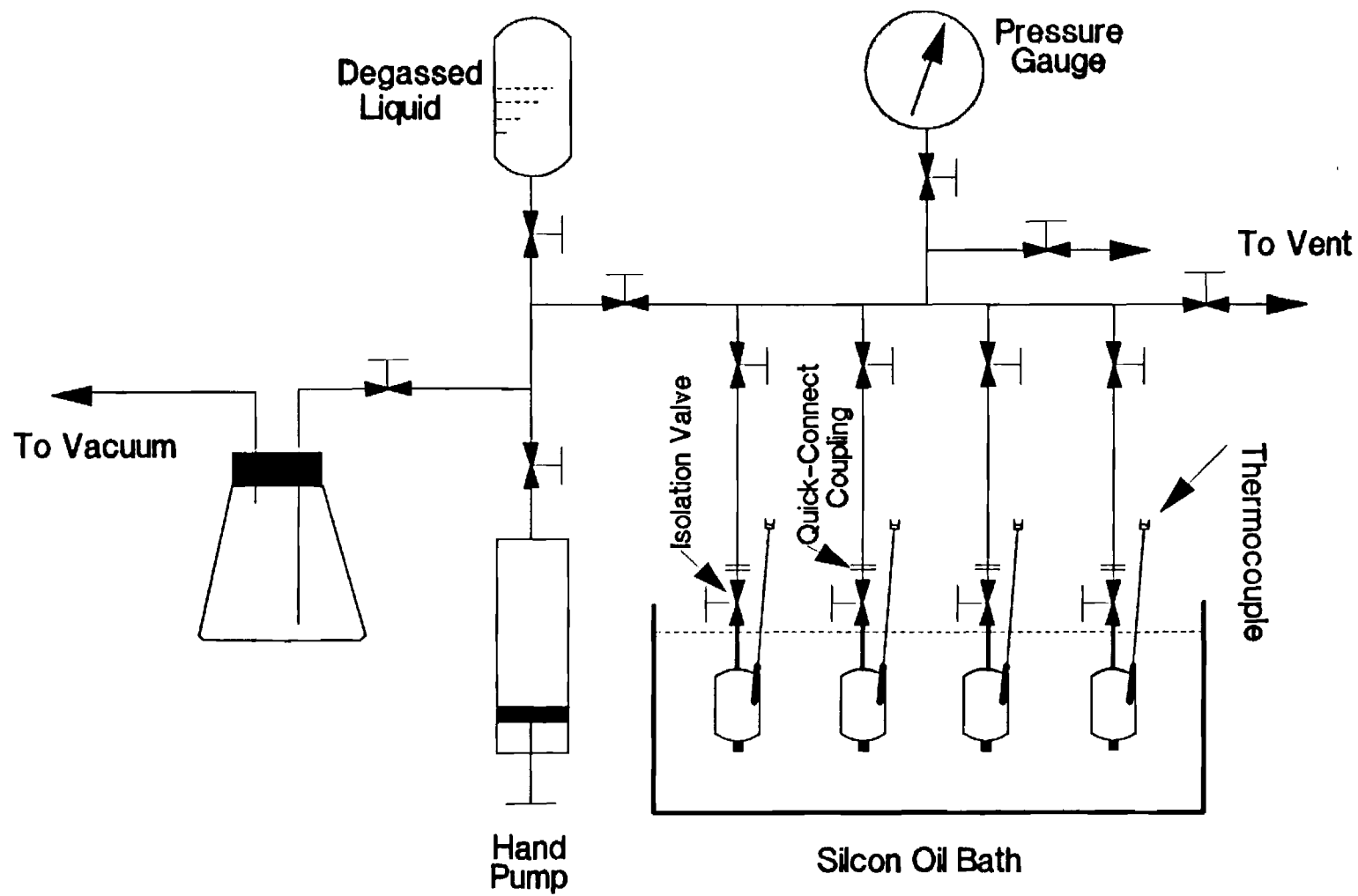


Figure 1. Schematic diagram of the high pressure pycnometer.

INTERNAL VOLUME OF DENSITY CELL 1

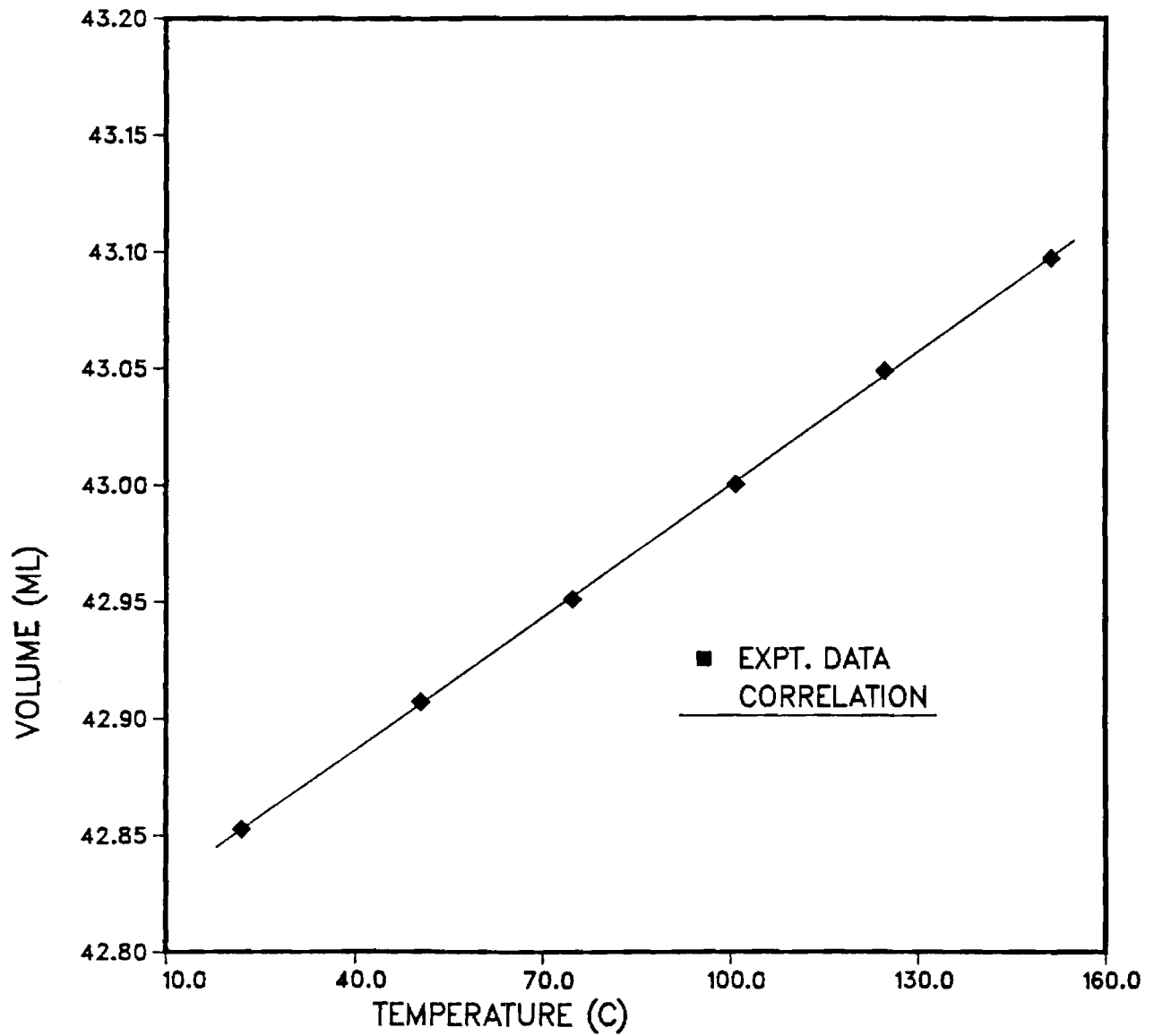


Figure 2. Volume of density cell 1.

DENSITY OF N-METHYLPYRROLIDINONE

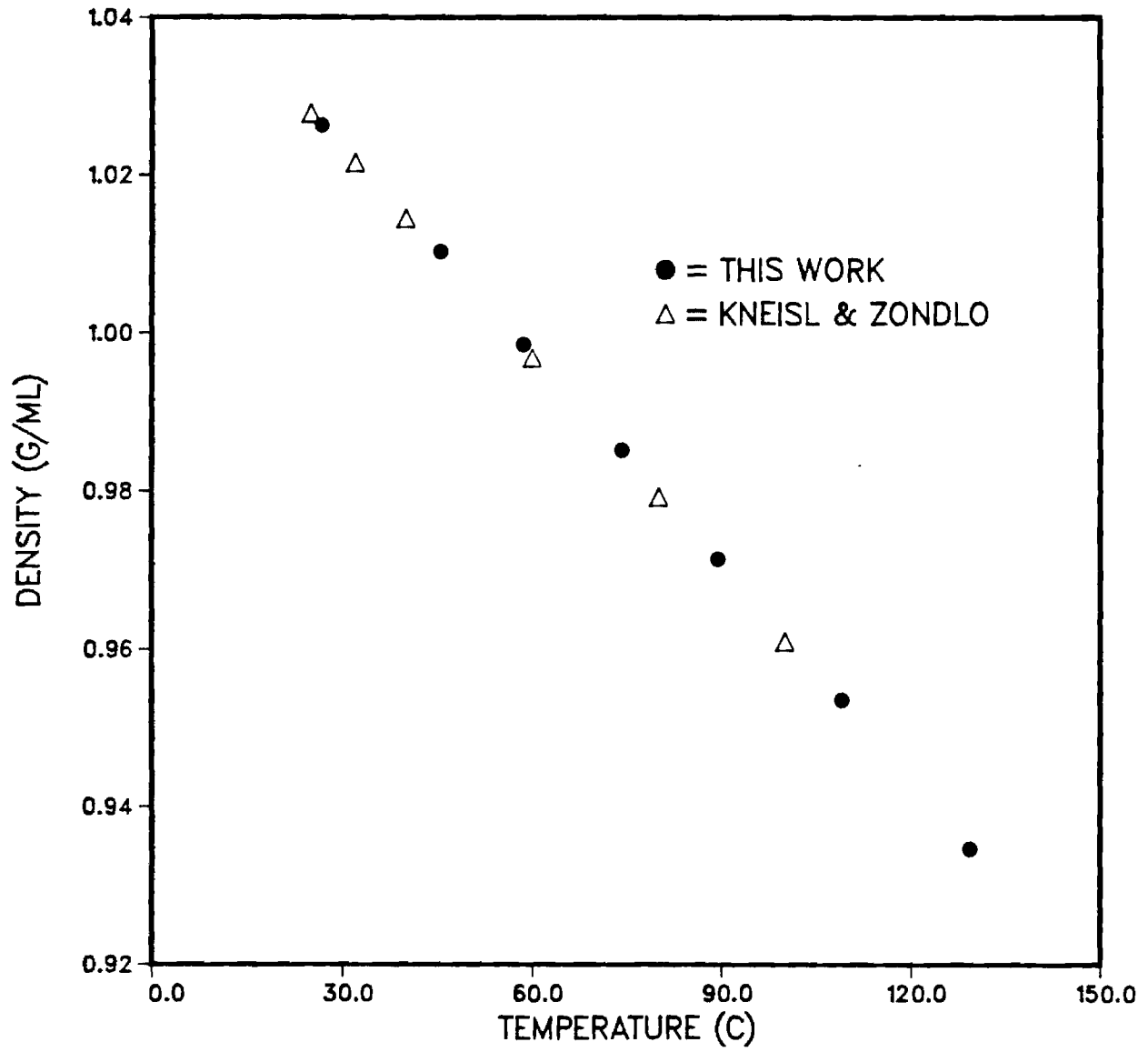


Figure 3. Liquid density of N-methylpyrrolidinone.

DENSITY OF AQUEOUS LiBr SOLUTION

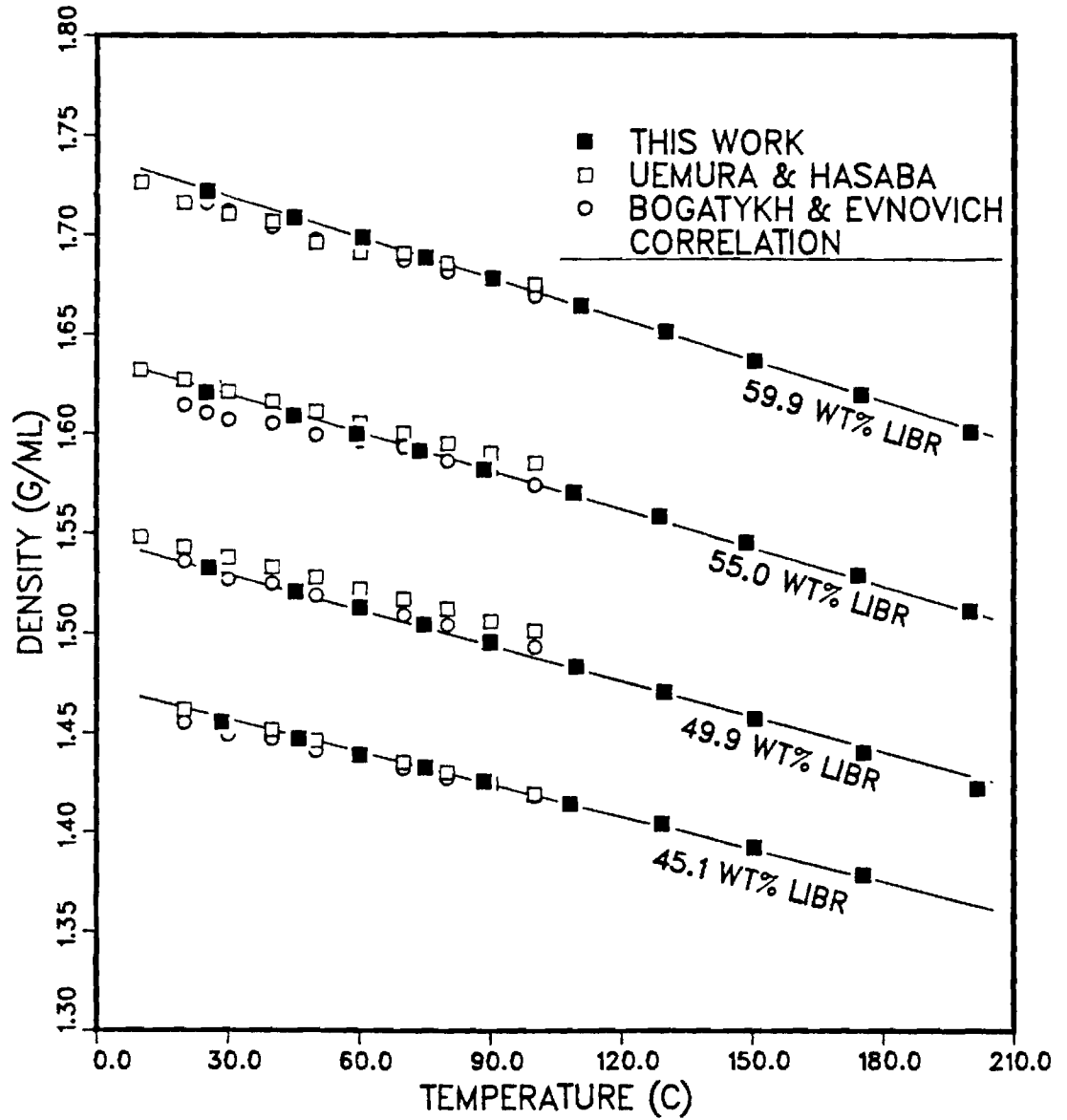


Figure 4. Liquid density of LiBr - water solutions.

DENSITY OF AQUEOUS LIBR SOLUTIONS

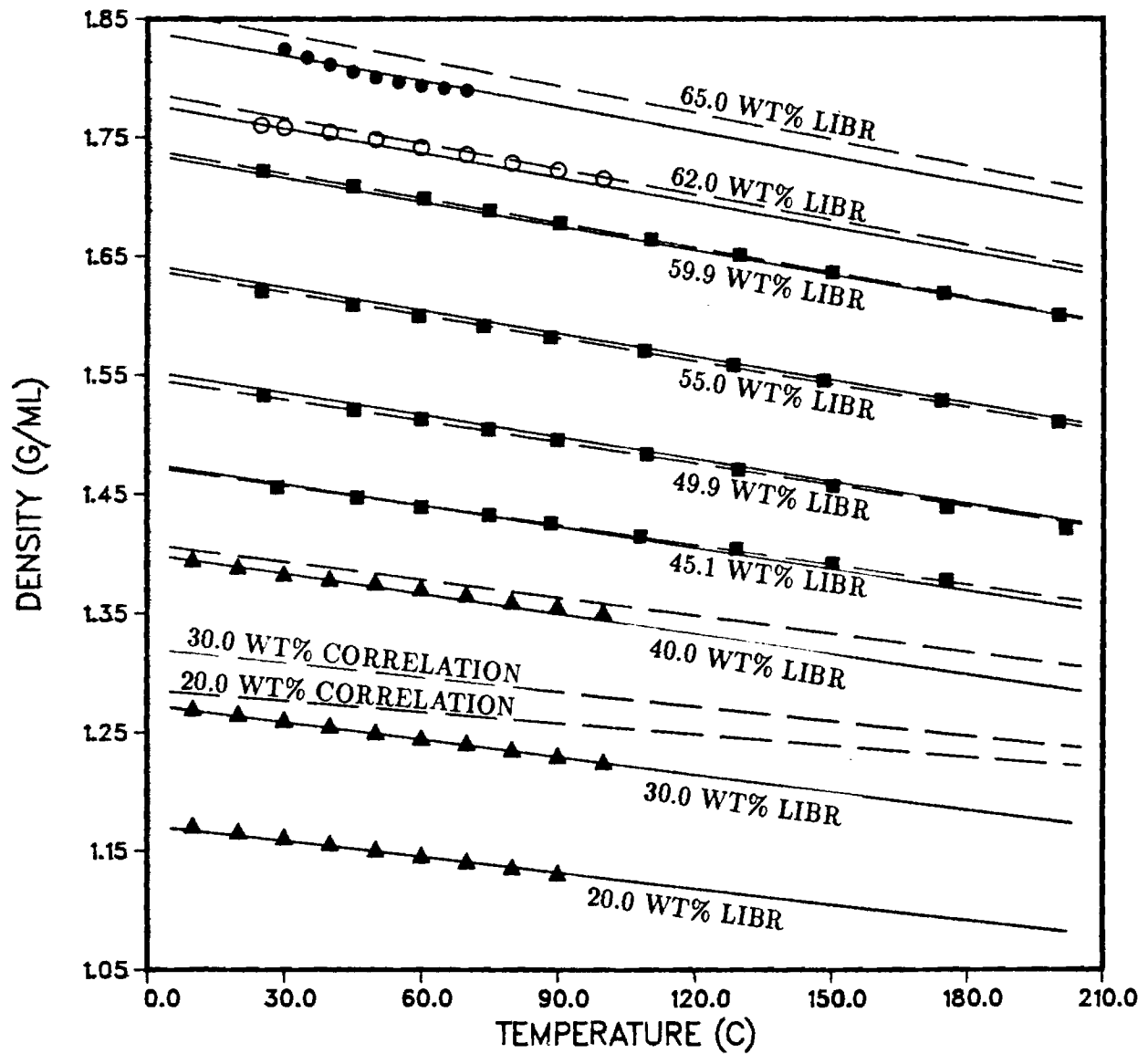


Figure 5. Alternative density correlation compared with experimental data. --- : limited correlation, Equation 8; ——— : inclusive correlation, Equation 9. Sources of Data: ■ this work; ○ Reference [1]; ● Reference [3]; ▲ composite of References [1], [3], and [4].

Chapter 4

Viscosity of Lithium Bromide - Water Solutions

1 Introduction

The transport properties of concentrated aqueous lithium bromide solutions are important in the design of absorption refrigeration systems. Although the viscosities of such solutions have been measured at low temperatures, more than 15% difference exists between values reported by different workers. Therefore, the viscosities of solutions with weight fractions of lithium bromide ranging from 0.45 to 0.65 and at temperatures up to 200 °C were measured in this work and are reported below.

2 Experiment

Principle of Operation The equation used to represent the absolute viscosity, μ , of a fluid flowing through a capillary is based on Poiseuille's law (1840),

$$\mu = \frac{\pi r^4 g h}{8LV} \rho t - \frac{\zeta V}{8\pi L} \frac{\rho}{t} \quad (1)$$

where

- r : radius of the capillary
- g : gravitational constant
- h : average head of the fluid
- L : length of the capillary
- V : efflux volume of the fluid
- t : efflux time
- ρ : density of the fluid
- ζ : kinetic energy coefficient

For a specific capillary viscometer, the kinematic viscosity ν can be related to the efflux time using:

$$\nu = \frac{\mu}{\rho} = C_1 t - \frac{C_2}{t} \quad (2)$$

where C_1 is the viscometric constant and is determined by calibration with a fluid of known viscosity. The second term on the right hand side represents the correction due to the kinetic energy and is usually neglected if an appropriately sized viscometer is used.

Apparatus and Procedure A high pressure viscometer was designed and constructed for viscosity measurement of highly corrosive solutions. The design of the apparatus is similar to that proposed by Al-Harbi (1982). Figure 1 shows the schematic diagram of this apparatus, which consists of a capillary viscometer, a pressure cell, a thermostated air bath, and a pressure distribution section. This apparatus was designed for temperatures up to 200 °C and pressures up to 30 atm.

A Size 1 Zeitfuchs (1946) cross-arm capillary viscometer (International Research Glassware) was used for determination of the kinematic viscosity (Figure 2). The calibration

factor was determined at room temperature using pure water. In order to repeat a measurement without reloading the liquid sample, the viscometer was calibrated with a wetted capillary. After calibration, the viscometer was placed inside the pressure cell and the capillary end was connected to the pressure distribution section through V5. The reservoir end was opened to the cell chamber such that the pressure over the viscometer could be balanced. The pressure cell is shown schematically in Figure 3. The cell was equipped with four glass view ports (tempered borosilicate glass) to allow visual observation of the reservoir and the measuring bulb of the viscometer. An insulated air bath, heated by a primary (800 W) and a secondary (200 W) heater, was used to establish the desired temperature. A stable temperature in the air bath was maintained by a commercial temperature control unit (Omega, model CN5000) and a circulating fan. Temperature fluctuations were minimized by the mass of the pressure cell, which was made of heavy steel. The test fluid was moved back and forth through the capillary tube by a high pressure hand pump (High Pressure Equipment Co., model 50-6-15) with helium as the pressurizing fluid.

The temperature was measured inside the cell by a chromel-alumel thermocouple, calibrated with a NBS calibrated Leeds and Northrop platinum resistance thermometer (Serial No. 709892). The accuracy of the temperature measurement was estimated to be ± 0.1 °C. Pressure measurement was accomplished by a precision gauge (3D Instruments Inc.) with an accuracy of 0.25% of full scale (0-1500 psi). An electronic timer accurate to 1/100 second was used to obtain the efflux time.

Before an experiment was performed, a clean dry viscometer loaded with the appropriate test solution was attached to the top flange of the pressure cell. The top flange was then bolted into place, and the cell was connected to the pressure distribution section and pressurized slowly to the desired pressure. To eliminate loss of vapor from the solution,

about 40 ml of slightly dilute lithium bromide solution was placed at the bottom of the cell chamber so that the solution in the viscometer was always under its vapor pressure.

At the beginning of an experiment, all valves were closed except for V4 and V5. The pressure on the capillary end was reduced by the use of the hand pump, causing the solution to flow into the reverse bend of the capillary. Once the flow had been initiated, valve V3 was opened to balance the pressures over both ends of the viscometer. The efflux time for the solution to flow between the timing marks on the measuring bulb was then measured. At the end of the measurement, valve V3 was closed and the solution was then forced to return to the reservoir by increasing the pressure on the capillary end with the hand pump. Measurements were repeated until consistent efflux times were obtained.

Material and Solution Preparation Anhydrous lithium bromide, with a certified purity of 99.3% from Alfa Products (lot No. F06H), was used for preparing the solutions. The lithium bromide - water solutions were prepared in the same way as described in the section on density measurement. The concentrations of the solutions were determined either by gravimetric or titrametric methods and are summarized in Table 1.

Reference Experiment To test the apparatus and procedures, the kinematic viscosity of pure water was measured and compared with values reported by the National Bureau of Standards (see CRC Handbook 1982). As illustrated in Figure 4, good agreement was obtained between the two sets of measurements. The density of water reported by Gildseth et al. (1972) was used to convert the measured kinematic viscosity to the absolute viscosity shown in this graph.

3 Results and Discussion

The experimental kinematic viscosities of aqueous lithium bromide solutions of 45.0, 50.0, 55.0, 59.9, 63.0, and 65.0 weight% (wt%) LiBr are presented in Table 2. The temperature range of the measurements varied from 40 to 200 °C, and the pressure was maintained at 200 psig throughout the experiments. Absolute viscosity data, in which the liquid densities were obtained from the correlation previously described, are also included in Table 2. The average of at least four samples was taken to obtain each value reported in this table. The viscosities were reproducible within $\pm 1.0\%$. A graphical presentation of the experimental results is given in Figure 5. As shown, a linear relationship between $\ln(\mu)$ and $1/T$ exists at low temperatures. However, the relationship is nonlinear at higher temperatures, in particular for less concentrated solutions (eg. 45.0 wt% LiBr).

The accuracy of the data was estimated as the sum of the bias error ϵ_b and the random error ϵ_r . The bias error was estimated from:

$$\epsilon_b = \epsilon_{b,LT} + \frac{\partial \epsilon_b}{\partial T} \Delta T_M \quad (3)$$

where $\epsilon_{b,LT}$ is the low temperature bias and the ΔT_M is the temperature difference between the low temperature reference test and the temperature range over which the data were measured. The low temperature bias error was estimated to be 0.5% by comparing our data on water with values of National Bureau of Standards. The comparison showed no apparent trend in the bias error with temperature. Thus, we concluded that $\frac{\partial \epsilon_b}{\partial T}$ is approximately zero and the bias error is 0.5% at all temperatures. Random error was estimated from three sources: the uncertainty in the measurement, the uncertainty in the reported concentration

and the uncertainty in the equilibrium temperature of the fluid, with

$$\epsilon_r^2 = \epsilon_m^2 + \left(\frac{\partial \mu}{\partial X} \frac{\partial X}{\mu}\right)^2 + \left(\frac{\partial \mu}{\partial T} \frac{\partial T}{\mu}\right)^2 \quad (4)$$

The uncertainty in the measurement ϵ_m^2 was 1%. The sensitivity of the viscosity to temperature and concentration were found using the correlation for viscosity reported in the next section of this paper. The maximum value of $\frac{\partial \mu}{\partial X} \frac{1}{\mu}$ was found to be 0.118 wt%⁻¹ and the maximum uncertainty in the composition was ± 0.8 wt%. The maximum value of $\frac{\partial \mu}{\partial T} \frac{1}{\mu}$ was found to be -0.026 K⁻¹ and the maximum uncertainty in the temperature measurement was ± 0.2 K. The total random error was then less than 1.5% and the total error was ± 2 %.

Comparison of our data with data available in the literature was attempted although the system pressures were different. Two sets of experimental data studied at atmospheric pressure by Uemura and Hasaba (1964), and by Bogatykh and Evnovich (1963) were selected. Figure 6 illustrates a comparison of 50.0 and 59.9 wt% LiBr solutions. The literature data shown in this figure were for 50.0 and 60.0 wt% LiBr respectively. The agreement between the literature data is poor, with the experimental data of Bogatykh and Evnovich being consistently lower than the data of Uemura and Hasaba. The literature data bracket our data at lower temperatures, while our data are higher at the higher temperatures. It is also apparent that our data are smoother than the literature data.

4 Correlation

The viscosity of lithium bromide - water solutions at each concentration can be described by the following equation

$$\ln \mu = A_1 + \frac{A_2}{T} + A_3 \ln T \quad (5)$$

where the unit of viscosity (μ) is in centipoise and temperature is in K. Values of A_1 , A_2 , and A_3 obtained by regression are listed in Table 3, as are the average absolute deviation (AAD%) and maximum absolute deviation (MAD%) between experimental and calculated viscosities. The MAD% was less than 1.1 % in all cases. The dependence of A_1 , A_2 , and A_3 on the weight fraction (X) is illustrated graphically in Figure 7. A regression of all data yields

$$A_1 = (-0.494122 + 1.63967X - 1.45110X^2) \times 10^3 \quad (6)$$

$$A_2 = (2.86064 - 9.34568X + 8.52755X^2) \times 10^4 \quad (7)$$

$$A_3 = (0.703848 - 2.35014X + 2.07809X^2) \times 10^2 \quad (8)$$

This correlation results in an AAD of 1.1% and a MAD of 3.1% over the entire region of T and X covered by this study. Figure 8 shows the good agreement between experimental data and the values calculated using the above correlation.

References

- [1] Al-Harbi, D. K., 1982. "Viscosity of Selected Hydrocarbons Saturated with Gas", Ph. D. Dissertation, Oklahoma State University, Stillwater, OK.
- [2] Bogatykh, S. A.; and Evnovich, I. D. 1963. *Zh. Prikl. Klim.*, Vol. 36, p. 186.
- [3] CRC Handbook of Chemistry and Physics, 63rd Edition, CRC Press, 1982.
- [4] Gildseth, W.; Habenschus, A.; and Spedding F. H. 1972. *J. Chem. Eng. Data*, Vol. 17, p. 402.
- [5] Poiseuille, J. 1840. *Compte Rendus*, Vol. 11, p. 961 and 1040.
- [6] Uemura, T.; and Hasaba, S. 1964. *Technol. Rept.*, Kansai, Univ., Vol. 6, p. 31.
- [7] Zeitfuchs, E. H. 1946. *Oil and Gas Journal*, Vol. 44, Jan., p. 99.

Table 1. Comparison of Solution Concentration
Determined by Different Methods.

No.	Weight Fraction of LiBr	
	Gravimetric	Titrametric
1	0.4500	0.4503
2	0.4999	0.5000
3	0.5499	0.5507
4	0.5993	0.6002
5	0.6300	0.6289
6	0.6495	0.6504

Table 2. Experimental Viscosities of Aqueous Lithium Bromide Solutions

Wt% LiBr	T [K]	ν [cst]	μ [cp]	Wt% LiBr	T [K]	ν [cst]	μ [cp]
45.0	312.9	1.325	1.919	50.0	314.9	1.605	2.446
	333.0	0.947	1.363		333.2	1.204	1.822
	353.2	0.738	1.054		353.7	0.932	1.400
	373.9	0.602	0.854		373.2	0.759	1.131
	393.2	0.515	0.725		393.3	0.637	0.942
	413.2	0.453	0.632		412.3	0.554	0.813
	433.0	0.407	0.564		432.6	0.490	0.712
	453.2	0.376	0.516		453.2	0.451	0.650
	472.5	0.353	0.480		472.6	0.413	0.589
55.0	314.2	2.120	3.418	59.9	316.0	2.897	4.952
	333.6	1.547	2.476		333.5	2.122	3.603
	353.1	1.193	1.895		353.6	1.577	2.657
	373.1	0.954	1.503		372.9	1.236	2.066
	393.5	0.786	1.228		394.3	0.986	1.634
	412.7	0.669	1.037		412.7	0.834	1.372
	433.0	0.586	0.900		433.0	0.714	1.164
	453.2	0.523	0.796		453.2	0.630	1.018
	472.3	0.477	0.720		472.9	0.553	0.886
63.0	333.1	2.826	4.964	65.0	333.4	3.162	5.680
	353.2	2.030	3.537		352.4	2.331	4.158
	373.6	1.542	2.665		372.3	1.749	3.095
	393.8	1.219	2.090		393.6	1.352	2.372
	413.2	1.011	1.720		413.2	1.106	1.925
	432.9	0.867	1.463		433.4	0.946	1.633
	452.9	0.744	1.245		452.6	0.820	1.405
	472.8	0.662	1.099		472.7	0.730	1.240

Table 3. Correlation of Experimental Data by Equation 5.

WT% LiBr	A_1	A_2	A_3	AAD%	MAD%
45.0	-49.8181	3813.29	6.66101	0.48	1.09
50.0	-40.1023	3357.43	5.27316	0.36	1.06
55.0	-33.6317	3118.48	4.33620	0.18	0.43
59.9	-32.5247	3222.14	4.15643	0.37	1.04
63.0	-37.3241	3605.41	4.83769	0.27	0.85
65.0	-46.3684	4167.00	6.13288	0.23	0.71

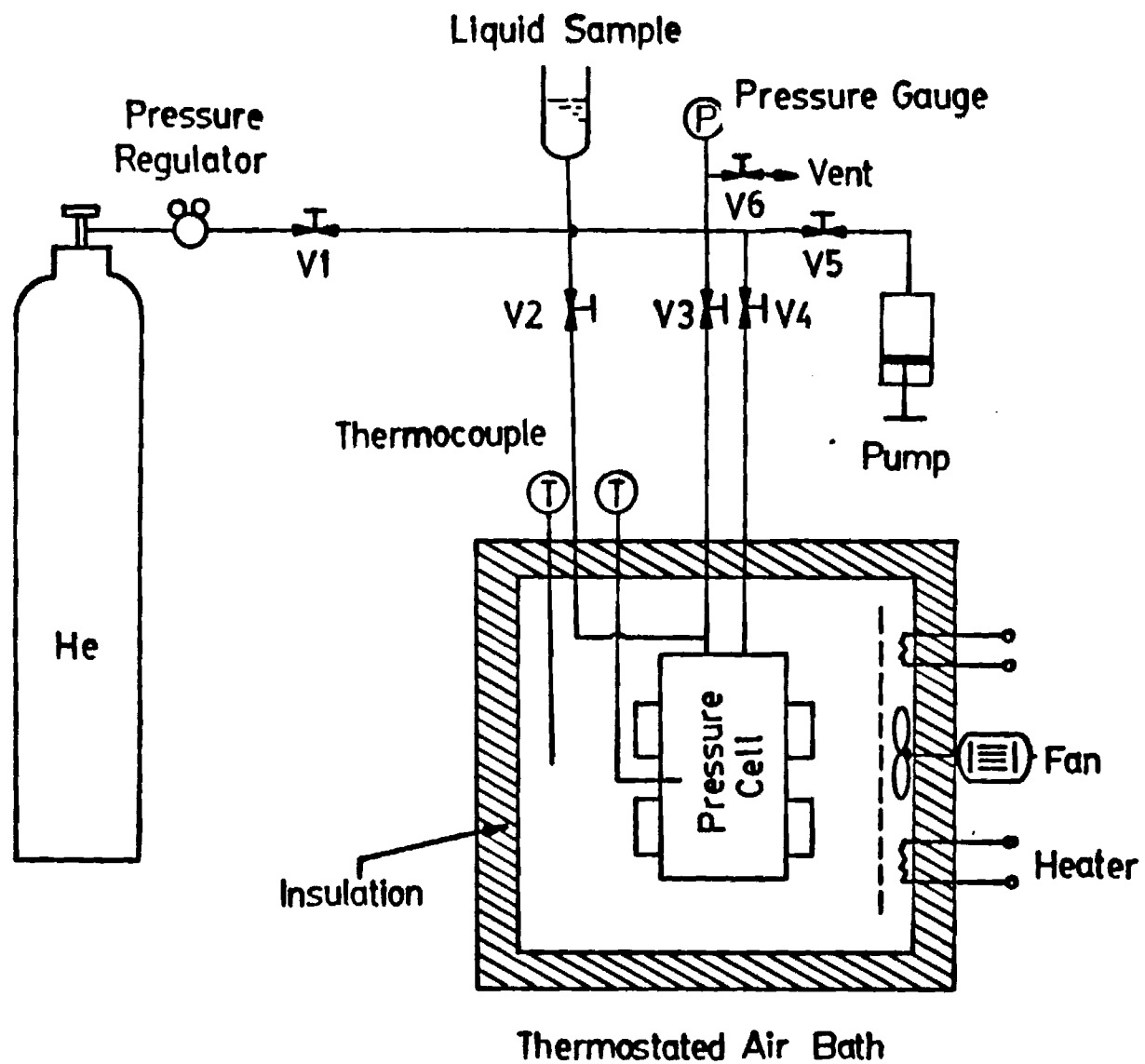


Figure 1. Schematic diagram of the high pressure viscometer.

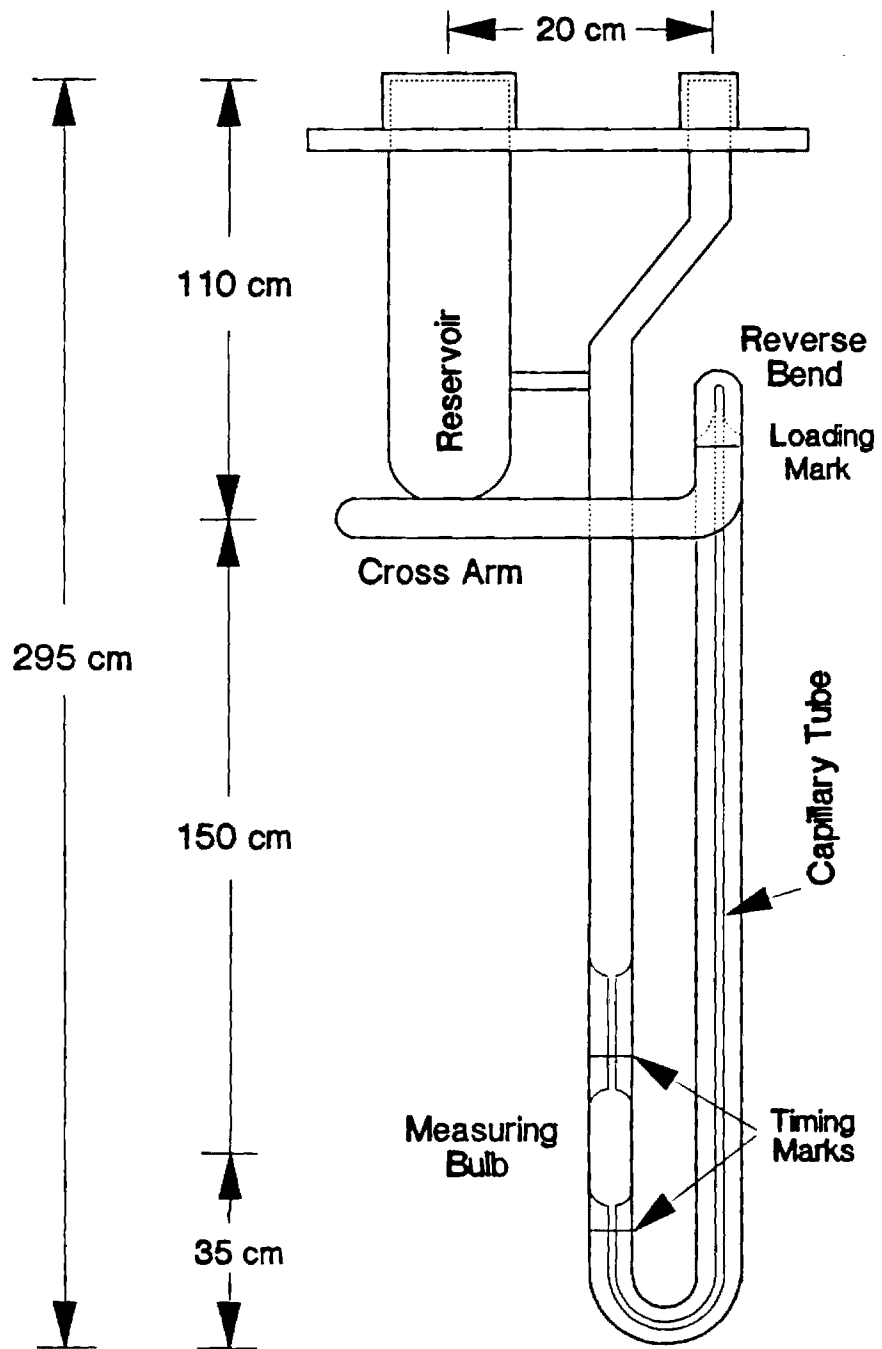


Figure 2. Zeitfuchs cross-arm viscometer.

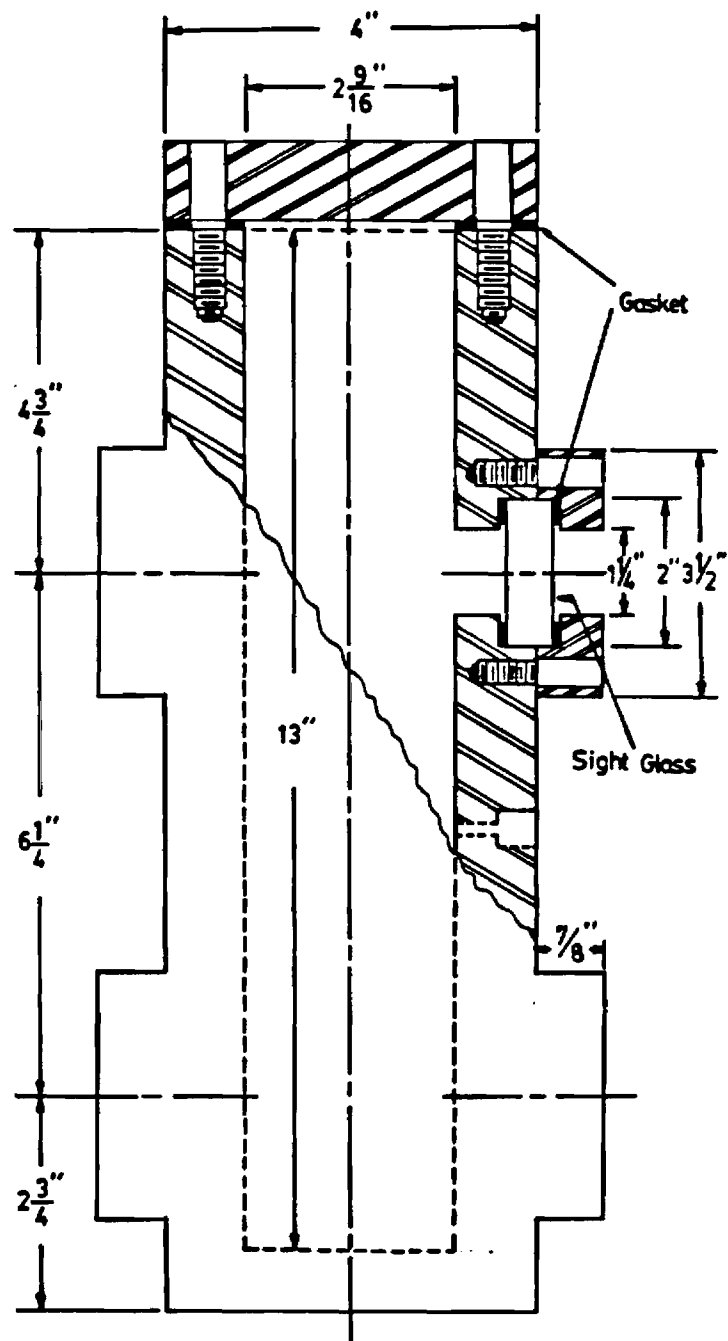


Figure 3. Detail design of the pressure cell.

VISCOSITY OF WATER

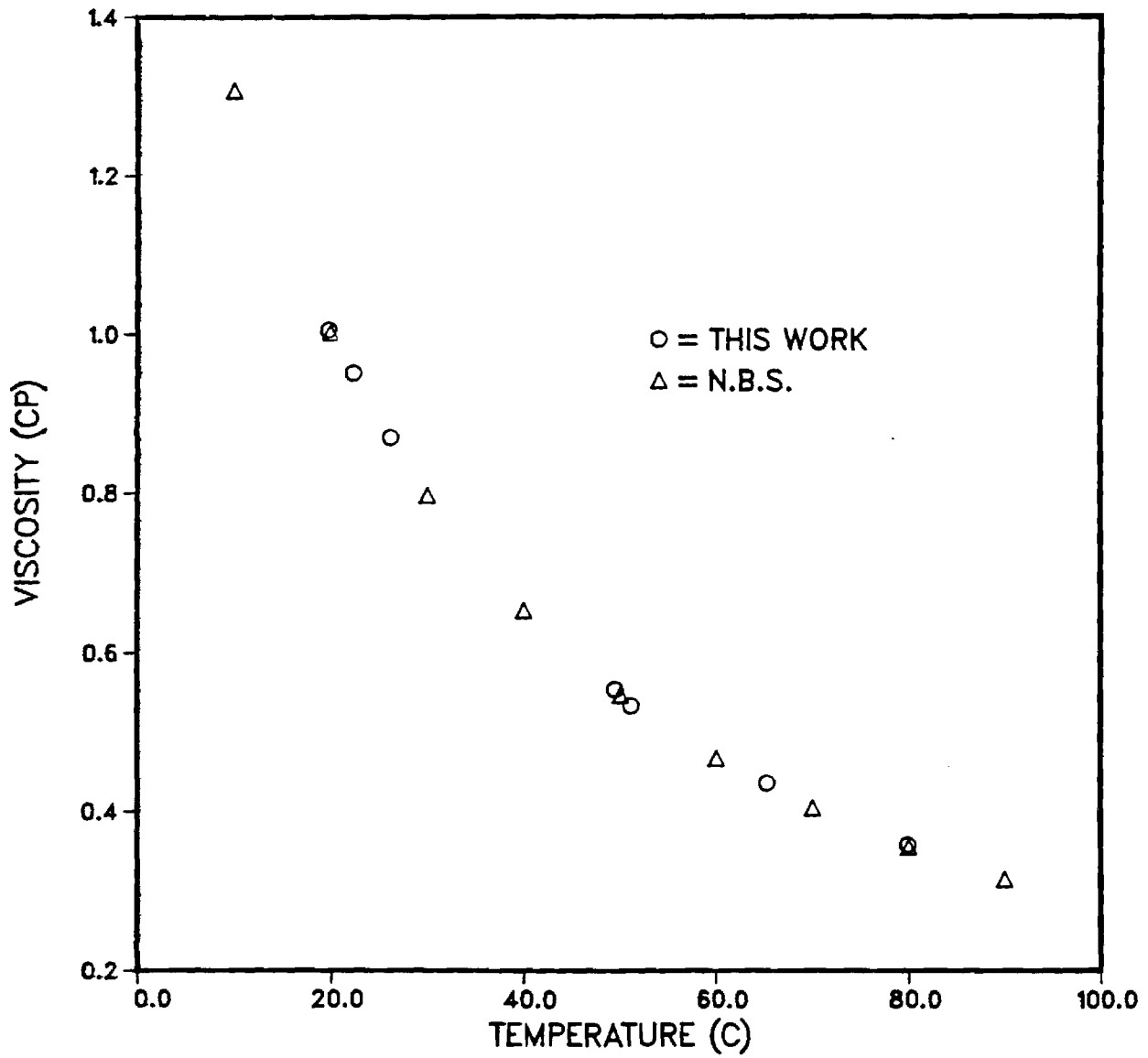


Figure 4. Viscosity of liquid water.

VISCOSITY OF AQUEOUS LiBr SOLUTION

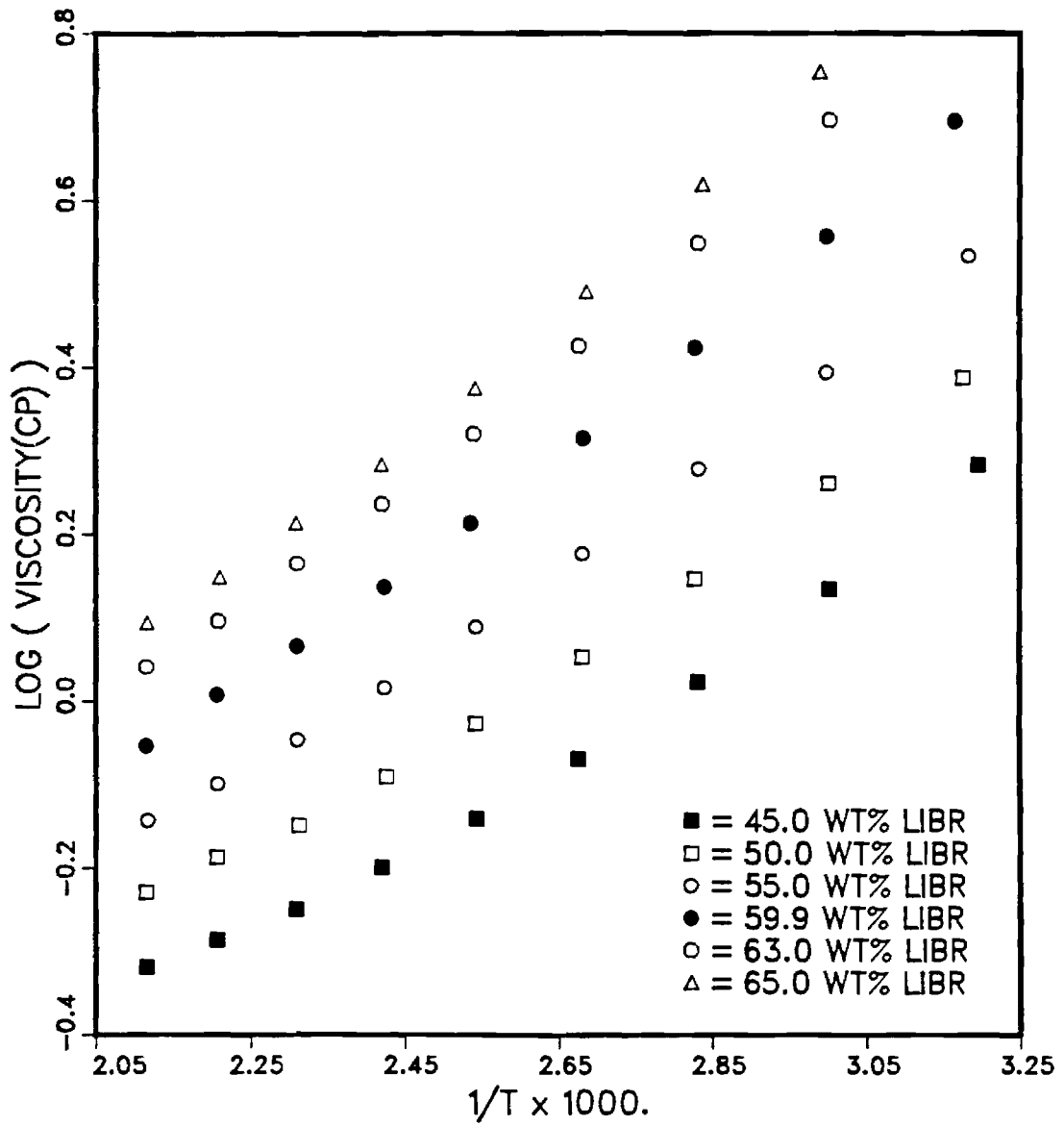


Figure 5. Viscosity of aqueous LiBr solutions.

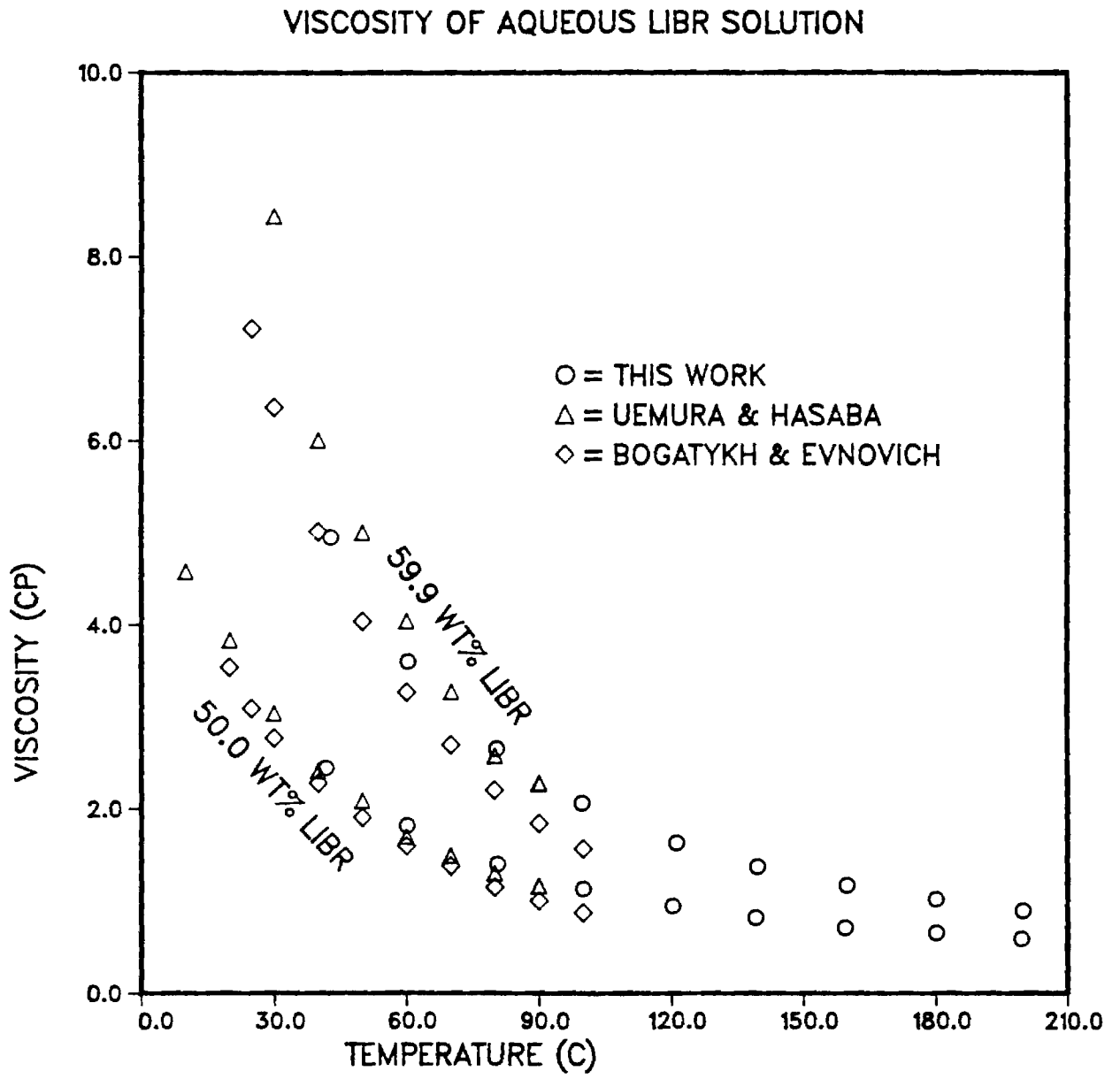


Figure 6. Comparison of the viscosity of LiBr - Water solutions obtained by different investigators.

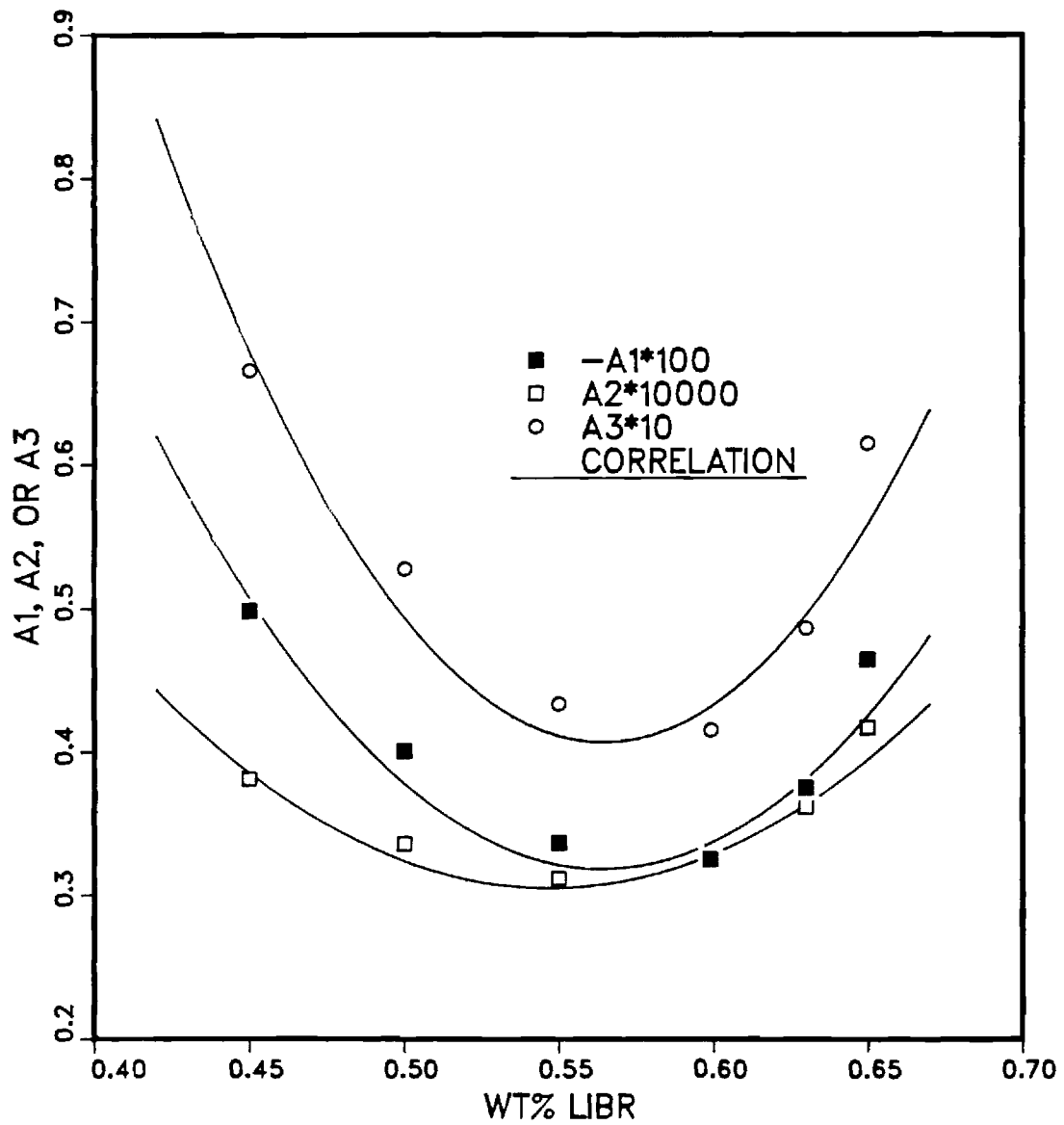


Figure 7. The values of A_1 , A_2 , and A_3 as a function of concentration.

VISCOSITY OF AQUEOUS LIBR SOLUTION

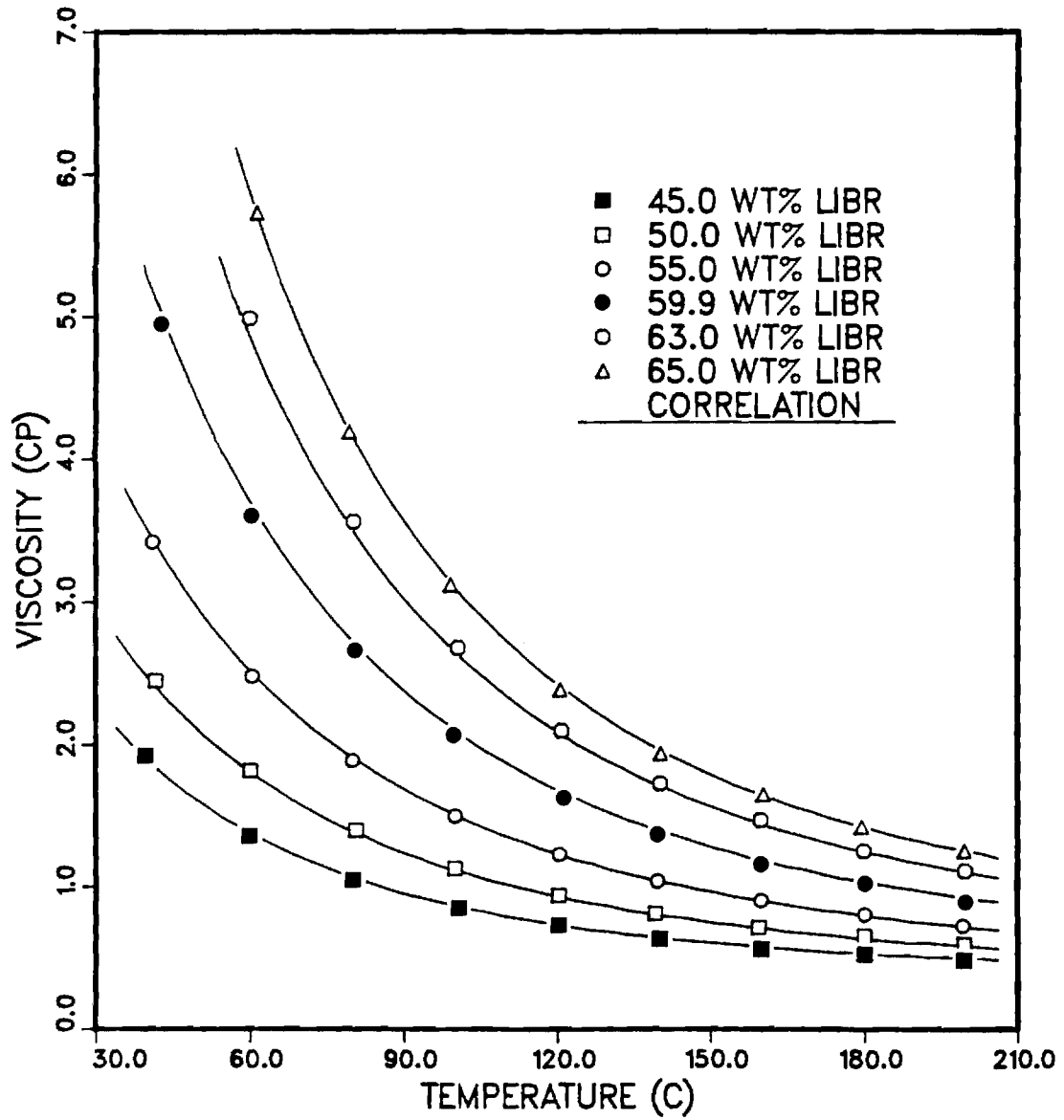


Figure 8. Comparison of the correlation with experimental data.

SPECIFIC HEAT MEASUREMENTS

1. INTRODUCTION:

As originally proposed, the specific heat measurements were conducted using a modified drop calorimeter. Proper application of this instrument produces accurate values for average specific heats over a finite temperature interval. These average specific heats can be fitted to a suitable function, such as a polynomial, of the temperature and concentration. Continuous values for the specific heat over the temperature range can be obtained by differentiating the average specific heat function. This general procedure has been followed resulting in data from this investigation that is in good agreement with independent data. The new data presented herein are compared with data from two alternative and independent sources and the three sets of data are demonstrated to be mutually confirming. The data from the three mutually confirming sets are also compared with two older data sets and the newer data do not confirm the older measurements.

A schematic of the particular instrument used in this investigation is shown in Figure 1. A drop calorimeter implements the classical "method of mixing" in which the system being "mixed" (i.e. brought to thermal equilibrium) consists of a small, ca. 100 gm, capsule containing the sample and a large, ca. 15 kg, receiver. For the apparatus used in this investigation, the receiver is well insulated but not quite adiabatic. In addition to the sample capsule and receiver, a drop calorimeter comprises a heater section and auxiliaries and controls. In operation, the material sample is confined in the rigid capsule or "bomb". The capsule containing the sample is brought up to an elevated temperature in the tube heater and inserted, by dropping, into the receiver. The receiver is a massive metal block, a copper cylinder in this case, with a central well to accept the capsule. The heat interaction between the sample and receiver is then monitored by a temperature probe installed in the receiver.

Quantitatively, the heat interaction can be interpreted in terms of energy changes in the receiver and the sample by consideration of two closed thermodynamic systems. The first system is the combination of the receiver and the capsule, which is charged with the sample. The second system is the capsule and sample alone. With reference to the closed system consisting of the charged capsule and the receiver, one has the following total energy at the instant before a drop:

$$E_{\text{com},i} = U_{\text{cs}}(T_s) + PE_{\text{cs}} + U_r(T_{ri})$$

Where:

$E_{\text{com},i}$ = energy of the combined system at the initial state, i

$U_{\text{cs}}(T_s)$ = internal energy of the capsule and sample at drop temperature, T_s

PE_{cs} = potential energy of the capsule and sample which are elevated with respect to the receiver

$U_r(T_{ri})$ = internal energy of the receiver at its initial temperature, before the drop, T_{ri} .

After the drop and later after the capsule, sample, and receiver have reached temperature equilibrium and have achieved a uniform final temperature, T_f , the energy is distributed as follows:

$$E_{\text{com},f} = U_{\text{cs}}(T_f) + U_r(T_f)$$

For the entire process beginning just before a drop and ending with temperature equilibrium, the principle of conservation of energy gives the following:

$$E_{\text{com},f} - E_{\text{com},i} + W_{\text{cs}} + W_r = Q_{\text{com}}$$

Where:

W_{cs} = work done by the capsule and sample during the process

W_r = work done by the receiver during the process

Q_{com} = heat interaction between combined system and its environment

Q_{com} is not quite zero, but a procedure to be explained below provides an empirical correction for a conditional assumption to be made that the combined system is adiabatic. Further simplifications are also possible. It can be verified that the change in potential energy of the sample due to its drop of about 0.5 meter is an entirely negligible .0049 kJ/kg. Additionally, the work terms can only involve boundary work on the atmosphere, $W_r = P_o \Delta V_r$ and $W_{\text{cs}} = P_o \Delta V_c$, and these quantities are also negligible. The potential energy change can be ignored, and the approximation that the combined system is adiabatic is now introduced. In consequence, the energy balance reduces to the following:

$$U_r(T_f) - U_r(T_i) + P_o \Delta V_r = - \{U_{\text{cs}}(T_f) - U_{\text{cs}}(T_s) + P_o \Delta V_c\}$$

or

$$\Delta H_r = - \Delta H_{\text{cs}}$$

Since the thermal expansion of both the receiver and capsule are entirely negligible, one could just as well write:

$$\Delta U_r = - \Delta U_{\text{cs}}$$

Clearly then, for the adiabatic case, the heat interaction from the capsule to the receiver, Q_x , is equal to the change in either the enthalpy or the energy of the sample and the capsule, or:

$$-Q_x = \Delta H_{\text{cs}} \text{ or } \Delta U_{\text{cs}}$$

Where the the indicated energy change is the sum of the component changes of the energies of the capsule and sample, or

$$\Delta U_{cs} = \Delta U_c + \Delta U_s$$

Proceeding from the assumption that the capsule undergoes an essentially constant volume process, the energy change of the sample, ΔU_s , can be readily evaluated. Ignoring the presence of a tiny quantity of air, the capsule can be considered to be filled with a known mass of fluid, m_s , such that:

$$V_s = m_s(v_f + x v_{fg})$$

Where V_s is the sample volume, 14.8 ml in this investigation.

Similarly, the internal energy of the sample is given as follows:

$$U_s = m_s(u_f + x u_{fg})$$

For a constant volume process proceeding from the initial sample temperature, T_s , and ending at T_f , the change in energy is as follows:

$$(U_s - U_f)/m_s = (u_{fs} - u_{ff}) + (x_s u_{fgs} - x_f u_{fgf})$$

Where:

u_{fs} = specific internal energy of the saturated liquid sample at T_s

u_{ff} = specific internal energy of the saturated liquid sample at T_f

x_s = quality of the sample at initial temperature, T_s

x_f = quality of the sample at final temperature, T_f

u_{fgs} = specific internal energy of evaporation of the sample at T_s

u_{fgf} = specific internal energy of evaporation of the sample at T_f

For a representative process, cooling a 12 gm sample of water from 200 C to 50 C, the first difference on the right is 641.33 kJ/kg while the second is around 1.02 kJ/kg. The influence of the phase change is only .0016 of the overall difference. Consequently, the heat effect on the sample can be considered to be just the change in energy of the saturated liquid. In terms of a heat capacity, the energy change can be quantified as the specific heat of the saturated liquid, often symbolized as " c_s ", as follows:

$$c_{s,ave} = (u_{fs} - u_{ff})/(T_s - T_f)$$

Generation of the saturated liquid specific heat data presented herein required a phased project beginning with a review of the pertinent literature, followed by upgrading and modifying the apparatus. The next steps were the development of a reliable experimental procedure and collecting the experimental data. The final step was the statistical analysis of the data and development of correlations for the average specific heats and the continuous specific heats. Work on the project has been proceeding since the summer of 1987. Preliminary work focused on a review of the pertinent literature. One source of data is especially well known, a dissertation by Löwer [1]. Specific heats at 50 WT% concentration from Löwer were relied upon by McNeely [2] in the production of enthalpy versus concentration and temperature charts. These charts were prepared

using a procedure developed by Haltenberger [3]. This procedure requires specific heats at only one concentration for the range of temperature along with vapor pressure data for the ranges of temperature and concentration. The data produced by McNeely have been fitted to a polynomial representation of the enthalpy by Patterson and Perez-Blanco [4]. Differentiation of these data provide an additional resource for specific heat data for ranges of temperature and concentration. A third alternative source is the previously unpublished data graciously provided by Dr. Uwe Rockenfeller, president of Rocky Research, Incorporated. An additional source of data is a report by Uemura and Hasaba [5] which includes data subsequently quoted elsewhere [6]. A final data source, by Pennington and Daetwyler [7], has been mentioned, but this data is for such a low temperature as to have no direct implication to the current work.

Our preliminary laboratory work involved rehabilitating the drop calorimeter, adapting it to this experiment, and interfacing to a personal computer (PC) based data acquisition system (DAS). The apparatus was functionally tested and found to be in basically good working condition. The receiver surface was oxidized after years of use so it was plated with a bright nickel alloy to minimize radiation losses. An attempt was made to repair the defective electromechanical printer that was supplied with the calorimeter. This was an effort to provide a redundant, independent data display in addition to the PC-based DAS to be used in production runs. This effort was not successful.

The next effort was to interface the calorimeter to the DAS. The DAS can accommodate calibrated thermocouple inputs as well as millivolt level inputs. A standard thermocouple input is used to monitor the sample temperature while in the furnace chamber. Precision resistance networks were constructed to condition the signal from the receiver thermistor. It was anticipated that initial runs would be made at low concentrations in open air while the heated enclosure necessary to elevate the calorimeter temperature to forestall phase change at high concentrations was under preparation. Consequently, it was necessary to design and build bridge circuits for two receiver temperature ranges, 0 to 40 C and 0 to 100 C.

Some upgrading of the calorimeter was accomplished to improve its performance and reliability. The most critical functional change is in the measurement of the sample temperature while the capsule is in the heater. In the original equipment design, a thermocouple is imbedded in the heating element outside the furnace tube. This arrangement is unsatisfactory for at least two reasons. Since the thermocouple is permanently installed, it cannot be removed for recalibration. Secondly, since the stock thermocouple is attached to the tube wall, it can not be assured that an accurate sample temperature measurement is being attained. To alleviate these problems, the apparatus was augmented with a calibrated thermocouple that is inserted directly into the capsule. To allow this access, a modified capsule was designed and fabricated. Some other minor improvements were made to insure the integrity of electrical connections, minimize mechanical problems caused by dust shedded from thermal insulation, and eliminate jams caused by interference between the heater tube and the capsule.

Some additional analytical work was also completed on the analysis of the receiver cooling curves and reduction of heat transfer data to energy changes and specific heats. These efforts completed our initial preparation and allowed for the initiation of the final tasks: development of the experimental procedure and collection of the data in production runs and analysis of the results and production of the property correlations.

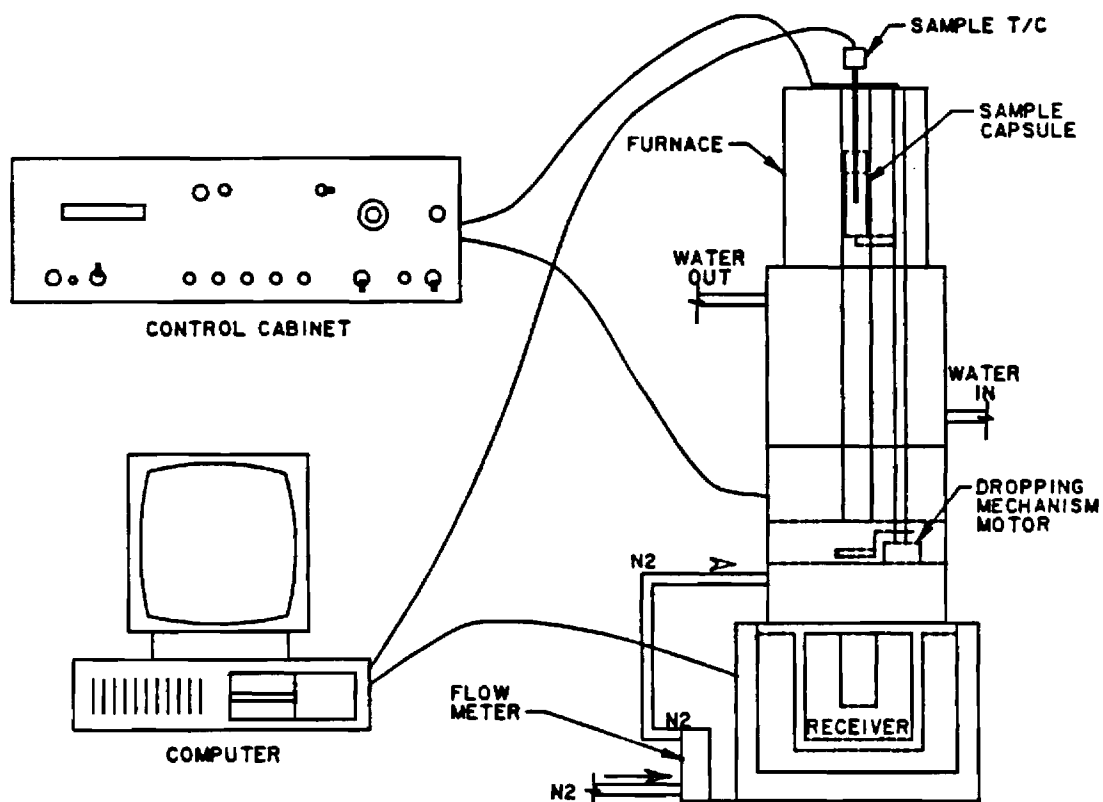


Figure 1. Schematic of Drop Calorimeter

2. EXPERIMENTAL DESIGN:

Experimental Apparatus. A single calorimeter, a Unitherm Model 7100 Drop Calorimeter, was used in all tests. For low concentrations, the calorimeter was operated in open air in the laboratory. For the higher concentrations, 60 WT% and 65 WT% by weight of LiBr, the calorimeter was operated in an elevated temperature enclosure as shown in Figure 2. The addition of the heated enclosure was necessary to prevent a phase transition to a crystalline hydrated complex, $\text{LiBr} \cdot n\text{H}_2\text{O}$, when the concentrated solutions are cooled to near room temperature. The enclosure was also thought desirable to provide a temperature stable environment.

Obtaining an accurate sample temperature is thought to be one of the important challenges in drop calorimetry. In the design of the original equipment, the sample thermocouple is installed outside the tube heater. This location is undesirable because the thermocouple cannot be removed for calibration and because an unknown temperature gradient must exist between the heater and capsule. To enhance this measurement, the capsule was modified to include a removable thermocouple well as shown in Figure 3. The entire construction is stainless steel. The thermowell port also serves as the capsule spout, and the thermowell tube serves as the stopper. A standard two piece, ring and ferrule, compression fitting secures the thermowell tubing. This reliable high pressure fitting can be reused indefinitely providing an inexpensive, leak-free assembly. In addition to the operational advantages, the integral thermowell has two thermometric advantages. In the modified design, the sample thermocouple can readily be removed for calibration and, as importantly, the thermocouple is immersed within the sample providing a highly accurate measure of the sample temperature. The sample thermocouple output from the DAS was calibrated by comparison with a field standard platinum RTD (Leeds and Northrop platinum resistance thermometer, Serial No. 709892) in a Muller bridge. The field standard RTD is traceable to the International Practical Temperature Scale in force when it was manufactured, the IPTS-48, and has been adjusted to correspond to IPTS-68, the current standard. Note that the calibration procedure used the production DAS in the calibration step. This allowed for the entire sample temperature measurement subsystem, including the thermocouple and its reference temperature compensation circuit as well as the instrumentation amplifier and ADC in the DAS, to be calibrated simultaneously. This overall calibration, while somewhat more demanding and inflexible than calibrating all the components individually, should allow for improved accuracy as calibration compensation is provided at once for all the critical measuring components and not just the temperature probe alone.

The other critical temperature measurement is the receiver temperature. For the present purposes, it is most important that the receiver temperature probe produce a linear response over the range of expected use, around 20 C to 30 C in open air or around 50 C to 60 C in the enclosure. A commercially packaged thermistor pair in a parallel arrangement with compensating resistors, similar to the manufacturers original equipment, was selected for the receiver temperature sensor. Semiconducting thermistors exhibit decreasing electrical resistance with increasing temperature. This resistance

change can be measured as a voltage change in a suitable auxiliary circuit. The parallel, compensated arrangement of the thermistors produces a very nearly linear temperature dependence in the overall resistance. This linear response is important for drop calorimetry. Circuits for both temperature ranges are similar. In the higher temperature device, the resistance is converted into a voltage signal in an external voltage divider with a nominal sensitivity of 6.7 mV/C°. The voltage divider was further incorporated into a Wheatstone bridge to allow the establishment of an arbitrary zero output voltage near 0 C. The completed circuit and DAS were calibrated by comparing computer output of the voltage with the field standard platinum RTD with the resulting relation:

$$T_r = 148.5964 \text{ (C/volt)} V_{\text{DAS}} + 5.781795 \text{ C}$$

This response allows service over a range of 5.8 C (at $V_{\text{DAS}} = 0$) to 80 C (at $V_{\text{DAS}} = 500$ mV) since the analog to digital converter will be used with a span of 0 to 500 mV. The temperature range is more than adequate in this or similar applications. The calibrated sensitivity of 6.73 mV/C° provides a resolution of .001 C°/count in the receiver temperature with the 16 bit ADC in use here. This is about .05 % of the expected temperature change in a typical drop and represents the limit of accuracy in the system due to resolution. In the room temperature device, a sensitivity of 9.92 mV/C° was obtained for a similar resolution of .0008 C°/count and an operating temperature range of 0 to 50 C.

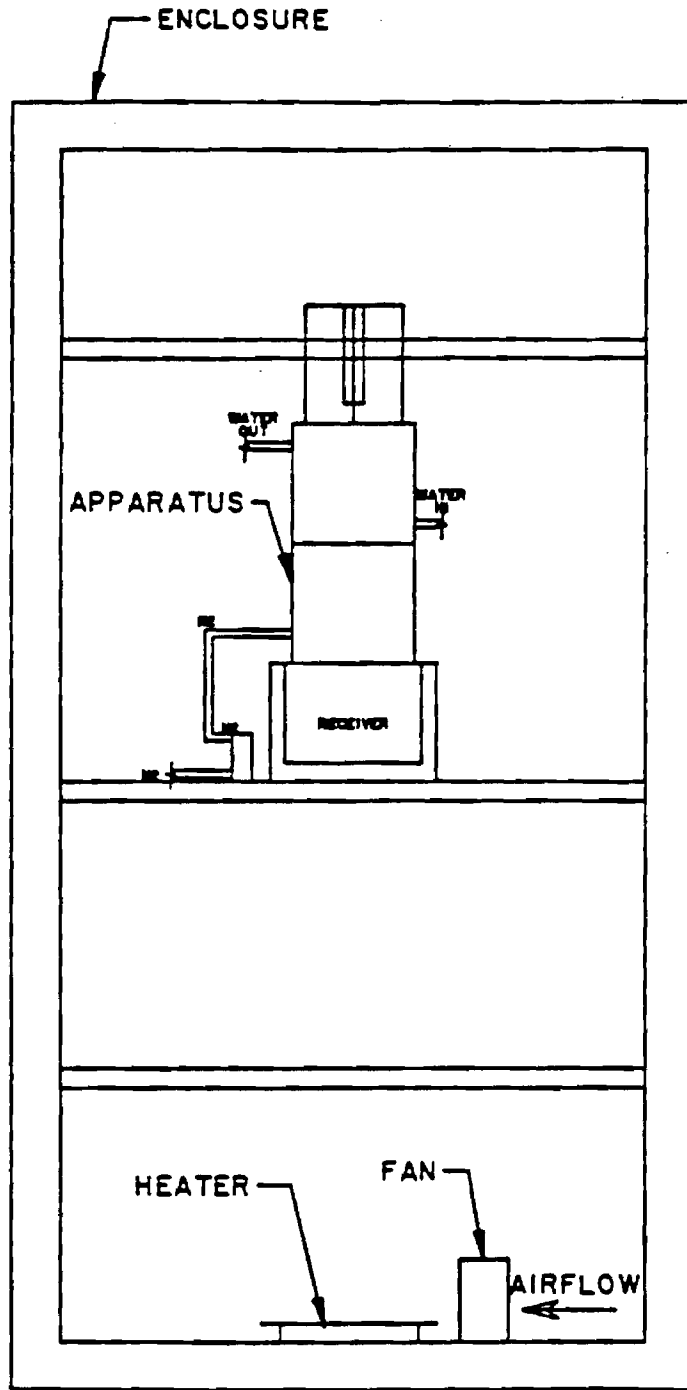
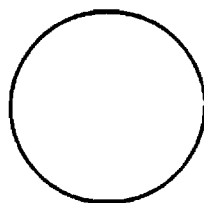
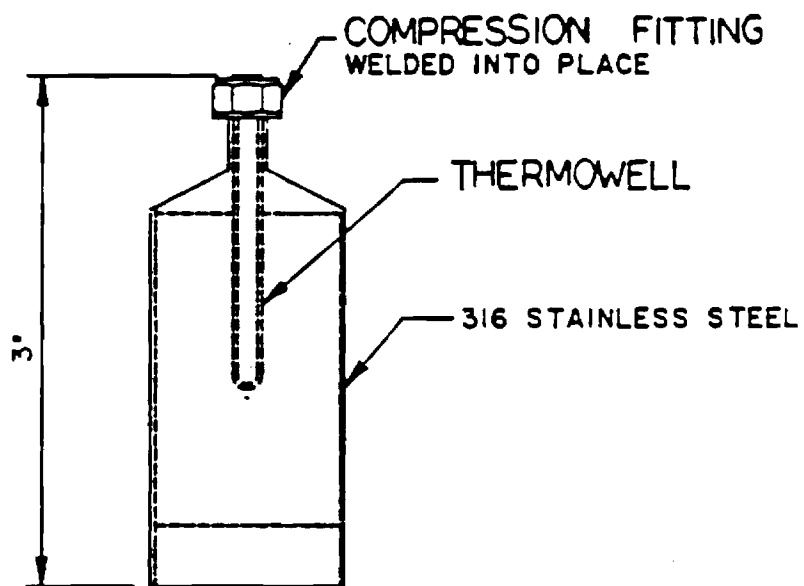


Figure 2. Drop Calorimeter in Temperature Controlled Enclosure



BOTTOM VIEW

Figure 3. Sample Capsule with Integral Thermowell

Experimental Procedure. The most crucial aspects of the experimental procedure are loading an accurate and appropriate mass of sample in the capsule and establishing stable sample and receiver temperatures before a drop and maintaining a stable environmental temperature during a drop.

The sample volume has been determined gravimetrically, using water, to be around 14.8 ml. A sample mass should be installed such that after thermal expansion a small ullage space remains as it is a practical impossibility to seal the capsule against the expansion of a compressed liquid. Typically, a volume of around 12 to 13 ml is installed. A minimal ullage volume is preferable primarily to maximize the mass of the sample and thereby increase the temperature response of the receiver and secondarily to reduce the effect of vaporization. The capsule is accurately weighed before and after installation of the sample to accurately determine the mass of the sample and to monitor against the possibility of leaks. No leaks have been observed in practice.

Establishing stable temperatures begins with the initial preparation for a drop with the receiver lowered after a previous drop. It is first necessary to return the receiver to near its environmental temperature whether this is room temperature or, preferably, the enclosure temperature. In the enclosure, it was found desirable to ventilate the exposed receiver with a small fan. Usually it was convenient to ventilate the receiver for several hours to allow complete cooling. During this cooling process, it is desirable to proceed with installing the sample capsule in the tube heater and preheating the sample. If the sample is preheated while the receiver is being ventilated, the heater will operate only intermittently later after the receiver has been raised and even later after the sample drop. Excessive operation of the sample heater later is likely to disturb the temperatures in the receiver or in the enclosure.

After the receiver is cooled and the sample preheated, the receiver is raised to its operational position where it is ready to accept the dropped capsule. Heat leak from the heater to the receiver cannot be eliminated by the insulation, water jacket, and cover gas so it is typical for the temperature of a properly cooled receiver to rise slightly subsequently to raising the receiver. In contrast, a receiver improperly left too warm from a previous drop will continue to cool even after being raised. It is critical to minimize any temperature drift prior to a drop. Otherwise the results of the drop will be impaired. Typically, the receiver is left in the raised position for at least 90 minutes to reestablish a stable receiver temperature. Prior to a drop, the receiver temperature should be closely monitored. Usually, the receiver temperature is studied for 10 minutes before the drop to verify a stable condition.

Once stable temperatures in the heated sample and receiver have been established, it is appropriate to drop the sample into the receiver. The drop mechanism can then be activated. The drop pin and insulated shutter move to allow the capsule to enter the receiver and then quickly return to their original position to allow the insulated shutter to continue to prevent excessive heat leak from the furnace tube to the receiver.

After the drop, the receiver temperature is monitored for several hours until the receiver has passed through its temperature maximum and is well along its cooling curve. For reference, the DAS continues to monitor the enclosure and room temperatures. After the cooling period, the temperature data is retrieved for further analysis.

3. DATA REDUCTION AND ANALYSIS:

Data reduction and analysis involves two steps, cooling curve analysis to determine the ultimate heat transfer from the capsule to the receiver followed by interpretation of the heat interaction in terms of calibration data for the capsule and receiver.

The cooling curve analysis results in an estimate of the ultimate temperature which would be reached by the receiver in the absence of heat loss. With this correction, the receiver, capsule, and sample constitute the adiabatic combined system envisaged as the principle of operation of the drop calorimeter. The correction is illustrated in Figure 4. The numerical procedure is as follows:

1. Identify the time, t_{max} , at which the maximum temperature is reached. For accuracy, this is done by fitting a smooth quadratic curve through the 10 data points nearest the peak and solving for the peak time and temperature analytically.

2. Next, identify the slope of the temperature versus time curve, also called the temperature drift, at some convenient instant. This slope should be evaluated well after the maximum so that the temperature drift due to heat loss from the receiver to the ambient is dominant and its trend is well established. A convenient time is $2 \cdot t_{max}$. Numerically this is done by fitting a straight line through the 11 data centering on $2 \cdot t_{max}$.

3. The temperature drift is next extrapolated backwards to a unique time after the drop at which time the extrapolated temperature is predicted to equal the ultimate receiver temperature that would have been achieved in a perfectly adiabatic process. The time suggested, [8] and [9], for this evaluation corresponds to the time at which the receiver has attained 60 % of its observed maximum value. Analysis of a thermal resistance network containing two lumped capacitances presented in [10] confirms this suggestion for the parameters of the drop calorimeter used in these measurements.

4. The temperature computed from the extrapolated drift, T_p , is used as the final temperature for the capsule and sample as well as the receiver. Note that this correction has the advantage of being strictly based on physical observations and current conditions, such as the temperature difference between the receiver and ambient, and should provide at least a first order correction for any casual environmental influences.

The cooling curve analysis also identifies the initial sample temperature, T_s , and the initial receiver temperature, T_{ri} . In later modifications, a linear fit was applied to minimize the effect of any initial drift or irregularity in these two measurements. The heat interaction is interpreted in terms of heat capacities from the following result of the energy balance:

$$-\Delta U_{cs} = (C_c + C_{sam})(T_s - T_f) = \Delta U_r = C_r(T_f - T_{ri})$$

Where:

C_c = the average heat capacity, $m \cdot c_{ave}$, of the capsule
 C_{sam} = the average heat capacity of the sample
 C_r = the average heat capacity of the receiver

Then solving for the average heat capacity of the sample:

$$C_{sam} = C_r(T_f - T_{ri}) / (T_s - T_f) - C_c$$

Upon introducing the experimentally convenient ratio, $K_{cr} = C_c/C_r$, which is the ratio of the average heat capacity of the capsule to that of the receiver one has:

$$C_{sam} = C_r(T_f - T_{ri}) / (T_s - T_f) - C_r K_{cr}$$

The specific heat of the saturated liquid sample can then be determined from the mass of the sample and its average heat capacity:

$$c_{s,ave} = C_{sam} / m_s$$

Clearly, the specific heat determination requires the two calibration values, C_r and K_{cr} . The values are determined as functions of the experimental conditions to further enhance accuracy in accord with the procedure suggested in [11]. The heat capacity ratio, K_{cr} , is determined by a series of empty capsule calibration drops. For a zero mass sample, the combined energy balance gives:

$$K_{cr} = C_c/C_r = (T_f - T_{ri}) / (T_s - T_f)$$

The results for a range of furnace temperatures, T_s , were correlated against the sample temperatures with the following results:

For the open air system:

$$K_{cr} = .0000088 T_s + .011551$$

For the temperature controlled enclosure:

$$K_{cr} = .0000085 T_s + .01149$$

The slight temperature dependency of this ratio is not necessarily due to thermal property differences alone but can also account for heat leaks from the furnace to the receiver during drops, when the insulated shutter is momentarily open, and any (much smaller) heat leak following the drop.

The heat capacity of the receiver can be calibrated by either a "relative" or an "absolute" procedure. An absolute calibration would rely on electric heating of the receiver and the subsequent temperature response. While the electric energy input can obviously be determined with great precision, the success of an absolute calibration is entirely dependent on a full understanding and characterization of the systematic behavior of the calorimeter. Accounting for systematic errors in the form of heat leaks between the

receiver and the ambient and the heater is enormously challenging; consequently, a relative calibration was adopted. In a relative calibration, the response of the receiver to a reference sample is measured. Two stable and well characterized materials were used as the reference substances, alumina and water. According to the energy balance, the receiver heat capacity for a calibration drop when the reference sample has a specific energy change of $u_{\text{ref}}(T_s)$ to $u_{\text{ref}}(T_f)$ is given by:

$$C_r = m_s [u_{\text{ref}}(T_s) - u_{\text{ref}}(T_f)] / [(T_f - T_{ri}) - K_{\text{cr}}(T_s - T_f)]$$

In accordance with the suggested procedure, C_r in units of kJ/K, was correlated against the overall temperature change of the receiver with the following results:

For the open air system:

$$C_r = 4.321664 + .052339 \Delta T_r$$

For the system in temperature controlled enclosure:

$$C_r = 4.312143 + .019233 \Delta T_r$$

The variation of apparent heat capacity of the receiver as explained by the receiver temperature change is unlikely to bear much relation to thermodynamic property changes since the receiver temperature rise is only a couple of degrees at most. More likely, this effect comes from a somewhat enhanced heat leak to the environment in higher temperature drops as well as from residual variation in the leak leak from the heater not accounted for by the K_{cs} correlation.

The calibration procedure described above represents one of the obstacles to rapid specific heat evaluations using the drop calorimeter since the entire calibration procedure for both K_{cr} and C_r should be repeated if the capsule or any other critical component such as the temperature sensors or their signal conditioning and data conversion circuits must be changed or significantly altered. In this investigation the calorimeter environment was changed once along with the receiver temperature circuit. This necessary change doubled the effort required for calibration. Obtaining stable initial conditions and collecting data for the extensive cooling curve analysis present another drawback. Several hours of phased cooling of the exposed receiver and an hour or two or more of temperature stabilization of the raised receiver must precede every drop, and several hours of monitored receiver response must follow the drop. Consequently, not even a single drop can be completed in an ordinary working day, and it takes considerable coordination to arrange for a drop to be prepared during the day and completed overnight. The resulting data rate, especially if allowing for interrupted data and spoiled drops, is not very high. An advantage is, however, that the physical principles of the device are simple and well founded in thermodynamic fundamentals. Another advantage is that an average specific heat is obtained which represents the behavior of the sample over a broad range, e.g. 100 Celsius degrees or more, on each drop.

The experimental data are presented in Tables 1 through 5 which present the measured average specific heat data, at specified concentrations near 45 WT%, 50 WT%,

55 WT%, 60 WT% and 65 WT%. Also tabulated are the initial and final sample temperatures T_s and T_f and the average temperature for the drop, $T_{ave} = (T_s + T_f)/2$.

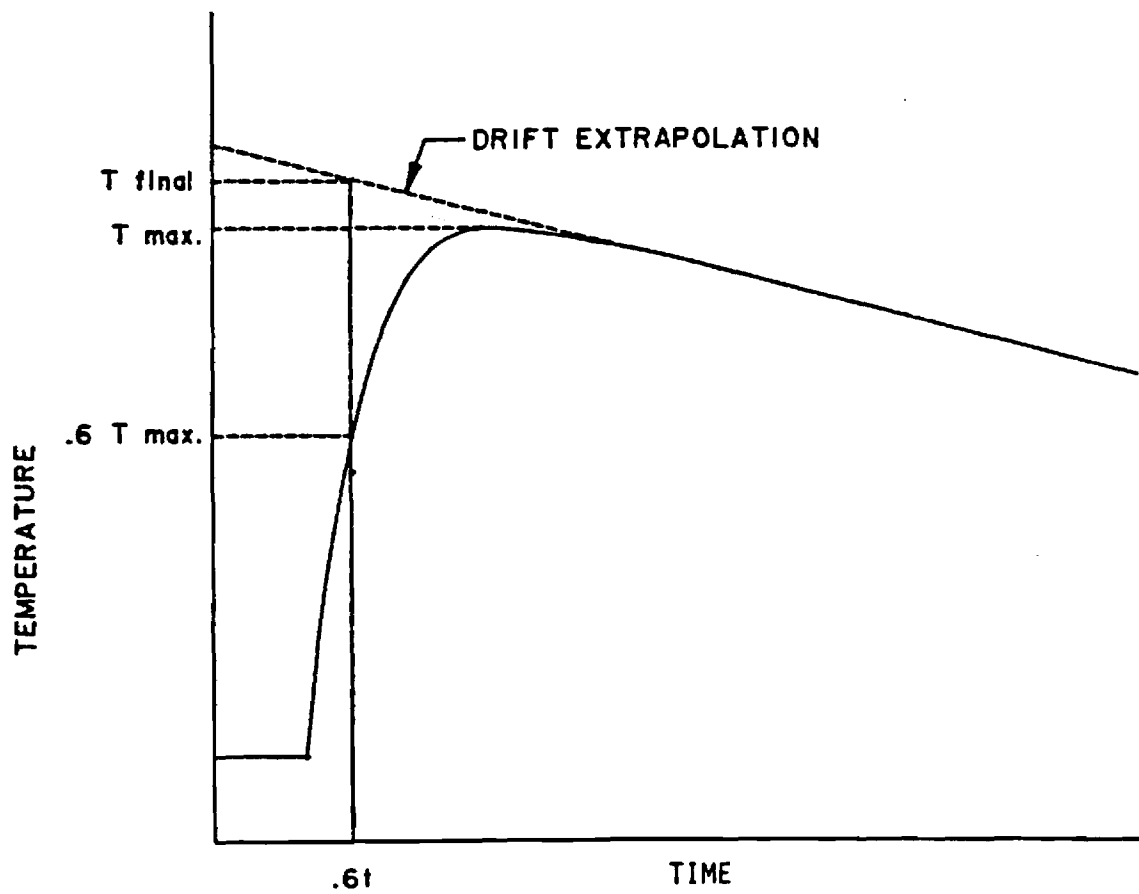


Figure 4. Graphical Representation of Cooling Curve Analysis

Table 1.
Average Specific Heat Results
for Concentrations near 45 WT%

Mass Fraction	Average Temperature	Average Specific Heat	Final Temperature	Sample Temperature
0.4395	61.9125	2.1924	23.741	100.084
0.4395	62.566	2.3932	25.193	99.939
0.4395	81.747	2.2153	25.345	138.149
0.4395	89.781	2.3525	26.454	153.108
0.4395	90.456	2.4056	26.627	154.285
0.4395	100.5785	2.4956	26.614	174.543
0.4395	114.605	2.3915	28.039	201.171
0.4395	105.7915	2.3589	28.402	183.181
0.4395	113.103	2.4931	25.701	200.505
0.4395	65.237	2.3546	25.603	104.871
0.4395	75.818	2.2437	26.324	125.312
0.4395	71.082	2.1682	25.461	116.703
0.4395	114.5565	2.5604	29.214	199.899
0.4395	84.36055	2.3824	49.0448	119.6763
0.4395	121.4709	2.3117	53.0417	189.9001
0.4395	121.4293	2.39	53.1895	189.669

Table 2.
Average Specific Heat Results
for Concentrations near 50 WT%

Mass Fraction	Average Temperature	Average Specific Heat	Final Temperature	Sample Temperature
0.5059	64.9115	2.4772	25.309	104.514
0.5059	85.564	2.3021	27.102	144.026
0.5059	108.394	2.2599	28.781	188.007
0.5059	71.2325	2.059	26.785	115.68
0.5059	93.616	2.2912	28.739	158.493
0.5059	116.522	2.3296	29.971	203.073
0.5059	78.5505	2.113	27.687	129.414
0.5059	101.093	2.3024	28.666	173.52
0.5059	64.6	2.029	23.094	106.106

Table 3.
Average Specific Heat Results
for Concentrations near 55 WT%

Mass Fraction	Average Temperature	Average Specific Heat	Final Temperature	Sample Temperature
0.541	68.3	2.0767	20.92	115.68
0.541	98.0085	1.9805	23.51	172.507
0.541	92.3355	2.1271	26.043	158.628
0.541	76.532	2.0097	23.988	129.076
0.541	87.2585	2.1565	25.443	149.074
0.541	114.661	2.167	27.089	202.233
0.541	64.459	1.949	22.281	106.637
0.541	71.3375	2.1536	22.449	120.226
0.541	105.565	2.2025	23.905	187.225
0.541	102.4675	2.0443	23.404	181.531

Table 4.
Average Specific Heat Results
for Concentrations near 60 WT%

Mass Fraction	Average Temperature	Average Specific Heat	Final Temperature	Sample Temperature
0.5948	88.001	1.8122	57.88	118.122
0.5948	95.21	1.9684	58.381	132.039
0.5948	103.0425	1.9254	59.318	146.767
0.5948	109.453	2.1008	61.387	157.519
0.5948	110.8975	2.0566	60.638	161.157
0.5948	117.207	1.9555	59.784	174.63
0.5948	118.488	2.0738	61.439	175.537
0.5948	126.6605	2.0113	63.731	189.59
0.5948	132.867	2.0438	62.42	203.314
0.5948	133.33	1.8606	62.593	204.067

Table 5.
Average Specific Heat Results
for Concentrations near 65 WT%

Mass Fraction	Average Temperature	Average Specific Heat	Final Temperature	Sample Temperature
0.6483	110.465	1.8476	60.796	160.134
0.6483	133.0425	1.7396	62.231	203.854
0.6483	100.1705	1.6356	59.307	141.034
0.6483	114.8285	1.7726	59.708	169.949
0.6483	127.694	1.7973	61.996	193.392
0.6483	104.864	1.6391	59.178	150.55
0.6483	120.3965	1.815	61.057	179.736
0.6483	87.973	1.4063	57.891	118.055
0.6483	126.0605	1.9652	62.222	189.899
0.6483	95.731	1.5161	59.539	131.923
0.6548	151.1252	1.863	62.4005	239.85
0.6548	150.1908	1.8308	60.3816	240.00
0.6548	149.7689	1.8518	59.7178	239.82
0.6548	150.0077	1.8587	59.9455	240.07
0.6548	150.5762	1.8237	60.5924	240.56
0.6548	125.1235	1.9023	58.637	191.61
0.6548	125.051	1.801	58.9119	191.19
0.6548	125.0617	1.8494	60.1435	189.98
0.6548	99.5894	1.8114	56.3988	142.78

4. CORRELATION OF DATA:

Inspection of the available data indicates that a polynomial temperature dependence constitutes an adequate model. For this behavior, the general dependence of the specific heat on temperature, T , is of the form:

$$c_s = a + b \cdot T$$

for a linear dependence on temperature, and

$$c_s = a + b \cdot T + c \cdot T^2$$

for a quadratic dependence.

In either case the coefficient functions can be polynomials in the salt concentration such as the following general formula:

$$a = \sum a_k \cdot w^k, \text{ with } k = 0 \text{ to } n.$$

In the current experimental work, statistically valid values for n were limited to 1 or 2 while in some numerical work quoted below values for n as large as 5 were used. As discussed below, no statistical support was found for a quadratic temperature dependence compared with the linear relationship; consequently, consideration of the models which are linear in temperature will be emphasized. In the preceding relationships, the coefficient functions, a and b and c , can be functions of the concentration. Herein, the concentration will be expressed in terms of mass fraction, w , of the salt (i.e. $0 < w < 1.0$). Both linear and quadratic functions of concentration, and combinations, have been investigated. Expanding the coefficient functions, the relationships that are linear in temperature can have one of the following functional forms:

A linear-linear (in w) model:

$$c_s = (a_0 + a_1 w) + (b_0 + b_1 w)T$$

A quadratic-linear model:

$$c_s = (a_0 + a_1 w + a_2 w^2) + (b_0 + b_1 w)T$$

A quadratic-quadratic model:

$$c_s = (a_0 + a_1 w + a_2 w^2) + (b_0 + b_1 w + b_2 w^2)T$$

For quantitative comparison, the following model quadratic in temperature was also considered:

T-Quadratic model:

$$c_s = (a_0 + a_1 w + a_2 w^2) + (b_0 + b_1 w + b_2 w^2)T + c_0 T^2$$

Regression calculation were performed on the four preceding models with the results tabulated in Table 6. In this table, salient statistical results are presented for each model. The first statistical result is the Coefficient of Determination which is the ratio of the variation explained by the model to the total variation in the data set. The balance of the variation is called the residual variation. The residual variation is due to any systematic or random errors in the data as well as any inadequacy in the model. Including extra parameters augments the model. An example of augmenting a model is shifting from a linear to a quadratic model. Any augmentation of the model is sure to decrease the residual variation because an additional term always provides some additional adaptability. In consequence, an enhanced model must result in a better fit to the data base, but unending augmentation of the model is not justifiable. According to the preceding results, the model with both coefficients linear in the concentration, the linear-linear model, is the only model linear in temperature that remains significant at the probability criterion well under .05, a conventional limit. The model with a leading term that is quadratic in composition and a coefficient function multiplying the temperature that is linear in composition, the quadratic-linear model, is marginally significant in a statistical sense. The model that has both coefficient functions quadratic in composition, the quadratic-quadratic model, is clearly insignificant statistically. In the last case, the additional parameter has reduced the residual variation so little that one can ascribe the minimal reduction merely to reduced random variation. Some reduction is guaranteed when the model is enhanced; but, when small, the better fit cannot be ascribed to an improved systematic fit to the data. The model quadratic in temperature is also not significant at a .05 level. This implies that the improvement in the Coefficient of Determination obtained by expanding the model to include the quadratic temperature term is no better than a random improvement. In addition, the Standard Error of Estimate is not improved at all. Furthermore, results from other investigations provide no support for a model quadratic in temperature. Therefore, it is the linear-linear model, the model that is linear in temperature with both coefficient functions linear in composition, that is the most likely model considering both the statistical and physical evidence. For any of the models with linear dependence on temperature such as the first three models, the average specific heat has the following especially simple form:

$$c_{s,ave} = a + b(T_s + T_f)/2$$

or using the linear-linear model as an example,

$$c_{s,ave} = (a_0 + a_1 w) + (b_0 + b_1 w)T_{ave}$$

This simple dependence conveniently allows even average specific heat data to be plotted as a function of the average temperature on a two dimensional graph. Figures 5, 6, 7, and 8 illustrate the correlation lines for all three linear models superimposed on the entire data set.

The linear-linear correlation results are plotted in Figures 9 to 13 for the five different concentrations. Plotted along with the correlation lines are confidence limits above and below the correlation line displaced by the amount of the Standard Error of Estimate. There is, unfortunately, some significant scatter in the data so the confidence limits are rather broad. Note that the error estimates are on the order of .10 kJ/kg. This uncertainty is about 5% of the typical value of the specific heat which is around 2 kJ/kg. Finally, the preferred, linear-linear, correlation model at evenly spaced values of the LiBr concentration is shown in Figure 14. Also shown in this figure is the c_s curve for water determined from quadratic interpolation of results from a program [12] that reproduces the 1967 version of the ASME Steam Tables. Note that the steady increase in c_s with temperature as exhibited by water is mimicked by the similar increase for the LiBr solutions.

Note that for completeness the correlation lines and correlation lines with error limits for the quadratic-linear and quadratic-quadratic models have been plotted and are included in an appendix. The coefficients for all three models are given in Table 7.

Table 6.

CORRELATION RESULTS FROM DROP CALORIMETER DATA

Model	Coefficient of Determination*	Statistical Significance Level**	Standard Error of Estimate***
Linear-Linear	.839594	ca. 0.	.0968 (ca. 4.8%)
Quadratic-Linear	.847687	.09	.0951 (ca. 4.8%)
Quadratic-Quadratic	.848925	.50	.0956 (ca. 4.8%)
T-Quadratic	.854556	.15	.0955 (ca. 4.8%)

* The Coefficient of Determination, R^2 , is the ratio of the unexplained variation to the total variation in a population for which a regression model has been developed. The total variation is the sum, $\sum (y_i - y_{ave})^2$, where y_i is the i th value of the dependent variable. The explained variation is the difference between the total variation and the residual variation, where the residual variation is the sum, $\sum (y_i - y_m(x_i))^2$, where y_m is the statistical model corresponding to the i th datum, y_i , which is evaluated at the i th value of the independent variables. A model that results in a perfect fit to the experimental data gives 1 for the Coefficient of Determination.

** The Statistical Significance Level is the probability, $P(z > t)$, that a random variable with some appropriate distribution, z , is greater than some pertinent value, t . In the current case, the appropriate distribution is the Student-t distribution and the pertinent value t is evaluated as follows:

$$t = \left(\frac{\Delta(R^2) \cdot DF}{1 - R^2} \right)^{\frac{1}{2}}$$

Where $\Delta(R^2)$ is the increase in R^2 due to the model

$$\Delta(R^2) = R^2(\text{enhanced model}) - R^2(\text{simpler model})$$

As an example, for a quadratic model:

$$\Delta(R^2) = R^2(\text{quadratic model}) - R^2(\text{linear model})$$

For the linear model use the special case:

$$\Delta(R^2) = R^2(\text{linear model}) - 0$$

DF = degrees of freedom

DF = number of data points - number of parameters

A high value of t leads to a low value of $P(z > t)$ and implies that an enhanced model, such as a quadratic model compared with a linear model, does not improve the R^2 merely by reducing some of the random model but provides a better systematic fit to the data.

*** The Standard Error of Estimate is analogous to the Standard Deviation from the mean of a simple distribution in that 68% of the data are expected to lie within one Standard Error of Estimate of the regression line.

Table 7

Coefficients for Three Models Linear in Temperature

		Algebraic Formulation of Model:		
		Linear- Linear	Quadratic- Linear	Quadratic- Quadratic
Coefficient:				
Symbol	Multiplies			
a_0		3.067819	1.938608	-.26642
a_1	w	-2.15232	2.692092	10.97101
a_2	w^2		-5.165042	-12.7661
b_0	T	0.06018	.002953	.02502
b_1	wT	-.00731	-.000805	-.08334
b_2	w^2T			.07541

Figure 5.

Linear-Linear Model with Data

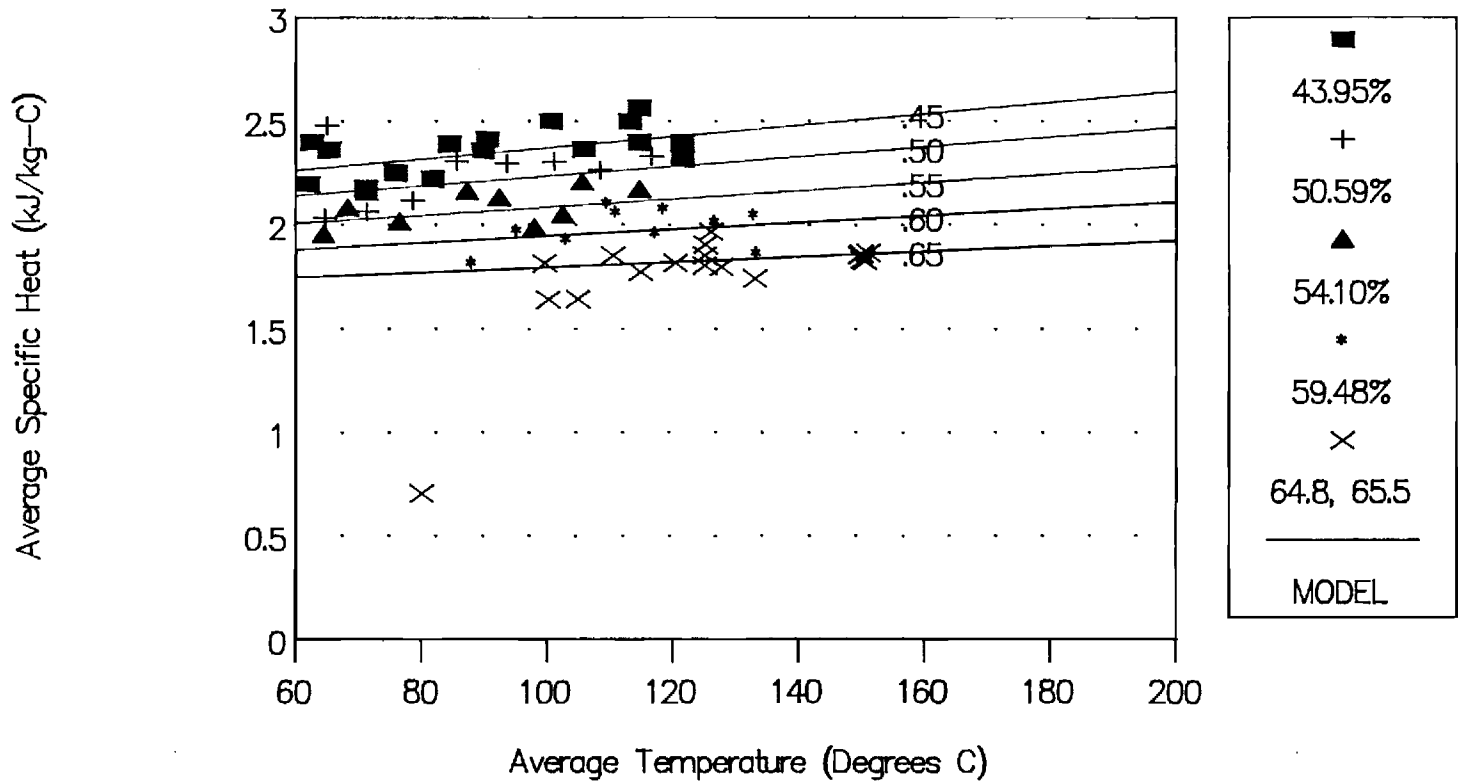


Figure 6. Data and Linear-Linear Model
at Concentrations Similar to Data

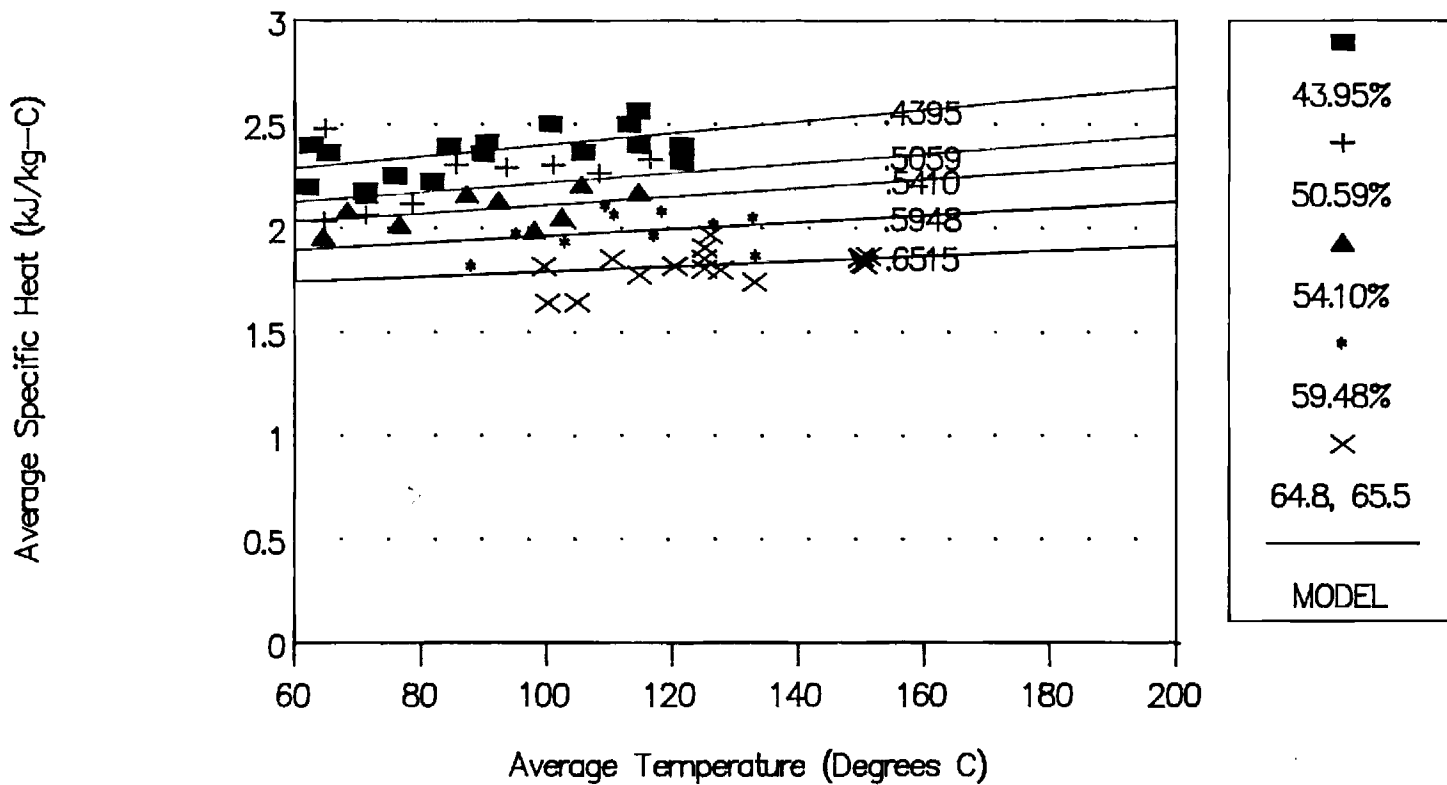


Figure 7.

Quadratic-Linear Model with Data

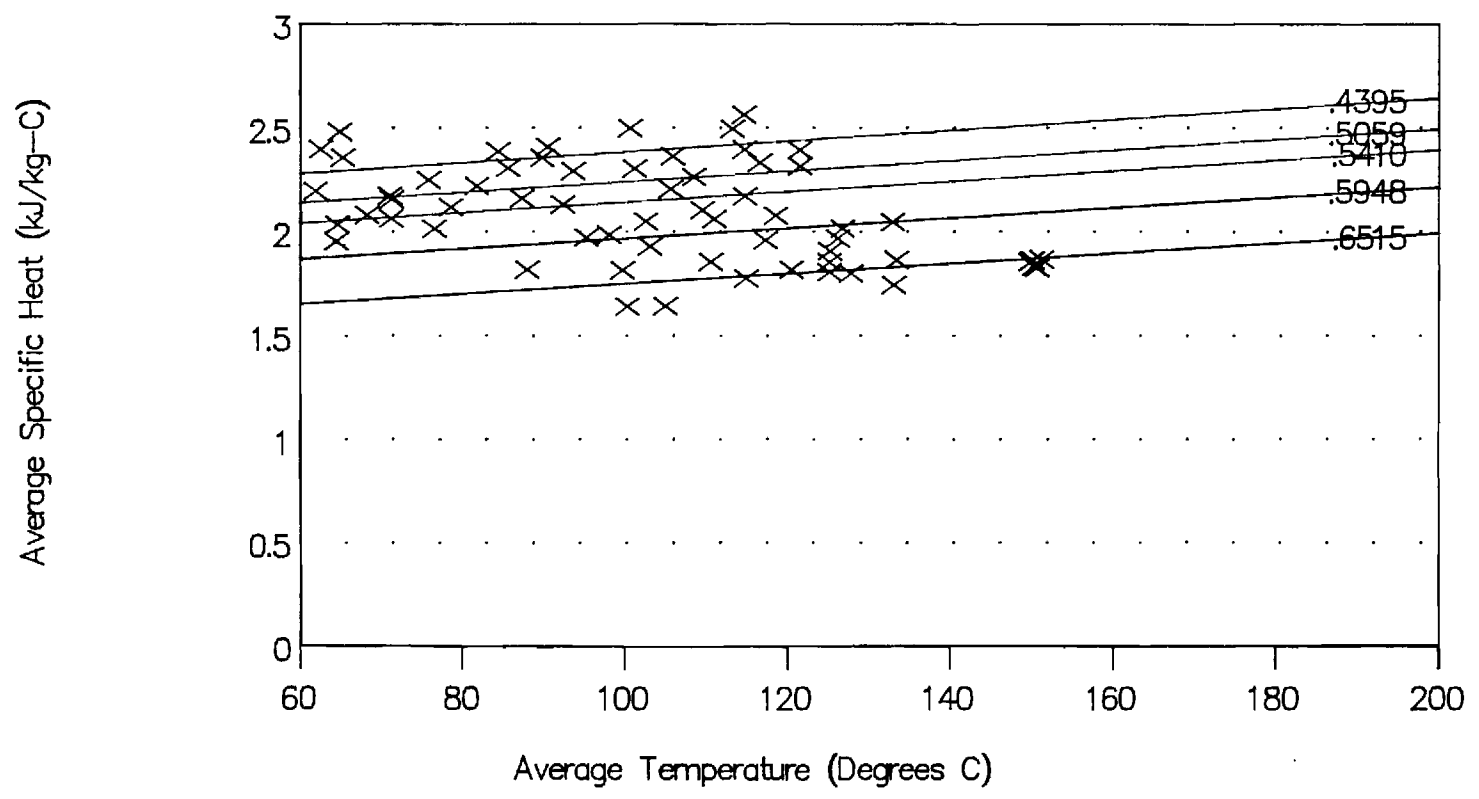


Figure 8.

Quadratic-Quadratic Model with Data

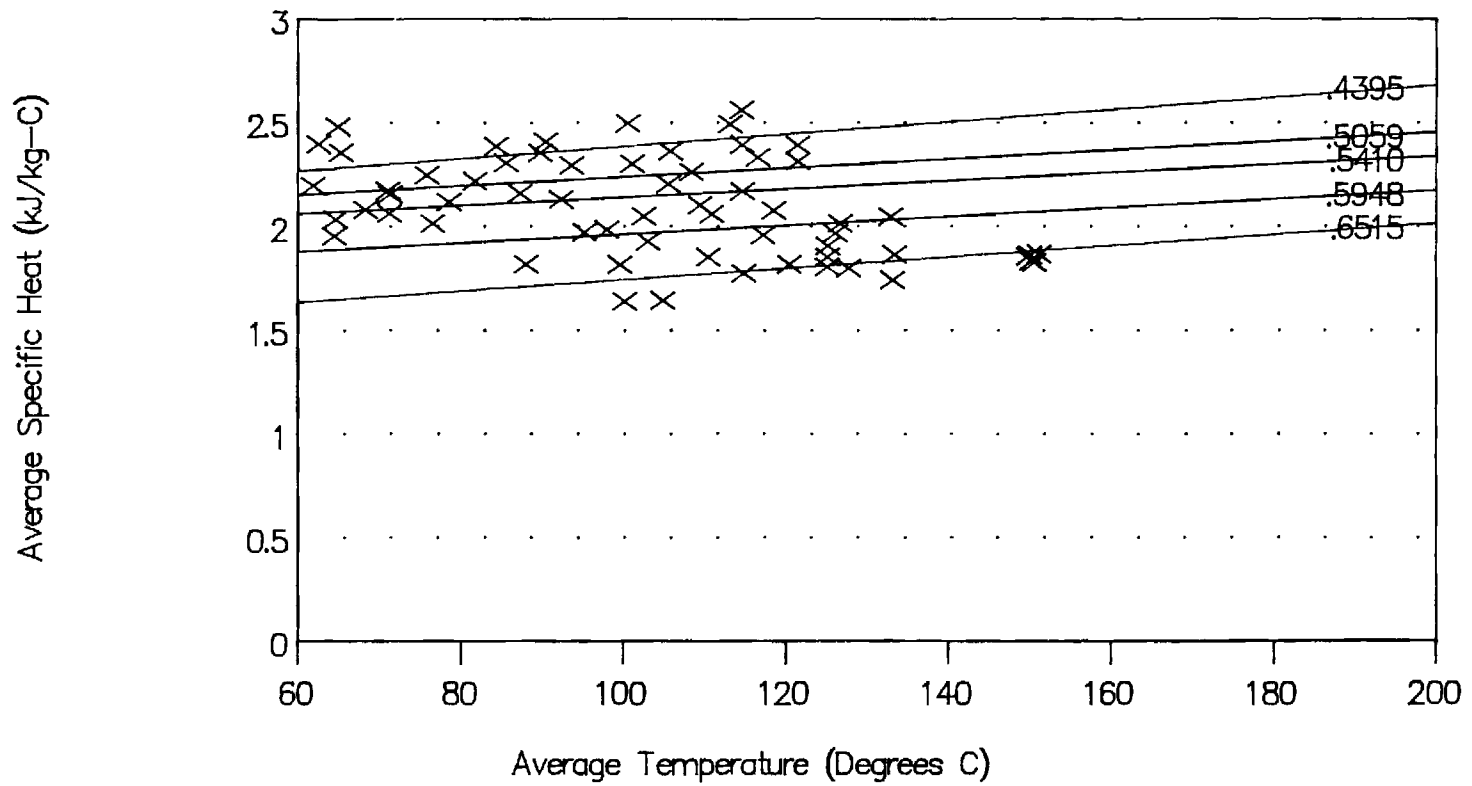


Fig. 9: 43.95% LiBr by weight

Linear-Linear Correlation

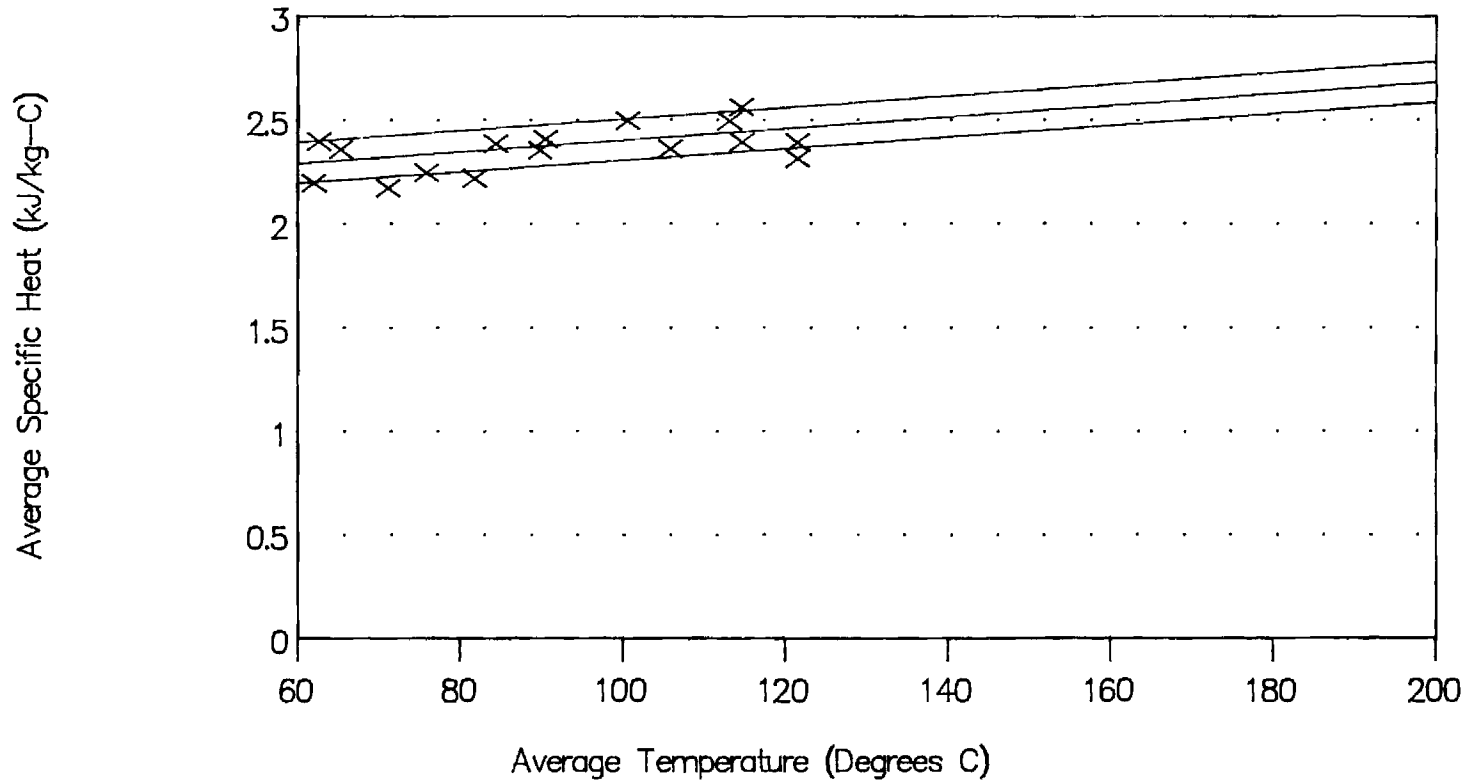


Fig. 10: 50.59% LiBr by weight

Linear-Linear Correlation

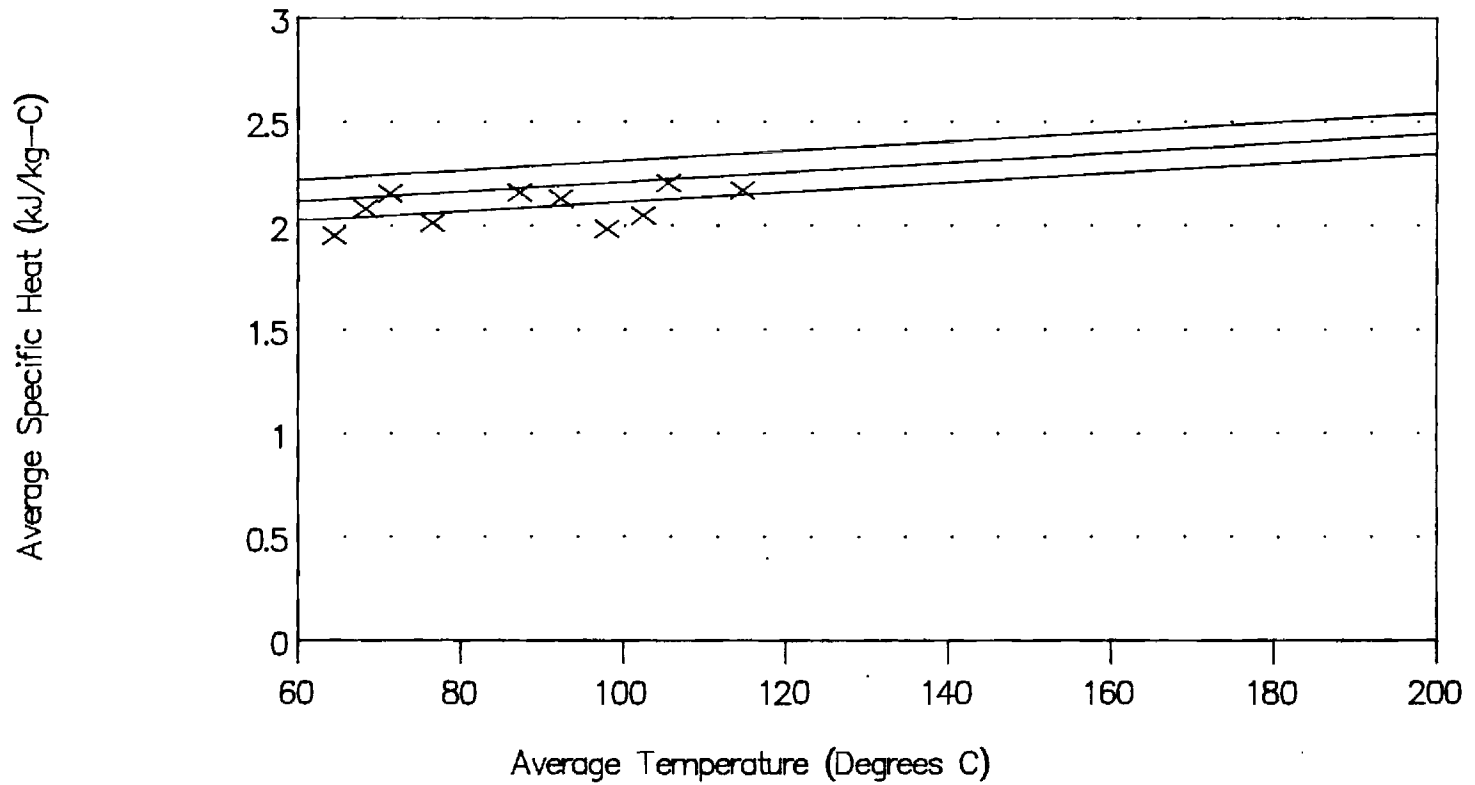


Fig. 11: 54.10% LiBr by weight

Linear-Linear Correlation

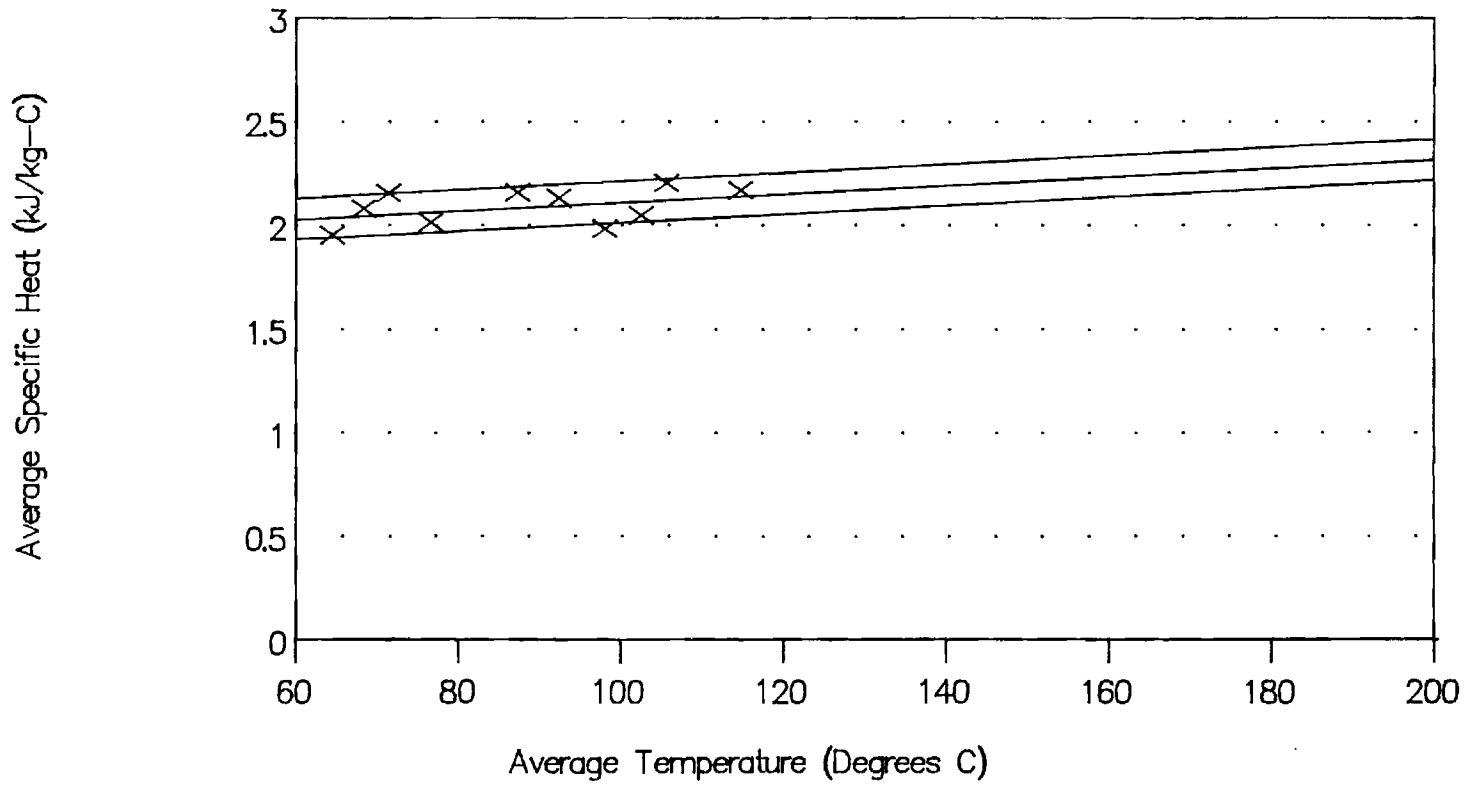


Fig 12: 59.48% LiBr by weight

Linear-Linear Correlation

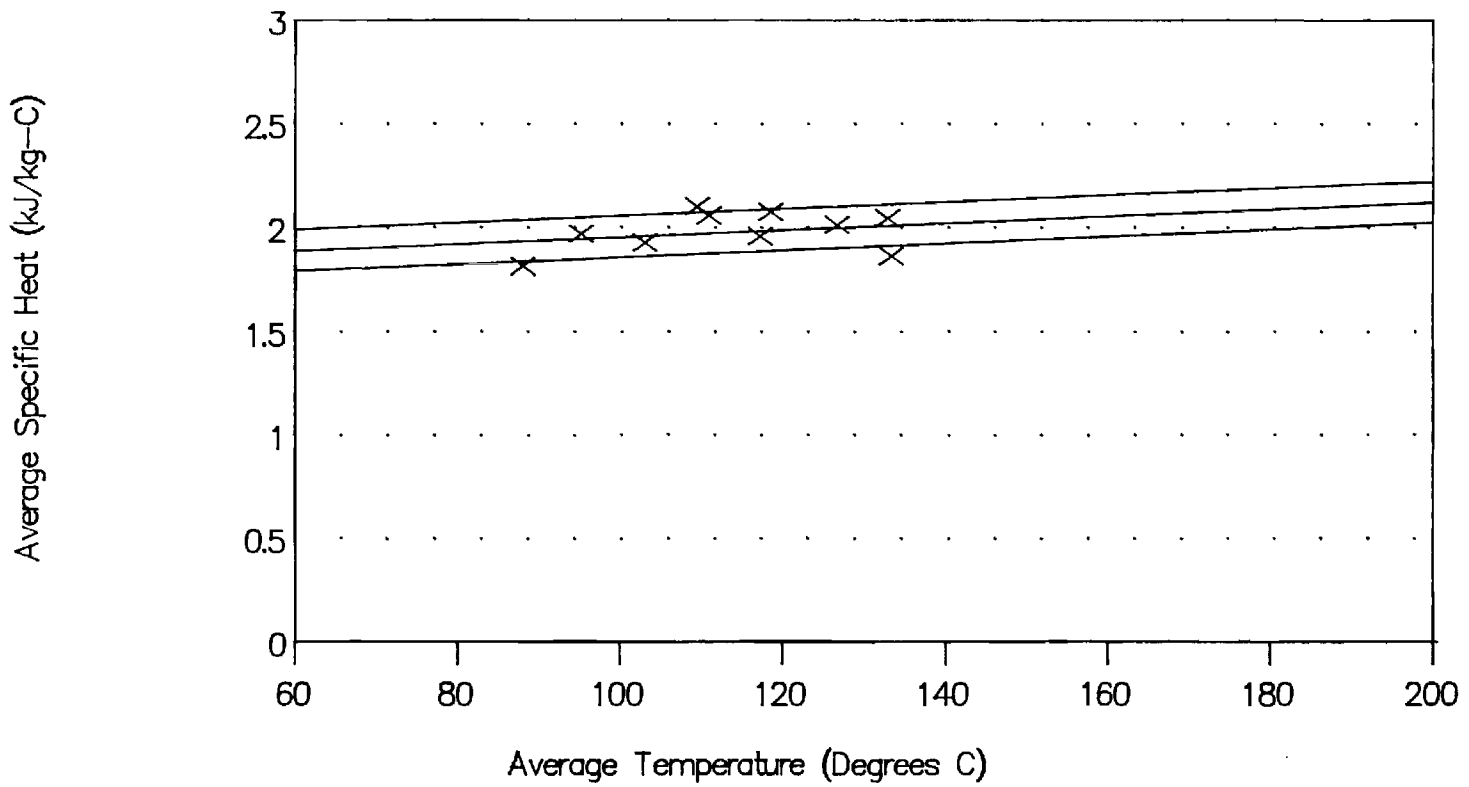


Fig. 13: 64.83wt% and 65.48wt% LiBr

Linear-Linear Correlation

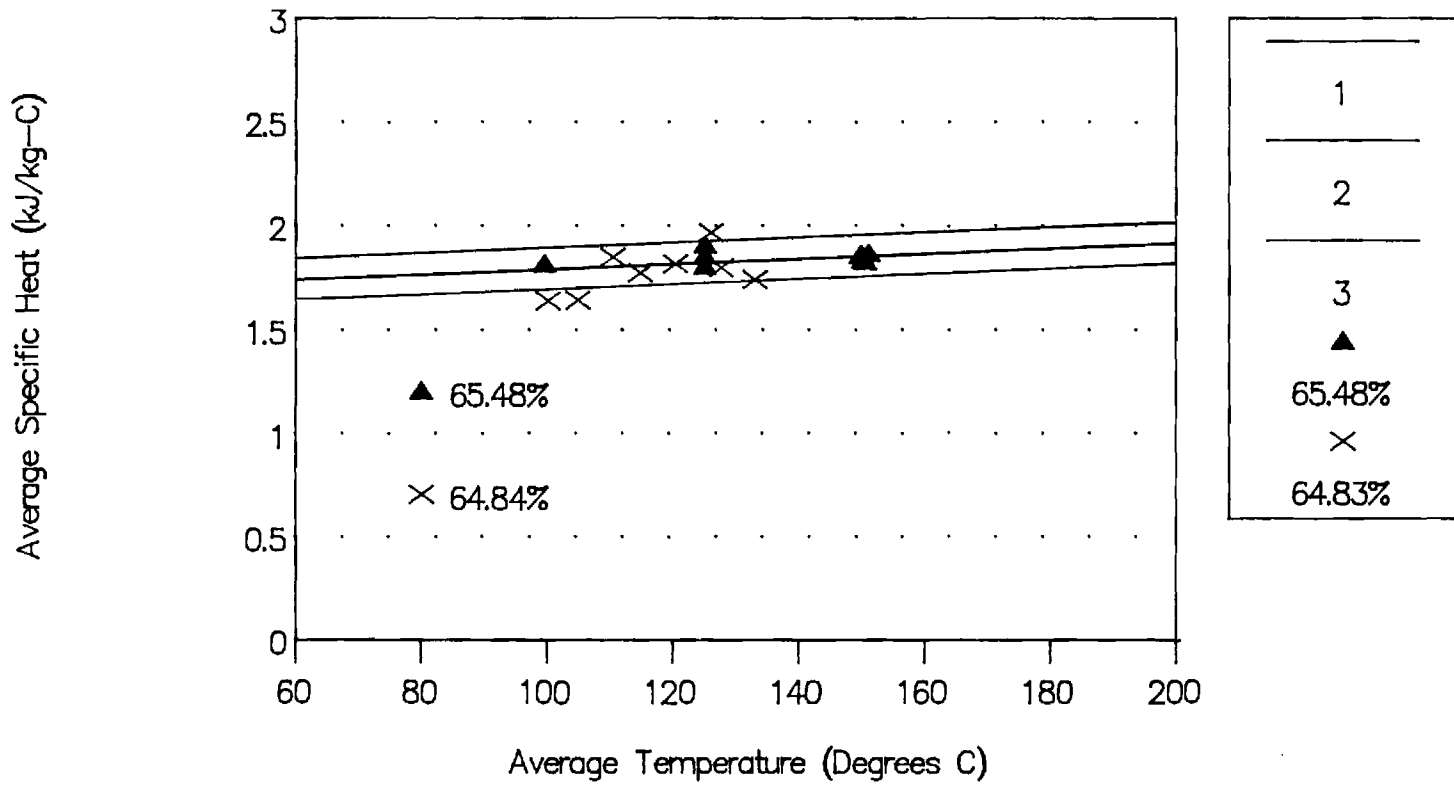
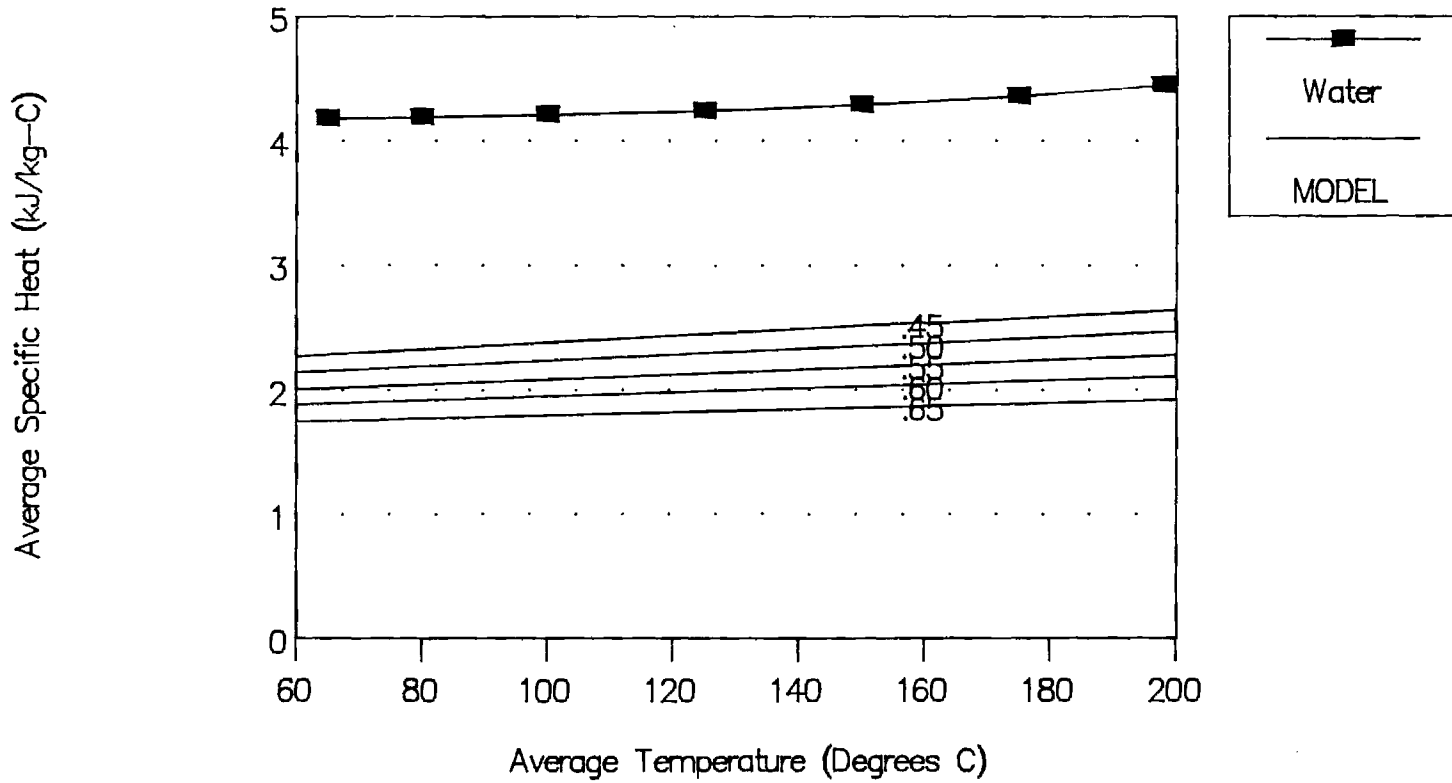


Figure 14. Linear-Linear Model
Compared with Data for Water



5. ERROR ANALYSIS AND COMPARISON WITH OTHER RESULTS:

Error Estimate. Since the drop calorimeter is a relatively complex device, especially as regards heat leaks to the environment, an error analysis based on and proceeding strictly from elementary principles appears to be formidably challenging at a minimum. Rather than attempt such an analysis, a series of drops using water as a standard reference fluid were conducted in November and December of 1988. Note that these drops are independent of the water drop used to calibrate the receiver: different samples were used and the latter drops were not used to adjust the calibration curves. Results of these drops are detailed in the following table.

Table 8

RESULTS OF STANDARDIZATION TESTS WITH WATER

Sample Temperature	Final Temperature	Empirical Average Specific Heat	Tabulated Average Specific Heat	Relative Error
142.77	51.59	4.21	4.219	-.002
165.98	52.36	4.29	4.239	.012
189.81	54.09	4.23	4.267	-.009
190.28	53.79	4.24	4.267	-.006
165.61	55.25	4.22	4.241	-.005
119.43	53.04	4.19	4.204	-.003
Root Mean Squared Error				.007

The preceding reveals an inherent calorimeter error on the order of $\pm 0.7\%$ with the samples of water. Over a similar temperature range, water has about twice the specific heat capacity of a typical LiBr solution (e.g. $4.2/2.4 = 1.75$). Consequently, for a typical LiBr solution the calorimeter error, ϵ_{cal} , is estimated to be about 1.2% (i.e. $.007 \cdot 1.75 = .012$).

In the current situation, inaccuracy in the composition of the solution is also a source of error. For the linear-linear model, the dependence of the specific heat on concentration is given by the following partial derivative:

$$\partial c_s / \partial w = a_1 + b_1 T$$

At 150 C, the value of the derivative is about $-3.2 \text{ kJ}/(\text{kg} \cdot \text{K} \cdot \text{kg}/\text{kg})$. Uncertainty in the composition is probably on the order of $0.1 \text{ WT}\%$; but even if it is as great as $1 \text{ WT}\%$, this component can contribute a relative composition error, ϵ_x , of only $.013$ (i.e. $3.2 \cdot .01/2.4$) which is only of the same order as the calorimeter error. Using the central limit theorem, the combined error is given as follows:

$$\epsilon = \{ \epsilon_{\text{cal}}^2 + \epsilon_x^2 \}^{1/2} = .018$$

In the production drops, this accuracy has not been achieved probably because of imperfect conditions during all procedures over the many months of effort required to complete the series of drops. The production drops have at least twice this inaccuracy as indicated by Standard Errors of Estimate in the correlations of around 5%.

Comparison with Other Results. As indicated above, five other sources of comparative data are available. The data of Pennington [7] are at room temperature and are not helpful for a comparison with the current results. The data of Uemura and Hasaba [5] are significantly lower than the values obtained herein or the values in the other three remaining sources. The comparison is illustrated in Figure 15 which shows both the reported data and the correlation provided by Uemura and Hasaba. Data obtained by Uemura and Hasaba are limited to the range of 51.7 C to 130.2 C for the concentration shown, 66.2 WT%. At lower concentrations, 110.4 C was the highest experimental temperature. Both the data and the correlation are 20% to 17% lower than the linear-linear correlation from this investigation over the the experimental range, which is approximately 50 C to 130 C. For example, Uemura and Hasaba obtained 1.51 kJ/(kg K) at $w = .662$ and $T = 130.2$ C compared with 1.79 kJ/(kg K) with the linear-linear correlation from the current investigation. The relative error between these data is 17%. Error limits are also plotted on the graph at one standard error above and below the correlation results from the present study. It is notable that all the data points reported by Uemura and Hasaba as well as their correlation line are fully outside the error bounds over their valid temperature range. This divergence from the present correlation indicates that there is no statistical support for the older results from the current data. The error in the results of Uemura and Hasaba appears to be excessive, and their results should probably not be employed. The reason for this error cannot be explained from the sketchy description in the literature. Possibly their apparatus was unsuitable for higher temperature operation since the temperature quoted above, only 130.2 C, was the highest in the data set. Note that the Uemura and Hasaba correlation converges on the linear-linear correlation at higher temperatures, but this is beyond the range of their experimental data base and is, therefore, only unsupported extrapolation.

A third source of comparative data is the thesis by Löwer [1]. These data at concentrations of 45, 50, 55, and 60 weight percent are plotted in Figure 16 along with the corresponding linear-linear correlation lines from the present investigation. Agreement between the two set of results of data is good but not perfect and ranges from better agreement near 45 WT% to poorer agreement near 60 WT%. In Figure 17, the standard error bands for the linear-linear correlation at 45 WT% and 60 WT% are plotted in comparison with the data of Löwer. As is evident in the figure, the data from Löwer is marginally in agreement with the results for the present study as illustrated by the bands near 45 WT% and 60 WT%; consequently, the data of Löwer are within marginal agreement with the results of the current study.

Two more important sources of data are the numerical results of Patterson and Perez-Blanco [4] and the experimental data provided by Dr. Uwe Rockenfeller of Rocky

Research Incorporated [13]. The Rocky Research data were measured with a Differential Scanning Calorimeter (DSC) manufactured by Perkin-Elmer. These data are reported to have been compensated for the difference in heat capacity between the cells holding the samples and the cell holding the reference. In addition, corrections have been applied for vaporization effects. The Rocky Research data are illustrated in Figure 18 along with linear-linear correlation lines for these same data. Because the DSC data are very smooth, the linear-linear correlation produces an excellent fit with a Coefficient of Determination over 99%. The numerical results of Patterson and Perez-Blanco are curve fits to the enthalpy data generated by McNeely [2]. Specific heats have been obtained from the enthalpy function by taking the partial derivative with respect to temperature while holding constant the concentration. McNeely employed the procedure of Haltenberger [3] to produce enthalpy-concentration charts from vapor pressure data over a range of temperatures and concentrations and specific heat data over a range of temperature. In particular, to produce the published results, McNeely used the specific heat data from Löwer at 50 WT% concentration. As shown in Figure 19, the results from differentiation of the correlations of Patterson and Perez-Blanco agree very well with the Rocky Research data. The Rocky Research data are slightly above the Patterson and Perez-Blanco curve fits. It is notable that the differentiation does not precisely return the specific heat data of Löwer. This is to be expected since both vapor properties and specific heat data are required to define the enthalpies, and the vapor properties have a significant impact. In addition, the numerical curve fit is defined over the entire range of the enthalpy chart which tends to somewhat obscure the influence of any particular contributing data. Table 9 provides the coefficients for both correlations and statistical results for the Rocky Research data along with the pertinent statistics.

Since the Rocky Research data agree very well with the correlation from Patterson and Perez-Blanco, it should be sufficient to illustrate and discuss the comparison between the results of the present investigation and the data from Rocky Research. The Rocky Research data are illustrated along with the corresponding linear-linear correlations in Figures 20 and 21. As is evident in the figure, there is good agreement between the two data sets which is very reassuring since such disparate equipment were used for the two measurements. The linear correlation ranges from ca. 4% above the Rocky Research correlation at 45.1 WT% and 150 C to a virtually identical value at 65 WT% and 150 C. The RMS error at mid range is only about 2%. This is hardly greater than the estimated inherent accuracy of the drop calorimeter and is less than the standard error estimate in the specific heat correlation for the drop calorimeter data. The Rocky Research data are illustrated in Figure 21 along with representative error bands for the linear-linear correlation. Nearly all of the Rocky Research data fall within the error bands. Consequently, the results of the current investigation are not statistically divergent from the Rocky Research data, and the two sets of data are mutually reinforcing. Indeed, at 65 WT% the two correlations are virtually identical. The principal difference is in the slope of the temperature dependence with the current investigation having the greater temperature effect. The specific heats from the enthalpy correlation of Patterson and Perez-Blanco are similarly in agreement with the current investigation and the with the Rocky Research data. As shown in Figure 22, four sources of data are in good agreement. At 60 WT%, the data of Löwer are slightly higher than the other data and the

formulation based on the Patterson and Perez-Blanco correlation being somewhat lower than the others. The nearly identical Rocky Research data and the linear-linear correlation of data from the current investigation occupy an intermediate position. Both the data of Löwer and the related Patterson and Perez-Blanco correlation have a nearly flat temperature dependence. The Rocky Research data and the linear-linear correlation increase with temperature, as does pure water in this temperature range. Since the increase with temperature is barely noticeable lower than approximately 100 C, even for pure water, it is possible that the limited temperature range of the Löwer data obscured this dependence. All the data shown lie within the error bounds of the current investigation. Error bounds on the other sources cannot be quantified, but they may be very small in the case of the Rocky Research data. In the absence of further uncertainty estimates, no statistical preference can be asserted among the four data bases at lower temperature or between the Rocky Research data and the current research at higher temperatures.

The ultimate goal of collecting specific heat data is constructing enthalpy-concentration charts and tables. This construction requires only specific heat data at a single concentration and a range of temperatures. Since the correlations for 65 WT% from this investigation and that based on the Rocky Research data are virtually identical, it is recommended that either of these be used for the computation of solution enthalpies.

Table 9

CORRELATION RESULTS FROM DATA OF OTHERS

Coefficient:		Regression of Rocky Research Data on Model of Form:		Differentiation of Enthalpy Fit by Patterson and Perez-Blanco
Symbol	Multiplies	Linear-Linear	Quadratic-Linear	
a_0		3.462023	3.818560	4.124891
a_1	w	-2.679895	-3.996355	-7.643903 E-02
a_2	w ²		1.195485	2.589577 E-03
a_3	w ³			-9.500522 E-05
a_4	w ⁴			1.708026 E-06
a_5	w ⁵			-1.102363 E-08
b_0	T	.0013499	.0013499	0.0011487386
b_1	wT	-.000655	-.000655	0.00011741842
b_2	w ² T			-1.4750638 E-05
b_3	w ³ T			6.555184 E-07
b_4	w ⁴ T			-1.2124608 E-08
b_5	w ⁵ T			7.803794 E-11
Standard Error of Estimate		.0096	.0081	
Coefficient of Correlation		.9977	.9984	

Fig 15. 66.2% Linear-Linear Correlation
Compared with Uemura and Hasaba

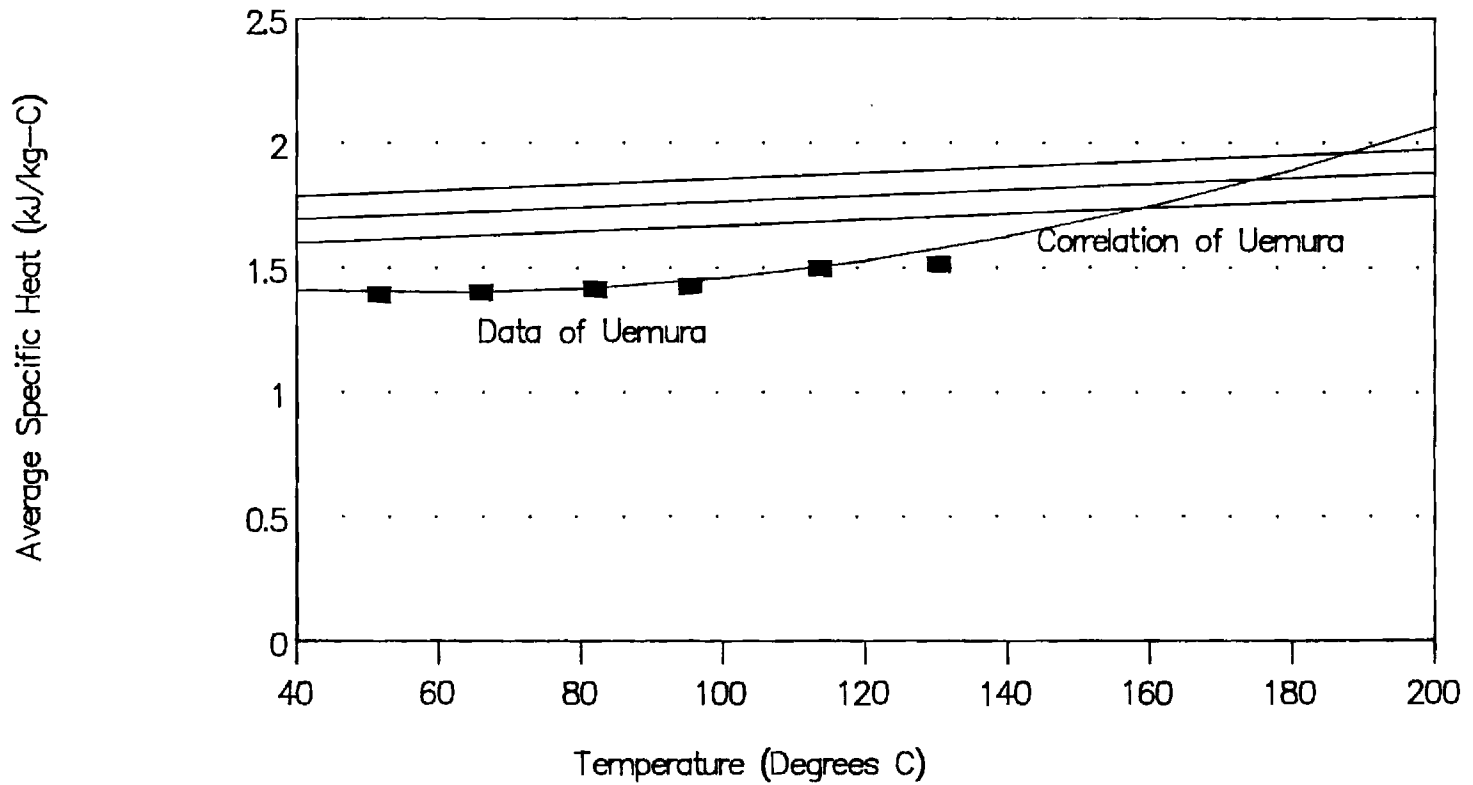


Figure 16. Data of Lower
and GIT Linear-Linear Correlation

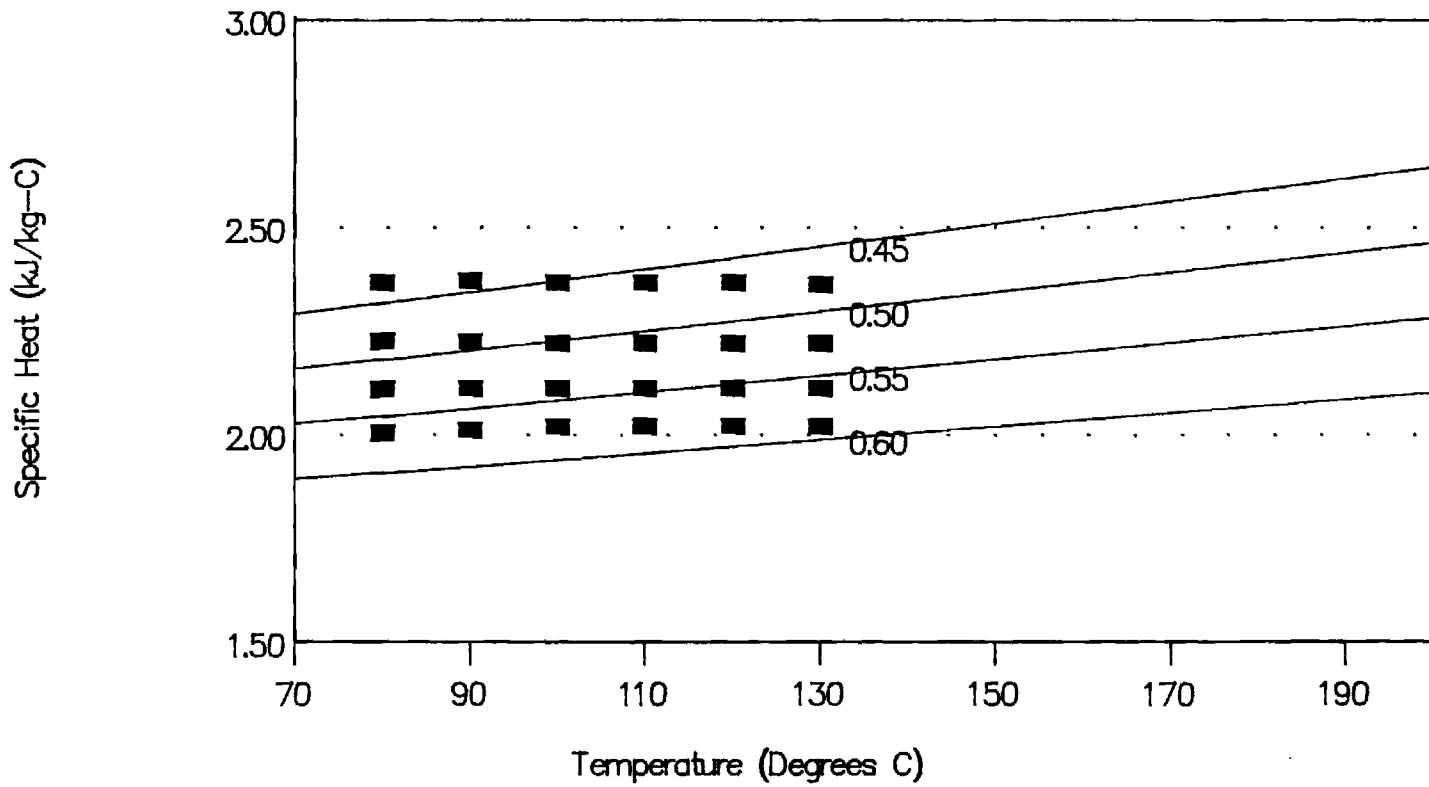


Figure 17. Data of Lower and GIT
Error Bands at 45 WT% and 60 WT%

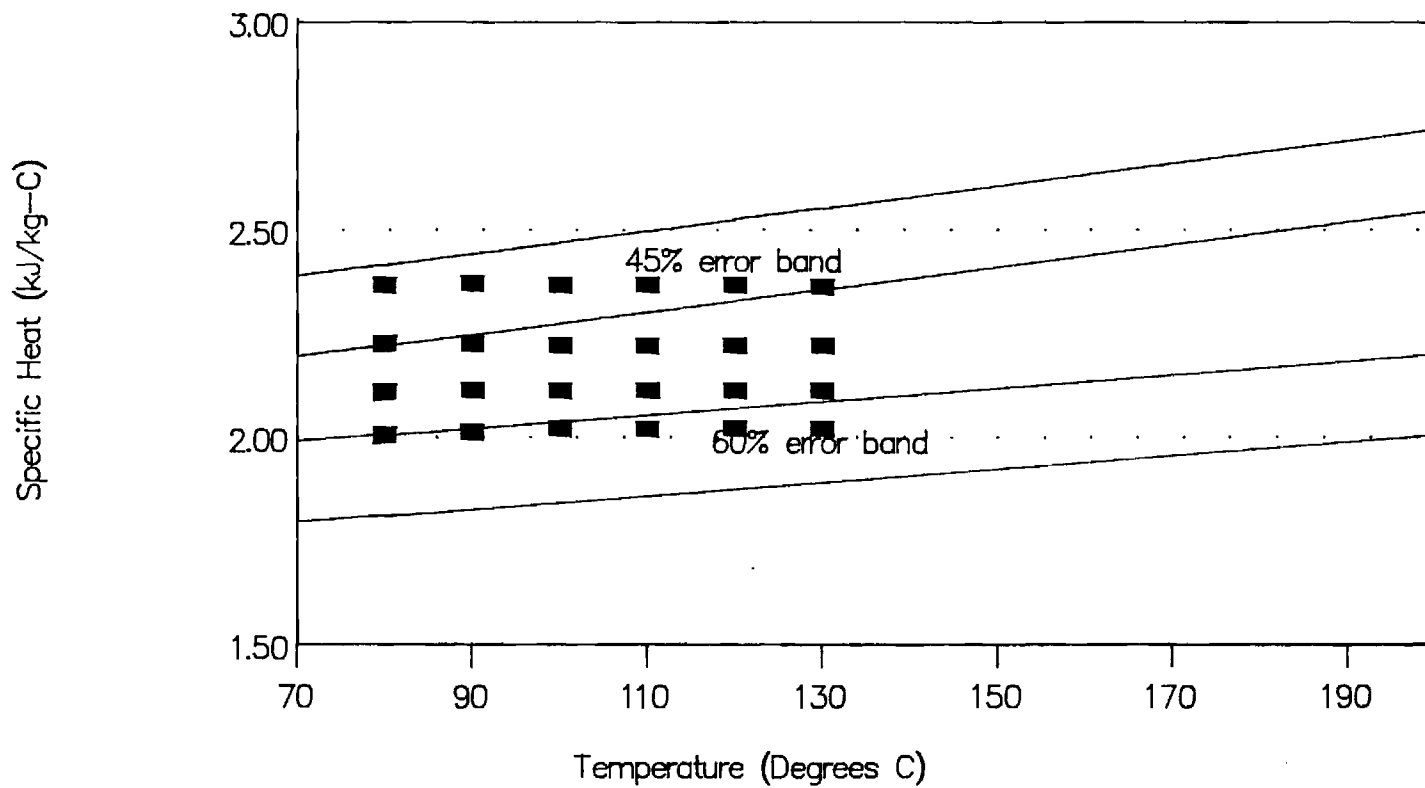


Figure 18.

Rocky Research Data and its Correlation

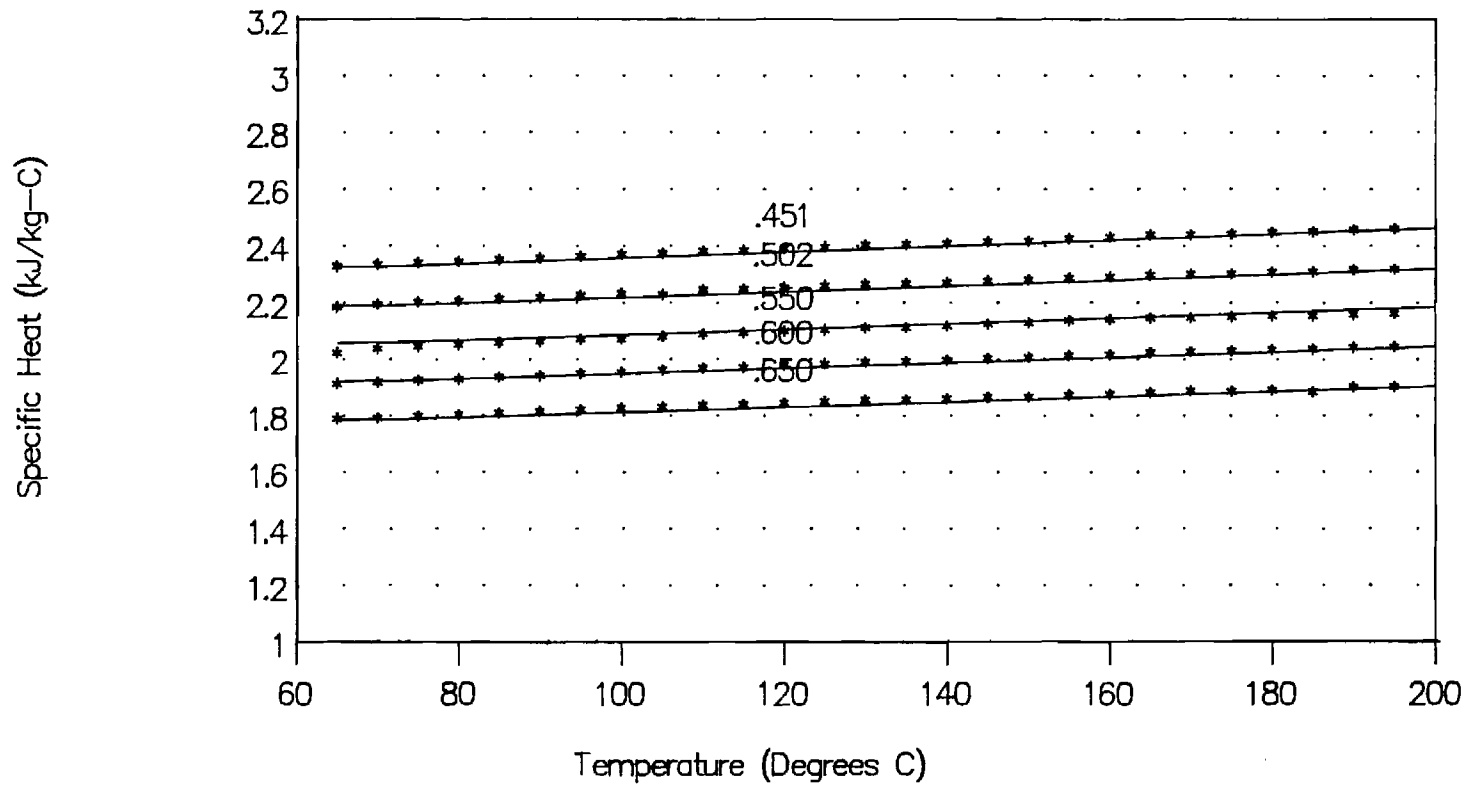


Figure 19: Rocky Research Data Compared
with Patterson and Perez-Blanco

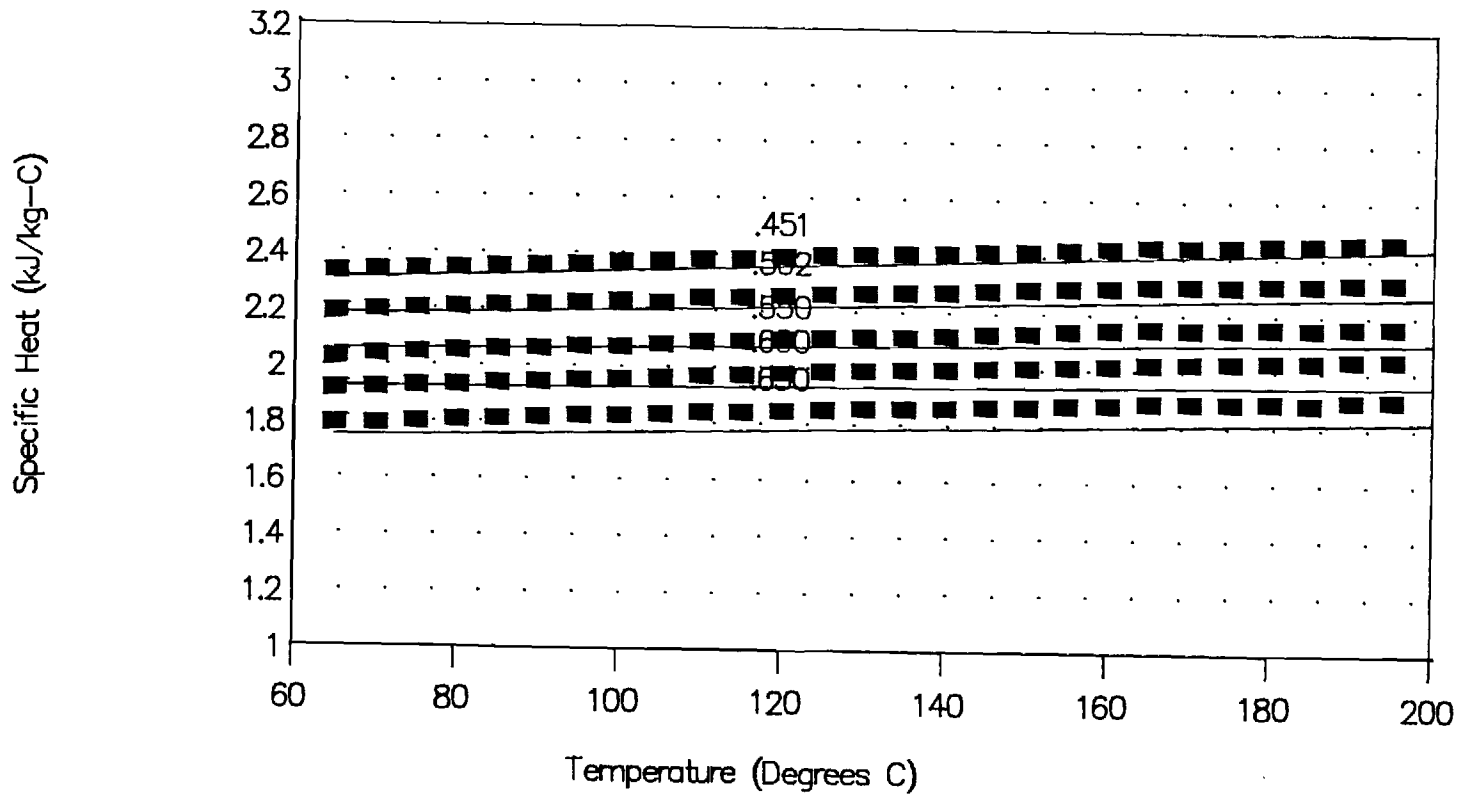


Fig. 20: Rocky Research data
and GIT linear-linear correlation

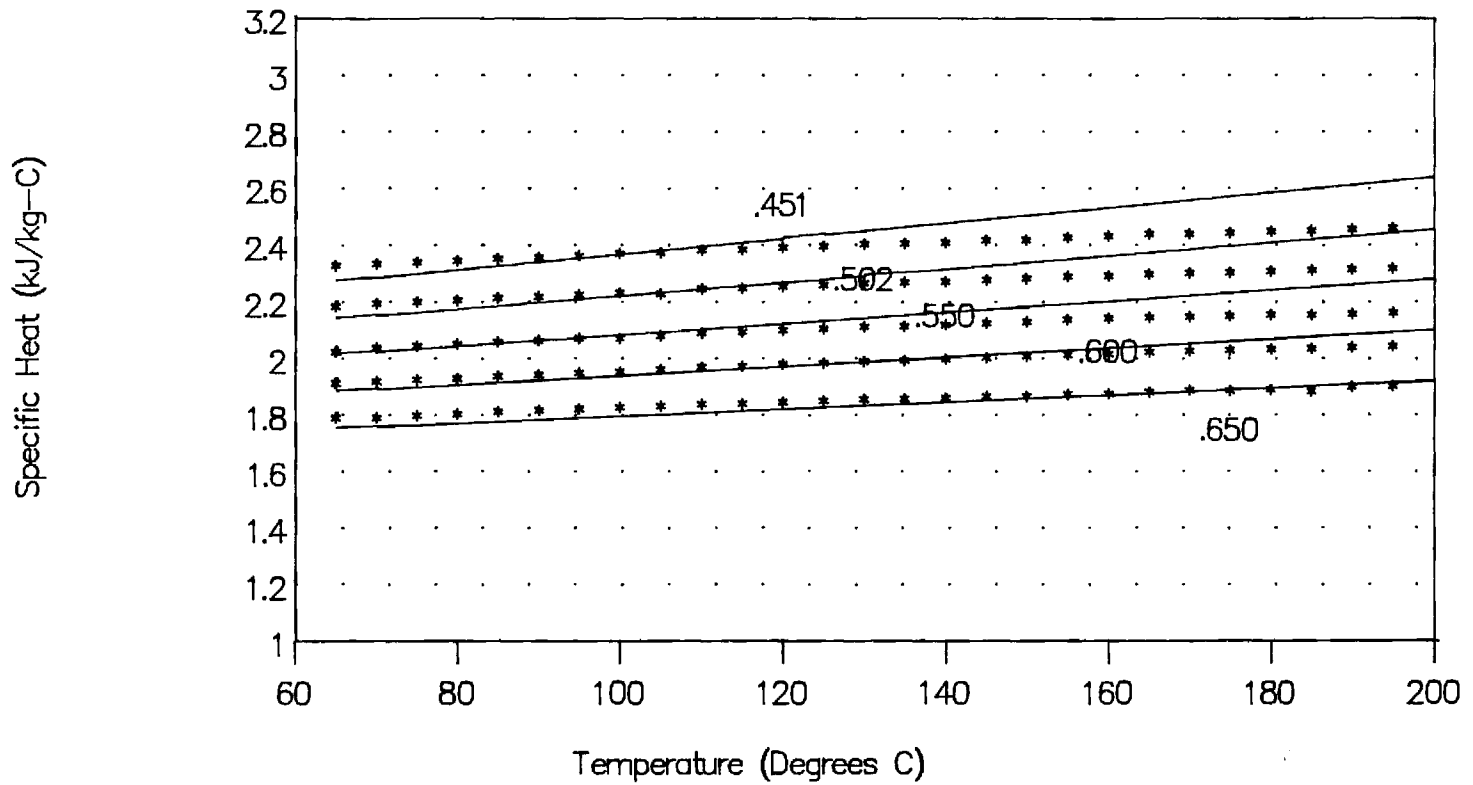


Fig. 21: Rocky Research data and GIT

linear-linear error bands

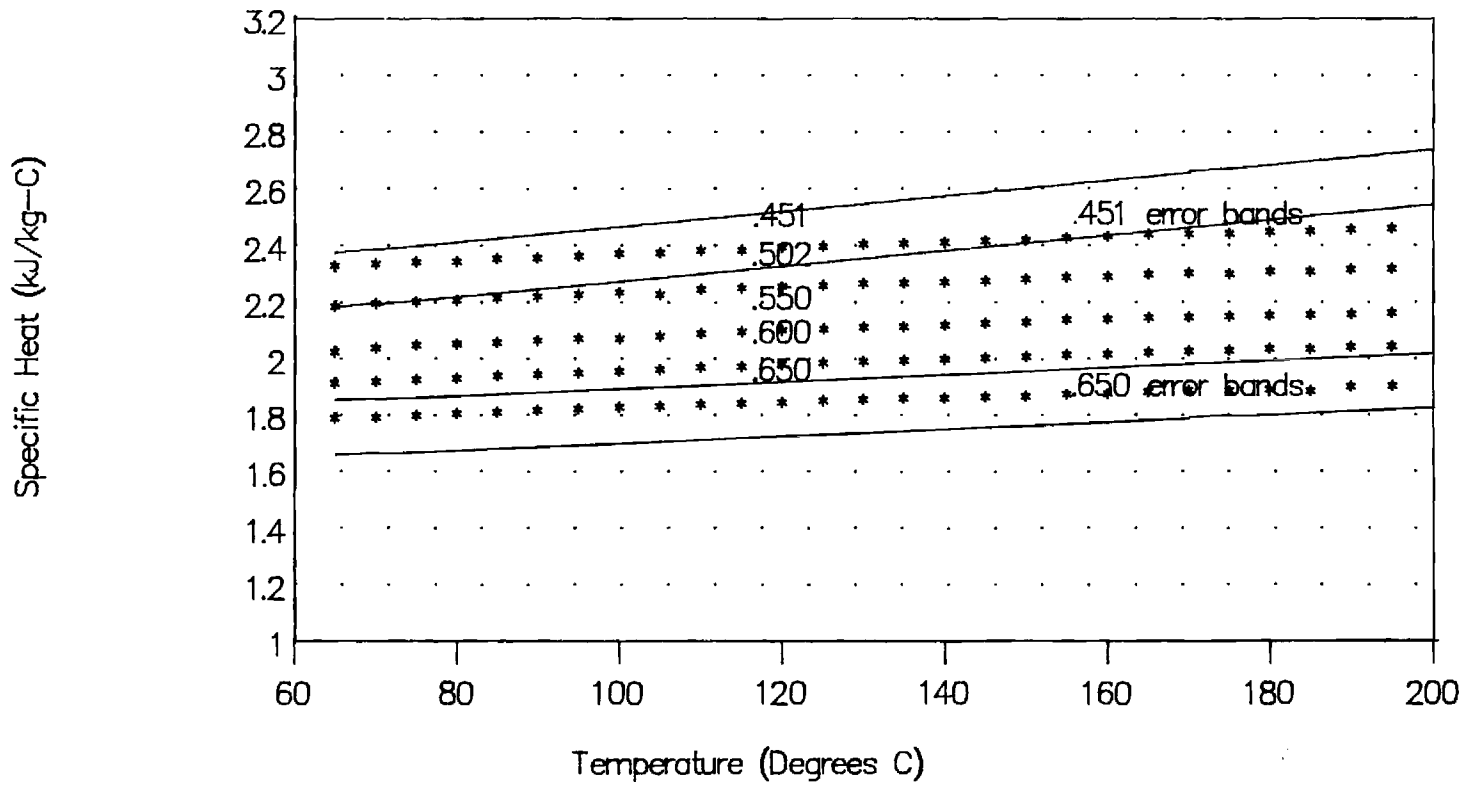
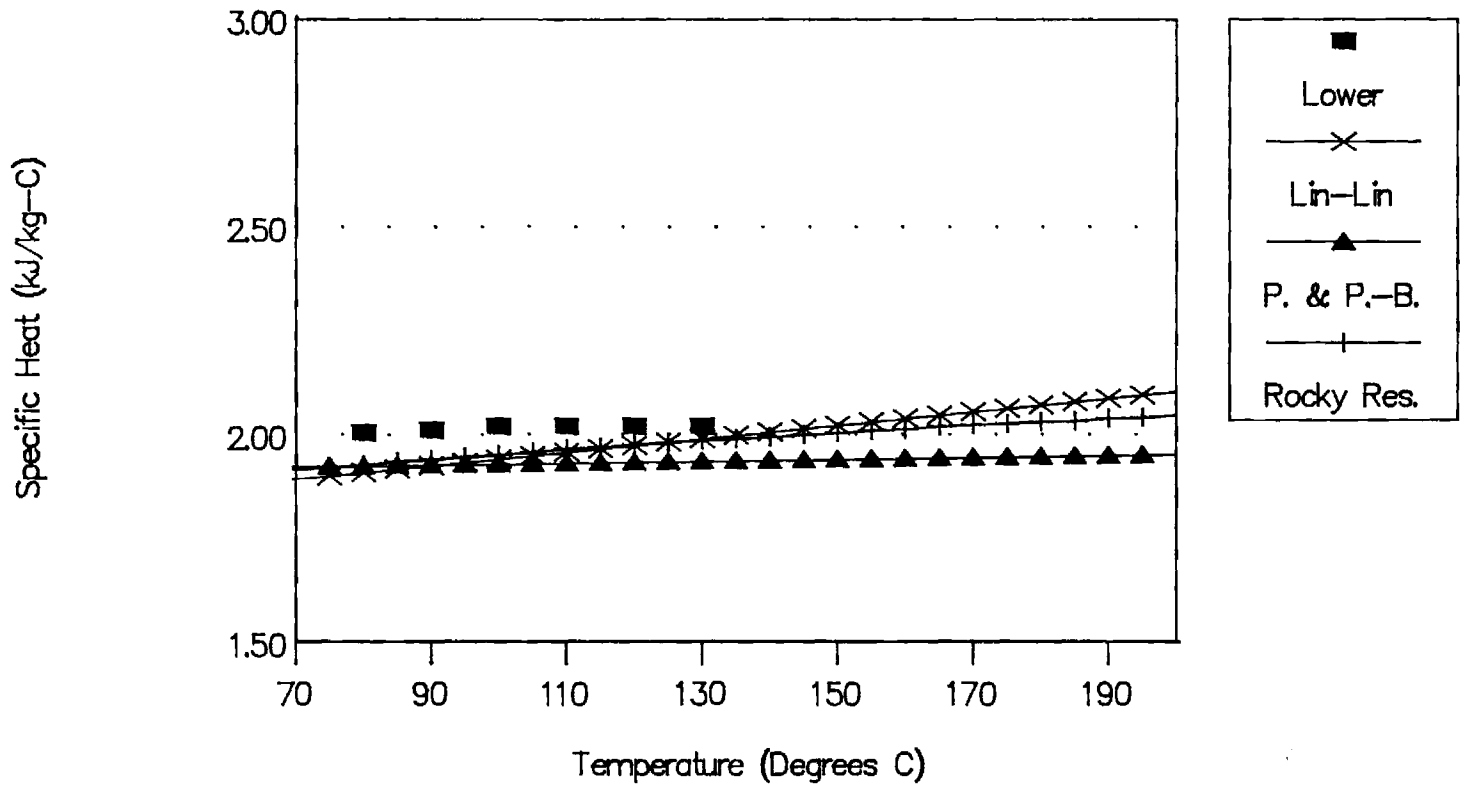


Figure 22. Comparison of Four Results
at 60 WT% Concentration



6. CONCLUSIONS:

Two data bases, the DSC measurements from Rocky Research and specific heats obtained by differentiation of enthalpy correlations prepared by Patterson and Perez-Blanco, are in agreement with the results of the current investigation. The data of Uemura and Hasaba are clearly lower than the results of the three mutually consistent data bases. The data of Löwer are at least marginally supported by the three later data bases, one of which, the enthalpy correlation, incorporated Löwer's data in computing the tabulated enthalpies on which the correlation was based. The data from Löwer, however, do not extend far enough into the temperature range under consideration here to be helpful. The Rocky Research data are supported by excellent agreement with the results from the Patterson and Perez-Blanco correlation and by good agreement with the results of the current investigation. Since the Rocky Research data are purely empirical, they should be preferred over the numerical results. In addition, the Rocky Research data occupy an intermediate position. They are slightly higher than the results from the enthalpy correlation and slightly lower than the results of the present investigation. In consequence, the Rocky Research data should represent an acceptable consensus data base. For practical purposes, specific heat data are needed at only one concentration, and at 65 WT% the correlation results from the present investigation are virtually identical with the correlation based on the Rocky Research data. Either correlation should be adequate and accurate for preparing enthalpy charts and tables.

It may be possible to make a finer distinction among the three preferred data bases by improving on the current measurements. Two possibilities have already been pursued. The temperature range of the measurements were extended for the higher concentrations where the vapor pressure is low enough for safe operation with the existing calorimeter capsule. This effort provided additional data points around 65 WT%. The additional data was helpful in its own right and also relieved some of the leverage of possible outliers at lower temperatures which can distort the temperature dependence. The evaluation of the specific heat from drop calorimeter data involves a ratio of the two temperature differences, the rise in receiver temperature and the drop in sample temperature. This situation makes measurements problematical at lower temperatures for which both temperature differences become smaller because the ratio of two small differences becomes very sensitive to experimental error. Additionally, the data base was scanned for outliers and suspected outliers were replaced with measurements from carefully conducted measurements. This effort required a few additional drops around 45 WT% and several additional drops around 65 WT%. Outliers are especially likely at higher concentrations where the lower specific heats magnify the influence of inadequate procedures or environmental influences. Further refinement of the measurements described herein with the present apparatus would be problematical; and, since an acceptable consensus specific heat correlation has been defined for evaluating the enthalpy, further work is beyond the scope of the present effort.

Further work, if attempted, might well proceed at lower concentrations, approaching pure water. The experimental results would be strongly confirmed if the highly regarded

and scrupulously measured specific heat of water emerges as the limiting case. This investigation should also alleviate uncertainty about the trend in temperature dependence if the dependence smoothly accelerates and approaches the trend for water as the amount of LiBr in the solution is decreased.

7. ACKNOWLEDGEMENTS

The contributions of Dr. Uwe Rockenfeller both for his guidance and encouragement as the technical monitor of this project and for providing the previously unpublished specific heat data is gratefully acknowledged. The assistance of Professor K. E. Herold for helpful discussions and his assistance with the literature review is also gratefully acknowledged.

7. REFERENCES:

1. Löwer, H., "Thermodynamische und physikalische Eigenschaften der wässrigen Lithiumbromid-Lösung", Dissertation, Technischen Hochschule Karlsruhe, Karlsruhe, Germany, 1960.
2. McNeely, L. A., "Thermodynamic Properties of Aqueous Solutions of Lithium Bromide", *ASHRAE Transactions*, Vol. 85, Part 2, pp. 413-434, 1979.
3. Haltenberger, W., "Enthalpy-Concentration Charts from Vapor Pressure Data", *Industrial and Engineering Chemistry*, pp. 783-786, June, 1939.
4. Patterson, M. R. and H. Perez-Blanco, "Numerical Fits of the Properties of Lithium-Bromide Water Solutions", *ASHRAE Transactions*, Vol. 94, Part 2, 1988.
5. Uemura, T. and S. Hasaba, "Studies on the Lithium Bromide-Water Absorption Refrigerating Machine", Technical Report, Kansai University, Vol. 6, pp. 31-55, 1964.
6. "Technical Data: Lithium Bromide", Commercial Brochure, Foote Mineral Company, Exton, PA.
7. Pennington, W. A. and C. Daetwyler, "Heat Capacity and Heat of Dilution of some Concentrated Water Solutions of LiBr at 25 C", Carrier Confidential Report, Project R1011-S1 Report No. 6, Carrier Corporation, Syracuse, NY, 18 April 1952.
8. "Operating Manual, Unitherm Model 7100 Calorimeter", Anter Laboratories, 15 December 1976.
9. Lee, M. C. and R. N. Maddox, "Measuring Heat Capacity Using the Unitherm Model 7100 Drop Calorimeter", Liquid Heat Capacity Report No. 6, Fluid Properties Research Institute, January 1979.
10. Moran, J. P., "Specific Heats of Aqueous Lithium Bromide Solutions", M. S. Thesis, The George W. Woodruff School of Mechanical Engineering, Georgia Institute of Technology, August 1988.
11. Pan, W. P. and R. N. Maddox, "Improved Technique for Heat Capacity Measurements using the Unitherm Model 7100 Drop Calorimeter", Liquid Heat Capacity Report No. 7, Fluid Properties Research Institute, August 1979.
12. McClintock, R. B. and G. J. Silvestri, "Some Improved Steam Property Calculation Procedures", *Journal of Engineering for Power*, American Society of Mechanical Engineers, pp. 123-134, April 1970.
13. Rockenfeller, U., "Laboratory Results: Solution = LiBr-H₂O, Properties = P-T-x, Heat Capacity", Unpublished Data, Rocky Research, Inc, Boulder City, NV, 1987.

8. APPENDIX:

For completeness, the following graphs are appended which illustrate the scatter plots of raw data along with correlation lines and error bands for the quadratic-quadratic and quadratic-linear models:

Figure A.1: Specific Heat Data for 43.95 WT% Solution of LiBr with Corresponding Quadratic-Quadratic Correlation Model.

Figure A.2: Specific Heat Data for 50.595 WT% Solution of LiBr with Corresponding Quadratic-Quadratic Correlation Model.

Figure A.3: Specific Heat Data for 54.10 WT% Solution of LiBr with Corresponding Quadratic-Quadratic Correlation Model.

Figure A.4: Specific Heat Data for 59.48 WT% Solution of LiBr with Corresponding Quadratic-Quadratic Correlation Model.

Figure A.5: Specific Heat Data for 64.83 WT% and 65.48 WT% Solution of LiBr with Corresponding Quadratic-Quadratic Correlation Model.

Figure A.6: Specific Heat Data for 43.95 WT% Solution of LiBr with Corresponding Quadratic-Linear Correlation Model.

Figure A.7: Specific Heat Data for 50.595 WT% Solution of LiBr with Corresponding Quadratic-Linear Correlation Model.

Figure A.8: Specific Heat Data for 54.10 WT% Solution of LiBr with Corresponding Quadratic-Linear Correlation Model.

Figure A.9: Specific Heat Data for 59.48 WT% Solution of LiBr with Corresponding Quadratic-Linear Correlation Model.

Figure A.10: Specific Heat Data for 64.83 WT% and 65.48 WT% Solution of LiBr with Corresponding Quadratic-Linear Correlation Model.

Figure A.1: 43.95% LiBr by weight

Quadratic-Quadratic Correlation

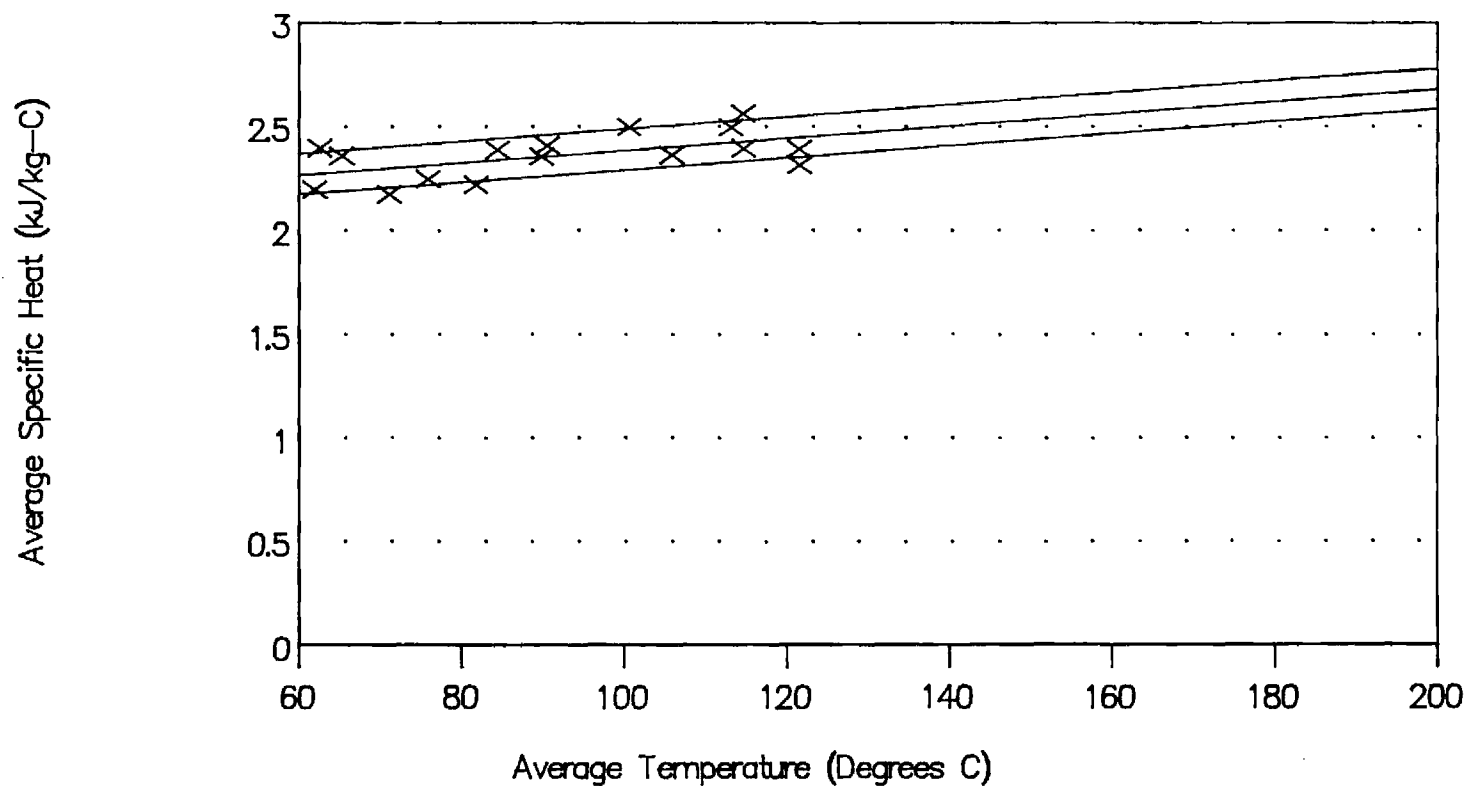


Figure A.2: 50.59% LiBr by weight

Quadratic-Quadratic Correlation

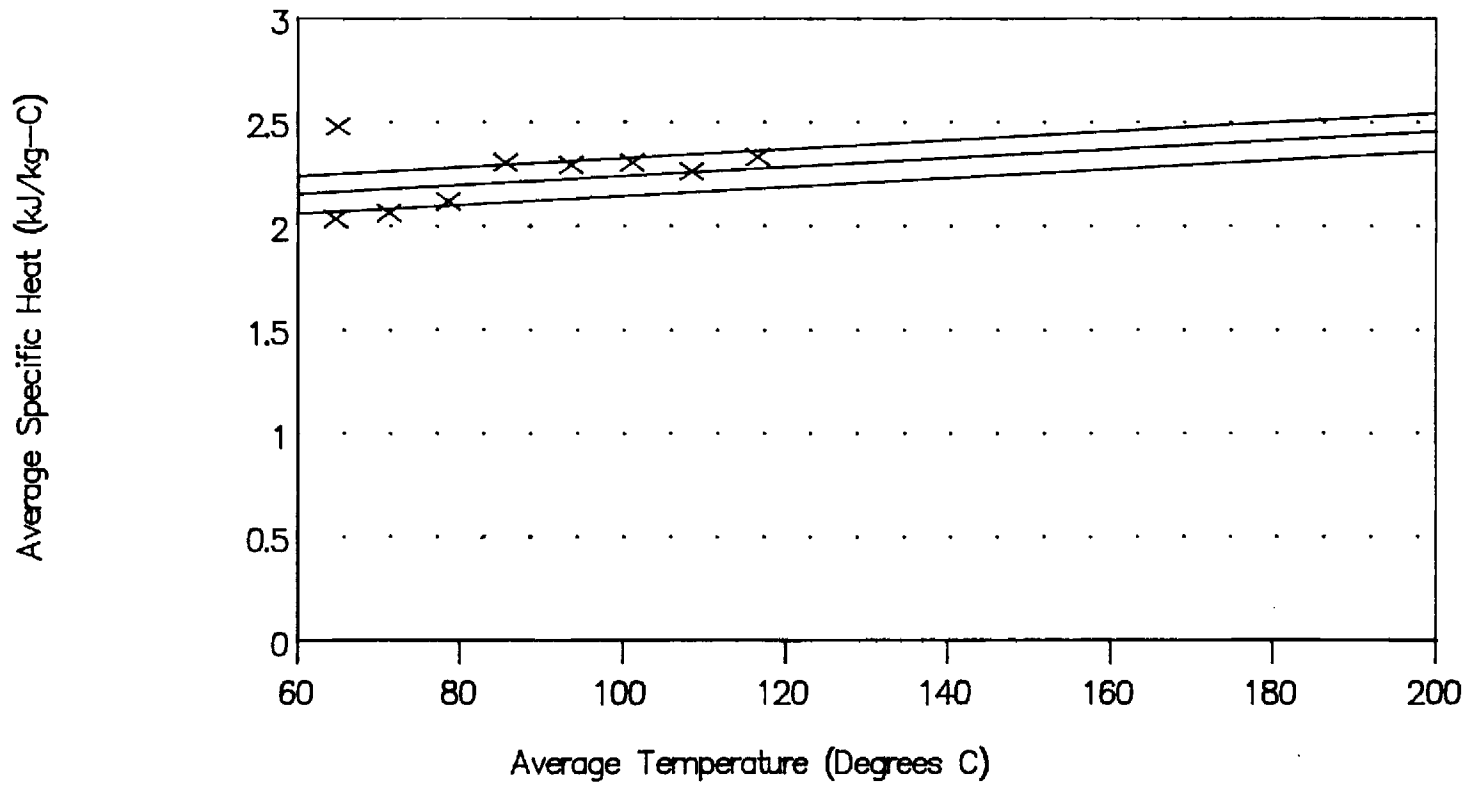


Figure A.3: 54.10% LiBr by weight

Quadratic-Quadratic Correlation

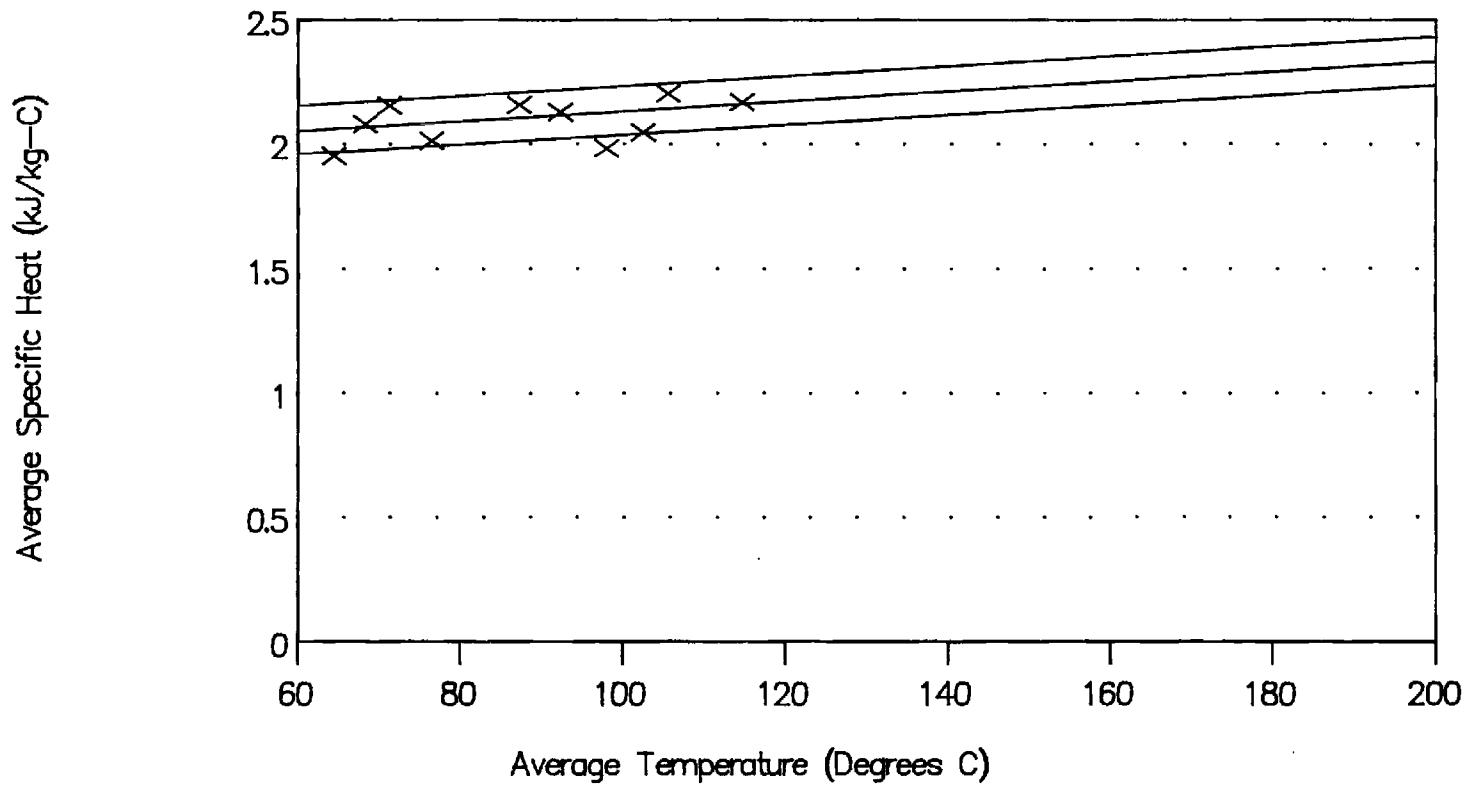


Figure A.4: 59.48% LiBr by weight

Quadratic-Quadratic Correlation

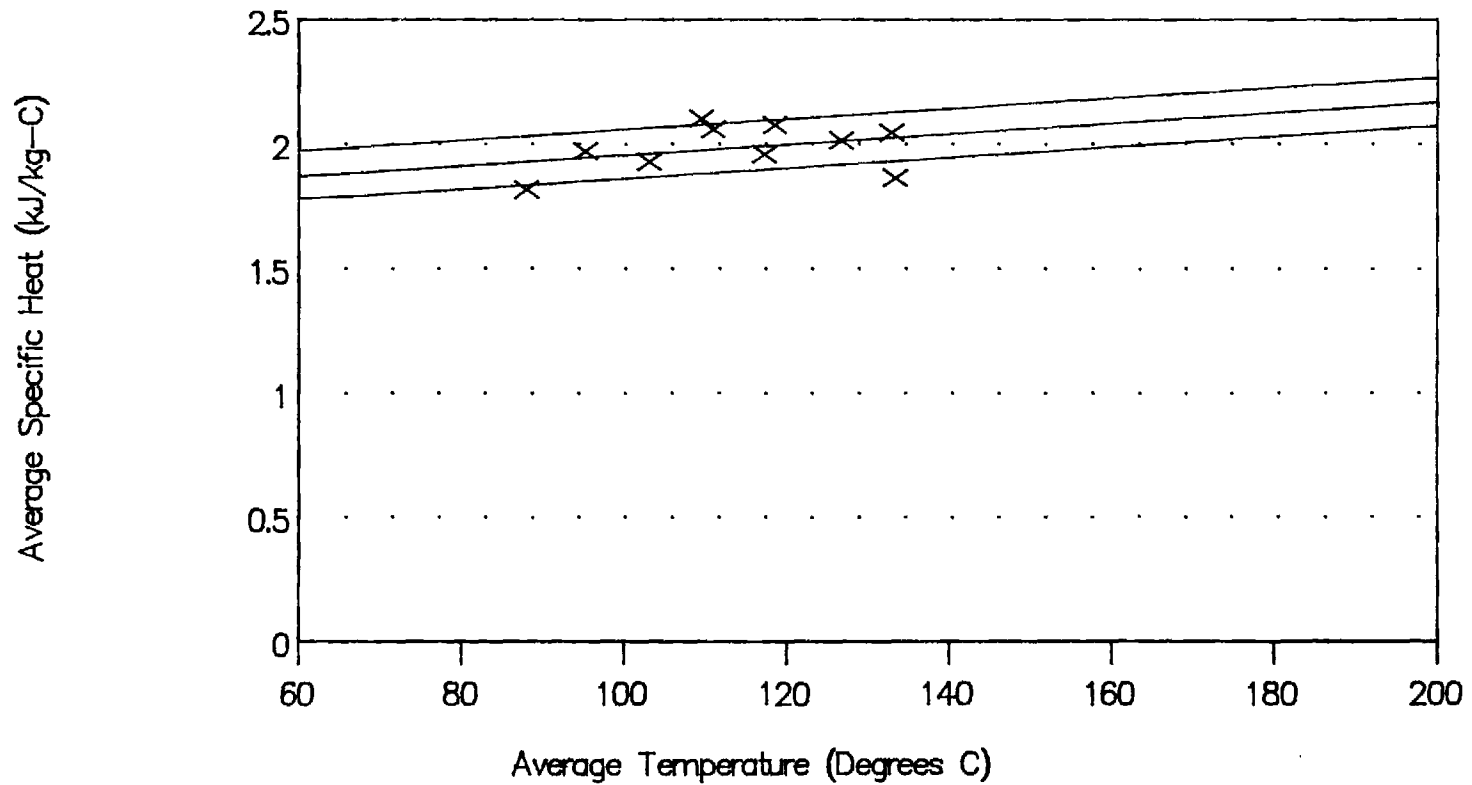


Figure A.5: 64.83% and 65.48% LiBr

Quadratic-Quadratic Correlation

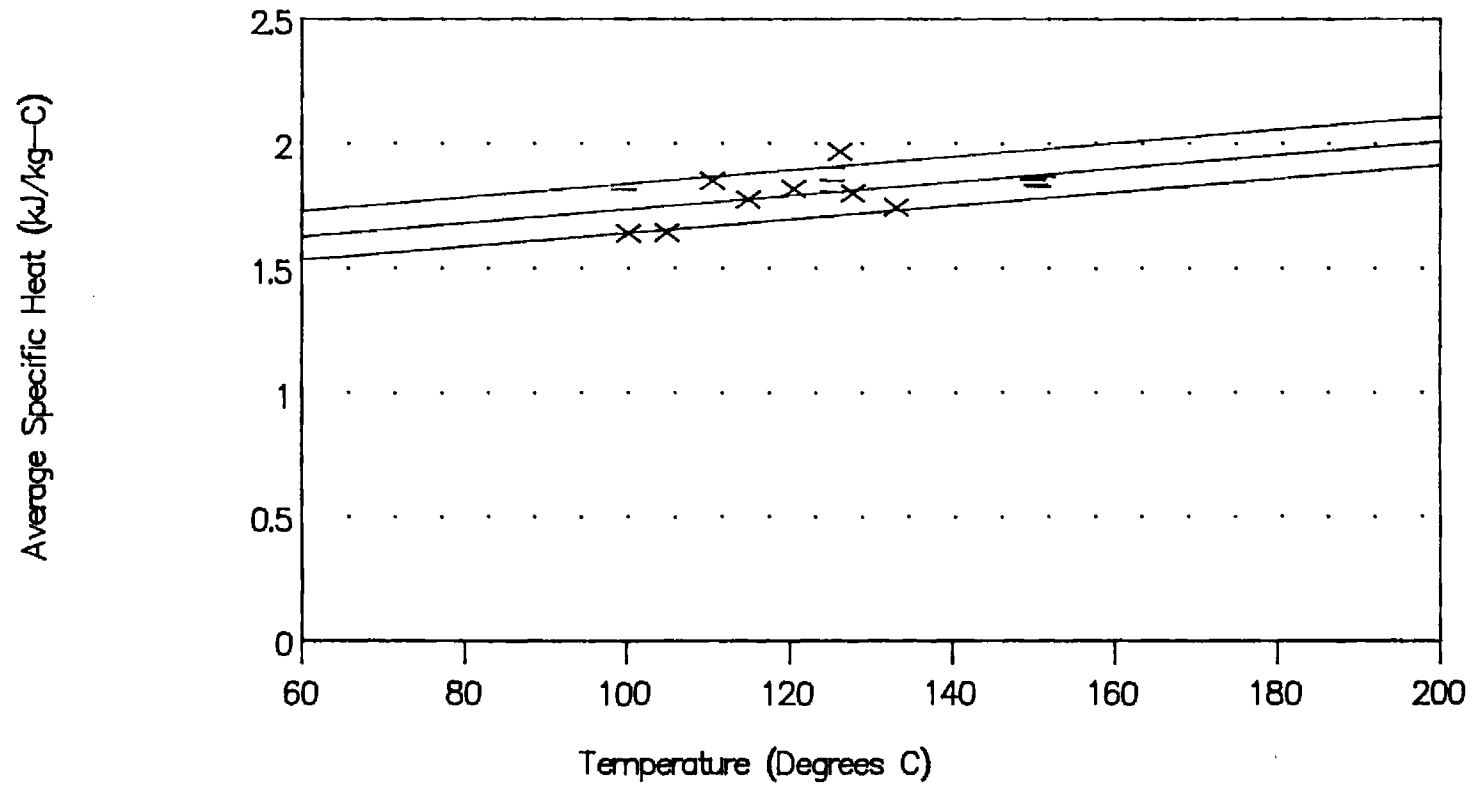


Figure A.6: 43.95% LiBr by weight

Quadratic-Linear Correlation

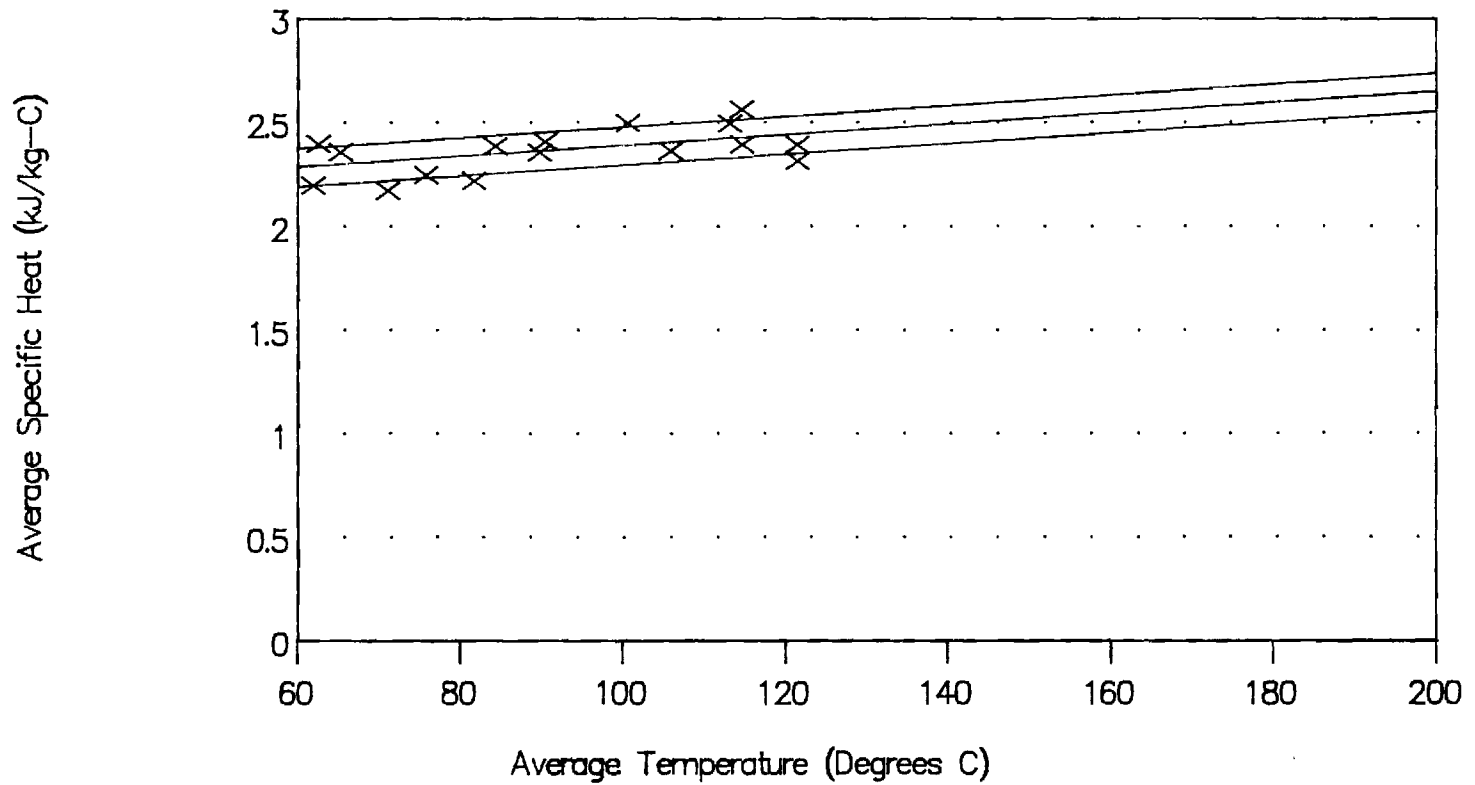


Figure A.7: 50.59% LiBr by weight

Quadratic-Linear Correlation

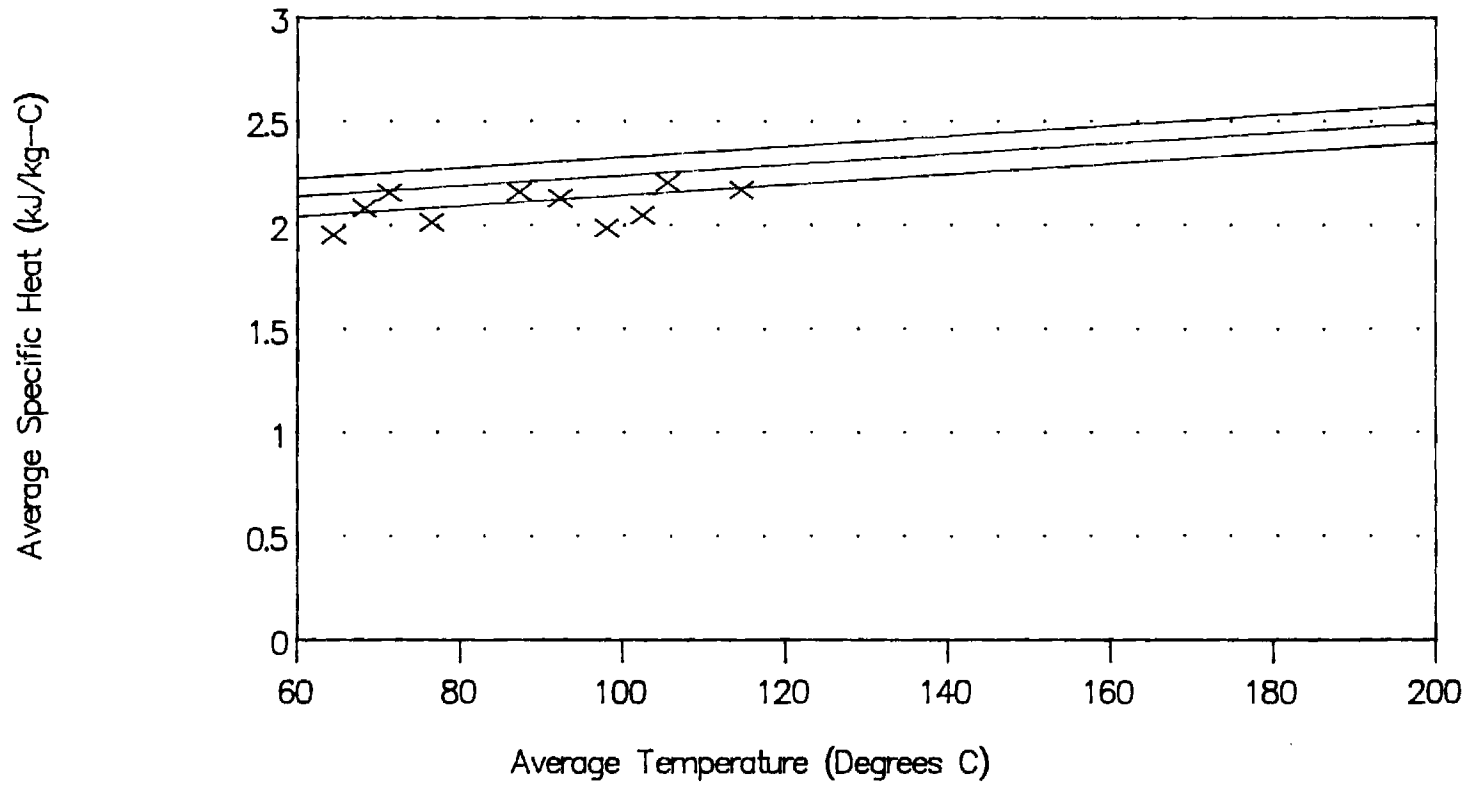


Figure A.8: 54.10% LiBr by weight

Quadratic-Linear Correlation

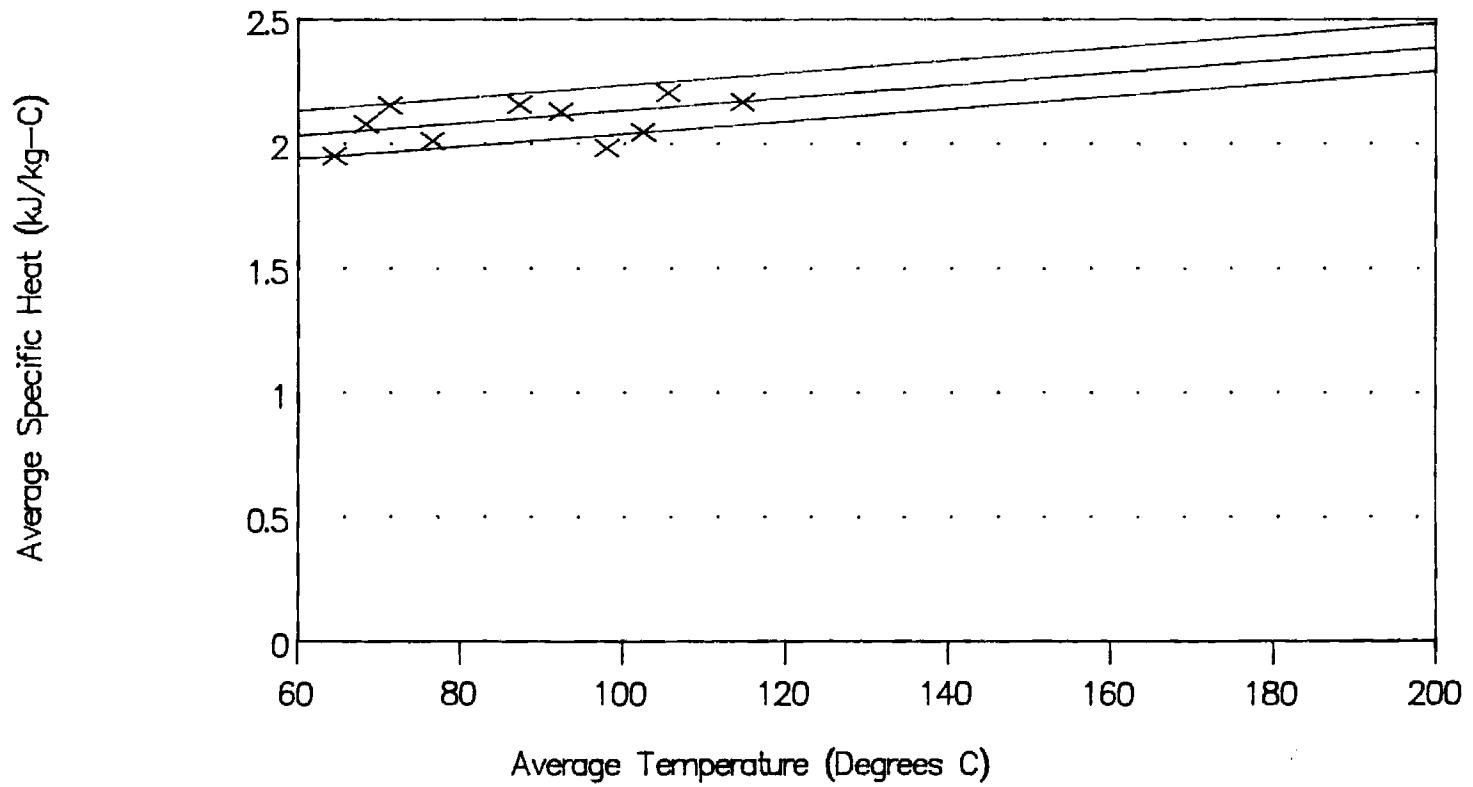


Figure A.9: 59.48% LiBr by weight

Quadratic-Linear Correlation

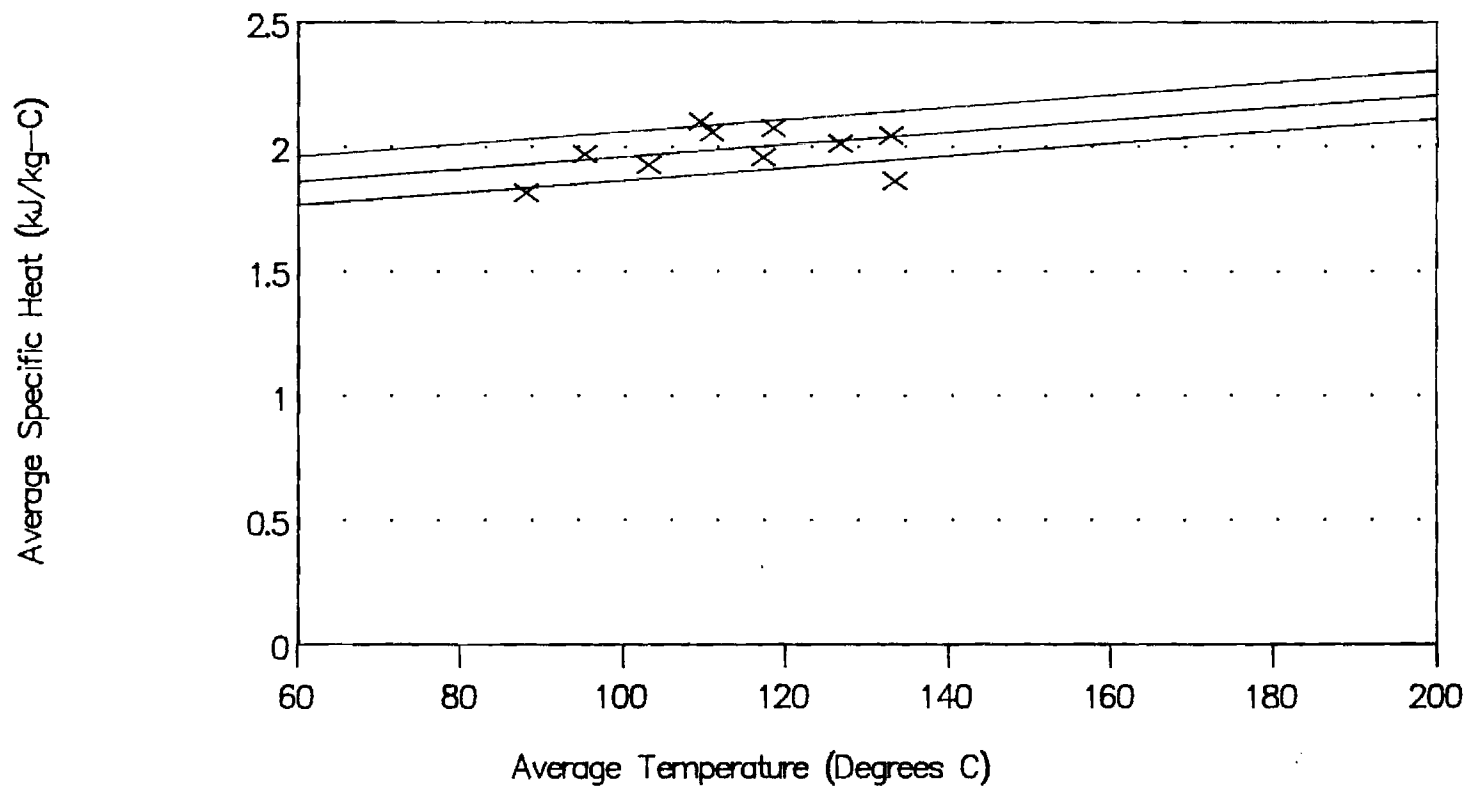
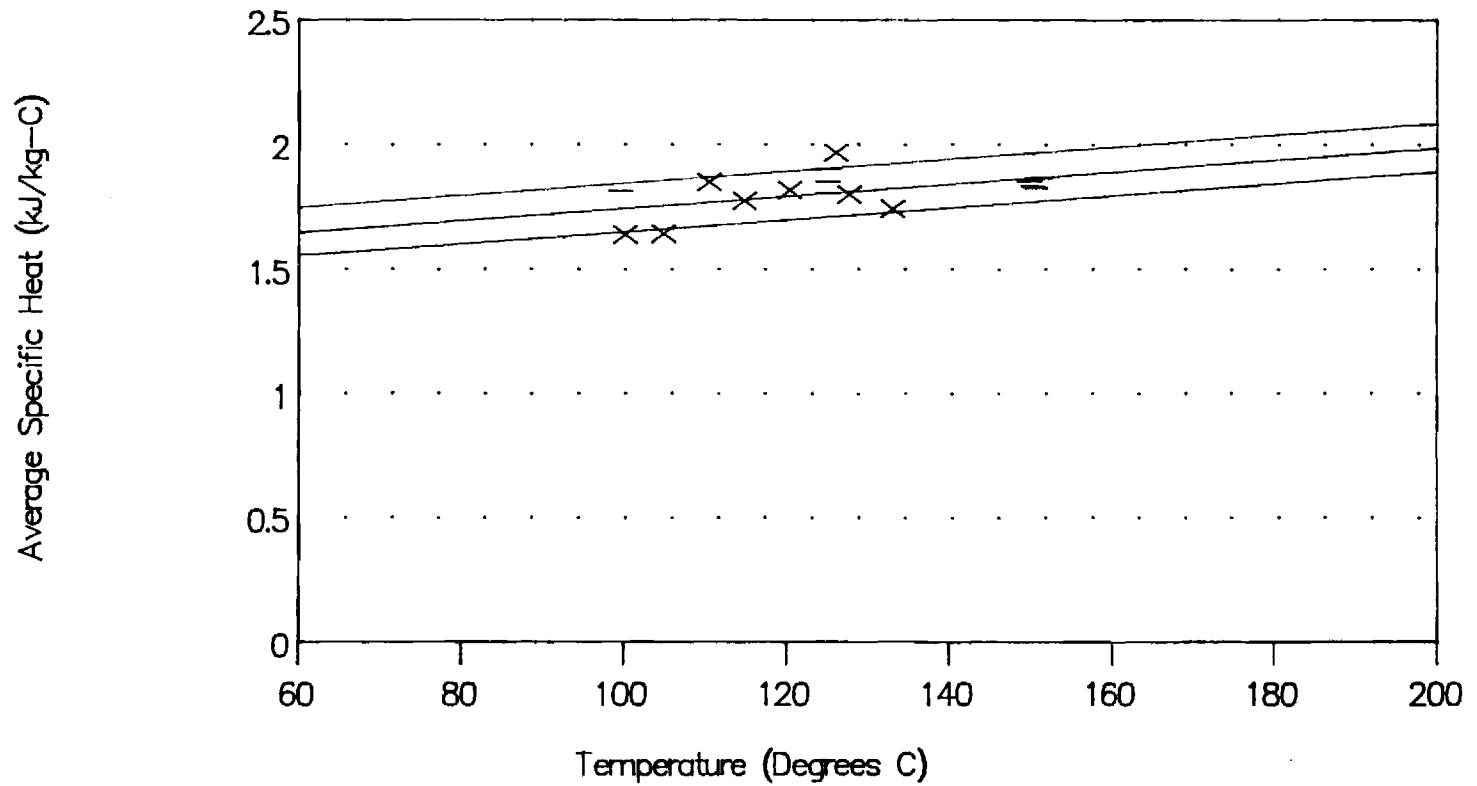


Figure A.10: 64.83% and 65.48% LiBr

Quadratic-Linear Correlation



VAPOR PRESSURES OF AQUEOUS LITHIUM BROMIDE SOLUTIONS

Abstract: The vapor pressures of concentrated aqueous lithium bromide solutions were measured at temperatures ranging from 120 °C to 210 °C. Five solutions of salt mass fractions 0.437, 0.494, 0.549, 0.608 and 0.652 were investigated. A novel representation of salt solution vapor pressure over a large range of temperature and concentration using a minimum number of parameters was developed. The data from this study were successfully correlated using the proposed model. Previously published vapor pressure measurements were also reviewed and checked for consistency. The most reliable literature data were combined with the measurements of the present study to develop a consistent database. The results of this work will allow the development of more reliable P-T-x chart for aqueous lithium bromide solutions and their extensions to higher temperatures.

Aqueous solutions of lithium bromide are common working fluids in absorption refrigeration applications. A knowledge of the physical properties and, in particular, of the P-T-x behavior of such solutions is required for process design and operation. To improve the efficiency of LiBr-water absorption refrigeration cycles, extensions of current processes to higher operating temperatures have been sought. However, very little reliable information on the thermophysical properties of lithium bromide solutions at high temperatures is available. The main objective of this work was to measure and correlate the vapor pressures of aqueous solutions of lithium bromide at temperatures ranging from 100 to 200 °C and concentrations ranging from 0.45 to 0.65 salt mass fraction. Previously reported data sets were reviewed and compared with the results obtained in this study. The most reliable literature data were combined with the measurements of the present study to develop a consistent database for the vapor pressure of concentrated aqueous lithium bromide solutions. The theory of electrolyte solutions is not yet sufficiently developed to allow a theoretical representation of thermophysical properties over a large range of temperature and concentration [Zemaitis,1986]. In the absence of a suitable theoretical model, a semi-empirical approach was adopted. A novel representation of the vapor pressure of salt solutions, suitable for large temperature and concentration ranges, was developed. The experimental results of this work were successfully correlated using the proposed semi-empirical model.

controller (Omega Programmable Temperature Controller, Model CN-2010) and could be maintained within ± 0.1 K of the set point for periods as long as 100 hours.

The pressure was transmitted from the cell to the pressure gauges through a high pressure manifold made from 2.11 mm (0.083 in) ID tubing (Autoclave Engineering HighPressure Tubings) and appropriate fittings (Autoclave Engineering HighPressure Fittings, Series F). For increased sensitivity, two pressure gauges (Heise 710-A, range 0-150 psig and Heise 710-A, range 0-200 bar) were used in this study. These pressure gauges were regularly calibrated against a dead weight tester (Budenberg, Model 380H) with rated accuracy of ± 0.05 % of the reading. During the experimental runs, the pressure gauges were zeroed periodically by opening the manifold to atmosphere. Barometric pressures were determined using a Fortin barometer; mercury elevations were corrected for temperature and local gravity effects.

In this work, it was decided to use pure degassed water as a pressure transmitting fluid. More classical choices, such as silicone oils or liquid metals, were initially tried but found to be inadequate (at the temperatures of interest in this study, the vapor pressure of mercury is no longer negligible and liquid gallium was found to react strongly with water vapor). Changes in solution composition due to transfer of water between the solution and the pressure transmitting fluid were avoided by controlling the position of the pressure transmitting liquid in the temperature gradient region present inside the oven wall (see Figure 2). When the valve of the cell (valve Vc in Figure 1) is closed, the pressure in the manifold is solely determined by the position of the pressure transmitting liquid inside the oven wall. This position can be adjusted freely by using the in-line variable volume generator (HIP Pressure Generator, Model 62-6-10). If the pre set pressure in the manifold is equal to the pressure in the cell, no transfer of water occurs as the valve of the cell is opened. If the pressure in the manifold is close to the pressure in the cell, only a negligible amount of water will be transferred, partly due to the very small flow area of the manifold tubing (3.50 mm^2 or 0.005 in^2). Furthermore, it was found that following the opening of the cell valve, mechanical equilibrium throughout the system, i.e. pressure equilibrium, is attained almost immediately. If the cell valve is left open after equalization of the pressure, some water transfer occurs as the water interface in the manifold tubing adjusts itself to a new equilibrium position. The rate of water transfer is however strongly limited by the rate of heat transfer into the oven wall or into the cell. Heat transfer occurs by conduction and is inherently much slower than pressure equalization. By closing the cell valve after mechanical equilibrium has

been attained and before any significant amount of water can be transferred, pressure measurements can be done without disturbing the solution composition.

This somewhat novel way of transmitting pressure was shown to be applicable to salt solutions. The pressure transmission was found to be accurate and very sensitive. Indeed, in our work, the sensitivity of the pressure transmission was only limited by the sensitivity of the pressure gauges, namely 0.7 mbar (or 0.01 psi). In addition, the attractiveness of this pressure transmitting technique lies mainly in the absence of limitations for its use at high pressure and high temperature.

2. Procedure

Before the start of a run, the high pressure equilibrium cell was cleaned with steam and baked under vacuum to remove any traces of surface contamination which might affect the measurements. 35 ml of a gravimetrically prepared aqueous lithium bromide solution was then transferred into the cell. The glass cell liner was plugged with some glass wool and the lid of the cell was secured with cap screws. The reliability of the graphite seal and of the cell fittings were then tested with extra dry nitrogen gas up to a pressure of 80 bar. This test pressure is more than four times greater than the maximum pressure encountered in the measurements. The pressurized cell was checked for leaks by immersing it in a tank of water.

Nitrogen gas and other inerts were removed from the cell by repeated pumping of the vapor phase present above the salt solutions. By keeping the solution at sufficiently low temperature (at the freezing point of water in this work), the amount of water present in the vapor phase and therefore removed from the cells during the pumping can be shown to be negligible. The absence of any significant water loss during the degassing procedure was checked by monitoring the mass of the contents of the cell. Above a salt mass fraction of 0.60, aqueous lithium bromide solutions were present at 0 °C in a state similar to a glassy state. Classical freeze-pump-thaw cycles were therefore used to degas the most concentrated solutions. Since thorough degassing is critical in static VLE experiments, the pressure inside the cell was monitored by a thermocouple vacuum gauge (Sargent-Welch Scientific Company, Model 1515) to assess the completeness of inert removal. Generally four to six cycles were found sufficient to obtain a constant residual pressure inside the cell.

Once the degassing had been completed, the cell was installed in the oven and attached to the manifold. The manifold and the pressure transmitting lines were tested for absence of leaks with nitrogen gas up to 80 bar and then evacuated. Pure degassed water was charged into the pressure transmitting lines. When the oven temperature had reached its set point, the valve connecting the manifold to the pressure transmitting lines (valve V_m in Figure 1) was opened and the water was allowed to penetrate into the manifold up to the temperature gradient region located inside the oven wall. Upon intrusion of water into the temperature gradient region, water vaporization occurred and pressure started to build up inside the manifold.

At this time the apparatus was ready for measurement. The position of the water vapor liquid interface inside the oven wall was adjusted to obtain the desired manifold pressure. The valve of the cell was then opened for five to ten seconds, time to record the total pressure in the system. After closing the cell valve, the absence of any significant water transfer was checked as the manifold pressure returned to its pre-set level. The solution inside the cell was allowed to equilibrate with its somewhat perturbed vapor phase and the manifold pressure was adjusted to a new value. Generally, three to four adjustments were sufficient to get a set manifold pressure equal to or very close to the pressure inside the cell. Once convergence had been obtained, the pressure determination procedure was continued with a set manifold pressure, first slightly higher and then slightly lower than the solution equilibrium pressure to check for hysteresis in the reading.

The temperature of the oven was then set to a new value and the pressure determination procedure repeated.

3. Materials

Lithium bromide was obtained in the anhydrous form from Morton Thiokol Inc. (lot F06H). The manufacturer's certificate of analysis stated a purity of 99.3 %w, the remaining being water (0.5 %w) and various salts. During the preparation of the lithium bromide solutions, the presence of fiber-like materials and black and orange pellets was noticed. These impurities seemed most likely to have come from the manufacturing process. However, their presence was not found to significantly affect the vapor pressure measurements. Before use, the required amount of salt was dried

by heating the sample under vacuum. This drying technique was found to be suitable for the particularly hygroscopic lithium bromide salt, as documented by Weintraub et al [1984] in their work on the determination of the water content of lithium salts. No further changes in the mass of the salt were observed after 24 to 48 hours of drying at temperatures ranging from 130 to 200 °C and pressure of the order of 100 mtorr. The drying was then considered complete. Analytical NaCl, used for the validation test, was purchased from Fisher Scientific (lot 851530) and was dried using the same procedure. The water used in this study was purified by distillation in an all-glass still (Corning Mega-Pure System, Model MP-6A).

II. Results and Discussion

The apparatus and the experimental procedure were validated by replicating vapor pressure measurements for the system NaCl-water. Our results were compared to the data of Liu and Lindsay [1972] (see Figure 3). The average relative deviation between the two data sets is 0.3%.

The vapor pressures of concentrated aqueous lithium bromide solutions were measured at temperatures ranging from their normal boiling temperature up to 210 °C. Five solutions with salt mass fraction ranging from 0.438 to 0.651 were investigated. The results of these measurements are given in Table 1. The solution composition was corrected for loss of water due to vaporization. The accuracy in the pressure measurement was estimated by error propagation analysis to be ± 15 mbar, whereas the uncertainty in the temperature determination is estimated to be $\pm 0.3\%$.

III. Correlation

Dilute and very dilute aqueous solutions of electrolytes have been extensively studied, especially at ambient conditions and numerous theoretically based models have been proposed for the representation of their thermophysical properties [Zemaitis, 1986]. Extensions of these models to higher salt concentrations and to higher temperatures is presently an active field of research. Dilute solution based models are, however, not yet suitable for representing thermophysical properties of electrolyte solutions over large ranges of temperature and concentration. An empirical or semi-empirical approach has therefore been traditionally preferred, and numerous empirical models have been proposed for correlating the vapor pressures of aqueous electrolyte solutions [Horvarth,1985].

For this study, a novel semi-empirical model, suitable for correlating the vapor pressures of aqueous electrolyte solutions over large ranges of temperature and concentration, has been developed. The ratio of the solution vapor pressure to the saturation pressure of pure water, namely P/P_w^{sat} , was found to be a particularly suitable dependent variable. The temperature dependence of this pressure ratio is well behaved, exhibiting a small and very linear dependence over large temperature ranges. Furthermore, as long as only a negligible amount of salt is present in the vapor phase, this pressure ratio is very closely related to the solvent activity and its value and behavior at the limits of the composition range are well known. When the amount of salt present in the solution approaches zero, the pressure ratio goes to one, and as the solution becomes more and more concentrated in salt, the pressure ratio approaches zero. By taking into account these limiting bounds, P/P_w^{sat} was expressed as a function of temperature and composition in the form:

$$P / P_w^{sat} = x_w + x_w(1 - x_w)g[T, x_w]$$

where x_w is the water mole fraction and g is an empirical function whose functional form is determined by stepwise regression analysis. In general, g is a simple function of the temperature and the water mole fraction, such as a polynomial in x_w and T , or a simple function containing terms such as $\ln(x_w)$, $\exp(x_w)$, $1/T$ or $\ln(T)$. It should be noted that the water mole fraction was defined in this work on a ionized basis as follows:

$$x_w = \frac{n_{water}}{n_{water} + n_{ion}}$$

where n_{water} is the amount of water present in the solution and n_{ion} is the total amount of ions assuming complete dissociation of the salt molecules. The correspondence between water mole fraction defined on an ionized basis and salt mass fraction, $\omega(\text{LiBr})$, is given by:

$$\frac{1}{\omega(\text{LiBr})} = 1 + 2 \frac{18.054}{86.85} \left(\frac{x_w}{1 - x_w} \right)$$

The experimental results of this work were correlated using this newly developed model. The stepwise regression analysis of the data resulted in the following correlation for P/P_w^{sat} :

$$P / P_w^{sat} = x_w + x_w(1 - x_w) \left[A_0 + A_1(x_w - 0.65) + A_2(x_w - 0.65)^2 + A_3(x_w - 0.65)^3 + A_4\left(\frac{T - 150}{150}\right) + A_5\left(\frac{T - 150}{150}\right)(x_w - 0.65)^2 \right]$$

where T is the temperature of the solution in °C. The parameters A_i are given in Table 2. The average relative deviation of the data set from the correlation is 0.21% (see Table 3). The quality of the fit is illustrated in Figure 5.

IV. Review of literature Data

1. Scope of the review

Numerous investigators have reported data for the vapor pressures of aqueous lithium bromide solutions. The International Critical Tables [I.C.T.,1928], published in 1928, mentions more than nine references related to this subject. Works done before 1970 were summarized by McNeely [1979], who compiled published data as well as data measured by the major manufacturers of lithium bromide absorption

equipment in USA. In this paper, more recent works will be reviewed. The data of Pennington [1955], on which the current PTx ASHRAE charts are generally based, were also included.

The temperature and concentration ranges studied by the different investigators included in this review are summarized in Figure 6. The data sets were analyzed to determine their intrinsic reliability and, to allow comparison on a common basis, were then correlated using the model proposed in this work. Statistical information characterizing the individual data sets is summarized in Table 3. The indicated number of data points refers to the total number of reported experimental determinations. The data set precision is expressed through its average absolute deviation (AAD) and its average relative deviation (ARD). The AAD and ARD computation were based on an optimized set of values, from which likely outliers and inconsistent results were removed. It should be noted that the AAD and the ARD criteria do not characterize the data sets in the same way, due to differences in temperature and composition ranges.

2. Measurements at subatmospheric conditions.

Most of the measurements, especially the earliest ones, were done at subatmospheric or atmospheric pressure. Pennington used three independent experimental techniques to measure the vapor pressure of aqueous lithium bromide solutions, which allowed him to span different ranges of temperature and pressure (for clarity purposes, his results at 30 °C were not included in Figure 6). The data sets are fairly consistent with each other and are remarkably free of scatter, as illustrated by their respective AAD or ARD. Boryta et al [1975] determined the vapor pressure of four aqueous lithium bromide solutions containing respectively 40, 50, 60 and 70 % of salt in mass, by a static and by a gas transport method. His data at 40 %w showed considerably more scatter than the ones at higher concentrations and a very unlikely temperature dependence (see Figure 7). They were not considered further. His gas transport results seemed less precise than the data obtained by the static method. However, within the scatter of the data, the results obtained by the two experimental methods seemed to agree. Renz [1981] measured the vapor pressure of aqueous lithium bromide solutions over an extended range of concentrations at subatmo-

spheric conditions. Since this review is mainly concerned with concentrated solutions, only his data pertaining to solutions having a salt mass fractions of 0.35 or more were considered.

3. Measurements above atmospheric pressure

Measurements above atmospheric pressure have been reported by three investigators. Fedorov et al [1976] measured the vapor pressure of aqueous lithium bromide solutions at temperature ranging from 150 to 350 °C for a wide range of compositions. However, only data interpolated to integral temperatures were reported. The absence of experimental scatter in the reported data did not permit a fair estimation of the data set precision. The individual correlation of the Fedorov et al measurements was based on the smoothed data. Rockenfeller [1988] determined the vapor pressure of aqueous lithium bromide solutions from 80 to 205 °C for solutions having a salt mass fraction ranging from 0.35 to 0.6470. His data under 95 °C showed considerably more scatter than the ones above 95 °C (see Figure 8). The data below 95 °C were not considered further. The reported precision of the measurements was ± 13 mbar. This value was found to be consistent with the derived AAD and ARD of the data set, and illustrates the high level of precision obtained in these measurements. However, it should be noted that two pressure gauges, with span range of respectively 25 and 250 psi, were used for these measurements and, small but clear discrepancies between the readings of the two pressure gauges were observed. Recently, Iyoki and Uemura [Iyoki, 1989] published measurements for the vapor pressure of concentrated aqueous lithium bromide solutions. The use of a thick wall glass still allowed them to measure vapor pressure up to 3 bar. The scatter in their data was found to be greater than in the previously discussed data sets. However, on the whole, the data seemed to be fairly reliable.

V. Comparison with literature data

Due to different temperature and composition conditions, a direct comparison of vapor pressure measurements is difficult. Therefore, agreements and disagreements between data sets were put in evidence by using the individual data set correlations. The vapor pressure measurements reported in the six reviewed studies were compared to the vapor pressure measurements obtained in this work. The results of the comparisons are shown in Figure 9a through Figure 9e. Large discrepancies are apparent. Rockenfeller's data are systematically higher. The bias is, on average, one order of magnitude greater than the precision of his data and therefore cannot be attributed simply to lack of fit of the data sets or to large scatter in the measurements. The data of Fedorov et al similarly exhibit strong discrepancies. The vapor pressure measurements of Renz and the ones of Iyoki and Uemura seem to agree consistently at the lowest concentrations, but discrepancies are apparent for the most concentrated solutions. The data set of Boryta et al and the one of Pennington do not show consistent agreement with any other data sets, but no clear bias can be shown. The experimental results of this work show good agreement with the data of Renz and with the data of Iyoki and Uemura at a salt mass fraction of 0.4375, 0.4940 and 0.5487. At a salt mass fraction of 0.6085 and especially at a salt mass fraction of 0.6515, our experimental results fall between the data of Renz and of Iyoki and Uemura. It should be added that the curvature in temperature of our experimental results, apparent in Figure 9a through 9e, is partly due to the increase of the salt mass fraction of the measured solution as the temperature is increased (see vaporization correction in the Results and Discussion paragraph).

VI. Conclusion

The vapor pressures of concentrated aqueous lithium bromide solutions were measured at temperatures ranging from their normal boiling temperature to 210 °C. Five solutions of salt mass fraction 0.437, 0.494, 0.549, 0.608 and 0.652 were investigated. The experimental results were successfully correlated using a novel semi-empirical model for the vapor pressure of electrolyte solutions. This model was shown particularly suitable for representing the vapor pressure of electrolyte solutions over large temperature and concentration ranges. And, although extrapolation in concentration should be used with caution, the proposed model was found to be useful for extrapolating data sets in temperature. Previously published vapor pressure measurements were also reviewed and checked for consistency. Our experimental results were found consistent with the most reliable literature data. The results of this work will allow the development of more reliable P-T-x chart for aqueous lithium bromide solutions and their extensions to higher temperatures.

Bibliography

Boryta D.A., Maas A.J. and Grant C.B., "Vapor Pressure-Temperature-Concentration Relationship for System Lithium Bromide and Water (40-70% Lithium Bromide)", *Journal of Chemical and Engineering Data*, Vol 20, 3:316-319, 1975

Federov M.K., Antonov N.A. and L'vov S.N., "Vapor Pressure of Saturated Aqueous Solutions of LiCl, LiBr, and LiI and Thermodynamic Characteristics of the Solvent in These Systems at Temperatures of 150-350 °C and Pressures up to 1500 bar", translated from *Zhurnal prikladnoi Khimii*, Vol 49, 6:1226-1232, 1976

Horvath A.L., "Handbook of Aqueous Electrolyte Solutions", Ellis Horwood Limited, Chichester, England, 1985

International Critical Tables, Vol 3, New-york, Mc Graw-Hill, 1928

Liu C. and Lindsay W.T., "Thermodynamics of Sodium Chloride Solutions at High Temperatures", *Journal of Solution Chemistry*, Vol 1, 1:45-69, 1972

Mc Neely L.A., "Thermodynamic Properties of Aqueous Solutions of Lithium Bromide", *ASHRAE Transactions*, 3:413-434, 1979

Pennington W., "How To Find Accurate Vapor Pressures of LiBr Water Solutions", *Refrigerating Engineering*, 63:57-61, 1955

Renz M., "Bestimmung Thermodynamischer Eigenschaften Wässriger und Methylalkoholischer Salzlösungen", Dissertation, University of Essen, 1981

Rockenfeller U., Private Communication, 1988

Iyoki S. and Uemura T., "Vapor Pressure of Water-Lithium Bromide System and the Water - Lithium Bromide - Zinc Bromide - Lithium Chloride System at High Temperatures", *Revue Internationale du Froid*, Vol 12, 278-282, 1989

Weintraub R., Apelblat A., Tamir A., "Determination of Water Content of Hygroscopic Lithium Salts", *Analytica Chimica Acta*, 166:325-327, 1984

Zemaitis J.F., Clark D.M., Rafal M., Scrivner N.C., "Handbook of Aqueous Electrolyte Thermodynamics", American Institute of Chemical Engineers Inc, New-York, USA, 1986

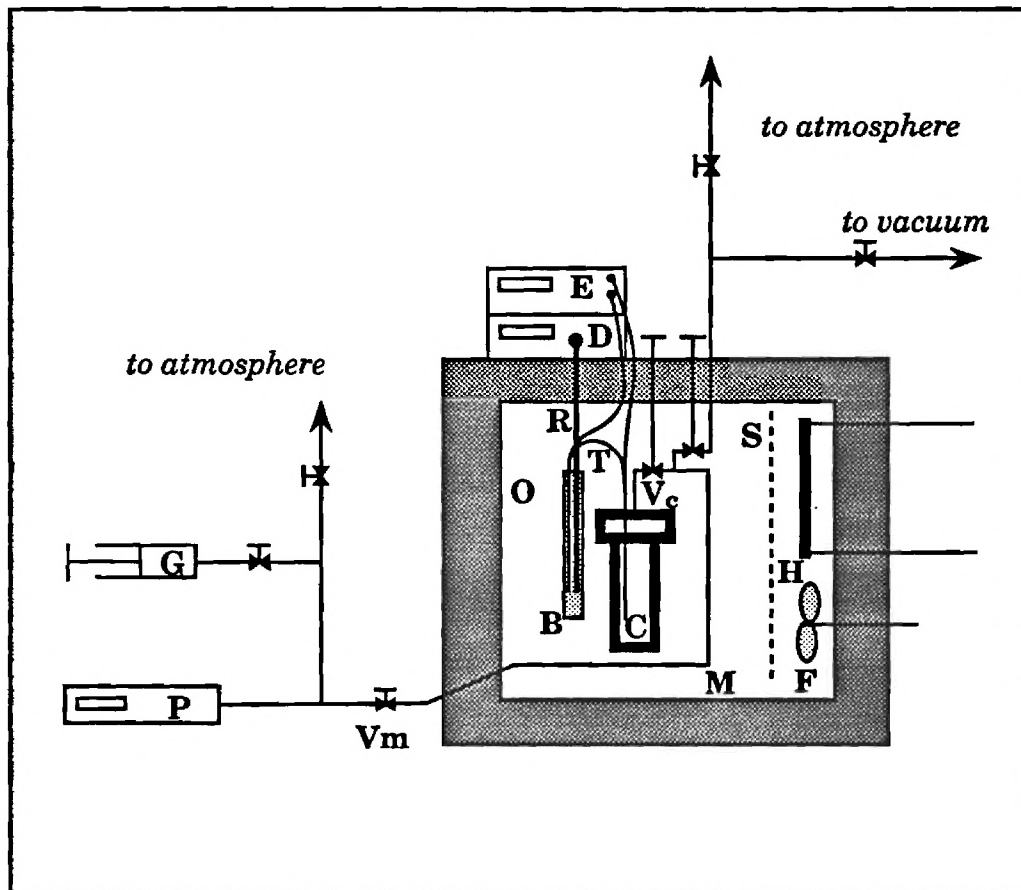


Fig 1 : Schematic of the static VLE apparatus:

(B) Metal Block, (C) Cell, (D) Digital thermometer, (E) Digital Multimeter, (F) Fan, (G) Variable Volume Generator, (H) Heater, (M) Manifold, (O) Oven, (P) Pressure Gauge, (R) Platinum Resistance Thermometer, (S) Screen, (T) Multijunction Thermocouple, (Vc) Cell Valve, (Vm) Manifold Valve.

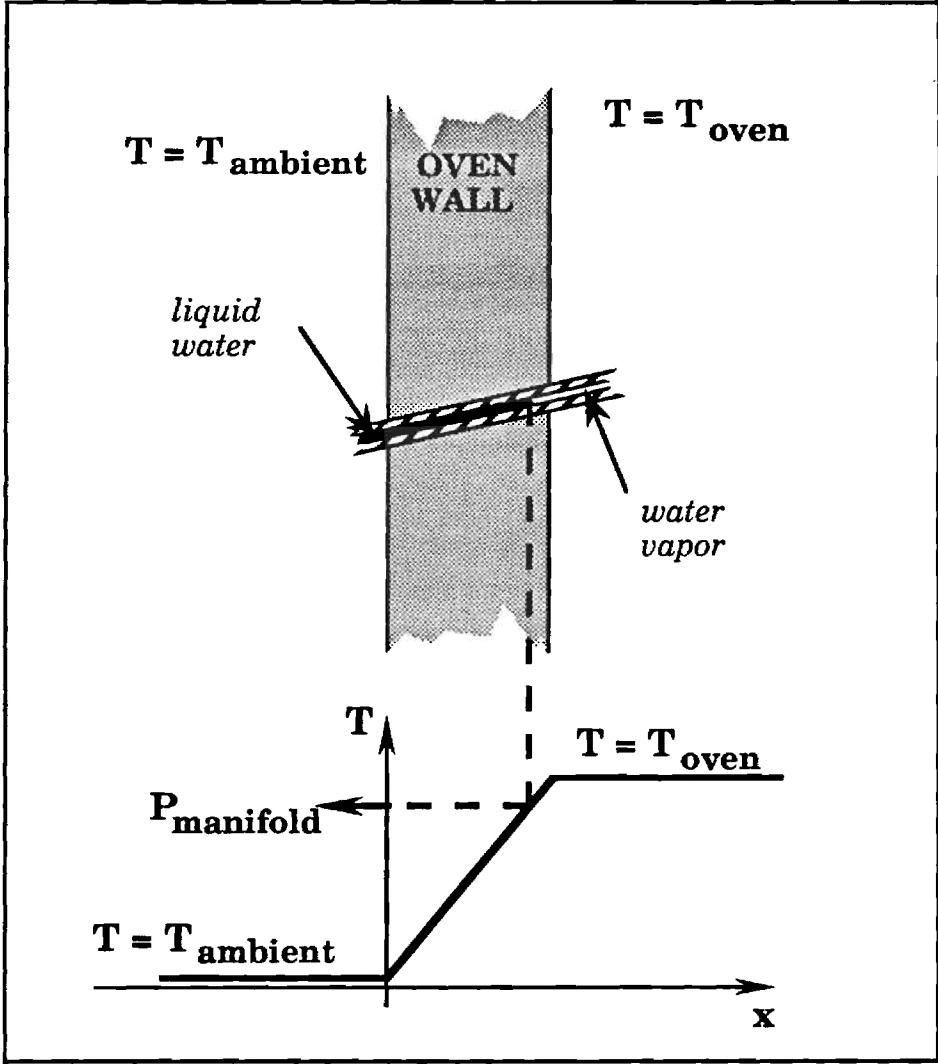


Fig 2: Pressure Transmitting Principle

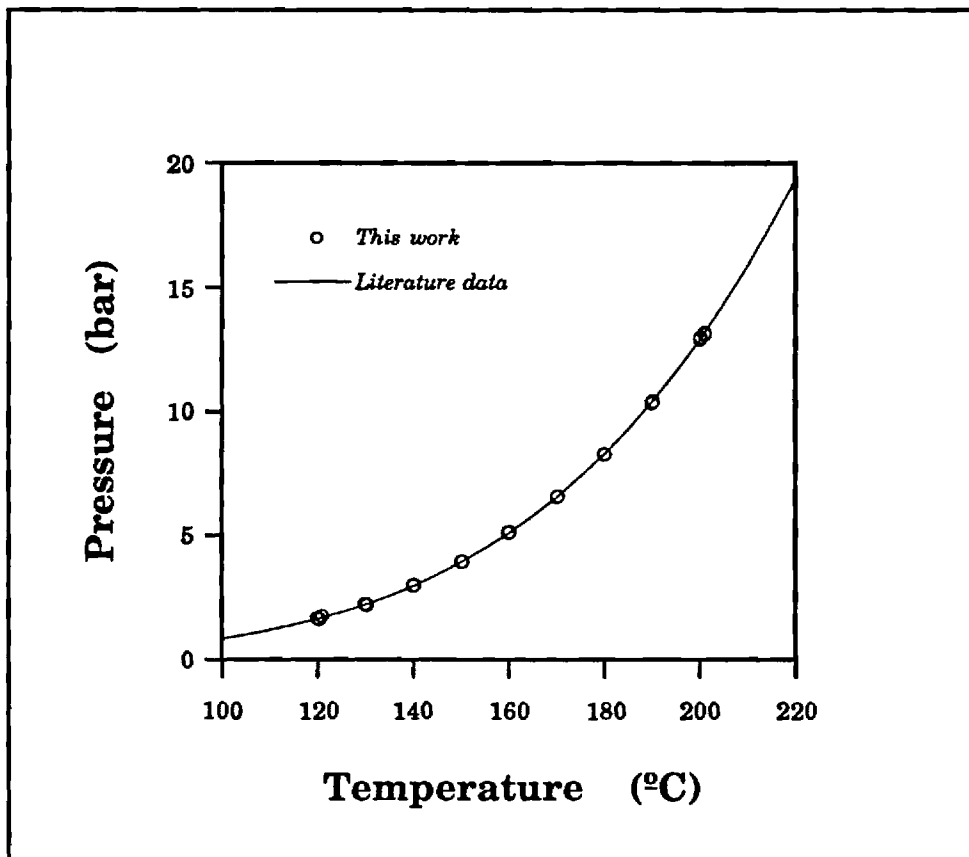


Fig 3: NaCl-Water system

The molality of the investigated solution was 4.6885 mol/kg. The literature data correlation was derived from the data of Liu and Lindsay [1972].

Table 1: Experimental Data

Salt Mass Fraction	Temperature (°C)	Pressure (bar)
0.4375 ±0.0045	125.0	1.121
0.4375 ±0.0045	134.9	1.525
0.4375 ±0.0045	149.9	2.352
0.4376 ±0.0045	165.0	3.518
0.4377 ±0.0045	180.3	5.133
0.4379 ±0.0045	210.4	10.002
0.4940 ±0.0040	135.0	1.134
0.4940 ±0.0040	150.1	1.775
0.4941 ±0.0040	165.1	2.688
0.4942 ±0.0040	180.3	3.959
0.4943 ±0.0040	195.3	5.652
0.4944 ±0.0040	210.3	7.857
0.5489 ±0.0025	150.0	1.253
0.5490 ±0.0025	165.0	1.944
0.5490 ±0.0025	180.2	2.913
0.5491 ±0.0025	195.2	4.227
0.5492 ±0.0025	210.5	6.001
0.6084 ±0.0030	165.0	1.305
0.6085 ±0.0030	180.4	2.013
0.6087 ±0.0030	195.5	2.980
0.6089 ±0.0030	210.6	4.295
0.6516 ±0.0030	179.7	1.451
0.6517 ±0.0030	194.9	2.188
0.6519 ±0.0030	209.9	3.167

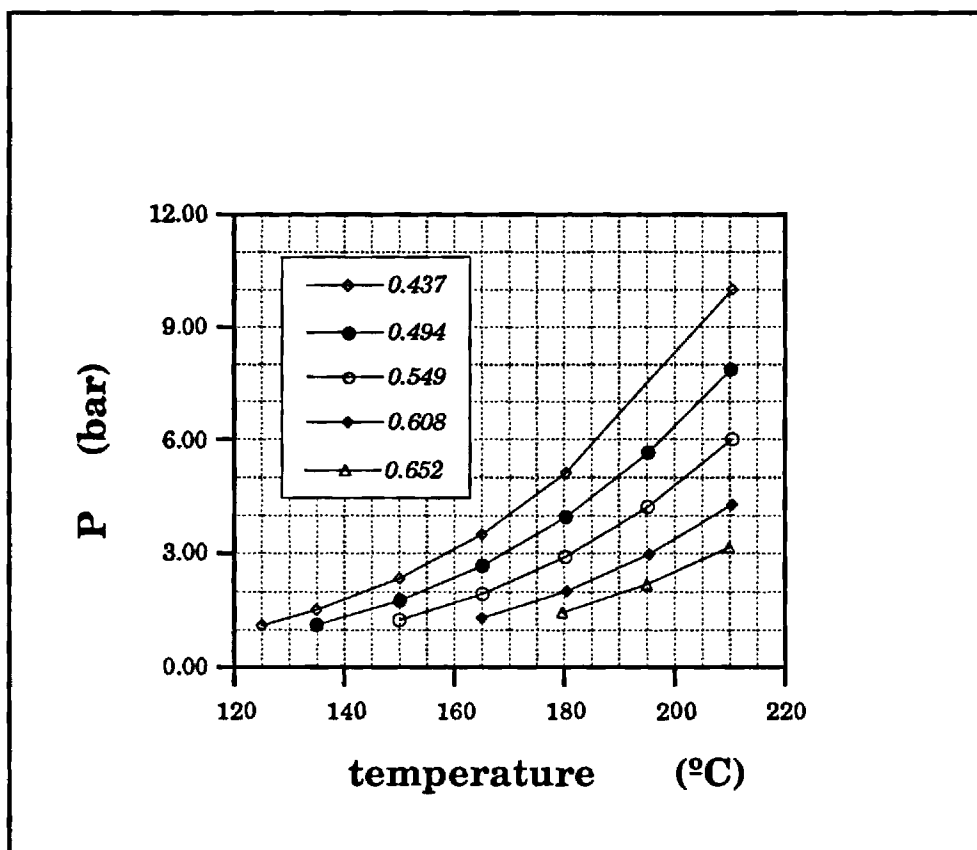


Fig 4: Experimental Data

The legend refers to the salt mass fraction of the investigated solutions.

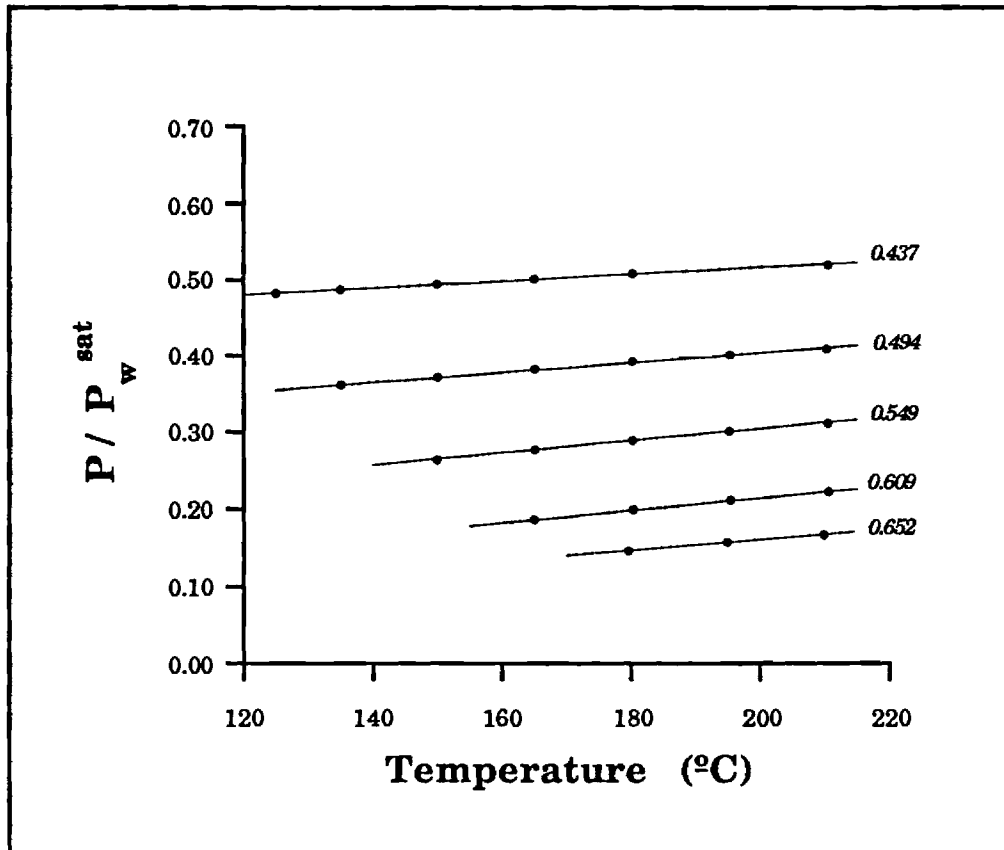


Fig 5: Correlation

(•) Experimental Data Point, (—) Correlation.

The number attached to a line indicates the salt mass fraction of the measured solution.

Table 2: Correlation Parameters.

A_0	-1.809784
A_1	1.059895
A_2	20.307708
A_3	43.314071
A_4	.536261
A_5	-15.298850

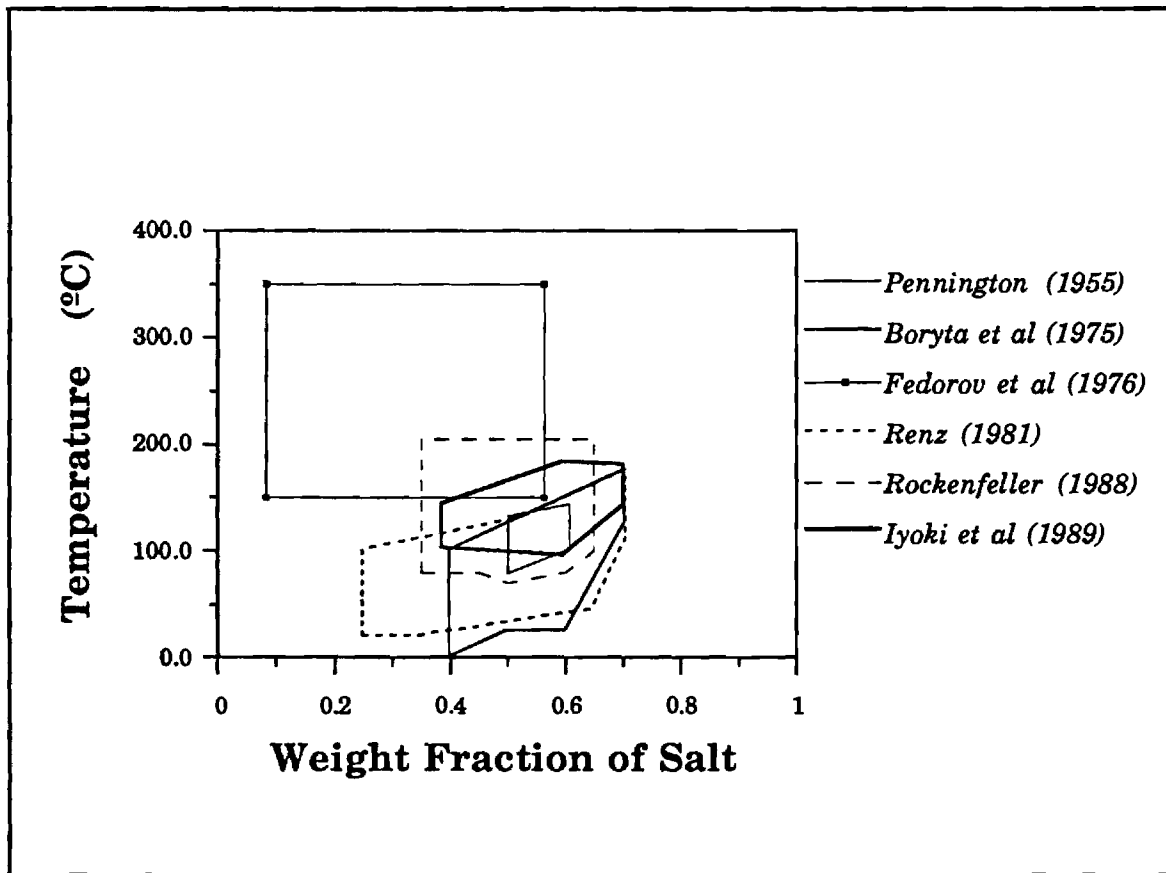


Fig 6: Temperature and composition ranges investigated in the reviewed works

Table 3: Summary of recent works

Investigator	Year	Experimental Technique	Number of data points	Precision	
				AAD	ARD
Pennington	1955	(1) Static Still	10	0.00144	0.56%
		(2) Ebulliometry	25	0.00196	0.82%
		(3) Water Absorbtion	11	0.00192	1.31%
Boryta et al.	1975	(1) Static Still	15	0.00238	1.81%
		(2) Gas Transport	17	0.00430	2.90%
Fedorov et al	1976	Static Still	35	—	—
Renz	1981	Static Still	96	0.00113	0.86%
Rockenfeller	1988	Unknown	199	0.00191	0.67%
Iyoki and Uemura	1989	Boiling Point	39	0.00380	2.24%
This work	1991	Static Still	24	0.00067	0.21%

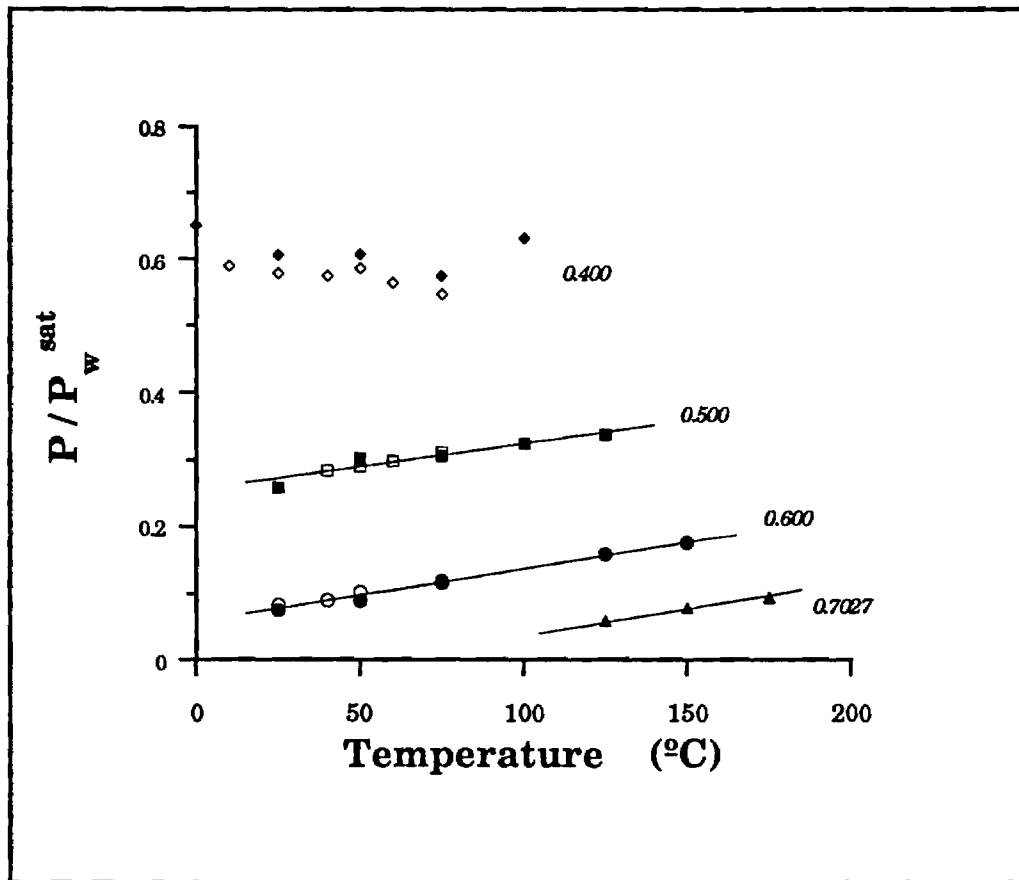


Fig 7: Experimental Results of Boryta et al

The open symbols represent the static still experimental results whereas the filled symbols represent measurements obtained by the gas transport technique. The correlation is based solely on the data of Boryta et al and was used to determine the intrinsic precision of the data set.

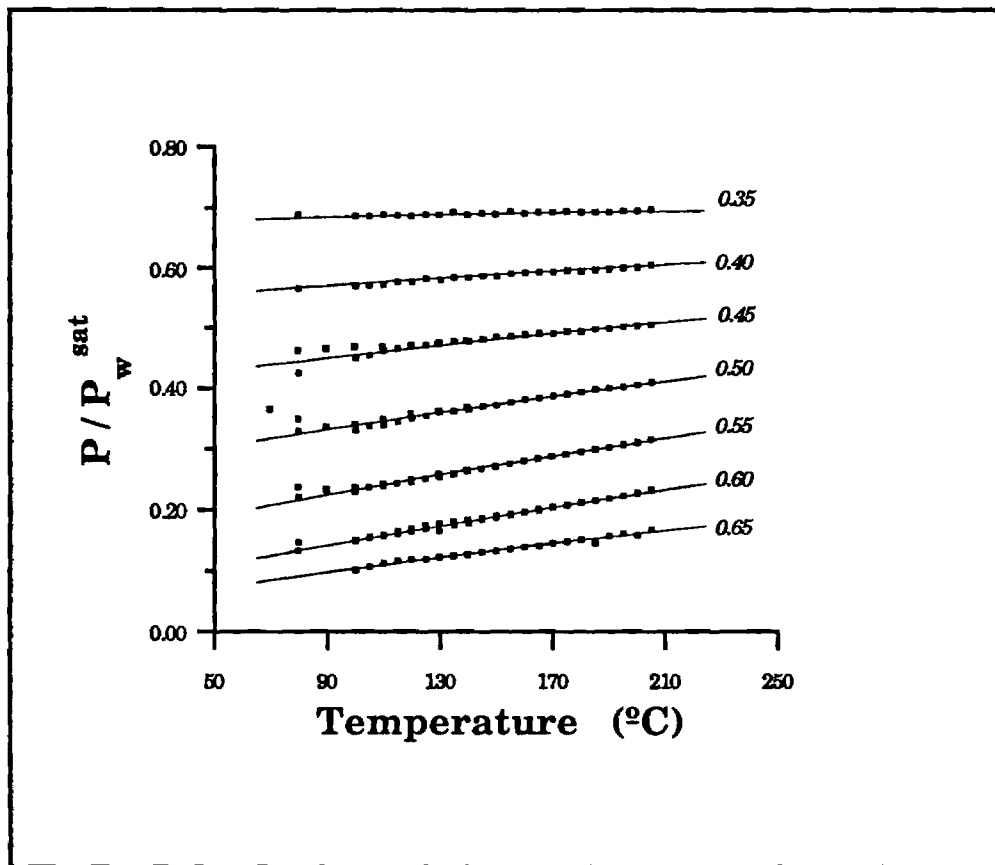


Fig 8: Experimental Results of Rockenfeller

(■) Experimental Data Point, (—) Correlation based on Rockenfeller's measurements. The number attached to a correlation line represents the salt mass fraction of the measured solution. Only measurements above 95°C were considered during the correlation of the data set.

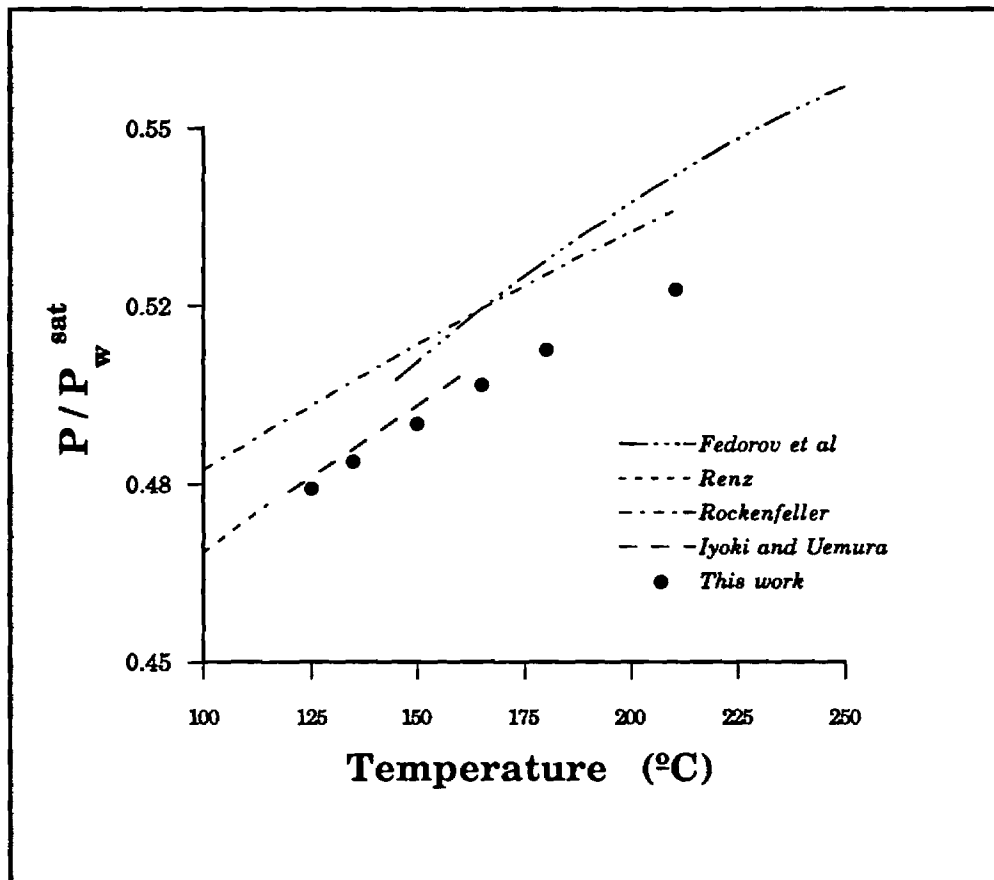


Fig 9a: Data Set Comparison

The comparison was made at a salt mass fraction of 0.4375.

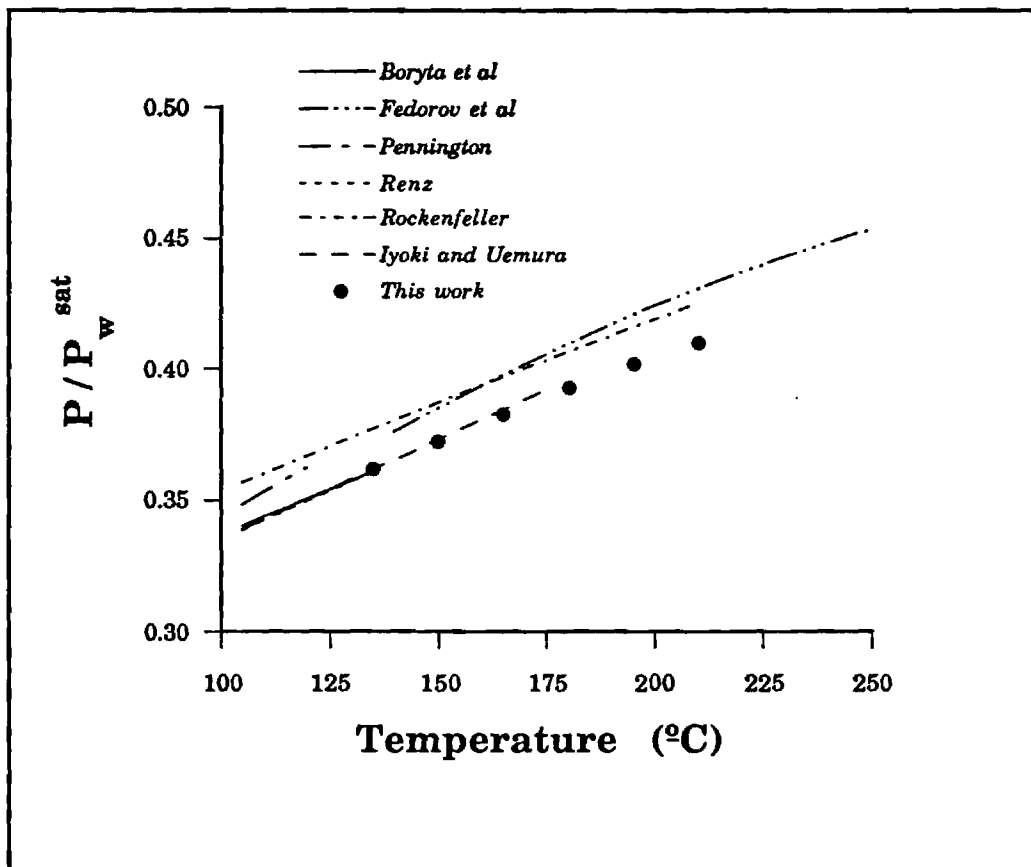


Fig 9b: Data Set Comparison

The comparison was made at a salt mass fraction of 0.4940.

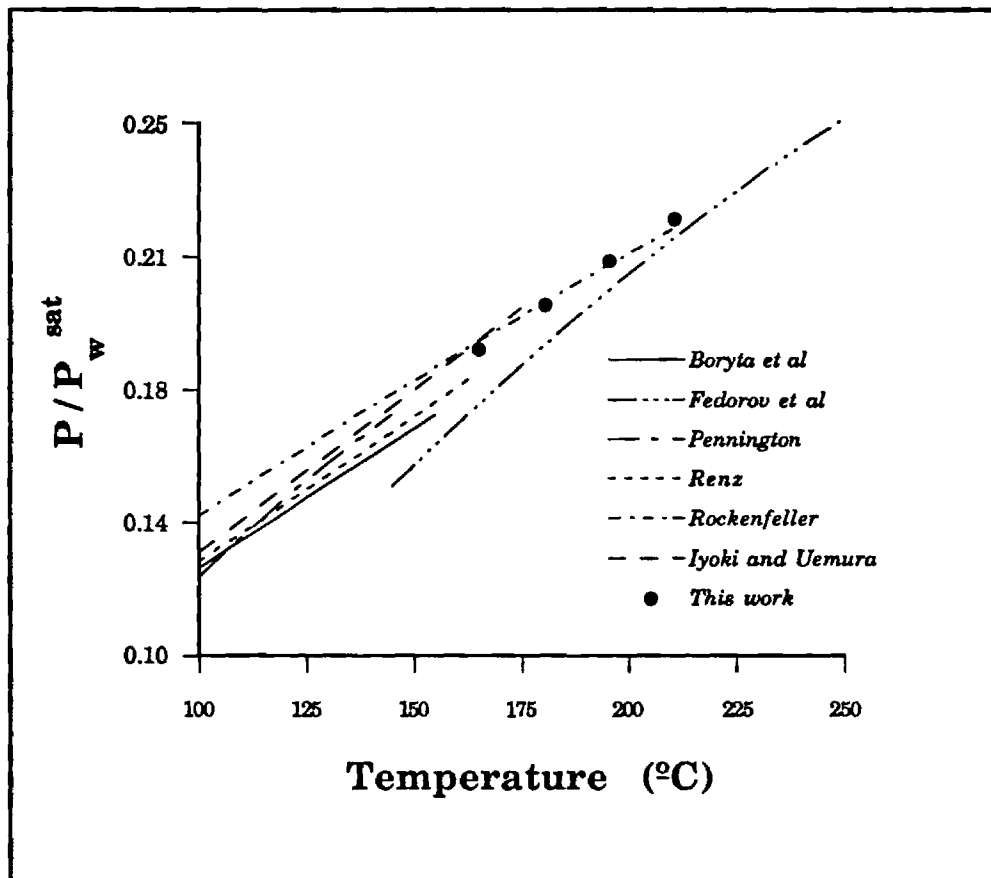


Fig 9d: Data Set Comparison

The comparison was made at a salt mass fraction of 0.6085.

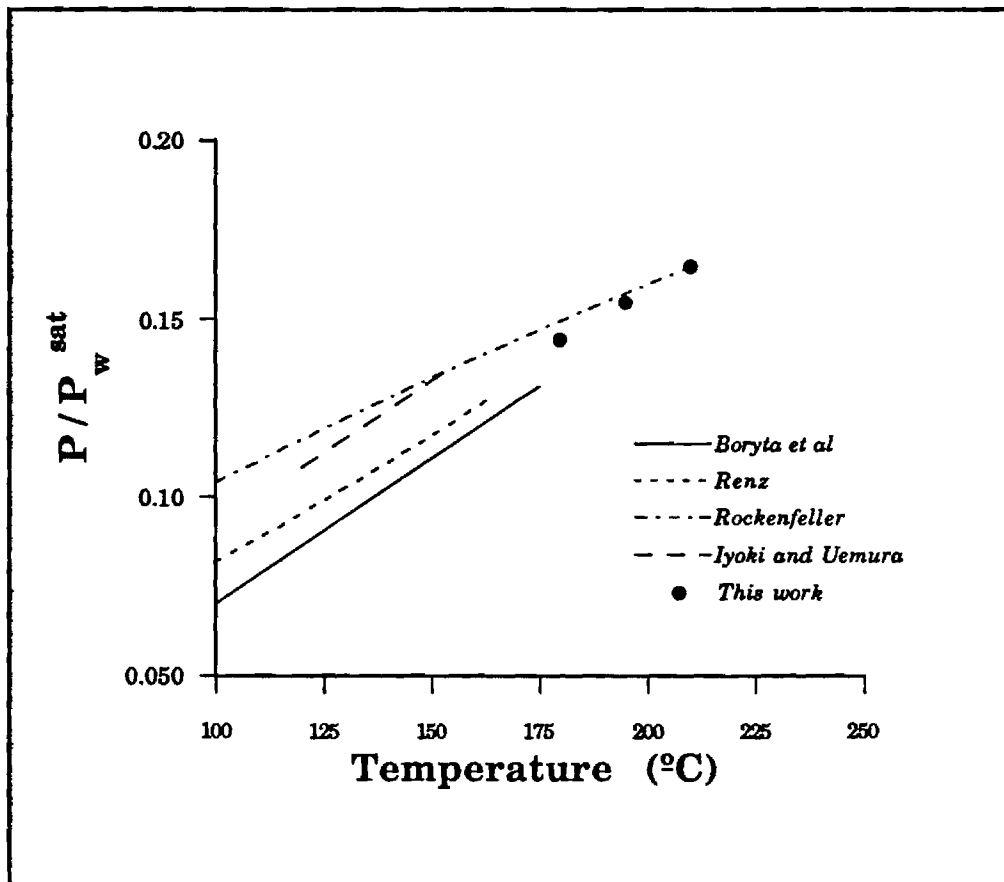


Fig 9e: Data Set Comparison.

The comparison was made at a salt mass fraction of 0.6515.

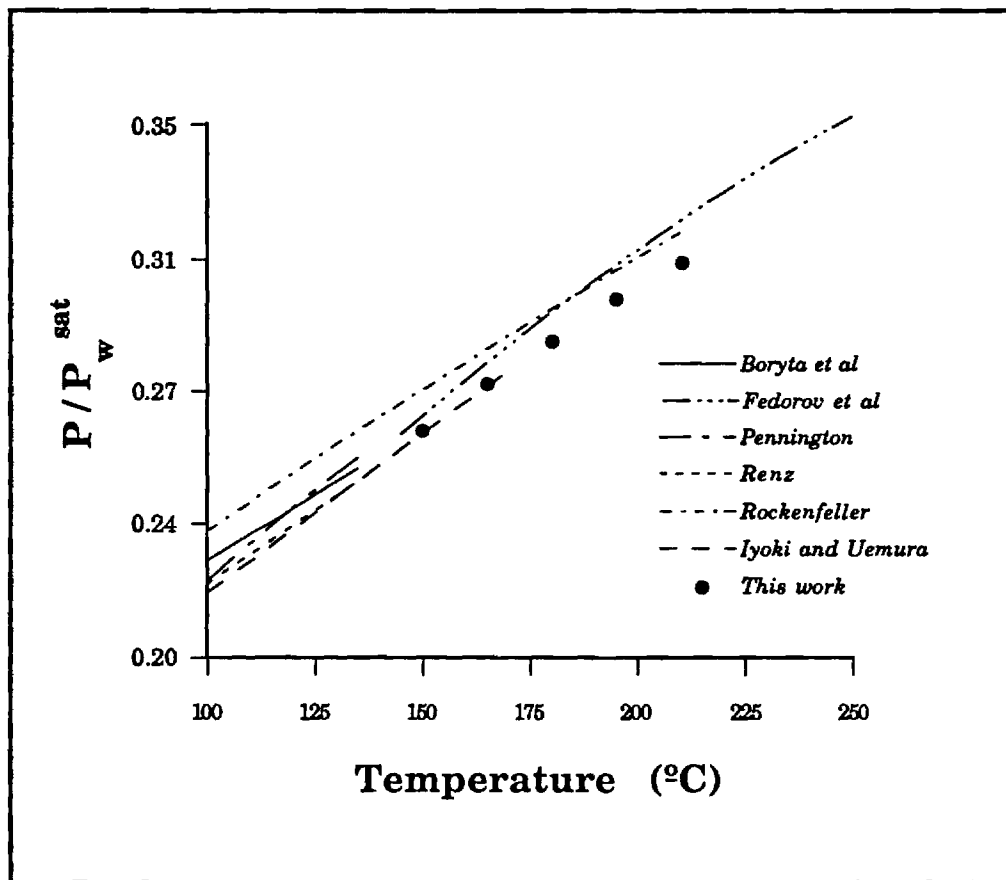


Fig 9c: Data Set Comparison

The comparison was made at a salt mass fraction of 0.5487.

Appendix I

ASHRAE Paper AT-90-30-4 (3380, RP-527): "Properties of Lithium Bromide - Water Solutions at High Temperatures and Concentrations - I. Thermal Conductivity", R. M. DiGuilio, R. J. Lee, S. M. Jeter, and A. S. Teja, ASHRAE Transactions 1990, Vol. 96, Part 1, 1990.

PROPERTIES OF LITHIUM BROMIDE-WATER SOLUTIONS AT HIGH TEMPERATURES AND CONCENTRATIONS—I. Thermal Conductivity

R.M. DiGullo

R.J. Lee, Ph.D.

S.M. Jeter, Ph.D., P.E.

A.S. Teja, Ph.D.

Associate Member ASHRAE

ABSTRACT

The thermal conductivity of lithium bromide-water solutions was measured over the temperature range 20° to 190°C using a modified hot wire technique. Solutions containing 30.2, 44.3, 49.1, 56.3, 60.0, 62.9, and 64.9 wt % lithium bromide were studied and comparisons were made with reported data on aqueous lithium bromide solutions at lower temperatures. The data were correlated as a function of temperature and weight percent lithium bromide with an average deviation of 0.6%. The accuracy of the measurements was estimated to be $\pm 2\%$. Subsequent papers in this series will report data on the density, viscosity, heat capacity, and vapor pressure of these mixtures.

INTRODUCTION

The design of refrigeration and heat pump systems that use aqueous lithium bromide (LiBr) solutions requires accurate thermal conductivity data. Most literature data, however, are limited to low temperatures and low concentrations of lithium bromide. The objectives of this work were, therefore, to measure the properties of lithium bromide solutions at high temperatures and concentrations.

An accepted and appropriate technique for the measurement of the thermal conductivity of liquids is the transient hot wire method (Nieto de Castro et al. 1986), in which a thin wire immersed in the liquid is electrically heated. The temperature rise of the wire is used to determine the thermal conductivity of the liquid. Electrically conducting solutions can be measured with this technique, if the wire is electrically insulated from the liquid under study. The insulation blocks the flow of current through the liquid, which would confuse the interpretation of the voltage measurements. However, the addition of an insulating layer to the wire has proved difficult to achieve in practice, especially at higher temperatures. Nagasaka and Nagashima (1981) successfully insulated a platinum wire with a polyester coating and reported measurements up to 150°C. Alloush et al. (1982) used a tantalum filament coated with a layer of tantalum oxide to obtain data on LiBr solutions at temperatures up to 80°C. Recently Kawamata

et al. (1988) used the tantalum-tantalum oxide filament to make measurements on LiBr solutions up to 100°C. However, they noted that the oxide coating failed to insulate the wire properly above 100°C. This limitation was confirmed by our own efforts to use the tantalum-tantalum oxide filament at temperatures above 100°C. This is shown in Figure 1, where the thermal conductivity of water measured with a tantalum wire is plotted as a function of temperature. Above 100°C, deviation from the ESDU (1967) recommended values occurs. The probable reasons for failure are the cracks that develop in the insulation due to the unequal expansion coefficients of the base metal and the oxide, and the decrease in dielectric strength with temperature of the oxide. Both effects might permit

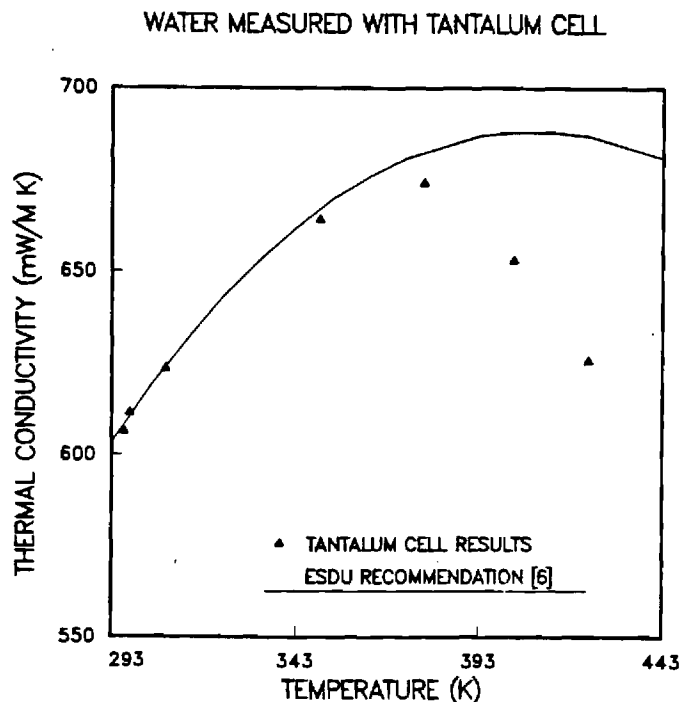


Figure 1 Thermal conductivity of water measured with a tantalum filament insulated with tantalum oxide. The oxide coating fails to insulate above 100°C.

R.M. DiGullo is a Graduate Research Assistant, R.J. Lee is a Research Engineer, and A.S. Teja is a Professor, all in the School of Chemical Engineering, and S.M. Jeter is an Associate Professor in the School of Mechanical Engineering, Georgia Institute of Technology, Atlanta.

THIS PREPRINT IS FOR DISCUSSION PURPOSES ONLY. FOR INCLUSION IN ASHRAE TRANSACTIONS 1990, V. 96, Pt. 1. Not to be reprinted in whole or in part without written permission of the American Society of Heating, Refrigerating and Air-Conditioning Engineers, Inc., 1791 Tullie Circle, NE, Atlanta, GA 30329. Opinions, findings, conclusions, or recommendations expressed in this paper are those of the author(s) and do not necessarily reflect the views of ASHRAE.

than 0.3 milliseconds. The program sampled the offset voltage on one channel, then switched channels to sample the applied voltage to ensure its constancy. The time between any two samples was 0.0084 s and that between two successive readings of the same channel was 0.0168 s. The delay between the closing of the relay and the first sampling was found to be 0.0132 s using an oscilloscope. Two hundred points were measured during each run and the experiment lasted about 3.4 s. From a previous calibration of the temperature vs. resistance, the temperature of the wire was found. A plot of ΔT vs. the logarithm of time was made and the slope in the time interval from 0.7 to 2.2 s was calculated using a least-squares fit, as described in the analysis section. The applied voltage was varied from about 2.5 to 3.5 V so that a more or less constant temperature rise in the quartz capillary surface of about 1.4°C was achieved. This resulted in offset voltages on the order of 5 mV. The A/D card has 16-bit resolution and the ± 25 mV range was used. Thus the card is capable of 0.8 μ V resolution.

SOURCE AND PURITY OF MATERIALS

Anhydrous lithium bromide with a minimum stated purity of 99 wt% LiBr was used in this work. Distilled water was used to prepare the solutions. Solutions were first prepared gravimetrically based on wt% LiBr. To ensure that no change in the composition of a solution occurred during the measurement procedure, samples of each composition were taken before and after the thermal conductivity measurement and checked using a computer-aided titrimeter. The precipitation titration was done using a 0.1 normal standard silver nitrate solution as the titrant. A silver-specific electrode was used to indicate the equivalence point, and a standard calomel electrode was used as the reference electrode. The compositions reported are the averages of a pair of titrations, one before and one after the thermal conductivity measurement. The average deviation between any pair of measurements was 0.4% and the maximum deviation was 0.8%. This agreement indicates that there was little variation in composition during the thermal conductivity measurement.

ANALYSIS

The model for the experiment is an infinite line source of heat submersed in an infinite fluid medium. By monitoring the temperature response of the wire to a step voltage input, the thermal conductivity of the fluid can be deduced. For an infinite line source of heat in an infinite fluid medium, the ideal temperature rise of the wire, ΔT_{id} , can be calculated using an expression derived by Carslaw and Jaeger (1959) and Healy et al. (1976) for $t \gg r_w^2/4\alpha$, where r_w is the radius of the filament and α is the thermal diffusivity of the fluid. The inequality is satisfied shortly after heating is started, that is, for 10 milliseconds $< t < 100$ milliseconds. The expression is:

$$\Delta T_{id} = \frac{q}{4\pi\lambda} \ln \left(\frac{4\lambda t}{r_w^2 \rho C_p C} \right) \quad (1)$$

where q is the heat dissipation per unit length, λ is the thermal conductivity, ρ is the density, C_p is the heat capacity, t is the time from the application of the step voltage, and C

is equal to $\exp(\gamma)$, where γ is Euler's constant. If it is assumed that all physical properties are independent of temperature over the small range of temperature considered (approximately 1.4°C), then,

$$\lambda = \frac{q}{4\pi \left(\frac{d\Delta T_{id}}{d \ln t} \right)} \quad (2)$$

where $d\Delta T_{id}/d \ln t$ is found experimentally from a plot of ΔT_{id} vs. $\ln t$.

Healy et al. (1976) also derived several corrections for the deviation of the model from reality. These may be written as:

$$\Delta T_{id} = \Delta T_w(t) + \sum_i \delta T_i \quad (3)$$

δT_1 accounts for the finite physical properties of the wire (liquid mercury) and is given by Healy et al. (1976):

$$\delta T_1 = \frac{r_w^2[(\rho C_p)_w - (\rho C_p)]}{2\lambda t} \Delta T_{id} - \frac{q}{4\pi\lambda} \frac{r_w^2}{4\alpha t} \left(2 - \frac{\alpha}{\alpha_w} \right) \quad (4)$$

where $(\rho C_p)_w$ is the volumetric heat capacity of the liquid mercury and α and α_w are the thermal diffusivity of the fluid and mercury, respectively.

The correction due to the finite extent of the fluid is given by Healy et al. (1976):

$$\delta T_2 = \frac{q}{4\pi\lambda} \left(\ln \frac{4\alpha t}{b^2 C} + \sum_{\nu=1}^{\infty} \exp^{-g_\nu^2 \alpha t/b^2} [\pi Y_0(g_\nu)]^2 \right) \quad (5)$$

where b is the inside diameter of the cell, Y_0 is the zero order Bessel function of the second kind, and g_ν are the roots of J_0 , the zero order Bessel function of the first kind. Although the first several roots are readily available, the higher roots can be found to sufficient accuracy using an expression from the work of Watson (1962):

$$g_\nu = (\pi\nu - \pi/4) + \frac{1}{8(\pi\nu - \pi/4)} - \frac{31}{385(\pi\nu - \pi/4)^3} + \frac{3779}{15366(\pi\nu - \pi/4)^5} \quad (6)$$

Values of Y_0 were calculated using the polynomial approximation given by Abramowitz and Stegun (1965).

The effect of the quartz capillary tube on the measurement has been evaluated analytically by Nagasaka and Nagashima (1981). The correction is given by:

(7)

with

$$\begin{aligned} A &= \frac{1}{t} (C_0 + B \ln t) \\ C_0 &= C_1 + C_2 + B \ln \left(\frac{4\alpha}{r_l^2 C} \right) \\ C_1 &= \frac{r_w^2}{8} \left[\left(\frac{\lambda - \lambda_l}{\lambda_w} \right) \left(\frac{1}{\alpha_w} - \frac{1}{\alpha_l} \right) + \frac{4}{\alpha_l} - \frac{2}{\alpha_w} \right] \\ C_2 &= \frac{r_l^2}{2} \left(\frac{1}{\alpha} - \frac{1}{\alpha_l} \right) + \frac{r_w^2}{\lambda_l} \left(\frac{\lambda_l}{\alpha_l} - \frac{\lambda_w}{\alpha_w} \right) \ln \left(\frac{r_l}{r_w} \right) \\ B &= \frac{r_w^2}{2\lambda} \left(\frac{\lambda_l}{\alpha_l} - \frac{\lambda_w}{\alpha_w} \right) + \frac{r_l^2}{2\lambda} \left(\frac{\lambda}{\alpha} - \frac{\lambda_w}{\alpha_w} \right) \end{aligned}$$

TEMPERATURE RISE VS LN(t)

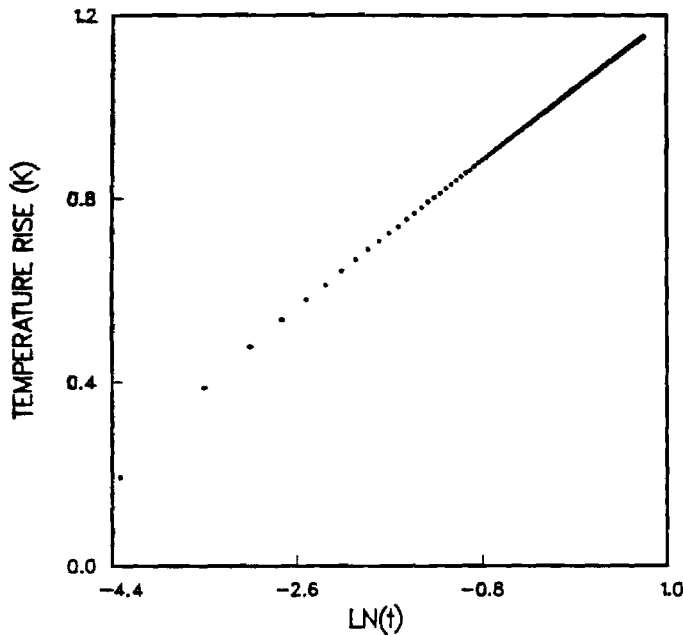


Figure 4 Plot of ΔT_M vs. $\ln t$ obtained from experiment. Only data from 0.7 s to 2.2 s (-.35 to .79) were used in the calculation of the slope.

thermal conductivity of the fluid and the adjusted temperature of the system. This series of calculations was repeated until no change in the thermal conductivity occurred. Three iterations were typically required for convergence.

RESULTS

Water was measured at room temperature to validate the liquid metal capillary technique. The agreement with the IUPAC data was excellent, with deviations between our measurements and IUPAC data being within 0.6%. However, the thermal conductivity of water at higher temperatures could not be measured because the low viscosity of water allowed convection to occur during the heating process. Fortunately, the viscosities of lithium bromide solutions were high enough to prevent the rapid onset of convection. In order to verify the linearity of the ΔT vs. $\ln t$ curves, the deviation from the linear fit was checked. Figure 5 shows a plot of the deviation from the fitted line for the same ΔT vs. $\ln t$ curve shown in Figure 4. The points are evenly scattered so that no bias is evident.

Seven compositions of lithium bromide-water solutions were measured (30.2, 44.3, 49.1, 56.3, 60.0, 62.9, and 64.9 wt% LiBr) in the temperature range from 20° to 190°C. The data are compiled in Table 1 and are shown graphically in Figure 5. Each data point represents the average of five experimental runs. The maximum deviation from the average value never exceeded 1.0%, and the precision of the data is therefore 1.0%.

The accuracy of the data was estimated from the sum of the bias error, ϵ_b , and the random error, ϵ_r . The bias error was estimated from:

$$\epsilon_b = \epsilon_{b,LT} + \frac{\partial \epsilon_b}{\partial T} \Delta T_M \quad (12)$$

LINEARITY OF TEMPERATURE VS LN(t) CURVE

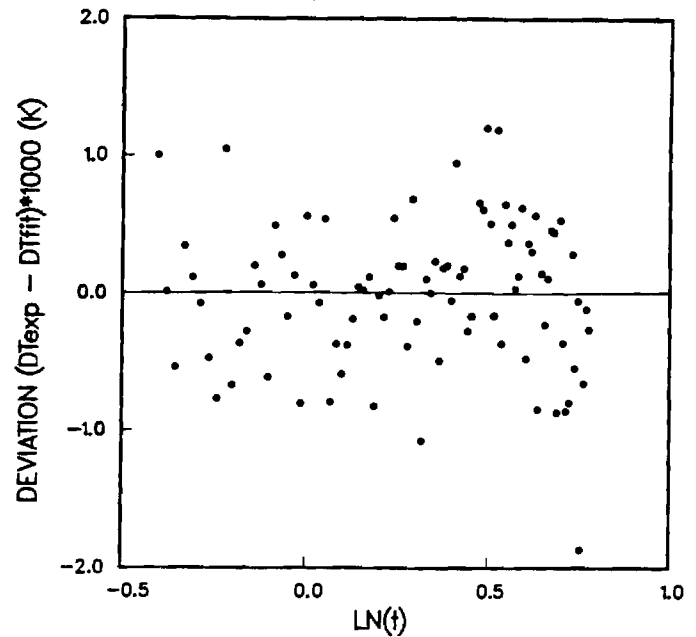


Figure 5 Plot of ΔT vs. $\ln t$ to verify function linearity

where $\epsilon_{b,LT}$ is the low-temperature bias and ΔT_M is the temperature difference between the highest temperature at which the thermal conductivity was measured and the reference temperature. The low-temperature bias was obtained by comparing our data on water with IUPAC data. Since our data were consistently about 0.6% high by comparison with the IUPAC data, we estimate the low-temperature bias error to be 0.6%. Comparison of our data with literature data for temperatures up to 100°C (see Table 2) showed no apparent trends in the bias error with temperature. Thus, we concluded that $\partial \epsilon_b / \partial T$ is approximately 0 and the bias is 0.6% at all temperatures. Random error was estimated from three sources: the uncertainty in the thermal conductivity measurement, the uncertainty in the reported concentration, and the uncertainty in the equilibrium temperature of the fluid, with

$$\epsilon_r^2 = \epsilon_m^2 + \left(\frac{\partial \lambda}{\partial W} \frac{\delta W}{\lambda} \right)^2 + \left(\frac{\partial \lambda}{\partial T} \frac{\delta T}{\lambda} \right)^2 \quad (13)$$

The uncertainty in the measurement, ϵ_m , was 1%. The sensitivity of the thermal conductivity to temperature and concentration was found using the correlation for thermal conductivity reported in the next section of this paper. The maximum value of $\partial \lambda / \partial W$ $1/\lambda$ was found to be -0.011 wt%⁻¹ and the maximum uncertainty in the composition was ± 0.8 wt%. The maximum value of $\partial \lambda / \partial T$ $1/\lambda$ was found to be 0.003 K⁻¹ and the maximum uncertainty in the temperature measurement was ± 0.2 K. The total random error was thus less than 1.4% and the total error was $\pm 2\%$.

Direct comparison of our data with literature data is difficult due to differences in concentrations. Table 2 is a comparison of the correlation found using only our data with the data of Kawamata et al. (1988), Alloush et al. (1982),

Nieto de Castro, C.A.; Li, S.F.Y.; Maitland, C.; and Wakeham, W.A. 1983. "Thermal conductivity of toluene in the temperature range 35-90°C at pressures up to 600 MPa." *Int. J. Thermophys.*, Vol. 4, p. 311.

Nieto de Castro, C.A.; Li, S.F.Y.; Nagashima, A.; Trengrove, R.D.; and Wakeham, W.A. 1986. "Standard reference data for the thermal conductivity of liquids." *J. Phys. Chem. Ref. Data*, Vol. 15, p. 1073.

Omotani, T.; Nagaska, Y.; and Nagashima, A. 1982. "Measurement of the thermal conductivity of KNO₃-NaNO₃ mixtures using a transient hot-wire method with a liquid metal in a capillary probe." *Int. J. Thermophys.*, Vol. 3, p. 17.

Riedel, L. 1951. "The heat conductivity of aqueous solutions of strong electrolytes." *Chem. Ingr. Tech.*, Vol. 23, p. 59.

Touloukian, Y.S., and Ho, C.Y., eds. 1972a. *Thermal conductivity of nonmetallic solids, vol. 2. The Thermophysical Properties Research Center Data Series*. New York: Plenum Press.

Touloukian, Y.S., and Ho, C.Y., eds. 1972b. *Specific heat of nonmetallic solids, vol. 5. The Thermophysical Properties Research Center Data Series*. New York: Plenum Press.

Tufeu, R.; Petitet, J.P.; Denielou, L.; and Le Neindre, B. 1985. "Experimental determination of the thermal conductivity of molten pure salts and salt mixtures." *Int. J. Thermophys.*, Vol. 6, p. 315.

Uemura, T., and Hasaba, S. 1965. "Studies on the lithium bromide-water absorptions refrigerating machine." *Refrig. Japan*, Vol. 40, p. 31.

Watson, G.N. 1962. *A treatise on the theory of Bessel functions*, 2d ed. Cambridge: Cambridge University Press.

Weast, R.C., ed. 1988. *CRC handbook of chemistry and physics*, 69th ed. Boca Raton, FL: CRC Press, Inc.

Williams, E.J. 1925. "The electrical conductivity of some dilute liquid amalgams." *Phil. Mag.*, Vol. 50, p. 589.

TABLE 1
Thermal Conductivity of LiBr-Water Solutions

Wt% LiBr	T [K]	λ [mW/(m·K)]	Wt% LiBr	T [K]	λ [mW/(m·K)]			
0.0	293.8	602.3	49.1	401.2	513.5			
	296.7	607.6		430.0	522.0			
	323.4	646.0		460.0	523.0			
	292.9	508.1		56.3	294.1	419.0		
	296.9	512.1			329.4	453.5		
	326.1	544.6			362.3	468.4		
	329.1	545.9			397.6	484.2		
	359.5	570.7			430.1	493.5		
	365.0	579.5			461.1	501.6		
	385.2	592.0			60.0	299.6	408.8	
388.9	592.8	329.2	432.9					
404.7	597.5	369.7	457.5					
434.0	591.1	402.5	473.4					
435.7	590.2	430.8	476.5					
461.3	573.8	460.6	485.8					
44.3	295.1	467.5	62.9	339.8		429.5		
	321.4	495.4		371.0		447.2		
	353.5	521.4		400.4		457.3		
	378.6	535.5		430.7		465.4		
	407.2	550.9		460.9	476.1			
	439.2	557.3		64.9	343.4	421.0		
	463.3	553.4			370.5	432.1		
	49.1	298.0			446.7	400.7	442.0	
		328.9			478.1		428.8	453.0
		371.6			503.9		461.0	458.2

TABLE 2
Comparison of This Work with the Literature [P = 1 atm]

T [K]	Wt% LiBr	λ [mW/(m·K)] Literature	Ref.	λ [mW/(m·K)] This Work ¹	Claimed Accuracy [± %]	% Dev.	
297.0	49.7	457	[2]	448.0	3.0	-2.01	
305.0		463	[2]	455.8	3.0	-1.57	
315.0		464	[2]	465.0	3.0	0.22	
335.0		478	[2]	481.6	3.0	0.75	
357.0		493	[2]	497.0	3.0	0.80	
297.0		53.8	452	[2]	432.9	3.0	-4.40
305.0			457	[2]	440.2	3.0	-3.82
315.0			461	[2]	448.7	3.0	-2.74
335.0			474	[2]	464.2	3.0	-2.11
313			54.25	444	[18]	445.2	0.28
302.8	428.6			[10]	427.3	0.5	-0.31
313.6	438.0			[10]	436.1	0.5	-0.43
333.5	452.4			[10]	451.0	0.5	-0.32
353.7	464.0			[10]	464.1	0.5	0.01
373.5	473.7			[10]	475.0	0.5	0.27
353	56.61	463		[18]	463.6	0.13	
323		442		[18]	443.3	0.30	
293		416		[18]	418.4	0.57	
303		429		[18]	427.0	-0.46	
333		451	[18]	450.0	-0.23		
313		60.35	418	[18]	420.0	0.47	

TABLE 2
Comparison of This Work with the Literature (Continued)

T [K]	Wt% LiBr	λ [mW/(m·K)] Literature	Ref.	λ [mW/(m·K)] This Work ¹	Claimed Accuracy [± %]	% Dev.	
293.8	0.0	599.1	[11]	602.3 ²		0.55	
296.7		604.1	[11]	607.6 ²		0.58	
323.4		642.6	[11]	646.0 ²		0.52	
323		26.04	557	[18]	558.0		0.18
313		26.05	551	[18]	545.5		-1.01
353		26.08	581	[18]	586.7		0.97
303		26.28	426	[18]	530.9		0.82
333		26.52	564	[18]	567.4		0.60
304.2		30.3	527.7	[10]	520.7	0.5	-1.35
313.9			536.0	[10]	533.2	0.5	-0.53
333.9	558.6		[10]	555.3	0.5	-0.60	
353.5	575.1		[10]	572.1	0.5	-0.53	
373.5	588.5		[10]	584.2	0.5	-0.73	
313	34.93		521	[18]	516.8		-0.81
303	35.61		503	[18]	502.6		-0.09
323	35.90		521	[18]	524.4		0.65
293	36.21		492	[18]	487.8		-0.87
333	36.29		533	[18]	532.8		-0.04
343	36.50	547	[18]	540.8		-1.15	
353	36.53	538	[18]	548.4		1.89	
293	41.4	471	[14]	476.2		1.08	
297.0		473	[2]	476.5	3.0	0.74	
305.0		478	[2]	485.7	3.0	1.58	
315.0		484	[2]	496.3	3.0	2.49	
335.0		500	[2]	515.1	3.0	2.94	
357.0		511	[2]	531.9	3.0	3.93	
303		44.84	465	[18]	471.5		1.37
333		44.94	501	[18]	499.5		-0.30
323		44.98	489	[18]	490.6		0.33
313		44.99	486	[18]	481.1		-1.01
353	45.42	509	[18]	512.6		0.71	
297.0	45.6	465	[2]	462.4	3.0	-0.56	
305.0		467	[2]	470.9	3.0	0.82	
315.0		469	[2]	480.8	3.0	2.45	
335.0		483	[2]	498.5	3.0	3.10	
357.0		499	[2]	514.6	3.0	3.02	
293		46.05	459	[18]	456.5		-0.55
302.4		46.5	468.2	[10]	464.9	0.5	-0.70
313.8			477.3	[10]	476.2	0.5	-0.22
333.3			490.8	[10]	493.4	0.5	0.54
353.6			501.4	[10]	508.5	0.5	1.40
373.2	510.9		[10]	520.3	0.5	1.81	

¹Values calculated from correlation of our data.

²Experimental value (pure water not included in correlation).

TABLE 3
Constants for Correlation

Constant	Value
a ₁	-1407.53
a ₂	11.0513
a ₃	-1.46741 × 10 ⁻²
b ₁	38.9855
b ₂	-0.240475
b ₃	3.48073 × 10 ⁻⁴
c ₁	-0.265025
c ₂	1.51915 × 10 ⁻³
c ₃	-2.32262 × 10 ⁻⁶

Appendix II

ASHRAE Paper AT-90-30-5 (3381, RP-527): "Properties of Lithium Bromide - Water Solutions at High Temperatures and Concentrations - II. Density and Viscosity", R. J. Lee, R. M. DiGuilio, S. M. Jeter, and A. S. Teja, **ASHRAE Transactions 1990**, Vol. 96, Part 1, 1990.

PROPERTIES OF LITHIUM BROMIDE-WATER SOLUTIONS AT HIGH TEMPERATURES AND CONCENTRATIONS—

II: Density and Viscosity

R.J. Lee, Ph.D.

R.M. DiGullio

S.M. Jeter, Ph.D., P.E.

A.S. Teja, Ph.D.

Associate Member ASHRAE

ABSTRACT

The densities and viscosities of lithium bromide-water solutions were measured at temperatures from 25°C to 200°C and concentrations from 45 wt% to 65 wt% lithium bromide. The data generally agreed with the data available in the literature at low temperatures in the case of density, but the agreement was only fair in the case of viscosity. Correlations of the experimental data are also reported in this paper.

INTRODUCTION

Improvements to the performance of absorption refrigeration equipment require a knowledge of the thermophysical properties of aqueous lithium bromide solutions. The literature data on density and viscosity of such solutions are limited to temperatures up to 100°C only (Uemura and Hasaba 1964; Bogatykh and Evnovich 1963, 1965). In a companion paper, Part I of this work, we reported our measurements of the thermal conductivity of these solutions at high temperatures and concentrations. Subsequent papers will cover the specific heats and vapor pressures. In this paper, we present our measurements of the density and viscosity. The densities and viscosities of solutions with weight percent (wt%) of lithium bromide ranging from 45 wt% to 65 wt% and at temperatures up to 200°C were measured. Correlations of the experimental data are also presented.

EXPERIMENT

Density Measurement

Principle of Operation The principle used to determine the liquid density (ρ) of a fluid in this study is based on the definition:

$$\rho = M/V \quad (1)$$

where M is the mass and V the volume of the fluid. Experimentally, we measured the mass of the fluid required to

fill a calibrated volume (density cell) in a high-pressure pycnometer.

Apparatus and Procedure The high-pressure pycnometer used in this study is shown schematically in Figure 1. The pycnometer is rated up to 300°C and 100 bar and consists of four sampling cylinders capped at one end by a high-pressure fitting. The other end of each cylinder was attached through a pipe nipple, an isolation valve, and a quick-connect coupling to a high-pressure hand pump. The pump was used to maintain pressure in the system in order to suppress boiling. Each stainless steel sampling cylinder, as modified with a thermowell for temperature measurement, had an internal volume of approximately 40 mL. The exact volume of each cell assembly was obtained by calibration with triple-distilled mercury at temperatures up to 150°C. The data were fitted to an appropriate function (either linear or quadratic) for interpolation or extrapolation. Temperature control within $\pm 0.05^\circ\text{C}$ was achieved by a constant-temperature circulating bath filled with silicon oil.

At the beginning of an experiment, the four density cells were cleaned thoroughly, weighed, and then connected to the system. The density cell assembly was then evacuated, filled with the test liquid, and placed in the oil bath. Usually, two hours were allowed for temperature equilibrium to be attained. Once equilibrium had been established, the isolation valves were closed and the pycnometers removed from the oil bath and weighed on an electronic balance.

The solution temperature was measured using a type-K thermocouple that had previously been calibrated against a platinum resistance thermometer. The accuracy of the temperature measurement was estimated to be $\pm 0.1^\circ\text{C}$. The system pressure was monitored by a precision pressure gauge rated at 1500 psi with an accuracy of $\pm 0.25\%$ of full scale. The electronic balance used for weight measurement has a precision of ± 0.001 g.

R.J. Lee is Research Engineer, R.M. DiGullio is Graduate Research Assistant, and A.S. Teja is Professor in the School of Chemical Engineering; S.M. Jeter is Associate Professor in the School of Mechanical Engineering, Georgia Institute of Technology, Atlanta, GA.

THIS PREPRINT IS FOR DISCUSSION PURPOSES ONLY, FOR INCLUSION IN ASHRAE TRANSACTIONS 1990, V. 96, Pt. 1. Not to be reprinted in whole or in part without written permission of the American Society of Heating, Refrigerating and Air-Conditioning Engineers, Inc., 1791 Tullie Circle, NE, Atlanta, GA 30329. Opinions, findings, conclusions, or recommendations expressed in this paper are those of the author(s) and do not necessarily reflect the views of ASHRAE.

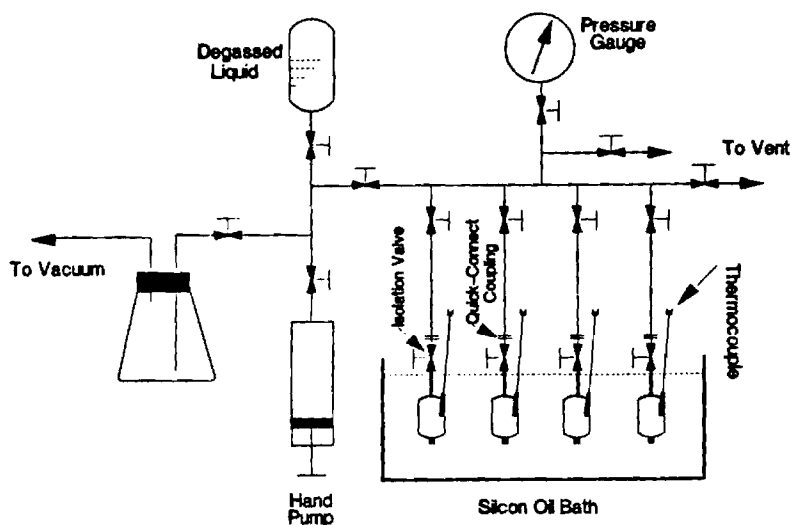


Figure 1 Schematic diagram of the high-pressure pycnometer

Reference Experiment In order to test the apparatus and procedure, the densities of 4 N-methylpyrrolidinone at atmospheric pressure were measured and compared with data in the literature. As illustrated in Figure 2, our measurements are in good agreement with those reported recently by Kneisl and Zondlo (1987).

Viscosity Measurement

Principle of Operation The equation used to represent the absolute viscosity, μ , of a fluid flowing through a capillary is based on Poiseuille's law (1840),

$$\mu = \frac{\pi r^4 g h}{8 L V} \rho t - \frac{\xi V}{8 \pi L} \frac{\rho}{t} \quad (2)$$

where r is the radius of the capillary, g is the gravitational constant, h is the average head of the fluid, L is the length

of the capillary, V is the efflux volume of the fluid, t is the efflux time, and ξ is the kinetic energy coefficient. For a specific capillary viscometer, the kinematic viscosity, ν , can be related to the efflux time using:

$$\nu = \mu/\rho = C_1 t - C_2 t^2 \quad (3)$$

where C_1 is the viscometric constant, which is determined by calibration with a fluid of known viscosity. The second term on the right-hand side represents the correction due to the kinetic energy and is usually neglected if an appropriately sized viscometer is used.

Apparatus and Procedure A high-pressure viscometer was designed and constructed for viscosity measurement of highly corrosive solutions. The design of the apparatus is similar to that proposed by Al-Harbi (1982). Figure 3 shows the schematic diagram of this apparatus, which consists of a capillary viscometer, a pressure cell, a thermostated air bath, and a pressure distribution section.

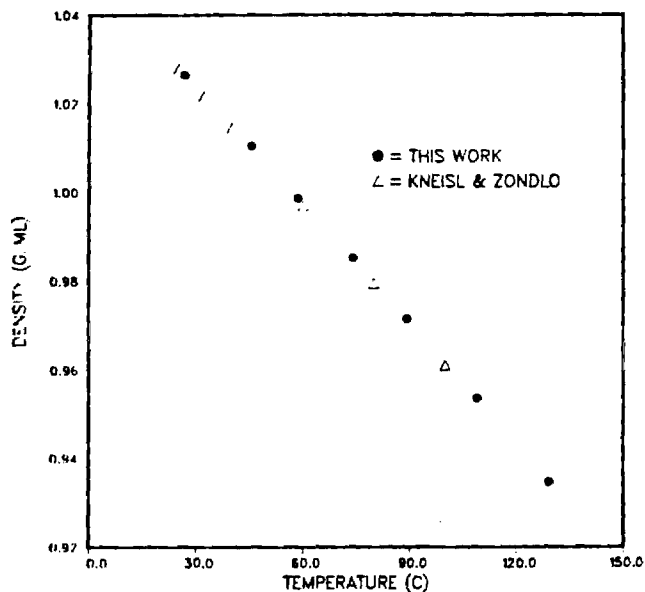


Figure 2 Density of liquid N-methylpyrrolidinone

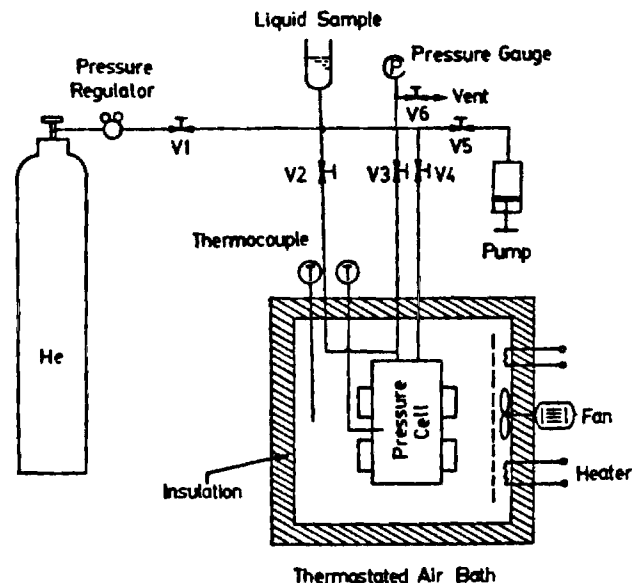


Figure 3 Schematic diagram of the high-pressure viscometer

This apparatus was designed for temperatures up to 200°C and pressures up to 30 atm.

A Size 1 Zeitfuchs (1946) cross-arm capillary viscometer was used for determination of the kinematic viscosity. The calibration factor was determined at room temperature using pure water. In order to repeat a measurement without reloading the liquid sample, the viscometer was calibrated with a wetted capillary. After calibration, the viscometer was placed inside the pressure cell and the capillary end was connected to the pressure distribution section through V5. The reservoir end was opened to the cell chamber such that the pressure over the viscometer could be balanced. The cell was equipped with four glass view ports (tempered borosilicate glass) to allow visual observation of the reservoir and the measuring bulb of the viscometer. An insulated air bath, heated by a primary (800 W) and a secondary (200 W) heater, was used to establish the desired temperature. A stable temperature in the air bath was maintained by a commercial temperature control unit and a circulating fan. Temperature fluctuations were minimized by the mass of the pressure cell, which was made of heavy steel. The test fluid was moved back and forth through the capillary tube by a high-pressure hand pump with helium as the pressurizing fluid.

The temperature was measured inside the cell by a chromel-alumel thermocouple, calibrated with an NBS-calibrated platinum resistance thermometer. The accuracy of the temperature measurement was estimated to be $\pm 0.1^\circ\text{C}$. Pressure measurement was accomplished by a precision gauge with an accuracy of 0.25% of full scale (0 to 1500 psi). An electronic timer accurate to 1/100 second was used to obtain the efflux time.

Before an experiment was performed, a clean, dry viscometer loaded with the appropriate test solution was attached to the top flange of the pressure cell. The top flange was then bolted into place, and the cell was connected to the pressure distribution section and pressurized slowly to the desired pressure. To eliminate loss of vapor from the solution, about 40 mL of slightly dilute lithium

bromide solution was placed at the bottom of the cell chamber so that the solution in the viscometer was always under its vapor pressure.

At the beginning of an experiment, all valves were closed except for V4 and V5. The pressure on the capillary end was reduced by the use of the hand pump, causing the solution to flow into the reverse bend of the capillary. Once the flow had been initiated, valve V3 was opened to balance the pressures over both ends of the viscometer. The efflux time for the solution to flow between the timing marks on the measuring bulb was then measured. At the end of the measurement, valve V3 was closed and the solution was then forced to return to the reservoir by increasing the pressure on the capillary end with the hand pump. Measurements were repeated until consistent efflux times were obtained.

Reference Experiment To test the apparatus and procedures, the kinematic viscosity of pure water was measured and compared with values reported by the National Institute of Standards and Technology (see CRC 1982). As illustrated in Figure 4, good agreement was obtained between the two sets of measurements. The density of water reported by Gildseth et al. (1972) was used to convert the measured kinematic viscosity to the absolute viscosity shown in this graph.

MATERIAL AND SOLUTION PREPARATION

N-methylpyrrolidinone (99.5% purity), mercury (99.999+% purity), and HPLC-grade water were purchased from three manufacturers. Anhydrous lithium bromide was provided and had a certified purity of 99.3% by weight. These chemicals were used without further purification. Aqueous lithium bromide solutions were prepared by adding degassed water to fresh anhydrous lithium bromide. The solutions were degassed by an alternating freeze-thaw procedure. About 0.2% of impurities by weight (excluding water) were ignored in calculating the concentrations of the prepared solutions. The concentrations were determined gravimetrically and checked on a computer-aided titrator. Solution concentrations determined by these two methods agreed within ± 0.1 wt% lithium bromide.

RESULTS AND DISCUSSION

Density

Table 1 summarizes the measured densities of four lithium bromide-water solutions containing 45.1, 49.9, 55.0, and 59.9 wt% of lithium bromide, respectively. Since high-concentration solutions are supersaturated at room temperature, the 65 wt% solution could not be measured with this apparatus because the solution would crystallize in unheated sections of the apparatus (such as the pressure gauge or exposed tubing). Measurements on the remaining solutions were performed at temperatures from ambient to 200°C. The system pressure was maintained at 150 psig throughout the experiments. At least three samples were taken at each condition to give the average reported in Table 1. The reproducibility of the results was $\pm 0.1\%$ and the accuracy of the data was estimated to be 0.25%.

The densities of aqueous lithium bromide solutions at lower temperatures have been reported by Uemura and Hasaba (1964) and Bogatykh and Evnovich (1965). Figure

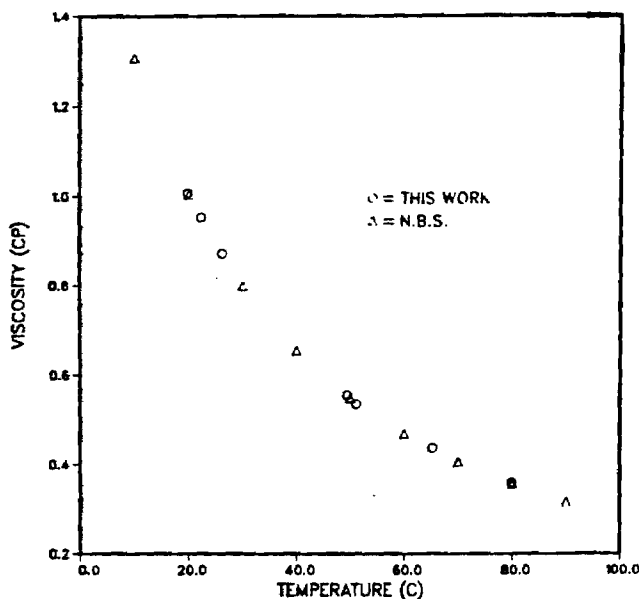


Figure 4 Viscosity of liquid water

TABLE 1
Experimental Densities of Aqueous Lithium Bromide Solutions

Wt% LiBr	T [K]	ρ [gm/mL]	Wt% LiBr	T [K]	ρ [gm/mL]
45.1	301.6	1.4554	49.9	298.7	1.5328
	319.1	1.4470		318.5	1.5206
	333.2	1.4389		333.2	1.5128
	348.1	1.4323		348.0	1.5042
	361.6	1.4255		363.1	1.4954
	381.3	1.4144		382.7	1.4833
	402.4	1.4041		402.8	1.4705
	423.5	1.3919		423.7	1.4568
	448.4	1.3782		448.6	1.4397
				474.8	1.4216
55.0	298.2	1.6205	59.9	298.5	1.7217
	318.2	1.6089		318.2	1.7087
	332.6	1.5997		333.7	1.6986
	346.9	1.5912		348.1	1.6884
	361.5	1.5816		363.6	1.6779
	382.1	1.5703		383.6	1.6642
	401.6	1.5584		403.0	1.6512
	421.6	1.5453		423.4	1.6365
	447.4	1.5287		447.9	1.6192
	473.1	1.5110		473.2	1.6008

5 shows that our data are in good agreement with those of the earlier workers. The average absolute deviation between our data and the data of Uemura and Hasaba was found to be 0.3%, while that between our data and the data of Bogatykh and Evnovich was 0.2%. Note that the data from these two references are at concentrations of 45.0, 50.0, 55.0, and 60.0 wt% LiBr, which differ only slightly from the experimental concentrations in this investigation (45.1, 49.9, 55.0, and 59.9 wt%).

Comparison of our data with the graphical data in the 1989 ASHRAE Fundamentals (ASHRAE 1989) was also made. Only low-temperature data for the density are available in the handbook. At 25°C the graphical handbook data and data from this experiment agree within $\pm 0.1\%$,

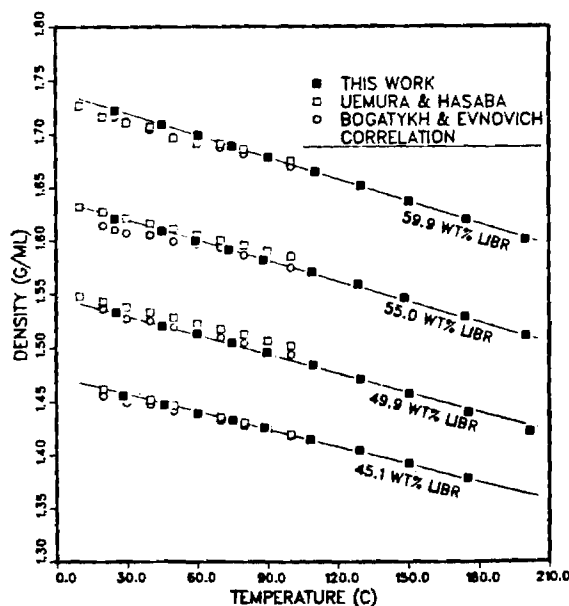


Figure 5 Density of aqueous LiBr solutions

while the agreement at 40°C ranges from the current data being +0.6% high to -0.2% low for concentrations of 45 wt% and 60 wt%, respectively. While this agreement is fairly good, the handbook data are only presented for two low temperatures and cannot reasonably be extrapolated to high temperatures where the correlation of Equation 8 (reported in the next section) should be used.

Viscosity

The experimental kinematic viscosities of aqueous lithium bromide solutions of 45.0, 50.0, 55.0, 59.9, 63.0, and 65.0 wt% lithium bromide are presented in Table 2. The temperature range of the measurements varied from 40°C to 200°C, and the pressure was maintained at 200 psig throughout the experiments. Absolute viscosity data, in which the liquid densities were obtained from the correlation described in the next section of this paper, are also included in Table 2. The average of at least four samples was taken to obtain each value reported in this table. The viscosities were reproducible within $\pm 1.0\%$. The accuracy of the data was estimated to be 2%. A graphical presentation of the experimental results is given in Figure 6.

Comparison of our data with data available in the literature was attempted, although the system pressures were different. Two sets of experimental data studied at atmospheric pressure by Uemura and Hasaba (1964) and by Bogatykh and Evnovich (1963) were selected. Figure 7 illustrates a comparison of 50.0 wt% and 59.9 wt% LiBr solutions. The literature data shown in this figure were for 50.0 wt% and 60.0 wt% LiBr, respectively. The agreement between the literature data is poor, with the experimental data of Bogatykh and Evnovich being consistently lower than the data of Uemura and Hasaba. The literature data bracket our data at lower temperatures, while our data are

TABLE 2
Experimental Viscosities of Aqueous Lithium Bromide Solutions

Wt% LiBr	T [K]	ν [cst]	μ [cp]	Wt% LiBr	T [K]	ν [cst]	μ [cp]
45.0	312.9	1.325	1.919	50.0	314.9	1.605	2.446
	333.0	0.947	1.363		333.2	1.204	1.822
	353.2	0.738	1.054		353.7	0.932	1.400
	373.9	0.602	0.854		373.2	0.759	1.131
	393.2	0.515	0.725		393.3	0.637	0.942
	413.2	0.453	0.632		412.3	0.554	0.813
	433.0	0.407	0.564		432.6	0.490	0.712
	453.2	0.376	0.516		453.2	0.451	0.650
	472.5	0.353	0.480		472.6	0.413	0.589
	55.0	314.2	2.120		3.418	59.9	316.0
333.6		1.547	2.476	333.5	2.122		3.603
353.1		1.193	1.895	353.6	1.577		2.657
373.1		0.954	1.503	372.9	1.236		2.066
393.5		0.786	1.228	394.3	0.986		1.634
412.7		0.669	1.037	412.7	0.834		1.372
433.0		0.586	0.900	433.0	0.714		1.164
453.2		0.523	0.796	453.2	0.630		1.018
472.3		0.477	0.720	472.9	0.553		0.886
63.0		333.1	2.826	4.964	65.0		333.4
	353.2	2.030	3.537	352.4		2.331	4.158
	373.6	1.542	2.665	372.3		1.749	3.095
	393.8	1.219	2.090	393.6		1.352	2.372
	413.2	1.011	1.720	413.2		1.106	1.925
	432.9	0.867	1.463	433.4		0.946	1.633
	452.9	0.744	1.245	452.6		0.820	1.405
	472.8	0.662	1.099	472.7		0.730	1.240

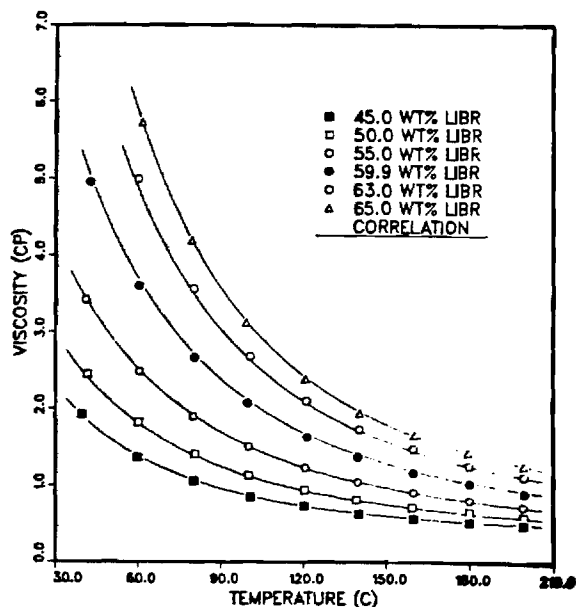


Figure 6 Viscosity of aqueous LiBr solutions

higher at the higher temperatures. It is also apparent that our data are smoother than the literature data.

Our data for viscosity agree fairly well with the graphical data in the 1989 ASHRAE *Fundamentals* (ASHRAE 1989). The handbook data are about 4% higher at 160°F (71.1°C) and 5% to 10% higher at 220°F (104.4°C) for concentrations of 45 wt% to 65 wt%. Because of the strong temperature dependence of viscosity on temperature, however, extrapolation of the handbook curves to higher temperatures is not recommended. Rather, the correlation of Equation 9, shown below, should be used.

CORRELATION

Density

Our results were fitted to the following polynomial function in temperature:

$$\rho = A_0 + A_1 T + A_2 T^2 \quad (4)$$

where ρ is in gm/mL and T is in K. The values of A_0 , A_1 , and A_2 were determined by minimizing the sum of squares of the relative deviations: $\sum_i [(\rho_{\text{expl},i} - \rho_{\text{cal},i})/\rho_{\text{expl},i}]^2$. The constants A_0 , A_1 , and A_2 were further interpolated in terms of wt% of lithium bromide (X) as follows:

$$A_0 = (10976.3 + 0.71244X + 2.21446X^2) \cdot 10^{-4} \quad (5)$$

$$A_1 = (6796.2 - 148.247X - 0.89696X^2) \cdot 10^{-7} \quad (6)$$

$$A_2 = (-350.97 - 324.312X + 4.97020X^2) \cdot 10^{-10} \quad (7)$$

All data could be correlated with the above equation with an overall average absolute deviation (AAD) of 0.06% and maximum absolute deviation (MAD) of 0.19%. Figure 5 shows the comparison between the values calculated by Equation 4 and the observed values.

It should be noted that the above correlation is based only on lithium bromide concentrations between 45 wt%

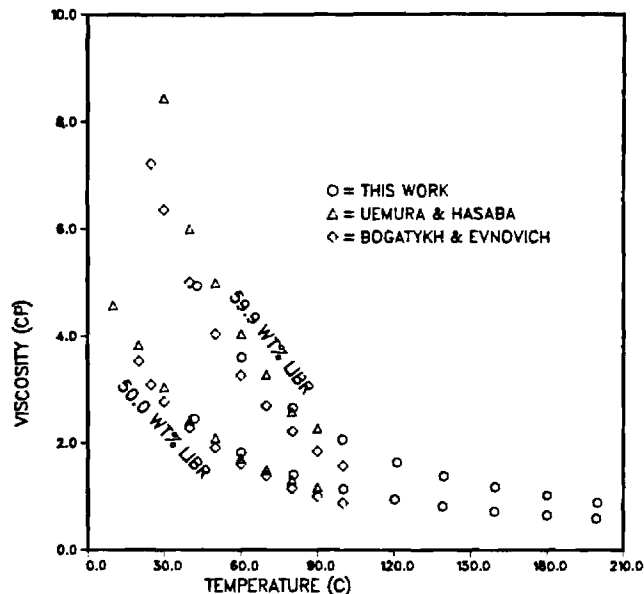


Figure 7 Comparison of the viscosity of LiBr-water solutions obtained by different investigators

and 60 wt% measured in this investigation. Extrapolation to other concentrations is not recommended. To cover a wider range of X , we included the data available in the literature at lower temperatures in the following simpler equation:

$$\rho = \frac{1145.36 + 4.7084X + 0.137479X^2}{1000} - \frac{33.3393 + 0.571749X}{100000} T \quad (8)$$

Figure 8 illustrates good agreement between the calculated values and experimental data of this work and of

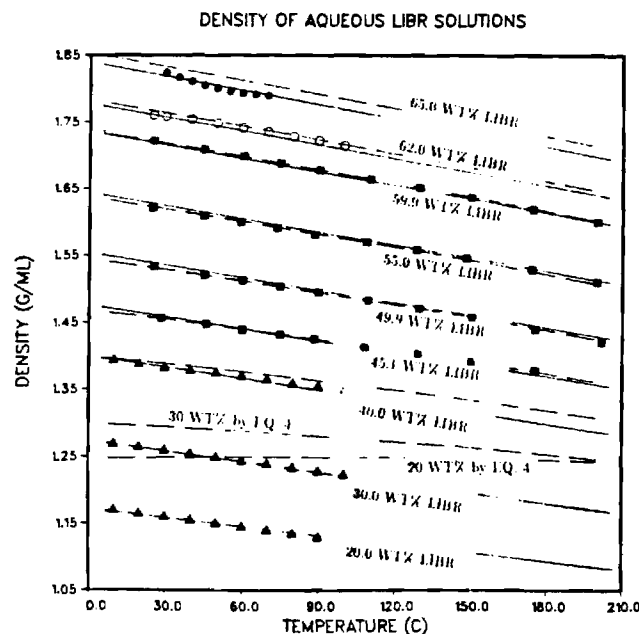


Figure 8 Comparison of density correlations with experimental data.

TABLE 3
Correlation of Experimental Data by Equation 9

WT% LiBr	A ₁	A ₂	A ₃	AAD%	MAD%
45.0	-49.8181	3813.29	6.66101	0.48	1.09
50.0	-40.1023	3357.43	5.27316	0.36	1.06
55.0	-33.6317	3118.48	4.33620	0.18	0.43
59.9	-32.5247	3222.14	4.15643	0.37	1.04
63.0	-37.3241	3605.41	4.83769	0.27	0.85
65.0	-46.3684	4167.00	6.13288	0.23	0.71

Bogatykh and Evnovich (1965), Sohnel and Novotny (1985), and Uemura and Hasaba (1964). The average deviation between the calculated and experimental values was found to be 0.19% for the 86 data points, which covered concentrations of LiBr from 20 wt% to 65 wt%. The maximum deviation was 0.51%. Note that Equation 4, which is also shown in this figure, does not extrapolate well to lower concentrations.

Viscosity

The viscosity of lithium bromide-water solutions at each concentration can be described by the following equation:

$$\ln \mu = A_1 + A_2/T + A_3 \ln T \quad (9)$$

where the unit of viscosity (μ) is in centipoise and temperature is in K. Values of A_1 , A_2 , and A_3 for each concentration obtained by regression are listed in Table 3, as are the AAD% and MAD% between experimental and calculated viscosities. The MAD% was less than 1.1 % in all cases. A regression of all data yields

$$A_1 = -494.122 + 16.3967X - 0.14511X^2 \quad (10)$$

$$A_2 = 28606.4 - 934.568X + 8.52755X^2 \quad (11)$$

$$A_3 = 70.3848 - 2.35014X + 0.0207809X^2 \quad (12)$$

This correlation results in an AAD of 1.1% and a MAD of 3.1% over the entire region of T and X covered by this study. Figure 6 shows the good agreement between experimental data and the values calculated using the above correlation.

CONCLUSION

The densities and viscosities of aqueous lithium bromide solutions at high temperatures and concentrations were measured in this work. The experiment covered

temperatures ranging from room temperature to 200°C, and concentrations from 45 wt% to 60 wt% for density measurements and 45 wt% to 65 wt% for viscosity measurements. Our density results generally agree with the literature data at low temperatures within $\pm 0.3\%$. However, the agreement for viscosity data is poor. It should be noted that more than 15% difference exists between values reported in the literature by different workers. Correlations for density and viscosity of these solutions were developed, which were able to describe the data reasonably well.

ACKNOWLEDGMENTS

The research reported herein was supported by ASHRAE Research Project 527-RP. This project was monitored by Technical Committee 8.3, Absorption Machines. The helpful suggestions and comments of the all committee members, including Dr. Uwe Rockenfeller, the technical monitor, Mr. Mark Fallek and Dr. Gary Vliet, present and former chairpersons, are gratefully acknowledged.

REFERENCES

- Al-Harbi, D.K. 1982. "Viscosity of selected hydrocarbons saturated with gas." Ph.D. dissertation, Oklahoma State University, Stillwater.
- ASHRAE. 1989. *ASHRAE handbook—1989 fundamentals*. Atlanta: American Society of Heating, Refrigerating, and Air-Conditioning Engineers, Inc.
- Bogatykh, S.A., and Evnovich, I.D. 1963. "The viscosity of aqueous solutions of LiCl, LiBr and CaCl₂, applicable to the conditions of drying of gases." *Zh. Prikl. Klim.*, Vol. 36, p. 186.
- Bogatykh, S.A., and Evnovich, I.D. 1965. "Investigation of densities of aqueous LiBr, LiCl, and CaCl₂ solutions in relation to conditions of gas drying." *Zh. Prikl. Klim.*, Vol. 38, p. 945.
- CRC. 1982. *CRC handbook of chemistry and physics*, 63d edition. Boca Raton, FL: CRC Press, Inc.
- Gildseth, W.; Habenschus, A.; and Spedding, F.H. 1972. "Precision measurements of densities and thermal dilation of water between 5°C and 80°C." *J. Chem. Eng. Data*, Vol. 17, p. 402.
- Kneisl, P., and Zondlo, J.W. 1987. "Vapor pressure, liquid density, and the latent heat of vaporization as functions of temperature for four dipolar aprotic solvents." *J. Chem. Eng. Data*, Vol. 32, p. 11.
- Poiseuille, J. 1840. *Compte rendus*, Vol. 11, pp. 961, 1040.
- Sohnel, O., and Novotny, P. 1985. *Densities of aqueous solutions of inorganic substances*. Amsterdam: Elsevier.
- Uemura, T., and Hasaba, S. 1964. "Studies on the lithium bromide-water absorption refrigeration machine." *Technol. Rept.*, Kansai Univ., Vol. 6, p. 31.
- Zeitfuchs, E. H. 1946. "Kinematic viscometer for opaque and very viscous liquids." *Oil and Gas Journal*, Vol. 44, January, p. 99.

FINAL REPORT

**THERMOPHYSICAL PROPERTY DATA FOR
LITHIUM BROMIDE/WATER SOLUTIONS
AT ELEVATED TEMPERATURES**

PREPARED FOR

**THE AMERICAN SOCIETY OF HEATING, REFRIGERATING AND
AIR-CONDITIONING ENGINEERS**

UNDER PROJECT 527-RP

PREPARED BY

**GEORGIA INSTITUTE OF TECHNOLOGY
SCHOOL OF CHEMICAL ENGINEERING
AND
THE GEORGE W. WOODRUFF SCHOOL
OF MECHANICAL ENGINEERING**

**MARCH 1991
(Revised July 1991)**

FINAL REPORT

**March 1991
(Revised July 1991)**

**THERMOPHYSICAL PROPERTY DATA FOR
LITHIUM BROMIDE/WATER SOLUTIONS
AT ELEVATED TEMPERATURES**

PREPARED FOR

**THE AMERICAN SOCIETY OF HEATING, REFRIGERATING AND
AIR-CONDITIONING ENGINEERS**

UNDER PROJECT 527-RP

SUPERVISED BY

**TECHNICAL COMMITTEE 8.3
(ABSORPTION AND HEAT OPERATED MACHINES)**

PREPARED BY

**GEORGIA INSTITUTE OF TECHNOLOGY
SCHOOL OF CHEMICAL ENGINEERING
AND
THE GEORGE W. WOODRUFF SCHOOL OF MECHANICAL ENGINEERING**

AUTHORS:

**A. S. TEJA, PRINCIPAL INVESTIGATOR
S. M. JETER, CO-PRINCIPAL INVESTIGATOR**

**R. J. LEE, RESEARCH ENGINEER
R. M. DIGUILIO, GRADUATE RESEARCH ASSISTANT
J.-L. Y. LENARD, GRADUATE RESEARCH ASSISTANT
J. P. MORAN, GRADUATE RESEARCH ASSISTANT**

TABLE OF CONTENTS

1. Introduction
2. Thermal Conductivity
3. Density
4. Kinematic Viscosity
5. Liquid Specific Heat
6. Vapor Pressure

Appendices

- I. ASHRAE Paper AT-90-30-4 (3380, RP-527): "Properties of Lithium Bromide - Water Solutions at High Temperatures and Concentrations - I. Thermal Conductivity", R. M. DiGuilio, R. J. Lee, S. M. Jeter, and A. S. Teja, **ASHRAE Transactions 1990**, Vol. 96, Part 1, 1990.
- II. ASHRAE Paper AT-90-30-5 (3381, RP-527): "Properties of Lithium Bromide - Water Solutions at High Temperatures and Concentrations - II. Density and Viscosity", R. J. Lee, R. M. DiGuilio, S. M. Jeter, and A. S. Teja, **ASHRAE Transactions 1990**, Vol. 96, Part 1, 1990.

INTRODUCTION

Aqueous lithium bromide (LiBr) solutions and similar mixtures have long been used in absorption refrigeration. Accurate thermophysical data including thermodynamic and transport data are needed for adequate design analysis and evaluations of such systems. In the past, little data was available at elevated temperatures and concentrations, and often the published thermophysical properties had been based on proprietary data or on the results of measurements that had not been fully disclosed or described. To alleviate this shortcoming, Technical Committee 8.3 initiated a project for the measurement of the following properties:

1. Thermal Conductivity
2. Density
3. Kinematic Viscosity
4. Liquid Specific Heat
5. Vapor Pressure

The Georgia Institute of Technology was selected as the contractor on this project. With assistance and forbearance from the sponsoring Technical Committee, the required measurements and data reduction and analysis have now been conducted. This report represents the completion of the project.

Important accomplishments of this project include the following:

1. The development and successful operation of a fused quartz thermal conductivity cell using a liquid metal thermometric fluid suitable for implementing the hot wire thermal conductivity measurement in an electrically conductive fluid.
2. The demonstration of a high pressure capillary viscometer system successfully used for measurements of the viscosity of a volatile fluid at elevated temperature.
3. Successful development and demonstration of an innovative static vapor pressure measurement system using water as the pressure transmitting fluid which is capable of highly accurate measurements of the pressure of water vapor above water solutions with non-volatile solutes.
4. Successful application of classical drop calorimetry with design improvements in temperature measurement and environmental control.

Details of the experimental procedures and designs are given in the following sections along with raw data and correlations. Two ASHRAE papers have already been generated reporting the results of this research. Copies of these papers are appended (see Appendix I and Appendix II).

The entire research team expresses its gratitude for the opportunity to be involved in this challenging and worthwhile project.

(This page intentionally left blank.)

Chapter 2

Thermal Conductivity of Lithium Bromide and Water Solutions

1 Introduction

The design of refrigeration and chiller systems which use aqueous lithium bromide solutions requires accurate thermal conductivity data. Most literature data, however, are limited to low temperatures and low concentrations of lithium bromide. The objectives of this work were therefore to measure the properties of lithium bromide solutions at high temperatures and concentrations of lithium bromide.

The most accurate technique for the measurement of the thermal conductivity of liquids is the transient hot wire method (Nieto de Castro et al. (1986)) in which a thin wire immersed in the liquid is electrically heated. The temperature rise of the wire is used to determine the thermal conductivity of the liquid. Electrically conducting solutions can be measured with this technique, if the wire is electrically insulated from the liquid under study. The insulation blocks the flow of current through the liquid, which would confuse the interpretation of the voltage measurements. However, the addition of an insulating layer to the wire has proved difficult to achieve in practice, especially at higher temperatures. Nagasaka and Nagashima (1981) successfully insulated a platinum wire with a polyester coating and reported measurements up to 150 °C. Alloush et al. (1982) used a tantalum

filament coated with a layer of tantalum oxide to obtain data on LiBr solutions at temperatures up to 80 °C. Recently Kawamata et al. (1988) used the tantalum - tantalum oxide filament to make measurements on LiBr solutions up to 100 °C. However, they noted that the oxide coating failed to insulate the wire properly above 100 °C. This limitation was confirmed by our own efforts to use the tantalum - tantalum oxide filament at temperatures above 100 °C. This is shown in Figure 1, where the thermal conductivity of water measured with a tantalum wire is plotted as a function of temperature. Above 100 °C, deviation from the ESDU (1967) recommended values occurs. The probable reasons for failure are the cracks that develop in the insulation due to the unequal expansion coefficients of the base metal and the oxide and the decrease in dielectric strength with temperature of the oxide. Both effects might permit current paths into the liquid and allow polarization of the fluid near the wire. A different technique was pioneered by Omotani et al. (1981, 1982). This technique uses a fine glass capillary filled with liquid mercury instead of the insulated wire. The apparatus was used to measure the thermal conductivity of molten salts up to 300 °C. The accuracy of these measurements was verified by Tufeu et al. (1985) using a coaxial cylinder method to measure the thermal conductivities of some of the same systems. Since the liquid metal technique has been validated at the temperatures of interest in this study, it was adopted in this work. Measurements were made in the range of concentration from 30 weight percent (wt%) to 65 wt% LiBr and of temperature between 20 °C to 190 °C.

2 Apparatus and Procedure

The transient hot wire apparatus employed in this work is shown in Figure 2. The major components of the apparatus are a Wheatstone bridge, a power supply, and a data acquisition system.

The Wheatstone bridge consists of two $100 \pm 0.01 \Omega$ precision resistors, a resistance decade box (General Radio Model 1433 U) with a range of 0 - 111.11 Ω , and a hot wire cell. The hot wire cell was constructed of quartz and is shown in Figure 3. The cell is in the shape of a U tube with one leg consisting of a quartz capillary tube (13.6 cm long, 0.05 mm ID, 0.08 mm OD) and the other a larger bore quartz tube (2 mm ID by 4 mm OD). The open end of the U tube is supported with a piece of machinable ceramic. The connection between the larger tube and the capillary tube is achieved by drawing down the larger tubing and sealing the capillary tubing into place with silicone rubber (General Electric RTV-106). Originally, it was intended to use liquid gallium to fill the U tube since liquid gallium has the advantages of low toxicity and very low vapor pressures. However, the reactivity of gallium with water vapor at high temperatures forced the choice of mercury as the liquid metal. The entire U tube was filled with liquid mercury with the thread of mercury in the capillary tube serving as the hot wire. Small pieces of tungsten wire were inserted into the liquid mercury at each end of the open U-tube to serve as electrodes. The tungsten wires were, in turn, connected to copper wires attached to the bridge. The cell itself was placed in a glass sleeve with ceramic supports at the top and bottom of the U-tube to ensure that the U-tube remained centered in the sleeve. The sleeve was then placed inside a pressure vessel. A 0.0625 inch diameter Type E thermocouple probe was inserted through both ceramic supports along the axis of the larger bore tube. The bridge was powered by a precision power supply (Hewlett-Packard Model 6213A) which served as a constant voltage source. The supply was used both to balance the bridge and provide the voltage for heating. A lab quality multimeter (Fluke Model 8840A) was used to indicate a balanced condition in the bridge. A data acquisition system consisting of an IBM PC XT with a 16 bit analog to digital converter card (Strawberry Tree ACPC-16) was used to read both the offset voltage and the applied voltage.

The test fluid was loaded into the glass sleeve and the sleeve was inserted into a stainless steel pressure vessel. The quartz cell was then lowered into the glass sleeve and the pressure vessel was sealed. The apparatus was then placed in a fluidized sand bath (Techne Model SBL-2D) which maintained the temperature to ± 0.1 °K. The sample was pressurized to 15 bar with nitrogen to prevent boiling during measurement. A Type E thermocouple, calibrated against a PRT (Leeds and Northrup SN 709892), was used to determine the stability of the bath and the sample equilibrium temperatures. After temperature equilibrium had been achieved, the air flow to the sand bath was stopped to prevent any vibration of the cell during measurement.

The procedure for each measurement was as follows. The bridge was first balanced and the computer program started. The program initiated a step input to the bridge using an electromechanical relay (Magnecraft W172DIP-1). The relay settled in less than 0.3 milliseconds. The program sampled the offset voltage on one channel, then switched channels to sample the applied voltage to insure its constancy. The time between any two samples was 0.0084 seconds and that between two successive readings of the same channel was 0.0168 seconds. The delay between the closing of the relay and the first sampling was found to be 0.0132 seconds using an oscilloscope. Two hundred points were measured during each run and the experiment lasted about 3.4 seconds. From a previous calibration of the temperature versus resistance, the temperature of the wire was found. A plot of ΔT versus the logarithm of time was made and the slope in the time interval from 0.7 to 2.2 seconds was calculated using a least squares fit as described in the analysis section. The applied voltage was varied from about 2.5 to 3.5 V so that a more or less constant temperature rise in the quartz capillary surface of about 1.4 °C was achieved. This resulted in offset voltages on the order of 5 mV. The A/D card has 16 bit resolution and the ± 25 mV range was used. Thus the card is capable of 0.8 μ V resolution.

3 Source and Purity of Materials

Anhydrous lithium bromide was obtained from Morton Thiokol Inc. (Lots F06H, L02F, and H26G). The minimum stated purity of the sample was 99 wt% LiBr. Distilled water was used to prepare the solutions. Solutions were first prepared gravimetrically based on weight percent LiBr. To ensure that no change in the composition of a solution occurred during the measurement procedure, samples of each composition were taken before and after the thermal conductivity measurement and checked using a computer aided titrimeter (Fisher CAT System including Controller Model 450, Buret Model 400 and Stirrer Model 460). The precipitation titration was done using a 0.1 Normal standard silver nitrate solution as the titrant (Fisher, Cat. No. SS72-500, .1000 \pm 0.0002 Normality). A silver specific electrode (Fisher Cat. No. 13-620-122) was used to indicate the equivalence point, and a standard calomel electrode (Fisher Cat. No. 13-620-51) was used as the reference electrode. The compositions reported are the averages of two titrations. The average deviation between any pair of measurements was 0.4% and the maximum deviation was 0.8%. This agreement indicates that there was little variation in composition during the thermal conductivity measurement.

4 Analysis

The model for the experiment is an infinite line source of heat submersed in an infinite fluid medium. By monitoring the temperature response of the wire to a step voltage input, the thermal conductivity of the fluid can be deduced. For an infinite line source of heat in an infinite fluid medium, the ideal temperature rise of the wire ΔT_{id} can be calculated using an expression derived by Carslaw and Jaeger (1959) and Healy et al. (1976) for $t \gg \frac{r_w^2}{4\alpha}$, where r_w is the radius of the filament and α is the thermal diffusivity of the fluid. The

inequality is satisfied shortly after heating is started, that is, for 10 milliseconds $< t <$ 100 milliseconds. The expression is:

$$\Delta T_{id} = \frac{q}{4\pi\lambda} \ln \left(\frac{4\lambda t}{r_w^2 \rho C_p C} \right) \quad (1)$$

where q is the heat dissipation per unit length, λ is the thermal conductivity, ρ the density, C_p the heat capacity, t the time from the application of the step voltage and C is equal to $\exp(\gamma)$ where γ is Euler's constant. If it is assumed that all physical properties are independent of temperature over the small range of temperature considered (ca. 1.4 °C), then,

$$\lambda = \frac{q}{4\pi \left(\frac{d\Delta T_{id}}{d \ln t} \right)} \quad (2)$$

where $\frac{d\Delta T_{id}}{d \ln t}$ is found experimentally from a plot of ΔT_{id} vs $\ln t$.

Healy et al. (1976) also derived several corrections for the deviation of the model from reality. These may be written as:

$$\Delta T_{id} = \Delta T_w(t) + \sum_i \delta T_i \quad (3)$$

δT_1 accounts for the finite physical properties of the wire (liquid mercury) and is given by Healy et al. (1976):

$$\delta T_1 = \frac{r_w^2 [(\rho C_p)_w - (\rho C_p)]}{2\lambda t} \Delta T_{id} - \frac{q}{4\pi\lambda} \frac{r_w^2}{4\alpha t} \left(2 - \frac{\alpha}{\alpha_w} \right) \quad (4)$$

where $(\rho C_p)_w$ is the volumetric heat capacity of the liquid mercury and α and α_w are the thermal diffusivity of the fluid and mercury respectively.

The correction due to the finite extent of the fluid is given by Healy et al. (1976):

$$\delta T_2 = \frac{q}{4\pi\lambda} \left(\ln \frac{4\alpha t}{b^2 C} + \sum_{\nu=1}^{\infty} \exp^{-g_\nu^2 \alpha t / b^2} [\pi Y_0(g_\nu)]^2 \right) \quad (5)$$

where b is the inside diameter of the cell, Y_0 is the zero order Bessel function of the second kind and g_ν are the roots of J_0 , the zero order Bessel function of the first kind. Although the

first several roots are readily available, the higher roots can be found to sufficient accuracy using an expression from the work of Watson (1962):

$$g_\nu = (\pi\nu - \pi/4) + \frac{1}{8(\pi\nu - \pi/4)} - \frac{31}{385(\pi\nu - \pi/4)^3} + \frac{3779}{15366(\pi\nu - \pi/4)^5} \quad (6)$$

Values of Y_0 were calculated using the polynomial approximation given by Abramowitz and Stegun (1965).

The effect of the quartz capillary tube on the measurement has been evaluated analytically by Nagasaka and Nagashima (1981). The correction is given by:

$$\delta T_3 = \frac{-q}{4\pi\lambda} \left[\ln \left(\frac{r_w}{r_l} \right)^2 + \frac{2\lambda}{\lambda_l} \ln \frac{r_l}{r_w} + \frac{\lambda}{\lambda_l} + A \right] \quad (7)$$

with :

$$A = \frac{1}{t} (C_0 + B \ln t)$$

$$C_0 = C_1 + C_2 + B \ln \left(\frac{4\alpha}{r_l^2 C} \right)$$

$$C_1 = \frac{r_w^2}{8} \left[\left(\frac{\lambda - \lambda_l}{\lambda_w} \right) \left(\frac{1}{\alpha_w} - \frac{1}{\alpha_l} \right) + \frac{4}{\alpha_l} - \frac{2}{\alpha_w} \right]$$

$$C_2 = \frac{r_l^2}{2} \left(\frac{1}{\alpha} - \frac{1}{\alpha_l} \right) + \frac{r_w^2}{\lambda_l} \left(\frac{\lambda_l}{\alpha_l} - \frac{\lambda_w}{\alpha_w} \right) \ln \left(\frac{r_l}{r_w} \right)$$

$$B = \frac{r_w^2}{2\lambda} \left(\frac{\lambda_l}{\alpha_l} - \frac{\lambda_w}{\alpha_w} \right) + \frac{r_l^2}{2\lambda} \left(\frac{\lambda}{\alpha} - \frac{\lambda_w}{\alpha_w} \right)$$

where r_l, α_l, λ_l are the radius, thermal diffusivity, and thermal conductivity of the quartz capillary.

Radiation by the fluid can be accounted for using an analytical expression for the temperature rise of the mercury thread given by Nieto de Castro et al. (1983):

$$\Delta T = \frac{q}{4\pi\lambda} \left(1 + \frac{Br_w^2}{4\alpha} \right) \ln \frac{4\alpha t}{r_w^2 C} + \frac{Bqr_w^2}{16\pi\alpha\lambda} - \frac{Bqt}{4\pi\lambda} \quad (8)$$

where B is the radiation parameter and is a measure of the contribution of radiant emission by the fluid to the heat transfer process. From Equation 8 Nieto de Castro et al. (1983) derived the following expression for the correction to the observed temperature rise:

$$\delta T_4 = \frac{-qB}{4\pi\lambda} \left(\frac{r_w^2}{4\alpha} \ln \frac{4\alpha t}{r_w^2 C} + \frac{r_w^2}{4\alpha} - t \right) \quad (9)$$

They used Equation 8 to show that emission from a fluid causes the ΔT vs $\ln t$ slope to exhibit a slight curvature, concave to the $\ln t$ axis.

ΔT , after correction for the other effects mentioned, can be fit to Equation 8 to obtain B as suggested by Nieto de Castro et al. (1983). Equation 9, then can be used to calculate δT_4 . If there is no radiation contribution, B is equal zero and thus there is no danger of biasing the data.

Since both sides of the U tube are made of quartz and the mercury is free to expand, there are no effects due to wire-slackening which must be accounted for in conventional hot wire methods. End effects however, must still be considered. These effects result mostly from conduction of heat axially away from the mercury thread to the thicker leads. No analytical correction exists for this source of error and it is generally compensated for experimentally using either potential leads at the top and bottom of the filament or by using a long and a short wire. However, liquid mercury has a thermal conductivity only about 10% of that of platinum, which is commonly used in hot wire apparatus. Therefore, any end effects were expected to be small or negligible in our experiments. This expectation was experimentally verified by the excellent agreement of our data with the IUPAC (1987) data for water and with the data of Kawamata et al. (1988) for LiBr solutions. Kawamata et al. (1988) used a two wire technique to account for end effects.

The actual temperature at which the thermal conductivity is reported is the average temperature of the fluid during the heating process. That is:

$$T_R = T_o + \frac{\Delta T(t_I) + \Delta T(t_F)}{2} \quad (10)$$

where T_o is the temperature of the fluid at the start of a measurement, and t_I and t_F refer to the initial and final times of the data used to find the slope of ΔT vs $\ln t$. In the case of an insulated wire, ΔT refers to the temperature at the surface of the insulation adjacent to the liquid. This temperature has been determined by Nagasaka and Nagashima (1981) and is given by:

$$\Delta T_i = \frac{q}{4\pi\lambda} \left[\frac{(P_3 + P_2 + P_1)}{t_i} + \ln \left(\frac{4\alpha t_i}{r_l^2 C} \right) \right] \quad (11)$$

with :

$$\begin{aligned} P_3 &= \frac{r_w^2}{4} \left(\frac{1}{\alpha_l} - \frac{1}{2\alpha_w} \right) + \frac{r_l^2}{4} \left(\frac{1}{\alpha} - \frac{1}{\alpha_l} \right) \\ P_2 &= \frac{r_w^2}{2\lambda_l} \left(\frac{\lambda_l}{\alpha_l} - \frac{\lambda_w}{\alpha_w} \right) \ln \left(\frac{r_l}{r_w} \right) \\ P_1 &= \ln \left(\frac{4\alpha t_i}{r_l^2 C} \right) \left[\frac{r_w^2}{2\lambda} \left(\frac{\lambda_l}{\alpha_l} - \frac{\lambda_w}{\alpha_w} \right) + \frac{r_l^2}{2\lambda} \left(\frac{\lambda}{\alpha} - \frac{\lambda_l}{\alpha_l} \right) \right] \end{aligned}$$

where the subscript i refers to t_I or t_F .

In order to apply the temperature corrections, various physical properties are required. The density and heat capacity of mercury were obtained from the CRC handbook (1988), and the thermal conductivity from the compilation of Ho et al. (1972), and the electrical resistivity from the work of Williams (1925). The thermal conductivity and the heat capacity of quartz were obtained from the Thermophysical Properties Research Center compilations (1972a,b). Finally, the heat capacity and density of lithium bromide solutions were measured in our laboratory.

The maximum correction δT_1 for the physical properties of the wire was 0.23% of ΔT_{id} . The correction for the finite extent of the fluid δT_2 was negligible, never exceeding 0.0002% of ΔT_{id} . The maximum correction for radiation δT_4 was less than 0.0004% of ΔT_{id} . Both δT_2 and δT_4 were included for consistency, although they were negligible. As expected, the correction for the insulation layer, δT_3 , was significant. The magnitude of δT_3 varied from about 12% to 16% of ΔT_{id} over the time interval of the measurement. Thus, the correction adds an offset to the temperature rise measured, although the slope $\frac{d\Delta T_{id}}{d \ln t}$ is only slightly affected. A typical ΔT_{id} vs $\ln t$ curve is shown in Figure 4. Only the data from about 0.7 seconds to 2.2 seconds were used to calculate $\frac{d\Delta T_{id}}{d \ln t}$. In order to calculate the corrections, an estimate of the thermal conductivity of the fluid is needed. This estimate was obtained by using ΔT_w , the measured temperature rise of the wire instead of ΔT_{id} to calculate the thermal conductivity. Using this estimate, the corrections δT_1 , δT_2 and δT_3 could be calculated and the corrected temperature rise data fit to Equation 8 to obtain B. The radiation parameter was then used to calculate δT_4 and hence ΔT_{id} . Finally, the thermal conductivity of the fluid was obtained using ΔT_{id} . This new thermal conductivity estimate generally differed from the original estimate. Furthermore, the physical properties required in the calculations had to be adjusted to reflect the actual average temperature of the system between 0.7 seconds and 2.2 seconds. This was done with Equation 10. In practice, the temperature of the system increased from about 0.8° to 1.2°C above the original equilibrium temperature during the time interval 0.7 seconds to 2.2 seconds. This resulted in an average temperature adjustment of about 1°C. The temperature corrections were re-evaluated using the new value of the thermal conductivity of the fluid and the adjusted temperature of the system. This series of calculations was repeated until no change in the thermal conductivity occurred. Three iterations were typically required for convergence.

5 Results

Water was measured at room temperature to validate the liquid metal capillary technique. The agreement with the IUPAC data was excellent, with deviations between our measurements and IUPAC data being within 0.6%. However, the thermal conductivity of water at higher temperatures could not be measured because the low viscosity of water allowed convection to occur during the heating process. Fortunately, the viscosities of lithium bromide solutions were high enough to prevent the rapid onset of convection. In order to verify the linearity of the ΔT vs $\ln t$ curves, the deviation from the linear fit was checked. Figure 5 shows a plot of the deviation from the fitted line for the same ΔT vs $\ln t$ curve shown in Figure 4. The points are evenly scattered so that no bias is evident.

Seven compositions of lithium bromide - water solutions were measured (30.2, 44.3, 49.1, 56.3, 60.0, 62.9, and 64.9 wt% LiBr) in the temperature range from 20 ° to 190 °C. The data are compiled in Table 1 and are shown graphically in Figure 5. Each data point represents the average of five experimental runs. The maximum deviation from the average value never exceeded 1.0%, and the precision of the data is therefore 1.0%.

The accuracy of the data was estimated from the sum of the bias error ϵ_b and the random error ϵ_r . The bias error was estimated from:

$$\epsilon_b = \epsilon_{b,LT} + \frac{\partial \epsilon_b}{\partial T} \Delta T_M \quad (12)$$

where $\epsilon_{b,LT}$ is the low temperature bias and ΔT_M is the temperature difference between the highest temperature at which the thermal conductivity was measured and the reference temperature. The low temperature bias was obtained by comparing our data on water with IUPAC data. Since our data were consistently about 0.6% high by comparison with the IUPAC data, we estimate the low temperature bias error to be 0.6%. Comparison of our data with literature data for temperatures up to 100°C (see Table 2) showed no apparent

trends in the bias error with temperature. Thus we concluded that $\frac{\partial \epsilon}{\partial T}$ is approximately zero and the bias is 0.6% at all temperatures. Random error was estimated from three sources: the uncertainty in the thermal conductivity measurement, the uncertainty in the reported concentration and the uncertainty in the equilibrium temperature of the fluid, with

$$\epsilon_r^2 = \epsilon_m^2 + \left(\frac{\partial \lambda}{\partial W} \frac{\delta W}{\lambda} \right)^2 + \left(\frac{\partial \lambda}{\partial T} \frac{\delta T}{\lambda} \right)^2 \quad (13)$$

The uncertainty in the measurement ϵ_m was 1%. The sensitivity of the thermal conductivity to temperature and concentration were found using the correlation for thermal conductivity reported in the next section of this paper. The maximum value of $\frac{\partial \lambda}{\partial W} \frac{1}{\lambda}$ was found to be $-0.011 \text{ wt}\%^{-1}$ and the maximum uncertainty in the composition was $\pm 0.8 \text{ wt}\%$. The maximum value of $\frac{\partial \lambda}{\partial T} \frac{1}{\lambda}$ was found to be 0.003 K^{-1} and the maximum uncertainty in the temperature measurement was $\pm 0.2 \text{ K}$. The total random error was thus less than 1.4% and the total error was $\pm 2\%$.

Direct comparison of our data with literature data is difficult due to differences in concentrations. Table 2 is a comparison of the correlation found using only our data with the data of Kawamata et al. (1988), Alloush et al. (1982), Uemura and Hasaba (1963), and Riedel (1951). The agreement between our data and Kawamata et al. who claim an accuracy of $\pm 0.5\%$ is excellent. The average deviation on 15 data points is 0.65% and the maximum is 1.8%. Agreement with Uemura and Hasaba is also excellent. The average deviation on 25 data points is 0.63% and the maximum is 1.9%. The single point from Riedel that lies in our concentration range agrees within 1.1%. The data of Alloush et al. show much larger deviation. The average deviation for 19 points is 2.1% with a maximum deviation of 4.4%. However, Alloush et al. claimed an accuracy of only $\pm 3.0\%$. Therefore, the overall agreement is within the accuracy of their experiments.

Kawamata et al. (1988) measured the thermal conductivity of LiBr solutions at three concentrations (30.3, 46.5, and 56.6 wt % LiBr) at pressures up to 40 MPa. The effect of pressure was found to be small. For example, at 56.6 wt% LiBr and 100 °C, the change in thermal conductivity from .1 MPa to 40 MPa was only 1.7%. Consequently, any dependence of the thermal conductivity on pressure is insignificant both in engineering calculations and as an influence on the measurements reported herein.

6 Correlation

The thermal conductivity of the lithium bromide solutions was correlated with temperature T in K and composition X in wt % as follows:

$$\lambda(T, X) = A(T) + B(T)X + C(T)X^2 \quad (14)$$

with :

$$A(T) = a_1 + a_2T + a_3T^2$$

$$B(T) = b_1 + b_2T + b_3T^2$$

$$C(T) = c_1 + c_2T + c_3T^2$$

Values of the constants $a_1, a_2, a_3, b_1, b_2, c_1, c_2, c_3$ were obtained by regression of the data obtained in this work and are given in Table 3. The average absolute deviation between correlation and experiment was found to be .6% for 47 data points and the maximum deviation was found to be 1.6%. The fitted curves are shown on Figure 6.

7 Conclusions

The thermal conductivity of aqueous solutions of lithium bromide ranging in composition from 30 to 65 wt % and in temperature from 20 ° to 190 °C were measured. The precision of the data is $\pm 1\%$ and the accuracy is estimated to be $\pm 2\%$. A correlation was developed which was able to fit the data with an average absolute deviation of 0.6% and a maximum deviation of 1.6%.

References

- [1] M. Abramowitz and I. A. Stegun, editors. *Handbook of Mathematical Functions*. Dover, New York, 1965.
- [2] A. Alloush, W. B. Gosney, and W. A. Wakeham. *Int J Thermophysics*, 3:225, 1982.
- [3] H. S. Carslaw and J. C. Jaeger. *Conduction of Heat in Solids*. Oxford University Press, London, second edition, 1959.
- [4] C. A. Nieto de Castro, S. F. Y. Li, C. Maitland, and W. A. Wakeham. *Int J Thermophysics*, 4:311, 1983.
- [5] C. A. Nieto de Castro, S. F. Y. Li, A. Nagashima, R. D. Trengrove, and W. A. Wakeham. *J Phys Chem Ref Data*, 15:1073, 1986.
- [6] ESDU. *Thermal Conductivity of Water Substance*. Technical Report 67031, Engineering Sciences Data Unit, London, 1967.
- [7] J. J. Healy, J. J. de Groot, and J. Kestin. *Physica*, 82C:392, 1976.
- [8] C. Y. Ho, R. W. Powell, and P. E. Liley. *J Phys Chem Ref Data*, 1:279, 1972.
- [9] M. Hoshi, T. Omotani, and A. Nagashima. *Rev Sci Instrum*, 52:755, 1981.
- [10] K. Kawamata, Y. Nagasaka, and A. Nagashima. *Int J Thermophysics*, 9:317, 1988.
- [11] K. N. Marsh, editor. *Recommended Reference Materials for the Realization of Physicochemical Properties*. Blackwell Scientific Publications, Boston, 1987.
- [12] Y. Nagasaka and A. Nagashima. *J Phys E: Sci Instrum*, 14:1435, 1981.
- [13] T. Omotani, Y. Nagasaka, and A. Nagashima. *Int J Thermophysics*, 3:17, 1982.

- [14] L. Riedel. *Chem Ingr Tech*, 23:59, 1951.
- [15] Y. S. Touloukian and C. Y. Ho, editors. *Specific Heat of Nonmetallic Solids*. Volume 5 of *The Thermophysical Properties Research Center Data Series*, Plenum Press, New York, 1972.
- [16] Y. S. Touloukian and C. Y. Ho, editors. *Thermal Conductivity of Nonmetallic Solids*. Volume 2 of *The Thermophysical Properties Research Center Data Series*, Plenum Press, New York, 1972.
- [17] R. Tufeu, J. P. Petitet, L. Denielou, and B. Le Neindre. *Int J Thermophysics*, 6:315, 1985.
- [18] T. Uemura and S. Hasaba. *Refrig Japan*, 38:19, 1963.
- [19] G. N. Watson. *A Treatise on the Theory of Bessel Functions*. Cambridge University Press, Cambridge, England, second edition, 1962.
- [20] R. C. Weast, editor. *CRC Handbook of Chemistry and Physics*. CRC Press, Inc., Boca Raton, Florida, 69 edition, 1988.
- [21] E. J. Williams. *Phil Mag*, 50:589, 1925.

Table I: Thermal Conductivity of LiBr - Water Solutions

Wt% LiBr	T [K]	λ [mW/M K]	Wt% LiBr	T [K]	λ [mW/M K]	
0.0	293.8	602.3	49.1	401.2	513.5	
	296.7	607.6		430.0	522.0	
	323.4	646.0		460.0	523.0	
30.2	292.9	508.1	56.3	294.1	419.0	
	296.9	512.1		329.4	453.5	
	326.1	544.6		362.3	468.4	
	329.1	545.9		397.6	484.2	
	359.5	570.7		430.1	493.5	
	365.0	579.5		461.1	501.6	
	385.2	592.0		60.0	299.6	408.8
	388.9	592.8			329.2	432.9
	404.7	597.5			369.7	457.5
	434.0	591.1			402.5	473.4
44.3	435.7	590.2	62.9	430.8	476.5	
	461.3	573.8		460.6	485.8	
	295.1	467.5		339.8	429.5	
	321.4	495.4		371.0	447.2	
	353.5	521.4		400.4	457.3	
	378.6	535.5		430.7	465.4	
	407.2	550.9		460.9	476.1	
	439.2	557.3		64.9	343.4	421.0
	463.3	553.4			370.5	432.1
	298.0	446.7			400.7	442.0
49.1	328.9	478.1	64.9	428.8	453.0	
	371.6	503.9		461.0	458.2	

Table II: Comparison of this Work with the Literature [P = 1 atm]

T [K]	Wt% LiBr	λ [mW/M K] Literature	Ref.	λ [mW/M K] This Work ¹	Claimed Accuracy (\pm %)	% Dev.
293.8	0.0	599.1	[14]	602.3 ²		0.55
296.7		604.1	[14]	607.6 ²		0.58
323.4		642.6	[14]	646.0 ²		0.52
323	26.04	557	[19]	558.0		0.18
313	26.05	551	[19]	545.5		-1.01
353	26.08	581	[19]	586.7		0.97
303	26.28	426	[19]	530.9		0.82
333	26.52	564	[19]	567.4		0.60
304.2	30.3	527.7	[4]	520.7	0.5	-1.35
313.9		536.0	[4]	533.2	0.5	-0.53
333.9		558.6	[4]	555.3	0.5	-0.60
353.5		575.1	[4]	572.1	0.5	-0.53
373.5		588.5	[4]	584.2	0.5	-0.73
313	34.93	521	[19]	516.8		-0.81
303	35.61	503	[19]	502.6		-0.09
323	35.90	521	[19]	524.4		0.65
293	36.21	492	[19]	487.8		-0.87
333	36.29	533	[19]	532.8		-0.04
343	36.50	547	[19]	540.8		-1.15
353	36.53	538	[19]	548.4		1.89
293	40	471	[20]	476.2		1.08
297.0	41.4	473	[3]	476.5	3.0	0.74
305.0		478	[3]	485.7	3.0	1.58
315.0		484	[3]	496.3	3.0	2.49
335.0		500	[3]	515.1	3.0	2.94
357.0		511	[3]	531.9	3.0	3.93
303	44.84	465	[19]	471.5		1.37
333	44.94	501	[19]	499.5		-0.30
323	44.98	489	[19]	490.6		0.33
313	44.99	486	[19]	481.1		-1.01
353	45.42	509	[19]	512.6		0.71
297.0	45.6	465	[3]	462.4	3.0	-0.56
305.0		467	[3]	470.9	3.0	0.82
315.0		469	[3]	480.8	3.0	2.45
335.0		483	[3]	498.5	3.0	3.10
357.0		499	[3]	514.6	3.0	3.02
293	46.05	459	[19]	456.5		-0.55
302.4	46.5	468.2	[4]	464.9	0.5	-0.70
313.8		477.3	[4]	476.2	0.5	-0.22
333.3		490.8	[4]	493.4	0.5	0.54
353.6		501.4	[4]	508.5	0.5	1.40
373.2		510.9	[4]	520.3	0.5	1.81

¹Values calculated from correlation of our data

²Experimental Value (pure water not included in correlation).

Table II: Comparison of this Work with the Literature (Continued)

T [K]	Wt% LiBr	λ [mW/M K] Literature	Ref.	λ [mW/M K] This Work ¹	Claimed Accuracy [\pm %]	% Dev.
297.0	49.7	457	[3]	448.0	3.0	-2.01
305.0		463	[3]	455.8	3.0	-1.57
315.0		464	[3]	465.0	3.0	0.22
335.0		478	[3]	481.6	3.0	0.75
357.0		493	[3]	497.0	3.0	0.80
297.0	53.8	452	[3]	432.9	3.0	-4.40
305.0		457	[3]	440.2	3.0	-3.82
315.0		461	[3]	448.7	3.0	-2.74
335.0		474	[3]	464.2	3.0	-2.11
313	54.25	444	[19]	445.2		0.28
302.8	56.6	428.6	[4]	427.3	0.5	-0.31
313.6		438.0	[4]	436.1	0.5	-0.43
333.5		452.4	[4]	451.0	0.5	-0.32
353.7		464.0	[4]	464.1	0.5	0.01
373.5		473.7	[4]	475.0	0.5	0.27
353	56.61	463	[19]	463.6		0.13
323	56.62	442	[19]	443.3		0.30
293	56.70	416	[19]	418.4		0.57
303	56.71	429	[19]	427.0		-0.46
333	56.75	451	[19]	450.0		-0.23
313	60.35	418	[19]	420.0		0.47

Table III: Constants for Correlation

Constant	Value
a_1	-1407.5255
a_2	11.051253
a_3	$-1.4674147 \times 10^{-2}$
b_1	38.985550
b_2	-0.24047484
b_3	3.4807273×10^{-4}
c_1	-0.26502516
c_2	1.5191536×10^{-3}
c_3	$-2.3226242 \times 10^{-6}$

WATER MEASURED WITH TANTALUM CELL

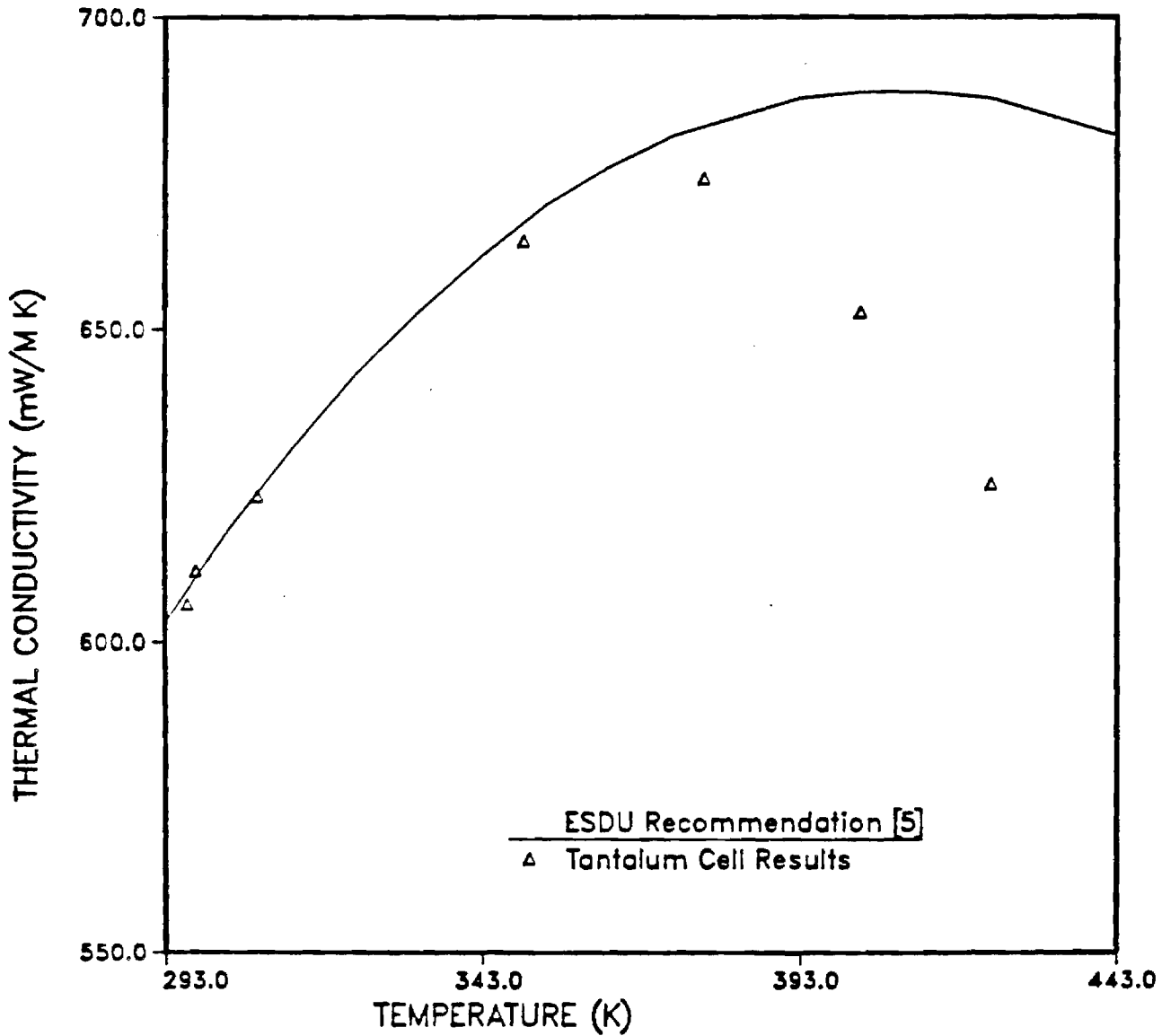


Figure 1: Thermal conductivity of water measured with a tantalum filament insulated with tantalum oxide. The oxide coating fails to insulate above 100 °C.

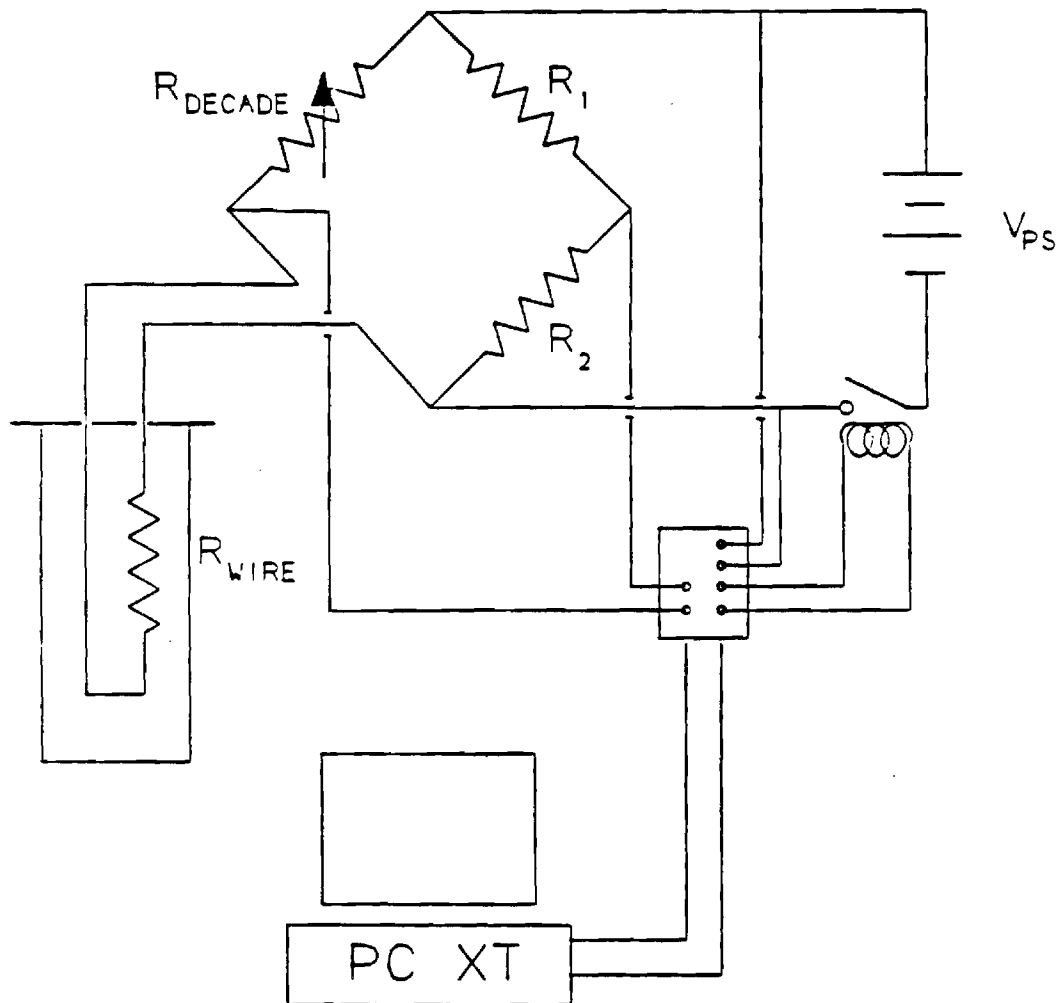


Figure 2: Schematic diagram of apparatus.

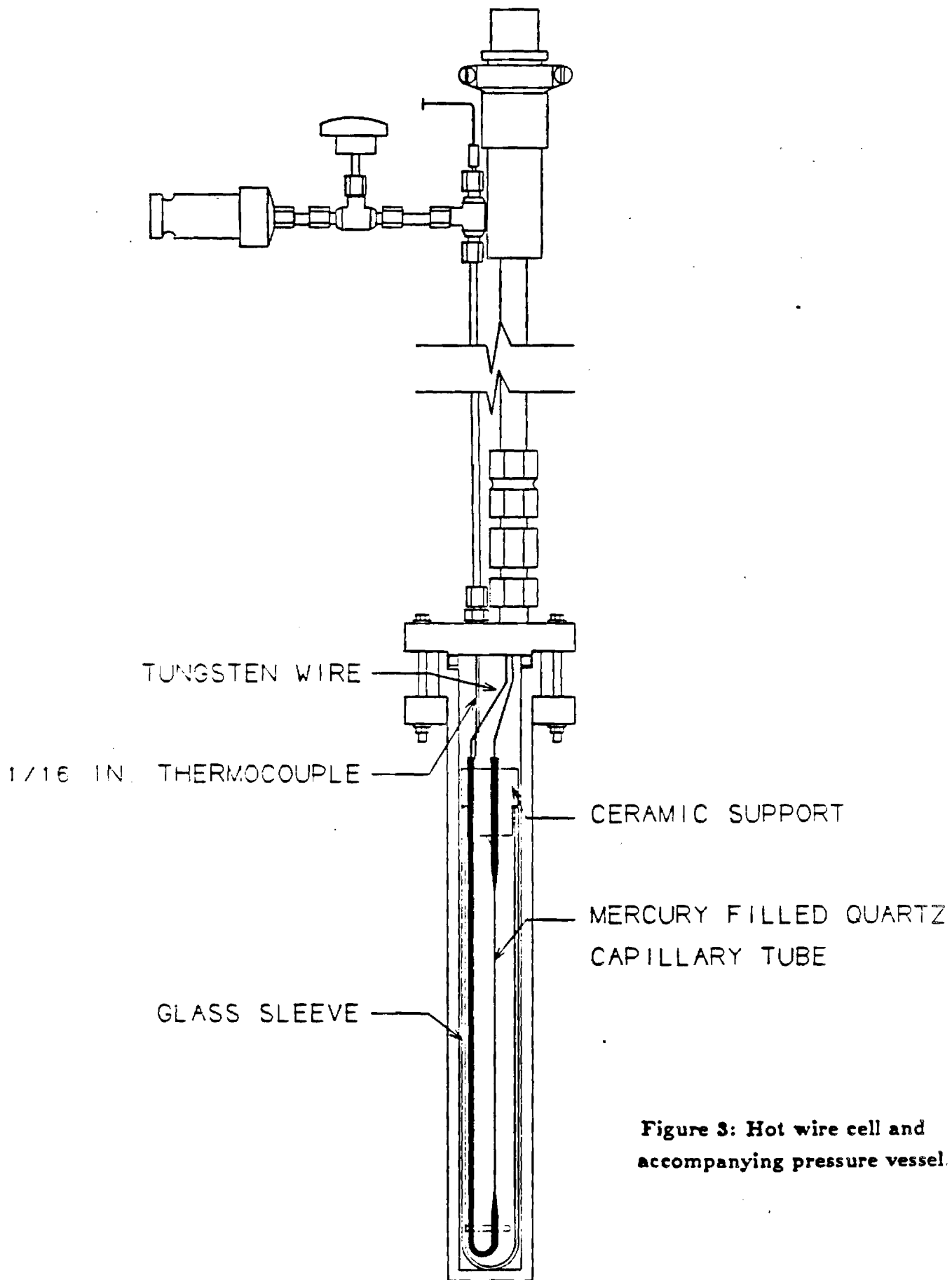


Figure 3: Hot wire cell and accompanying pressure vessel.

TEMPERATURE RISE VS $\ln(t)$

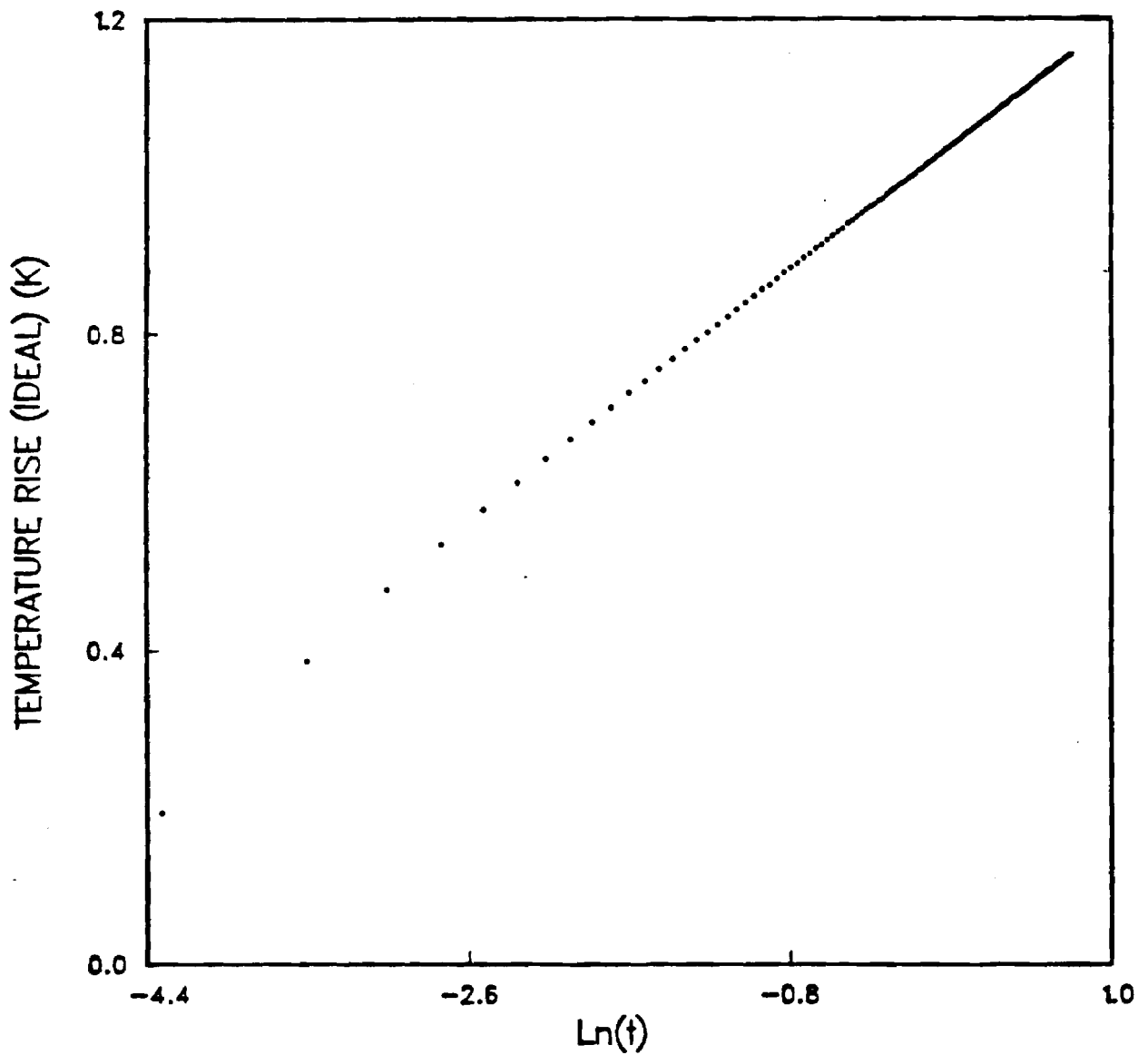


Figure 4: Plot of ΔT_{id} vs $\ln t$ obtained from experiment. Only data from 0.7 s to 2.2 s (-.35 to .79) was used in the calculation of the slope.

LINEARITY OF TEMPERATURE VS LN(t) CURVE

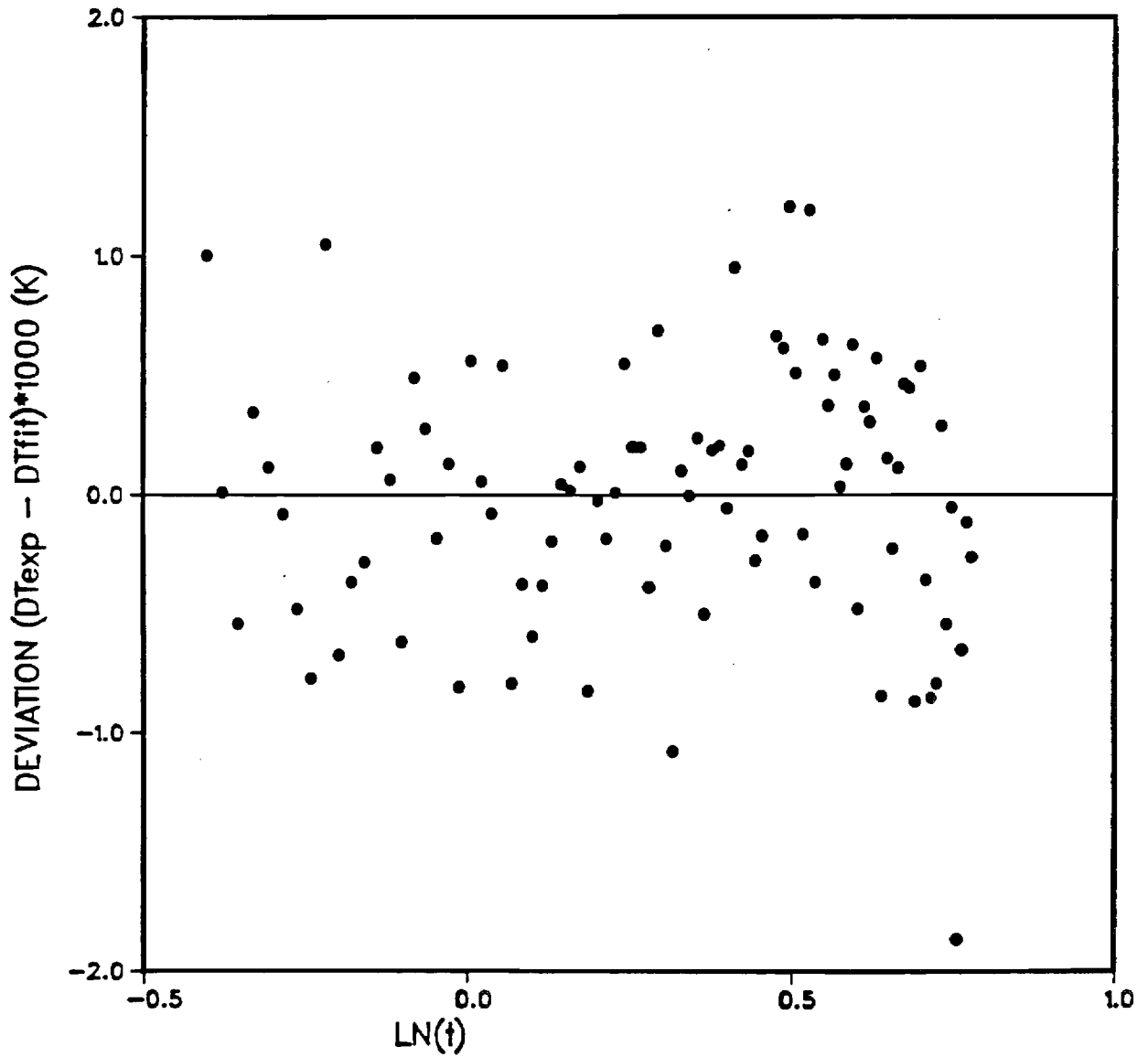


Figure 5: Plot of ΔT vs $\ln t$ to verify function linearity.

THERMAL CONDUCTIVITY OF AQUEOUS LiBr

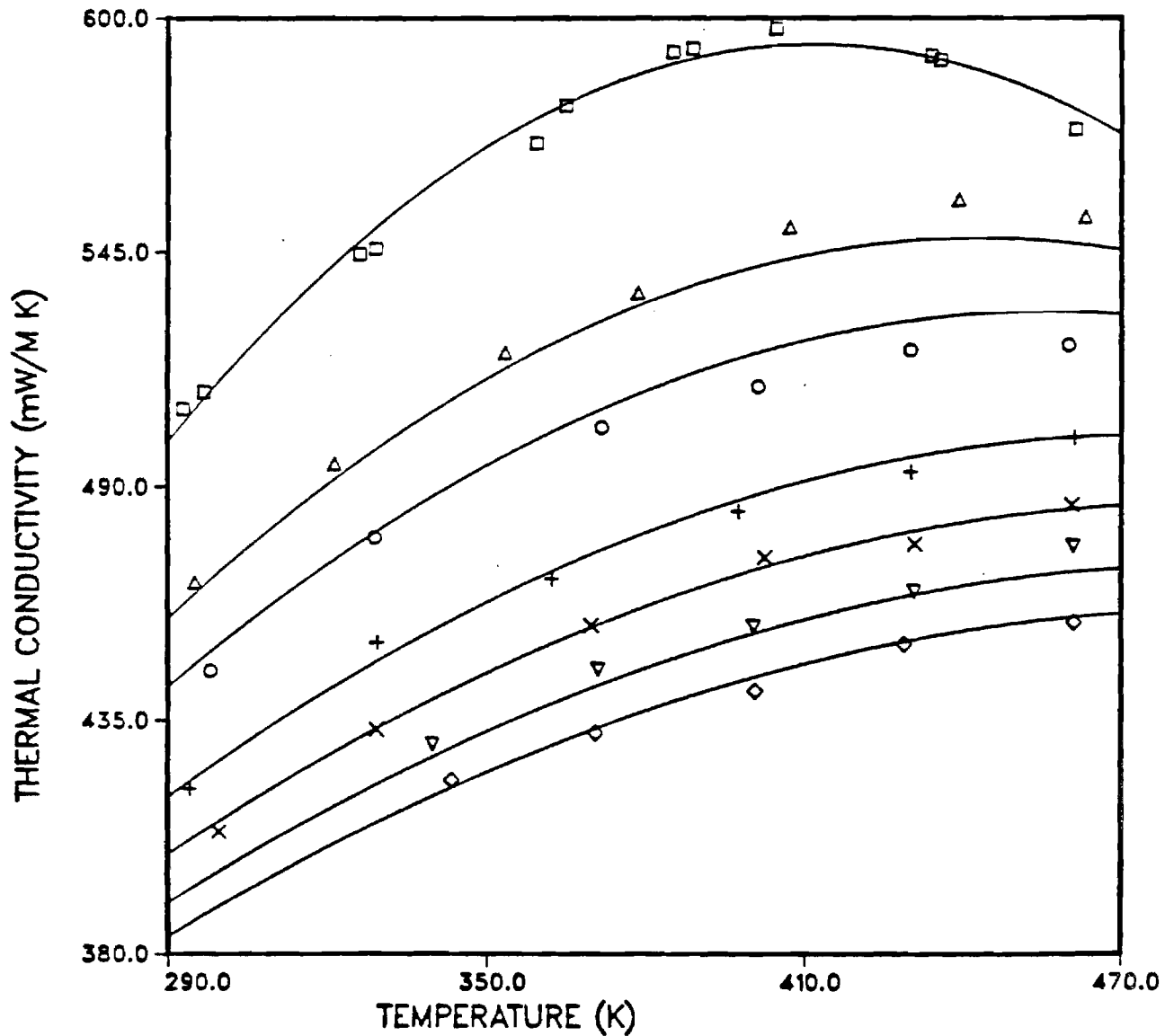


Figure 6: Thermal Conductivity of aqueous lithium bromide solutions. Solid curves are from the correlation. \square = 30.2 wt% LiBr, Δ = 44.3 wt% LiBr, \circ = 49.1 wt% LiBr, $+$ = 56.3 wt% LiBr, \times = 60.0 wt% LiBr, ∇ = 62.9 wt% LiBr, \diamond = 64.9 wt% LiBr.

Chapter 3

Density of Lithium Bromide - Water Solutions

1 Introduction

Improvements to the performance of absorption refrigeration equipment require a knowledge of the thermophysical properties of aqueous lithium bromide solutions. The density of such solutions at temperatures up to 100 °C has been investigated by Uemura and Hasaba (1964) and by Bogatykh and Evnovich (1965). An extension of these measurements to higher temperatures and concentrations is reported in this paper. The densities of aqueous lithium bromide solutions at four concentrations, namely 45.1, 49.9, 55.0, and 59.9 weight % (wt%) and temperatures up to 200 °C were measured. A correlation of the experimental data is also presented.

2 Experiment

Principle of Operation The principle used to determine the liquid density (ρ) of a fluid in this study is based on the definition:

$$\rho = \frac{M}{V} \quad (1)$$

where M is the mass and V the volume of the fluid. Experimentally, we measured the mass of the fluid required to fill a calibrated volume (density cell).

Apparatus and Procedure The densities of lithium bromide - water solutions were measured in a high pressure pycnometer shown schematically in Figure 1. The pycnometer is rated up to 300 °C and 100 bar and consists of four sampling cylinders (Whitey, HDF2-40) capped at one end by a high pressure fitting. The other end of each cylinder was attached through a pipe nipple (Cajon HLN), an isolation valve (Whitey, ORF2), and a quick connect coupling to a high pressure hand pump (High Pressure Equipment Co., model 50-6-15). The pump was used to maintain pressure in the system in order to suppress boiling. Each stainless steel sampling cylinder was equipped with a thermowell for temperature measurement and had an internal volume of approximately 40 ml. The exact volume of each cell assembly was obtained by calibration with triple-distilled mercury at temperatures up to 150 °C. Figure 2 shows a typical calibration curve for density cell No. 1. The data were fitted to an appropriate function (either linear, as in Figure 1, or quadratic) for interpolation or extrapolation. Temperature control within ± 0.05 °C was achieved by a constant temperature circulating bath (Haake-Buchler, model N3B) filled with silicone oil.

At the beginning of an experiment, the four density cells were cleaned thoroughly, weighed, and then connected to the system. The density cell assembly was then evacuated, filled with the test liquid and placed in the oil bath. Usually, two hours were allowed for temperature equilibrium to be attained. Once equilibrium had been established, the isolation valves were closed and the pycnometers removed from the oil bath and weighed on an electronic balance (Sartorius, type 1580).

The solution temperature was measured using a type K thermocouple which had previously been calibrated against a platinum resistance thermometer (Leeds and Northrup Co., Serial No. 709892). The accuracy of the temperature measurement was estimated to be ± 0.1 °C. The system pressure was monitored by a precision pressure gauge (3D Instruments

Inc.) rated at 1500 psi with an accuracy of $\pm 0.25\%$ of full scale. The electronic balance used for weight measurement has a precision of $\pm 0.001\text{g}$.

Material and Solution Preparation N-Methylpyrrolidinone (99.5% purity), mercury (99.999+% purity) and HPLC grade water were purchased from Pfatz & Bauer, Inc., Bethlehem Apparatus Co., and Fisher Scientific, respectively. Anhydrous lithium bromide was provided by Alfa Products (lot No. H26G) and had a certified purity of 99.5 % by weight. These chemicals were used without further purification. Aqueous lithium bromide solutions were prepared by adding degassed water to fresh anhydrous lithium bromide. The solutions were degassed by an alternating freeze-thaw procedure. About 0.2% of impurities by weight (excluding water) were ignored in calculating the concentrations of the prepared solutions. The concentrations were determined gravimetrically and checked on a computer-aided titrameter (Fisher Scientific, CAT system). As shown in Table 1, excellent agreement between solution concentrations determined by these two methods was obtained. The precision of concentration measurement was estimated to be ± 0.1 wt% lithium bromide.

Reference Experiment In order to test the apparatus and procedure, the densities of N-methylpyrrolidinone at atmospheric pressure were measured and compared with data in the literature. As illustrated in Figure 3, our measurements are in good agreement with those reported recently by Kneisl and Zondlo (1987).

3 Results and Discussion

Table 2 summarizes the measured densities of four lithium bromide - water solutions containing 45.1, 49.9, 55.0, and 59.9 wt% of lithium bromide, respectively. Since high concen-

tration solutions are supersaturated at room temperature, the 65 wt% solution could not be measured with this apparatus because the solution would crystallize in unheated sections of the apparatus (such as the pressure gauge or exposed tubing). Measurements on the remaining solutions were performed at temperatures from ambient to 200 °C. The system pressure was maintained at 150 psig throughout the experiments. At least three samples were taken at each condition to give the average reported in Table 2. The reproducibility of the results was $\pm 0.1\%$.

The accuracy of the data was estimated as the sum of the bias error ϵ_b and the random error ϵ_r . The bias error was estimated from:

$$\epsilon_b = \epsilon_{b,MT} + \frac{\partial \epsilon_b}{\partial T} \Delta T_M \quad (2)$$

where $\epsilon_{b,MT}$ is the moderate temperature bias and the ΔT_M is the temperature difference between the moderate temperature reference test and the temperature range over which the data were measured. The moderate temperature bias error was estimated to be 0.1% by comparing our data on N-methylpyrrolidinone with data of Kneisl and Zondlo at temperatures up to 100 °C. The comparison showed no apparent trend in the bias error with temperature. Thus, we concluded that $\frac{\partial \epsilon_b}{\partial T}$ is approximately zero and the bias error is 0.1% at all temperatures. Random error was estimated from three sources: the uncertainty in the measurement, the uncertainty in the reported concentration and the uncertainty in the equilibrium temperature of the fluid, with

$$\epsilon_r^2 = \epsilon_m^2 + \left(\frac{\partial \rho}{\partial X} \frac{\partial X}{\rho}\right)^2 + \left(\frac{\partial \rho}{\partial T} \frac{\partial T}{\rho}\right)^2 \quad (3)$$

The uncertainty in the measurement ϵ_m^2 was 0.1%. The sensitivity of the density to temperature and concentration were found using the correlation for density reported in the next section of this chapter. The maximum value of $\frac{\partial \rho}{\partial X} \frac{1}{\rho}$ was found to be 0.012 wt%⁻¹. Allowing

for experimental variation, the maximum uncertainty in the composition was ± 0.5 wt%. The maximum value of $\frac{\partial \rho}{\partial T} \frac{1}{\rho}$ was found to be -0.0002 K^{-1} and the maximum uncertainty in the temperature measurement was ± 0.2 K. The total random error was then less than 0.15% and the total error was ± 0.25 %.

The densities of aqueous lithium bromide solutions at lower temperatures have been reported by Uemura and Hasaba (1964) and Bogatykh and Evnovich (1965). Figure 4 shows that our data are in good agreement with those of the earlier workers. The average absolute deviation between our data and the data of Uemura and Hasaba was found to be 0.3%, while that between our data and the data of Bogatykh and Evnovich was 0.2%. Note that the data from these two references are at concentrations of 45.0, 50.0, 55.0, and 60.0 wt% LiBr which differ only slightly from the experimental concentrations in this investigation (45.1, 49.9, 55.0, and 59.9 wt%).

4 Correlation

Our results were fitted to the following polynomial function in temperature

$$\rho = A_0 + A_1T + A_2T^2 \quad (4)$$

where ρ is in gm/ml and T is in K. The values of A_0 , A_1 , and A_2 were determined by minimizing the sum of squares of the relative deviations: $\sum_i [(\rho_{\text{expt},i} - \rho_{\text{cal},i})/\rho_{\text{expt},i}]^2$. The constants A_0 , A_1 , and A_2 were further interpolated in terms of weight fraction of lithium bromide (X) as follows

$$A_0 = 1.09763 + 0.071244X + 2.21446X^2 \quad (5)$$

$$A_1 = (0.679620 - 1.48247X - 0.89696X^2) \times 10^{-3} \quad (6)$$

$$A_2 = (-0.035097 - 3.24312X + 4.97020X^2) \times 10^{-6} \quad (7)$$

All data could be correlated with the above equation with an overall average absolute deviation (AAD) of 0.06% and maximum absolute deviation (MAD) of 0.19%. However, nine parameters are required. A simpler form with five parameters is given by:

$$\rho = 1.40818 - 0.713995X + 2.64232X^2 - \frac{(0.12318 + 0.946268X)T}{1000} \quad (8)$$

with an AAD of 0.08% and MAD of 0.39%. Figure 4 shows the comparison between the values calculated by this equation and the observed values.

It should be noted that the correlation of Equation 8 is based only on lithium bromide concentrations between 45 wt% and 60 wt% measured in this investigation. Extrapolation to other concentrations is not recommended. To cover a wider range of X, we included the data available in the literature at lower temperatures in the following equation:

$$\rho = 1.14536 + 0.47084X + 1.37479X^2 - \frac{(0.333393 + 0.571749X)T}{1000} \quad (9)$$

Figure 5 illustrates good agreement between the calculated values and experimental data of this work and of Bogatykh and Evnovich (1965), Sohnel and Novotny (1985), and Uemura and Hasaba (1964). The average deviation (AAD%) between the calculated and experimental values was found to be 0.19% for the 86 data points, which covered a weight fraction of LiBr from 0.2 to 0.65. The maximum deviation was 0.51%. Note that Equation 9, which is also shown in the figure, does not extrapolate well to lower concentrations.

References

- [1] Bogatykh, S. A.; and Evnovich, I. D. 1965. *Zh. Prikl. Klim.*, Vol. 38, p. 945.
- [2] Kneisl, P.; and Zondlo J. W. 1987. *J. Chem. Eng. Data*, Vol. 32, p. 11.
- [3] Sohnel, O.; and Novotny P. 1985. "Densities of Aqueous Solutions of Inorganic Substances", Elsevier, Amsterdam.
- [4] Uemura, T.; and Hasaba S. 1964. *Technol. Rept.*, Kansai Univ., Vol. 6, p. 31.

**Table 1. Comparison of Solution Concentration
Determined by Different Methods.**

No.	Weight Fraction of LiBr	
	Gravimetric	Titrametric
1	0.4506	0.4507
2	0.4985	0.4993
3	0.5500	0.5495
4	0.5990	0.5988

Table 2. Experimental Densities of Aqueous Lithium Bromide Solutions.

Wt% LiBr	T [K]	ρ [gm/ml]	Wt% LiBr	T [K]	ρ [gm/ml]
45.1	301.6	1.4554	49.9	298.7	1.5328
	319.1	1.4470		318.5	1.5206
	333.2	1.4389		333.2	1.5128
	348.1	1.4323		348.0	1.5042
	361.6	1.4255		363.1	1.4954
	381.3	1.4144		382.7	1.4833
	402.4	1.4041		402.8	1.4705
	423.5	1.3919		423.7	1.4568
	448.4	1.3782		448.6	1.4397
				474.8	1.4216
55.0	298.2	1.6205	59.9	298.5	1.7217
	318.2	1.6089		318.2	1.7087
	332.6	1.5997		333.7	1.6986
	346.9	1.5912		348.1	1.6884
	361.5	1.5816		363.6	1.6779
	382.1	1.5703		383.6	1.6642
	401.6	1.5584		403.0	1.6512
	421.6	1.5453		423.4	1.6365
	447.4	1.5287		447.9	1.6192
	473.1	1.5110		473.2	1.6008

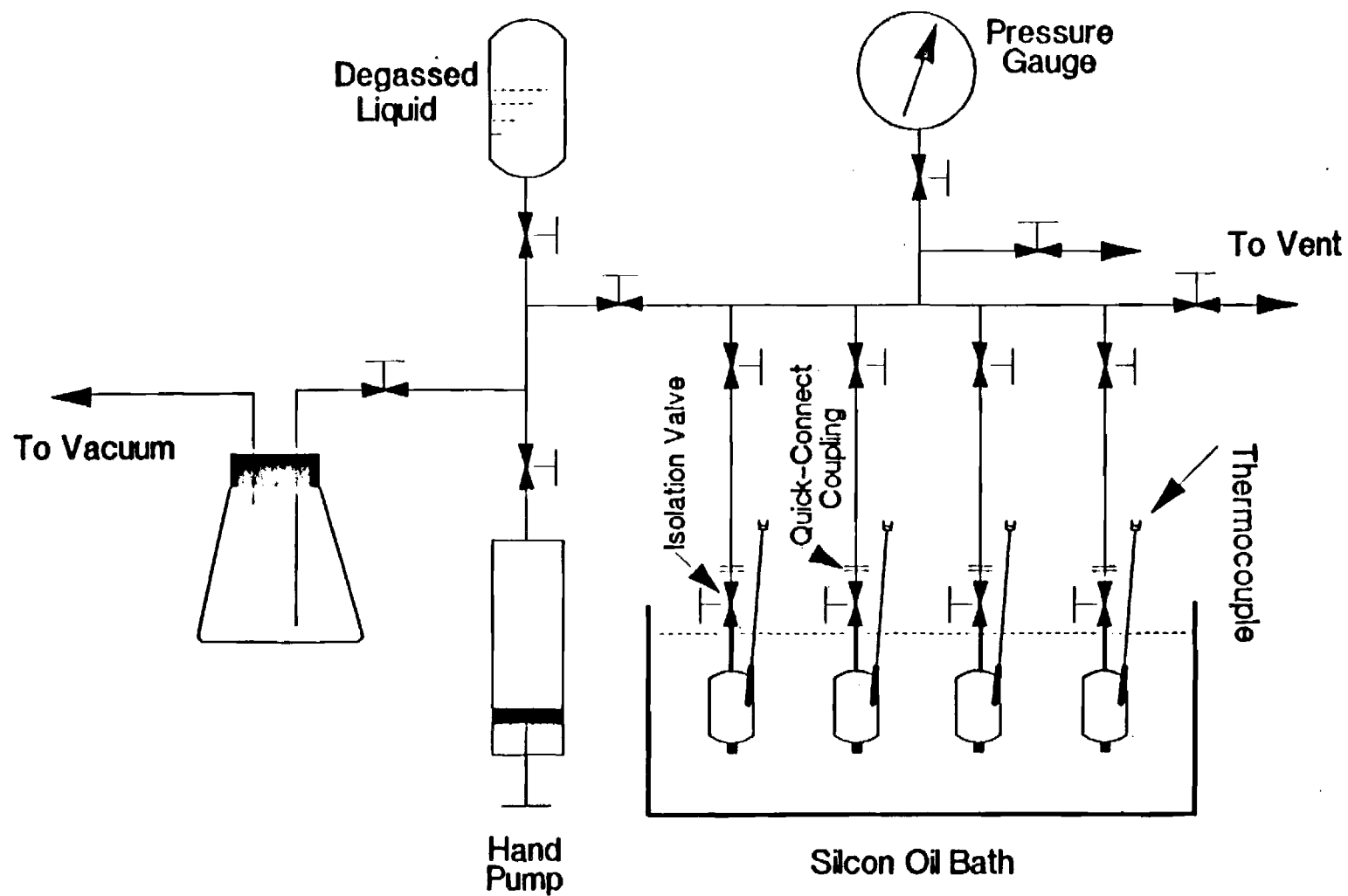


Figure 1. Schematic diagram of the high pressure pycnometer.

INTERNAL VOLUME OF DENSITY CELL 1

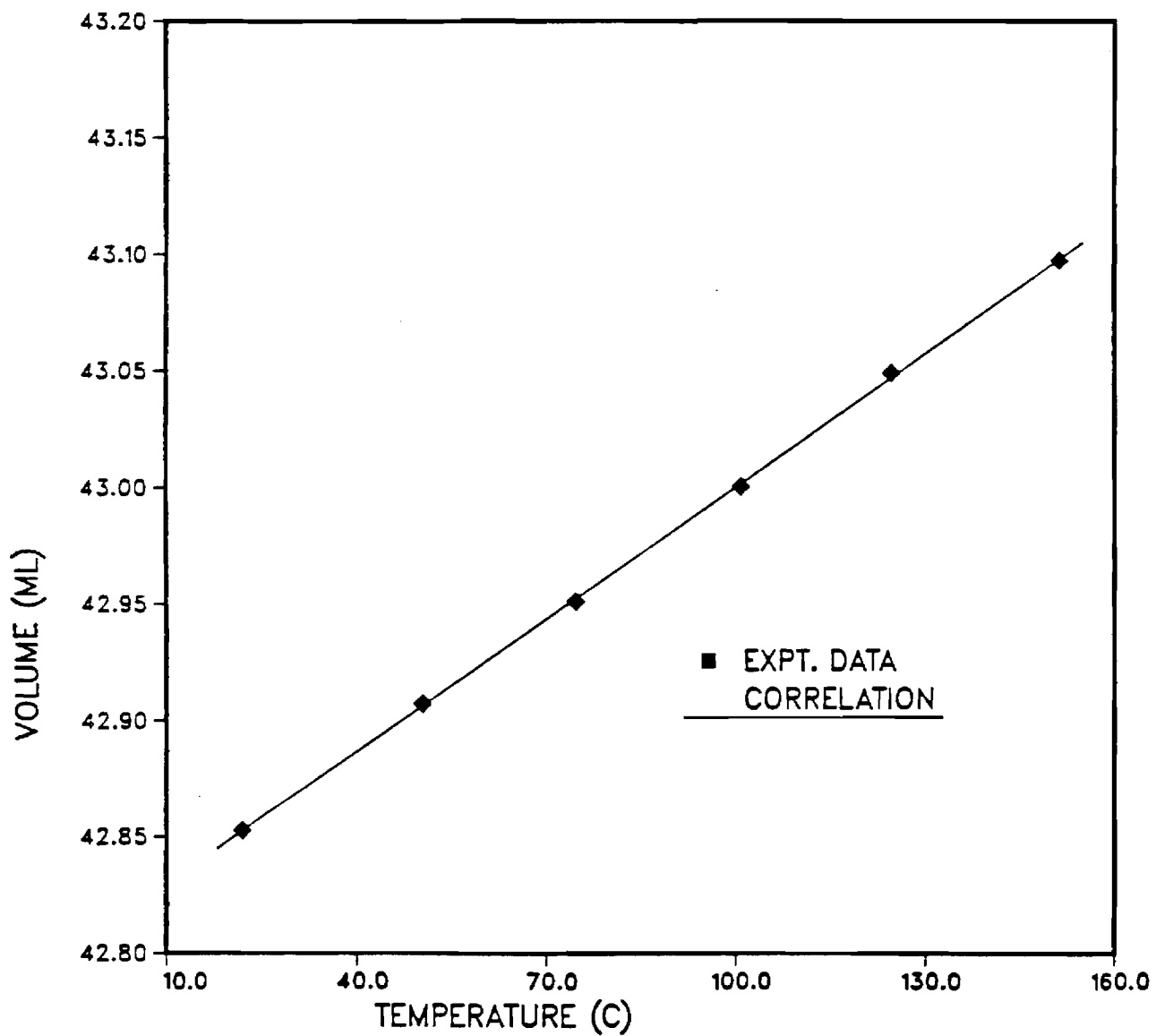


Figure 2. Volume of density cell 1.

DENSITY OF N-METHYLPYRROLIDINONE

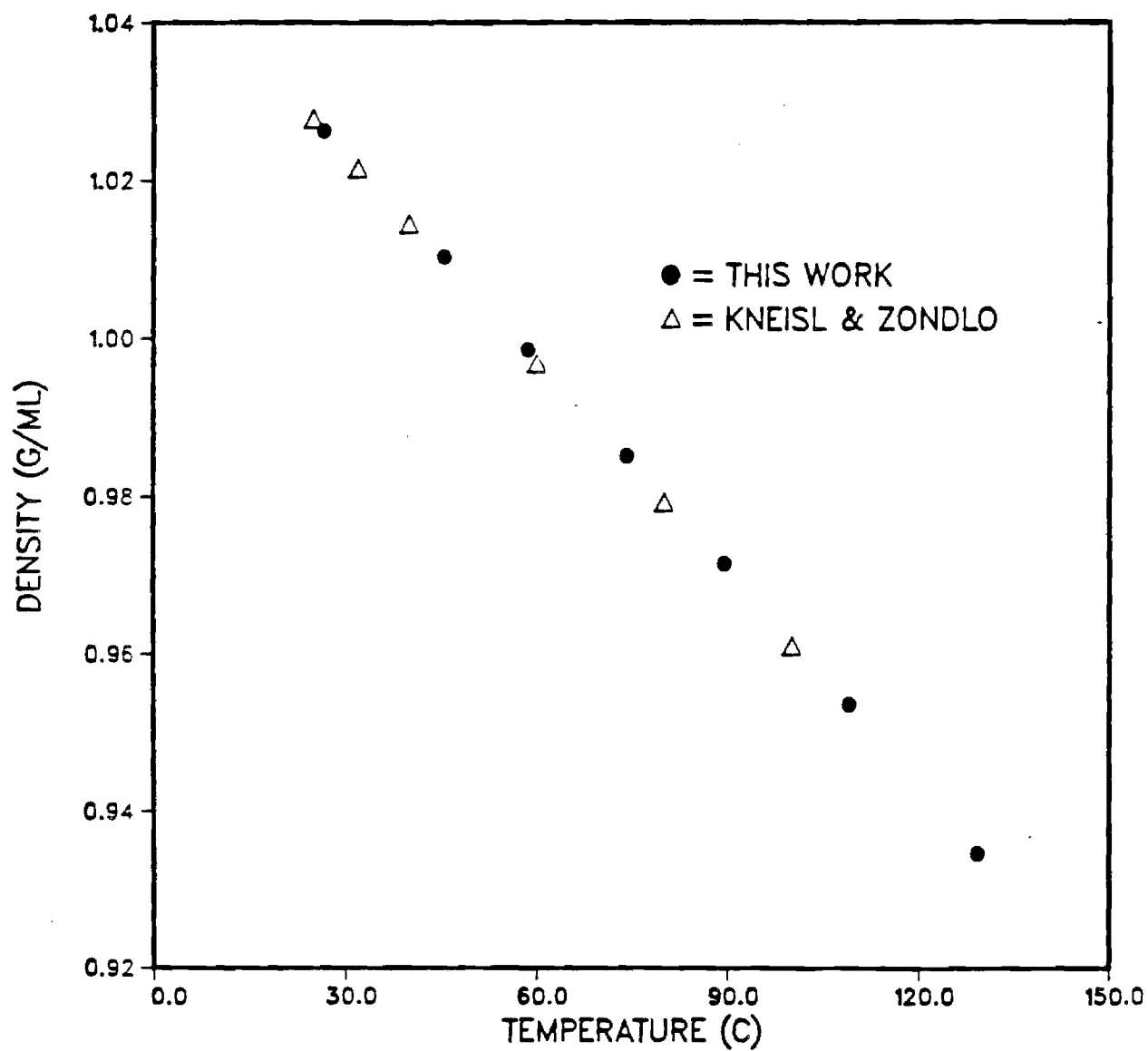


Figure 3. Liquid density of N-methylpyrrolidinone.

DENSITY OF AQUEOUS LiBr SOLUTION

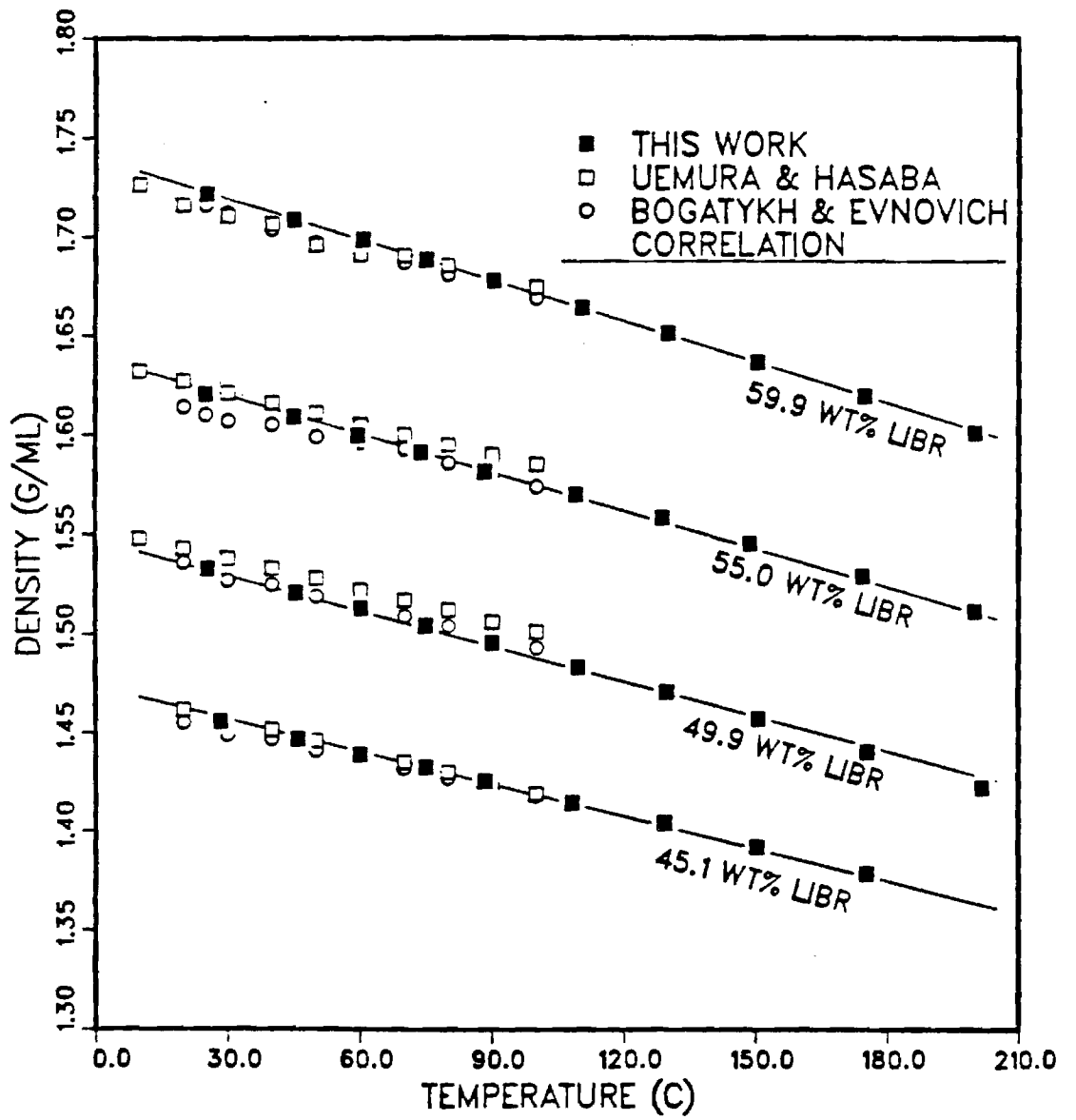


Figure 4. Liquid density of LiBr - water solutions.

DENSITY OF AQUEOUS LIBR SOLUTIONS

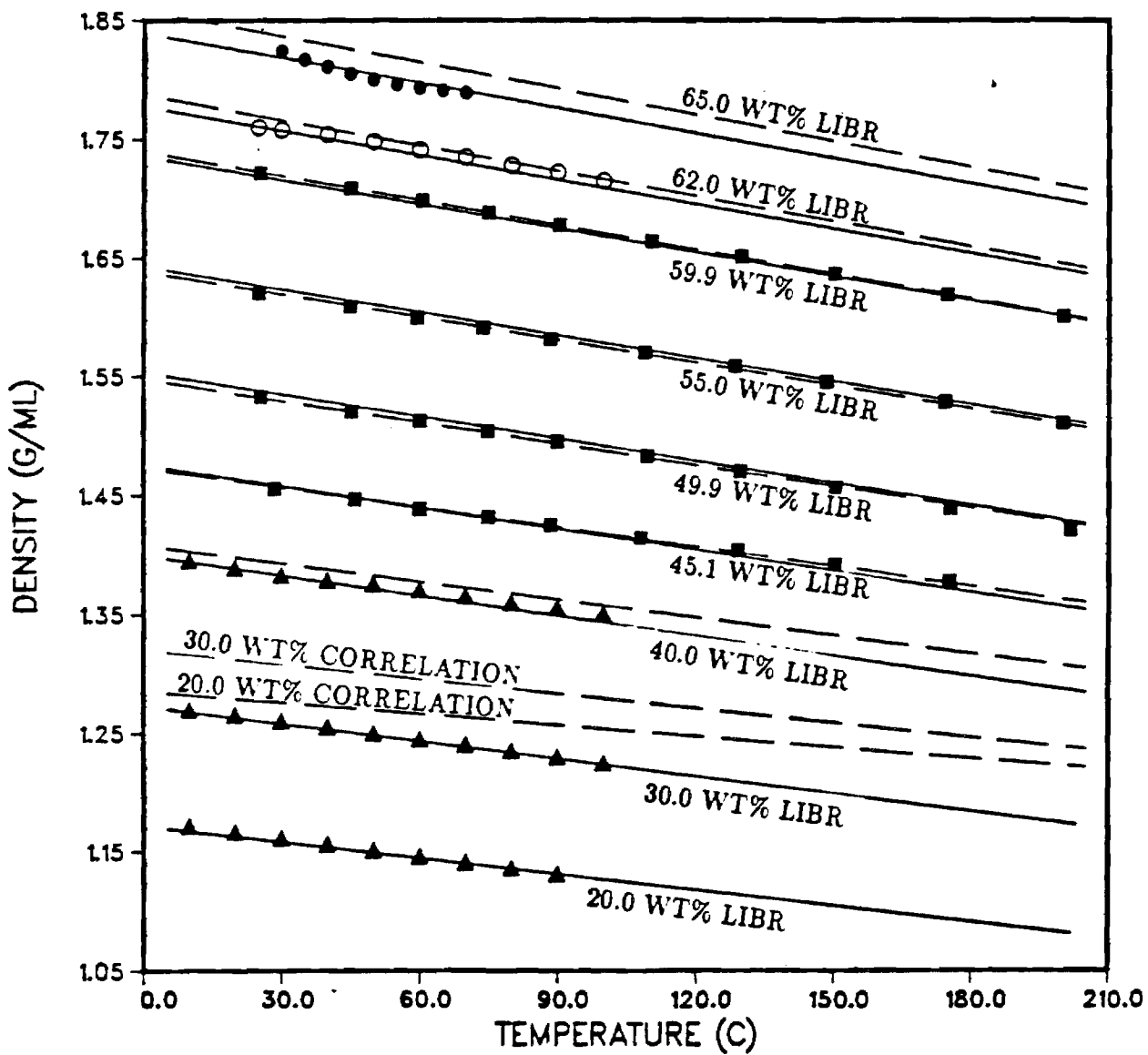


Figure 5. Density correlations compared with experimental data. Equation 8 — ; Equation 9. — — —. Sources of Data: ■ this work; ○ Reference [1]; ● Reference [3]; ▲ composite of References [1], [3], and [4].

Chapter 4

Viscosity of Lithium Bromide - Water Solutions

1 Introduction

The transport properties of concentrated aqueous lithium bromide solutions are important in the design of absorption refrigeration systems. Although the viscosities of such solutions have been measured at low temperatures, more than 15% difference exists between values reported by different workers. Therefore, the viscosities of solutions with weight fractions of lithium bromide ranging from 0.45 to 0.65 and at temperatures up to 200 °C were measured in this work and are reported below.

2 Experiment

Principle of Operation The equation used to represent the absolute viscosity, μ , of a fluid flowing through a capillary is based on Poiseuille's law (1840),

$$\mu = \frac{\pi r^4 g h}{8LV} \rho t - \frac{\zeta V}{8\pi L} \frac{\rho}{t} \quad (1)$$

where

- r : radius of the capillary
 g : gravitational constant
 h : average head of the fluid
 L : length of the capillary
 V : efflux volume of the fluid
 t : efflux time
 ρ : density of the fluid
 ζ : kinetic energy coefficient

For a specific capillary viscometer, the kinematic viscosity ν can be related to the efflux time using:

$$\nu = \frac{\mu}{\rho} = C_1 t - \frac{C_2}{t} \quad (2)$$

where C_1 is the viscometric constant and is determined by calibration with a fluid of known viscosity. The second term on the right hand side represents the correction due to the kinetic energy and is usually neglected if an appropriately sized viscometer is used.

Apparatus and Procedure A high pressure viscometer was designed and constructed for viscosity measurement of highly corrosive solutions. The design of the apparatus is similar to that proposed by Al-Harbi (1982). Figure 1 shows the schematic diagram of this apparatus, which consists of a capillary viscometer, a pressure cell, a thermostated air bath, and a pressure distribution section. This apparatus was designed for temperatures up to 200 °C and pressures up to 30 atm.

A Size 1 Zeitfuchs (1946) cross-arm capillary viscometer (International Research Glassware) was used for determination of the kinematic viscosity (Figure 2). The calibration

factor was determined at room temperature using pure water. In order to repeat a measurement without reloading the liquid sample, the viscometer was calibrated with a wetted capillary. After calibration, the viscometer was placed inside the pressure cell and the capillary end was connected to the pressure distribution section through V5. The reservoir end was opened to the cell chamber such that the pressure over the viscometer could be balanced. The pressure cell is shown schematically in Figure 3. The cell was equipped with four glass view ports (tempered borosilicate glass) to allow visual observation of the reservoir and the measuring bulb of the viscometer. An insulated air bath, heated by a primary (800 W) and a secondary (200 W) heater, was used to establish the desired temperature. A stable temperature in the air bath was maintained by a commercial temperature control unit (Omega, model CN5000) and a circulating fan. Temperature fluctuations were minimized by the mass of the pressure cell, which was made of heavy steel. The test fluid was moved back and forth through the capillary tube by a high pressure hand pump (High Pressure Equipment Co., model 50-6-15) with helium as the pressurizing fluid.

The temperature was measured inside the cell by a chromel-alumel thermocouple, calibrated with a NBS calibrated Leeds and Northrop platinum resistance thermometer (Serial No. 709892). The accuracy of the temperature measurement was estimated to be ± 0.1 °C. Pressure measurement was accomplished by a precision gauge (3D Instruments Inc.) with an accuracy of 0.25% of full scale (0-1500 psi). An electronic timer accurate to 1/100 second was used to obtain the efflux time.

Before an experiment was performed, a clean dry viscometer loaded with the appropriate test solution was attached to the top flange of the pressure cell. The top flange was then bolted into place, and the cell was connected to the pressure distribution section and pressurized slowly to the desired pressure. To eliminate loss of vapor from the solution,

about 40 ml of slightly dilute lithium bromide solution was placed at the bottom of the cell chamber so that the solution in the viscometer was always under its vapor pressure.

At the beginning of an experiment, all valves were closed except for V4 and V5. The pressure on the capillary end was reduced by the use of the hand pump, causing the solution to flow into the reverse bend of the capillary. Once the flow had been initiated, valve V3 was opened to balance the pressures over both ends of the viscometer. The efflux time for the solution to flow between the timing marks on the measuring bulb was then measured. At the end of the measurement, valve V3 was closed and the solution was then forced to return to the reservoir by increasing the pressure on the capillary end with the hand pump. Measurements were repeated until consistent efflux times were obtained.

Material and Solution Preparation Anhydrous lithium bromide, with a certified purity of 99.3% from Alfa Products (lot No. F06H), was used for preparing the solutions. The lithium bromide - water solutions were prepared in the same way as described in the section on density measurement. The concentrations of the solutions were determined either by gravimetric or titrametric methods and are summarized in Table 1.

Reference Experiment To test the apparatus and procedures, the kinematic viscosity of pure water was measured and compared with values reported by the National Bureau of Standards (see CRC Handbook 1982). As illustrated in Figure 4, good agreement was obtained between the two sets of measurements. The density of water reported by Gildseth et al. (1972) was used to convert the measured kinematic viscosity to the absolute viscosity shown in this graph.

3 Results and Discussion

The experimental kinematic viscosities of aqueous lithium bromide solutions of 45.0, 50.0, 55.0, 59.9, 63.0, and 65.0 weight% (wt%) LiBr are presented in Table 2. The temperature range of the measurements varied from 40 to 200 °C, and the pressure was maintained at 200 psig throughout the experiments. Absolute viscosity data, in which the liquid densities were obtained from the correlation previously described, are also included in Table 2. The average of at least four samples was taken to obtain each value reported in this table. The viscosities were reproducible within $\pm 1.0\%$. A graphical presentation of the experimental results is given in Figure 5. As shown, a linear relationship between $\ln(\mu)$ and $1/T$ exists at low temperatures. However, the relationship is nonlinear at higher temperatures, in particular for less concentrated solutions (eg. 45.0 wt% LiBr).

The accuracy of the data was estimated as the sum of the bias error ϵ_b and the random error ϵ_r . The bias error was estimated from:

$$\epsilon_b = \epsilon_{b,LT} + \frac{\partial \epsilon_b}{\partial T} \Delta T_M \quad (3)$$

where $\epsilon_{b,LT}$ is the low temperature bias and the ΔT_M is the temperature difference between the low temperature reference test and the temperature range over which the data were measured. The low temperature bias error was estimated to be 0.5% by comparing our data on water with values of National Bureau of Standards. The comparison showed no apparent trend in the bias error with temperature. Thus, we concluded that $\frac{\partial \epsilon_b}{\partial T}$ is approximately zero and the bias error is 0.5% at all temperatures. Random error was estimated from three sources: the uncertainty in the measurement, the uncertainty in the reported concentration

and the uncertainty in the equilibrium temperature of the fluid, with

$$\epsilon_r^2 = \epsilon_m^2 + \left(\frac{\partial \mu}{\partial X} \frac{\partial X}{\mu}\right)^2 + \left(\frac{\partial \mu}{\partial T} \frac{\partial T}{\mu}\right)^2 \quad (4)$$

The uncertainty in the measurement ϵ_m^2 was 1%. The sensitivity of the viscosity to temperature and concentration were found using the correlation for viscosity reported in the next section of this paper. The maximum value of $\frac{\partial \mu}{\partial X} \frac{1}{\mu}$ was found to be $0.118 \text{ wt}\%^{-1}$ and the maximum uncertainty in the composition was $\pm 0.8 \text{ wt}\%$. The maximum value of $\frac{\partial \mu}{\partial T} \frac{1}{\mu}$ was found to be -0.026 K^{-1} and the maximum uncertainty in the temperature measurement was $\pm 0.2 \text{ K}$. The total random error was then less than 1.5% and the total error was $\pm 2 \%$.

Comparison of our data with data available in the literature was attempted although the system pressures were different. Two sets of experimental data studied at atmospheric pressure by Uemura and Hasaba (1964), and by Bogatykh and Evnovich (1963) were selected. Figure 6 illustrates a comparison of 50.0 and 59.9 wt% LiBr solutions. The literature data shown in this figure were for 50.0 and 60.0 wt% LiBr respectively. The agreement between the literature data is poor, with the experimental data of Bogatykh and Evnovich being consistently lower than the data of Uemura and Hasaba. The literature data bracket our data at lower temperatures, while our data are higher at the higher temperatures. It is also apparent that our data are smoother than the literature data.

4 Correlation

The viscosity of lithium bromide - water solutions at each concentration can be described by the following equation

$$\ln \mu = A_1 + \frac{A_2}{T} + A_3 \ln T \quad (5)$$

where the unit of viscosity (μ) is in centipoise and temperature is in K. Values of A_1 , A_2 , and A_3 obtained by regression are listed in Table 3, as are the average absolute deviation (AAD%) and maximum absolute deviation (MAD%) between experimental and calculated viscosities. The MAD% was less than 1.1 % in all cases. The dependence of A_1 , A_2 , and A_3 on the weight fraction (X) is illustrated graphically in Figure 7. A regression of all data yields

$$A_1 = (-0.494122 + 1.63967X - 1.45110X^2) \times 10^3 \quad (6)$$

$$A_2 = (2.86064 - 9.34568X + 8.52755X^2) \times 10^4 \quad (7)$$

$$A_3 = (0.703848 - 2.35014X + 2.07809X^2) \times 10^2 \quad (8)$$

This correlation results in an AAD of 1.1% and a MAD of 3.1% over the entire region of T and X covered by this study. Figure 8 shows the good agreement between experimental data and the values calculated using the above correlation.

References

- [1] Al-Harbi, D. K., 1982. "Viscosity of Selected Hydrocarbons Saturated with Gas", Ph. D. Dissertation, Oklahoma State University, Stillwater, OK.
- [2] Bogatykh, S. A.; and Evnovich, I. D. 1963. *Zh. Prikl. Klim.*, Vol. 36, p. 186.
- [3] CRC Handbook of Chemistry and Physics, 63rd Edition, CRC Press, 1982.
- [4] Gildseth, W.; Habenschus, A.; and Spedding F. H. 1972. *J. Chem. Eng. Data*, Vol. 17, p. 402.
- [5] Poiseuille, J. 1840. *Compte Rendus*, Vol. 11, p. 961 and 1040.
- [6] Uemura, T.; and Hasaba, S. 1964. *Technol. Rept.*, Kansai, Univ., Vol. 6, p. 31.
- [7] Zeitfuchs, E. H. 1946. *Oil and Gas Journal*, Vol. 44, Jan., p. 99.

Table 1. Comparison of Solution Concentration
Determined by Different Methods.

No.	Weight Fraction of LiBr	
	Gravimetric	Titrametric
1	0.4500	0.4503
2	0.4999	0.5000
3	0.5499	0.5507
4	0.5993	0.6002
5	0.6300	0.6289
6	0.6495	0.6504

Table 2. Experimental Viscosities of Aqueous Lithium Bromide Solutions

Wt% LiBr	T [K]	ν [cst]	μ [cp]	Wt% LiBr	T [K]	ν [cst]	μ [cp]
45.0	312.9	1.325	1.919	50.0	314.9	1.605	2.446
	333.0	0.947	1.363		333.2	1.204	1.822
	353.2	0.738	1.054		353.7	0.932	1.400
	373.9	0.602	0.854		373.2	0.759	1.131
	393.2	0.515	0.725		393.3	0.637	0.942
	413.2	0.453	0.632		412.3	0.554	0.813
	433.0	0.407	0.564		432.6	0.490	0.712
	453.2	0.376	0.516		453.2	0.451	0.650
	472.5	0.353	0.480		472.6	0.413	0.589
55.0	314.2	2.120	3.418	59.9	316.0	2.897	4.952
	333.6	1.547	2.476		333.5	2.122	3.603
	353.1	1.193	1.895		353.6	1.577	2.657
	373.1	0.954	1.503		372.9	1.236	2.066
	393.5	0.786	1.228		394.3	0.986	1.634
	412.7	0.669	1.037		412.7	0.834	1.372
	433.0	0.586	0.900		433.0	0.714	1.164
	453.2	0.523	0.796		453.2	0.630	1.018
	472.3	0.477	0.720		472.9	0.553	0.886
63.0	333.1	2.826	4.964	65.0	333.4	3.162	5.680
	353.2	2.030	3.537		352.4	2.331	4.158
	373.6	1.542	2.665		372.3	1.749	3.095
	393.8	1.219	2.090		393.6	1.352	2.372
	413.2	1.011	1.720		413.2	1.106	1.925
	432.9	0.867	1.463		433.4	0.946	1.633
	452.9	0.744	1.245		452.6	0.820	1.405
	472.8	0.662	1.099		472.7	0.730	1.240

Table 3. Correlation of Experimental Data by Equation 5.

WT% LiBr	A_1	A_2	A_3	AAD%	MAD%
45.0	-49.8181	3813.29	6.66101	0.48	1.09
50.0	-40.1023	3357.43	5.27316	0.36	1.06
55.0	-33.6317	3118.48	4.33620	0.18	0.43
59.9	-32.5247	3222.14	4.15643	0.37	1.04
63.0	-37.3241	3605.41	4.83769	0.27	0.85
65.0	-46.3684	4167.00	6.13288	0.23	0.71

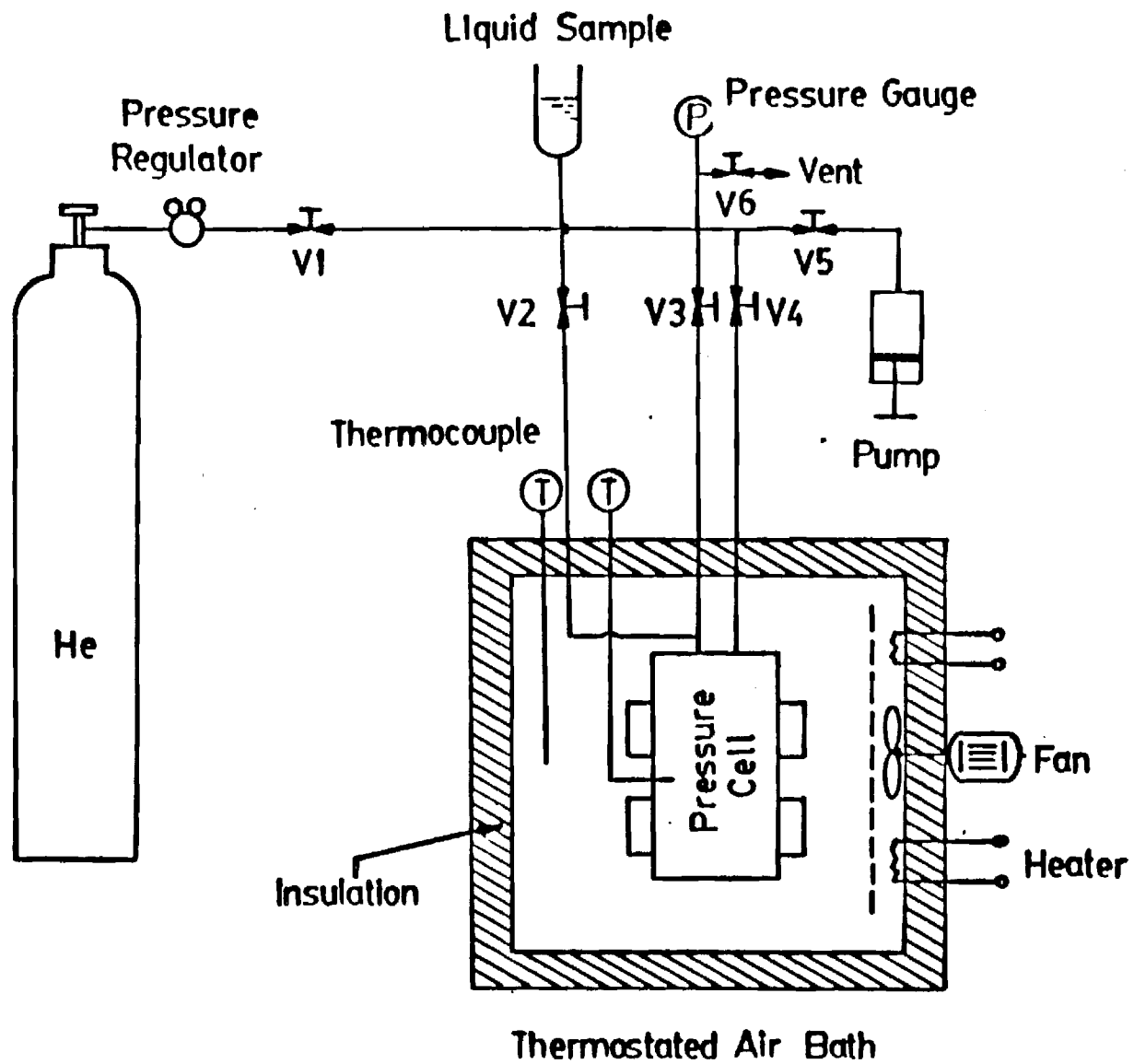


Figure 1. Schematic diagram of the high pressure viscometer.

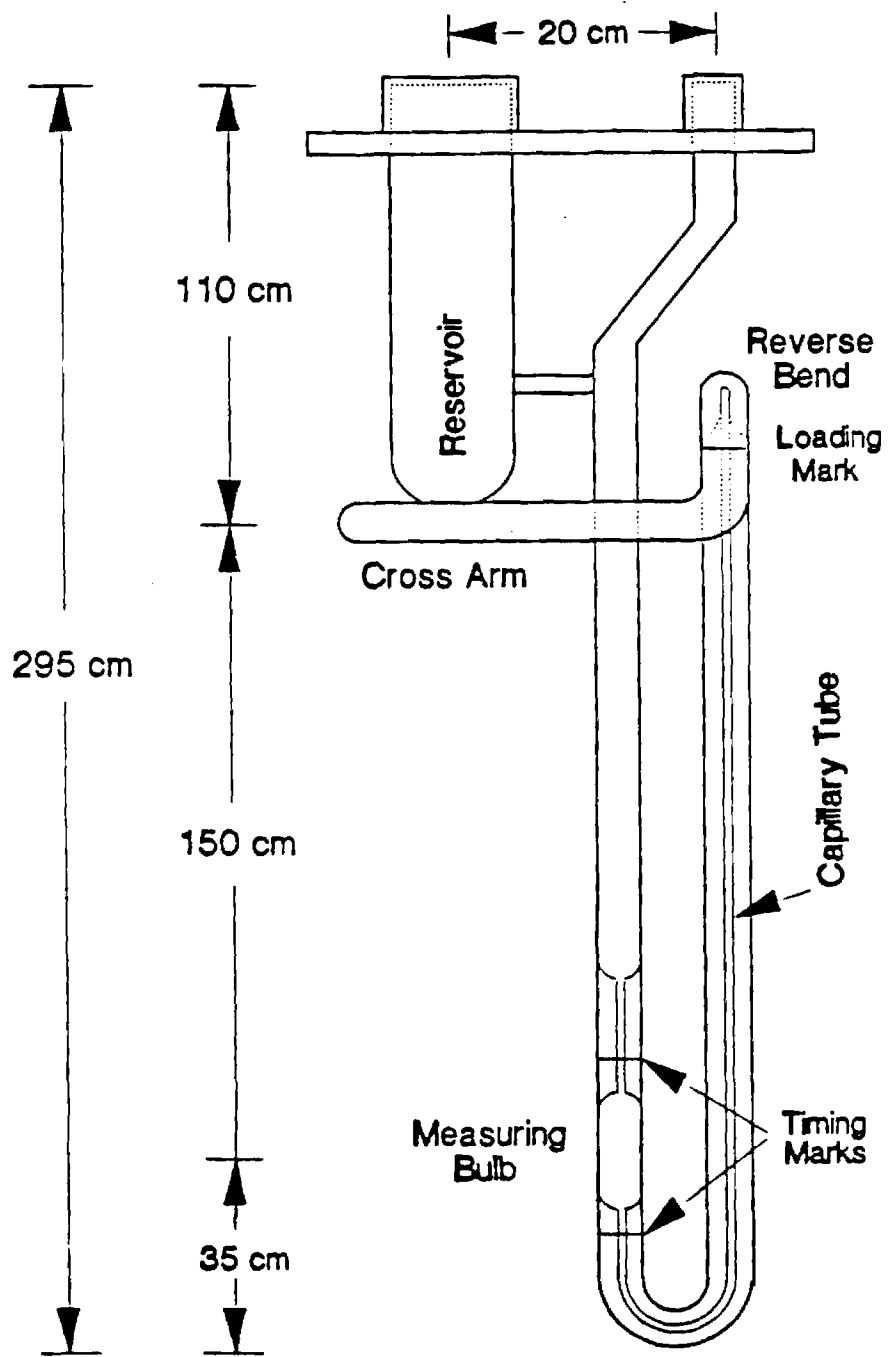


Figure 2. Zeitzuchs cross-arm viscometer.

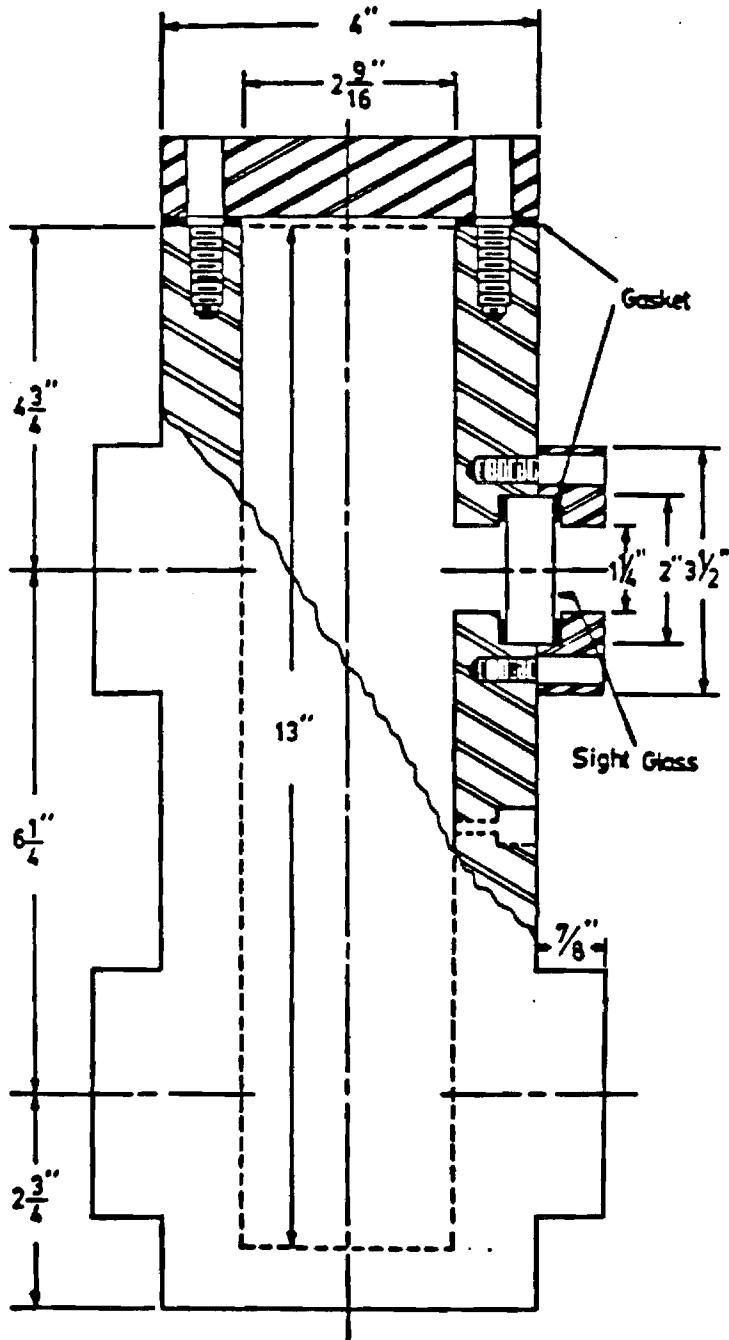


Figure 3. Detail design of the pressure cell.

VISCOSITY OF WATER

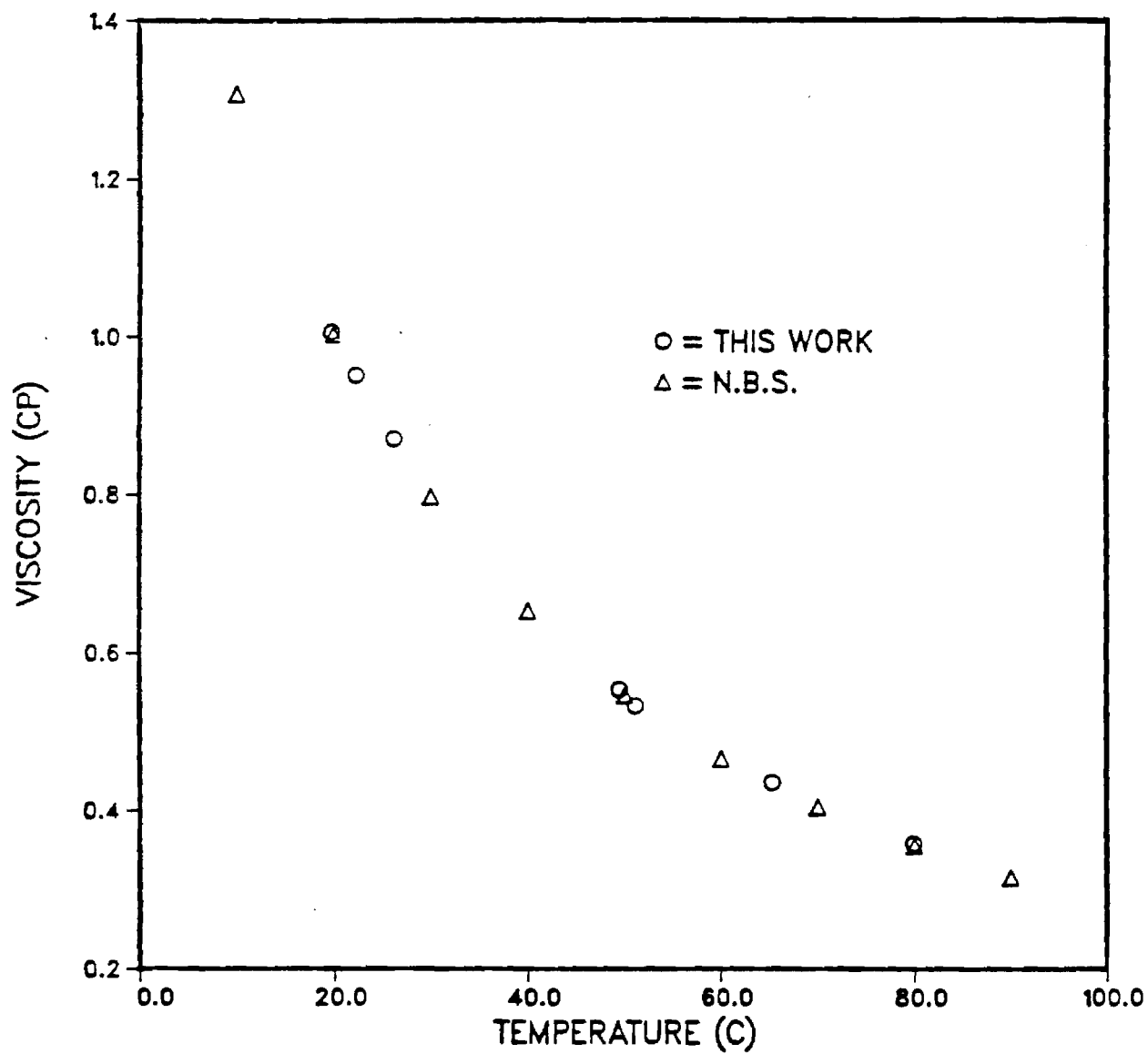


Figure 4. Viscosity of liquid water.

VISCOSITY OF AQUEOUS LiBr SOLUTION

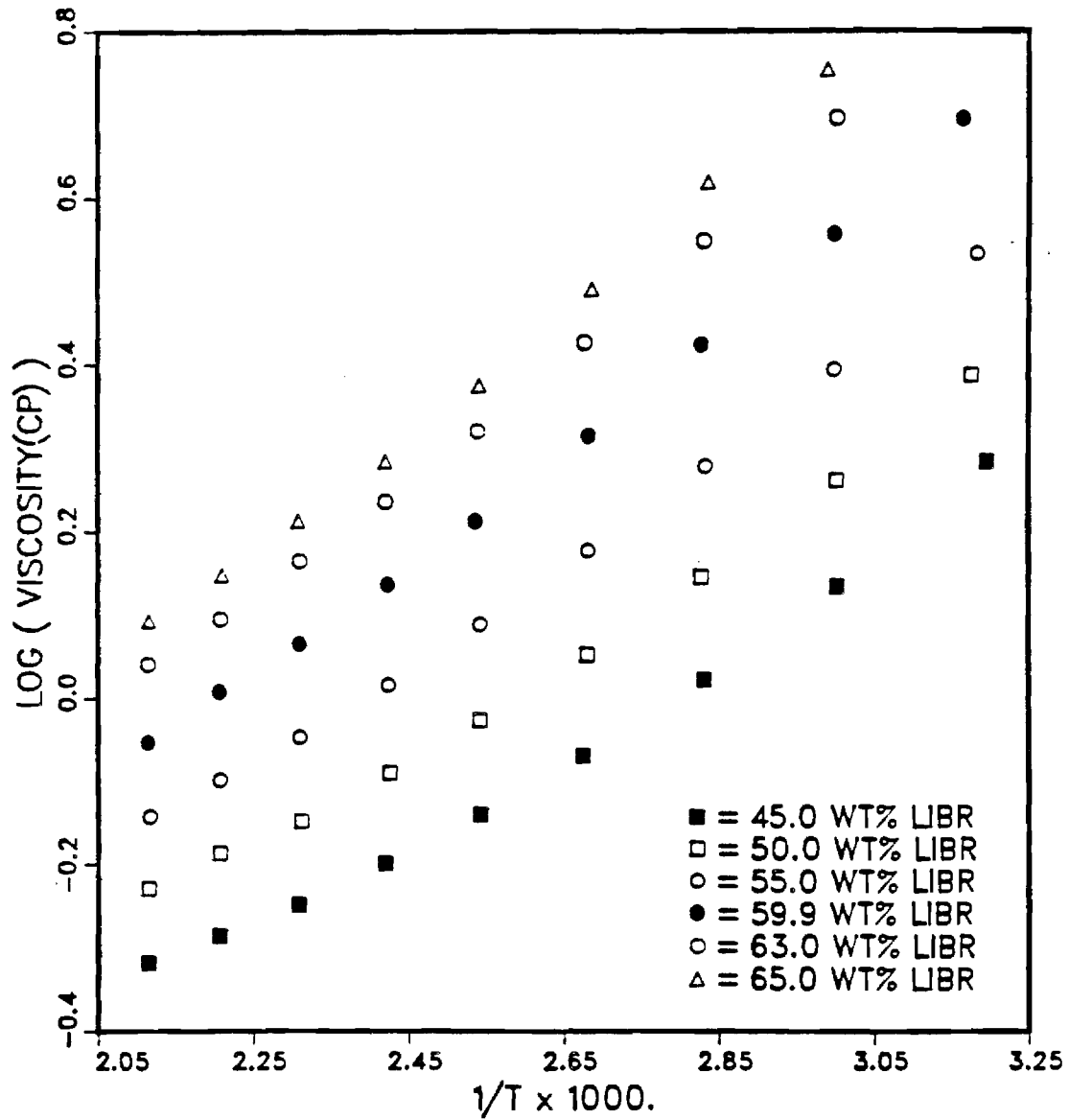


Figure 5. Viscosity of aqueous LiBr solutions.

VISCOSITY OF AQUEOUS LiBr SOLUTION

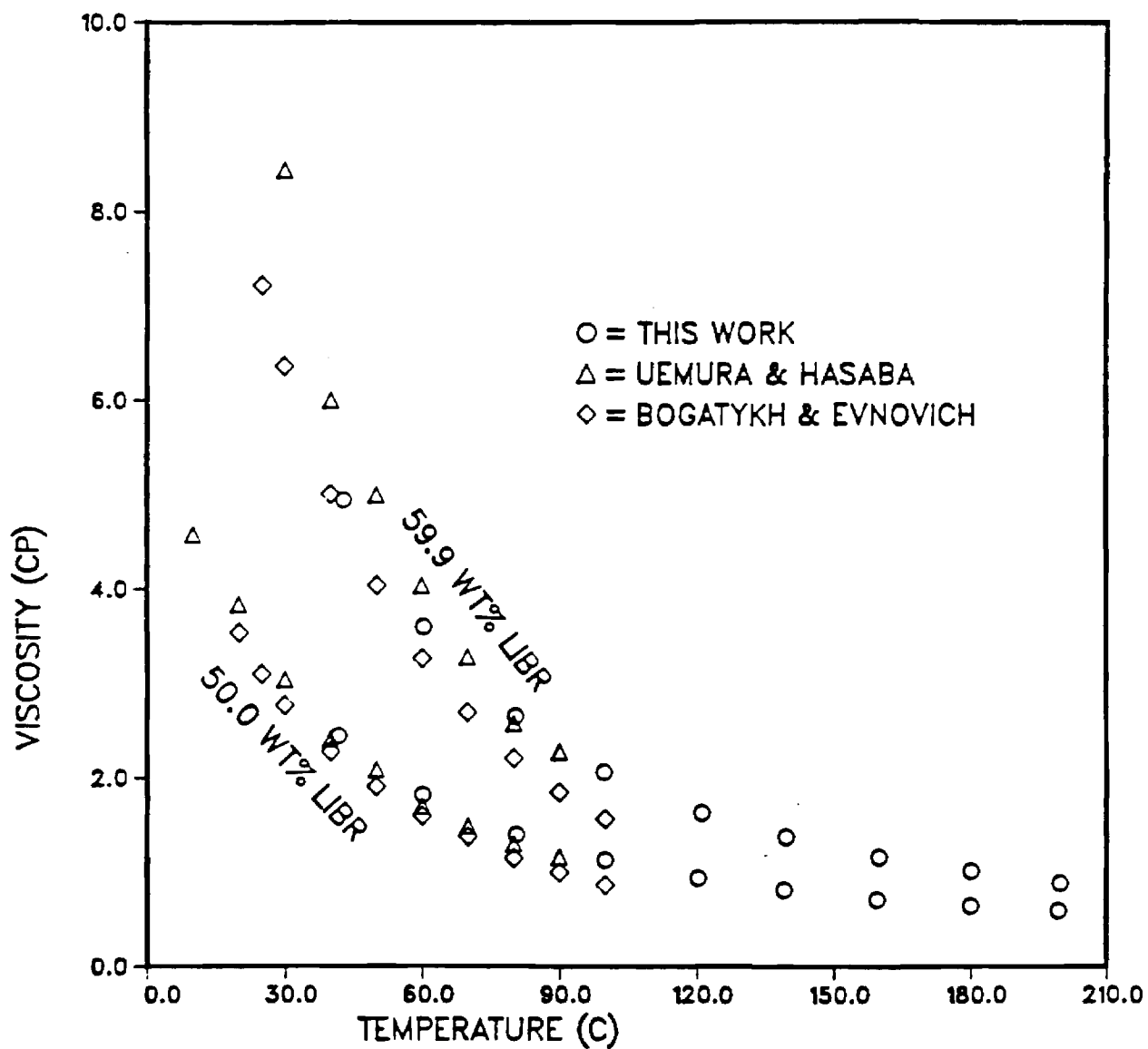


Figure 6. Comparison of the viscosity of LiBr - Water solutions obtained by different investigators.

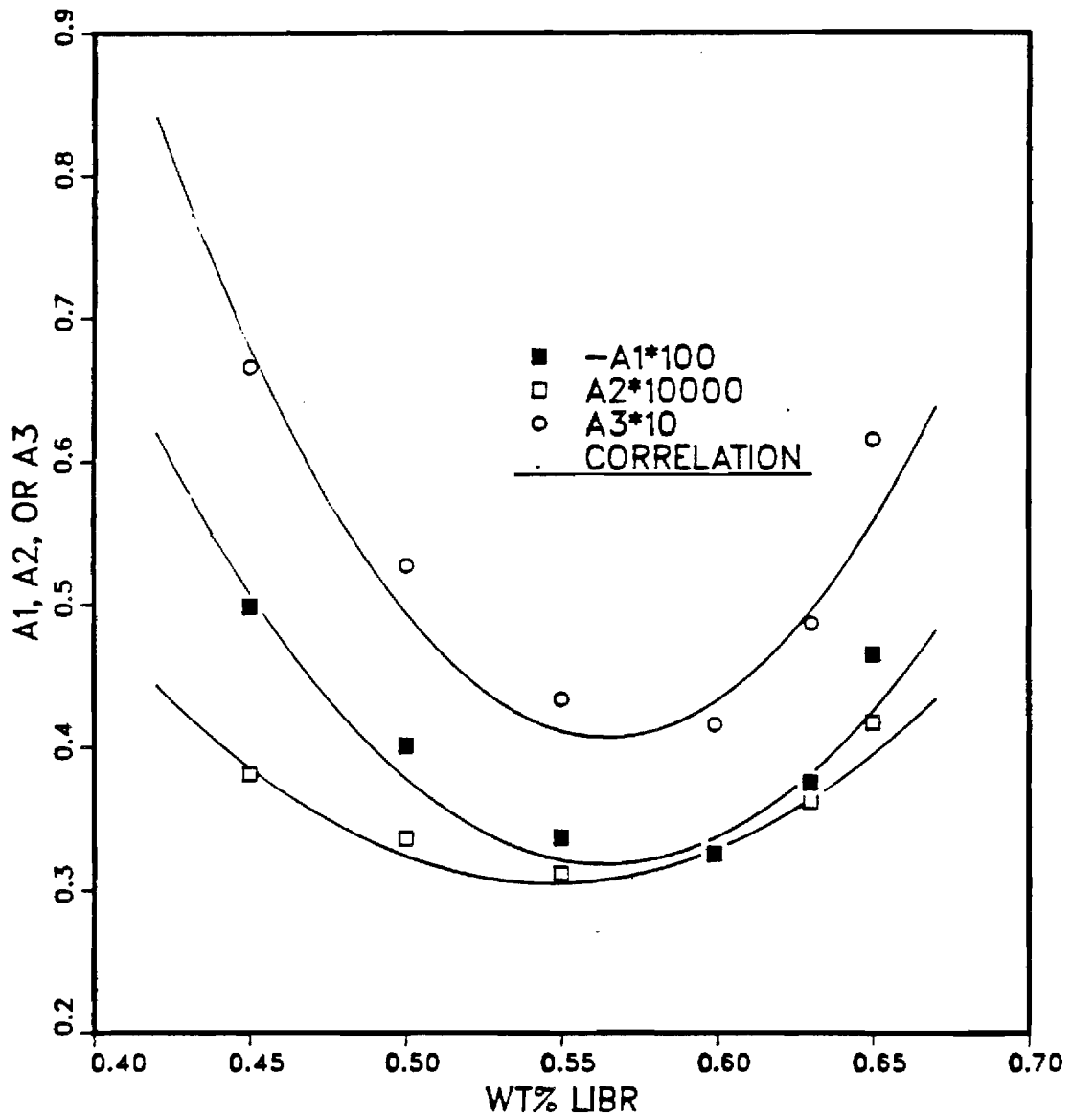


Figure 7. The values of A_1 , A_2 , and A_3 as a function of concentration.

VISCOSITY OF AQUEOUS LIBR SOLUTION

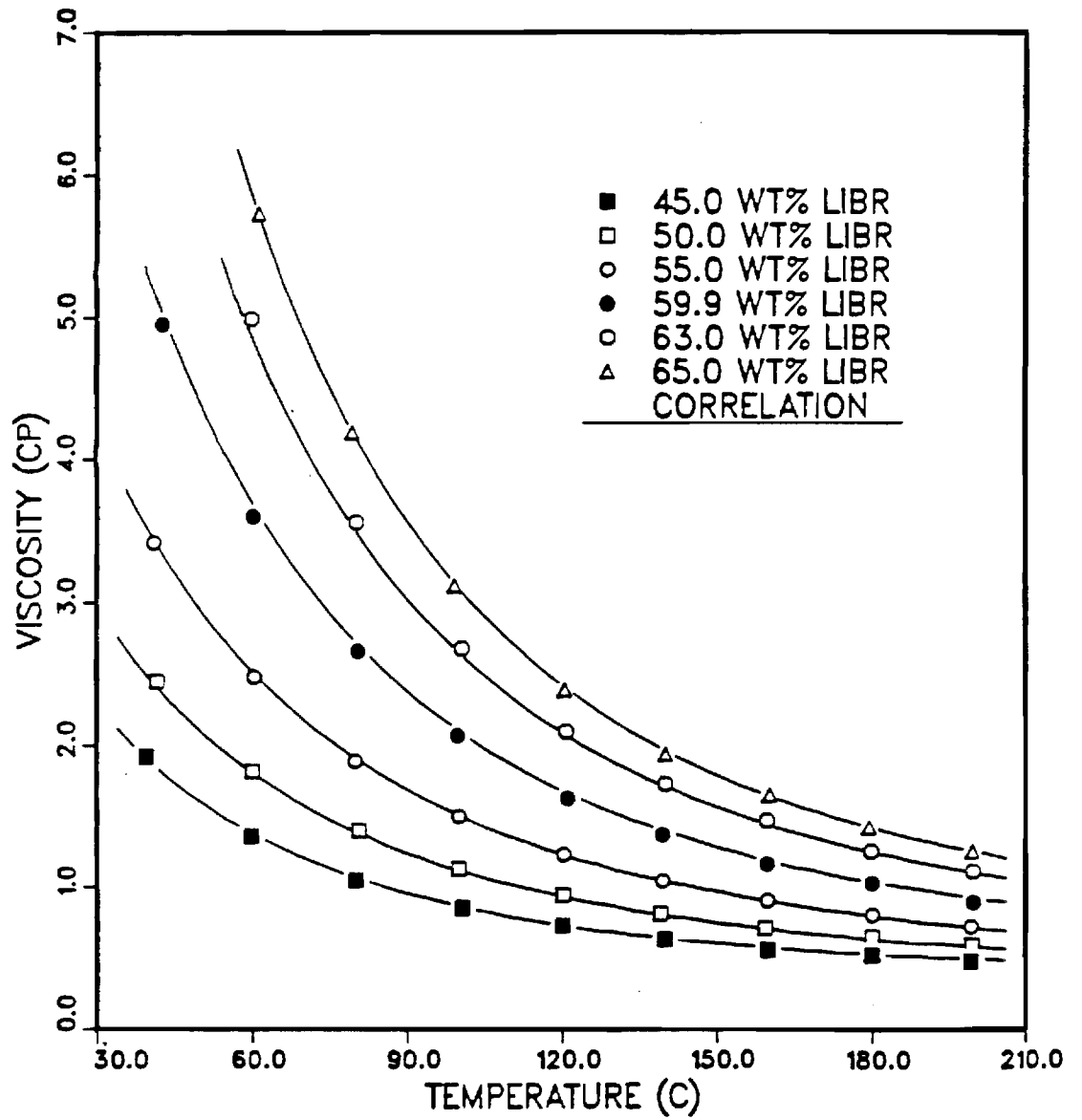


Figure 8. Comparison of the correlation with experimental data.

CHAPTER 5 SPECIFIC HEAT MEASUREMENTS

1. INTRODUCTION:

As originally proposed, the specific heat measurements were conducted using a modified drop calorimeter. Proper application of this instrument produces accurate values for average specific heats over a finite temperature interval. These average specific heats can be fitted to a suitable function, such as a polynomial, of the temperature and concentration. Continuous values for the specific heat over the temperature range can be obtained by differentiating the average specific heat function. This general procedure has been followed resulting in data from this investigation that is in good agreement with independent data. The new data presented herein are compared with data from two alternative and independent sources and the three sets of data are demonstrated to be mutually confirming. The data from the three mutually confirming sets are also compared with two older data sets and the newer data do not confirm the older measurements.

A schematic of the particular instrument used in this investigation is shown in Figure 1. A drop calorimeter implements the classical "method of mixing" in which the system being "mixed" (i.e. brought to thermal equilibrium) consists of a small, ca. 100 gm, capsule containing the sample and a large, ca. 15 kg, receiver. For the apparatus used in this investigation, the receiver is well insulated but not quite adiabatic. In addition to the sample capsule and receiver, a drop calorimeter comprises a heater section and auxiliaries and controls. In operation, the material sample is confined in the rigid capsule or "bomb". The capsule containing the sample is brought up to an elevated temperature in the tube heater and inserted, by dropping, into the receiver. The receiver is a massive metal block, a copper cylinder in this case, with a central well to accept the capsule. The heat interaction between the sample and receiver is then monitored by a temperature probe installed in the receiver.

Quantitatively, the heat interaction can be interpreted in terms of energy changes in the receiver and the sample by consideration of two closed thermodynamic systems. The first system is the combination of the receiver and the capsule, which is charged with the sample. The second system is the capsule and sample alone. With reference to the closed system consisting of the charged capsule and the receiver, one has the following total energy at the instant before a drop:

$$E_{\text{com},i} = U_{\text{cs}}(T_s) + PE_{\text{cs}} + U_r(T_{ri})$$

Where:

$E_{\text{com},i}$ = energy of the combined system at the initial state, i

$U_{\text{cs}}(T_s)$ = internal energy of the capsule and sample at drop temperature, T_s

PE_{cs} = potential energy of the capsule and sample which are elevated with respect to the receiver

$U_r(T_{ri})$ = internal energy of the receiver at its initial temperature, T_{ri} .

After the drop and later after the capsule, sample, and receiver have reached temperature equilibrium and have achieved a uniform final temperature, T_f , the energy is distributed as follows:

$$E_{\text{com},f} = U_{\text{cs}}(T_f) + U_r(T_f)$$

For the entire process beginning just before a drop and ending with temperature equilibrium, the principle of conservation of energy gives the following:

$$E_{\text{com},f} - E_{\text{com},i} + W_{\text{cs}} + W_r = Q_{\text{com}}$$

Where:

W_{cs} = work done by the capsule and sample during the process

W_r = work done by the receiver during the process

Q_{com} = heat interaction between combined system and its environment

Q_{com} is not quite zero, but a procedure to be explained below provides an empirical correction for a conditional assumption to be made that the combined system is adiabatic. Further simplifications are also possible. It can be verified that the change in potential energy of the sample due to its drop of about 0.5 meter is an entirely negligible .0049 kJ/kg. Additionally, the work terms can only involve boundary work on the atmosphere, $W_r = P_o \Delta V_r$ and $W_{\text{cs}} = P_o \Delta V_c$, and these quantities are also negligible. The potential energy change can be ignored, and the approximation that the combined system is adiabatic is now introduced. In consequence, the energy balance reduces to the following:

$$U_r(T_f) - U_r(T_i) + P_o \Delta V_r = - \{U_{\text{cs}}(T_f) - U_{\text{cs}}(T_s) + P_o \Delta V_c\}$$

or

$$\Delta H_r = - \Delta H_{\text{cs}}$$

Since the thermal expansion of both the receiver and capsule are entirely negligible, one could just as well write:

$$\Delta U_r = - \Delta U_{\text{cs}}$$

Clearly then, for the adiabatic case, the heat interaction from the capsule to the receiver, Q_x , is equal to the change in either the enthalpy or the energy of the sample and the capsule, or:

$$-Q_x = \Delta H_{\text{cs}} \text{ or } \Delta U_{\text{cs}}$$

Where the the indicated energy change is the sum of the component changes of the energies of the capsule and sample, or

$$\Delta U_{cs} = \Delta U_c + \Delta U_s$$

Proceeding from the assumption that the capsule undergoes an essentially constant volume process, the energy change of the sample, ΔU_s , can be readily evaluated. Ignoring the presence of a tiny quantity of air, the capsule can be considered to be filled with a known mass of fluid, m_s , such that:

$$V_s = m_s(v_f + x v_{fg})$$

Where V_s is the sample volume, 14.8 ml in this investigation.

Similarly, the internal energy of the sample is given as follows:

$$U_s = m_s(u_f + x u_{fg})$$

For a constant volume process proceeding from the initial sample temperature, T_s , and ending at T_f , the change in energy is as follows:

$$(U_s - U_f)/m_s = (u_{fs} - u_{ff}) + (x_s u_{fgs} - x_f u_{fgf})$$

Where:

u_{fs} = specific internal energy of the saturated liquid sample at T_s

u_{ff} = specific internal energy of the saturated liquid sample at T_f

x_s = quality of the sample at initial temperature, T_s

x_f = quality of the sample at final temperature, T_f

u_{fgs} = specific internal energy of evaporation of the sample at T_s

u_{fgf} = specific internal energy of evaporation of the sample at T_f

For a representative process, cooling a 12 gm sample of water from 200 C to 50 C, the first difference on the right is 641.33 kJ/kg while the second is around 1.02 kJ/kg. The influence of the phase change is only .0016 of the overall difference. Consequently, the heat effect on the sample can be considered to be just the change in energy of the saturated liquid. In terms of a heat capacity, the energy change can be quantified as the specific heat of the saturated liquid, often symbolized as " c_s ", as follows:

$$c_{s,ave} = (u_{fs} - u_{ff})/(T_s - T_f)$$

Generation of the saturated liquid specific heat data presented herein required a phased project beginning with a review of the pertinent literature, followed by upgrading and modifying the apparatus. The next steps were the development of a reliable experimental procedure and collecting the experimental data. The final step was the statistical analysis of the data and development of correlations for the average specific heats and the continuous specific heats. Work on the project has been proceeding since the summer of 1987. Preliminary work focused on a review of the pertinent literature. One source of data is especially well known, a dissertation by Löwer [1]. Specific heats at 50 WT% concentration from Löwer were relied upon by McNeely [2] in the production of enthalpy versus concentration and temperature charts. These charts were prepared

using a procedure developed by Haltenberger [3]. This procedure requires specific heats at only one concentration for the range of temperature along with vapor pressure data for the ranges of temperature and concentration. The data produced by McNeely have been fitted to a polynomial representation of the enthalpy by Patterson and Perez-Blanco [4]. Differentiation of these data provide an additional resource for specific heat data for ranges of temperature and concentration. A third alternative source is the previously unpublished data graciously provided by Dr. Uwe Rockenfeller, president of Rocky Research. An additional source of data is a report by Uemura and Hasaba [5] which includes data subsequently quoted elsewhere [6]. A final data source, by Pennington and Daetwyler [7], has been mentioned, but this data is for such a low temperature as to have no direct implication to the current work.

Our preliminary laboratory work involved rehabilitating the drop calorimeter, adapting it to this experiment, and interfacing to a personal computer (PC) based data acquisition system (DAS). The apparatus was functionally tested and found to be in basically good working condition. The receiver surface was oxidized after years of use so it was plated with a bright nickel alloy to minimize radiation losses. An attempt was made to repair the defective electromechanical printer that was supplied with the calorimeter. This was an effort to provide a redundant, independent data display in addition to the PC-based DAS to be used in production runs. This effort was not successful.

The next effort was to interface the calorimeter to the DAS. The DAS can accommodate calibrated thermocouple inputs as well as millivolt level inputs. A standard thermocouple input is used to monitor the sample temperature while in the furnace chamber. Precision resistance networks were constructed to condition the signal from the receiver thermistor. It was anticipated that initial runs would be made at low concentrations in open air while the heated enclosure necessary to elevate the calorimeter temperature to forestall phase change at high concentrations was under preparation. Consequently, it was necessary to design and build bridge circuits for two receiver temperature ranges, 0 to 40 C and 0 to 100 C.

Some upgrading of the calorimeter was accomplished to improve its performance and reliability. The most critical functional change is in the measurement of the sample temperature while the capsule is in the heater. In the original equipment design, a thermocouple is imbedded in the heating element outside the furnace tube. This arrangement is unsatisfactory for at least two reasons. Since the thermocouple is permanently installed, it cannot be removed for recalibration. Secondly, since the stock thermocouple is attached to the tube wall, it can not be assured that an accurate sample temperature measurement is being attained. To alleviate these problems, the apparatus was augmented with a calibrated thermocouple that is inserted directly into the capsule. To allow this access, a modified capsule was designed and fabricated. Some other minor improvements were made to insure the integrity of electrical connections, minimize mechanical problems caused by dust shedded from thermal insulation, and eliminate jams caused by interference between the heater tube and the capsule.

Some additional analytical work was also completed on the analysis of the receiver cooling curves and reduction of heat transfer data to energy changes and specific heats. These efforts completed our initial preparation and allowed for the initiation of the final tasks: development of the experimental procedure and collection of the data in production runs and analysis of the results and production of the property correlations.

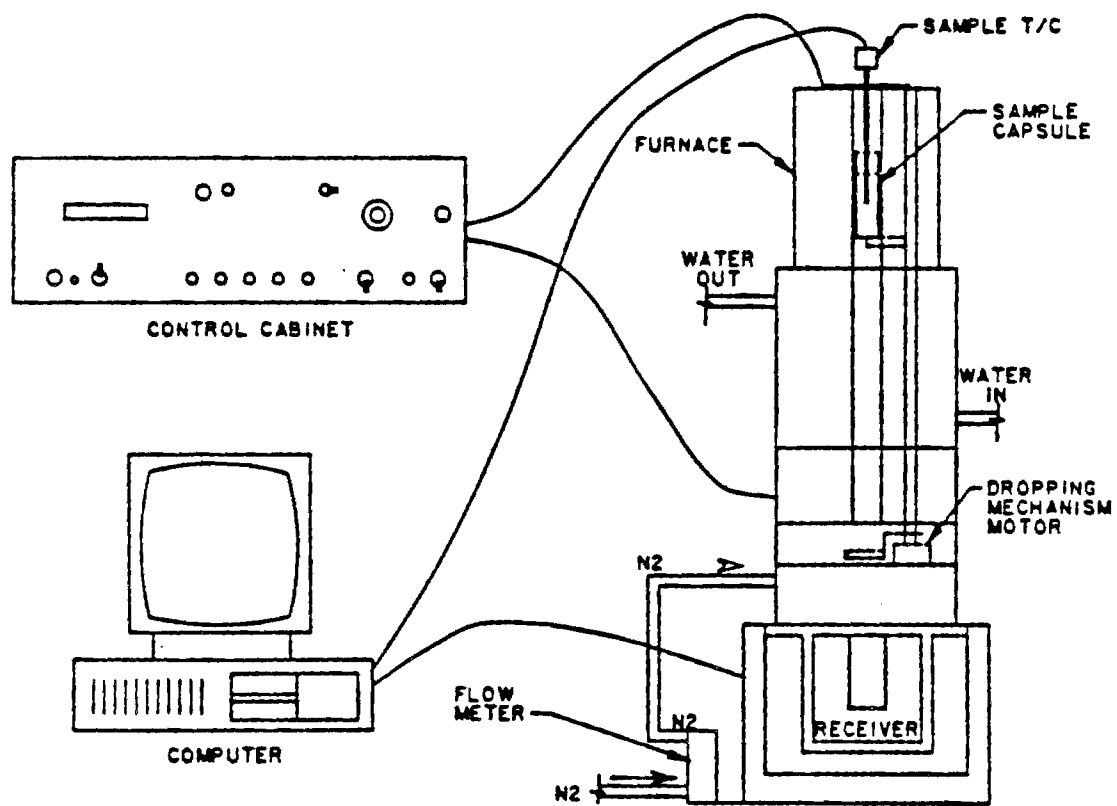


Figure 1. Schematic of Drop Calorimeter

2. EXPERIMENTAL DESIGN:

Experimental Apparatus. A single calorimeter, a Unitherm Model 7100 Drop Calorimeter, was used in all tests. For low concentrations, the calorimeter was operated in open air in the laboratory. For the higher concentrations, 60 WT% and 65 WT% by weight of LiBr, the calorimeter was operated in an elevated temperature enclosure as shown in Figure 2. The addition of the heated enclosure was necessary to prevent a phase transition to a crystalline hydrated complex, $\text{LiBr} \cdot n\text{H}_2\text{O}$, when the concentrated solutions are cooled to near room temperature. The enclosure was also thought desirable to provide a temperature stable environment.

Obtaining an accurate sample temperature is thought to be one of the important challenges in drop calorimetry. In the design of the original equipment, the sample thermocouple is installed outside the tube heater. This location is undesirable because the thermocouple cannot be removed for calibration and because an unknown temperature gradient must exist between the heater and capsule. To enhance this measurement, the capsule was modified to include a removable thermocouple well as shown in Figure 3. The entire construction is stainless steel. The thermowell port also serves as the capsule spout, and the thermowell tube serves as the stopper. A standard two piece, ring and ferrule, compression fitting secures the thermowell tubing. This reliable high pressure fitting can be reused indefinitely providing an inexpensive, leak-free assembly. In addition to the operational advantages, the integral thermowell has two thermometric advantages. In the modified design, the sample thermocouple can readily be removed for calibration and, as importantly, the thermocouple is immersed within the sample providing a highly accurate measure of the sample temperature. The sample thermocouple output from the DAS was calibrated by comparison with a field standard platinum RTD (Leeds and Northrop platinum resistance thermometer, Serial No. 709892) in a Muller bridge. The field standard RTD is traceable to the International Practical Temperature Scale in force when it was manufactured, the IPTS-48, and has been adjusted to correspond to IPTS-68, the current standard. Note that the calibration procedure used the production DAS in the calibration step. This allowed for the entire sample temperature measurement subsystem, including the thermocouple and its reference temperature compensation circuit as well as the instrumentation amplifier and ADC in the DAS, to be calibrated simultaneously. This overall calibration, while somewhat more demanding and inflexible than calibrating all the components individually, should allow for improved accuracy as calibration compensation is provided at once for all the critical measuring components and not just the temperature probe alone.

The other critical temperature measurement is the receiver temperature. For the present purposes, it is most important that the receiver temperature probe produce a linear response over the range of expected use, around 20 C to 30 C in open air or around 50 C to 60 C in the enclosure. A commercially packaged thermistor pair in a parallel arrangement with compensating resistors, similar to the manufacturers original equipment, was selected for the receiver temperature sensor. Semiconducting thermistors exhibit decreasing electrical resistance with increasing temperature. This resistance

change can be measured as a voltage change in a suitable auxiliary circuit. The parallel, compensated arrangement of the thermistors produces a very nearly linear temperature dependence in the overall resistance. This linear response is important for drop calorimetry. Circuits for both temperature ranges are similar. In the higher temperature device, the resistance is converted into a voltage signal in an external voltage divider with a nominal sensitivity of 6.7 mV/C°. The voltage divider was further incorporated into a Wheatstone bridge to allow the establishment of an arbitrary zero output voltage near 0 C. The completed circuit and DAS were calibrated by comparing computer output of the voltage with the field standard platinum RTD with the resulting relation:

$$T_r = 148.5964 \text{ (C/volt)} V_{\text{DAS}} + 5.781795 \text{ C}$$

This response allows service over a range of 5.8 C (at $V_{\text{DAS}} = 0$) to 80 C (at $V_{\text{DAS}} = 500$ mV) since the analog to digital converter will be used with a span of 0 to 500 mV. The temperature range is more than adequate in this or similar applications. The calibrated sensitivity of 6.73 mV/C° provides a resolution of .001 C°/count in the receiver temperature with the 16 bit ADC in use here. This is about .05 % of the expected temperature change in a typical drop and represents the limit of accuracy in the system due to resolution. In the room temperature device, a sensitivity of 9.92 mV/C° was obtained for a similar resolution of .0008 C°/count and an operating temperature range of 0 to 50 C.

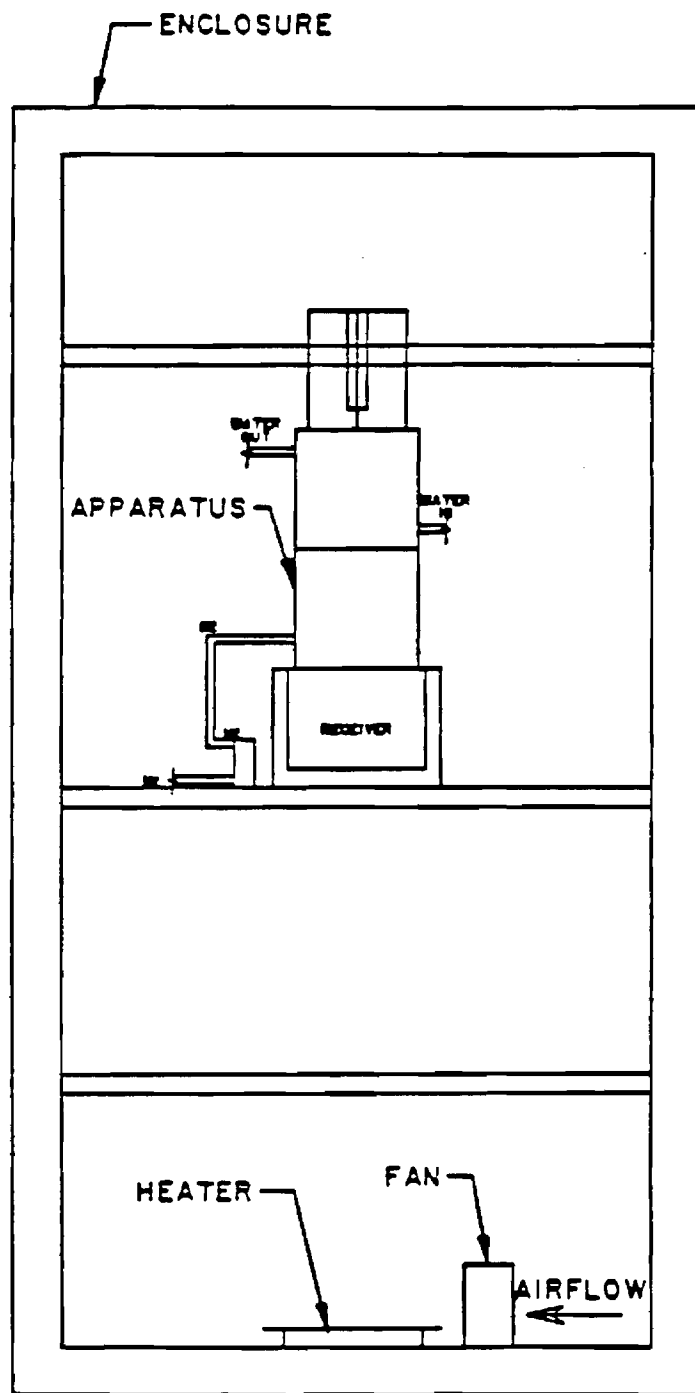
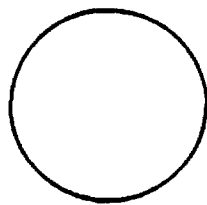
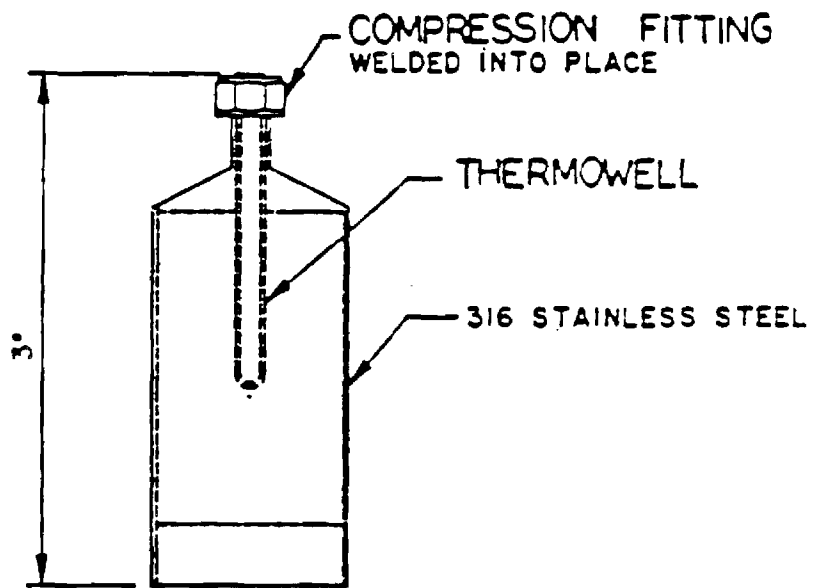


Figure 2. Drop Calorimeter in Temperature Controlled Enclosure



BOTTOM VIEW

Figure 3. Sample Capsule with Integral Thermowell

Experimental Procedure. The most crucial aspects of the experimental procedure are loading an accurate and appropriate mass of sample in the capsule and establishing stable sample and receiver temperatures before a drop and maintaining a stable environmental temperature during a drop.

The sample volume has been determined gravimetrically, using water, to be around 14.8 ml. A sample mass should be installed such that after thermal expansion a small ullage space remains as it is a practical impossibility to seal the capsule against the expansion of a compressed liquid. Typically, a volume of around 12 to 13 ml is installed. A minimal ullage volume is preferable primarily to maximize the mass of the sample and thereby increase the temperature response of the receiver and secondarily to reduce the effect of vaporization. The capsule is accurately weighed before and after installation of the sample to accurately determine the mass of the sample and to monitor against the possibility of leaks. No leaks have been observed in practice.

Establishing stable temperatures begins with the initial preparation for a drop with the receiver lowered after a previous drop. It is first necessary to return the receiver to near its environmental temperature whether this is room temperature or, preferably, the enclosure temperature. In the enclosure, it was found desirable to ventilate the exposed receiver with a small fan. Usually it was convenient to ventilate the receiver for several hours to allow complete cooling. During this cooling process, it is desirable to proceed with installing the sample capsule in the tube heater and preheating the sample. If the sample is preheated while the receiver is being ventilated, the heater will operate only intermittently later after the receiver has been raised and even later after the sample drop. Excessive operation of the sample heater later is likely to disturb the temperatures in the receiver or in the enclosure.

After the receiver is cooled and the sample preheated, the receiver is raised to its operational position where it is ready to accept the dropped capsule. Heat leak from the heater to the receiver cannot be eliminated by the insulation, water jacket, and cover gas so it is typical for the temperature of a properly cooled receiver to rise slightly subsequently to raising the receiver. In contrast, a receiver improperly left too warm from a previous drop will continue to cool even after being raised. It is critical to minimize any temperature drift prior to a drop. Otherwise the results of the drop will be impaired. Typically, the receiver is left in the raised position for at least 90 minutes to reestablish a stable receiver temperature. Prior to a drop, the receiver temperature should be closely monitored. Usually, the receiver temperature is studied for 10 minutes before the drop to verify a stable condition.

Once stable temperatures in the heated sample and receiver have been established, it is appropriate to drop the sample into the receiver. The drop mechanism can then be activated. The drop pin and insulated shutter move to allow the capsule to enter the receiver and then quickly return to their original position to allow the insulated shutter to continue to prevent excessive heat leak from the furnace tube to the receiver.

After the drop, the receiver temperature is monitored for several hours until the receiver has passed through its temperature maximum and is well along its cooling curve. For reference, the DAS continues to monitor the enclosure and room temperatures. After the cooling period, the temperature data is retrieved for further analysis.

3. DATA REDUCTION AND ANALYSIS:

Data reduction and analysis involves two steps, cooling curve analysis to determine the ultimate heat transfer from the capsule to the receiver followed by interpretation of the heat interaction in terms of calibration data for the capsule and receiver.

The cooling curve analysis results in an estimate of the ultimate temperature which would be reached by the receiver in the absence of heat loss. With this correction, the receiver, capsule, and sample constitute the adiabatic combined system envisaged as the principle of operation of the drop calorimeter. The correction is illustrated in Figure 4. The numerical procedure is as follows:

1. Identify the time, t_{\max} , at which the maximum temperature is reached. For accuracy, this is done by fitting a smooth quadratic curve through the 10 data points nearest the peak and solving for the peak time and temperature analytically.
2. Next, identify the slope of the temperature versus time curve, also called the temperature drift, at some convenient instant. This slope should be evaluated well after the maximum so that the temperature drift due to heat loss from the receiver to the ambient is dominant and its trend is well established. A convenient time is $2 \cdot t_{\max}$. Numerically this is done by fitting a straight line through the 11 data centering on $2 \cdot t_{\max}$.
3. The temperature drift is next extrapolated backwards to a unique time after the drop at which time the extrapolated temperature is predicted to equal the ultimate receiver temperature that would have been achieved in a perfectly adiabatic process. The time suggested, [8] and [9], for this evaluation corresponds to the time at which the receiver has attained 60 % of its observed maximum value. Analysis of a thermal resistance network containing two lumped capacitances presented in [10] confirms this suggestion for the parameters of the drop calorimeter used in these measurements.
4. The temperature computed from the extrapolated drift, T_f , is used as the final temperature for the capsule and sample as well as the receiver. Note that this correction has the advantage of being strictly based on physical observations and current conditions, such as the temperature difference between the receiver and ambient, and should provide at least a first order correction for any casual environmental influences.

The cooling curve analysis also identifies the initial sample temperature, T_s , and the initial receiver temperature, T_{ri} . In later modifications, a linear fit was applied to minimize the effect of any initial drift or irregularity in these two measurements. The heat interaction is interpreted in terms of heat capacities from the following result of the energy balance:

$$-\Delta U_{cs} = (C_c + C_{sam})(T_s - T_f) = \Delta U_r = C_r(T_f - T_{ri})$$

Where:

C_c = the average heat capacity, $m \cdot c_{ave}$, of the capsule
 C_{sam} = the average heat capacity of the sample
 C_r = the average heat capacity of the receiver

Then solving for the average heat capacity of the sample:

$$C_{sam} = C_r(T_f - T_{ri}) / (T_s - T_f) - C_c$$

Upon introducing the experimentally convenient ratio, $K_{cr} = C_c/C_r$, which is the ratio of the average heat capacity of the capsule to that of the receiver one has:

$$C_{sam} = C_r(T_f - T_{ri}) / (T_s - T_f) - C_r K_{cr}$$

The specific heat of the saturated liquid sample can then be determined from the mass of the sample and its average heat capacity:

$$c_{s,ave} = C_{sam} / m_s$$

Clearly, the specific heat determination requires the two calibration values, C_r and K_{cr} . The values are determined as functions of the experimental conditions to further enhance accuracy in accord with the procedure suggested in [11]. The heat capacity ratio, K_{cr} , is determined by a series of empty capsule calibration drops. For a zero mass sample, the combined energy balance gives:

$$K_{cr} = C_c/C_r = (T_f - T_{ri}) / (T_s - T_f)$$

The results for a range of furnace temperatures, T_s , were correlated against the sample temperatures with the following results:

For the open air system:

$$K_{cr} = .0000088 T_s + .011551$$

For the temperature controlled enclosure:

$$K_{cr} = .0000085 T_s + .01149$$

The slight temperature dependency of this ratio is not necessarily due to thermal property differences alone but can also account for heat leaks from the furnace to the receiver during drops, when the insulated shutter is momentarily open, and any (much smaller) heat leak following the drop.

The heat capacity of the receiver can be calibrated by either a "relative" or an "absolute" procedure. An absolute calibration would rely on electric heating of the receiver and the subsequent temperature response. While the electric energy input can obviously be determined with great precision, the success of an absolute calibration is entirely dependent on a full understanding and characterization of the systematic behavior of the calorimeter. Accounting for systematic errors in the form of heat leaks between the

receiver and the ambient and the heater is enormously challenging; consequently, a relative calibration was adopted. In a relative calibration, the response of the receiver to a reference sample is measured. Two stable and well characterized materials were used as the reference substances, alumina and water. According to the energy balance, the receiver heat capacity for a calibration drop when the reference sample has a specific energy change of $u_{ref}(T_s)$ to $u_{ref}(T_f)$ is given by:

$$C_r = m_s [u_{ref}(T_s) - u_{ref}(T_f)] / [(T_f - T_{ri}) - K_{cr}(T_s - T_f)]$$

In accordance with the suggested procedure, C_r in units of kJ/K, was correlated against the overall temperature change of the receiver with the following results:

For the open air system:

$$C_r = 4.321664 + .052339 \Delta T_r$$

For the system in temperature controlled enclosure:

$$C_r = 4.312143 + .019233 \Delta T_r$$

The variation of apparent heat capacity of the receiver as explained by the receiver temperature change is unlikely to bear much relation to thermodynamic property changes since the receiver temperature rise is only a couple of degrees at most. More likely, this effect comes from a somewhat enhanced heat leak to the environment in higher temperature drops as well as from residual variation in the leak leak from the heater not accounted for by the K_{cs} correlation.

The calibration procedure described above represents one of the obstacles to rapid specific heat evaluations using the drop calorimeter since the entire calibration procedure for both K_{cr} and C_r should be repeated if the capsule or any other critical component such as the temperature sensors or their signal conditioning and data conversion circuits must be changed or significantly altered. In this investigation the calorimeter environment was changed once along with the receiver temperature circuit. This necessary change doubled the effort required for calibration. Obtaining stable initial conditions and collecting data for the extensive cooling curve analysis present another drawback. Several hours of phased cooling of the exposed receiver and an hour or two or more of temperature stabilization of the raised receiver must precede every drop, and several hours of monitored receiver response must follow the drop. Consequently, not even a single drop can be completed in an ordinary working day, and it takes considerable coordination to arrange for a drop to be prepared during the day and completed overnight. The resulting data rate, especially if allowing for interrupted data and spoiled drops, is not very high. An advantage is, however, that the physical principles of the device are simple and well founded in thermodynamic fundamentals. Another advantage is that an average specific heat is obtained which represents the behavior of the sample over a broad range, e.g. 100 Celsius degrees or more, on each drop.

The experimental data are presented in Tables 1 through 5 which present the measured average specific heat data, at specified concentrations near 45 WT%, 50 WT%,

55 WT%, 60 WT% and 65 WT%. Also tabulated are the initial and final sample temperatures T_s and T_f and the average temperature for the drop, $T_{ave} = (T_s + T_f)/2$.

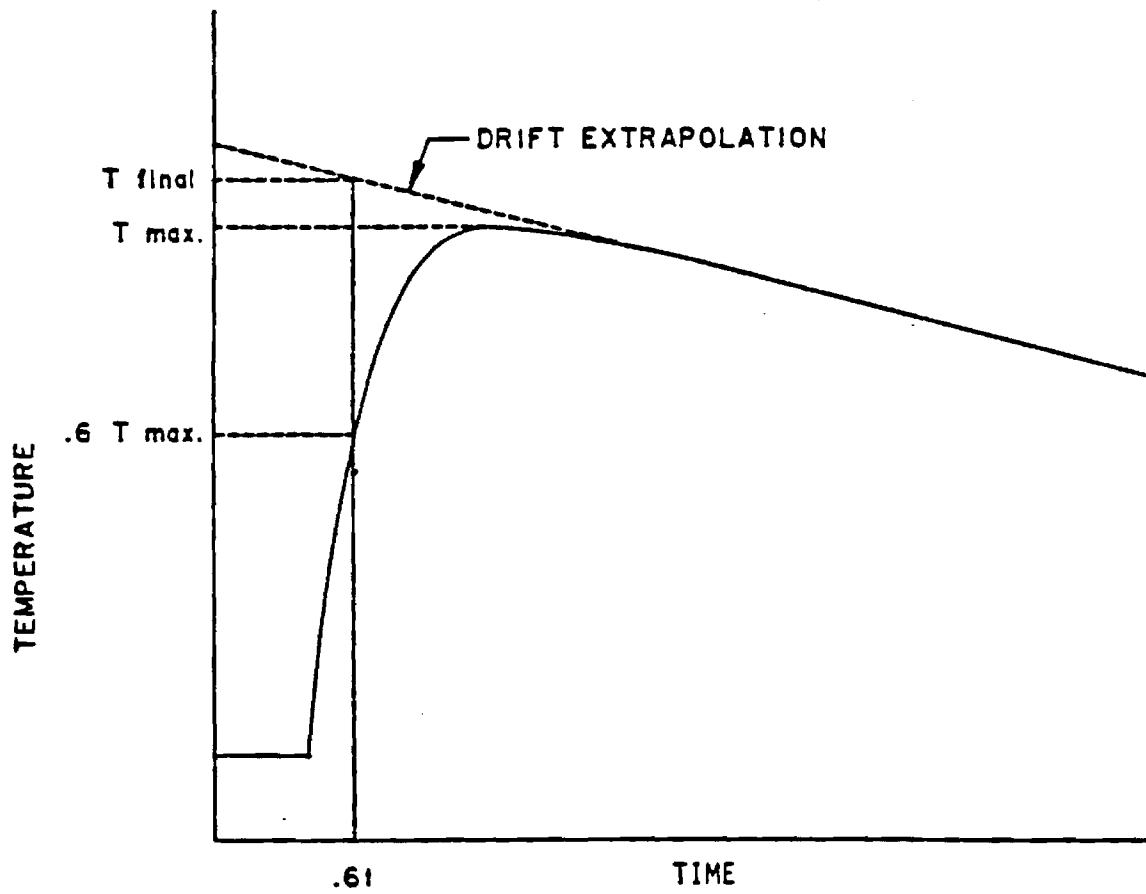


Figure 4. Graphical Representation of Cooling Curve Analysis

Table 1.
Average Specific Heat Results
for Concentrations near 45 WT%

Mass Fraction	Average Temperature	Average Specific Heat	Final Temperature	Sample Temperature
0.4395	61.9125	2.1924	23.741	100.084
0.4395	62.566	2.3932	25.193	99.939
0.4395	81.747	2.2153	25.345	138.149
0.4395	89.781	2.3525	26.454	153.108
0.4395	90.456	2.4056	26.627	154.285
0.4395	100.5785	2.4956	26.614	174.543
0.4395	114.605	2.3915	28.039	201.171
0.4395	105.7915	2.3589	28.402	183.181
0.4395	113.103	2.4931	25.701	200.505
0.4395	65.237	2.3546	25.603	104.871
0.4395	75.818	2.2437	26.324	125.312
0.4395	71.082	2.1682	25.461	116.703
0.4395	114.5565	2.5604	29.214	199.899
0.4395	84.36055	2.3824	49.0448	119.6763
0.4395	121.4709	2.3117	53.0417	189.9001
0.4395	121.4293	2.39	53.1895	189.669

Table 2.
Average Specific Heat Results
for Concentrations near 50 WT%

Mass Fraction	Average Temperature	Average Specific Heat	Final Temperature	Sample Temperature
0.5059	64.9115	2.4772	25.309	104.514
0.5059	85.564	2.3021	27.102	144.026
0.5059	108.394	2.2599	28.781	188.007
0.5059	71.2325	2.059	26.785	115.68
0.5059	93.616	2.2912	28.739	158.493
0.5059	116.522	2.3296	29.971	203.073
0.5059	78.5505	2.113	27.687	129.414
0.5059	101.093	2.3024	28.666	173.52
0.5059	64.6	2.029	23.094	106.106

Table 3.
Average Specific Heat Results
for Concentrations near 55 WT%

Mass Fraction	Average Temperature	Average Specific Heat	Final Temperature	Sample Temperature
0.541	68.3	2.0767	20.92	115.68
0.541	98.0085	1.9805	23.51	172.507
0.541	92.3355	2.1271	26.043	158.628
0.541	76.532	2.0097	23.988	129.076
0.541	87.2585	2.1565	25.443	149.074
0.541	114.661	2.167	27.089	202.233
0.541	64.459	1.949	22.281	106.637
0.541	71.3375	2.1536	22.449	120.226
0.541	105.565	2.2025	23.905	187.225
0.541	102.4675	2.0443	23.404	181.531

Table 4.
Average Specific Heat Results
for Concentrations near 60 WT%

Mass Fraction	Average Temperature	Average Specific Heat	Final Temperature	Sample Temperature
0.5948	88.001	1.8122	57.88	118.122
0.5948	95.21	1.9684	58.381	132.039
0.5948	103.0425	1.9254	59.318	146.767
0.5948	109.453	2.1008	61.387	157.519
0.5948	110.8975	2.0566	60.638	161.157
0.5948	117.207	1.9555	59.784	174.63
0.5948	118.488	2.0738	61.439	175.537
0.5948	126.6605	2.0113	63.731	189.59
0.5948	132.867	2.0438	62.42	203.314
0.5948	133.33	1.8606	62.593	204.067

Table 5.
Average Specific Heat Results
for Concentrations near 65 WT%

Mass Fraction	Average Temperature	Average Specific Heat	Final Temperature	Sample Temperature
0.6483	110.465	1.8476	60.796	160.134
0.6483	133.0425	1.7396	62.231	203.854
0.6483	100.1705	1.6356	59.307	141.034
0.6483	114.8285	1.7726	59.708	169.949
0.6483	127.694	1.7973	61.996	193.392
0.6483	104.864	1.6391	59.178	150.55
0.6483	120.3965	1.815	61.057	179.736
0.6483	87.973	1.4063	57.891	118.055
0.6483	126.0605	1.9652	62.222	189.899
0.6483	95.731	1.5161	59.539	131.923
0.6548	151.1252	1.863	62.4005	239.85
0.6548	150.1908	1.8308	60.3816	240.00
0.6548	149.7689	1.8518	59.7178	239.82
0.6548	150.0077	1.8587	59.9455	240.07
0.6548	150.5762	1.8237	60.5924	240.56
0.6548	125.1235	1.9023	58.637	191.61
0.6548	125.051	1.801	58.9119	191.19
0.6548	125.0617	1.8494	60.1435	189.98
0.6548	99.5894	1.8114	56.3988	142.78

4. CORRELATION OF DATA:

Inspection of the available data indicates that a polynomial temperature dependence constitutes an adequate model. For this behavior, the general dependence of the specific heat on temperature, T , is of the form:

$$c_s = a + b \cdot T$$

for a linear dependence on temperature, and

$$c_s = a + b \cdot T + c \cdot T^2$$

for a quadratic dependence.

In either case the coefficient functions can be polynomials in the salt concentration such as the following general formula:

$$a = \sum a_k \cdot w^k, \text{ with } k = 0 \text{ to } n.$$

In the current experimental work, statistically valid values for n were limited to 1 or 2 while in some numerical work quoted below values for n as large as 5 were used. As discussed below, no statistical support was found for a quadratic temperature dependence compared with the linear relationship; consequently, consideration of the models which are linear in temperature will be emphasized. In the preceding relationships, the coefficient functions, a and b and c , can be functions of the concentration. Herein, the concentration will be expressed in terms of mass fraction, w , of the salt (i.e. $0 < w < 1.0$). Both linear and quadratic functions of concentration, and combinations, have been investigated. Expanding the coefficient functions, the relationships that are linear in temperature can have one of the following functional forms:

A linear-linear (in w) model:

$$c_s = (a_0 + a_1 w) + (b_0 + b_1 w)T$$

A quadratic-linear model:

$$c_s = (a_0 + a_1 w + a_2 w^2) + (b_0 + b_1 w)T$$

A quadratic-quadratic model:

$$c_s = (a_0 + a_1 w + a_2 w^2) + (b_0 + b_1 w + b_2 w^2)T$$

For quantitative comparison, the following model quadratic in temperature was also considered:

T-Quadratic model:

$$c_s = (a_0 + a_1 w + a_2 w^2) + (b_0 + b_1 w + b_2 w^2)T + c_0 T^2$$

Regression calculations were performed on the four preceding models with the results tabulated in Table 6. In this table, salient statistical results are presented for each model. The first statistical result is the Coefficient of Determination which is the ratio of the variation explained by the model to the total variation in the data set. The balance of the variation is called the residual variation. The residual variation is due to any systematic or random errors in the data as well as any inadequacy in the model. Including extra parameters augments the model. An example of augmenting a model is shifting from a linear to a quadratic model. Any augmentation of the model is sure to decrease the residual variation because an additional term always provides some additional adaptability. In consequence, an enhanced model must result in a better fit to the data base, but unending augmentation of the model is not justifiable. According to the preceding results, the model with both coefficients linear in the concentration, the linear-linear model, is the only model linear in temperature that remains significant at the probability criterion well under .05, a conventional limit. The model with a leading term that is quadratic in composition and a coefficient function multiplying the temperature that is linear in composition, the quadratic-linear model, is marginally significant in a statistical sense. The model that has both coefficient functions quadratic in composition, the quadratic-quadratic model, is clearly insignificant statistically. In the last case, the additional parameter has reduced the residual variation so little that one can ascribe the minimal reduction merely to reduced random variation. Some reduction is guaranteed when the model is enhanced; but, when small, the better fit cannot be ascribed to an improved systematic fit to the data. The model quadratic in temperature is also not significant at a .05 level. This implies that the improvement in the Coefficient of Determination obtained by expanding the model to include the quadratic temperature term is no better than a random improvement. In addition, the Standard Error of Estimate is not improved at all. Furthermore, results from other investigations provide no support for a model quadratic in temperature. Therefore, it is the linear-linear model, the model that is linear in temperature with both coefficient functions linear in composition, that is the most likely model considering both the statistical and physical evidence. For any of the models with linear dependence on temperature such as the first three models, the average specific heat has the following especially simple form:

$$c_{s,ave} = a + b(T_s + T_f)/2$$

or using the linear-linear model as an example,

$$c_{s,ave} = (a_0 + a_1 w) + (b_0 + b_1 w)T_{ave}$$

This simple dependence conveniently allows even average specific heat data to be plotted as a function of the average temperature on a two dimensional graph. Figures 5, 6, 7, and 8 illustrate the correlation lines for all three linear models superimposed on the entire data set.

The linear-linear correlation results are plotted in Figures 9 to 13 for the five different concentrations. Plotted along with the correlation lines are confidence limits above and below the correlation line displaced by the amount of the Standard Error of Estimate. There is, unfortunately, some significant scatter in the data so the confidence limits are rather broad. Note that the error estimates are on the order of .10 kJ/kg. This uncertainty is about 5% of the typical value of the specific heat which is around 2 kJ/kg. Finally, the preferred, linear-linear, correlation model at evenly spaced values of the LiBr concentration is shown in Figure 14. Also shown in this figure is the c_p curve for water determined from quadratic interpolation of results from a program [12] that reproduces the 1967 version of the ASME Steam Tables. Note that the steady increase in c_p with temperature as exhibited by water is mimicked by the similar increase for the LiBr solutions.

Note that for completeness the correlation lines and correlation lines with error limits for the quadratic-linear and quadratic-quadratic models have been plotted and are included in an appendix. The coefficients for all three models are given in Table 7.

Table 6.

CORRELATION RESULTS FROM DROP CALORIMETER DATA

Model	Coefficient of Determination*	Statistical Significance Level**	Standard Error of Estimate***	
Linear-Linear	.839594	ca. 0.	.0968	(ca. 4.8%)
Quadratic-Linear	.847687	.09	.0951	(ca. 4.8%)
Quadratic-Quadratic	.848925	.50	.0956	(ca. 4.8%)
T-Quadratic	.854556	.15	.0955	(ca. 4.8%)

* The Coefficient of Determination, R^2 , is the ratio of the unexplained variation to the total variation in a population for which a regression model has been developed. The total variation is the sum, $\sum (y_i - y_{ave})^2$, where y_i is the i th value of the dependent variable. The explained variation is the difference between the total variation and the residual variation, where the residual variation is the sum, $\sum (y_i - y_m(x_i))^2$, where y_m is the statistical model corresponding to the i th datum, y_i , which is evaluated at the i th value of the independent variables. A model that results in a perfect fit to the experimental data gives 1 for the Coefficient of Determination.

** The Statistical Significance Level is the probability, $P(z > t)$, that a random variable with some appropriate distribution, z , is greater than some pertinent value, t . In the current case, the appropriate distribution is the Student-t distribution and the pertinent value t is evaluated as follows:

$$t = \left[\frac{\Delta(R^2) \cdot DF}{1 - R^2} \right]^{\frac{1}{2}}$$

Where $\Delta(R^2)$ is the increase in R^2 due to the model

$$\Delta(R^2) = R^2(\text{enhanced model}) - R^2(\text{simpler model})$$

As an example, for a quadratic model:

$$\Delta(R^2) = R^2(\text{quadratic model}) - R^2(\text{linear model})$$

For the linear model use the special case:

$$\Delta(R^2) = R^2(\text{linear model}) - 0$$

DF = degrees of freedom

DF = number of data points - number of parameters

A high value of t leads to a low value of $P(z > t)$ and implies that an enhanced model, such as a quadratic model compared with a linear model, does not improve the R^2 merely by reducing some of the random model but provides a better systematic fit to the data.

*** The Standard Error of Estimate is analogous to the Standard Deviation from the mean of a simple distribution in that 68% of the data are expected to lie within one Standard Error of Estimate of the regression line.

Table 7

Coefficients for Three Models Linear in Temperature

Coefficient: Symbol Multiplies		Algebraic Formulation of Model:		
		Linear- Linear	Quadratic- Linear	Quadratic- Quadratic
a_0		3.067819	1.938608	-.26642
a_1	w	-2.15232	2.692092	10.97101
a_2	w^2		-5.165042	-12.7661
b_0	T	0.006018	.002953	.02502
b_1	wT	-.00731	-.000805	-.08334
b_2	w^2T			.07541

Figure 5.

Linear-Linear Model with Data

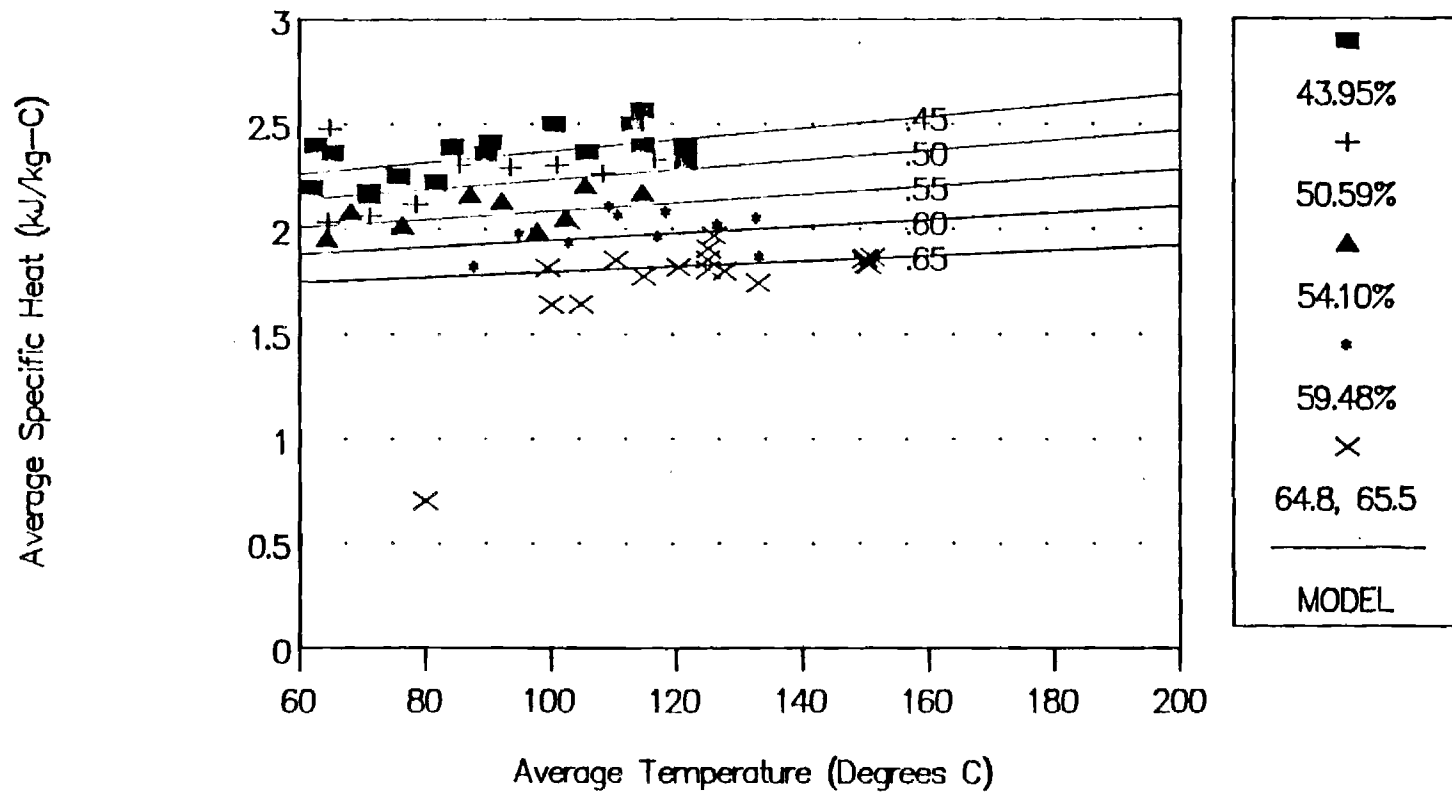


Figure 6. Data and Linear-Linear Model
at Concentrations Similar to Data

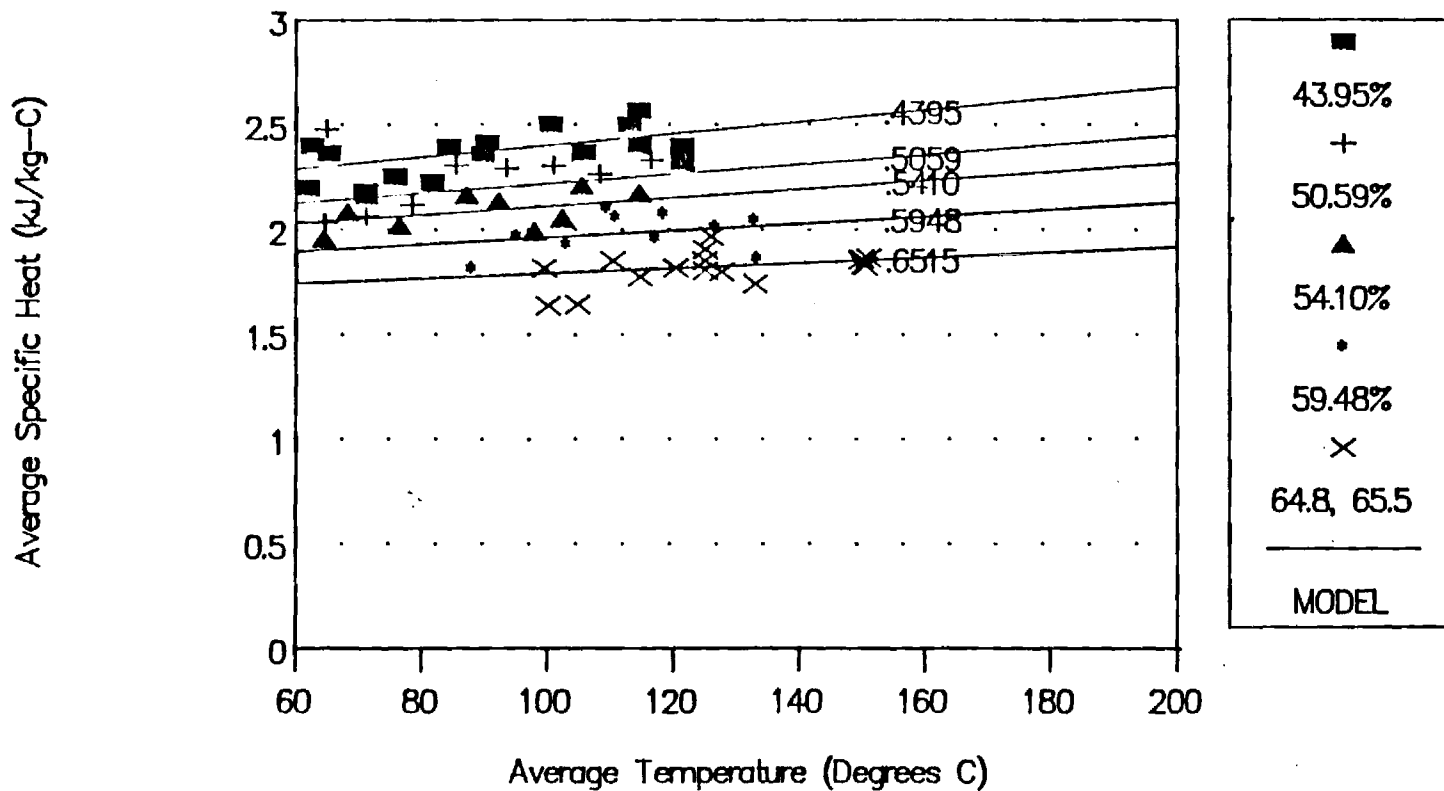


Figure 7.

Quadratic-Linear Model with Data

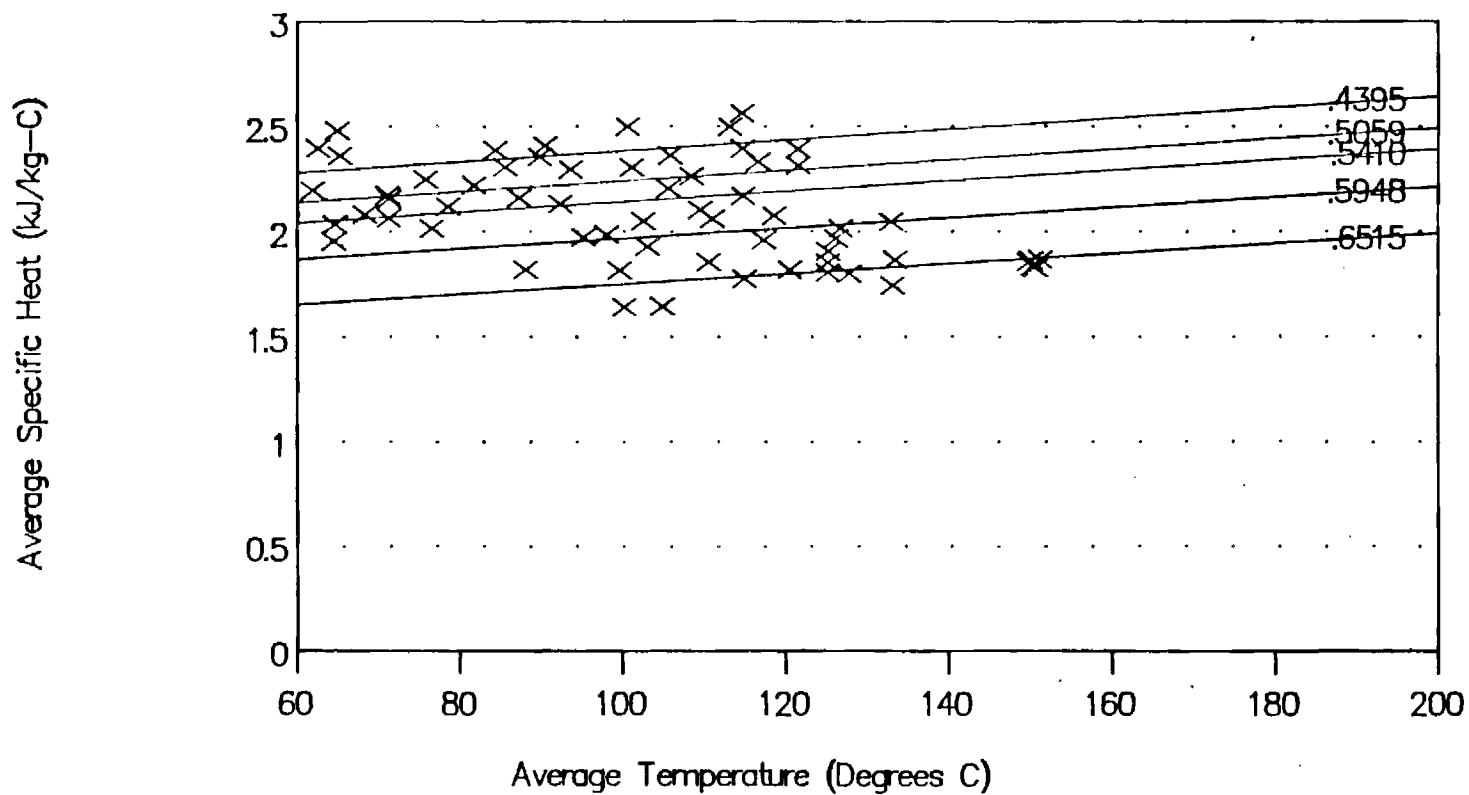


Figure 8.

Quadratic-Quadratic Model with Data

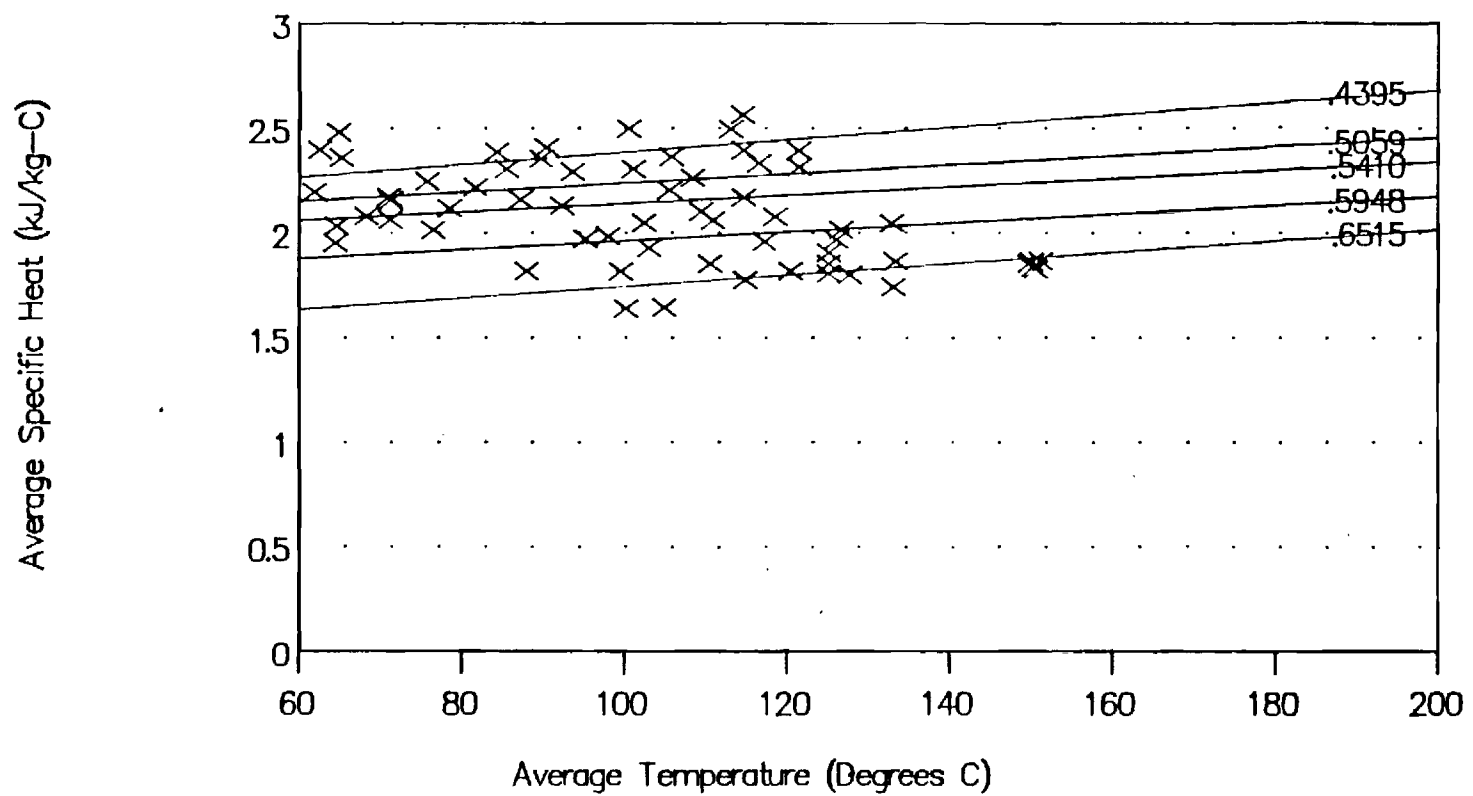


Fig. 9: 43.95% LiBr by weight

Linear-Linear Correlation

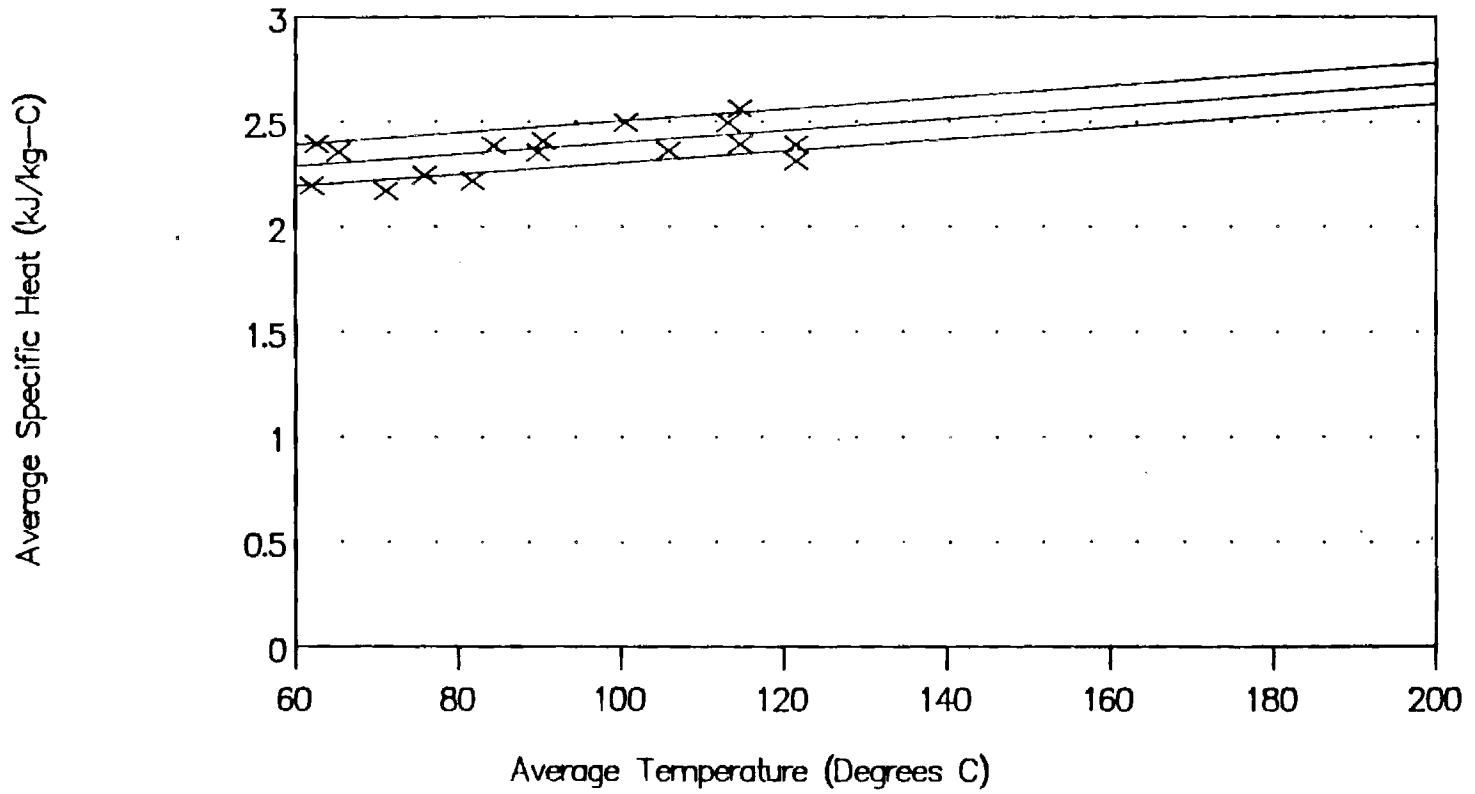


Fig. 10: 50.59% LiBr by weight

Linear-Linear Correlation

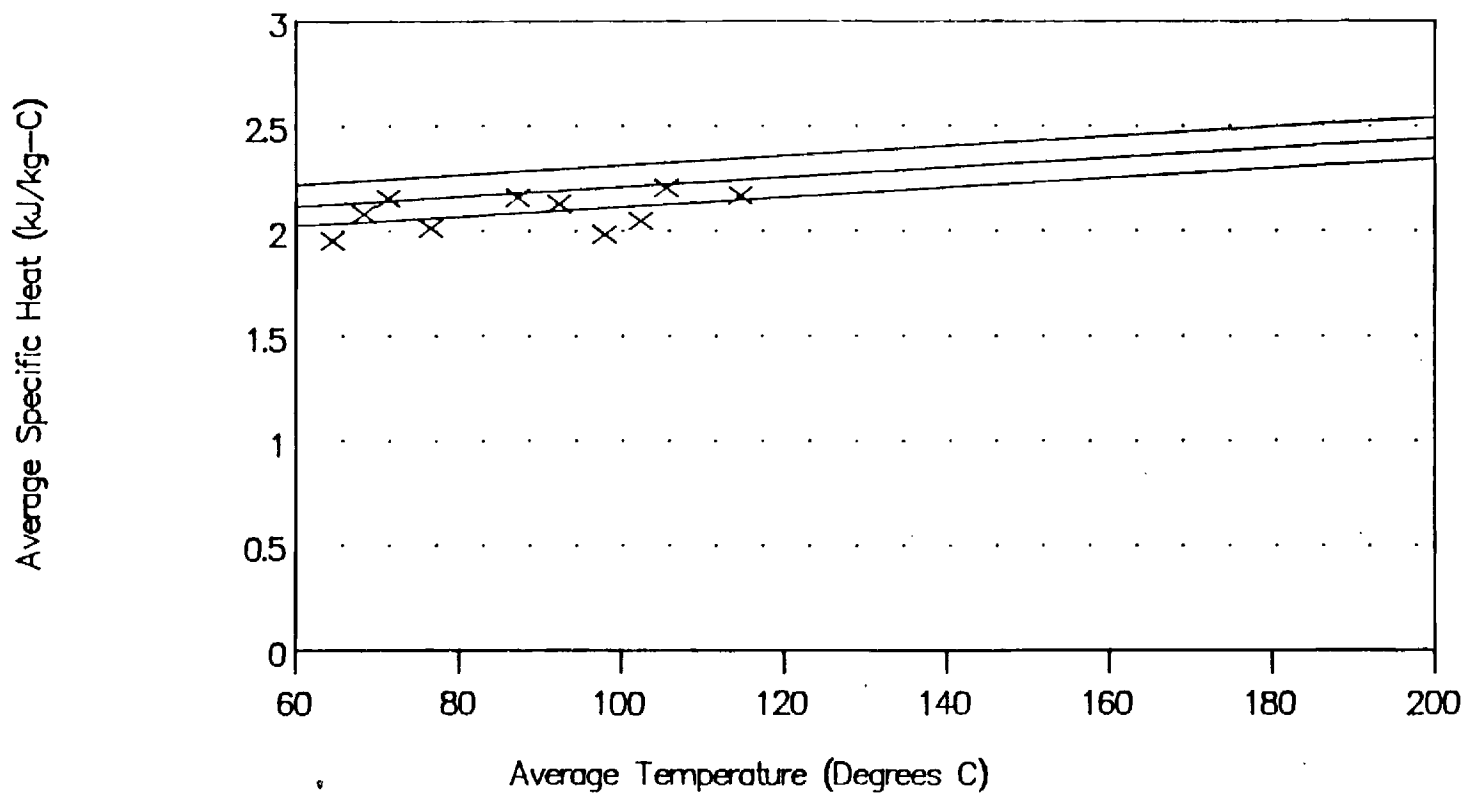


Fig. 11: 54.10% LiBr by weight

Linear-Linear Correlation

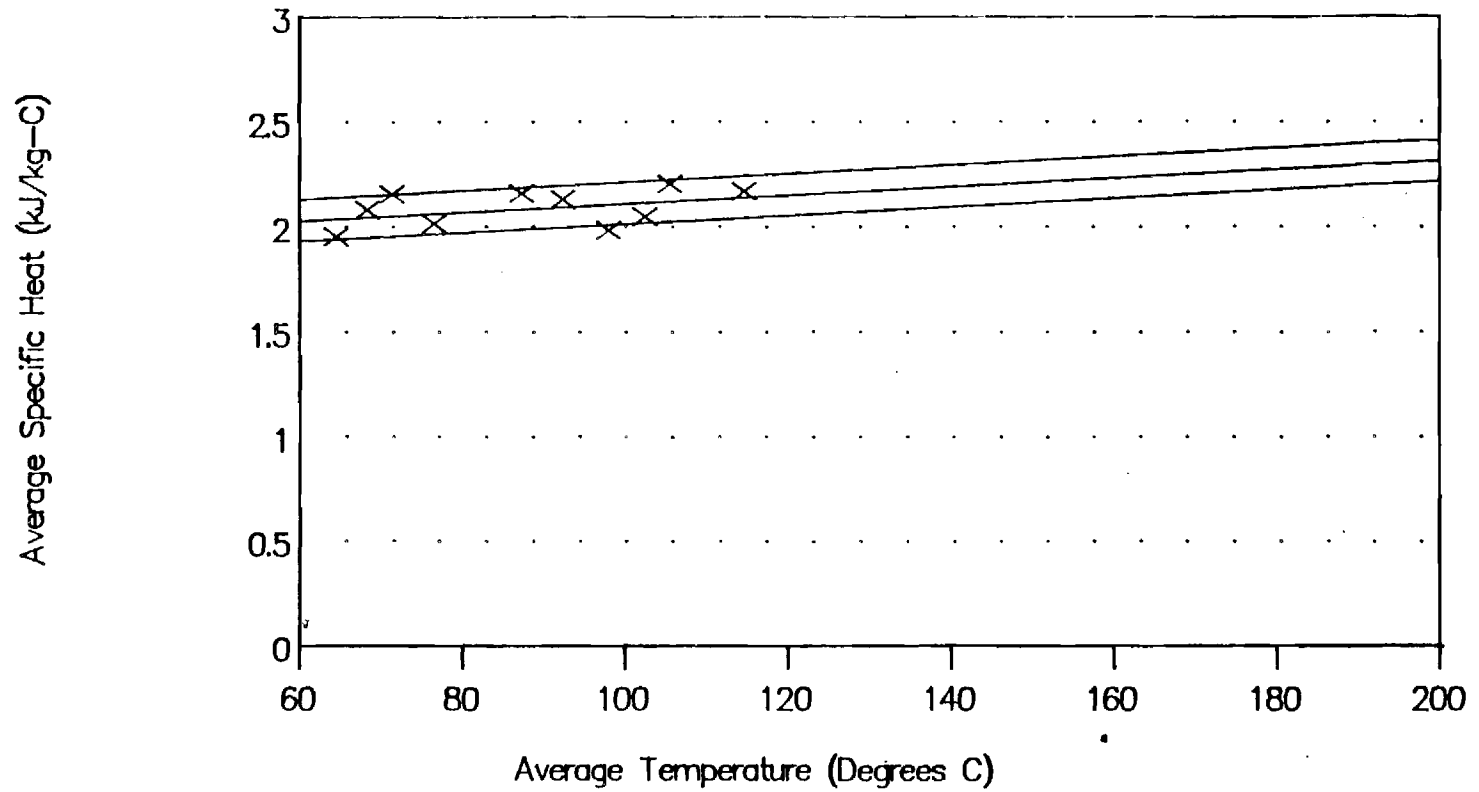


Fig 12: 59.48% LiBr by weight

Linear-Linear Correlation

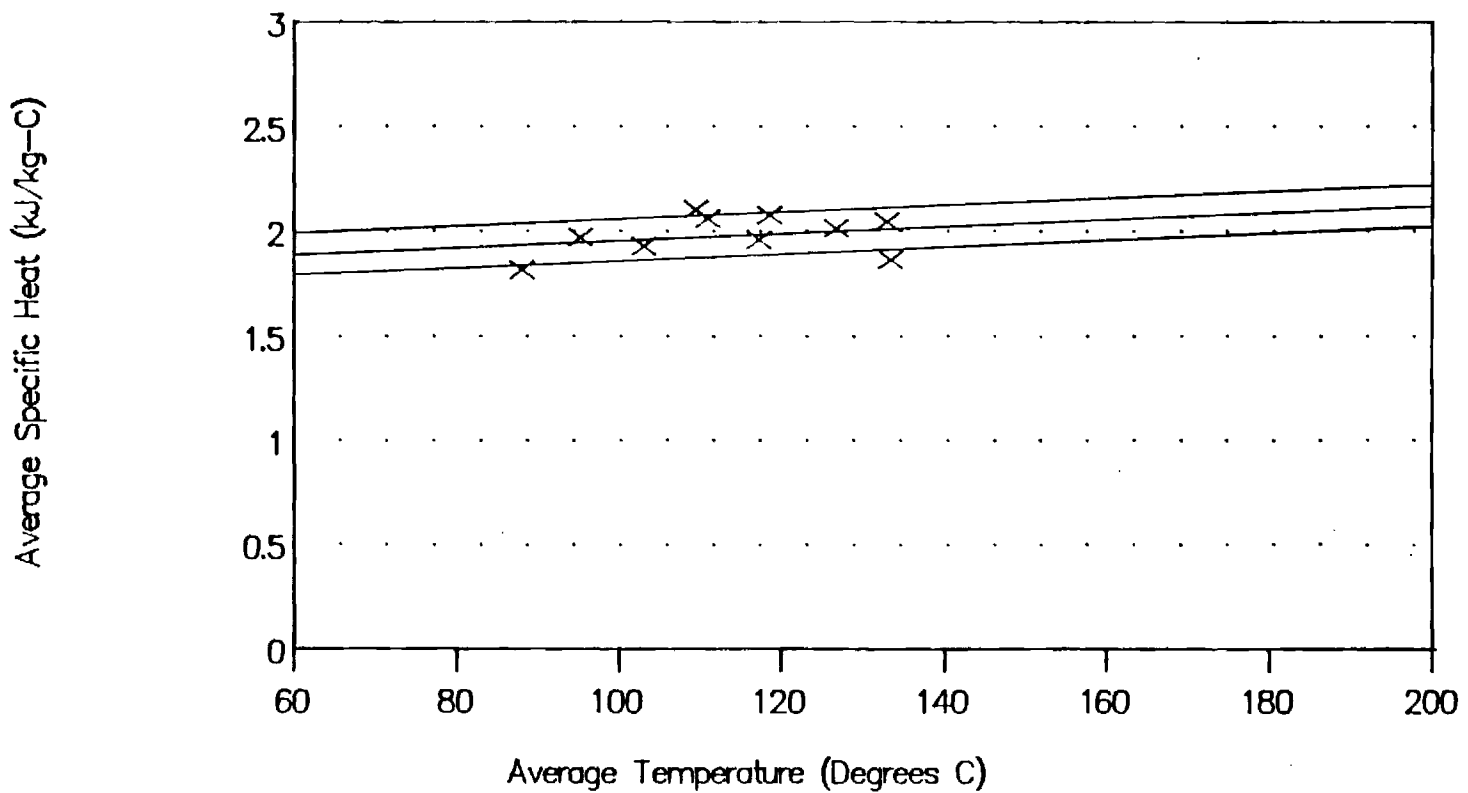


Fig. 13: 64.83wt% and 65.48wt% LiBr

Linear-Linear Correlation

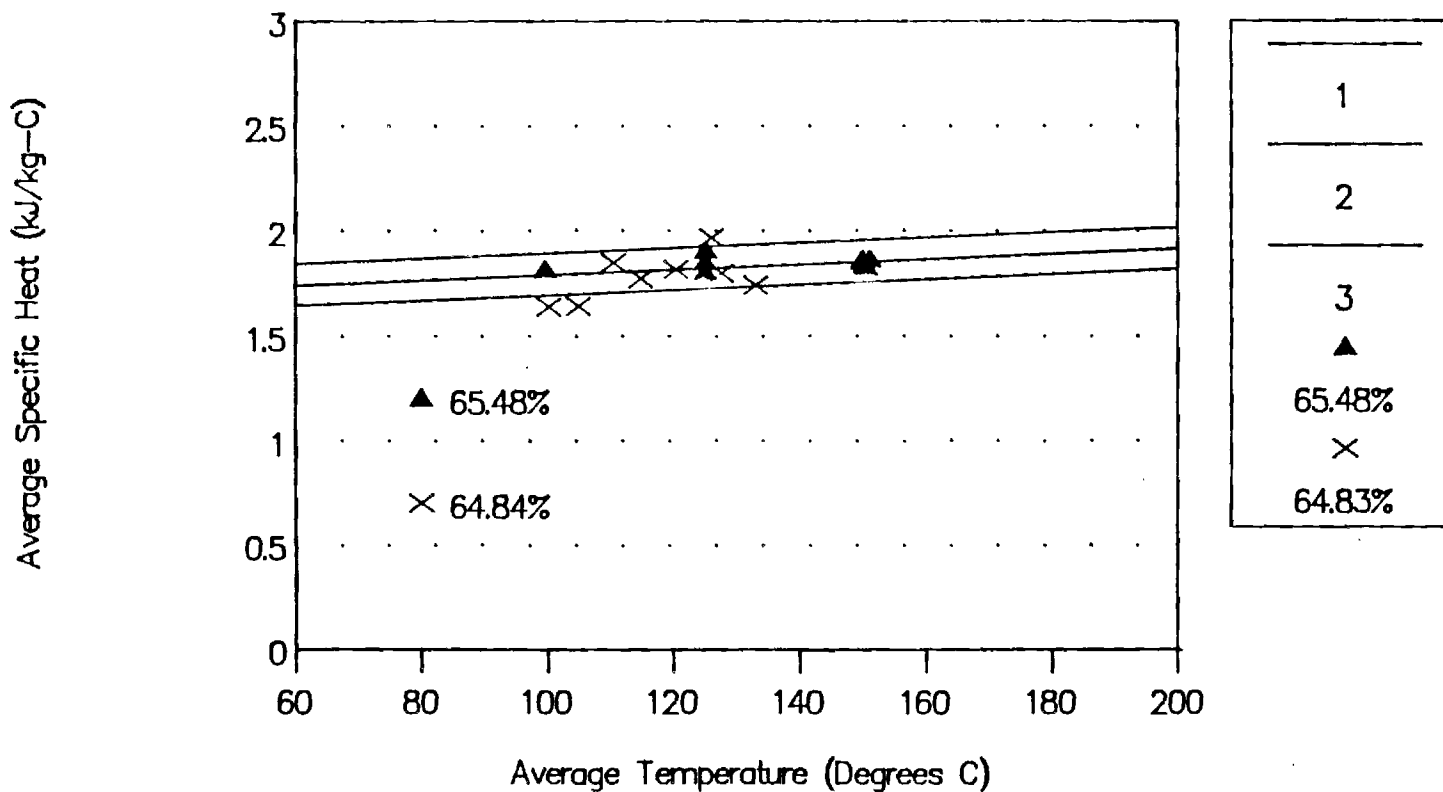
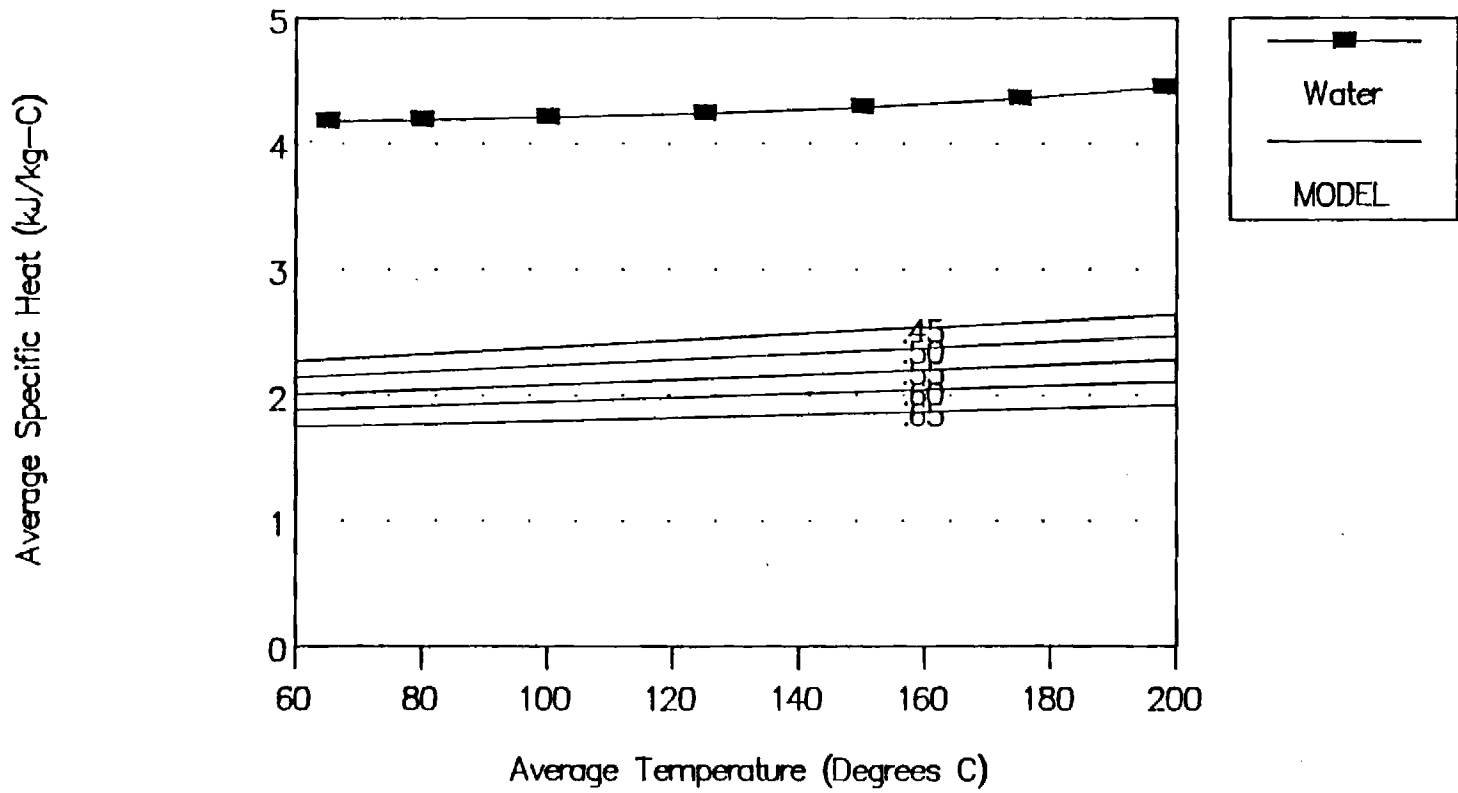


Figure 14. Linear-Linear Model
 Compared with Data for Water



5. ERROR ANALYSIS AND COMPARISON WITH OTHER RESULTS:

Error Estimate. Since the drop calorimeter is a relatively complex device, especially as regards heat leaks to the environment, an error analysis based on and proceeding strictly from elementary principles appears to be formidably challenging at a minimum. Rather than attempt such an analysis, a series of drops using water as a standard reference fluid were conducted in November and December of 1988. Note that these drops are independent of the water drop used to calibrate the receiver: different samples were used and the latter drops were not used to adjust the calibration curves. Results of these drops are detailed in the following table.

Table 8

RESULTS OF STANDARDIZATION TESTS WITH WATER

Sample Temperature	Final Temperature	Empirical Average Specific Heat	Tabulated Average Specific Heat	Relative Error
142.77	51.59	4.21	4.219	-.002
165.98	52.36	4.29	4.239	.012
189.81	54.09	4.23	4.267	-.009
190.28	53.79	4.24	4.267	-.006
165.61	55.25	4.22	4.241	-.005
119.43	53.04	4.19	4.204	-.003
Root Mean Squared Error				.007

The preceding reveals an inherent calorimeter error on the order of $\pm 0.7\%$ with the samples of water. Over a similar temperature range, water has about twice the specific heat capacity of a typical LiBr solution (e.g. $4.2/2.4 = 1.75$). Consequently, for a typical LiBr solution the calorimeter error, ϵ_{cal} , is estimated to be about 1.2% (i.e. $.007 \cdot 1.75 = .012$).

In the current situation, inaccuracy in the composition of the solution is also a source of error. For the linear-linear model, the dependence of the specific heat on concentration is given by the following partial derivative:

$$\partial c_s / \partial w = a_1 + b_1 T$$

At 150 C, the value of the derivative is about $-3.2 \text{ kJ}/(\text{kg} \cdot \text{K} \cdot \text{kg}/\text{kg})$. Uncertainty in the composition is probably on the order of 0.1 WT%; but even if it is as great as 1 WT%, this component can contribute a relative composition error, ϵ_x , of only .013 (i.e. $3.2 \cdot .01/2.4$) which is only of the same order as the calorimeter error. Using the central limit theorem, the combined error is given as follows:

$$\epsilon = \{ \epsilon_{\text{cal}}^2 + \epsilon_x^2 \}^{1/2} = .018$$

In the production drops, this accuracy has not been achieved probably because of imperfect conditions during all procedures over the many months of effort required to complete the series of drops. The production drops have at least twice this inaccuracy as indicated by Standard Errors of Estimate in the correlations of around 5%.

Comparison with Other Results. As indicated above, five other sources of comparative data are available. The data of Pennington [7] are at room temperature and are not helpful for a comparison with the current results. The data of Uemura and Hasaba [5] are significantly lower than the values obtained herein or the values in the other three remaining sources. The comparison is illustrated in Figure 15 which shows both the reported data and the correlation provided by Uemura and Hasaba. Data obtained by Uemura and Hasaba are limited to the range of 51.7 C to 130.2 C for the concentration shown, 66.2 WT%. At lower concentrations, 110.4 C was the highest experimental temperature. Both the data and the correlation are 20% to 17% lower than the linear-linear correlation from this investigation over the the experimental range, which is approximately 50 C to 130 C. For example, Uemura and Hasaba obtained 1.51 kJ/(kg K) at $w = .662$ and $T = 130.2$ C compared with 1.79 kJ/(kg K) with the linear-linear correlation from the current investigation. The relative error between these data is 17%. Error limits are also plotted on the graph at one standard error above and below the correlation results from the present study. It is notable that all the data points reported by Uemura and Hasaba as well as their correlation line are fully outside the error bounds over their valid temperature range. This divergence from the present correlation indicates that there is no statistical support for the older results from the current data. The error in the results of Uemura and Hasaba appears to be excessive, and their results should probably not be employed. The reason for this error cannot be explained from the sketchy description in the literature. Possibly their apparatus was unsuitable for higher temperature operation since the temperature quoted above, only 130.2 C, was the highest in the data set. Note that the Uemura and Hasaba correlation converges on the linear-linear correlation at higher temperatures, but this is beyond the range of their experimental data base and is, therefore, only unsupported extrapolation.

A third source of comparative data is the thesis by Löwer [1]. These data at concentrations of 45, 50, 55, and 60 weight percent are plotted in Figure 16 along with the corresponding linear-linear correlation lines from the present investigation. Agreement between the two sets of results of data is good but not perfect and ranges from better agreement near 45 WT% to poorer agreement near 60 WT%. In Figure 17, the standard error bands for the linear-linear correlation at 45 WT% and 60 WT% are plotted in comparison with the data of Löwer. As is evident in the figure, the data from Löwer is marginally in agreement with the results for the present study as illustrated by the bands near 45 WT% and 60 WT%; consequently, the data of Löwer are within marginal agreement with the results of the current study.

Two more important sources of data are the numerical results of Patterson and Perez-Blanco [4] and the experimental data provided by Dr. Uwe Rockenfeller of Rocky

Research Incorporated [13]. The Rocky Research data were measured with a Differential Scanning Calorimeter (DSC) manufactured by Perkin-Elmer. These data are reported to have been compensated for the difference in heat capacity between the cells holding the samples and the cell holding the reference. In addition, corrections have been applied for vaporization effects. The Rocky Research data are illustrated in Figure 18 along with linear-linear correlation lines for these same data. Because the DSC data are very smooth, the linear-linear correlation produces an excellent fit with a Coefficient of Determination over 99%. The numerical results of Patterson and Perez-Blanco are curve fits to the enthalpy data generated by McNeely [2]. Specific heats have been obtained from the enthalpy function by taking the partial derivative with respect to temperature while holding constant the concentration. McNeely employed the procedure of Haltenberger [3] to produce enthalpy-concentration charts from vapor pressure data over a range of temperatures and concentrations and specific heat data over a range of temperature. In particular, to produce the published results, McNeely used the specific heat data from Löwer at 50 WT% concentration. As shown in Figure 19, the results from differentiation of the correlations of Patterson and Perez-Blanco agree very well with the Rocky Research data. The Rocky Research data are slightly above the Patterson and Perez-Blanco curve fits. It is notable that the differentiation does not precisely return the specific heat data of Löwer. This is to be expected since both vapor properties and specific heat data are required to define the enthalpies, and the vapor properties have a significant impact. In addition, the numerical curve fit is defined over the entire range of the enthalpy chart which tends to somewhat obscure the influence of any particular contributing data. Table 9 provides the coefficients for both correlations and statistical results for the Rocky Research data along with the pertinent statistics.

Since the Rocky Research data agree very well with the correlation from Patterson and Perez-Blanco, it should be sufficient to illustrate and discuss the comparison between the results of the present investigation and the data from Rocky Research. The Rocky Research data are illustrated along with the corresponding linear-linear correlations in Figures 20 and 21. As is evident in the figure, there is good agreement between the two data sets which is very reassuring since such disparate equipment were used for the two measurements. The linear correlation ranges from ca. 4% above the Rocky Research correlation at 45.1 WT% and 150 C to a virtually identical value at 65 WT% and 150 C. The RMS error at mid range is only about 2%. This is hardly greater than the estimated inherent accuracy of the drop calorimeter and is less than the standard error estimate in the specific heat correlation for the drop calorimeter data. The Rocky Research data are illustrated in Figure 21 along with representative error bands for the linear-linear correlation. Nearly all of the Rocky Research data fall within the error bands. Consequently, the results of the current investigation are not statistically divergent from the Rocky Research data, and the two sets of data are mutually reinforcing. Indeed, at 65 WT% the two correlations are virtually identical. The principal difference is in the slope of the temperature dependence with the current investigation having the greater temperature effect. The specific heats from the enthalpy correlation of Patterson and Perez-Blanco are similarly in agreement with the current investigation and the with the Rocky Research data. As shown in Figure 22, four sources of data are in good agreement. At 60 WT%, the data of Löwer are slightly higher than the other data and the

formulation based on the Patterson and Perez-Blanco correlation being somewhat lower than the others. The nearly identical Rocky Research data and the linear-linear correlation of data from the current investigation occupy an intermediate position. Both the data of Löwer and the related Patterson and Perez-Blanco correlation have a nearly flat temperature dependence. The Rocky Research data and the linear-linear correlation increase with temperature, as does pure water in this temperature range. Since the increase with temperature is barely noticeable lower than approximately 100 C, even for pure water, it is possible that the limited temperature range of the Löwer data obscured this dependence. All the data shown lie within the error bounds of the current investigation. Error bounds on the other sources cannot be quantified, but they may be very small in the case of the Rocky Research data. In the absence of further uncertainty estimates, no statistical preference can be asserted among the four data bases at lower temperature or between the Rocky Research data and the current research at higher temperatures.

The ultimate goal of collecting specific heat data is constructing enthalpy-concentration charts and tables. This construction requires only specific heat data at a single concentration and a range of temperatures. Since the correlations for 65 WT% from this investigation and that based on the Rocky Research data are virtually identical, it is recommended that either of these be used for the computation of solution enthalpies.

Table 9

CORRELATION RESULTS FROM DATA OF OTHERS

Coefficient:		Regression of Rocky Research Data on Model of Form: Linear-Linear Quadratic-Linear		Differentiation of Enthalpy Fit by Patterson and Perez-Blanco
Symbol	Multiplies			
a_0		3.462023	3.818560	4.124891
a_1	w	-2.679895	-3.996355	-7.643903 E-02
a_2	w^2		1.195485	2.589577 E-03
a_3	w^3			-9.500522 E-05
a_4	w^4			1.708026 E-06
a_5	w^5			-1.102363 E-08
b_0	T	.0013499	.0013499	0.0011487386
b_1	wT	-.000655	-.000655	0.00011741842
b_2	w^2T			-1.4750638 E-05
b_3	w^3T			6.555184 E-07
b_4	w^4T			-1.2124608 E-08
b_5	w^5T			7.803794 E-11
Standard Error of Estimate		.0096	.0081	
Coefficient of Correlation		.9977	.9984	

Fig 15. 66.2% Linear-Linear Correlation
Compared with Uemura and Hasaba

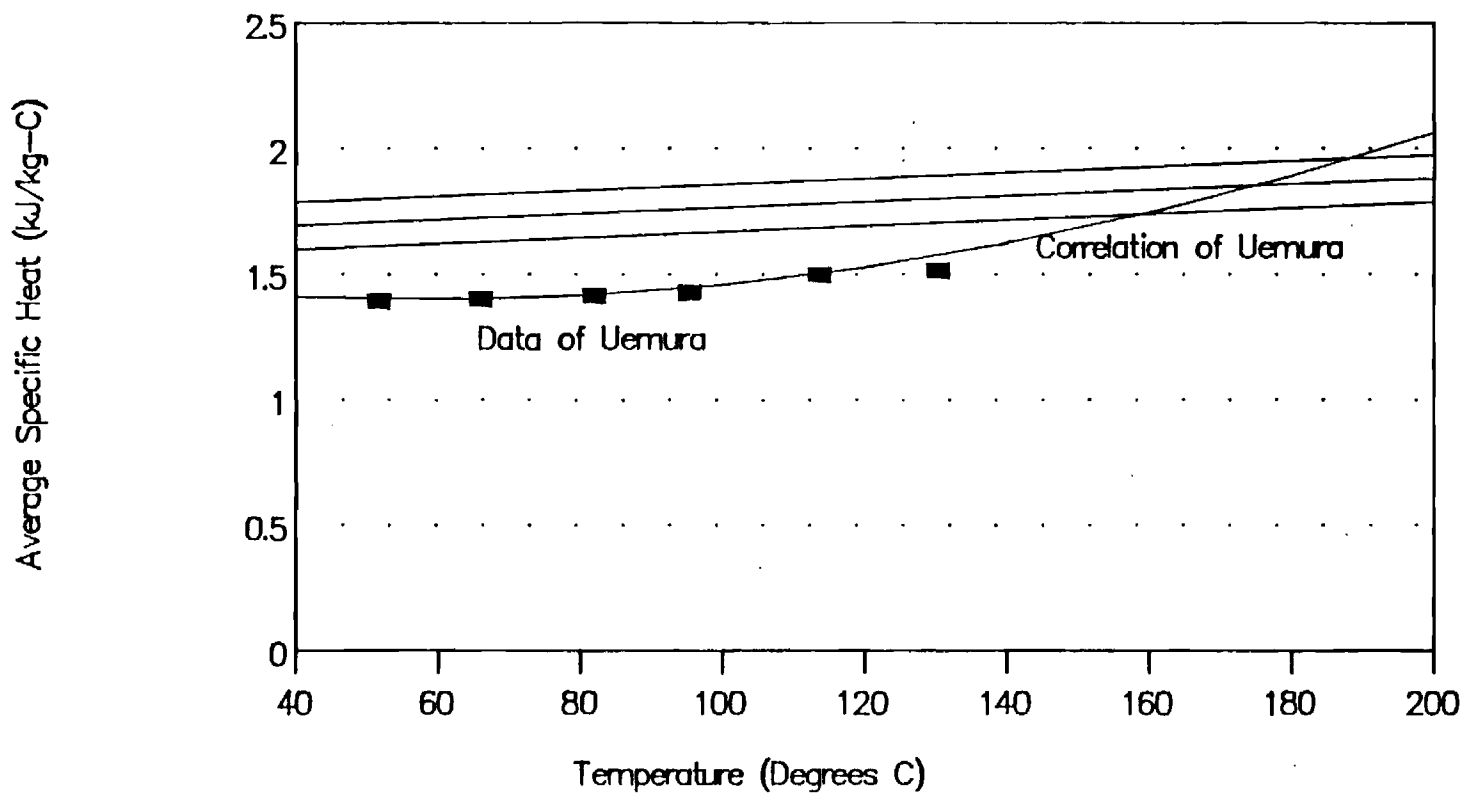


Figure 16. Data of Lower
and GIT Linear-Linear Correlation

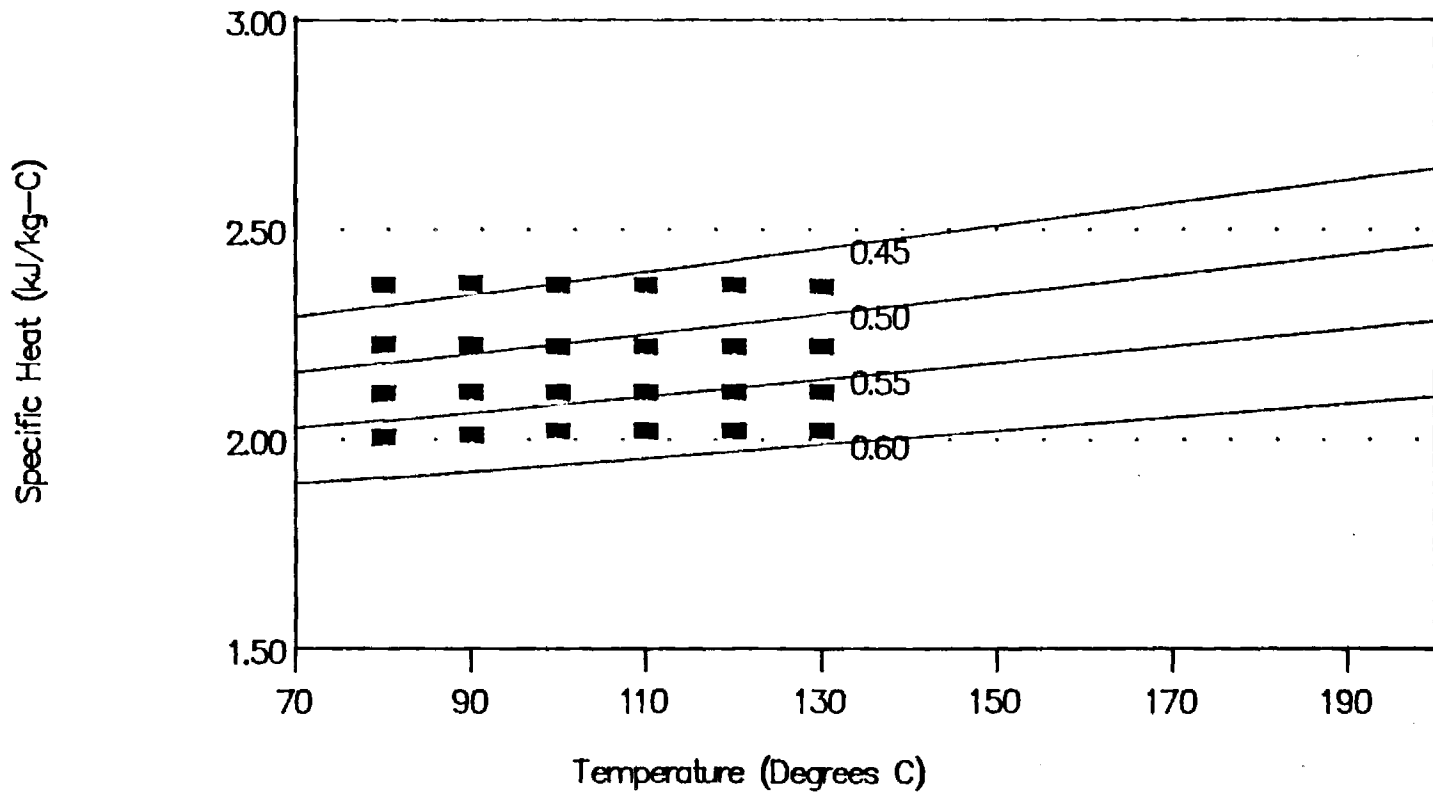


Figure 17. Data of Lower and GIT
Error Bands at 45 WT% and 60 WT%

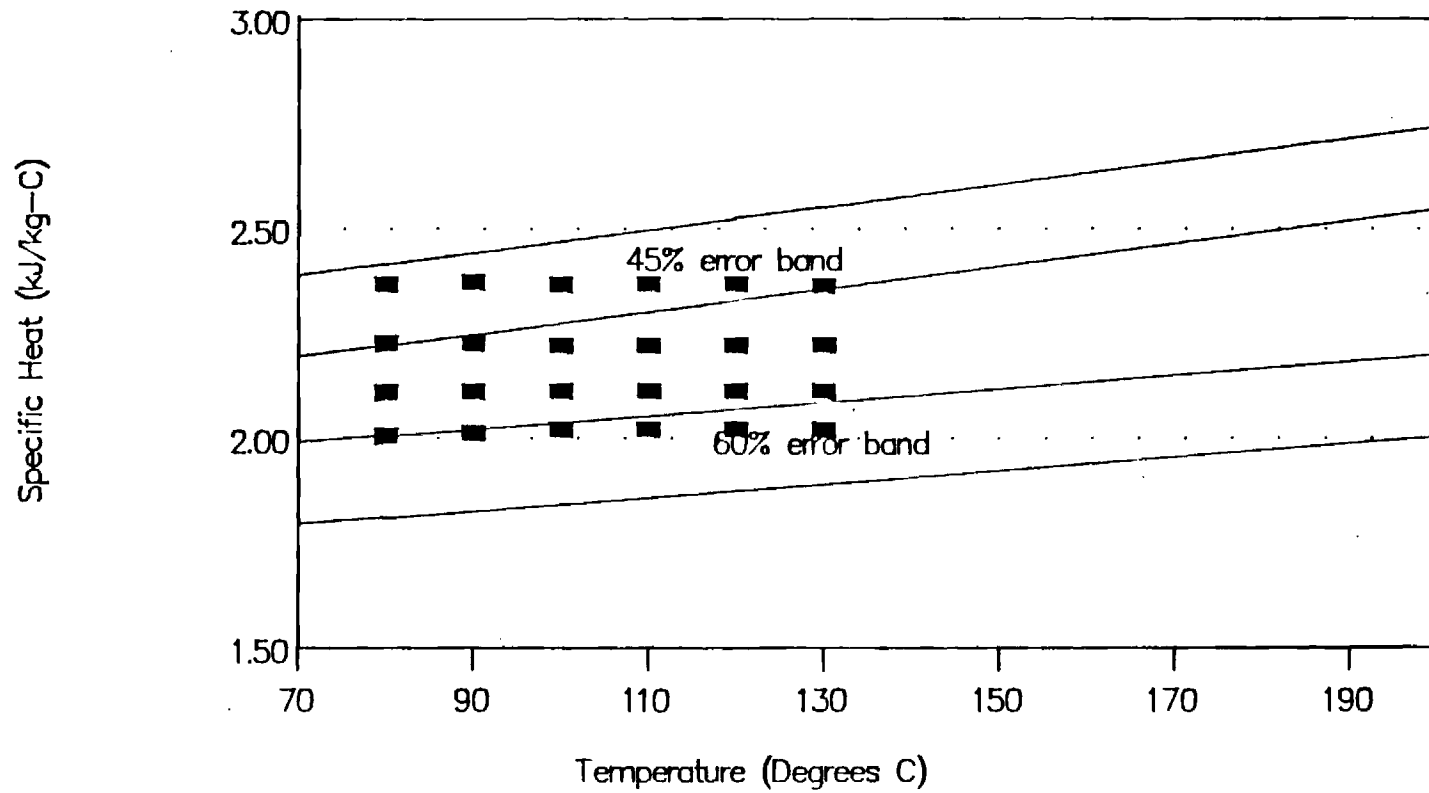


Figure 18.

Rocky Research Data and its Correlation

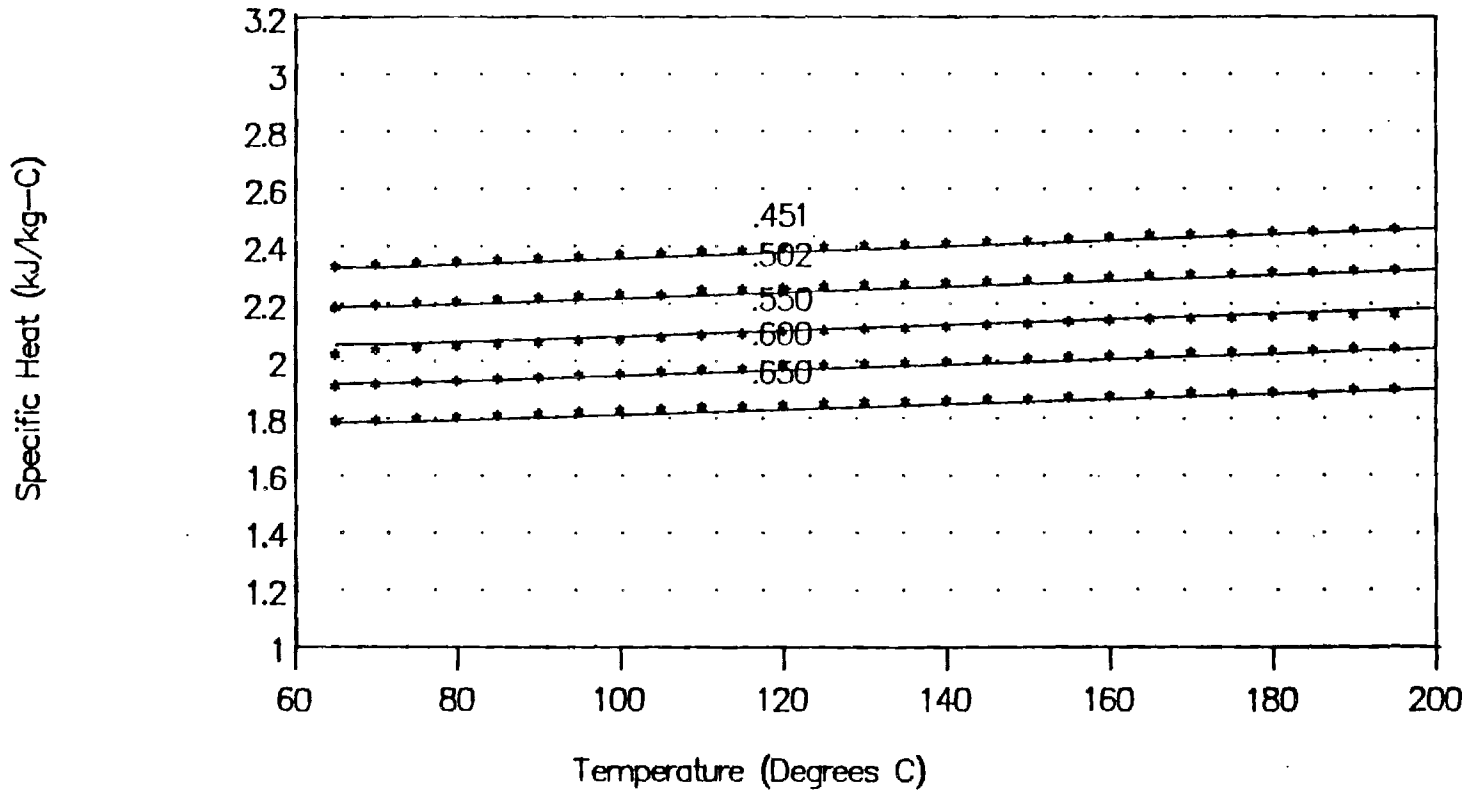


Figure 19: Rocky Research Data Compared
with Patterson and Perez-Blanco

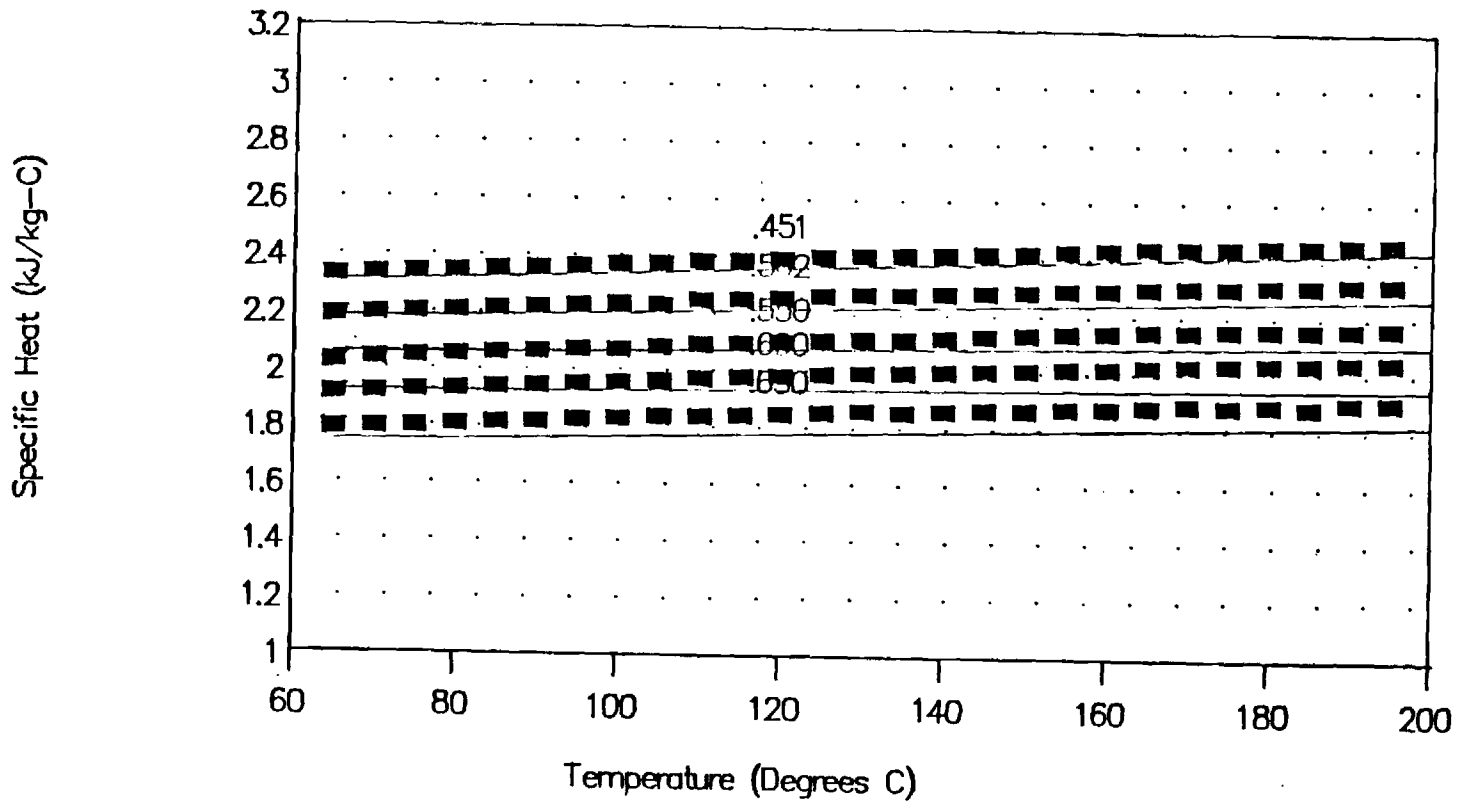


Fig. 20: Rocky Research data
and GIT linear-linear correlation

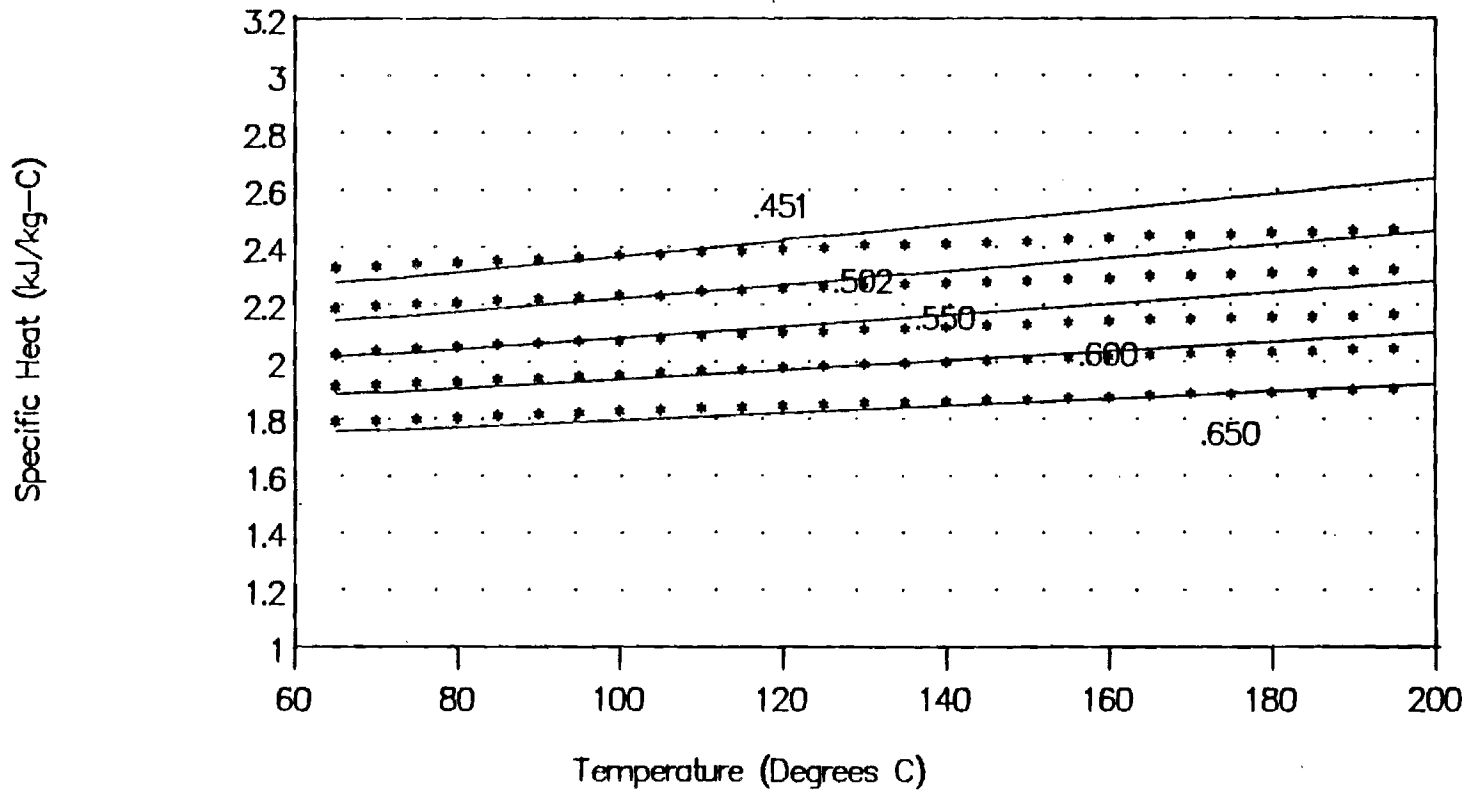


Fig. 21: Rocky Research data and GIT

linear-linear error bands

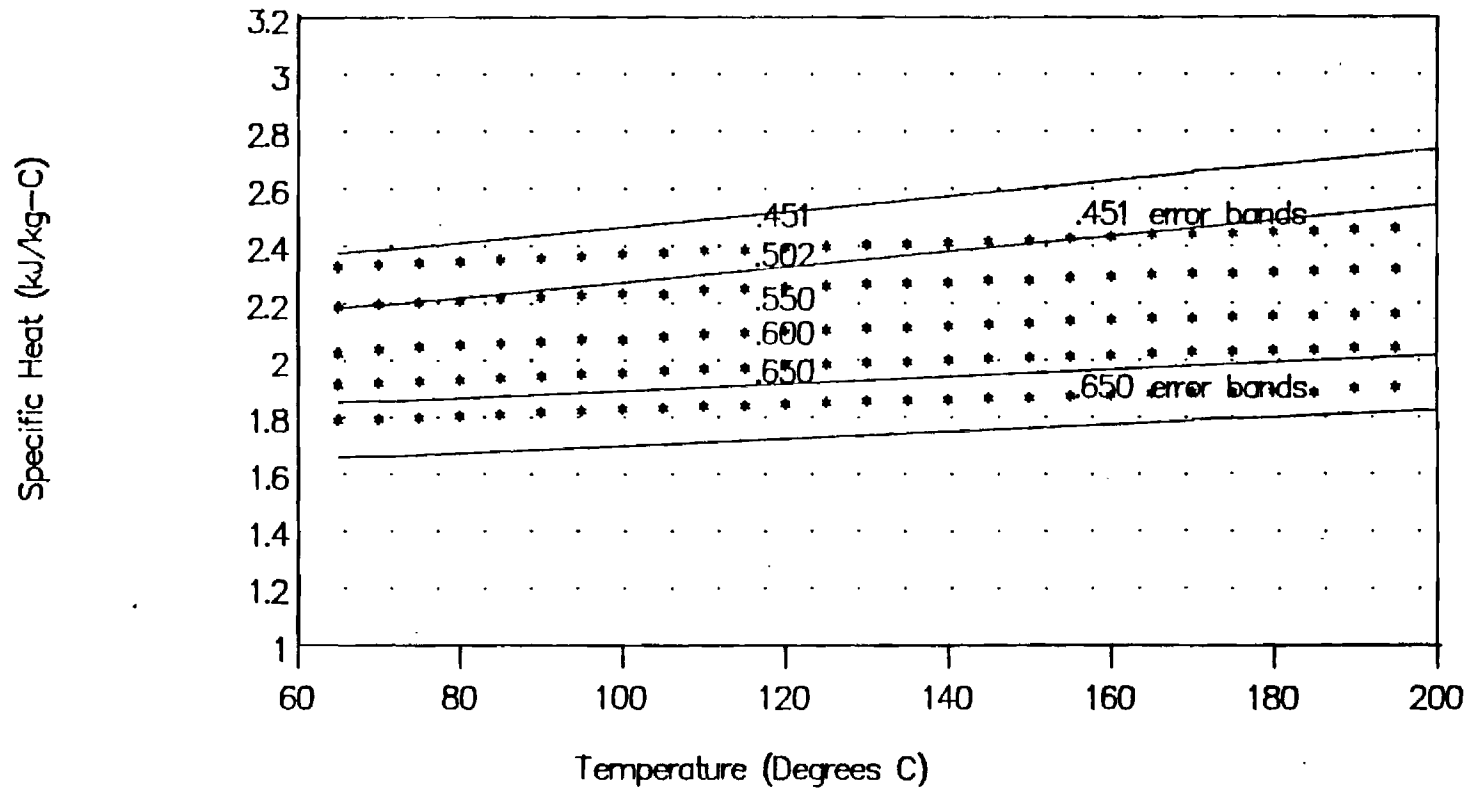
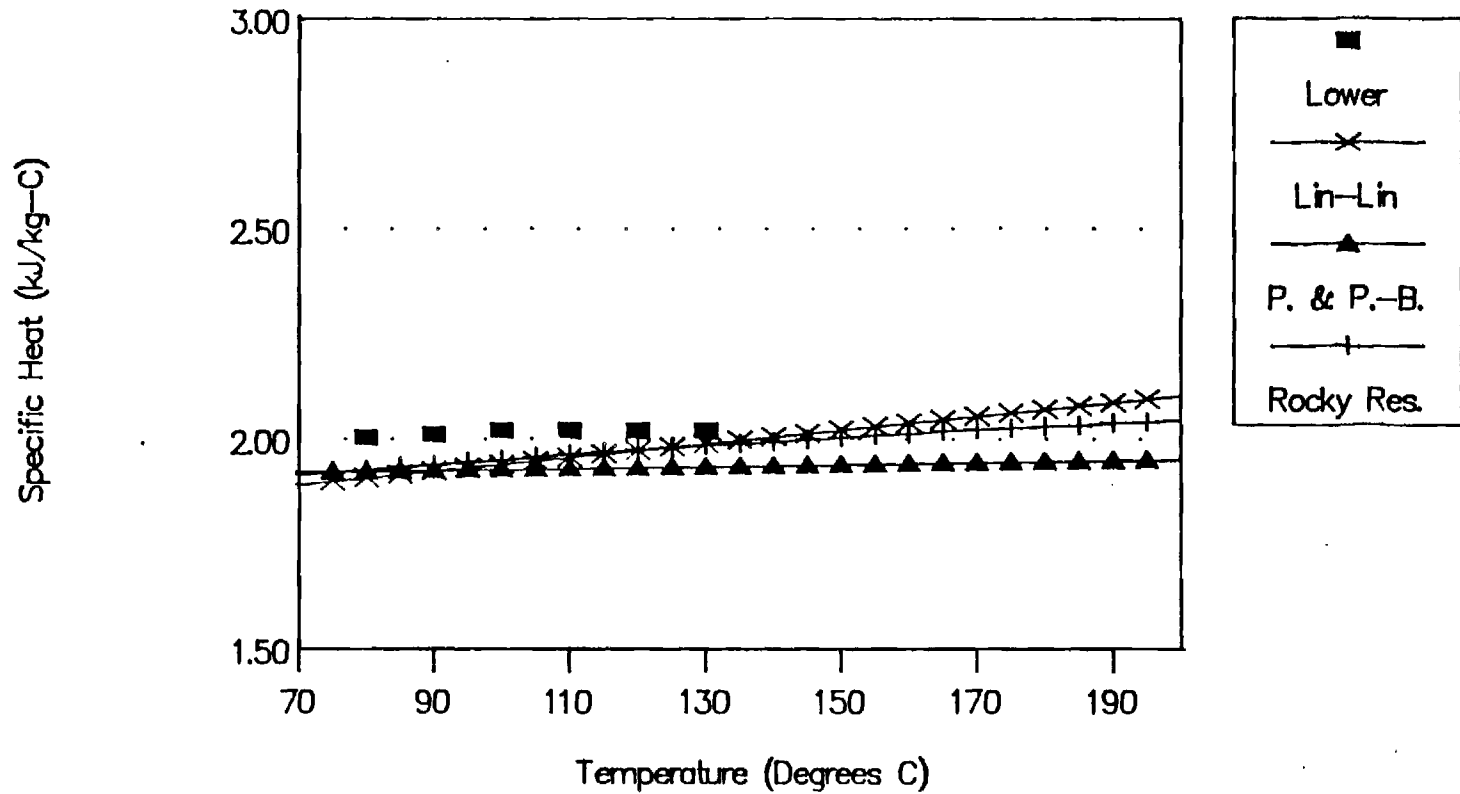


Figure 22. Comparison of Four Results
at 60 WT% Concentration



6. CONCLUSIONS:

Two data bases, the DSC measurements from Rocky Research and specific heats obtained by differentiation of enthalpy correlations prepared by Patterson and Perez-Blanco, are in agreement with the results of the current investigation. The data of Uemura and Hasaba are clearly lower than the results of the three mutually consistent data bases. The data of Löwer are at least marginally supported by the three later data bases, one of which, the enthalpy correlation, incorporated Löwer's data in computing the tabulated enthalpies on which the correlation was based. The data from Löwer, however, do not extend far enough into the temperature range under consideration here to be helpful. The Rocky Research data are supported by excellent agreement with the results from the Patterson and Perez-Blanco correlation and by good agreement with the results of the current investigation. Since the Rocky Research data are purely empirical, they should be preferred over the numerical results. In addition, the Rocky Research data occupy an intermediate position. They are slightly higher than the results from the enthalpy correlation and slightly lower than the results of the present investigation. In consequence, the Rocky Research data should represent an acceptable consensus data base. For practical purposes, specific heat data are needed at only one concentration, and at 65 WT% the correlation results from the present investigation are virtually identical with the correlation based on the Rocky Research data. Either correlation should be adequate and accurate for preparing enthalpy charts and tables.

It may be possible to make a finer distinction among the three preferred data bases by improving on the current measurements. Two possibilities have already been pursued. The temperature range of the measurements were extended for the higher concentrations where the vapor pressure is low enough for safe operation with the existing calorimeter capsule. This effort provided additional data points around 65 WT%. The additional data was helpful in its own right and also relieved some of the leverage of possible outliers at lower temperatures which can distort the temperature dependence. The evaluation of the specific heat from drop calorimeter data involves a ratio of the two temperature differences, the rise in receiver temperature and the drop in sample temperature. This situation makes measurements problematical at lower temperatures for which both temperature differences become smaller because the ratio of two small differences becomes very sensitive to experimental error. Additionally, the data base was scanned for outliers and suspected outliers were replaced with measurements from carefully conducted measurements. This effort required a few additional drops around 45 WT% and several additional drops around 65 WT%. Outliers are especially likely at higher concentrations where the lower specific heats magnify the influence of inadequate procedures or environmental influences. Further refinement of the measurements described herein with the present apparatus would be problematical; and, since an acceptable consensus specific heat correlation has been defined for evaluating the enthalpy, further work is beyond the scope of the present effort.

Further work, if attempted, might well proceed at lower concentrations, approaching pure water. The experimental results would be strongly confirmed if the highly regarded

and scrupulously measured specific heat of water emerges as the limiting case. This investigation should also alleviate uncertainty about the trend in temperature dependence if the dependence smoothly accelerates and approaches the trend for water as the amount of LiBr in the solution is decreased.

7. ACKNOWLEDGEMENTS

The contributions of Dr. Uwe Rockenfeller both for his guidance and encouragement as the technical monitor of this project and for providing the previously unpublished specific heat data is gratefully acknowledged. The assistance of Professor K. E. Herold for helpful discussions and his assistance with the literature review is also gratefully acknowledged.

7. REFERENCES:

1. Löwer, H., "Thermodynamische und physikalische Eigenschaften der wässrigen Lithiumbromid-Lösung", Dissertation, Technischen Hochschule Karlsruhe, Karlsruhe, Germany, 1960.
2. McNeely, L. A., "Thermodynamic Properties of Aqueous Solutions of Lithium Bromide", *ASHRAE Transactions*, Vol. 85, Part 2, pp. 413-434, 1979.
3. Haltenberger, W., "Enthalpy-Concentration Charts from Vapor Pressure Data", *Industrial and Engineering Chemistry*, pp. 783-786, June, 1939.
4. Patterson, M. R. and H. Perez-Blanco, "Numerical Fits of the Properties of Lithium-Bromide Water Solutions", *ASHRAE Transactions*, Vol. 94, Part 2, 1988.
5. Uemura, T. and S. Hasaba, "Studies on the Lithium Bromide-Water Absorption Refrigerating Machine", Technical Report, Kansai University, Vol. 6, pp. 31-55, 1964.
6. "Technical Data: Lithium Bromide", Commercial Brochure, Foote Mineral Company, Exton, PA.
7. Pennington, W. A. and C. Daetwyler, "Heat Capacity and Heat of Dilution of some Concentrated Water Solutions of LiBr at 25 C", Carrier Confidential Report, Project R1011-S1 Report No. 6, Carrier Corporation, Syracuse, NY, 18 April 1952.
8. "Operating Manual, Unitherm Model 7100 Calorimeter", Anter Laboratories, 15 December 1976.
9. Lee, M. C. and R. N. Maddox, "Measuring Heat Capacity Using the Unitherm Model 7100 Drop Calorimeter", Liquid Heat Capacity Report No. 6, Fluid Properties Research Institute, January 1979.
10. Moran, J. P., "Specific Heats of Aqueous Lithium Bromide Solutions", M. S. Thesis, The George W. Woodruff School of Mechanical Engineering, Georgia Institute of Technology, August 1988.
11. Pan, W. P. and R. N. Maddox, "Improved Technique for Heat Capacity Measurements using the Unitherm Model 7100 Drop Calorimeter", Liquid Heat Capacity Report No. 7, Fluid Properties Research Institute, August 1979.
12. McClintock, R. B. and G. J. Silvestri, "Some Improved Steam Property Calculation Procedures", *Journal of Engineering for Power*, American Society of Mechanical Engineers, pp. 123-134, April 1970.
13. Rockenfeller, U., "Laboratory Results: Solution = LiBr-H₂O, Properties = P-T-x, Heat Capacity", Unpublished Data, Rocky Research, Inc, Boulder City, NV, 1987.

8. APPENDIX:

For completeness, the following graphs are appended which illustrate the scatter plots of raw data along with correlation lines and error bands for the quadratic-quadratic and quadratic-linear models:

Figure A.1: Specific Heat Data for 43.95 WT% Solution of LiBr with Corresponding Quadratic-Quadratic Correlation Model.

Figure A.2: Specific Heat Data for 50.595 WT% Solution of LiBr with Corresponding Quadratic-Quadratic Correlation Model.

Figure A.3: Specific Heat Data for 54.10 WT% Solution of LiBr with Corresponding Quadratic-Quadratic Correlation Model.

Figure A.4: Specific Heat Data for 59.48 WT% Solution of LiBr with Corresponding Quadratic-Quadratic Correlation Model.

Figure A.5: Specific Heat Data for 64.83 WT% and 65.48 WT% Solution of LiBr with Corresponding Quadratic-Quadratic Correlation Model.

Figure A.6: Specific Heat Data for 43.95 WT% Solution of LiBr with Corresponding Quadratic-Linear Correlation Model.

Figure A.7: Specific Heat Data for 50.595 WT% Solution of LiBr with Corresponding Quadratic-Linear Correlation Model.

Figure A.8: Specific Heat Data for 54.10 WT% Solution of LiBr with Corresponding Quadratic-Linear Correlation Model.

Figure A.9: Specific Heat Data for 59.48 WT% Solution of LiBr with Corresponding Quadratic-Linear Correlation Model.

Figure A.10: Specific Heat Data for 64.83 WT% and 65.48 WT% Solution of LiBr with Corresponding Quadratic-Linear Correlation Model.

Figure A.1: 43.95% LiBr by weight

Quadratic-Quadratic Correlation

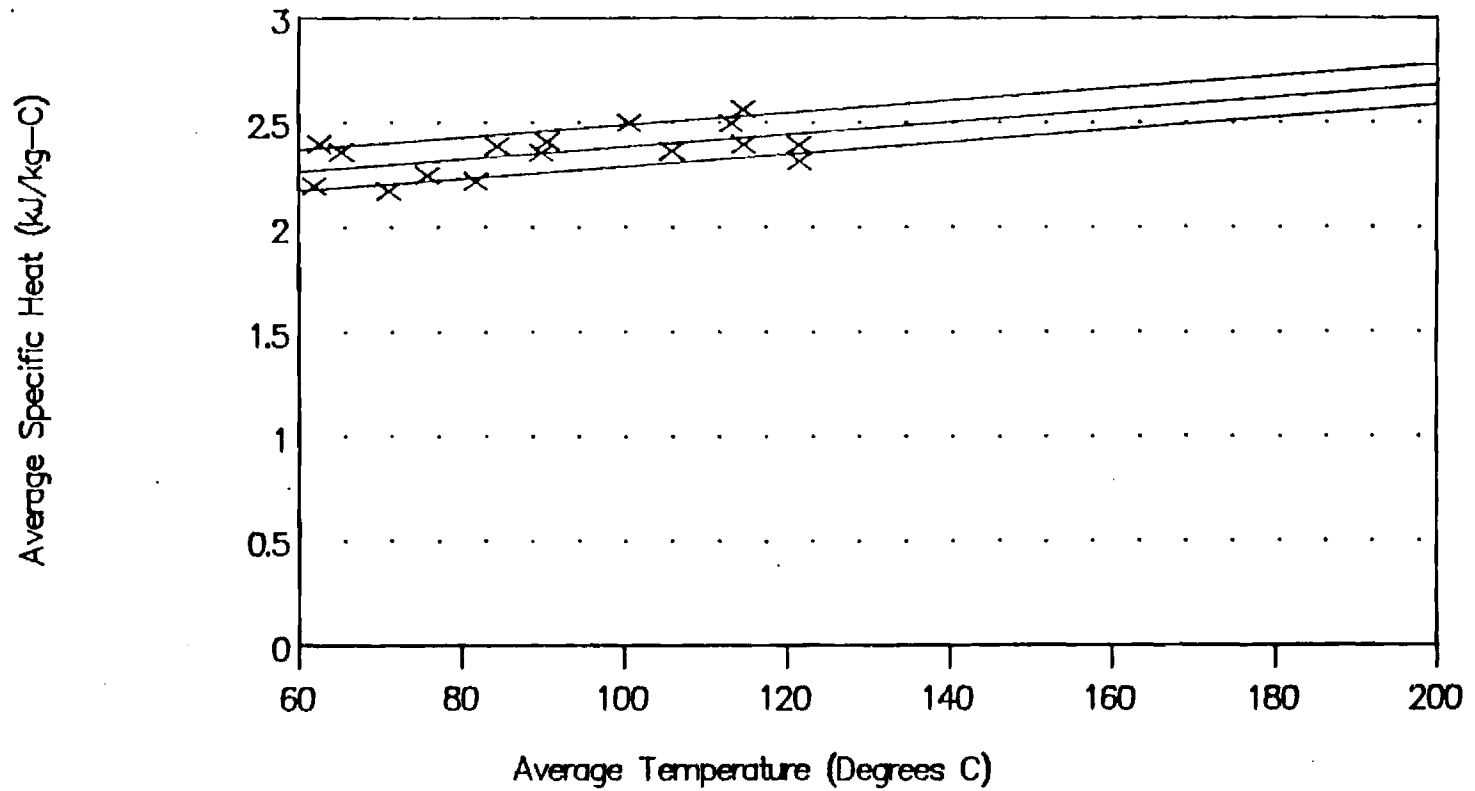


Figure A.2: 50.59% LiBr by weight

Quadratic-Quadratic Correlation

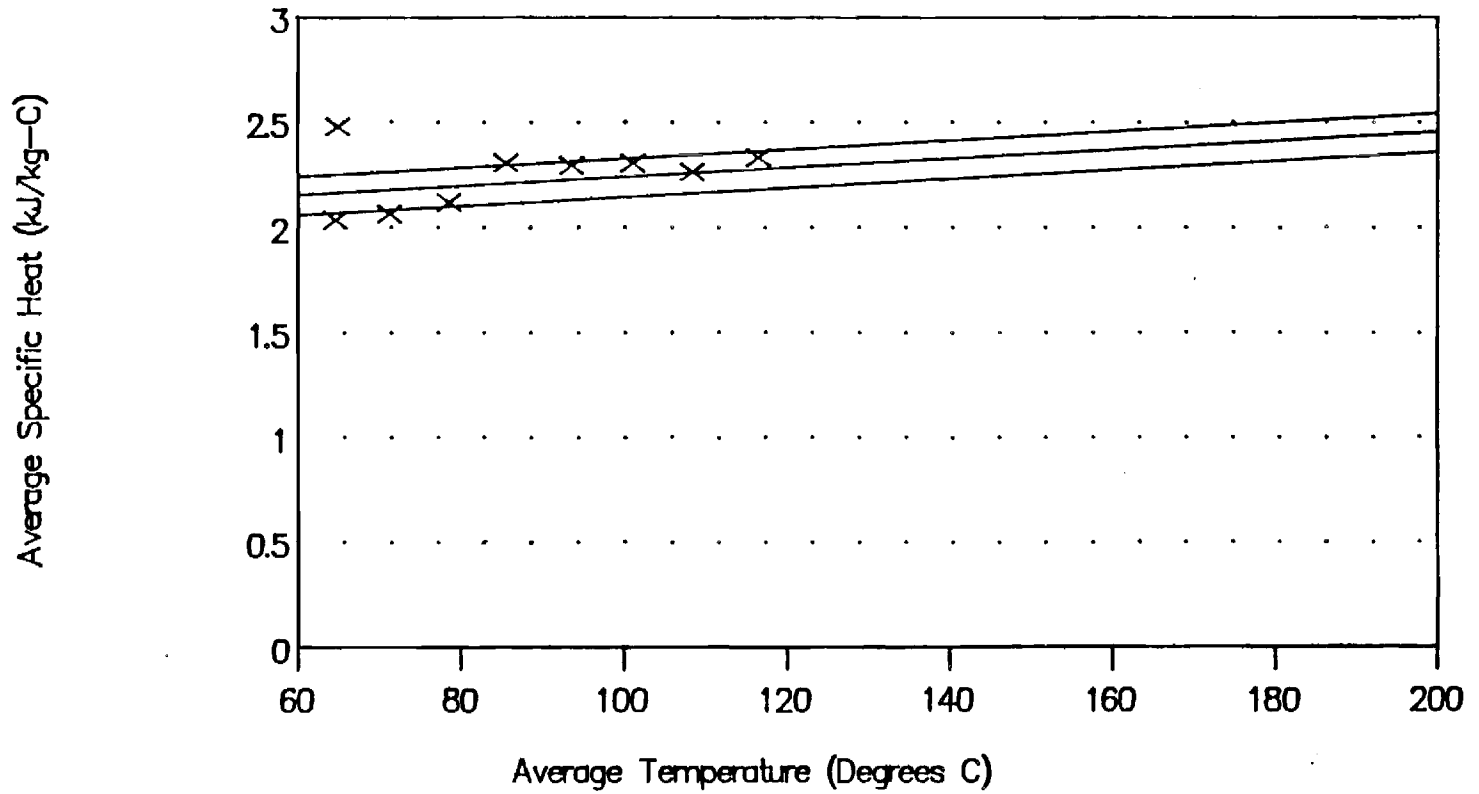


Figure A.3: 54.10% LiBr by weight

Quadratic-Quadratic Correlation

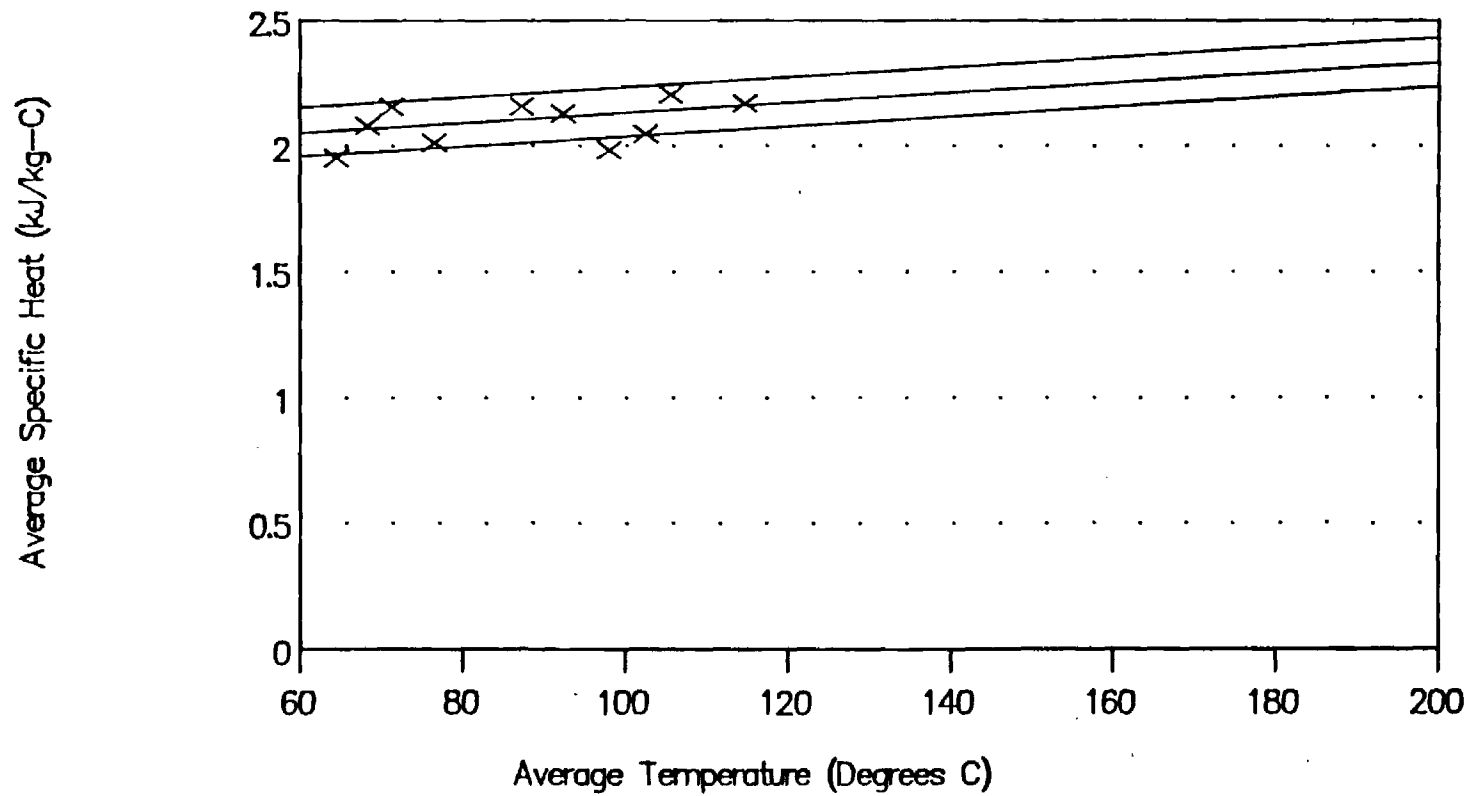


Figure A.4: 59.48% LiBr by weight

Quadratic-Quadratic Correlation

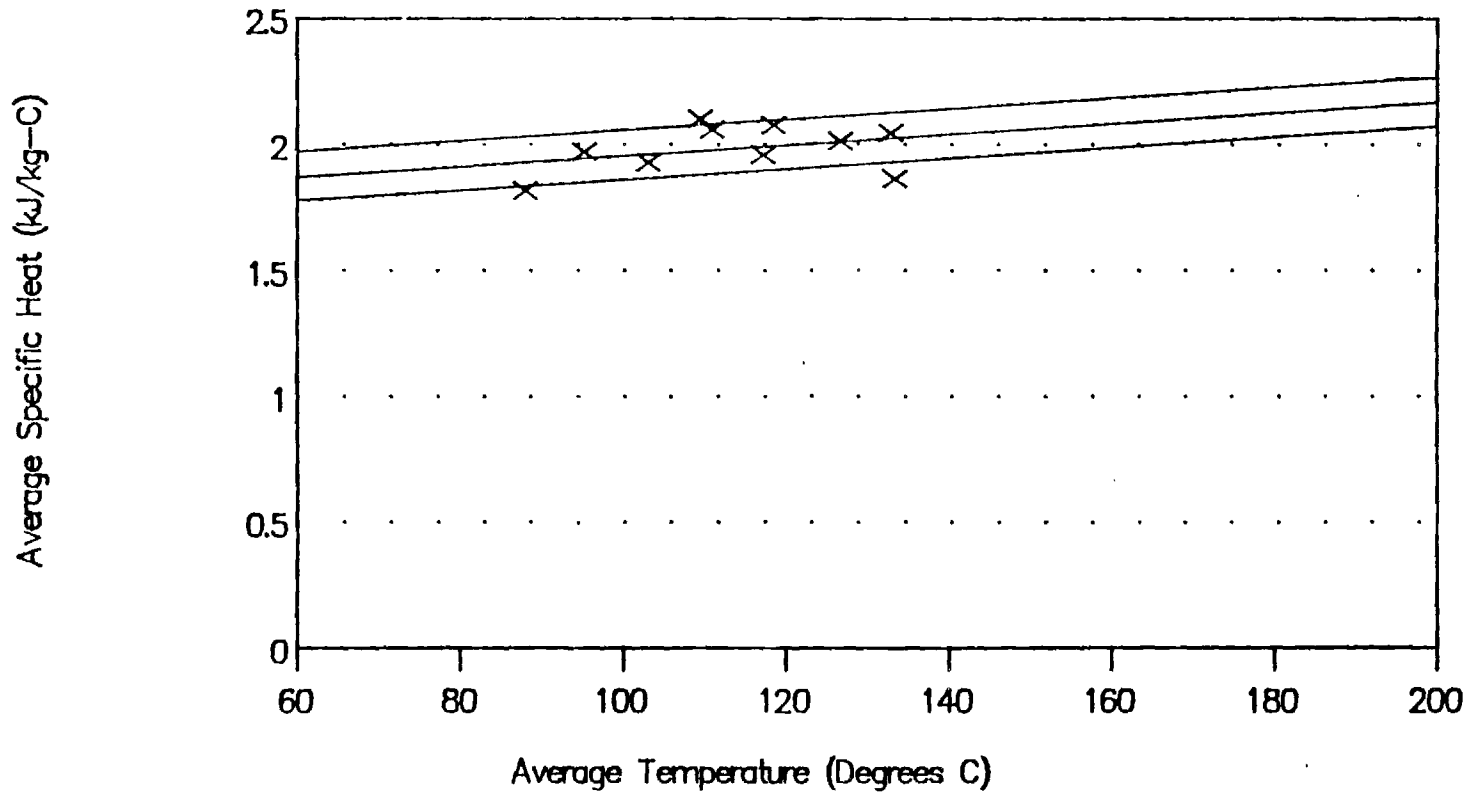


Figure A.5: 64.83% and 65.48% LiBr

Quadratic-Quadratic Correlation

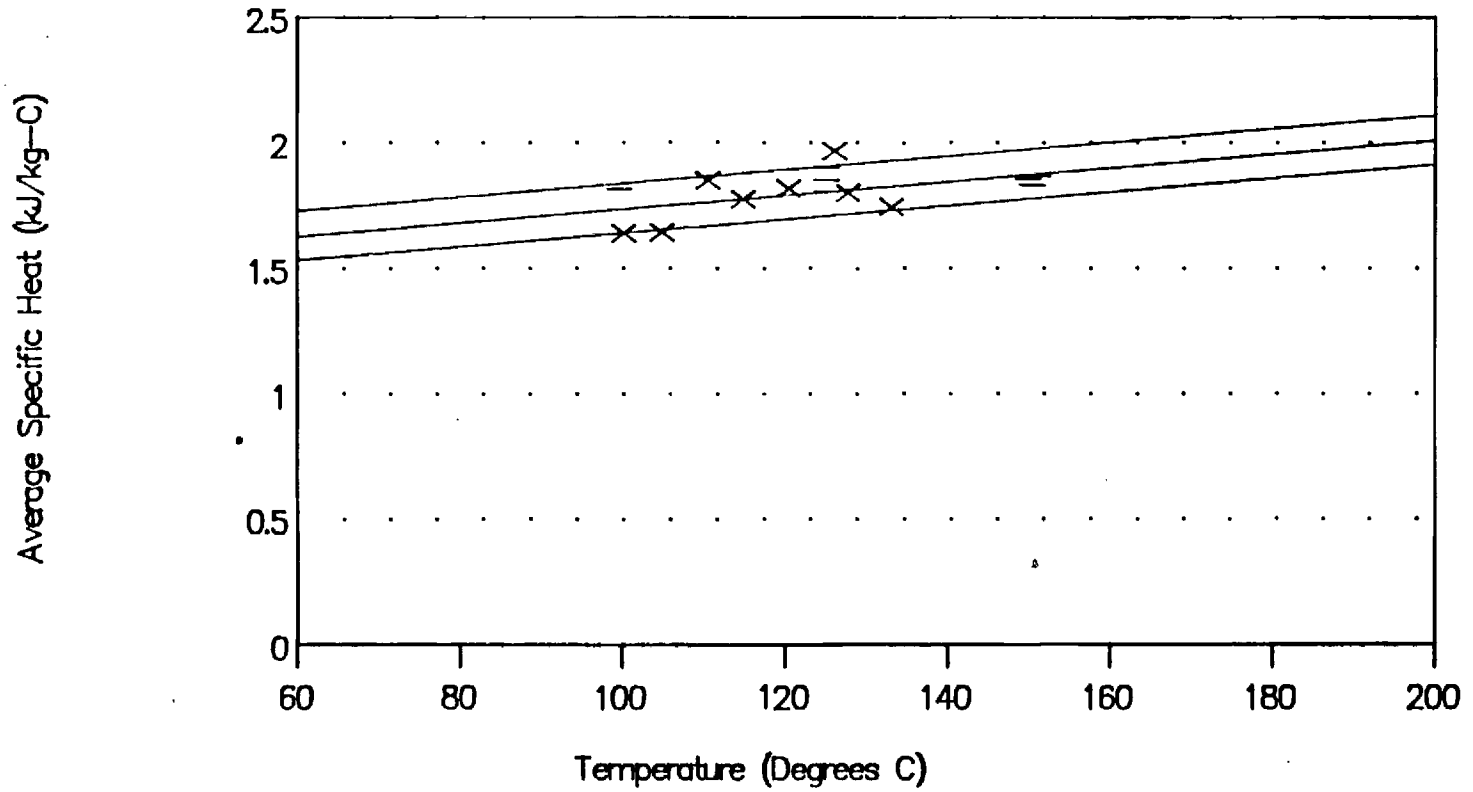


Figure A.6: 43.95% LiBr by weight

Quadratic-Linear Correlation

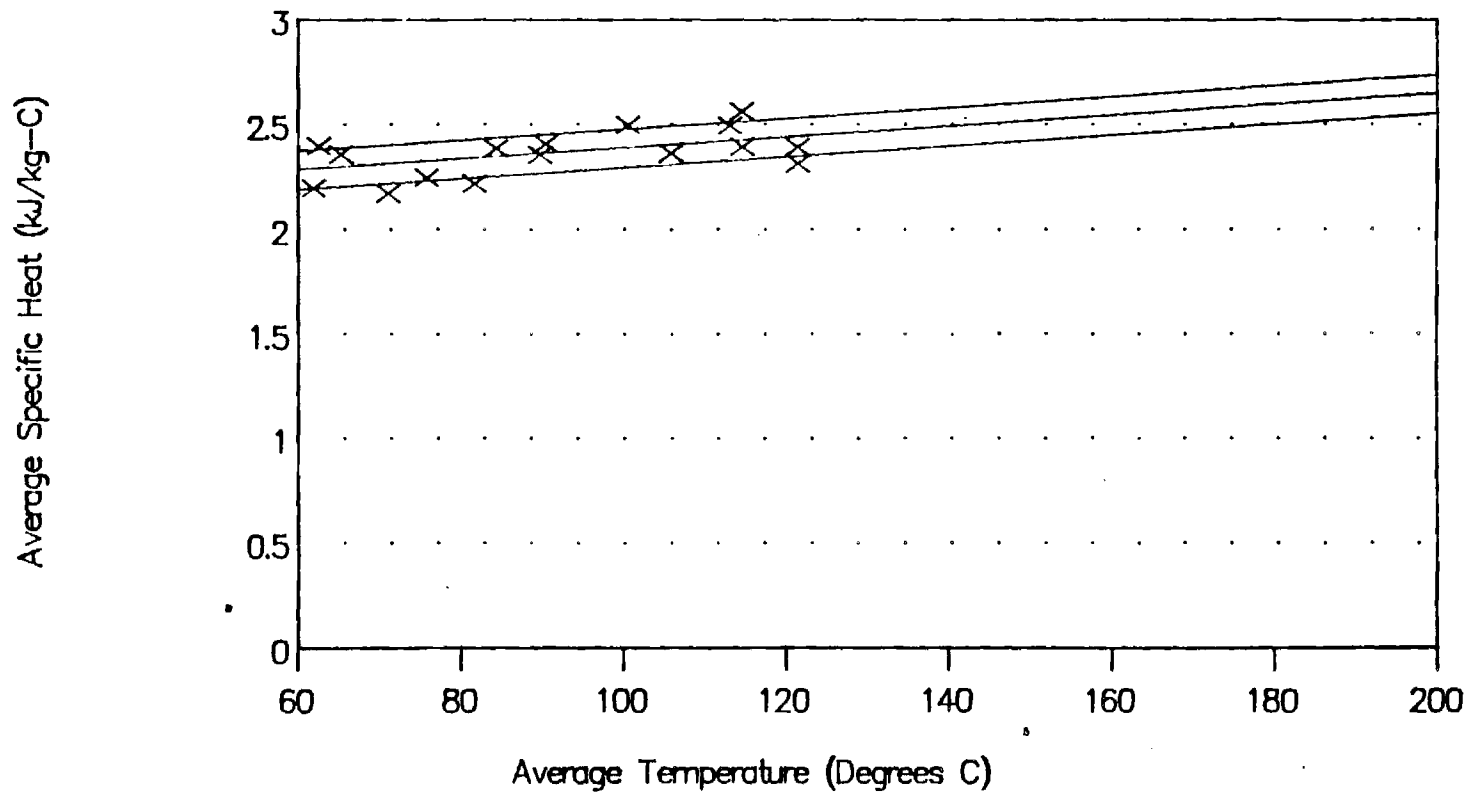


Figure A.7: 50.59% LiBr by weight

Quadratic-Linear Correlation

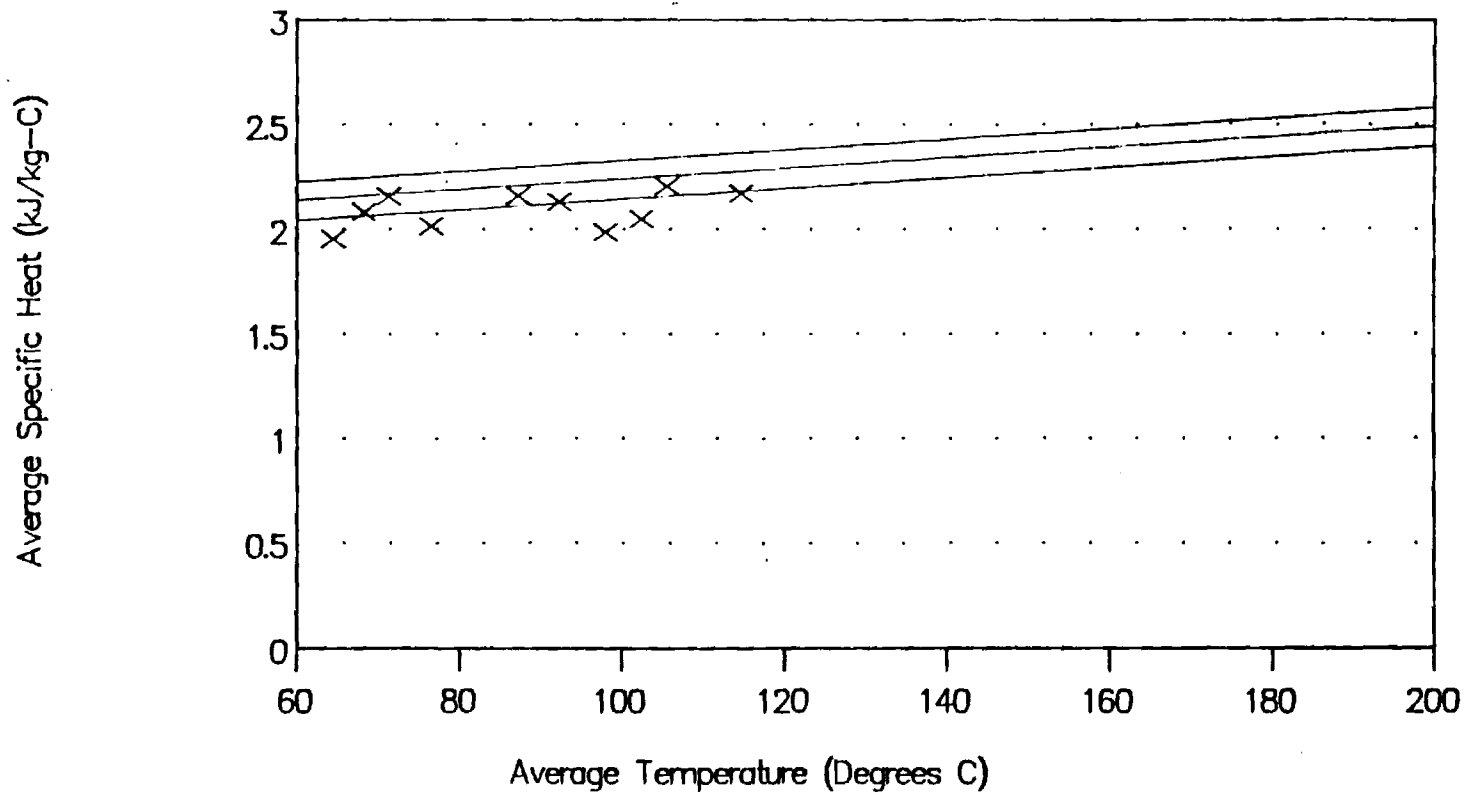


Figure A.8: 54.10% LiBr by weight

Quadratic-Linear Correlation

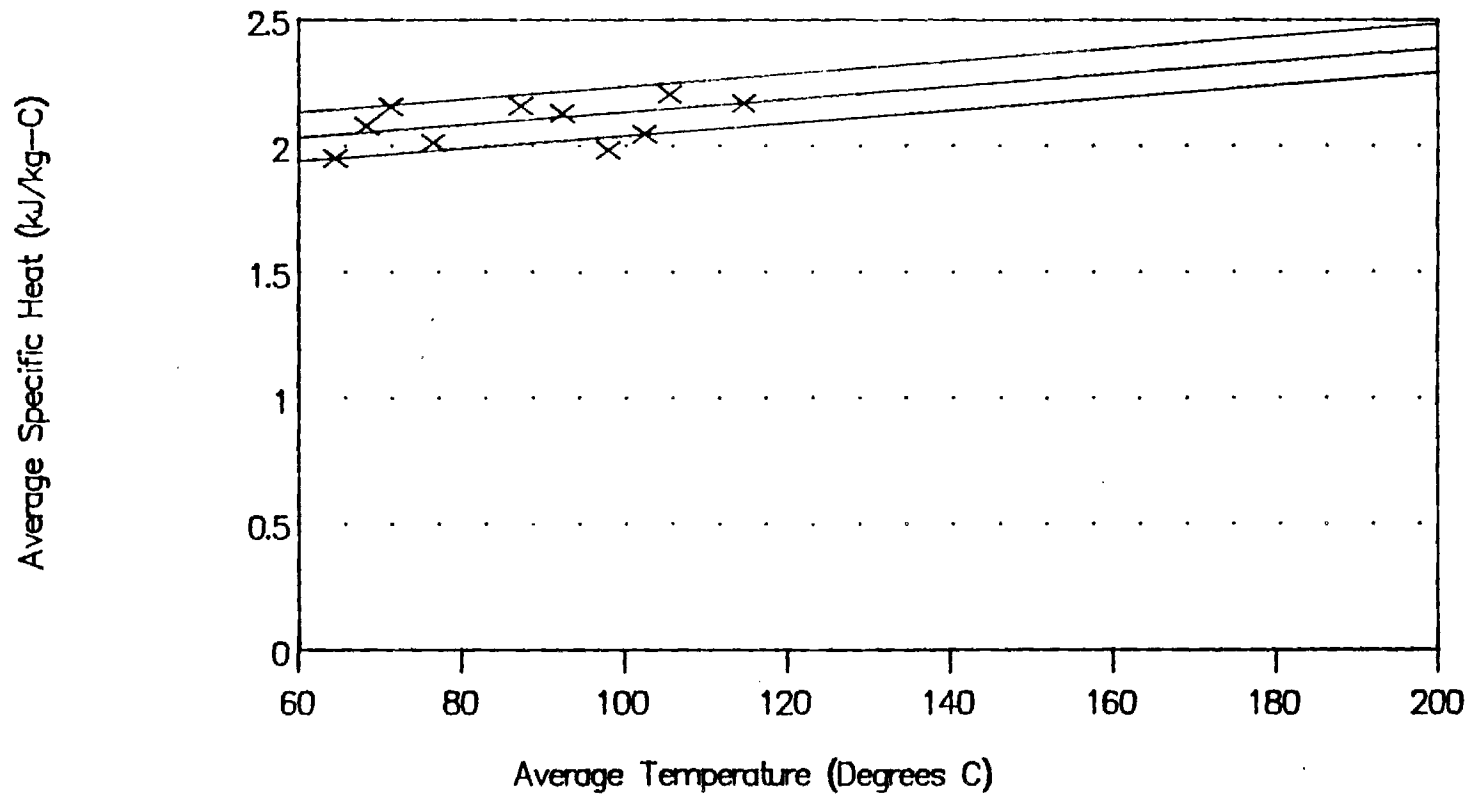


Figure A.9: 59.48% LiBr by weight

Quadratic-Linear Correlation

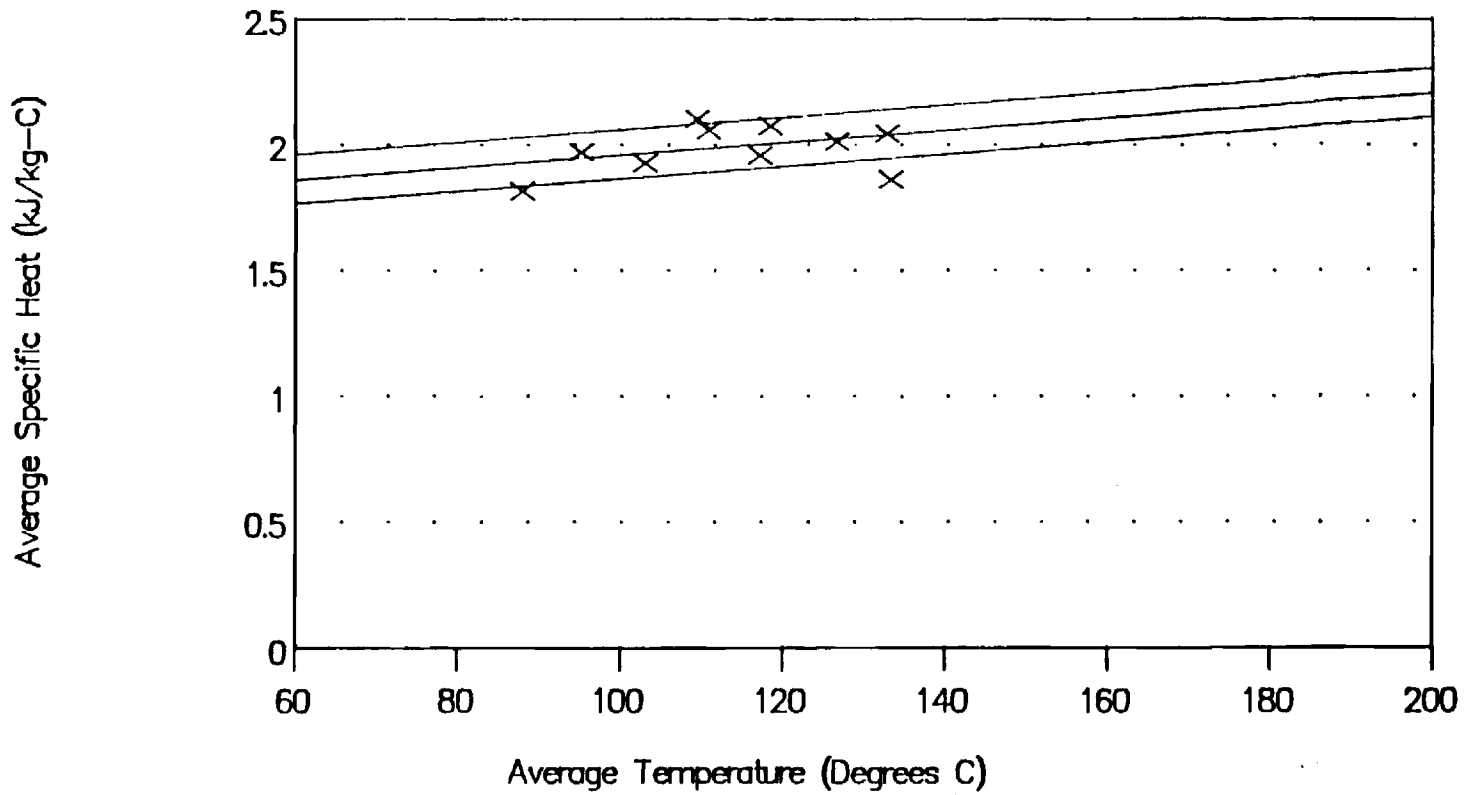
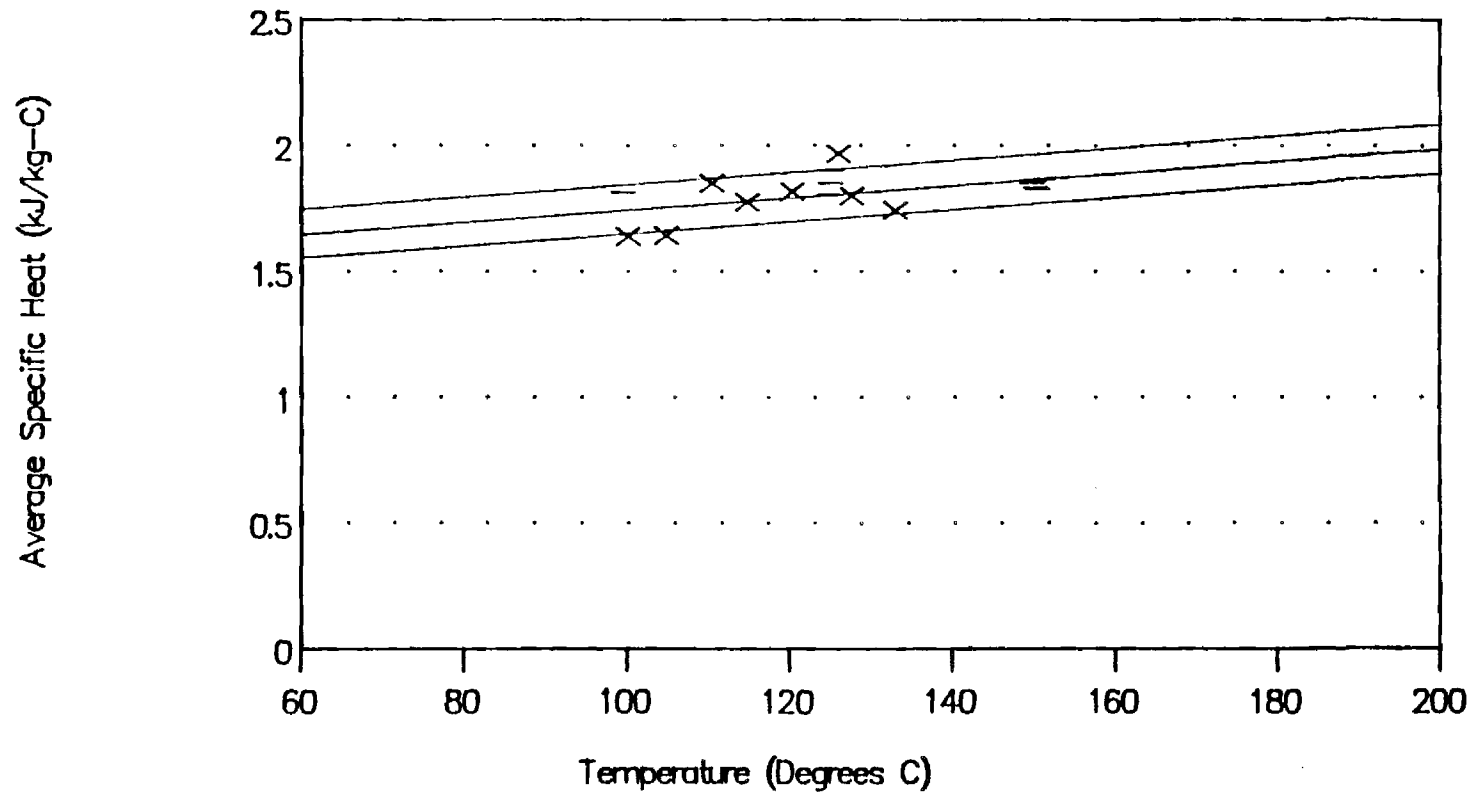


Figure A.10: 64.83% and 65.48% LiBr

Quadratic-Linear Correlation



Chapter 6

Vapor Pressures of Aqueous Lithium Bromide Solutions

1. Introduction

Aqueous solutions of lithium bromide are common working fluids in absorption refrigeration applications. A knowledge of the physical properties and, in particular, of the P-T-x behavior of such solutions is required for process design and operation. To improve the efficiency of LiBr-water absorption cycles, extensions of current processes to higher operating temperatures have been sought. However, very little reliable information on the thermophysical properties of lithium bromide solutions at high temperatures is available. The main objective of this work was to measure and correlate the vapor pressures of aqueous solutions of lithium bromide at temperatures ranging from 100 to 200 °C and concentrations ranging from 0.45 to 0.65 salt mass fraction. Five solutions of salt mass fractions 0.437, 0.494, 0.549, 0.608 and 0.652 were investigated. Previously reported data sets were reviewed and compared with the results obtained in this study. The most reliable literature data were combined with the measurements of this study to develop a consistent database for the vapor pressure of concentrated electrolyte solutions. The theory of electrolyte solutions is not yet sufficiently developed to allow a theoretical representation of thermophysical properties over a large range of temperature and concentration [Zemaitis,1986]. In the absence of a suitable theoretical model, a semi-empirical

approach was adopted. A novel representation of the vapor pressure of salt solutions, suitable for large temperature and concentration ranges, was developed. The experimental results of this work were successfully correlated using the proposed semi-empirical model. The results of this work will allow the development of more reliable P-T-x charts for aqueous lithium bromide solutions and their extensions to higher temperatures.

2. Experimental

Apparatus

The experimental apparatus used in this work is shown in Figure 1. It is based on the static vapor liquid equilibrium principle and was developed specifically for the measurement of the vapor pressure of salt solutions at high temperatures and high pressures. The apparatus comprises five parts: the equilibrium cell, the manifold, the pressure transducer, the temperature transducer and the oven.

The heart of the system is a high pressure equilibrium cell made of 316 stainless steel with a wall thickness of 0.635 cm (1/4 in). Borosilicate glass liners for the cell and passivation of the steel by nitric acid were used to minimize corrosion problems inherent to the system LiBr-H₂O. A glass coated magnet was used to stir the solution inside the cell. The magnet was driven externally by a permanent magnet translating up and down along the side of the cell. A glass wool plug on top of the glass cell liner prevented salt from being splashed onto the steel walls. The internal volume of the cell was 54.6 ml. A 0.16 cm (1/16 in) thick graphite washer (Grafoil) was employed to provide a reliable pressure and vacuum seal between the lid and the bottom of the cell. A high pressure non-rotating stem valve (High pressure Autoclave Engineering, model 30-VM) connected the cell to the manifold.

The temperature inside the cell was determined by differential thermometry. The reference temperature was given by a platinum resistance thermometer (Fluke Model Y2039) buried in a metal block located in the immediate vicinity of the cell. The platinum resistance thermometer was connected to a high precision digital

thermometer (Fluke, Model 2180A) allowing direct and accurate reading of the temperature. The temperature difference between the cell and the metal block was measured with a six junction type E thermocouple, whose output voltage was monitored by a digital multimeter (Fluke, Model 8840A). During the experimental runs, the accuracy of the platinum resistance thermometer reading was checked regularly at the freezing point of water.

The oven consists of an insulated metal cabinet containing a heater and a fan. The heater and the fan were separated from the remaining contents of the oven by a fine screen mesh. The cell temperature was controlled by a PID temperature controller (Omega Programmable Temperature Controller, Model CN-2010) and could be maintained within ± 0.1 K of the set point for periods as long as 100 hours.

The pressure was transmitted from the cell to the pressure gauges through a high pressure manifold made from 2.11 mm (0.083 in) ID tubing (Autoclave Engineering HighPressure Tubings) and appropriate fittings (Autoclave Engineering HighPressure Fittings, Series F). For increased sensitivity, two pressure gauges (Heise 710-A, range 0-150 psig with a sensitivity of ± 0.01 psi and Heise 710-A, range 0-200 bar with a sensitivity of 0.01 bar) were used in this study. These pressure gauges were regularly calibrated against a dead weight tester (Budenberg, Model 380H) with rated accuracy of ± 0.05 % of the reading. During the experimental runs, the pressure gauges were zeroed periodically by opening the manifold to atmosphere. Barometric pressures were determined using a Fortin barometer; mercury elevations were corrected for temperature and local gravity effects. Since the pressure gauges were kept at room temperature, no temperature correction of the readings were necessary.

In this work, it was decided to use pure degassed water as a pressure transmitting fluid. More classical choices, such as silicone oils or liquid metals, were initially tried but found to be inadequate (at the temperatures of interest in this study, the vapor pressure of mercury is no longer negligible and liquid gallium was found to react strongly with water vapor). Changes in solution composition due to transfer of water between the solution and the pressure transmitting fluid were avoided by controlling the position of the pressure transmitting liquid in the temperature gradient region present inside the oven wall (see Figure 2). When the valve of the cell (valve Vc in Figure 1) is closed, the pressure in the manifold is solely determined by the position of the pressure transmitting liquid inside the oven wall. This position can be adjusted freely by using the in-line variable volume generator (HIP Pressure Generator, Model 62-6-10). If the pre set pressure in the manifold is equal to the

pressure in the cell, no transfer of water occurs as the valve of the cell is opened. If the pressure in the manifold is close to the pressure in the cell, only a negligible amount of water will be transferred, partly due to the very small flow area of the manifold tubing (3.50 mm^2 or 0.005 in^2). Furthermore, it was found that following the opening of the cell valve, mechanical equilibrium throughout the system, i.e. pressure equilibrium, is attained almost immediately. If the cell valve is left open after equalization of the pressure, some water transfer occurs as the water interface in the manifold tubing adjusts itself to a new equilibrium position. The rate of water transfer is however strongly limited by the rate of heat transfer into the oven wall or into the cell. Heat transfer occurs by conduction and is inherently much slower than pressure equalization. By closing the cell valve after mechanical equilibrium has been attained and before any significant amount of water can be transferred, pressure measurements can be done without disturbing the solution composition.

This somewhat novel way of transmitting pressure was shown to be applicable to salt solutions. The pressure transmission was found to be accurate and very sensitive. Indeed, in our work, the sensitivity of the pressure transmission was only limited by the sensitivity of the pressure gauges, namely 0.7 mbar (or 0.01 psi). In addition, the attractiveness of this pressure transmitting technique lies mainly in the absence of limitations for its use at high pressure and high temperature.

Procedure

Before the start of a run, the high pressure equilibrium cell was cleaned with steam and baked under vacuum to remove any traces of surface contamination which might affect the measurements. 35 ml of a gravimetrically prepared aqueous lithium bromide solution was then transferred into the cell. The glass cell liner was plugged with some glass wool and the lid of the cell was secured with cap screws. The reliability of the graphite seal and of the cell fittings were then tested with extra dry nitrogen gas up to a pressure of 80 bar . This test pressure is more than four times greater than the maximum pressure encountered in the measurements. The pressurized cell was checked for leaks by immersing it in a tank of water.

Nitrogen gas and other inerts were removed from the cell by repeated pumping of the vapor phase present above the salt solutions. By keeping the solution at sufficiently low temperature (at the freezing point of water in this work), the amount

of water present in the vapor phase and therefore removed from the cells during the pumping can be shown to be negligible. The absence of any significant water loss during the degassing procedure was checked by monitoring the mass of the contents of the cell. Above a salt mass fraction of 0.60, aqueous lithium bromide solutions were present at 0 °C in a state similar to a glassy state. Classical freeze-pump-thaw cycles were therefore used to degas the most concentrated solutions. Since thorough degassing is critical in static VLE experiments, the pressure inside the cell was monitored by a thermocouple vacuum gauge (Sargent-Welch Scientific Company, Model 1515) to assess the completeness of inert removal. Generally four to six cycles were found sufficient to obtain a constant residual pressure inside the cell.

Once the degassing had been completed, the cell was installed in the oven and attached to the manifold. The manifold and the pressure transmitting lines were tested for absence of leaks with nitrogen gas up to 80 bar and then evacuated. Pure degassed water was charged into the pressure transmitting lines. When the oven temperature had reached its set point, the valve connecting the manifold to the pressure transmitting lines (valve Vm in Figure 1) was opened and the water was allowed to penetrate into the manifold up to the temperature gradient region located inside the oven wall. Upon intrusion of water into the temperature gradient region, water vaporization occurred and pressure started to build up inside the manifold.

At this time the apparatus was ready for measurement. The position of the water vapor liquid interface inside the oven wall was adjusted to obtain the desired manifold pressure. The valve of the cell was then opened for five to ten seconds, time to record the total pressure in the system. After closing the cell valve, the absence of any significant water transfer was checked as the manifold pressure returned to its pre-set level. The solution inside the cell was allowed to equilibrate with its somewhat perturbed vapor phase and the manifold pressure was adjusted to a new value. Generally, three to four adjustments were sufficient to get a set manifold pressure equal to or very close to the pressure inside the cell. Once convergence had been obtained, the pressure determination procedure was continued with a set manifold pressure, first slightly higher and then slightly lower than the solution equilibrium pressure to check for hysteresis in the reading.

The temperature of the oven was then set to a new value and the pressure determination procedure repeated.

Materials

Lithium bromide was obtained in the anhydrous form from Morton Thiokol Inc. (lot F06H). The manufacturer's certificate of analysis stated a purity of 99.3 %w, the remaining being water (0.5 %w) and various salts. During the preparation of the lithium bromide solutions, the presence of fiber-like materials and black and orange pellets was noticed. These impurities seemed most likely to have come from the manufacturing process. However, their presence was not found to significantly affect the vapor pressure measurements. Before use, the required amount of salt was dried by heating the sample under vacuum. This drying technique was found to be suitable for the particularly hygroscopic lithium bromide salt, as documented by Weintraub et al [1984] in their work on the determination of the water content of lithium salts. No further changes in the mass of the salt were observed after 24 to 48 hours of drying at temperatures ranging from 130 to 200 °C and pressure of the order of 100 mtorr. The drying was then considered complete. Analytical NaCl, used for the validation test, was purchased from Fisher Scientific (lot 851530) and was dried using the same procedure. The water used in this study was purified by distillation in an all-glass still (Corning Mega-Pure System, Model MP-6A).

3. Results and Discussion

The apparatus and the experimental procedure were validated by replicating vapor pressure measurements for the system NaCl-water. Our results were compared to the data of Liu and Lindsay [1972] (see Figure 3). The average relative deviation between the two data sets is 0.3%.

The vapor pressures of concentrated aqueous lithium bromide solutions were measured at temperatures ranging from their normal boiling temperature up to 210 °C. Five solutions with salt mass fraction ranging from 0.438 to 0.651 were investigated. The results of these measurements are given in Table 1. The solution composition was corrected for loss of water due to vaporization. The accuracy in the pressure measurement was estimated by error propagation analysis to be ± 15 mbar, whereas the uncertainty in the temperature determination is estimated to be $\pm 0.3\%$.

4. Correlation

Dilute and very dilute aqueous solutions of electrolytes have been extensively studied, especially at ambient conditions and numerous theoretically based models have been proposed for the representation of their thermophysical properties [Zemaitis, 1986]. Extensions of these models to higher salt concentrations and to higher temperatures is presently an active field of research. Dilute solution based models are, however, not yet suitable for representing thermophysical properties of electrolyte solutions over large ranges of temperature and concentration. An empirical or semi-empirical approach has therefore been traditionally preferred, and numerous empirical models have been proposed for correlating the vapor pressures of aqueous electrolyte solutions [Horvarth,1985].

For this study, a novel semi-empirical model, suitable for correlating the vapor pressures of aqueous electrolyte solutions over large ranges of temperature and concentration, has been developed. The ratio of the solution vapor pressure to the saturation pressure of pure water, namely P/P_w^{sat} , was found to be a particularly suitable dependent variable. The temperature dependence of this pressure ratio is well behaved, exhibiting a small and very linear dependence over large temperature ranges. Furthermore, as long as only a negligible amount of salt is present in the vapor phase, this pressure ratio is very closely related to the solvent activity and its value and behavior at the limits of the composition range are well known. When the amount of salt present in the solution approaches zero, the pressure ratio goes to one, and as the solution becomes more and more concentrated in salt, the pressure ratio approaches zero. By taking into account these limiting bounds, P/P_w^{sat} was expressed as a function of temperature and composition in the form:

$$P / P_w^{sat} = x_w + x_w(1 - x_w)g[T, x_w]$$

where x_w is the water mole fraction and g is an empirical function whose functional form is determined by stepwise regression analysis. In general, g is a simple function of the temperature and the water mole fraction, such as a polynomial in x_w and T , or a simple function containing terms such as $\ln(x_w)$, $\exp(x_w)$, $1/T$ or $\ln(T)$. It should be noted that the water mole fraction was defined in this work on a ionized basis as follows:

$$x_w = \frac{n_{water}}{n_{water} + n_{ion}}$$

where n_{water} is the amount of water present in the solution and n_{ion} is the total amount of ions assuming complete dissociation of the salt molecules. The correspondence between water mole fraction defined on an ionized basis and salt mass fraction, $\omega(\text{LiBr})$, is given by:

$$\frac{1}{\omega(\text{LiBr})} = 1 + 2 \frac{18.054}{86.85} \left(\frac{x_w}{1 - x_w} \right)$$

The experimental results of this work were correlated using this newly developed model. The stepwise regression analysis of the data resulted in the following correlation for P/P_w^{sat} :

$$P / P_w^{sat} = x_w + x_w (1 - x_w) \left[A_0 + A_1 (x_w - 0.65) + A_2 (x_w - 0.65)^2 + A_3 (x_w - 0.65)^3 + A_4 \left(\frac{T - 150}{150} \right) + A_5 \left(\frac{T - 150}{150} \right) (x_w - 0.65)^2 \right]$$

where T is the temperature of the solution in °C. The parameters A_i are given in Table 2. The average relative deviation of the data set from the correlation is 0.21% (see Table 3). The quality of the fit is illustrated in Figure 5.

5. Review of literature Data

Scope of the review

Numerous investigators have reported data for the vapor pressures of aqueous lithium bromide solutions. The International Critical Tables [I.C.T.,1928], published in 1928, mentions more than nine references related to this subject. Works done before 1970 were summarized by McNeely [1979], who compiled published data as well as data measured by the major manufacturers of lithium bromide absorption

equipment in USA. In this paper, more recent works will be reviewed. The data of Pennington [1955], on which the current PTx ASHRAE charts are generally based, were also included.

The temperature and concentration ranges studied by the different investigators included in this review are summarized in Figure 6. The data sets were analyzed to determine their intrinsic reliability and, to allow comparison on a common basis, were then correlated using the model proposed in this work. Statistical information characterizing the individual data sets is summarized in Table 3. The indicated number of data points refers to the total number of reported experimental determinations. The data set precision is expressed through its average absolute deviation (AAD) and its average relative deviation (ARD). The AAD and ARD computation were based on an optimized set of values, from which likely outliers and inconsistent results were removed. It should be noted that the AAD and the ARD criteria do not characterize the data sets in the same way, due to differences in temperature and composition ranges.

Measurements at subatmospheric conditions.

Most of the measurements, especially the earliest ones, were done at subatmospheric or atmospheric pressure. Pennington used three independent experimental techniques to measure the vapor pressure of aqueous lithium bromide solutions, which allowed him to span different ranges of temperature and pressure (for clarity purposes, his results at 30 °C were not included in Figure 6). The data sets are fairly consistent with each other and are remarkably free of scatter, as illustrated by their respective AAD or ARD. Boryta et al [1975] determined the vapor pressure of four aqueous lithium bromide solutions containing respectively 40, 50, 60 and 70 % of salt in mass, by a static and by a gas transport method. His data at 40 %w showed considerably more scatter than the ones at higher concentrations and a very unlikely temperature dependence (see Figure 7). They were not considered further. His gas transport results seemed less precise than the data obtained by the static method. However, within the scatter of the data, the results obtained by the two experimental methods seemed to agree. Renz [1981] measured the vapor pressure of aqueous lithium bromide solutions over an extended range of concentrations at subatmo-

spheric conditions. Since this review is mainly concerned with concentrated solutions, only his data pertaining to solutions having salt mass fractions of 0.35 or more were considered.

Measurements above atmospheric pressure

Measurements above atmospheric pressure have been reported by three investigators. Fedorov et al [1976] measured the vapor pressure of aqueous lithium bromide solutions at temperature ranging from 150 to 350 °C for a wide range of compositions. However, only data interpolated to integral temperatures were reported. The absence of experimental scatter in the reported data did not permit a fair estimation of the data set precision. The individual correlation of the Fedorov et al measurements was based on the smoothed data. Rockenfeller [1988] determined the vapor pressure of aqueous lithium bromide solutions from 80 to 205 °C for solutions having a salt mass fraction ranging from 0.35 to 0.6470. His data under 95 °C showed considerably more scatter than the ones above 95 °C (see Figure 8). The data below 95 °C were not considered further. The reported precision of the measurements was ± 13 mbar. This value was found to be consistent with the derived AAD and ARD of the data set, and illustrates the high level of precision obtained in these measurements. However, it should be noted that two pressure gauges, with span range of respectively 25 and 250 psi, were used for these measurements and, small but clear discrepancies between the readings of the two pressure gauges were observed. Recently, Iyoki and Uemura [Iyoki, 1989] published measurements for the vapor pressure of concentrated aqueous lithium bromide solutions. The use of a thick wall glass still allowed them to measure vapor pressure up to 3 bar. The scatter in their data was found to be greater than in the previously discussed data sets. However, on the whole, the data seemed to be fairly reliable.

6. Comparison with literature data

Due to different temperature and composition conditions, a direct comparison of vapor pressure measurements is difficult. Therefore, agreements and disagreements between data sets were put in evidence by using the individual data set correlations. The vapor pressure measurements reported in the six reviewed studies were compared to the vapor pressure measurements obtained in this work. The results of the comparisons are shown in Figure 9a through Figure 9e. Large discrepancies are apparent. Rockenfeller's data are systematically higher. The bias is, on average, one order of magnitude greater than the precision of his data and therefore cannot be attributed simply to lack of fit of the data sets or to large scatter in the measurements. The data of Fedorov et al similarly exhibit strong discrepancies. The vapor pressure measurements of Renz and the ones of Iyoki and Uemura seem to agree consistently at the lowest concentrations, but discrepancies are apparent for the most concentrated solutions. The data set of Boryta et al and the one of Pennington do not show consistent agreement with any other data sets, but no clear bias can be shown. The experimental results of this work show good agreement with the data of Renz and with the data of Iyoki and Uemura at a salt mass fraction of 0.4375, 0.4940 and 0.5487. At a salt mass fraction of 0.6085 and especially at a salt mass fraction of 0.6515, our experimental results fall between the data of Renz and of Iyoki and Uemura. It should be added that the curvature in temperature of our experimental results, apparent in Figure 9a through 9e, is partly due to the increase of the salt mass fraction of the measured solution as the temperature is increased (see vaporization correction in the Results and Discussion paragraph).

7. Conclusion

The vapor pressures of concentrated aqueous lithium bromide solutions were measured at temperatures ranging from their normal boiling temperature to 210 °C. Five solutions of salt mass fraction 0.437, 0.494, 0.549, 0.608 and 0.652 were investigated. The experimental results were successfully correlated using a novel semi-empirical model for the vapor pressure of electrolyte solutions. This model was shown particularly suitable for representing the vapor pressure of electrolyte solutions over large temperature and concentration ranges. And, although extrapolation in concentration should be used with caution, the proposed model was found to be useful for extrapolating data sets in temperature. Previously published vapor pressure measurements were also reviewed and checked for consistency. Our experimental results were found consistent with the most reliable literature data. The results of this work will allow the development of more reliable P-T-x charts for aqueous lithium bromide solutions and their extensions to higher temperatures.

8. Bibliography

Boryta D.A., Maas A.J. and Grant C.B., "Vapor Pressure-Temperature-Concentration Relationship for System Lithium Bromide and Water (40-70% Lithium Bromide)", *Journal of Chemical and Engineering Data*, Vol 20, 3:316-319, 1975

Federov M.K., Antonov N.A. and L'vov S.N., "Vapor Pressure of Saturated Aqueous Solutions of LiCl, LiBr, and LiI and Thermodynamic Characteristics of the Solvent in These Systems at Temperatures of 150-350 °C and Pressures up to 1500 bar", translated from *Zhurnal prikladnoi Khimii*, Vol 49, 6:1226-1232, 1976

Horvath A.L., "Handbook of Aqueous Electrolyte Solutions", Ellis Horwood Limited, Chichester, England, 1985

International Critical Tables, Vol 3, New-york, Mc Graw-Hill, 1928

Liu C. and Lindsay W.T., "Thermodynamics of Sodium Chloride Solutions at High Temperatures", *Journal of Solution Chemistry*, Vol 1, 1:45-69, 1972

Mc Neely L.A., "Thermodynamic Properties of Aqueous Solutions of Lithium Bromide", *ASHRAE Transactions*, 3:413-434, 1979

Pennington W., "How To Find Accurate Vapor Pressures of LiBr Water Solutions", *Refrigerating Engineering*, 63:57-61, 1955

Renz M., "Bestimmung Thermodynamischer Eigenschaften Wässriger und Methylalkoholischer Salzlösungen", Dissertation, University of Essen, 1981

Rockenfeller U., Private Communication, 1988

Iyoki S. and Uemura T., "Vapor Pressure of Water-Lithium Bromide System and the Water - Lithium Bromide - Zinc Bromide - Lithium Chloride System at High Temperatures", *Revue Internationale du Froid*, Vol 12, 278-282, 1989

Weintraub R., Apelblat A., Tamir A., "Determination of Water Content of Hygroscopic Lithium Salts", *Analytica Chimica Acta*, 166:325-327, 1984

Zemaitis J.F., Clark D.M., Rafal M., Scrivner N.C., "Handbook of Aqueous Electrolyte Thermodynamics", American Institute of Chemical Engineers Inc, New-York, USA, 1986

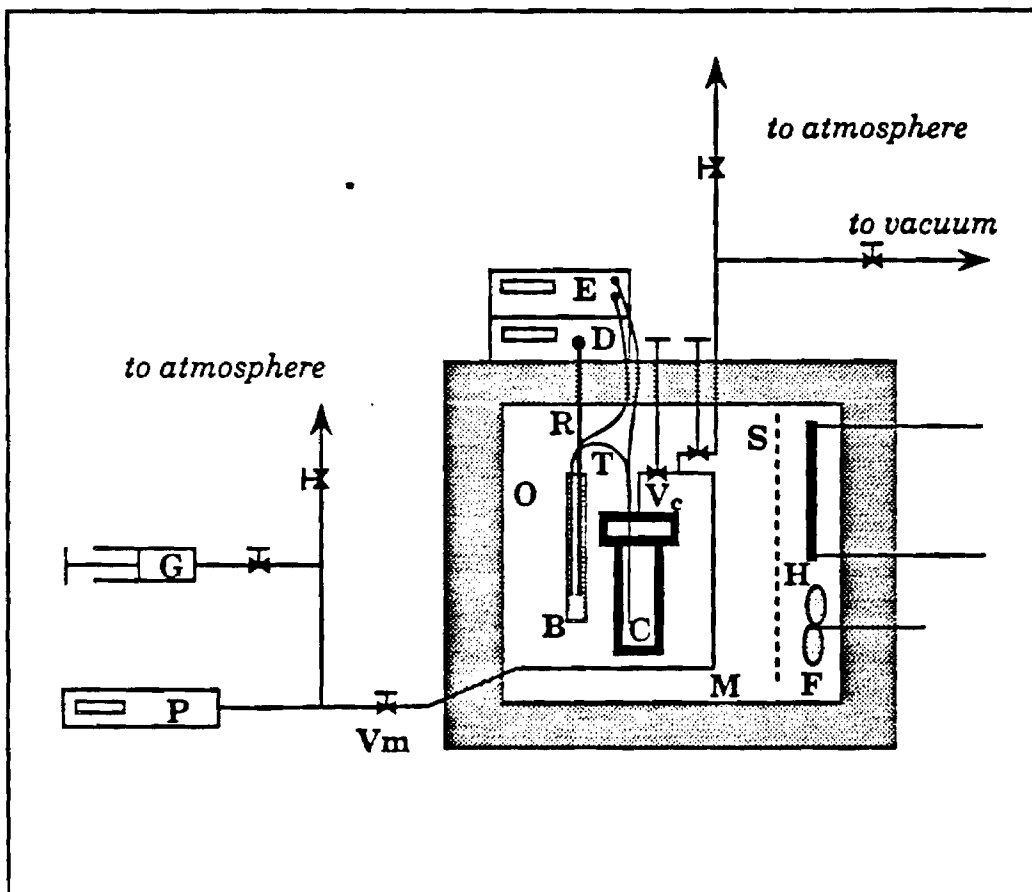


Fig 1 : Schematic of the static VLE apparatus:

(B) Metal Block, (C) Cell, (D) Digital thermometer, (E) Digital Multimeter, (F) Fan, (G) Variable Volume Generator, (H) Heater, (M) Manifold, (O) Oven, (P) Pressure Gauge, (R) Platinum Resistance Thermometer, (S) Screen, (T) Multijunction Thermocouple, (Vc) Cell Valve, (Vm) Manifold Valve.

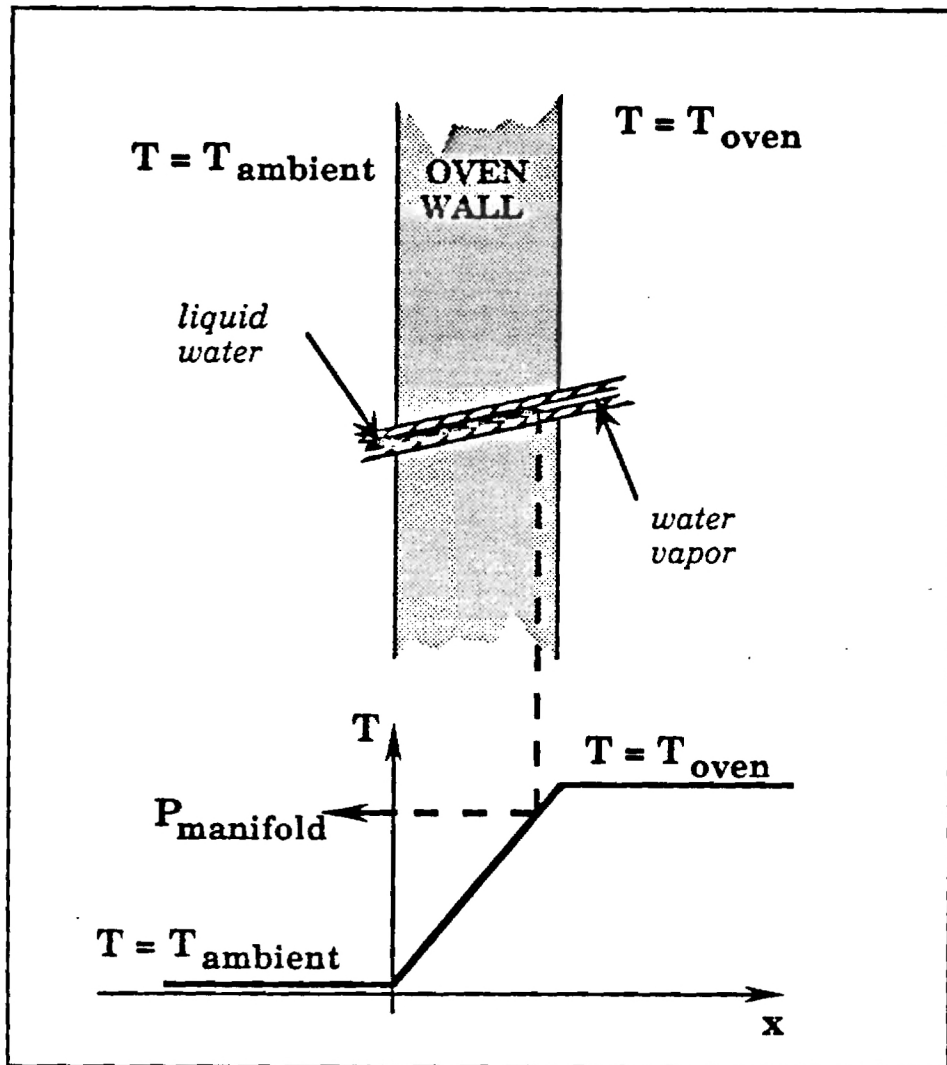


Fig 2: Pressure Transmitting Principle

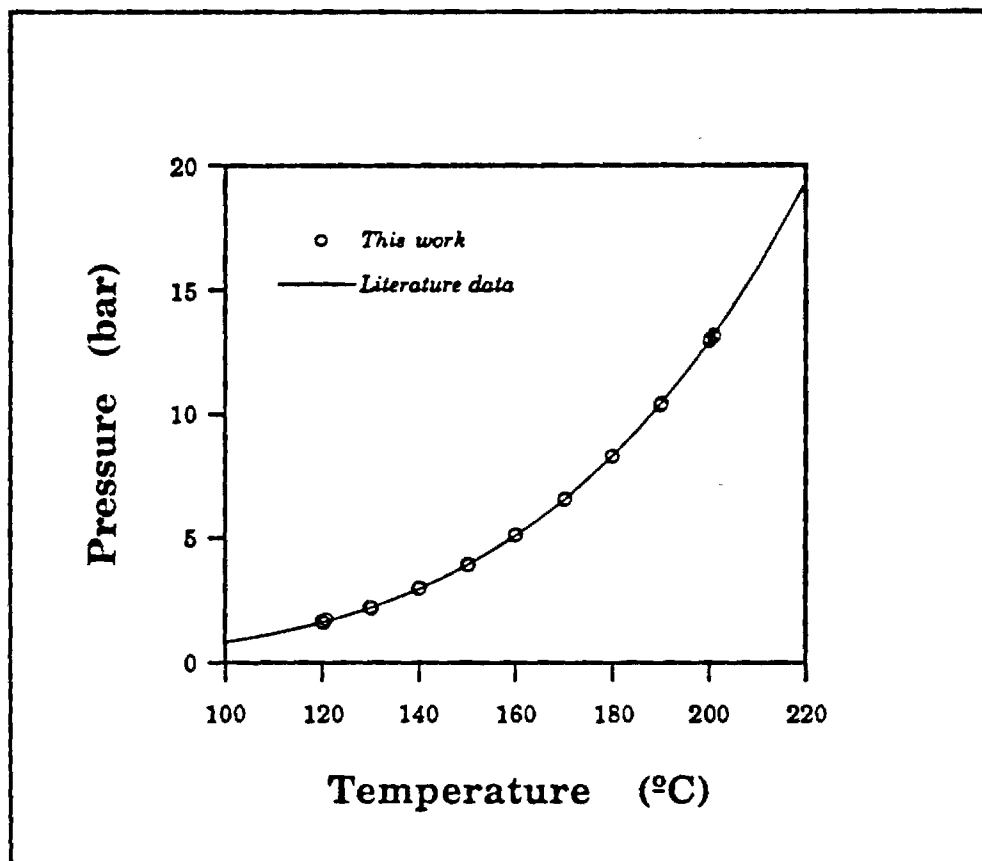


Fig 3: NaCl-Water system

The molality of the investigated solution was 4.6885 mol/kg. The literature data correlation was derived from the data of Liu and Lindsay [1972].

Table 1: Experimental Data

Salt Mass Fraction	Temperature (°C)	Pressure (bar)
0.4375 ±0.0045	125.0	1.121
0.4375 ±0.0045	134.9	1.525
0.4375 ±0.0045	149.9	2.352
0.4376 ±0.0045	165.0	3.518
0.4377 ±0.0045	180.3	5.133
0.4379 ±0.0045	210.4	10.002
0.4940 ±0.0040	135.0	1.134
0.4940 ±0.0040	150.1	1.775
0.4941 ±0.0040	165.1	2.688
0.4942 ±0.0040	180.3	3.959
0.4943 ±0.0040	195.3	5.652
0.4944 ±0.0040	210.3	7.857
0.5489 ±0.0025	150.0	1.253
0.5490 ±0.0025	165.0	1.944
0.5490 ±0.0025	180.2	2.913
0.5491 ±0.0025	195.2	4.227
0.5492 ±0.0025	210.5	6.001
0.6084 ±0.0030	165.0	1.305
0.6085 ±0.0030	180.4	2.013
0.6087 ±0.0030	195.5	2.980
0.6089 ±0.0030	210.6	4.295
0.6516 ±0.0030	179.7	1.451
0.6517 ±0.0030	194.9	2.188
0.6519 ±0.0030	209.9	3.167

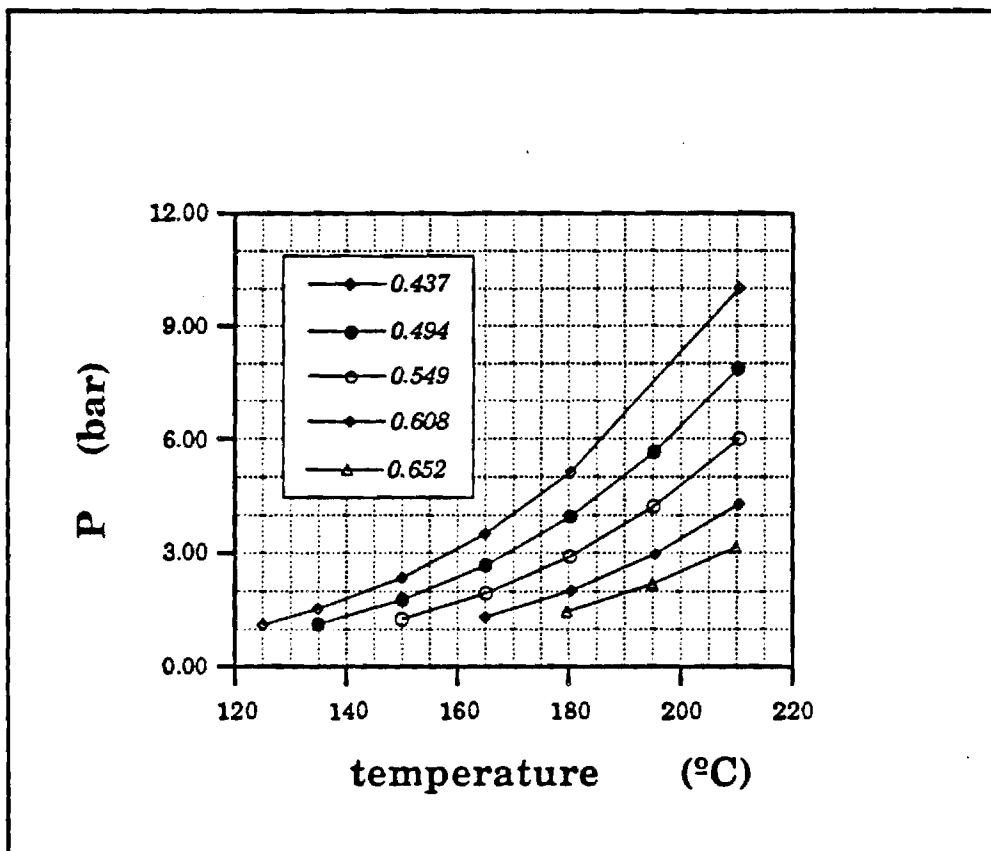


Fig 4: Experimental Data

The legend refers to the salt mass fraction of the investigated solutions.

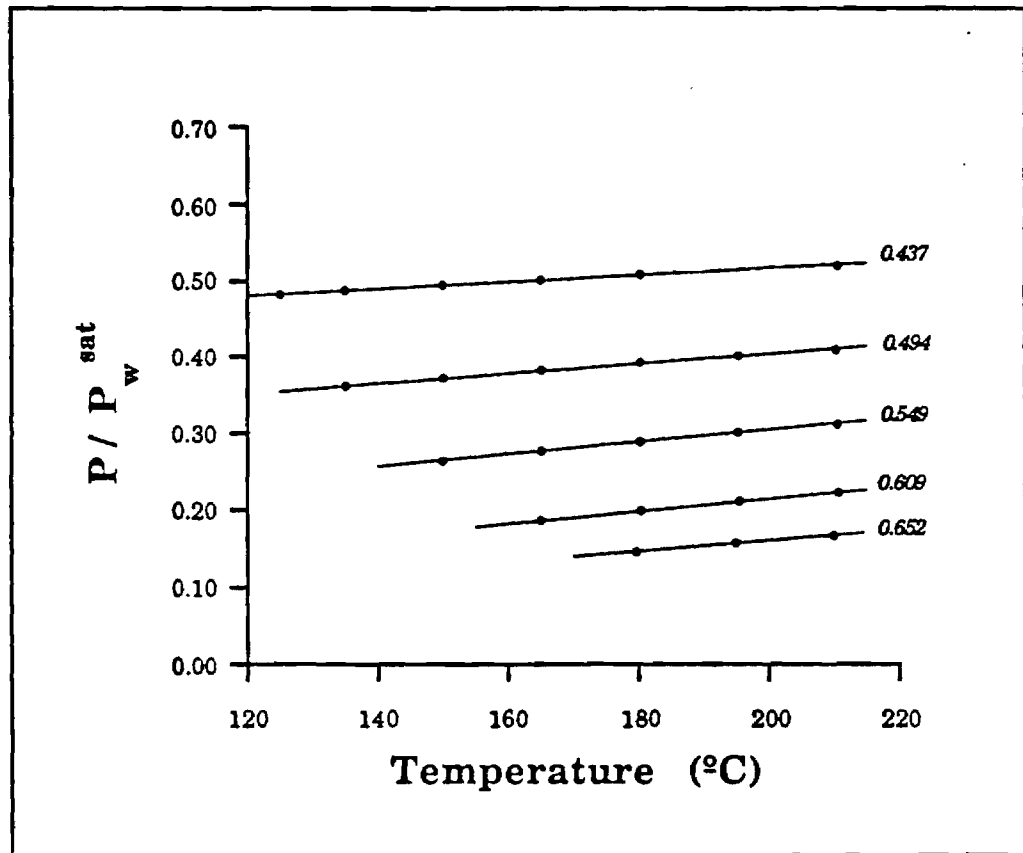


Fig 5: Correlation

(•) Experimental Data Point, (—) Correlation.

The number attached to a line indicates the salt mass fraction of the measured solution.

Table 2: Correlation Parameters.

A_0	-1.809784
A_1	1.059895
A_2	20.307708
A_3	43.314071
A_4	.536261
A_5	-15.298850

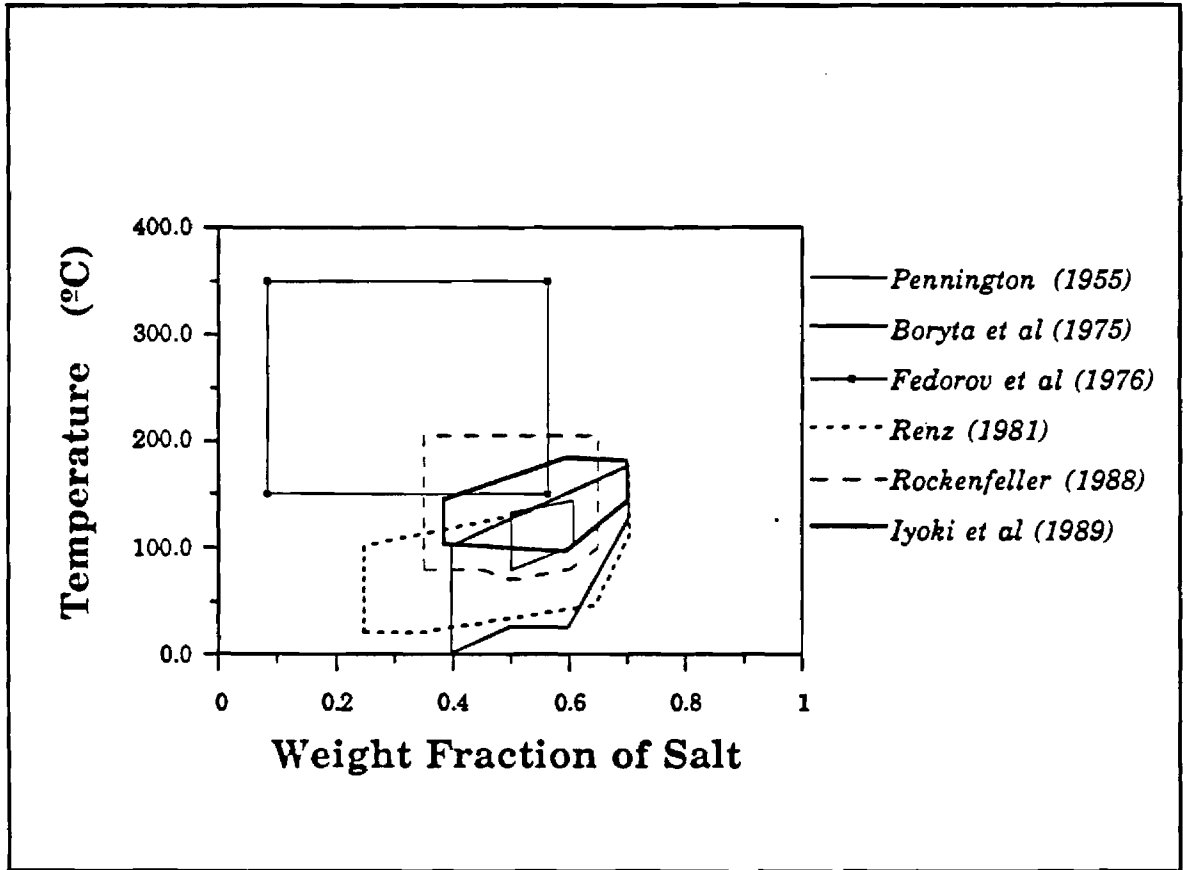


Fig 6: Temperature and composition ranges investigated in the reviewed works

Table 3: Summary of recent works

Investigator	Year	Experimental Technique	Number of data points	Precision	
				AAD	ARD
Pennington	1955	(1) Static Still	10	0.00144	0.56%
		(2) Ebulliometry	25	0.00196	0.82%
		(3) Water Absorbtion	11	0.00192	1.31%
Boryta et al.	1975	(1) Static Still	15	0.00238	1.81%
		(2) Gas Transport	17	0.00430	2.90%
Fedorov et al	1976	Static Still	35	-	-
Renz	1981	Static Still	96	0.00113	0.86%
Rockenfeller	1988	Static Still	199	0.00191	0.67%
Iyoki and Uemura	1989	Boiling Point	39	0.00380	2.24%
This work	1991	Static Still	24	0.00067	0.21%

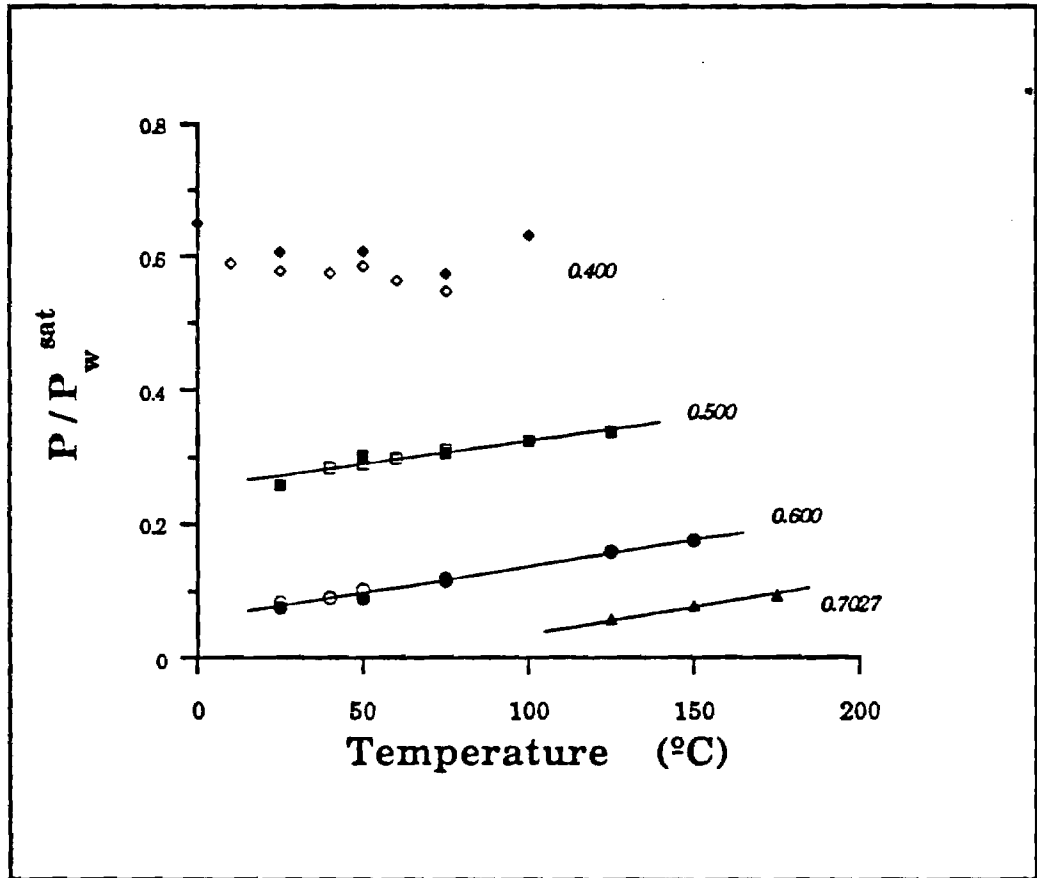


Fig 7: Experimental Results of Boryta et al

The open symbols represent the static still experimental results whereas the filled symbols represent measurements obtained by the gas transport technique. The correlation is based solely on the data of Boryta et al and was used to determine the intrinsic precision of the data set.

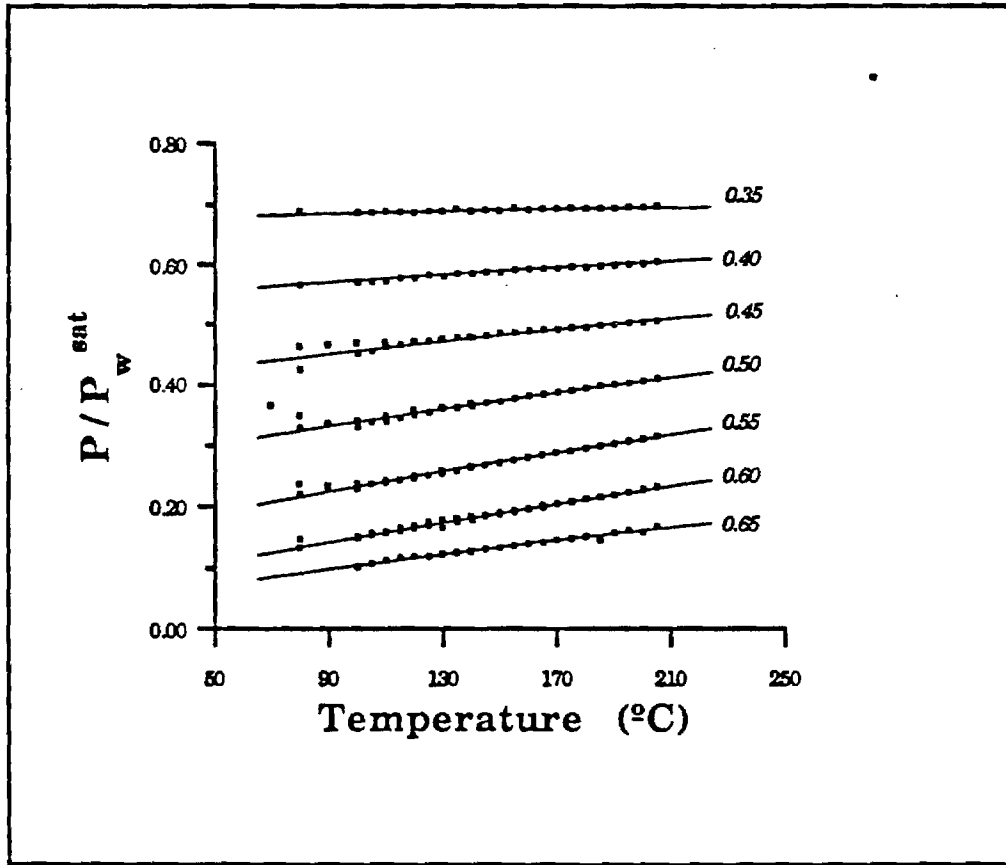


Fig 8: Experimental Results of Rockenfeller

(■) Experimental Data Point, (—) Correlation based on Rockenfeller's measurements. The number attached to a correlation line represents the salt mass fraction of the measured solution. Only measurements above 95°C were considered during the correlation of the data set.

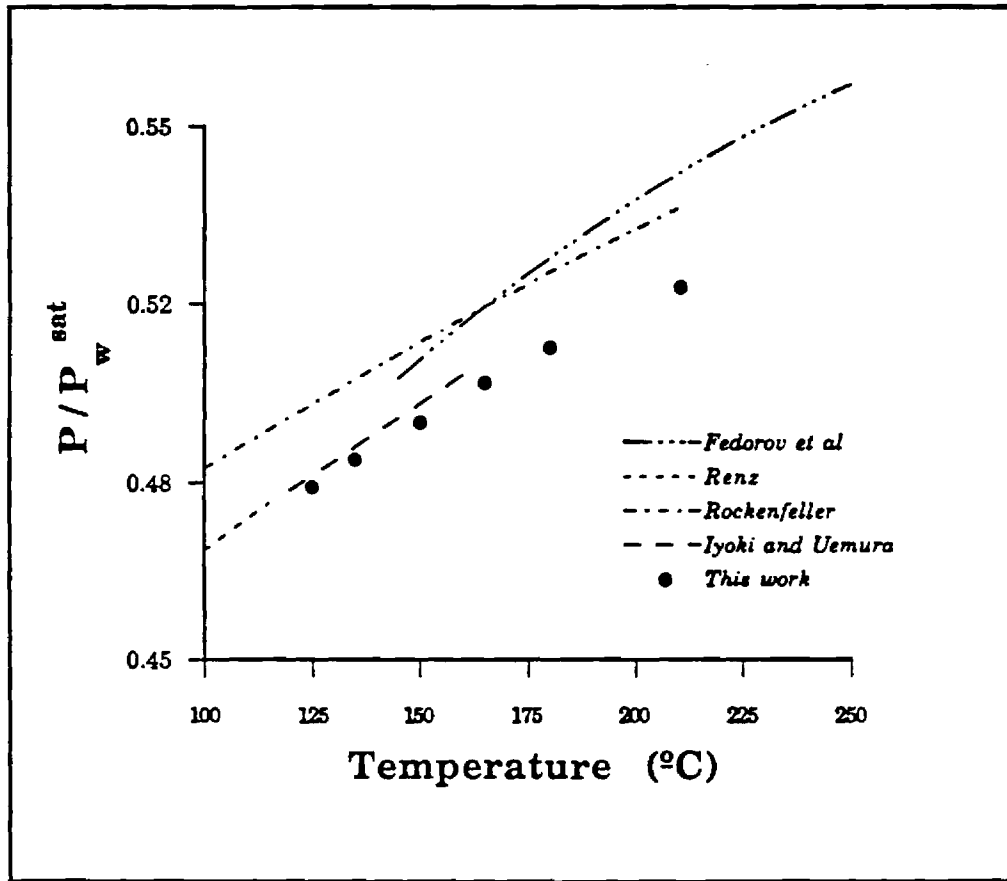


Fig 9a: Data Set Comparison

The comparison was made at a salt mass fraction of 0.4375.

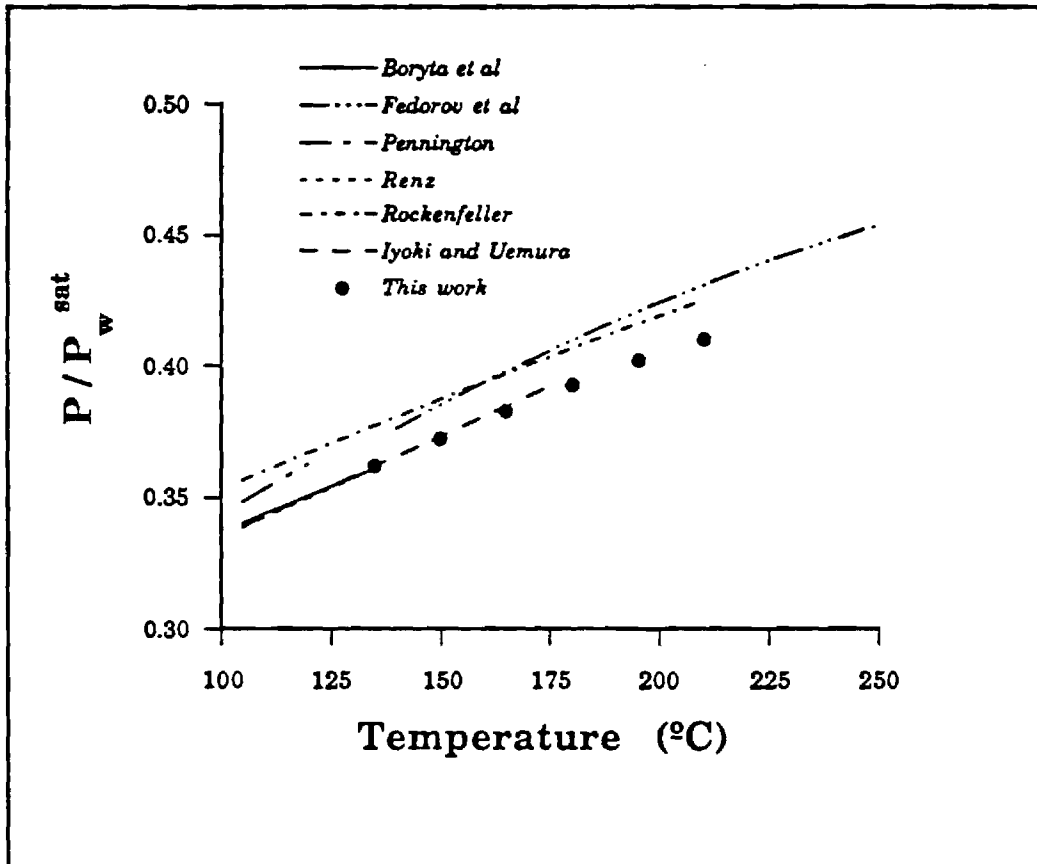


Fig 9b: Data Set Comparison

The comparison was made at a salt mass fraction of 0.4940.

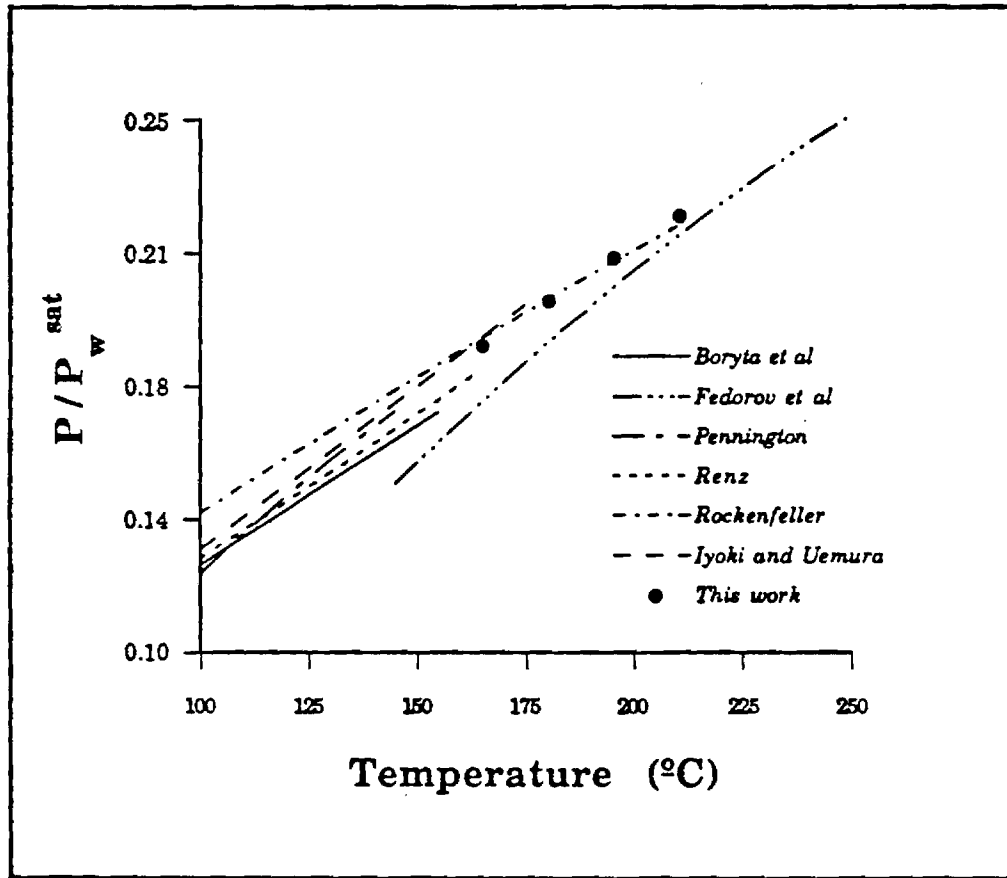


Fig 9d: Data Set Comparison

The comparison was made at a salt mass fraction of 0.6085.

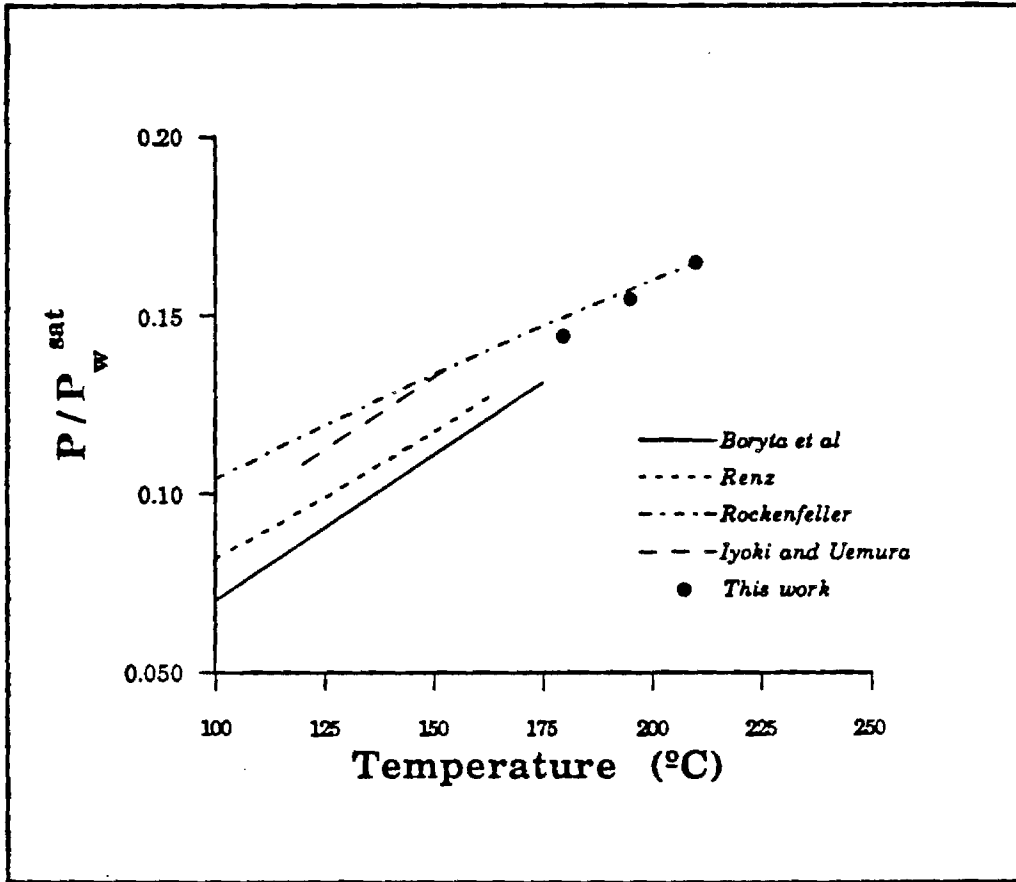


Fig 9e: Data Set Comparison.
 The comparison was made at a salt mass fraction of 0.6515.

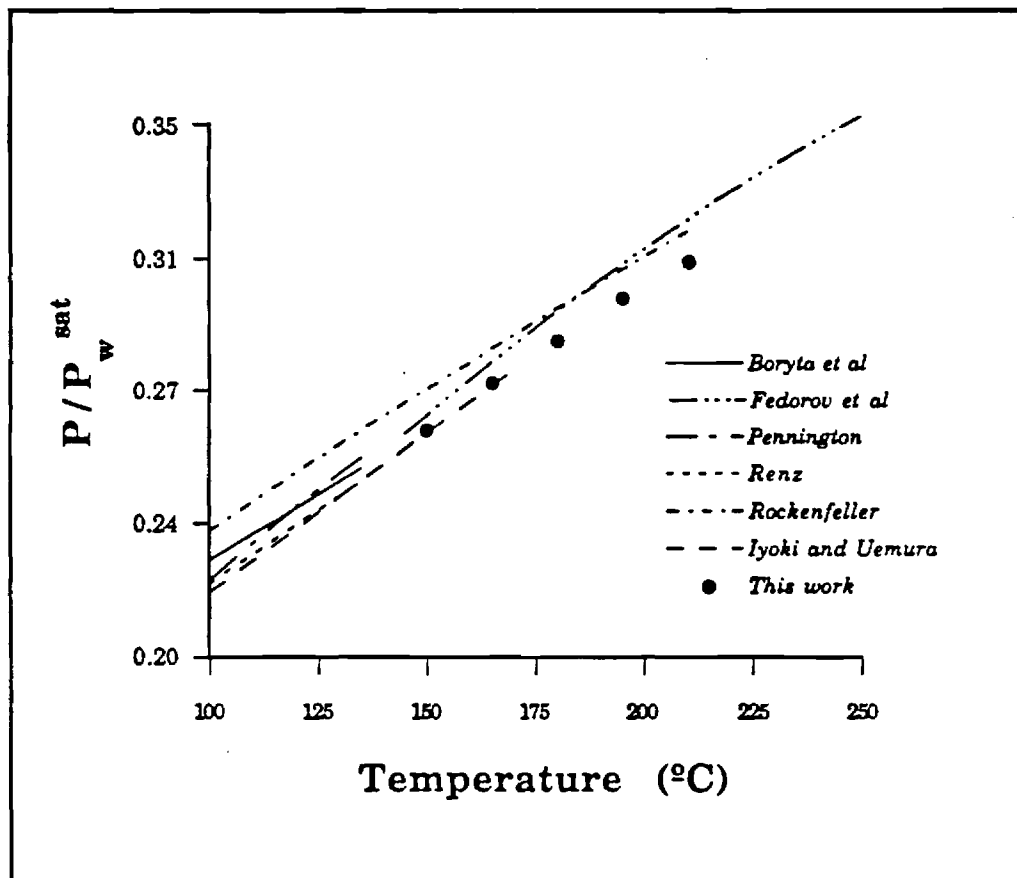


Fig 9c: Data Set Comparison

The comparison was made at a salt mass fraction of 0.5487.



Appendix I

ASHRAE Paper AT-90-30-4 (3380, RP-527): "Properties of Lithium Bromide - Water Solutions at High Temperatures and Concentrations - I. Thermal Conductivity", R. M. DiGuilio, R. J. Lee, S. M. Jeter, and A. S. Teja, **ASHRAE Transactions 1990**, Vol. 96, Part 1, 1990.

PROPERTIES OF LITHIUM BROMIDE-WATER SOLUTIONS AT HIGH TEMPERATURES AND CONCENTRATIONS—I. Thermal Conductivity

R.M. DiGullio

R.J. Lee, Ph.D.

S.M. Jeter, Ph.D., P.E.

A.S. Teja, Ph.D.

Associate Member ASHRAE

ABSTRACT

The thermal conductivity of lithium bromide-water solutions was measured over the temperature range 20° to 190°C using a modified hot wire technique. Solutions containing 30.2, 44.3, 49.1, 56.3, 60.0, 62.9, and 64.9 wt % lithium bromide were studied and comparisons were made with reported data on aqueous lithium bromide solutions at lower temperatures. The data were correlated as a function of temperature and weight percent lithium bromide with an average deviation of 0.6%. The accuracy of the measurements was estimated to be $\pm 2\%$. Subsequent papers in this series will report data on the density, viscosity, heat capacity, and vapor pressure of these mixtures.

INTRODUCTION

The design of refrigeration and heat pump systems that use aqueous lithium bromide (LiBr) solutions requires accurate thermal conductivity data. Most literature data, however, are limited to low temperatures and low concentrations of lithium bromide. The objectives of this work were, therefore, to measure the properties of lithium bromide solutions at high temperatures and concentrations.

An accepted and appropriate technique for the measurement of the thermal conductivity of liquids is the transient hot wire method (Nieto de Castro et al. 1986), in which a thin wire immersed in the liquid is electrically heated. The temperature rise of the wire is used to determine the thermal conductivity of the liquid. Electrically conducting solutions can be measured with this technique, if the wire is electrically insulated from the liquid under study. The insulation blocks the flow of current through the liquid, which would confuse the interpretation of the voltage measurements. However, the addition of an insulating layer to the wire has proved difficult to achieve in practice, especially at higher temperatures. Nagasaka and Nagashima (1981) successfully insulated a platinum wire with a polyester coating and reported measurements up to 150°C. Alloush et al. (1982) used a tantalum filament coated with a layer of tantalum oxide to obtain data on LiBr solutions at temperatures up to 80°C. Recently Kawamata

et al. (1988) used the tantalum-tantalum oxide filament to make measurements on LiBr solutions up to 100°C. However, they noted that the oxide coating failed to insulate the wire properly above 100°C. This limitation was confirmed by our own efforts to use the tantalum-tantalum oxide filament at temperatures above 100°C. This is shown in Figure 1, where the thermal conductivity of water measured with a tantalum wire is plotted as a function of temperature. Above 100°C, deviation from the ESDU (1967) recommended values occurs. The probable reasons for failure are the cracks that develop in the insulation due to the unequal expansion coefficients of the base metal and the oxide, and the decrease in dielectric strength with temperature of the oxide. Both effects might permit

WATER MEASURED WITH TANTALUM CELL

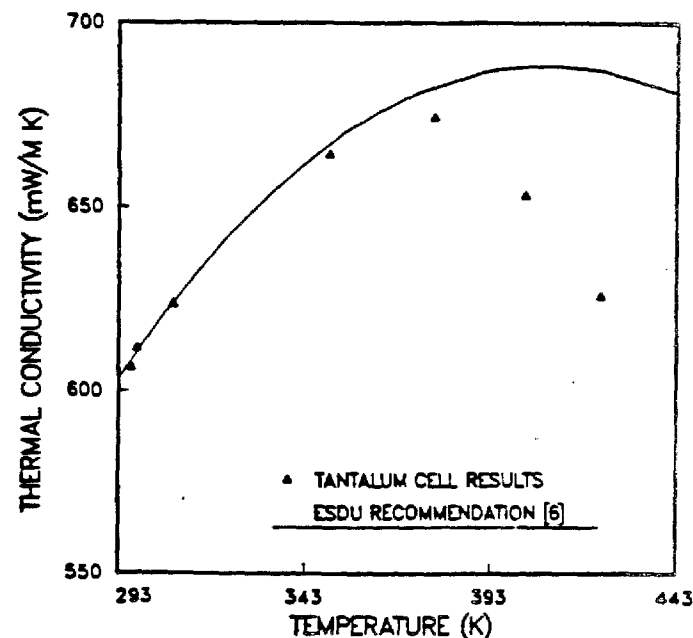


Figure 1 Thermal conductivity of water measured with a tantalum filament insulated with tantalum oxide. The oxide coating fails to insulate above 100°C.

R.M. DiGullio is a Graduate Research Assistant, R.J. Lee is a Research Engineer, and A.S. Teja is a Professor, all in the School of Chemical Engineering, and S.M. Jeter is an Associate Professor in the School of Mechanical Engineering, Georgia Institute of Technology, Atlanta.

THIS PREPRINT IS FOR DISCUSSION PURPOSES ONLY, FOR INCLUSION IN ASHRAE TRANSACTIONS 1990, V. 96, Pt. 1. Not to be reprinted in whole or in part without written permission of the American Society of Heating, Refrigerating and Air-Conditioning Engineers, Inc., 1791 Tullie Circle, NE, Atlanta, GA 30329. Opinions, findings, conclusions, or recommendations expressed in this paper are those of the author(s) and do not necessarily reflect the views of ASHRAE.

than 0.3 milliseconds. The program sampled the offset voltage on one channel, then switched channels to sample the applied voltage to ensure its constancy. The time between any two samples was 0.0084 s and that between two successive readings of the same channel was 0.0168 s. The delay between the closing of the relay and the first sampling was found to be 0.0132 s using an oscilloscope. Two hundred points were measured during each run and the experiment lasted about 3.4 s. From a previous calibration of the temperature vs. resistance, the temperature of the wire was found. A plot of ΔT vs. the logarithm of time was made and the slope in the time interval from 0.7 to 2.2 s was calculated using a least-squares fit, as described in the analysis section. The applied voltage was varied from about 2.5 to 3.5 V so that a more or less constant temperature rise in the quartz capillary surface of about 1.4°C was achieved. This resulted in offset voltages on the order of 5 mV. The A/D card has 16-bit resolution and the ± 25 mV range was used. Thus the card is capable of 0.8 μ V resolution.

SOURCE AND PURITY OF MATERIALS

Anhydrous lithium bromide with a minimum stated purity of 99 wt% LiBr was used in this work. Distilled water was used to prepare the solutions. Solutions were first prepared gravimetrically based on wt% LiBr. To ensure that no change in the composition of a solution occurred during the measurement procedure, samples of each composition were taken before and after the thermal conductivity measurement and checked using a computer-aided titrimeter. The precipitation titration was done using a 0.1 normal standard silver nitrate solution as the titrant. A silver-specific electrode was used to indicate the equivalence point, and a standard calomel electrode was used as the reference electrode. The compositions reported are the averages of a pair of titrations, one before and one after the thermal conductivity measurement. The average deviation between any pair of measurements was 0.4% and the maximum deviation was 0.8%. This agreement indicates that there was little variation in composition during the thermal conductivity measurement.

ANALYSIS

The model for the experiment is an infinite line source of heat submersed in an infinite fluid medium. By monitoring the temperature response of the wire to a step voltage input, the thermal conductivity of the fluid can be deduced. For an infinite line source of heat in an infinite fluid medium, the ideal temperature rise of the wire, ΔT_w , can be calculated using an expression derived by Carslaw and Jaeger (1959) and Healy et al. (1976) for $t \gg r_w^2/4\alpha$, where r_w is the radius of the filament and α is the thermal diffusivity of the fluid. The inequality is satisfied shortly after heating is started, that is, for 10 milliseconds $< t < 100$ milliseconds. The expression is:

$$\Delta T_{id} = \frac{q}{4\pi\lambda} \ln \left(\frac{4\lambda t}{r_w^2 \rho C_p C} \right) \quad (1)$$

where q is the heat dissipation per unit length, λ is the thermal conductivity, ρ is the density, C_p is the heat capacity, t is the time from the application of the step voltage, and C

is equal to $\exp(\gamma)$, where γ is Euler's constant. If it is assumed that all physical properties are independent of temperature over the small range of temperature considered (approximately 1.4°C), then,

$$\lambda = \frac{q}{4\pi \left(\frac{d\Delta T_{id}}{d \ln t} \right)} \quad (2)$$

where $d\Delta T_w/d \ln t$ is found experimentally from a plot of ΔT_w vs. $\ln t$.

Healy et al. (1976) also derived several corrections for the deviation of the model from reality. These may be written as:

$$\Delta T_{id} = \Delta T_w(t) + \sum_i \delta T_i \quad (3)$$

δT_1 accounts for the finite physical properties of the wire (liquid mercury) and is given by Healy et al. (1976):

$$\delta T_1 = \frac{r_w^2 [(\rho C_p)_w - (\rho C_p)]}{2\lambda t} \Delta T_{id} - \frac{q}{4\pi\lambda} \frac{r_w^2}{4\alpha t} \left(2 - \frac{\alpha}{\alpha_w} \right) \quad (4)$$

where $(\rho C_p)_w$ is the volumetric heat capacity of the liquid mercury and α and α_w are the thermal diffusivity of the fluid and mercury, respectively.

The correction due to the finite extent of the fluid is given by Healy et al. (1976):

$$\delta T_2 = \frac{q}{4\pi\lambda} \left(\ln \frac{4\alpha t}{b^2 C} + \sum_{\nu=1}^{\infty} \exp^{-g_\nu^2 \alpha t / b^2} [\pi Y_0(g_\nu)]^2 \right) \quad (5)$$

where b is the inside diameter of the cell, Y_0 is the zero order Bessel function of the second kind, and g_ν are the roots of J_0 , the zero order Bessel function of the first kind. Although the first several roots are readily available, the higher roots can be found to sufficient accuracy using an expression from the work of Watson (1962):

$$g_\nu = (\pi\nu - \pi/4) + \frac{1}{8(\pi\nu - \pi/4)} - \frac{31}{385(\pi\nu - \pi/4)^3} + \frac{3779}{15360(\pi\nu - \pi/4)^5} \quad (6)$$

Values of Y_0 were calculated using the polynomial approximation given by Abramowitz and Stegun (1965).

The effect of the quartz capillary tube on the measurement has been evaluated analytically by Nagasaka and Nagashima (1981). The correction is given by:

(7)

with

$$\begin{aligned} A &= \frac{1}{t} (C0 + B \ln t) \\ C0 &= C1 + C2 + B \ln \left(\frac{4\alpha}{r_w^2 C} \right) \\ C1 &= \frac{r_w^2}{8} \left[\left(\frac{\lambda - \lambda_l}{\lambda_w} \right) \left(\frac{1}{\alpha_w} - \frac{1}{\alpha_l} \right) + \frac{4}{\alpha_l} - \frac{2}{\alpha_w} \right] \\ C2 &= \frac{r_w^2}{2} \left(\frac{1}{\alpha} - \frac{1}{\alpha_l} \right) + \frac{r_w^2}{\lambda_l} \left(\frac{\lambda_l}{\alpha_l} - \frac{\lambda_w}{\alpha_w} \right) \ln \left(\frac{r_l}{r_w} \right) \\ B &= \frac{r_w^2}{2\lambda} \left(\frac{\lambda_l}{\alpha_l} - \frac{\lambda_w}{\alpha_w} \right) + \frac{r_l^2}{2\lambda} \left(\frac{\lambda}{\alpha} - \frac{\lambda_w}{\alpha_w} \right) \end{aligned}$$

TEMPERATURE RISE VS LN(t)

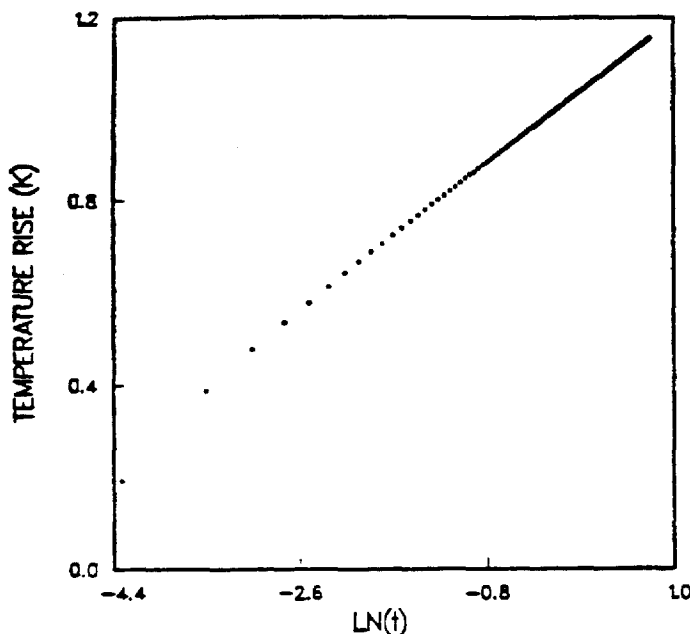


Figure 4 Plot of ΔT_M vs. $\ln t$ obtained from experiment. Only data from 0.7 s to 2.2 s (-35 to .79) were used in the calculation of the slope.

thermal conductivity of the fluid and the adjusted temperature of the system. This series of calculations was repeated until no change in the thermal conductivity occurred. Three iterations were typically required for convergence.

RESULTS

Water was measured at room temperature to validate the liquid metal capillary technique. The agreement with the IUPAC data was excellent, with deviations between our measurements and IUPAC data being within 0.6%. However, the thermal conductivity of water at higher temperatures could not be measured because the low viscosity of water allowed convection to occur during the heating process. Fortunately, the viscosities of lithium bromide solutions were high enough to prevent the rapid onset of convection. In order to verify the linearity of the ΔT vs. $\ln t$ curves, the deviation from the linear fit was checked. Figure 5 shows a plot of the deviation from the fitted line for the same ΔT vs. $\ln t$ curve shown in Figure 4. The points are evenly scattered so that no bias is evident.

Seven compositions of lithium bromide-water solutions were measured (30.2, 44.3, 49.1, 56.3, 60.0, 62.9, and 64.9 wt% LiBr) in the temperature range from 20° to 190°C. The data are compiled in Table 1 and are shown graphically in Figure 5. Each data point represents the average of five experimental runs. The maximum deviation from the average value never exceeded 1.0%, and the precision of the data is therefore 1.0%.

The accuracy of the data was estimated from the sum of the bias error, ϵ_b , and the random error, ϵ_r . The bias error was estimated from:

$$\epsilon_b = \epsilon_{b,LT} + \frac{\partial \epsilon_b}{\partial T} \Delta T_M \quad (12)$$

LINEARITY OF TEMPERATURE VS LN(t) CURVE

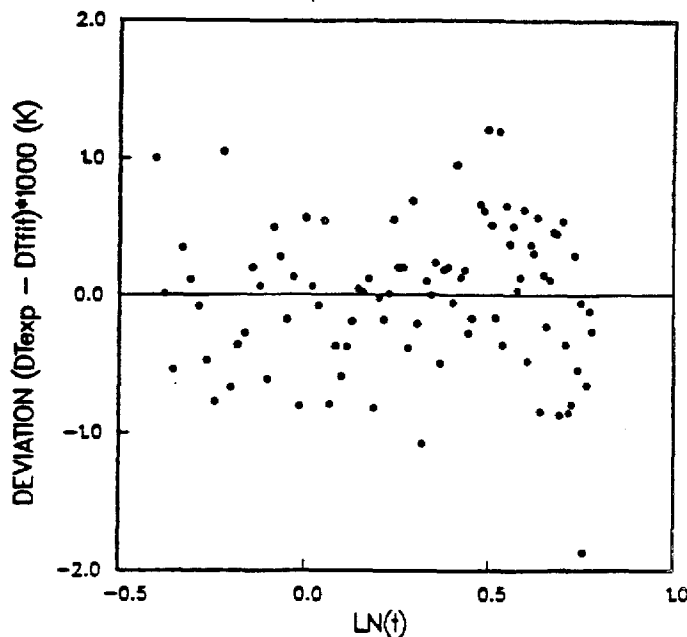


Figure 5 Plot of ΔT vs. $\ln t$ to verify function linearity

where $\epsilon_{b,LT}$ is the low-temperature bias and ΔT_M is the temperature difference between the highest temperature at which the thermal conductivity was measured and the reference temperature. The low-temperature bias was obtained by comparing our data on water with IUPAC data. Since our data were consistently about 0.6% high by comparison with the IUPAC data, we estimate the low-temperature bias error to be 0.6%. Comparison of our data with literature data for temperatures up to 100°C (see Table 2) showed no apparent trends in the bias error with temperature. Thus, we concluded that $\partial \epsilon_b / \partial T$ is approximately 0 and the bias is 0.6% at all temperatures. Random error was estimated from three sources: the uncertainty in the thermal conductivity measurement, the uncertainty in the reported concentration, and the uncertainty in the equilibrium temperature of the fluid, with

$$\epsilon_r^2 = \epsilon_m^2 + \left(\frac{\partial \lambda}{\partial W} \frac{\delta W}{\lambda} \right)^2 + \left(\frac{\partial \lambda}{\partial T} \frac{\delta T}{\lambda} \right)^2 \quad (13)$$

The uncertainty in the measurement, ϵ_m , was 1%. The sensitivity of the thermal conductivity to temperature and concentration was found using the correlation for thermal conductivity reported in the next section of this paper. The maximum value of $\partial \lambda / \partial W$ $1/\lambda$ was found to be -0.011 wt%⁻¹ and the maximum uncertainty in the composition was ± 0.8 wt%. The maximum value of $\partial \lambda / \partial T$ $1/\lambda$ was found to be 0.003 K⁻¹ and the maximum uncertainty in the temperature measurement was ± 0.2 K. The total random error was thus less than 1.4% and the total error was $\pm 2\%$.

Direct comparison of our data with literature data is difficult due to differences in concentrations. Table 2 is a comparison of the correlation found using only our data with the data of Kawamata et al. (1988), Alloush et al. (1982),

Nieto de Castro, C.A.; Li, S.F.Y.; Maitland, C.; and Wakeham, W.A. 1983. "Thermal conductivity of toluene in the temperature range 35-90°C at pressures up to 600 MPa." *Int. J. Thermophys.* Vol. 4, p. 311.

Nieto de Castro, C.A.; Li, S.F.Y.; Nagashima, A.; Trengrove, R.D.; and Wakeham, W.A. 1986. "Standard reference data for the thermal conductivity of liquids." *J. Phys. Chem. Ref. Data*, Vol. 15, p. 1073.

Omotani, T.; Nagaska, Y.; and Nagashima, A. 1982. "Measurement of the thermal conductivity of KNO₃-NaNO₃ mixtures using a transient hot-wire method with a liquid metal in a capillary probe." *Int. J. Thermophys.* Vol. 3, p. 17.

Riedel, L. 1951. "The heat conductivity of aqueous solutions of strong electrolytes." *Chem. Ingr. Tech.*, Vol. 23, p. 59.

Touloukian, Y.S., and Ho, C.Y., eds. 1972a. *Thermal conductivity of nonmetallic solids, vol. 2. The Thermophysical Properties Research Center Data Series*. New York: Plenum Press.

Touloukian, Y.S., and Ho, C.Y., eds. 1972b. *Specific heat of nonmetallic solids, vol. 5. The Thermophysical Properties Research Center Data Series*. New York: Plenum Press.

Tufeu, R.; Petitot, J.P.; Denielou, L.; and Le Neindre, B. 1985. "Experimental determination of the thermal conductivity of molten pure salts and salt mixtures." *Int. J. Thermophys.* Vol. 6, p. 315.

Uemura, T., and Hasaba, S. 1965. "Studies on the lithium bromide-water absorptions refrigerating machine." *Refrig. Japan*, Vol. 40, p. 31.

Watson, G.N. 1962. *A treatise on the theory of Bessel functions*, 2d ed. Cambridge: Cambridge University Press.

Weast, R.C., ed. 1988. *CRC handbook of chemistry and physics*, 69th ed. Boca Raton, FL: CRC Press, Inc.

Williams, E.J. 1925. "The electrical conductivity of some dilute liquid amalgams." *Phil. Mag.*, Vol. 50, p. 589.

TABLE 1
Thermal Conductivity of LiBr-Water Solutions

Wt% LiBr	T [K]	λ [mW/(m·K)]	Wt% LiBr	T [K]	λ [mW/(m·K)]	
0.0	293.8	602.3	49.1	401.2	513.5	
	296.7	607.6		430.0	522.0	
	323.4	646.0		460.0	523.0	
30.2	292.9	508.1	56.3	294.1	419.0	
	296.9	512.1		329.4	453.5	
	326.1	544.6		362.3	468.4	
	329.1	545.9		397.6	484.2	
	359.5	570.7		430.1	493.5	
	365.0	579.5		461.1	501.6	
	385.2	592.0		60.0	299.6	408.8
	388.9	592.8			329.2	432.9
	404.7	597.5			369.7	457.5
	44.3	434.0		591.1	62.9	402.5
435.7		590.2	430.8	476.5		
461.3		573.8	460.6	485.8		
295.1		467.5	64.9	339.8		429.5
321.4		495.4		371.0		447.2
353.5		521.4		400.4		457.3
378.6		535.5	430.7	465.4		
407.2		550.9	460.9	476.1		
439.2		557.3	343.4	421.0		
463.3		553.4	370.5	432.1		
49.1	298.0	446.7	400.7	442.0		
	328.9	478.1	428.8	453.0		
	371.6	503.9	461.0	458.2		

TABLE 2
Comparison of This Work with the Literature [P = 1 atm]

T [K]	Wt% LiBr	λ [mW/(m·K)] Literature	Ref.	λ [mW/(m·K)] This Work ¹	Claimed Accuracy (± %)	% Dev.
297.0	49.7	457	[2]	448.0	3.0	-2.01
305.0		463	[2]	455.8	3.0	-1.57
315.0		464	[2]	465.0	3.0	0.22
335.0		478	[2]	481.6	3.0	0.75
357.0		493	[2]	497.0	3.0	0.80
297.0	53.8	452	[2]	432.9	3.0	-4.40
305.0		457	[2]	440.2	3.0	-3.82
315.0		461	[2]	448.7	3.0	-2.74
335.0		474	[2]	464.2	3.0	-2.11
313		444	[18]	445.2	0.28	0.28
302.5	56.6	428.6	[10]	427.3	0.5	-0.31
313.6		438.0	[10]	436.1	0.5	-0.43
333.5	56.75	452.4	[10]	451.0	0.5	-0.32
353.7		464.0	[10]	464.1	0.5	0.01
373.5		473.7	[10]	475.0	0.5	0.27
353	56.61	463	[18]	463.6	0.13	0.13
323		442	[18]	443.3	0.30	0.30
293	416	[18]	418.4	0.57	0.57	
303	429	[18]	427.0	-0.46	-0.46	
333	451	[18]	450.0	-0.23	-0.23	
313	60.35	418	[18]	420.0	0.47	0.47

TABLE 2
Comparison of This Work with the Literature (Continued)

T [K]	Wt% LiBr	λ [mW/(m·K)] Literature	Ref.	λ [mW/(m·K)] This Work ¹	Claimed Accuracy (± %)	% Dev.	
293.8	0.0	599.1	[11]	602.3 ²		0.55	
296.7		604.1	[11]	607.6 ²		0.58	
323.4	26.04	642.6	[11]	646.0 ²		0.52	
323		557	[18]	558.0		0.18	
313		551	[18]	545.5		-1.01	
353		581	[18]	586.7		0.97	
303		426	[18]	530.9		0.82	
333		564	[18]	567.4		0.60	
304.2		30.3	527.7	[10]	520.7	0.5	-1.35
313.9			536.0	[10]	533.2	0.5	-0.53
333.9			558.6	[10]	555.3	0.5	-0.60
353.5			575.1	[10]	572.1	0.5	-0.53
373.5	588.5		[10]	584.2	0.5	-0.73	
313	521		[18]	516.8		-0.81	
303	503		[18]	502.6		-0.09	
323	521		[18]	524.4		0.65	
293	492		[18]	487.8		-0.87	
333	533		[18]	532.8		-0.04	
343	547	[18]	540.8		-1.15		
353	538	[18]	548.4		1.89		
293	471	[14]	476.2		1.08		
297.0	41.4	473	[2]	476.5	3.0	0.74	
305.0		478	[2]	485.7	3.0	1.58	
315.0		484	[2]	496.3	3.0	2.49	
335.0		500	[2]	515.1	3.0	2.94	
357.0		511	[2]	531.9	3.0	3.93	
303		465	[18]	471.5		1.37	
333		501	[18]	499.5		-0.30	
323		489	[18]	490.6		0.33	
313		486	[18]	481.1		-1.01	
353		509	[18]	512.6		0.71	
297.0	45.6	465	[2]	462.4	3.0	-0.56	
305.0		467	[2]	470.9	3.0	0.82	
315.0		469	[2]	480.8	3.0	2.45	
335.0		483	[2]	498.5	3.0	3.10	
357.0		499	[2]	514.6	3.0	3.02	
293		459	[18]	456.5		-0.55	
302.4		46.5	468.2	[10]	464.9	0.5	-0.70
313.8			477.3	[10]	476.2	0.5	-0.22
333.3		490.8	[10]	493.4	0.5	0.54	
353.6		501.4	[10]	508.5	0.5	1.40	
373.2	510.9	[10]	520.3	0.5	1.81		

¹Values calculated from correlations of our data.

²Experimental value (pure water not included in correlation).

TABLE 3
Constants for Correlation

Constant	Value
a ₁	-1407.53
a ₂	11.0513
a ₃	-1.46741 × 10 ⁻²
b ₁	38.9855
b ₂	-0.240475
b ₃	3.48073 × 10 ⁻⁴
c ₁	-0.265025
c ₂	1.51915 × 10 ⁻³
c ₃	-2.32262 × 10 ⁻⁶

Appendix II

ASHRAE Paper AT-90-30-5 (3381, RP-527): "Properties of Lithium Bromide - Water Solutions at High Temperatures and Concentrations - II. Density and Viscosity", R. J. Lee, R. M. DiGuilio, S. M. Jeter, and A. S. Teja, *ASHRAE Transactions* 1990, Vol. 96, Part 1, 1990.

PROPERTIES OF LITHIUM BROMIDE-WATER SOLUTIONS AT HIGH TEMPERATURES AND CONCENTRATIONS—

II: Density and Viscosity

R.J. Lee, Ph.D.

R.M. DiGullio

S.M. Jeter, Ph.D., P.E.

A.S. Teja, Ph.D.

Associate Member ASHRAE

ABSTRACT

The densities and viscosities of lithium bromide-water solutions were measured at temperatures from 25°C to 200°C and concentrations from 45 wt% to 65 wt% lithium bromide. The data generally agreed with the data available in the literature at low temperatures in the case of density, but the agreement was only fair in the case of viscosity. Correlations of the experimental data are also reported in this paper.

INTRODUCTION

Improvements to the performance of absorption refrigeration equipment require a knowledge of the thermophysical properties of aqueous lithium bromide solutions. The literature data on density and viscosity of such solutions are limited to temperatures up to 100°C only (Uemura and Hasaba 1964; Bogatykh and Evnovich 1963, 1965). In a companion paper, Part I of this work, we reported our measurements of the thermal conductivity of these solutions at high temperatures and concentrations. Subsequent papers will cover the specific heats and vapor pressures. In this paper, we present our measurements of the density and viscosity. The densities and viscosities of solutions with weight percent (wt%) of lithium bromide ranging from 45 wt% to 65 wt% and at temperatures up to 200°C were measured. Correlations of the experimental data are also presented.

EXPERIMENT

Density Measurement

Principle of Operation The principle used to determine the liquid density (ρ) of a fluid in this study is based on the definition:

$$\rho = M/V \quad (1)$$

where M is the mass and V the volume of the fluid. Experimentally, we measured the mass of the fluid required to

fill a calibrated volume (density cell) in a high-pressure pycnometer.

Apparatus and Procedure The high-pressure pycnometer used in this study is shown schematically in Figure 1. The pycnometer is rated up to 300°C and 100 bar and consists of four sampling cylinders capped at one end by a high-pressure fitting. The other end of each cylinder was attached through a pipe nipple, an isolation valve, and a quick-connect coupling to a high-pressure hand pump. The pump was used to maintain pressure in the system in order to suppress boiling. Each stainless steel sampling cylinder, as modified with a thermowell for temperature measurement, had an internal volume of approximately 40 mL. The exact volume of each cell assembly was obtained by calibration with triple-distilled mercury at temperatures up to 150°C. The data were fitted to an appropriate function (either linear or quadratic) for interpolation or extrapolation. Temperature control within $\pm 0.05^\circ\text{C}$ was achieved by a constant-temperature circulating bath filled with silicon oil.

At the beginning of an experiment, the four density cells were cleaned thoroughly, weighed, and then connected to the system. The density cell assembly was then evacuated, filled with the test liquid, and placed in the oil bath. Usually, two hours were allowed for temperature equilibrium to be attained. Once equilibrium had been established, the isolation valves were closed and the pycnometers removed from the oil bath and weighed on an electronic balance.

The solution temperature was measured using a type-K thermocouple that had previously been calibrated against a platinum resistance thermometer. The accuracy of the temperature measurement was estimated to be $\pm 0.1^\circ\text{C}$. The system pressure was monitored by a precision pressure gauge rated at 1500 psi with an accuracy of $\pm 0.25\%$ of full scale. The electronic balance used for weight measurement has a precision of ± 0.001 g.

R.J. Lee is Research Engineer, R.M. DiGullio is Graduate Research Assistant, and A.S. Teja is Professor in the School of Chemical Engineering; S.M. Jeter is Associate Professor in the School of Mechanical Engineering, Georgia Institute of Technology, Atlanta, GA.

THIS PREPRINT IS FOR DISCUSSION PURPOSES ONLY. FOR INCLUSION IN ASHRAE TRANSACTIONS 1990, V. 96, Pt. 1. Not to be reprinted in whole or in part without written permission of the American Society of Heating, Refrigerating and Air-Conditioning Engineers, Inc., 1791 Tullie Circle, NE, Atlanta, GA 30329. Opinions, findings, conclusions, or recommendations expressed in this paper are those of the author(s) and do not necessarily reflect the views of ASHRAE.

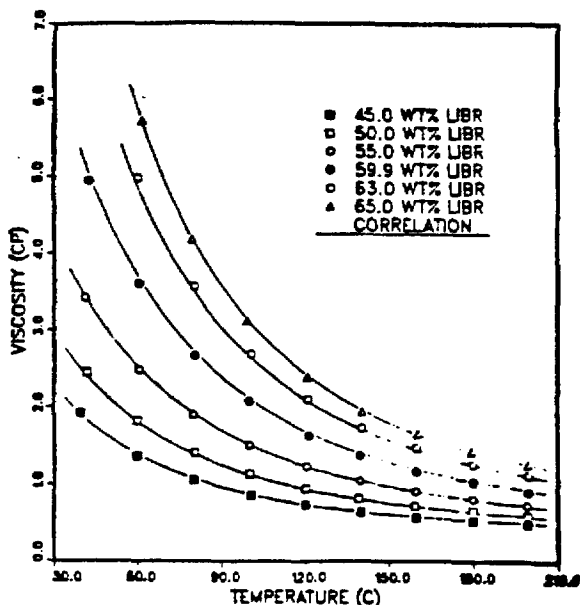


Figure 6 Viscosity of aqueous LiBr solutions

higher at the higher temperatures. It is also apparent that our data are smoother than the literature data.

Our data for viscosity agree fairly well with the graphical data in the 1989 *ASHRAE Fundamentals* (ASHRAE 1989). The handbook data are about 4% higher at 160°F (71.1°C) and 5% to 10% higher at 220°F (104.4°C) for concentrations of 45 wt% to 65 wt%. Because of the strong temperature dependence of viscosity on temperature, however, extrapolation of the handbook curves to higher temperatures is not recommended. Rather, the correlation of Equation 9, shown below, should be used.

CORRELATION

Density

Our results were fitted to the following polynomial function in temperature:

$$\rho = A_0 + A_1T + A_2T^2 \quad (4)$$

where ρ is in gm/mL and T is in K. The values of A_0 , A_1 , and A_2 were determined by minimizing the sum of squares of the relative deviations: $\sum_i [(\rho_{\text{expt},i} - \rho_{\text{calc},i})/\rho_{\text{expt},i}]^2$. The constants A_0 , A_1 , and A_2 were further interpolated in terms of wt% of lithium bromide (X) as follows:

$$A_0 = (10976.3 + 0.71244X + 2.21446X^2) \cdot 10^{-4} \quad (5)$$

$$A_1 = (6796.2 - 148.247X - 0.89696X^2) \cdot 10^{-7} \quad (6)$$

$$A_2 = (-350.97 - 324.312X + 4.97020X^2) \cdot 10^{-10} \quad (7)$$

All data could be correlated with the above equation with an overall average absolute deviation (AAD) of 0.06% and maximum absolute deviation (MAD) of 0.19%. Figure 5 shows the comparison between the values calculated by Equation 4 and the observed values.

It should be noted that the above correlation is based only on lithium bromide concentrations between 45 wt%

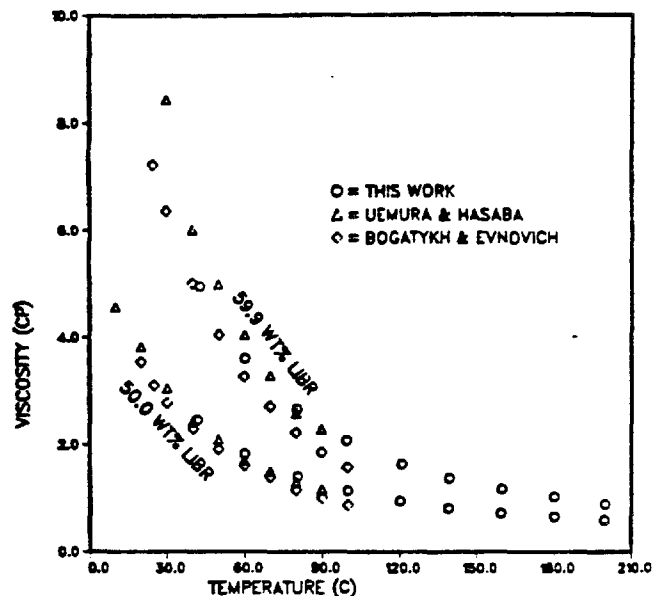


Figure 7 Comparison of the viscosity of LiBr-water solutions obtained by different investigators

and 60 wt% measured in this investigation. Extrapolation to other concentrations is not recommended. To cover a wider range of X , we included the data available in the literature at lower temperatures in the following simpler equation:

$$\rho = \frac{1145.36 + 4.7084X + 0.137479X^2}{1000} - \frac{33.3393 + 0.571749X}{100000} T \quad (8)$$

Figure 8 illustrates good agreement between the calculated values and experimental data of this work and of

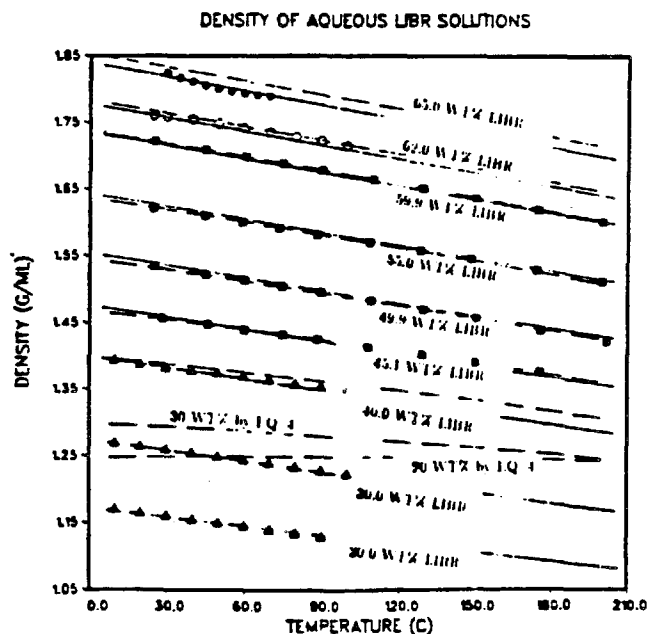


Figure 8 Comparison of density correlations with experimental data.

This apparatus was designed for temperatures up to 200°C and pressures up to 30 atm.

A Size 1 Zeiffuchs (1946) cross-arm capillary viscometer was used for determination of the kinematic viscosity. The calibration factor was determined at room temperature using pure water. In order to repeat a measurement without reloading the liquid sample, the viscometer was calibrated with a wetted capillary. After calibration, the viscometer was placed inside the pressure cell and the capillary end was connected to the pressure distribution section through V5. The reservoir end was opened to the cell chamber such that the pressure over the viscometer could be balanced. The cell was equipped with four glass view ports (tempered borosilicate glass) to allow visual observation of the reservoir and the measuring bulb of the viscometer. An insulated air bath, heated by a primary (800 W) and a secondary (200 W) heater, was used to establish the desired temperature. A stable temperature in the air bath was maintained by a commercial temperature control unit and a circulating fan. Temperature fluctuations were minimized by the mass of the pressure cell, which was made of heavy steel. The test fluid was moved back and forth through the capillary tube by a high-pressure hand pump with helium as the pressurizing fluid.

The temperature was measured inside the cell by a chromel-alumel thermocouple, calibrated with an NBS-calibrated platinum resistance thermometer. The accuracy of the temperature measurement was estimated to be $\pm 0.1^\circ\text{C}$. Pressure measurement was accomplished by a precision gauge with an accuracy of 0.25% of full scale (0 to 1500 psi). An electronic timer accurate to 1/100 second was used to obtain the efflux time.

Before an experiment was performed, a clean, dry viscometer loaded with the appropriate test solution was attached to the top flange of the pressure cell. The top flange was then bolted into place, and the cell was connected to the pressure distribution section and pressurized slowly to the desired pressure. To eliminate loss of vapor from the solution, about 40 mL of slightly dilute lithium

bromide solution was placed at the bottom of the cell chamber so that the solution in the viscometer was always under its vapor pressure.

At the beginning of an experiment, all valves were closed except for V4 and V5. The pressure on the capillary end was reduced by the use of the hand pump, causing the solution to flow into the reverse bend of the capillary. Once the flow had been initiated, valve V3 was opened to balance the pressures over both ends of the viscometer. The efflux time for the solution to flow between the timing marks on the measuring bulb was then measured. At the end of the measurement, valve V3 was closed and the solution was then forced to return to the reservoir by increasing the pressure on the capillary end with the hand pump. Measurements were repeated until consistent efflux times were obtained.

Reference Experiment To test the apparatus and procedures, the kinematic viscosity of pure water was measured and compared with values reported by the National Institute of Standards and Technology (see CRC 1982). As illustrated in Figure 4, good agreement was obtained between the two sets of measurements. The density of water reported by Gildseth et al. (1972) was used to convert the measured kinematic viscosity to the absolute viscosity shown in this graph.

MATERIAL AND SOLUTION PREPARATION

N-methylpyrrolidinone (99.5% purity), mercury (99.999+ % purity), and HPLC-grade water were purchased from three manufacturers. Anhydrous lithium bromide was provided and had a certified purity of 99.3% by weight. These chemicals were used without further purification. Aqueous lithium bromide solutions were prepared by adding degassed water to fresh anhydrous lithium bromide. The solutions were degassed by an alternating freeze-thaw procedure. About 0.2% of impurities by weight (excluding water) were ignored in calculating the concentrations of the prepared solutions. The concentrations were determined gravimetrically and checked on a computer-aided titrator. Solution concentrations determined by these two methods agreed within ± 0.1 wt% lithium bromide.

RESULTS AND DISCUSSION

Density

Table 1 summarizes the measured densities of four lithium bromide-water solutions containing 45.1, 49.9, 55.0, and 59.9 wt% of lithium bromide, respectively. Since high-concentration solutions are supersaturated at room temperature, the 65 wt% solution could not be measured with this apparatus because the solution would crystallize in unheated sections of the apparatus (such as the pressure gauge or exposed tubing). Measurements on the remaining solutions were performed at temperatures from ambient to 200°C. The system pressure was maintained at 150 psig throughout the experiments. At least three samples were taken at each condition to give the average reported in Table 1. The reproducibility of the results was $\pm 0.1\%$ and the accuracy of the data was estimated to be 0.25%.

The densities of aqueous lithium bromide solutions at lower temperatures have been reported by Uemura and Hasaba (1964) and Bogatykh and Evnovich (1965). Figure

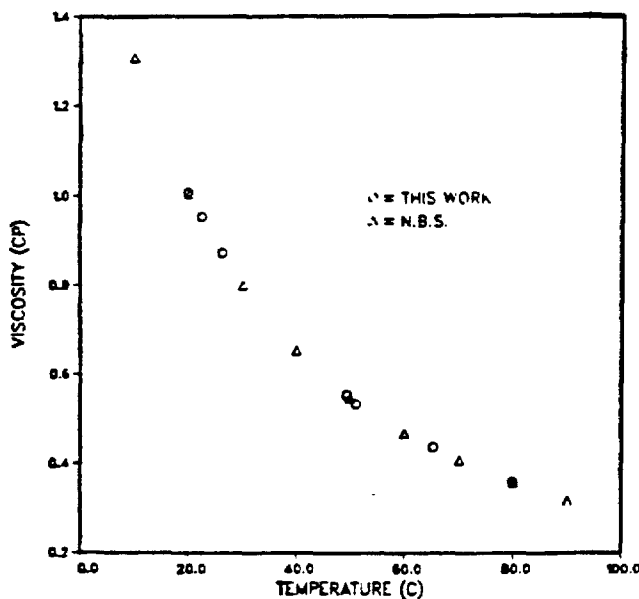


Figure 4 Viscosity of liquid water